



## City Research Online

### City, University of London Institutional Repository

---

**Citation:** Kimambo, C. (1996). Modelling of linebreak in high-pressure gas pipes.  
(Unpublished Doctoral thesis, City University London)

This is the accepted version of the paper.

This version of the publication may differ from the final published version.

---

**Permanent repository link:** <https://openaccess.city.ac.uk/id/eprint/7934/>

**Link to published version:**

**Copyright:** City Research Online aims to make research outputs of City, University of London available to a wider audience. Copyright and Moral Rights remain with the author(s) and/or copyright holders. URLs from City Research Online may be freely distributed and linked to.

**Reuse:** Copies of full items can be used for personal research or study, educational, or not-for-profit purposes without prior permission or charge. Provided that the authors, title and full bibliographic details are credited, a hyperlink and/or URL is given for the original metadata page and the content is not changed in any way.

# **MODELLING OF LINEBREAK IN HIGH-PRESSURE GAS PIPES**

**by**

**Cuthbert Z M Kimambo**

**A thesis submitted to  
City University  
in partial fulfilment of the  
requirement for the degree of  
Doctor of Philosophy**

**July, 1996**

**Department of Mechanical  
Engineering & Aeronautics**

**City University  
London**

# TABLE OF CONTENTS

	Page
TABLE OF CONTENTS	2
LIST OF TABLES	6
LIST OF FIGURES	7
ACKNOWLEDGMENTS	10
DECLARATION	11
ABSTRACT	12
NOMENCLATURE	13
 <b>CHAPTER 1: INTRODUCTION</b>	 16
1.1 TRANSPORTATION OF NATURAL GAS IN PIPELINES	16
1.2 RUPTURE AND BLOWDOWN OF GAS PIPELINES	17
1.3 COMPUTER CODES FOR ANALYSIS OF FLUID FLOW IN PIPES	19
1.4 PREVIOUS WORK AT CITY UNIVERSITY	22
 <b>CHAPTER 2: THEORETICAL DEVELOPMENT OF THE BASIC EQUATIONS FOR UNSTEADY FLOW</b>	 27
2.1 INTRODUCTION	27
2.2 MAJOR ASSUMPTIONS AND SIMPLIFICATIONS	32
2.2.1 Dimension of Flow	32
2.2.2 Flow Phase	34
2.2.3 Fluid Structure Interaction	36
2.2.4 Minor Losses and Changes in Cross-section	38
2.3 DERIVATION OF THE BASIC EQUATIONS FOR UNSTEADY FLOW OF A COMPRESSIBLE FLUID IN A PIPE	39
2.4 THERMODYNAMIC AND TRANSPORT PROPERTIES	48
2.4.1 Introduction	48
2.4.2 Thermal Equations of State for Real Gases	50
2.4.3 Theoretical Approach to the Equation of State	53
2.4.3.1 Introduction to the Basic Principles and Equations	53
2.4.3.2 The Principle of Corresponding States	56
2.4.3.3 Extension of the Principle of Corresponding States	57
2.4.3.4 Commercial Computer Software	58
2.4.3.4.1 IUPAC	58
2.4.3.4.2 QUANT	58
2.4.3.4.3 PREPROP	59
2.4.4 Other Approaches for Real-Gas Mixtures	60
2.4.5 Caloric Equations of State	60

2.5	<b>FRICTIONAL FORCE</b>	62
2.5.1	Introduction	62
2.5.2	Steady Flow Friction Factor	63
2.5.3	Flow-Dependent Friction Factor	64
2.5.4	Frequency-Dependent Friction Factor	68
2.5.5	Friction Factor for Two-Phase Homogeneous Flow	69
2.5.6	Friction Factor With Respect to Fluid Structure Interaction	70
2.5.7	Approximation of Friction Factor When Solving the Basic Equations	70
2.6	<b>HEAT TRANSFER</b>	71
2.6.1	Introduction	71
2.6.2	Heat Transfer Process	71
2.6.3	Calculation of Heat Transfer	74
2.7	<b>OTHER APPROACHES TO THE BASIC EQUATIONS</b>	79
	<b>CHAPTER 3: METHODS FOR SOLUTION OF THE BASIC EQUATIONS</b>	82
3.1	<b>INTRODUCTION</b>	82
3.2	<b>NUMERICAL METHODS OF SOLUTION</b>	83
3.2.1	Finite-Difference Methods	83
3.2.1.1	General Description	83
3.2.1.2	Explicit Finite-Difference Methods	84
3.2.1.3	Method of Characteristics	86
3.2.1.4	Lax-Wendroff Second-Order Two-Step Method	88
3.2.1.5	Implicit Finite-Difference Methods	89
3.2.2	Finite-Element Methods	90
3.2.3	Flux-Difference Splitting Schemes	92
3.2.4	Method of Lines	94
3.2.5	Wave-Plan Method	96
3.3	<b>A REVIEW OF SOME NUMERICAL STUDIES</b>	97
3.3.1	General Studies on Transient Flow	97
3.3.2	Studies on Pipeline Rupture and Blowdown	109
3.4	<b>DISCUSSION OF NUMERICAL METHODS</b>	118
	<b>CHAPTER 4: THE COMPUTER MODEL FOR LINEBREAK ANALYSIS</b>	122
4.1	<b>SIMPLIFICATION OF THE BASIC EQUATIONS OF FLOW</b>	122
4.1.1	Should the Small Terms be Neglected?	122
4.1.2	Solution Procedure	124
4.1.3	Representation of Non-Linear Terms	126
4.2	<b>INITIAL AND BOUNDARY CONDITIONS</b>	126
4.2.1	Introduction	126
4.2.2	Steady State Analysis	128



4.2.2.1 Basic Equations for Steady State Flow	128
4.2.2.2 Incompressible Flow	130
4.2.2.3 Isothermal Compressible Flow	130
4.2.2.4 Adiabatic Compressible Flow	132
4.2.2.5 Non-isothermal Non-adiabatic Compressible Flow	139
4.2.3 Break Boundary Conditions	140
4.3 NUMERICAL SOLUTION OF THE BASIC EQUATIONS FOR UNSTEADY FLOW	146
4.3.1 Introduction	146
4.3.2 Method of Characteristics	148
4.3.3 MacCormack Second-order Two-step Method	179
4.3.4 Warming-Kutler-Lomax Third-order Method	182
4.4 VARIABLE GRID SIZE	184
4.5 APPLICATION OF THE QUANT SOFTWARE FOR THERMODYNAMIC AND TRANSPORT PROPERTIES OF FLUIDS	187
4.6 COMPUTER CODES	192
4.7 PREPARATION OF GENERAL GAS AND SYSTEM DATA	205
<b>CHAPTER 5: A REVIEW OF SOME EXPERIMENTAL AND NUMERICAL DATA</b>	<b>212</b>
5.1 INTRODUCTION	212
5.2 LABORATORY EXPERIMENTS	213
5.2.1 Description of the Shock Tube Test	213
5.2.2 Review of Some Laboratory Experiment	214
5.3 REVIEW OF SOME FULL-SCALE PIPELINE EXPERIMENTS	217
5.4 REVIEW OF SOME NUMERICAL DATA	220
5.5 SELECTION OF TEST DATA	222
<b>CHAPTER 6: VALIDATION OF THE COMPUTER MODEL</b>	<b>226</b>
6.1 VALIDATION PROCEDURE	226
6.2 COMPARISON OF COMPUTER MODEL PREDICTIONS WITH EXPERIMENTAL RESULTS	227
6.2.1 Foothills Test Data	227
6.2.2 British Gas Test Data	231
6.2.3 SNGSO Test Data	237
6.2.4 API Test Data	244
6.3 DISCUSSION OF VALIDATION RESULTS	249

<b>CHAPTER 7: CASE STUDY: THE SONGO SONGO-DAR ES SALAAM NATURAL GAS PIPELINE</b>	<b>272</b>
7.1 A BRIEF OVERVIEW OF TANZANIA'S ENERGY SECTOR	272
7.2 DESCRIPTION OF THE SONGO SONGO GAS DEVELOPMENT PROJECT	274
7.2.1 Background Information	274
7.2.2 Gas Properties	275
7.2.3 Preliminary Pipeline Design	277
7.3 COMPUTER SIMULATION OF A LINEBREAK IN THE SONGO SONGO-DAR ES SALAAM GAS PIPELINE	281
7.4 DISCUSSION OF SIMULATION RESULTS	286
<b>CHAPTER 8: RECOMMENDATIONS FOR FURTHER WORK</b>	<b>288</b>
<b>CHAPTER 9: CONCLUSIONS</b>	<b>291</b>
<b>REFERENCES AND BIBLIOGRAPHY</b>	<b>297</b>
<b>APPENDICES</b>	<b>309</b>
A General Equations	309
B Expressions for Equation of State	310
C Expressions for Friction Factor	314
D List of Programmes and Sub-routines	318
E Programme Listings (in a floppy disk)	

## **LIST OF TABLES**

<b>Table 2.1</b>	<b>McAdams Constants for Natural Convection to Air</b>
<b>Table 4.1</b>	<b>Possible Boundary Conditions</b>
<b>Table 4.2</b>	<b>General Gas and System Data Layout</b>
<b>Table 6.1</b>	<b>Foothills Tests General Data</b>
<b>Table 6.2</b>	<b>Average Gas Composition for Foothills Tests</b>
<b>Table 7.1</b>	<b>Average (Mol. %) Composition of Songo Songo Gas</b>
<b>Table 7.2</b>	<b>Songo Songo Gas Properties</b>
<b>Table 7.3</b>	<b>Projected Gas Demand for the Three Scenarios for Years 2011 and 2016</b>
<b>Table 7.4</b>	<b>Estimated Gas Velocities and Pipe Sizes</b>
<b>Table 7.5</b>	<b>Pipe Parameters</b>
<b>Table 7.6</b>	<b>Block Valve Parameters</b>



## **LIST OF FIGURES**

Figure 2.1	Flow Pattern for Air-water Mixture Flowing in a Pipe
Figure 2.2	Sketch Showing the Control Volume at the Beginning of a Time Step
Figure 2.3	Sketch Illustrating Equation 2.2
Figure 2.4	Conical Control Volume Illustrating Body Forces
Figure 2.5	Control Volume Illustrating Heat and Work Transfer
Figure 2.6	Distribution of Pressure, Temperature and Velocity Along the Pipe Diameter
Figure 2.7	Radial Temperature Distribution Across a Pipe Section and its Surroundings
Figure 3.1	Finite-difference Grid Illustrating the Two-step Lax-Wendroff Method
Figure 4.1	Grid Illustrating Steady State Analysis
Figure 4.2	Pressure and Velocity Variations Illustrating Flatt's Decompression Model
Figure 4.3	Decompression Curve at the Break Boundary
Figure 4.4	Grid Illustrating Hybrid Method of Characteristics Solution at Interior Points
Figure 4.5	Solution Domain Using Interior Points Only
Figure 4.6	Grid Illustrating Hybrid Method of Characteristics Solution at Boundary Points
Figure 4.7	Finite-difference Grid Illustrating the MacCormack Method Solution
Figure 4.8	Finite-difference Grid Illustrating the Warming-Kutler-Lomax Method Solution
Figure 4.9	Grid Illustrating Hybrid Method of Characteristics Solution at Interior Boundary Points Without Interpolation
Figure 4.10	Grid Illustrating Hybrid Method of Characteristics Solution at Interior Boundary Points With Interpolation
Figure 4.11	Flow Chart for Tiley's Computer Programme
Figure 4.12	Flow Chart for the Main Computer Code for the New Model
Figure 4.13	Flow Chart for Sub-programme STEAD
Figure 4.14	Flow Chart for Sub-programmes TRANS and BREAK for Transient Analysis
Figure 4.15	Flow Chart for a Typical Method of Characteristics Programme
Figure 4.16	Flow Chart for Sub-routines S..MOC..1 and S..MOC..2
Figure 4.17	Dimensions of the Test Section of the Pipe
Figure 4.18	Diameters of the Pipe in the Test Section
Figure 4.19	Test Section of the Pipe After the Break Illustrating a Variable Grid
Figure 6.1	Schematic of Foothills Test NABTF1



Figure 6.2	Schematic of Foothills Test NABTF7
Figure 6.3	p-t Curves for Foothills Test NABTF1 East Comparison with First-order Method of Characteristics Predictions
Figure 6.4	p-t Curves for Foothills Test NABTF1 East Comparison with MacCormack Method Predictions
Figure 6.5	Pressure Wave Propagation Speed for Foothills Test NABTF1 East
Figure 6.6	p-t Curves for Foothills Test NABTF7 West Comparison with First-order Method of Characteristics Predictions
Figure 6.7	Pressure Wave Propagation Speed for Foothills Test NABTF7 West
Figure 6.8	Schematic of British Gas Tests BGT1, BGT2 and BGT3
Figure 6.9	p-t Curves for British Gas Test BGT1 Comparison with First-order Method of Characteristics Predictions
Figure 6.10	p-t Curves for British Gas Test BGT1 Comparison with Second-order Method of Characteristics Predictions
Figure 6.11	p-t Curves for British Gas Test BGT1 Comparison with MacCormack Method (Alternative 1) Predictions
Figure 6.12	p-t Curves for British Gas Test BGT2 Comparison with MacCormack Method (Alternative 1) Predictions
Figure 6.13	p-t Curves for British Gas Test BGT2 Comparison with MacCormack Method (Alternative 2) Predictions
Figure 6.14	p-t Curves for British Gas Test BGT2 Comparison with MacCormack Method (Alternative 3) Predictions
Figure 6.15	p-t Curves for British Gas Test BGT3 Comparison with MacCormack Method (Alternative 3) Predictions
Figure 6.16	p-t Curves for British Gas Test BGT3 Comparison with Warming-Kutler-Lomax Method Predictions
Figure 6.17	p-t Curves for British Gas Test BGT3 Comparison with First-order Method of Characteristics Predictions ( $\Delta x=0.01\text{m}$ )
Figure 6.18	p-t Curves for British Gas Test BGT3 Comparison with Second-order Method of Characteristics Predictions ( $\Delta x=0.01\text{m}$ )
Figure 6.19	p-t Curves for British Gas Test BGT3 Comparison with Second-order Method of Characteristics Predictions ( $\Delta x=0.1\text{m}$ )
Figure 6.20	Pressure Wave Propagation Speed Curves for BMI Tests
Figure 6.21	Pressure Wave Propagation Speed Curves for University of Calgary Tests
Figure 6.22	Schematic of SNGSO Test
Figure 6.23	u-t Curves for SNGSO Test Comparison with First-order Method of Characteristics Predictions

Figure 6.24	p-t Curves for SNGSO Test Comparison with First-order Method of Characteristics Predictions
Figure 6.25	Velocity Head Curves for SNGSO Test Comparison with First-order Method of Characteristics Predictions
Figure 6.26	Schematic of Alberta Petroleum Industry Tests APIT1 and APIT2
Figure 6.27	Schematic of Alberta Petroleum Industry Tests APIT3
Figure 6.28	Mass Flow Rate for Alberta Petroleum Industry Test APIT1 Comparison with Second-order Method of Characteristics Predictions
Figure 6.29	Pressure at Intact End for Alberta Petroleum Industry Test APIT1 Comparison with Second-order Method of Characteristics Predictions
Figure 6.30	Mass Flow Rate for Alberta Petroleum Industry Test APIT2 Comparison with First-order Method of Characteristics Predictions
Figure 6.31	Pressure at Intact End for Alberta Petroleum Industry Test APIT2 Comparison with First-order Method of Characteristics Predictions
Figure 6.32	Mass Flow Rate for Alberta Petroleum Industry Test APIT3 Comparison with First-order Method of Characteristics Predictions
Figure 6.33	Pressure at Intact End for Alberta Petroleum Industry Test APIT3 Comparison with First-order Method of Characteristics Predictions
Figure 7.1	Map of Africa Showing the Location of Tanzania
Figure 7.2	Map of Tanzania Indicating the Location of the Songo Songo Gas Development Project
Figure 7.3	Kilwa Kivinje-Dar es Salaam Gas Pipeline Location Map
Figure 7.4	Pipeline Route from Songo Songo Island to Dar es Salaam
Figure 7.5	Line Pressure Profile for Low Scenario
Figure 7.6	Line Pressure Profile for Medium Scenario
Figure 7.7	Block Valves Location
Figure 7.8	Line Pressure Profile for High Scenario Comparison with Model Predictions
Figure 7.9	Line Pressure Profile for Simulated Break in the Songo Songo-Dar es Salaam Pipeline
Figure 7.10	Mass Flow Rate Profile for Simulated Break in the Songo Songo-Dar es Salaam Pipeline



## **ACKNOWLEDGMENTS**

I wish to express my sincere gratitude and appreciation to all individuals and organizations who contributed to the successful completion of this study.

I wish to express special thanks and appreciation to my supervisor, Prof. A. R. D. Thorley, first for providing the research topic; for his continuous encouragement; guidance; criticisms; and support, even in matters beyond academic life.

I also wish to extend particular thanks to the German Government who, through the German Academic Exchange Service (DAAD) provided generous financial support for the study programme and also for the purchase of the QUANT software for thermodynamic and transport properties of fluids.

Particular thanks also go to the University of Dar es Salaam for granting study leave, support and encouragement during the study period.

It is not possible to mention every individual and organization who assisted but I am very much indebted to Mr. Renè Flatt of the Swiss Federal Institute of Lausanne, whose untiring contribution in various academic aspects of the project has been invaluable. In this regard I also wish to mention Prof. Stephen Richardson of Imperial College, London.

I wish to thank all organizations which generously provided various literature and data used in this study. In particular I would like to mention British Gas Plc, the Energy Resources Conservation Board, and the NOVA Gas Transmission both of Alberta, Canada for providing experimental data; and the Ministry of Water, Energy and Mineral, and Hardy BBT Ltd. in Dar es Salaam for providing information about the proposed Songo Songo to Dar es Salaam natural gas pipeline.

# **DECLARATION**

I grant powers of discretion to the University Librarian to allow the thesis to be copied in whole or in part without further reference to the author. The permission covers only single copies made for study purposes, subject to normal conditions of acknowledgment.



## ABSTRACT

Although there are many computer codes available for analysis of fluid transients, only a few are known to be applicable to linebreak situations and their scope is limited. There is, therefore, still a big potential for development work in the subject. Discrepancies between different models which have been developed have mainly centred on the assumptions used in developing the basic partial differential equations of flow, and subsequent simplifications; the thermophysical model used; representation of various terms in the equations such as the friction term; and the numerical method of solution of the basic partial differential equations.

A previous model developed by Tiley (1989), overestimated the actual wave speeds and had problems of instability of the solution. A new approach, in which the three basic partial differential equation of flow are derived, based on the assumption of an unsteady quasi-one-dimensional flow of a real gas through a rigid constant cross-section area pipe, and using the Gamma Delta method is used. No further simplification is made on the basic equations. Significant improvements have been made on the type of equation of state, thermodynamic model, heat transfer approximation and friction factor representation. The QUANT software for thermodynamic and transport properties of real gases is used. A flow dependent explicit equation of Chen (1979) is used to calculate the frictional force and heat transfer is calculated using the concept of recovery factor and adiabatic wall temperature. Numerical solution of the basic equations is performed using the third-order Warming-Kutler-Lomax method, the second-order MacCormack method and the method of characteristics. A pc based computer coding with the C language is used.

The QUANT software has successfully been incorporated with the programme. The full benefits of the software could not be realised with linebreak problems due to limitation of the range within which it gives output at present, but satisfactory results have nevertheless been attained.

An improved and more accurate way of calculating the break boundary condition has been used. A non-uniform grid spacing has been used, which allow fine grid spacing in the vicinity of the break in order to enable accurate modelling of the rapid transients occurring in that part. Two different models for calculating the heat transfer i.e. one for the case of pipes exposed to the atmosphere and buried pipes have been incorporated with the model.

Experimental data from full-scale pipeline tests is used to validate the computer models. Results from the computer model simulations show good agreement with the experimental data. The MacCormack method has been found to be unsuitable for modelling transient flow following linebreak in high-pressure gas pipelines. The method of characteristics has proved to be the method of solution for such applications. A better understanding of the flow following a break in high-pressure gas pipes is achieved, especially the decompression behaviour at the break boundary. Data gathered from feasibility studies conducted in the late 1980's for a pipeline in Tanzania is used to validate the steady state analysis model and to simulate a linebreak in the pipeline. Results of the computer simulation are discussed and recommendations made on the suitability the pipeline design.

Additional work is recommended on refining and further testing of the computer programmes and using the Gamdeleps method which covers all the three phases region i.e. gas, liquid and gas/liquid.

# NOMENCLATURE

Symbol	Description	Units
A	Cross-section area of pipe	$m^2$
$a$	Wave speed	$m/s$
$c$	Pipe wall thickness	$m$
$C_n$	Courant number	-
$C_p$	Specific heat of gas at constant pressure	$J/kgK$
$C_v$	Specific heat of gas at constant volume	$J/kgK$
$d$	Pipe diameter	$m$
$D$	Depth of pipe	$m$
$E$	Energy of the system	$J$
$e$	Specific internal energy of gas	$J/kg$
$F$	Force	$N$
$f$	Friction factor	-
$g$	Gravitational acceleration	$m/s^2$
$H$	Vertical height/piezometric height	$m$
$h$	Specific enthalpy of gas	$J/kg$
$h_{BL}$	Heat transfer coefficient through the boundary layer	$W/mK$
$h_{CA}$	Convective heat transfer to the atmosphere	$W/mK$
$I$	Inventory/mass of gas in the pipeline	$kg$
$k$	Thermal conductivity	$W/mK$
$L$	Length of pipeline/wetted perimeter	$m$
$M$	Molecular weight of gas	$kg/mol$
$M_a$	Mach number	-
$m$	Mass flow rate of gas	$kg/s$
$N_L$	Avogadro's number	-
$p$	Static pressure of gas	$Pa$
$Pr$	Prandtl number	-
$Q$	Heat transfer rate per unit volume	$J/m^3s$
$q$	Pseudo-viscosity variable	$N/m^2$
$r$	Radial distance of the pipe	$m$
$R$	Specific gas constant	$J/kg$



$R_c$	Recovery factor	-
$Re$	Reynolds number	-
$S$	Specific entropy of gas	J/kgK
$St$	Stanton number	-
$T$	Temperature of gas	K
$t$	Time	s
$U$	Overall heat transfer coefficient	W/mK
$u$	Flow velocity of gas	m/s
$V$	Volume flow rate of gas	m <sup>3</sup> /s
$W$	Work done by the system	J
$x$	Horizontal distance along the pipe	m
$Z$	Compressibility factor of gas	-

### Greek Symbols

$\alpha$	Polytropic alpha coefficient	-
$\beta$	Polytropic beta coefficient	-
$\gamma$	Polytropic gamma coefficient	-
$\Delta$	Small change in the quantity	-
$\Delta E$	Change in energy of the system	J
$\delta$	Polytropic delta coefficient	-
$\epsilon$	Polytropic epsalon coefficient	-
$\epsilon$	Roughness of pipe	m
$\theta$	Angle of inclination of pipe to horizontal	radians
$K$	Ratio of specific heats	-
$\mu$	Coefficient of dynamic viscosity	kg/ms
$\nu$	Kinematic viscosity	m <sup>2</sup> /s
$\rho$	Density of gas	kg/m <sup>3</sup>
$\nu$	Specific volume of gas	m <sup>3</sup> /kg
$\Phi$	Viscous dissipation function	-
$\chi$	Thermodynamic quantity/dryness fraction	-
$\psi$	Conical angle of the pipe	radians
$\varphi$	Free parameter	-
$\Omega$	Heat flow into the pipe per unit length of pipe per unit time	J/m s
$\omega$	Frictional force per unit length of pipe	N/m

### **Subscripts**

A	Atmosphere
aw	Adiabatic-wall
BL	Boundary layer
c	Critical
CA	Convection to atmosphere
D	Darcy's
e	Equalization
eff	Effective
F	Fanning's
m	surrounding media
o	Stagnation/initial
p	At constant pressure/pipe
pw	Pipe wall
R	Reduced (ratio to critical value)
r	radial
S	Isentropic
wo	Outer pipe wall
wi	Inner pipe wall

### **Superscripts**

-	mean
---	------



# **CHAPTER 1**

## **INTRODUCTION**

### **1.1 TRANSPORTATION OF NATURAL GAS IN PIPELINES**

Transportation of natural gas in pipelines takes place at very high pressures (typically 35-150bar, though higher pressures are also used). In main transmission lines, the gas mixture normally exists in one phase (liquid phase), thus avoiding problems such as multi phase flow and reduction in pipe capacity. These high pressure pipelines, normally cover very long distances. The largest natural gas pipeline network in the world is the USA one, with a total length of more than 1.5 million kilometres. The former USSR network is the second largest in the world. In the United Kingdom, the national transmission system covers approximately 5000 kilometres plus another 12000 kilometres, with pressures of up to 7bar in the regional distribution systems. In the Netherlands, the high-pressure system consists of a series of transmission lines with a total length of over 6000 kilometres. Following recent discoveries of natural gas in the South Eastern Coast of Africa, plans are now well underway to construct pipelines to transport the gas to areas with highest market potential. In Tanzania, a 200km pipeline is under construction for transportation of natural gas from Songo Songo Island to Dar es Salaam and in Mozambique, a 900km pipeline will be constructed from Pande to the Republic of South Africa.

The amounts of natural gas stored in the transmission lines are enormous. In the Netherlands system described above, the yearly flow amounts to over  $7 \times 10^{10}$  kilogramme of natural gas. To give a feeling of the amounts and their qualities, a 145 kilometre typical high-pressure pipeline would contain about 7000 tonnes of natural gas, which is equivalent to 100MW of heat power for 40 days. With such large amounts of natural gas contained in pipeline systems, potential hazards such as pollution, fire and economic losses due to the spilling of the gas in case of a rupture are of great concern and need to be thoroughly and accurately assessed. This will in turn be the basis for designing and implementing preventive measures for such hazards. One example of such cases was in Alberta, Canada, where it was necessary to accurately model sour gas (natural gas containing hydrogen sulphide) pipeline rupture, in order to set guidelines for land development policy.

At present, there are over a dozen computer codes for analysing transient flow behaviour of fluids in pipelines. Some work which has been done in the past three decades, on pipe rupture and blowdown in gas transmission lines, is summarised in Section 1.2.

## **1.2 RUPTURE AND BLOWDOWN OF GAS PIPELINES**

It has been stated in section 1.1 that the amounts of natural gas stored in the transmission lines are enormous and the potential hazards, such as pollution, fire and economic losses due to the spilling of the gas in case of a rupture, are of great concern. Assessment of the flow situation following a linebreak in such pipelines is crucial, in order to be able to design and implement preventive measures and to plan corrective action for such hazards.

Most pipeline ruptures occur accidentally due to causes such as material failure; poor or lack of maintenance, faulty operation; damage to pipelines due to excavation work; and damage of pipelines by falling objects from platforms, ships and icebergs. Within the last decade, the world has witnessed several disasters resulting from accidental pipeline ruptures. These include the Piper Alpha disaster on the night of 6<sup>th</sup> July 1986 and more recently (April and May 1995) in Russia and South Korea respectively. The South Korean rupture was caused by pipeline damage, due to excavation work and it resulted in many deaths. The Russian pipeline rupture is thought to have been caused by pipe failure due to corrosion. After the Russian pipeline rupture, flames could be seen up to 25000ft high and several square miles of forest were set on fire. Pipe blowdown is a controlled venting to the atmosphere and is usually done prior to shutdown or repair. In this report, both rupture and blowdown are referred to as linebreak.

Analysis of the flow following a linebreak in a gas pipeline is done using computer models which have been validated with the best available experimental data. A review of experimental data which is available on linebreak has shown that it consists of data from shock tube tests; laboratory experiments on short sections of pipes; linebreak simulation experiments on full-scale pipelines such as those reported by Bisgaard, Sørensen and Spangenberg (1987) and Van Deen & Reintsema (1983); rupture and blowdown tests on sections of full-scale pipeline such as the Foothills Pipe Lines (Yukon) Ltd. (1981); and measurements on full-scale pipeline system during accidental rupture such as the Piper Alpha disaster during which some data was recorded.

One essential requirement before performing computer modelling of a given pipeline rupture is that the test data, specific gas data and pipeline system data must be prepared in the form required by the computer programme. Often this involves making a number of assumptions and simplifications, such as assuming some parameters to be constant for some interval. Computer software such as QUANT, PPDS-IUPAC, ASPEN PLUS and



PREPROP for calculation of thermophysical properties of fluids are available and make the process much easier and accurate, while maintaining a sound computation speed. System data such as pipeline dimensions, is usually included in experimental data. However, some variables such as grid size, friction factor, Stanton number etc. need to be determined. A suitable grid size needs to be chosen in order to produce stable results and to adequately model the physical behaviour such as the shock wave fronts. Transient analysis in the vicinity of the break is very crucial. However, it is often not easy to obtain the required experimental data and with the required accuracy in this area. Consequently, the only available option is to use computer models. In the more recent studies, such as those by Picard and Bishnoi (1989), Tiley (1989) and Chen, Richardson and Saville (1992) variable grid sizes were used in the vicinity of the break, in order to enable close monitoring of the expansion waves.

The flow of gas following a rupture in a high-pressure gas pipeline is one case of rapid transient flow of compressible fluids in pipelines. Such flows are governed by the well known set of three partial differential equations derived from the principles of conservation of mass, momentum and energy. The gas properties are described by an equation of state. These, together with appropriate auxiliary conditions, determine the mathematical state of the gas. Many assumptions and simplifications are involved in the process of formulating and manipulating these equations. All these aspects are presented in this thesis.

When a rupture occurs, the operating parameters such as pressure ( $p$ ), flow velocity ( $u$ ), density ( $\rho$ ) and temperature ( $T$ ) at different parts of the system vary considerably. For example,  $T$  could fall to such an extent that it could render part of the pipeline unusable after the rupture, due to changes in its material properties. It is therefore very important to be able to determine these variations in order to be able to decide which parts of the pipeline should not be used and thus avoid further disaster. In modelling a linebreak in a gas pipeline system, questions such as what is the magnitude of the flow rate at the broken pipe end, how quickly will it diminish with time, what is the pressure, what is the temperature and how are these going to affect the rest of the system have to be answered. Another important parameter is the speed of propagation of pressure waves in the system, which also has a bearing on the fracture behaviour of the pipe material.

Results of transient analysis in ruptured pipelines, whether produced by experiments or computer models, are normally presented in a set of graphs. The more commonly used are the pressure, temperature, flow velocity, mass flow rate, pressure wave speed and mass of gas in the pipeline as functions of position and time.

### **1.3 COMPUTER CODES FOR ANALYSIS OF FLUID FLOW IN PIPES**

Nearly thirty computer codes, for the analysis of fluid transient situations in gaseous and/or multi-phase flows, are known to have been used; and some of these are available commercially. These include PIPENET, PIPESIM, PIPESIM PLUS, SURGE, EXPRES, PIPETE, IMF, IPSA, TOFFEA, SIMPLE-2P, PISO-2P, PIPETRAN, TRANSFLOW, TRAC, FLASH, RODFLOW, RELAP, FEAT, OLGA, PLAC, FLUENT, FLOW-3D, PHOENICS, PRO-II, HYSIM, FLOWMASTER, TGNET, PIPE1, PIPE2, BLOWDOWN and PIPEBREAK. In addition, some organisations, such as British Gas [Mallinson (1996)] and GASUNIE of the Netherlands [De Bakker (1993)], have developed their own models suited to their own pipeline operations.

FLUENT, FLOW-3D and PHOENICS are general purpose codes for multi-dimensional two-phase flow, but limited to dispersed flow or particle tracking. Algorithms for separated and stratified flow analysis include IMF, IPSA, TOFFEA, SIMPLE-2P and PISO-2P. OLGA and PLAC are one-dimensional flow codes which do not assume homogeneous two-phase flow and are therefore suited to low-speed two-phase fluid flow. FLASH, RELAP, RODFLOW and TRAC are normally used for Loss-Of-Coolant-Analysis (LOCA) in nuclear power plants. They are therefore suited for situations where the two-phase fluid is primarily a steam-water mixture. FLOWMASTER, of the British Hydromechanics Research Group (BHRG), can handle fluid systems where both rapid and slow changes occur in the boundary condition. FEAT is based on a finite-element numerical method of solution.

TGNET, PIPE1, PIPE2 and BLOWDOWN are among the group of codes for analysis of transients following high-pressure gas pipeline ruptures. PIPE1 and PIPE2 were developed by Flatt (1985-1989) at the Swiss Federal Institute of Technology, Lausanne. PIPE1 is for perfect gases whereas PIPE2 is for real gases. It is known that at least one company has offered to acquire the codes. BLOWDOWN is a computer code which can be used to simulate the emergency blowdown of vessels and pipelines containing hydrocarbons. The programme can predict pressure, temperature and multi-phase composition within a vessel or a pipeline; temperature of the wall; and efflux: all as



functions of time. Development of the code [Richardson (1993-96)] started in 1984 at Imperial College, London; and the first version of the code was produced in 1988. It has since then undergone constant modifications and testing, which it is claimed have not yet involved any correction, but have extended considerably the range of problems which it can handle. An independent study commissioned to compare BLOWDOWN with PRO-II and HYSIM concluded that it is BLOWDOWN alone which is capable of dealing with systems containing liquid condensate or comprising more than one vessel. BLOWDOWN is now used by many gas and oil companies for the simulation of depressurisation systems. Applications have included a large number of individual vessels on offshore platforms and onshore installations, a number of multiple vessels connected to a common blowdown header, complete platforms and sub-sea pipelines. BLOWDOWN is being used throughout the SHELL Group of Companies. British Gas has decided that it will only use BLOWDOWN for depressurisation calculations. BLOWDOWN can also be used to simulate the repressurisation of a system (which is effectively just depressurisation in reverse) and the whole programme is common to repressurisation and depressurisation. The main physical difference between the two is that the fluid tends to get warmer (and much warmer if the process is fast enough) in the former, while in the latter it tends to get colder (and much colder if the depressurisation is fast enough).

PIPEBREAK is a computer programme which was developed and is being used by British Gas Plc for linebreak analysis. The GASUNIE pc model for hazard assessment can model gas outflow for complex pipeline networks with different elements and different outflow scenarios, all in one model. It can model linebreak, venting and leakage. It can handle elements defining different boundary conditions, which can represent, for example, the simplified behaviour of a compressor. The emphasis in developing this model was put on user friendliness, robustness and the ability to model complex networks. The basic relations are solved using implicit finite-difference schemes and a graphical user interface makes inputting of the network very easy. An estimate of the accuracy is claimed to be 5 to 20 per cent, and in the GASUNIE context, this is considered to be sufficient for hazard analysis purposes.

There are numerous studies in which attempts were made to develop computer codes for analysis of transients in ruptured high-pressure gas pipelines. Perhaps the earliest published model for the analysis of gas linebreak is that by Sens, Jouve and Pelletier (1970). There have since then been several attempts to develop computer models for gas linebreak analysis, including that by Tiley (1989) which was the starting point of this study. Sens, Jouve and Pelletier (1970) claimed that results from their model were identical with their

experimental results. Arrison, Hancox, Sulatisky and Banerjee (1977) compared predictions from their RODFLOW code with experimental data for blowdown of a recirculating water loop containing two pumps, two heated sections and two heat exchangers arranged in a figure-of-eight geometry. Groves, Bishnoi and Wallbridge (1978) developed a computer model to calculate decompression wave velocities in natural gas pipelines. The model was validated with the experimental data of Groves (1976). Cheng and Bowyer (1978) used their quasi-one-dimensional unsteady compressible fluid flow code to simulate two cases of transient flow. Transients caused by a sudden pipe rupture at the left hand side of a three duct steam system were predicted. Lyczkowski, Grimesey and Solbrig (1978) presented comparative results of their alternating gradient method with analytical results and also their experimental results.

A study by Alberta Petroleum Industry, Government Environmental Committee (1978) reported on two existing hydrogen sulphide isopleth (constant concentration of hydrogen sulphide lines) prediction models, one blowdown model and a simplified blowdown model developed during the study. Predictions from the blowdown models were validated with experimental results in a subsequent study [Alberta Petroleum Industry, Government Environmental Committee (1979)]. Knox, Atwell, Angle, Willoughby and Dielwart (1980), presented results of their theoretical model and compared them with their experimental data. Cronje, Bishnoi and Svrcek (1980) presented their adiabatic model and compared its results with the experimental data of Groves (1976). Other studies include those by Fanneløp and Ryhming (1982), Van Deen and Reintsema (1983), Bisgaard, Sørensen and Spangenberg (1987), Lang and Fanneløp (1987), Picard and Bishnoi (1988 and 1989), Tiley (1989), Botros, Jungowski and Weiss (1989), Lang (1991), Kunsch, Sjøen and Fanneløp (1991 and 1995) and Olorunmaiye and Imide (1993).

Whereas the physical phenomena of a pipeline system response following a rapid transient event is well explained for the other cases such as pump trip, rapid valve closure etc., the contrary applies for the case of a linebreak, despite all the studies mentioned in this section. It is stated that when a break occurs in a high-pressure pipeline, the pressure drops virtually instantaneously at the break and rarefaction waves are transmitted up and down the pipeline and are rapidly dissipated when the fluid in the pipe is a gas. Expansion waves are created in the section of the pipe upstream of the break and flow reversal occurs in the section of the pipe downstream of the break. This study investigates further the linebreak phenomenon, especially at the break boundary with the aim of achieving a better understanding of the phenomenon and a more accurate and stable model.



The process of developing a computer model for analysis of transient flow of gas in pipelines entails three main steps, namely formulation of the basic governing equations, numerical solution of the equations and finally validation of the model with experimental data. Discrepancies between different models which have been developed for analysis of transients following a linebreak in gas pipelines have mainly centred on the assumptions made in developing the basic partial differential equations of flow, and subsequent simplifications; the thermophysical model used; representation of various terms of the equations such as the friction term etc.; and the numerical methods used for solution of the basic partial differential equations.

Following a critical review of the previous study by Tiley (1989) a new approach, based on the Gamma Delta method developed by Flatt (1989), is used. The three basic partial differential equations of flow are derived for unsteady quasi-one-dimensional flow of real gases through a non-rigid variable cross-section area pipe. The only subsequent simplification are assumptions of constant cross-section area and rigid pipe walls. The QUANT software for thermodynamic and transport properties of real gases is used. The software is based on the virial equation of state and also contains the isentropic gamma and delta coefficients ( $\gamma_s$  and  $\delta_s$ ) required for the Gamma Delta method. A flow dependent explicit equation is used to calculate the friction losses. Numerical solution of the basic equations is done using the method of characteristics; the second-order MacCormack and third-order Warming-Kutler-Lomax explicit finite-difference methods.

## **1.4 PREVIOUS WORK AT CITY UNIVERSITY**

This work [Tiley (1989)] was an attempt to develop a computer model which can simulate a linebreak occurring in a gas pipeline. The procedure involved derivation of the basic simultaneous partial differential equations of motion which mathematically model unsteady fluid flow in a pipeline, by assuming a one-dimensional homogeneous flow, constant value steady flow friction factor, constant value Stanton number and neglecting minor losses and changes in cross-section area of the pipe. The equations were solved numerically using the method of characteristics. A computer code was written in FORTRAN 77 and a Gould PN 9005 mainframe computer was used to solve the mathematical model. Finally, the model was tested using experimental data. It is reported that although the theoretical model successfully simulated the rapid expansion of a gas following a linebreak in a high-pressure pipeline, comparison of the model results with experimental data which was available, did



highlight some areas of concern. These include overestimating actual wave speeds and problems of instability of the solution. Further work was recommended in the two areas mentioned above and also further refinement and testing of the model.

In this study, the whole approach used by Tiley (1989) has been critically reviewed. The subjects which have been explored include the following:

- (a) One-dimensional flow assumption.
- (b) Homogeneous flow assumption.
- (c) Neglecting minor losses and changes in cross-section area of the pipe.
- (d) Classification of the partial differential equations.
- (e) Use of a constant value steady flow friction factor to calculate friction losses.
- (f) Use of a constant value Stanton number to account for heat transfer (simplified model of heat transfer).
- (g) Use of the method of characteristics for numerical solution of the basic partial differential equations.
- (h) Use of FORTRAN 77 and Gould N 9005 mainframe computer.
- (i) Estimation of the gas constants specific heat at constant pressure ( $C_p$ ), specific gas constant ( $R$ ), critical temperature ( $T_c$ ) and critical pressure ( $P_c$ ).
- (j) Physical modelling of a linebreak situation.
- (k) Assumption that pipe walls are inelastic.
- (l) Determination of compressibility factor.
- (m) Limitation in the amount and scope of experimental data.
- (n) Simplification of the basic equations.

The one-dimensional flow approximation was used on the basis that for high Reynolds number flows, as in gas transmission lines, the approximation has been shown to be very good for steady and slowly varying flows. This was despite the fact that in the region of influence on flow of bends and fittings and particularly where there are large, rapid changes in conditions, as in the case of a linebreak, larger discrepancies are expected from the one-dimensional approximation. An alternative to this approximation is to apply the method used in turbulent boundary-layer theory which is lengthy and complicated. Some workers have used this method. A review of their work has been done in order to find out the limitations of using this method and the significance of errors introduced in the model by assuming a one-dimensional flow.

Homogeneous one-dimensional flow means that property distribution is uniform over the cross-section. This includes assumption about velocity profile, which is to be examined in more detail presently. The study by Tiley assumed a homogeneous flow. The validity of this assumption was investigated. Darcy's steady flow friction factor was used on the basis that there had been no friction factors defined for transient gas flows. It was stated that the use of steady flow friction factor for transient flow causes very little error when the flow variations are of relatively low frequency and amplitude, but it was also admitted that when large, rapid disturbances are occurring, a significant error may be incurred. The latter fact was considered when selecting the steady flow friction factor and also in subsequent calculations. From the review made, in this study, of flow (Reynolds number) and frequency-dependent friction, it is strongly felt that the use of constant value steady flow friction factor for transient flow could introduce quite considerable error in the model results and could in fact be one of the major causes of the inaccuracies observed with the model. A considerable amount of work on frequency-dependent friction in transient fluid flow simulation has been identified. This has been reviewed but not used in this study because the effects of unsteady friction, in addition to steady friction, are very small. The other issues raised by Tiley concerning the friction factor such as friction factor for two-phase flow and approximation of the friction term have also been critically reviewed.

The three partial differential equations describing the transient flow were classified as "non-linear hyperbolic partial differential equations", while they are in fact "first-order quasi-linear hyperbolic partial differential equations". However, this variation in classification of the equations had no impact on the solution and results obtained. An investigation has been made on the relative magnitudes of the minor losses and changes in cross-section area in a practical situation in order to assess the significance of the error introduced by neglecting them. The decision on whether or not to neglect them has been reviewed based on the findings of the above investigation and other factors affecting the development and execution of the model.

A constant value Stanton number was used to account for heat transfer on the basis that variations in Stanton number with flow rate are not sufficient to warrant the additional computation involved, and that the heat transfer term in the basic equations is comparatively small. Also in deriving the equation for the heat transfer term, it was assumed that in a rapid transient, the pressure changes occur instantaneously, allowing no time for heat transfer to take place between the pipe and the surroundings (adiabatic flow). It has been argued by others that no models are known for the general case of heat transfer in non-steady flows, where there is no thermal equilibrium between the pipe and the



surroundings. The literature search made has revealed that there has been previous works on this subject. A review of these has been done in Section 2.6 and, as a result, the heat transfer model has been improved.

The Berthelot equation of state was used to determine the compressibility factor, since it was said to produce comparatively accurate results for gases and vapours at low temperatures. It was stated previously by Thorley and Tiley (1987), that since the terms involving compressibility factor in the basic equations are usually relatively small, a complex equation of state would be uneconomical in terms of computer time. Therefore, only the relatively simple equations were examined. Also equations of state were preferred to compressibility charts because the former can easily be programmed into a computer and can be solved for derivatives. The equation of state for a real gas and the thermodynamic identity were used before applying the Berthelot equation of state. In this study, other approaches and equations of state which could be used to produce better results have been considered.

The isobaric heat constant ( $C_p$ ), isochoric heat constant ( $C_v$ ), specific gas constant ( $R$ ), critical temperature ( $T_c$ ) and critical pressure ( $p_c$ ) of the gases used in various experiments employed to validate the model were estimated by assuming constant values for pressure and temperature ranges encountered for  $C_p$ ; dividing the universal gas constant by the mean molecular weight of gas for  $R$ ; Grieves and Thodes method for  $T_c$ ; and Rausnitz and Gunn method for  $p_c$ . A recommendation was made for this to be one of the areas to be experimented in, in an attempt to improve the model. In this work, different methods of estimating these parameters have been reviewed and the QUANT software for thermodynamic and transport properties of fluid has been chosen. Also test data in which as many as possible gas constants are specified, has been selected.

The assumption that the pipe walls are inelastic was made without any discussion to justify its validity. It is known that the transient behaviour of a pipeline system depends upon the elastic properties of the conduit (including conduit size, wall thickness and wall material), external constraints (including type of supports) and the freedom of conduit movement in the longitudinal direction. These have been discussed in Section 2.2.3. In deriving the basic equations the terms  $\partial(\rho u^2 A)/\partial x$  and  $\partial(\rho u A)/\partial t$  were neglected on the basis that they are very small. Studies are known which have argued for the retention of each and both of these terms. These have been reviewed in this study and it has been decided that they should both be retained because the error introduced by neglecting them is very significant.



Tiley reviewed some of the popular numerical methods used for modelling fluid transients and selected the method of characteristics. The main merits of this method were said to be the ability to handle small time steps required for rapid transients; relatively more accuracy; and ability to pose the boundary conditions properly. It was also stated that the method of characteristics is more suited to single pipelines. Since the conclusion of the study by Tiley, there has been more studies employing and comparing different numerical methods of solution available. It was therefore found necessary to update the review carried out by Tiley, in order to decide on the most suitable numerical method.

A novel feature of Tiley's model, compared to those which were previously available is that it allows for the possibility of flow reversal downstream of the break as well as handling grid size reduction in the vicinity of the break. Both these features have been adopted in the model developed in this study. Tiley's main code consists of two programmes, one performing a transient analysis on a given shock tube or single pipe, and the other converting the required section of the numerical output of the first programme into graphical form.

## CHAPTER 2

# THEORETICAL DEVELOPMENT OF THE BASIC EQUATIONS FOR UNSTEADY FLOW

### 2.1 INTRODUCTION

Unsteady flow of compressible fluids in pipelines is described by a set of three partial differential equations, derived from the principles of conservation of mass (continuity equation), conservation of momentum or Newton's second law of motion (equation of motion or momentum equation) and conservation of energy or First Law of Thermodynamics (energy equation). The gas properties are described by an equation of state. These together with appropriate auxiliary conditions, determine the mathematical state of the gas. Many assumptions and simplifications are involved in the process of formulating and manipulating these equations. The form of the equation varies with the assumptions made regarding the condition of operation of the gas pipeline and any simplifications made. Based on the above the equations may, in the more general classification, be linear, quasi-linear or non-linear; parabolic or hyperbolic; and first- or second-order.

It is generally preferred to keep the equations as simple as possible, without significantly reducing the accuracy of results in a particular model, in order to economise on computational labour and time and also to minimise the computer memory requirement. This rule is very effective for modelling of slow transients, but there seems to be not much room for manoeuvre in the case of rapid transients, and especially linebreak problems. In the latter case, the equations have to be used almost without any simplification in order to achieve the required accuracy criteria. In most of the studies reviewed, it is generally felt that researchers have made various assumptions and simplifications; used one form of the basic equations or the other; represented the various terms in particular ways; in order to suit a particular method of solution or application and vice versa. Suwan and Anderson (1992) argued that alternative formulations, interpolations, friction force representation, or time integration, which may be appropriate for parabolic problems, will all violate the basic information carrying physics of a hyperbolic problem. Most cases of unsteady one-dimensional flow, where disturbance propagation velocities do not vary significantly, are characterised by quasi-linear hyperbolic partial differential equations for continuity and momentum. On the other hand, complex phenomena such as stratified and intermittent stratified-bubble (slug) flows require a two-dimensional transient analysis.

Various analytical techniques have been used to reduce the number of equations before employing the relevant numerical procedure. Van Deen and Reintsema (1983), for example, introduced a technique which reduces the energy equation to a single parameter-in-mass equation without the assumption of isothermal or isentropic flow. It was stated in section 1.3, that the process of developing a computer model for transient analysis of gas pipelines entails three main steps, namely formulation of the basic governing equations, solution of the equations and finally validation of the model with experimental data. This chapter deals entirely with the first step. Essentially the same approach as used by Tiley (1989) is used but an improvement is made on the assumptions used and representation of the various terms, with an overall objective of achieving more accurate and numerically stable results.

Tiley (1989) assumed a one-dimensional homogeneous flow in an inelastic pipe and neglected minor losses and changes of cross-section area of the pipe. Three simultaneous non-linear (Though the equations have been classified by Tiley (1989) as non-linear, they are in actual fact quasi-linear) partial differential equations which mathematically model pressure transients in a non-perfect gas were derived. A constant value steady flow Darcy's friction factor was used to calculate frictional losses. Heat transfer into the pipe was approximated by a constant value Stanton number. The Berthelot equation of state was considered to be the most suitable for this application. A formulation using the general equation of state for a perfect gas and the thermodynamic identity from the Joule-Kelvin effect was used.

Since the development of the Tiley model and even before, there has been a considerable amount of research activity on theoretical modelling of fluid transients, and in particular those aspects related to linebreak in gas transmission systems. A great number of these have been thoroughly and critically reviewed and considered in this study. Following this review a new approach based on the gamma delta method developed by Flatt (1989), is used. The three basic partial differential equations of flow are derived for unsteady quasi-one-dimensional flow of real gases through a rigid constant cross-section area pipe. No further simplification is made on the basic equations and the QUANT software for thermodynamic and transport properties of real gases is used. The software is based on the virial equation of state and also contains the coefficients required for the gamma delta method. A flow dependent explicit equation is used to calculate the friction losses. Numerical solution of the basic equations is effected using explicit finite-difference methods.



There are three basic approaches by which fluid flow problems are formulated; namely the control volume, integral or large-scale analysis; infinitesimal system, differential or small-scale analysis; and experimental or dimensional analysis. In all these cases, the three basic conservation laws of mechanics i.e. conservation of mass, momentum and energy plus the thermodynamic equation of state and associated boundary conditions must be satisfied. A control volume is a finite region chosen carefully with open boundaries which mass, momentum and energy are allowed to cross. A balance is made between the incoming and outgoing fluid and the resultant changes within the control volume, and details of the flow are normally ignored. In the infinitesimal approach, the conservation laws are written for an infinitesimal system of fluid in motion and become the basic differential equations of the fluid flow. To apply them to a specific problem, one must integrate these equations mathematically over the volume, subject to the boundary conditions of the particular problem. Exact analytical solutions are often possible only for very simple geometries and boundary conditions, otherwise numerical integration on a digital computer is used. Experimental study may be full-scale or laboratory based.

The differential approach can be used for any problem but in practice the lack of mathematical tools and the inability of digital computers to model small-scale processes makes the application of the differential approach rather limited. Even computer programmes sometimes fail to provide accurate simulation because of either the inadequate storage or inability to model the finely detailed flow structure characteristics of irregular geometries or turbulent flow patterns. The dimensional analysis approach can similarly be applied to any problem but lack of time and money and generality often makes the experimental approach limited. The control-volume analysis is considered the most useful of all the three approaches as far as practical engineering applications are concerned. It gives useful results in a reasonable amount of time, though sometimes gross and crude. In applications such as modelling of a linebreak in high-pressure gas pipelines, the differential or infinitesimal approach is normally used and later validated with experimental results.

In fluid flow problems the dependent variables, i.e.  $p$ ,  $\rho$ ,  $u$  etc., are functions of the independent variables i.e.  $t$  and  $x$ , in the case of one-dimensional flow. In any given flow situation, the determination by experiment or theory of the fluid properties as a function of position and time is considered to be the solution to the problem. There are two distinct fundamental methods of specifying the flow field, namely the Eulerian description and the Lagrangian description. In the Eulerian form, the independent space variables refer to a coordinate system assumed to be fixed in space or translating and through which the fluid is moving. The flow is characterised by a time-dependent velocity field which is to be found



by solving the initial value problem. In the Lagrangian form, the independent space variables refer to a coordinate system fixed in the fluid and undergoing all the motion and distortion of the fluid, so that the particles of the fluid are permanently identified by their Lagrangian variables, while their actual positions in space are among the dependent variables to be solved for.

Although the Eulerian and Lagrangian forms are essentially equivalent, the Lagrangian form gives more information i.e. it tells where each bit of fluid came from initially and has the virtue that conservation of mass is automatic. This results in considerably greater accuracy in some problems. Ritchmyer (1957) stated that for the above reasons, the Lagrangian form is generally preferred for some problems in a one space variable. For problems in two or more space variables and time, the Lagrangian method encounters serious difficulties. In particular, the accuracy usually decreases seriously as time goes on, due to distortions, unless a new Lagrangian point-net is defined from time to time, which requires difficult and usually rather inaccurate interpolations. From this point of view, the Eulerian form is more attractive. However, the Eulerian form is almost useless if there are interfaces between fluids having different thermodynamic properties because it provides no simple mechanism for telling which kind of fluid is to be found at a given instant at a given net-point (for problems in one space variable, such a mechanism can easily be provided). Many schemes had been tried, some combining the features of the Lagrangian and Eulerian forms but there was no satisfactory universal method that had been found for general multi-dimensional problems.

Fashbaugh and Widawsky (1972) stated that the Eulerian formulation is usually used in steady-state fluid flow problems and the Lagrangian formulation is used more extensively in unsteady flow and is more desired for solution of shock propagation problems. Also the fact that the Lagrangian formulation yields more information, such as where each bit of fluid originates initially, facilitates locating temperature contact surfaces propagated in the pipe. The study compared two methods namely the pseudo-viscosity and the Lax-Wendroff numerical method in modelling the effects of duct area change on shock strength in one-dimensional viscous air flow. It was concluded that a one-dimensional variable area Lagrange analysis is adequate for predicting shock flow through a duct area increase of up to at least area ratios of 10 to 1. In addition, the Lagrangian formulation using the pseudo-viscosity numerical method of solution was recommended and preferred to the Eulerian formulation with the Lax-Wendroff numerical method of solution for accurate predictions in very long ducts, where an appropriate function for the friction factor should be used.



Ames (1977) stated that until the early 1960's, the only known stable difference approximations for the Eulerian form were less accurate than those for the Lagrangian form. Consequently, the Lagrangian forms were preferred. Both systems have approximately the same complexity. The major disadvantage of the Eulerian system arises when interfaces (shocks) occur separating fluids of different density. The Lagrangian form does not have the spatial coordinate mesh fixed in advance and may require refinement of the mesh as computation advances. This possibility of regridding arises since the Lagrange form is constructed so that mass between two successive mesh points is approximately conserved. White (1988) stated that certain numerical analyses of sharply bounded fluid flow, such as the motion of isolated fluid droplets are very conveniently computed in Lagrangian coordinates. Other more recent writers, including Batchelor (1992) argued that the Lagrangian type of specification is useful in certain special contexts but it leads to rather cumbersome analysis and in general is at a disadvantage in not giving directly the spatial gradients of velocity in the fluid.

In fluid dynamics measurements, the Eulerian method is the most suitable. To simulate a Lagrangian measurement, the probe would have to move downstream at the fluid particle speeds. However, this is sometimes done in oceanographic measurements, where flow meters drift along with the prevailing current. The Eulerian formulation has almost exclusively been used in all recent studies and literature, even in such cases where according to the above discussion, the Lagrangian description would seem more appropriate. For the sake of convenience, the continuity equation has been derived based on the Eulerian approach, while derivation of the momentum and energy equations is based on the Lagrangian approach.

The equations of flow of fluid in a pipe can be quite complex, especially for cases such as high-pressure gas pipeline ruptures. This is more so if all aspects of the flow are to be taken into consideration. However, the equations can be handled conveniently by making a set of assumptions and simplifications regarding the condition of the flow. In this particular case for example, one has got to decide whether to use a one-dimensional or multi-dimensional flow approximation, single phase or multi-phase flow, include structural effects of the system, consider minor losses and changes in cross-section area etc. The inclusion of viscous and thermal effects has been well discussed by among others Tiley (1989) and Issa (1970), and therefore need not be repeated here. It is therefore being assumed that in the equations being formulated, viscous and thermal effects are included i.e. non-isothermal viscous flow. Further simplifications could be made, for example by neglecting body forces etc. Various workers have made different assumptions when



developing the basic flow equations, depending on their particular flow situations. Tiley (1989) assumed a one-dimensional homogeneous flow in an inelastic pipe, neglecting minor losses and changes in cross-section area, when developing a model for pressure transients in a ruptured high-pressure gas pipeline. The same assumptions were made by Goldwater and Fincham (1981) and Osiadacz (1987). They all arrived at the same set of equations. White (1988) gave a detailed description of the derivation of similar equations for three-dimensional flow and Moe and Bendiksen (1993) used equations for three-dimensional two-phase flow to develop their model. Chen, Richardson and Saville (1993) presented a set of equations for a transient homogeneous two-phase flow model.

## **2.2 MAJOR ASSUMPTIONS AND SIMPLIFICATIONS**

### **2.2.1 DIMENSION OF FLOW**

In one-dimensional flow, the components of the fluid velocity in the circumferential and radial directions are ignored. A flow can be assumed to be one-dimensional if the rate of change of gas properties normal to the streamline direction is negligible compared with the rate of change along the streamline. This means that over any cross-section of the pipe all the gas properties can be assumed to be uniform. The assumption of one-dimensional flow gives satisfactory solutions to many problems where either the cross-section area changes slowly along the path of the stream of gas, the radius of curvature of the pipe is large compared with its diameter or the shape of the velocity and temperature profiles are approximately constant along the pipe. For one-dimensional flow of a fluid;  $p$ ,  $\rho$ ,  $u$  etc. are only functions of  $t$  and  $x$ . The one-dimensional model enables derivation of the basic equations of pipeline flow in a simple fashion.

In real fluid flow situations, especially in the case of high-pressure natural gas flow in pipelines, the flow cannot be truly one-dimensional because viscous effects will produce a velocity profile across the pipe with the local velocity zero at the pipe wall and reaching a maximum in the centre. Moreover, the flow is turbulent so that there are random motions superimposed upon the mean flow. Ansari (1972) investigated the influence of including radial flow on the solution of unsteady pipe flow equations. It was shown that neglecting the radial velocity can lead to substantial error in the determination of the axial velocity of flow. The effect of the assumption of negligible radial flow was also investigated in relation to another assumption which is commonly made, i.e. the gradient of the axial velocity in the



axial direction, in viscous flow, is negligibly small compared to the gradient in radial direction. It was found that for slow transients the latter assumption is valid while the former is not and vice versa for the case of rapid transients. The departure from the one-dimensional flow assumption will be even more pronounced where there are bends and fittings in the pipeline. Nevertheless, despite the foregoing, the one-dimensional approximation in gas transmission systems has been shown to be very good for steady and slowly varying flows. When the variations in flow are large and rapid, such as in high-pressure gas pipeline ruptures, larger discrepancies are expected from the one-dimensional approximation. A more rigorous approach is to apply the integrated equation method used in the turbulent boundary layer theory.

There are many studies and computer models developed for multi-dimensional flow analysis. A few computer codes based on multi-dimensional flow models such as FLOW-3D are commercially available. However, these models can only be applied to some special cases with confidence. Shin (1978) discussed the extension of the one-dimensional method of characteristics to two space dimensions. The extended method uses the same simplifications and retains the similar simplicity and efficiency as in the conventional one. The two-dimensional method is applicable to both the cartesian and axisymmetric systems and includes the conventional method as a special case. Wylie (1982) presented a similar numerical method for analysis of low-velocity two-dimensional transient fluid flow problems. The method contains similarities to the one-dimensional method of characteristics but does not follow the traditional characteristics theory for two-dimensional problems. The most up to date and comprehensive study is that by Moe and Bendiksen (1993), which presented the physical basis of a new type of multi-dimensional two-fluid model, particularly suited for transient flow problems. A basic difference between this model and the other models is in the solution procedure, aiming in particular at improved predictions of transient problems. The numerical scheme is based on an extension of an earlier one-dimensional model and employs an implicit finite-difference scheme.

It follows from the above discussion that the three-dimensional approximation is the natural method for the linebreak problem being modelled. However, for the sake of simplicity, the one-dimensional model is used with the aim of extending it to three-dimensions in the future. As shown in the above mentioned studies, the extension of one-dimensional models to two- and three-dimensional models could, in principle, be achieved especially if caution is made in representation of the other terms of the equations.

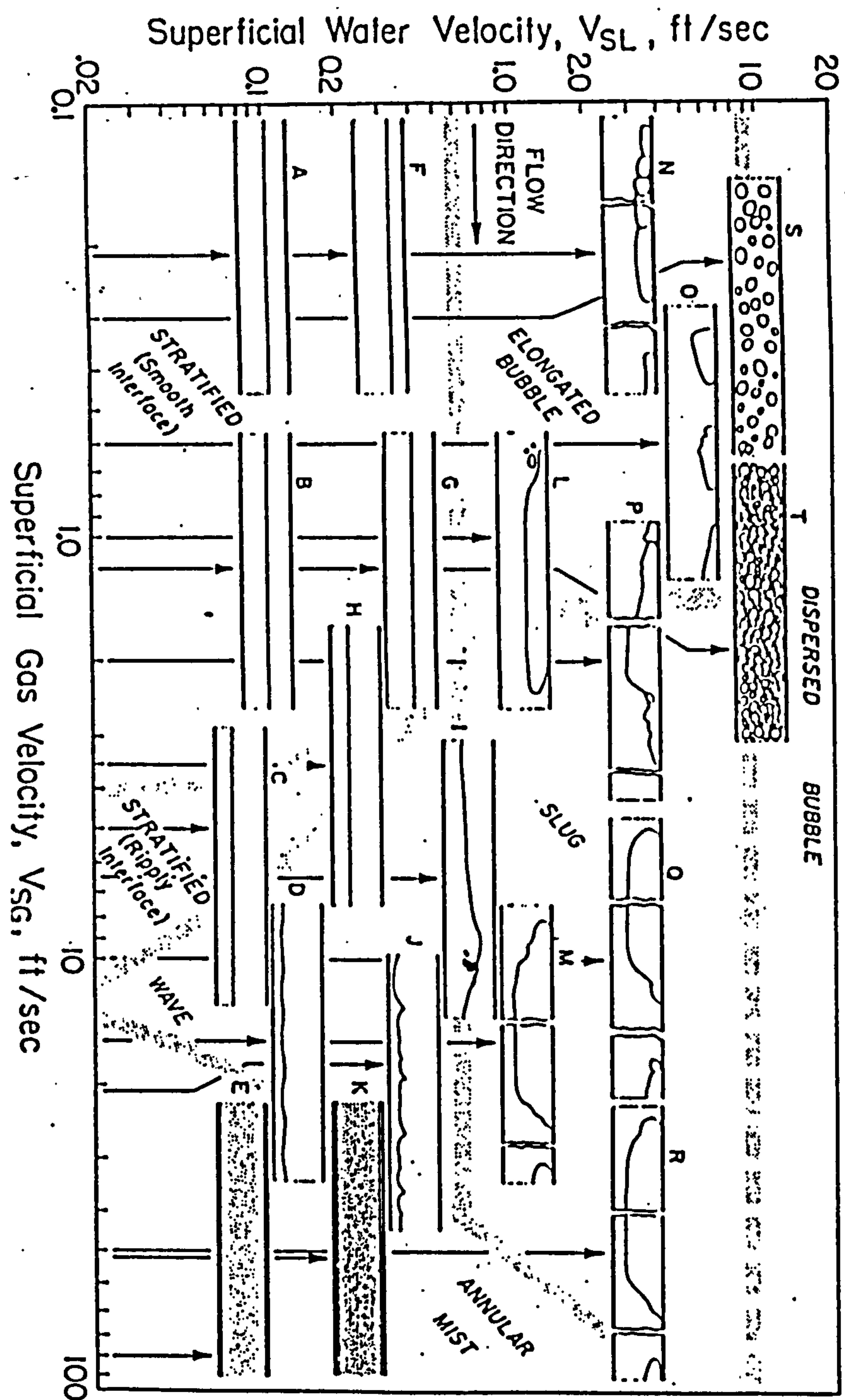


### 2.2.2 FLOW PHASE

When a high-pressure natural gas pipeline is ruptured, the temperature falls hence condensation occurs. A multi-phase flow situation is therefore likely to be encountered. Multi-phase flow in general is a very complicated phenomenon. It is conveniently classified into flow regimes which may be further grouped into two main types, namely dispersed (particles, bubbles and droplets) and separated (stratified, annular and elongated bubbles) flows. More complex flow regimes often occur as combinations of these, such as stratified and annular flows with entrainment and slug flow. Flow regimes that are commonly encountered are stratified (wavy or smooth), annular dispersed, intermittent (slug) and dispersed bubble flows. These are shown in Figure 2.1. In relatively long pipelines, with possibly large pressure losses, several of these flow regimes may exist simultaneously as a result of changing in situ flow rates and physical properties of the fluids. A gas-liquid mixture may be treated as a pseudo-fluid, if the mixture and its motion may be treated as homogeneous.

Dispersed flow regimes have been quite extensively studied recently using two- and three-dimensional models. For two-phase flow, however, at least three general purpose codes are available namely FLUENT, FLOW-3D and PHOENICS. For separated or stratified flow, there has been several studies, including those by Oliemans (1987); Wu, Pots, Holdenberg & Meerhoff (1987); and Moe & Bendiksen (1993). In the multi-dimensional Moe-Bendiksen model, the general two-fluid equations have been applied with the assumption of a single pressure field. The modelling of constitutive laws at the interface is not general but focused on separated or stratified flows. A volume equation is applied for the pressure, enabling a direct two-step solution procedure. Oliemans (1987) investigated the accuracy of two-phase flow trunk line predictions by a one-dimensional steady model for stratified wavy flow in horizontal and inclined pipes. Wu, Pots, Holdenberg and Meerhoff (1987) investigated the exact location of the transition from stratified to non-stratified flow for a high-pressure gas-condensate system in a large pipe both experimentally and using the Taitel-Dukler mechanistic model and the Wallis one-dimensional wave theory.

According to the one-dimensional linear wave stability criterion for high-pressure gas-condensate flow in an 8 inch pipe, unstable (non-stratified) flow occurs at much higher liquid fractions than according to the Taitel-Dukler flow regime map. This is confirmed by



Source: Govier and Aziz (1972)

Fig. 2.1 Flow Pattern for Air-water Mixture Flowing in a Pipe



measurements in a pipe using natural gas and live condensate at a pressure of 75 bar. Experimentally, at the theoretical transition to unstable waves, stratified flow shifts to a flow pattern featuring pipe wall wetting and liquid entrainment. The transition to intermittent flow was observed at still larger liquid loadings. It was concluded that a proper theoretical description of this flow regime transition most likely requires a more sophisticated modelling with due account being taken of two-dimensional effects, liquid entrainment and non-linearity. For the intermittent flow boundary, some promising results have been obtained by determining the unstable solution of the one-dimensional transient stratified model.

In analysing pressure transients in bubbly air-water mixtures; Padmanabhan, Ames and Martin (1978) used a homogeneous model which consists of one-dimensional equations of conservation of mass for each of the phases and conservation of momentum for the mixture. Bhallamudi and Chaudhry (1990) developed a third-order accurate explicit finite-difference scheme for transient flows in one-dimensional homogeneous gas-liquid mixtures in pipes. The gas-liquid mixture was treated as a pseudo-liquid. Chen, Richardson and Saville (1993) used a two-phase model called the two-fluid model, in which the local instantaneous conservation equations are formulated for each phase. In the model by Tiley (1989), the fluid was assumed to be homogeneous and no provision was made in the representation of the various terms such as friction, for the possibility of a two-phase mixture being present. For the sake of simplicity, the same approach is used in this study. However, significant errors could be introduced in the solution because of this simplification.

### **2.2.3 FLUID STRUCTURE INTERACTION**

The classical waterhammer theory only predicts the extreme loading on a system as long as it is rigidly anchored. When a piping system has certain degrees of freedom severe deviation from the classical theory may occur due to motion of the system. Pressure waves exert forces which cause a compliant system to move. As a result of the motion, pressure waves are formed. This phenomenon is known as Fluid Structure Interaction. Fluid Structure Interaction is essentially a dynamic phenomenon, the interaction being caused by dynamic forces which act conversely on fluid and pipe. The forces in such a piping system are classified in two groups namely distributed forces and local forces. Typical examples

of distributed forces are fluid pressure and friction. In the case of fluid pressure, rapid pressure fluctuations cause a pipe to expand or contract thereby creating axial stress waves in the pipe wall. The stress waves in return generate pressure fluctuations in the enclosed fluid, resulting in a coupling known as Poisson Coupling. Similarly, friction force is responsible for friction coupling. In most practical systems, frictional coupling is weak. Local forces act on specific points in a system, such as elbows, tees or valves and cause axial and lateral motions which generate pressure waves in the fluid resulting in an interaction called junction coupling. Junction coupling is generally dominant compared with Poisson and friction couplings. Lawooij and Tijsselling (1990) conducted a study of Fluid Structure Interaction in compliant piping systems. They concluded that the most significant coupling mechanisms are Poisson and junction coupling. A simple guideline which states when interaction is important is formulated in terms of three time scales i.e., the time in which the pressure is built up, the eigenperiods of the structure and the time scale of the waterhammer waves. They also concluded that Poisson coupling is important for the fluid when significant modes of interaction are dominated by stiffness.

To consider the motion of the pipe, three main displacements are distinguished namely axial displacement, lateral displacement and rotation. Therefore in general, the dynamics of a pipe system are influenced by four wave families, i.e. axial, flexural and torsional waves in the pipe wall and pressure waves in the fluid. These co-exist during transience and have different degrees of influence on the transient behaviour. Fluid Structure Interaction in compliant piping systems is modelled by extended waterhammer theory for the fluid and by beam theory for the pipes. In buried pipelines, the lateral restraint is usually sufficient to ensure that the overall behaviour is dominated by axial effects. Hence most analyses of Fluid Structure Interaction have focused on the propagation of axial waves i.e. pressure waves propagating along the walls of the pipe. In suspended pipelines however, few lateral restraints exist and account should be taken of flexural and torsional waves.

In a study on Fluid Structure Interaction in flexible curved pipes, Stittgen and Zielke (1990) concluded that the influence of structural motion on the internal pressure is smaller than the time dependent internal pressure but can still be of influence in particular cases. They also concluded that pressure waves in flexible pipes are quite dependent on visco-elastic wall properties. Rachid and Stuchenbruck (1990) stated that the mechanical properties of the material, the temperature and the degree of stiffness of the supports, have



a significant influence on the response of the system. Stiffer pipe materials i.e. those with mechanical damping will experience higher pressures than more compliant pipe systems. They also found that Poisson effects can induce significant piping motion especially in long pipe reaches and cause high frequency peaks for pressure and stress in visco-elastic pipes, e.g. up to 25% above the rigid pipe model. However, mechanical damping of the pipe material tends to degrade the solid wave front quite quickly. In most cases, high frequencies generated by the Fluid Structure Interaction mechanism are virtually eliminated before the first fluid cycle.

In practice the value of the sonic velocity in the fluid in a pipe is influenced by the elasticity of the confining walls and the compressibility of the fluid. As the elasticity of the wall materials increases, the effective value of sonic velocity decreases. This effect is commonly neglected for typical high-pressure gas pipelines. However, some workers including Wood, Dorsch and Lightner (1966), Zielke (1968), Hirose (1971) and Beauchemin and Marche (1992) have all taken into consideration the effect of pipe elasticity. This has resulted in an additional term in the continuity equation. In the Beauchemin-Marche model, no simplification was made on the basic equations and in addition the effect of variable cross-section area was included. Despite this, the model could still be implemented with acceptable computational costs.

In the study by Tiley (1989) the effects of Fluid Structure Interaction were not considered. The same approach is followed here in order to maintain simplicity of the model and also because the review made does not conclude any significant justification for incorporating Fluid Structure Interaction in the model. A consideration of the wall elasticity is taken into account when developing the basic equations of fluid flow. It should be noted however, that in the study by Tiley (1989) the pipe was assumed to be inelastic i.e. elasticity of the pipe walls is negligible compared with the compressibility of the fluid.

#### **2.2.4 MINOR LOSSES AND CHANGES IN CROSS-SECTION**

Another effect worth considering in the formulation of the basic equation of the flow, is that arising from minor losses and changes in cross-section area. Swaffield (1967 and 1968-69) investigated the influence of bends on fluid transients which were propagated by a rapid valve closure in a long pipeline. He used a short dimensional analysis and a series of experimental tests which were designed to record the pipe diameter to thickness ratio, pipe

elasticity to fluid bulk modulus ratio, restraint applied to the pipe, bend radius of curvature to pipe bore ratio, included angle of the bend and initial flow velocity. He concluded that the influence of a bend is solely dependent on its geometry. Empirical formulae were developed to express the reflection and transmission of a transient at a bend in terms of the bend radius of curvature to pipe bore ratio and included angle. Otwell, Wiggert and Hatfield (1985) investigated the effect of elbow restraint on pressure transients. They observed that if an elbow was fully restrained, there was no alteration of a pressure transient travelling through the elbow. However, if an elbow was not fully restrained, there was a significant alteration of the liquid transient. The alteration was related to the direction and amplitude of the motion of the elbow and it was therefore thought to be dependent on the mechanical characteristics of the piping and pipe support structure. A numerical model was developed, which accurately predicted pressure and velocity responses.

Since in this case we are dealing with relatively long and straight lines (rather than networks), the assumption that minor losses are negligible is reasonable. Tiley (1989) assumed that the above losses were small compared with the distributed frictional losses and therefore neglected them. The same assumption is used in this study. Generally, most workers have assumed that the cross-section area of the pipe is not a function of the axial distance or varies slowly. In some special cases such as in cooling ducts etc. where the cross-section area varies appreciably with distance, the effect has been incorporated into the basic equations. However, in some studies on compressible flow, including those by Zielke (1968) and Flatt (1989), the equations are based on a variable change in cross-section area. Tiley (1989) neglected changes in cross-section area of the pipe. Also in this study, it is assumed that the cross-section area of the pipe is not a function of the axial distance. However, the basic equations of flow have been derived with provision for varying cross-section area with axial distance.

## **2.3 DERIVATION OF THE BASIC EQUATIONS FOR UNSTEADY FLOW OF A COMPRESSIBLE FLUID IN A PIPE**

Derivation of the basic equations describing a homogeneous compressible fluid flow in a pipe from first principles is very well known. For one-dimensional flow in an inelastic pipe with minor losses and changes in cross sectional area neglected, Tiley (1989) and Osiadacz (1987) derived the three conservation equations, in the conventional form using different



approaches. Nevertheless, they both arrived at similar equations. Zucrow (1977) derived the basic governing equations for unsteady one-dimensional and quasi-one-dimensional isentropic flow and also for generalised flow. White (1988) described the derivation of similar equations but for the case of a three-dimensional flow.

Literature on derivation from first principles of more complex phenomena such as the one being proposed in this study is rather scarce, but the equations concerned have been stated by various workers who used them. In this study, the basic equations for unsteady quasi-one-dimensional flow of real gases through non-rigid non-constant area pipes, using the gamma delta method, are used. The gravity term, is also included. These equations are valid for three fluid forms namely, real (or perfect) gas, homogeneous liquid/vapour mixture and liquid. This form of the equations simplifies considerably computer codes and is conceived to deal with problems where several of the three fluid forms appear simultaneously. The approach is rigorous from the thermodynamic point of view and takes into account the compressibility of the fluid and considers the vapour as a real gas. Formulation of the energy equation for unsteady flow of fluid in pipes has commonly contained either specific internal energy or specific enthalpy. Each of the above mentioned dependent variables is related to the other dependent variables  $p$ ,  $\rho$  and  $T$  by a caloric equation of state which is often a complicated non-linear empirical correlation in integral form. This procedure sometimes involves as many as 20 or more gas dependent coefficients. With the help of the two non-dimensional coefficients  $\gamma$  and  $\delta$ , it is possible to eliminate the specific internal energy and specific enthalpy from the energy equation, resulting in considerable computing economy.

The three basic equations of conservation for unsteady flow are derived from first principles, assuming that the cross-section area of the pipe varies with  $t$  as well as with  $x$ . The approach used in deriving the basic equations is very similar to that used by Flatt (1993a). The major difference between this derivation and that of Flatt is that the gravity term has been included, whereas Flatt neglected the gravity term. The centre line of the pipe is assumed to be stationary. Depending on which one is more convenient, either the Euler concept which is denoted by  $(\partial./\partial t)$  and  $(\partial./\partial x)$  or the Lagrange concept of full derivatives which is denoted by  $(d./dt)$  are used. It is possible to transform from one of the two approaches to the other, by using the following mathematical equivalence:

$$\frac{d\bullet\bullet}{dt} = \frac{\partial\bullet\bullet}{\partial t} + u \frac{\partial\bullet\bullet}{\partial x} \quad (2.1)$$

In this derivation, the control volume is regarded to be fixed in space (according to the Euler concept) and attached to moving particles of the fluid (according to the Lagrange concept).

### Continuity equation:

The continuity equation is derived using the Eulerian approach. An infinitesimal control volume for a pipe with varying cross-section area, which is depicted in Fig. 2.2 is used.

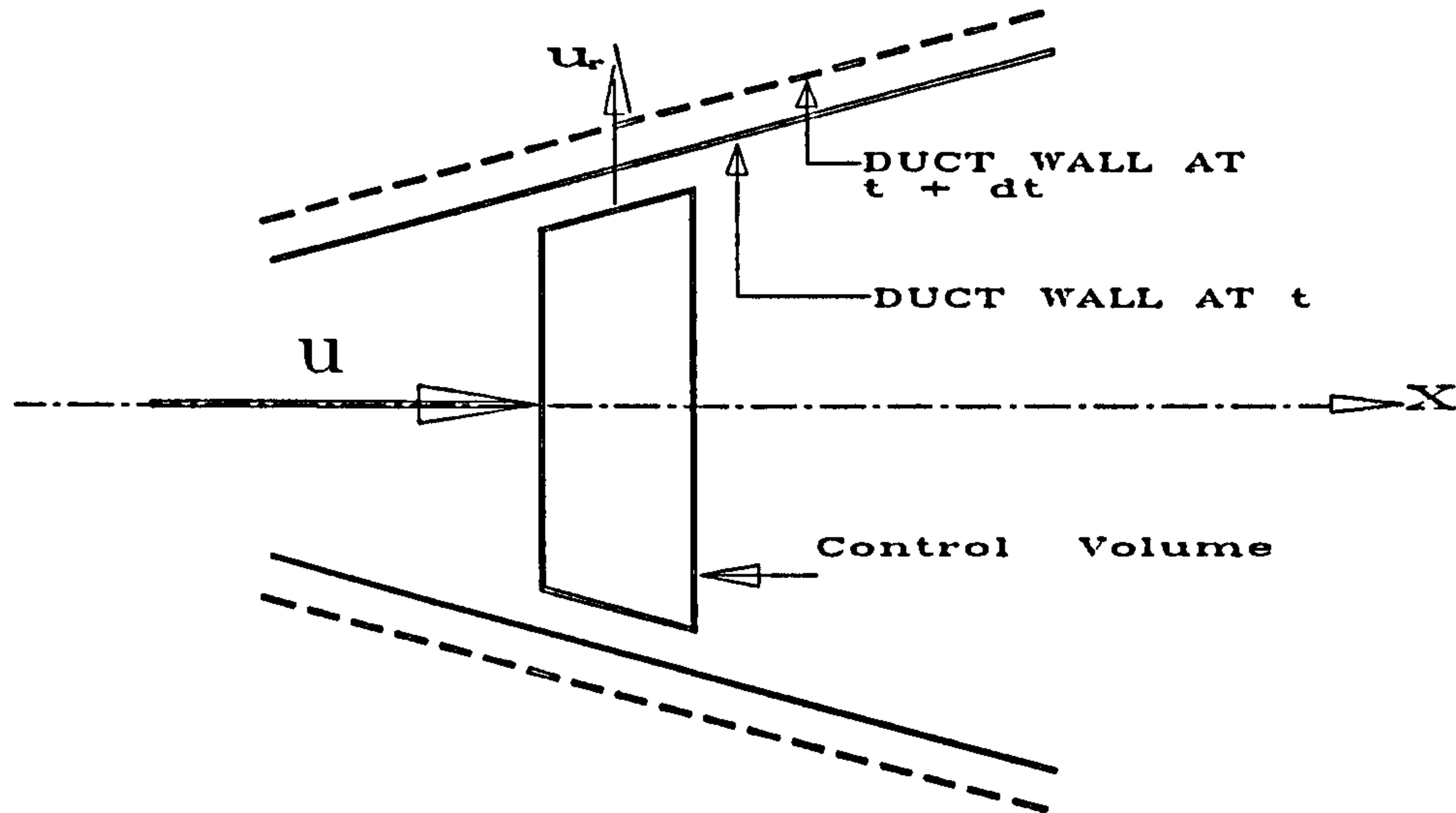


Fig.2.2 Sketch Showing the Control Volume at the Beginning of a Time Step

Mass balance is performed across the control volume. The total mass of the control volume with length  $dx$  after time  $dt$  is the sum of mass flux into the control volume, mass leaving the control volume and mass flux through the fictitious stationary pipe wall. In equation form, this is represented as follows:

$$\left[ \left( A + \frac{\partial A}{\partial x} \frac{dx}{2} \right) dx \right] \frac{\partial \rho}{\partial t} = A \rho u - \left[ A \rho u + \frac{\partial (A \rho u)}{\partial x} dx \right] - (L dx) \rho u_r \quad (2.2)$$

where

$L$  = wetted perimeter

$u_r$  = radial velocity of the pipe



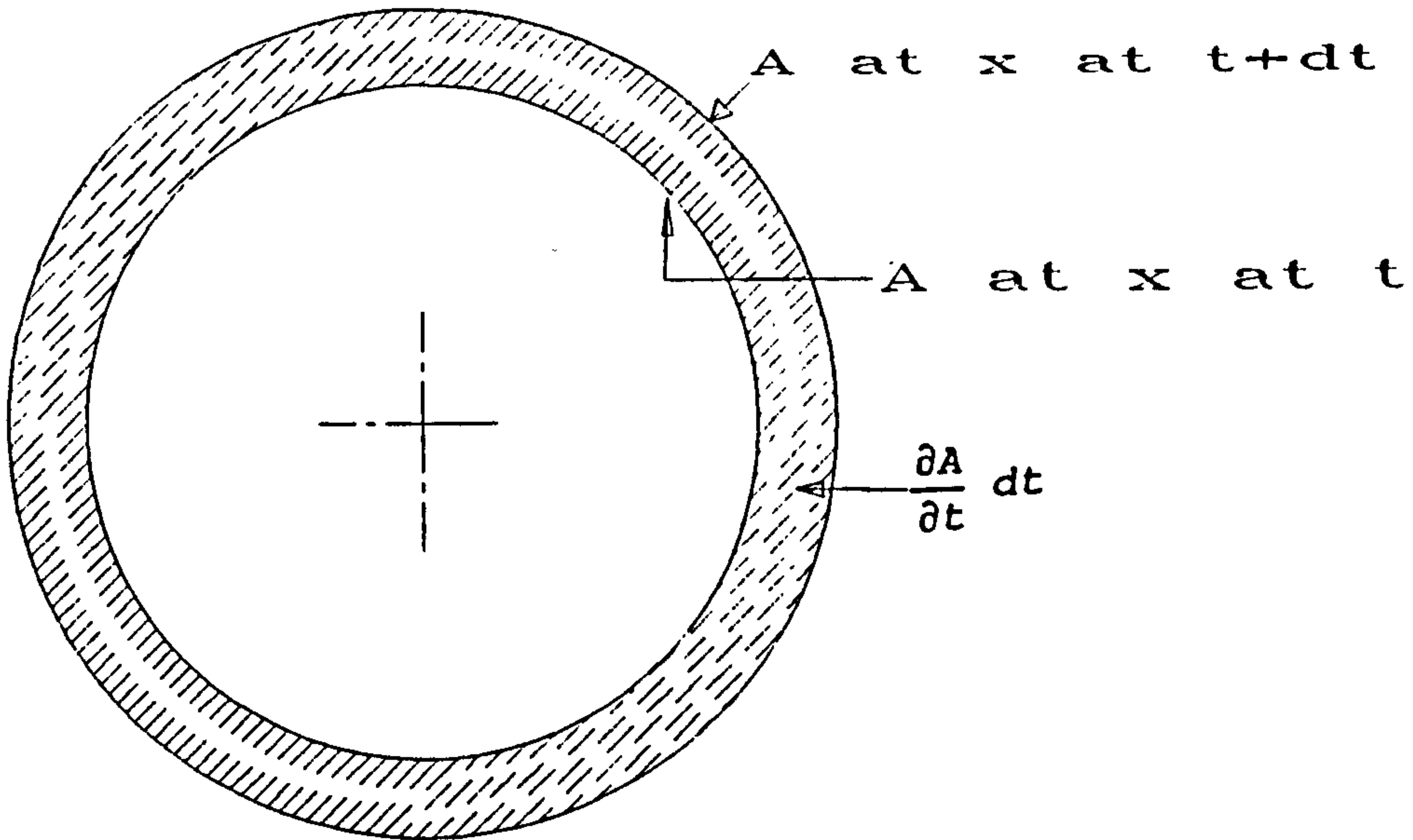


Fig. 2.3 Sketch Illustrating Equation (2.2)

The two parameters are related through the following equation:

$$\frac{\partial A}{\partial t} = Lu_r \quad (2.3)$$

Neglecting the small terms i.e. those containing  $(dx)^2$ , substituting equation (2.3) and dividing throughout by  $A dx$ , equation (2.2) reduces to the following equation:

$$\frac{\partial \rho}{\partial t} + \frac{\partial A}{\partial x} \frac{\rho u}{A} + \frac{\partial \rho}{\partial x} u + \rho \frac{\partial u}{\partial x} + \frac{\partial A}{\partial t} \frac{\rho}{A}$$

Rearranging and using equation (2.1) we get the following equation:

$$\frac{\partial \rho}{\partial t} + u \frac{\partial \rho}{\partial x} + \frac{d\rho}{dt} = -\rho \frac{\partial u}{\partial x} - \frac{\partial A}{\partial x} \frac{\rho u}{A} - \frac{\partial A}{\partial t} \frac{\rho}{A} \quad (2.4)$$

Let the last two terms of equation (2.4) be represented by the notation  $\xi$ . Therefore

$$\xi = -\rho \left[ \frac{\partial A}{\partial t} \frac{1}{A} + \frac{u}{A} \frac{\partial A}{\partial x} \right] \quad (2.5)$$

For rigid and cylindrical pipes  $\xi = 0$ . The continuity equation is obtained by substituting equation (2.5) into equation (2.4), resulting into the following equation:

$$\frac{\partial \rho}{\partial t} + u \frac{\partial \rho}{\partial x} + \rho \frac{\partial u}{\partial x} = \xi \quad (2.6)$$

### Momentum equation:

The momentum equation is derived according to the Lagrange concept. The forces acting on the control volume are shown in Fig. 2.4.

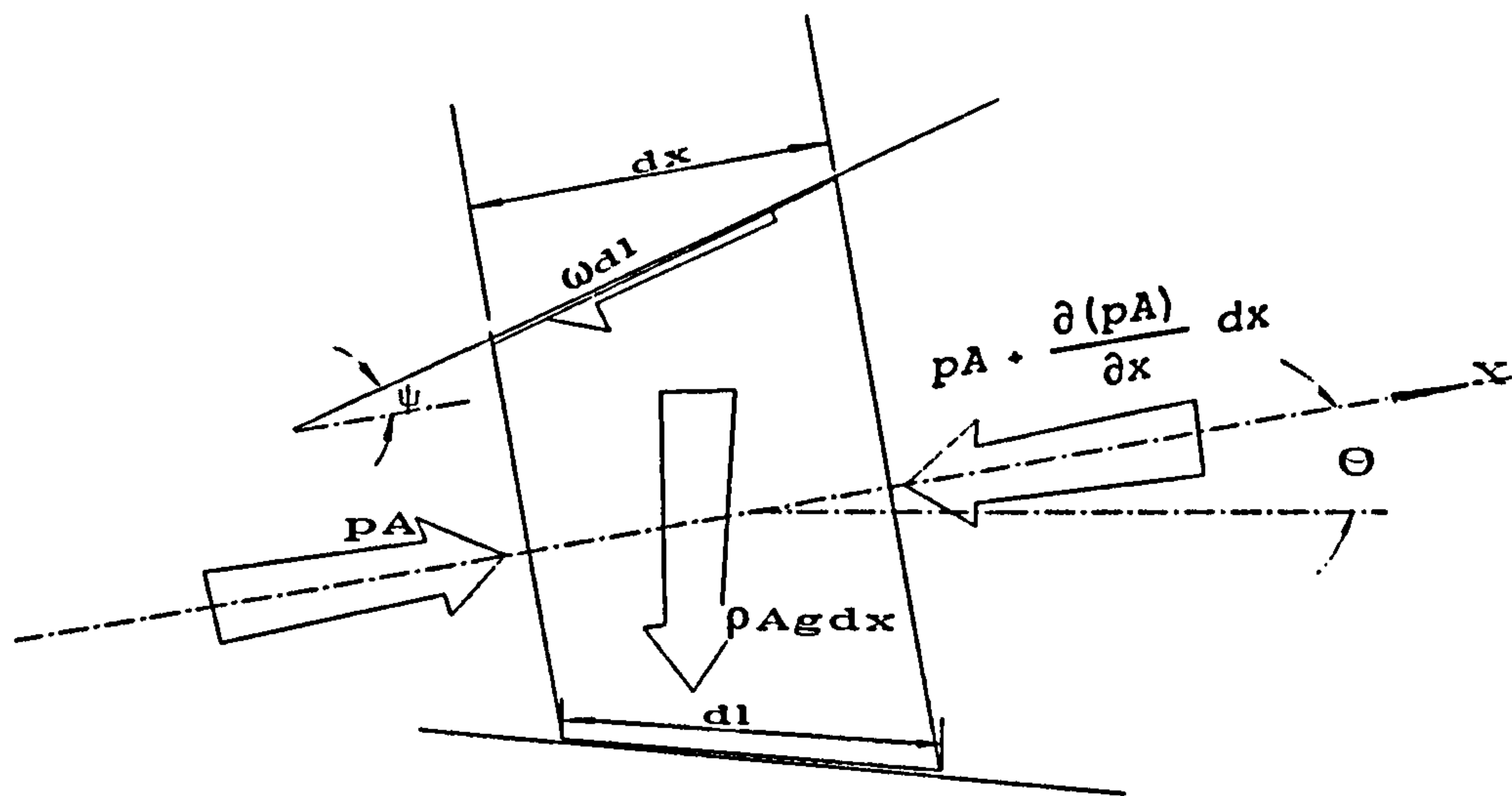


Fig. 2.4 Conical Control Volume Illustrating Body Forces

Applying Newton's second law of motion to the control volume, in x direction, the following equation is obtained:

$$(A \rho dx) \frac{du}{dt} = pA - \left[ pA + \frac{\partial(pA)}{\partial x} dx \right] + \frac{p \partial A}{\partial x} dx - \omega dl - \rho Ag \sin \theta dx$$

Substituting the value of  $dl = dx / \cos \psi$  and simplifying we get the following equation:

$$A \rho dx \frac{du}{dt} = -A \frac{\partial p}{\partial x} dx - p \frac{\partial A}{\partial x} dx + p \frac{\partial A}{\partial x} dx - \omega \frac{dx}{\cos \psi} - \rho Ag \sin \theta dx$$

Dividing throughout by  $A dx$  we get the following equation:

$$\rho \frac{du}{dt} = - \frac{\partial p}{\partial x} - \frac{\omega}{A \cos \psi} - \rho g \sin \theta$$

Using equation (2.1) for  $du/dt$  and dividing throughout by  $\rho$ , we get the following equation:

$$\frac{\partial u}{\partial t} + \frac{1}{\rho} \frac{\partial p}{\partial x} + u \frac{\partial u}{\partial x} = - \frac{\omega}{\rho A \cos \psi} - g \sin \theta \quad (2.7)$$

For a uniform diameter pipe,  $\cos \psi = 1$ .



### Energy equation:

The Lagrangian approach is used in deriving the energy equation, and heat transfer into the control volume in x direction is neglected. This assumption is very common for gaseous flows.

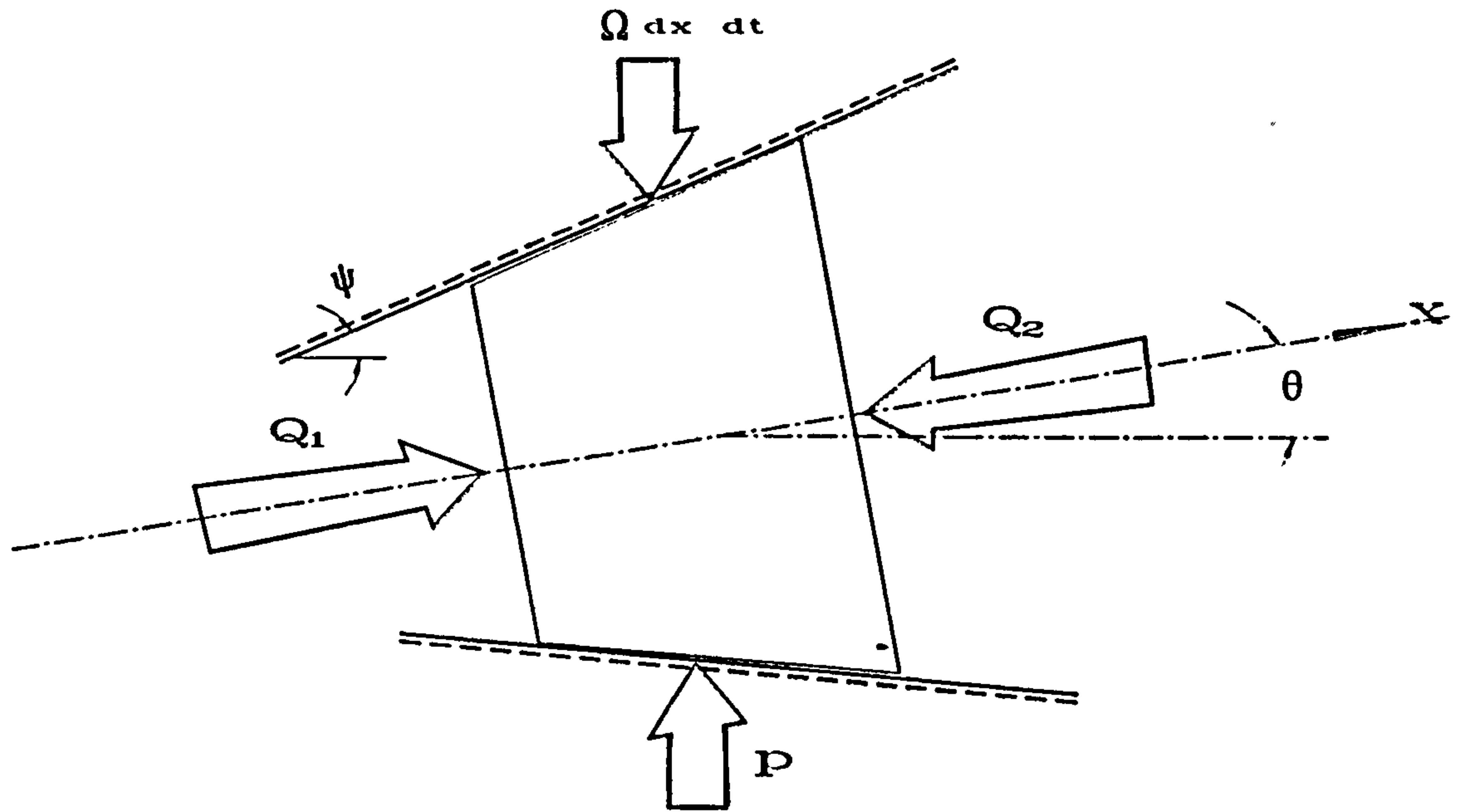


Fig. 2.5 Control Volume Illustrating Heat and Work Transfer

Applying the first law of thermodynamics to the control volume, the following equation results:

$$\rho A dx \frac{de_o}{dt} = p A u - \left[ p A u + \frac{\partial(p A u)}{\partial x} dx \right] - p L dx u_r + \frac{\Omega dx dt}{dt} - \rho A g u dx \sin \theta \quad (2.8)$$

The specific internal energy at stagnation conditions,  $e_o$ , is given by the following equation:

$$e_o = e + \frac{1}{2}u^2 \quad (2.9)$$

Dividing throughout equation (2.8) by  $A dx$  and using equation (2.3), we get the following equation:

$$\rho \frac{de_o}{dt} = -u \frac{\partial p}{\partial x} - \frac{pu}{A} \frac{\partial A}{\partial x} - p \frac{\partial u}{\partial x} - \frac{p}{A} \frac{\partial A}{\partial t} + \frac{\Omega}{A} - \rho g u \sin \theta \quad (2.10)$$

Rearranging equation (2.6) for  $\partial u / \partial x$  we get the following equation:

$$\frac{\partial u}{\partial x} = - \left[ \frac{1}{\rho} \frac{d\rho}{dt} + \frac{1}{A} \frac{\partial A}{\partial t} + \frac{u}{A} \frac{\partial A}{\partial x} \right] \quad (2.11)$$

Similarly, rearranging equation (2.7) for  $\partial p/\partial x$  we get the following equation:

$$\frac{\partial p}{\partial x} = - \left[ \rho \frac{du}{dt} + \frac{\omega}{A \cos \psi} + \rho g \sin \theta \right] \quad (2.12)$$

Substituting equation (2.9), (2.11) and (2.12) into equation (2.10) we get the following equation:

$$\begin{aligned} \rho \frac{de}{dt} + \rho u \frac{du}{dt} = & \left( \rho u \frac{du}{dt} + \frac{\omega u}{A \cos \psi} + \rho u g \sin \theta \right) - \frac{pu}{A} \frac{\partial A}{\partial x} \\ & + \left( \frac{p}{\rho} \frac{d\rho}{dt} + \frac{p}{A} \frac{\partial A}{\partial t} + \frac{pu}{A} \frac{\partial A}{\partial x} \right) - \frac{p}{A} \frac{\partial A}{\partial t} + \frac{\Omega}{A} - \rho u g \sin \theta \end{aligned}$$

Simplifying and rearranging results in the following equation:

$$\rho \frac{de}{dt} - \frac{p}{\rho} \frac{d\rho}{dt} = \frac{\omega u}{A \cos \psi} + \frac{\Omega}{A} \quad (2.13)$$

The specific internal energy is related to specific enthalpy through the following thermodynamic relationship:

$$e = h - \frac{p}{\rho} \quad (2.14)$$

Differentiating equation (2.14) with respect to  $t$  we get the following equation:

$$\frac{de}{dt} = \frac{dh}{dt} - \frac{1}{\rho} \frac{dp}{dt} + \frac{p}{\rho^2} \frac{d\rho}{dt} \quad (2.15)$$

Both the continuity and momentum equations i.e. equations (2.6) and (2.7) contain only  $p$ ,  $u$  and  $\rho$  as the dependent variables and neither of these equations contain the variable  $h$ . It would therefore be convenient to eliminate  $h$  from equation (2.15) by replacing it with the variables used in the continuity and momentum equations. This is achieved by using the gamma delta method, which was developed by Flatt (1993b) and which is derived in the following part of this section. For small changes in the domain as is the case in this model,  $\gamma$  and  $\delta$  are assumed to be constant.



In deriving the basic relationship for the gamma delta method, the polytropic coefficients of Dzung (1944) which are described in Section 2.4.5, for the particular case of isentropic process are used. The coefficients are as follows:

$$\alpha_s = \frac{T}{v} \left( \frac{\partial v}{\partial T} \right)_s \quad (2.16)$$

$$\beta_s = \frac{T}{p} \left( \frac{\partial p}{\partial T} \right)_s \quad (2.17)$$

$$\gamma_s = - \frac{v}{p} \left( \frac{\partial p}{\partial v} \right)_s \quad (2.18)$$

The three coefficients are related to each other by the following relationship:

$$\beta_s = - \alpha_s \gamma_s \quad (2.19)$$

Flatt (1989) derived a relationship for the coefficient  $\delta_s$  which is expressed as follows:

$$\delta_s = 1 - \frac{1}{\alpha_s} = 1 - \frac{v}{T} \left( \frac{\partial T}{\partial v} \right)_s \quad (2.20)$$

Another expression relating the specific enthalpy to the isentropic alpha and beta coefficients was derived by Flatt (1985b) and is as follows:

$$dh = (1 - \alpha_s) v dp + \beta_s p dv \quad (2.21)$$

From equation (2.20)

$$1 - \alpha_s = 1 + \frac{1}{\delta_s - 1} = \frac{\delta_s}{\delta_s - 1} \quad (2.22)$$

and from equations (2.19) and (2.20)

$$\beta_s = \frac{\gamma_s}{\delta_s - 1} \quad (2.23)$$

Substituting equations (2.22) and (2.23) into equation (2.21) we get the following equation:

$$dh = \frac{\delta_s}{\delta_s - 1} v dp + \frac{\gamma_s}{\delta_s - 1} p dv$$

Rewriting using  $\rho$  we get the following relationship:

$$dh = \frac{\delta_s}{\delta_s - 1} \frac{1}{\rho} dp - \frac{\gamma_s}{\delta_s - 1} \frac{p}{\rho^2} d\rho \quad (2.24)$$

Differentiating equation (2.24) with respect to  $t$ , the following equation is obtained:

$$\frac{dh}{dt} = \frac{\delta_s}{\delta_s - 1} \frac{1}{\rho} \frac{dp}{dt} - \frac{\gamma_s}{\delta_s - 1} \frac{p}{\rho^2} \frac{d\rho}{dt} \quad (2.25)$$

Substituting equation (2.25) into equation (2.15) and subsequently substituting the resulting equation into equation (2.13) we get the following equation:

$$\frac{\delta_s}{\delta_s - 1} \frac{dp}{dt} - \frac{\gamma_s}{\delta_s - 1} \frac{p}{\rho} \frac{d\rho}{dt} - \frac{dp}{dt} + \frac{p}{\rho} \frac{d\rho}{dt} - \frac{p}{\rho} \frac{d\rho}{dt} = \frac{\omega u}{A \cos \psi} + \frac{\Omega}{A}$$

Simplifying we get the following equation:

$$\frac{\delta_s - (\delta_s - 1)}{\delta_s - 1} \frac{dp}{dt} - \frac{1}{\delta_s - 1} \left( \gamma_s \frac{p}{\rho} \right) \frac{d\rho}{dt} = \frac{\omega u}{A \cos \psi} + \frac{\Omega}{A} \quad (2.26)$$

The speed of sound is related to  $\gamma_s$  by the following equation:

$$a^2 = \gamma_s \frac{p}{\rho} \quad (2.27)$$

Substituting equation (2.27) into equation (2.26), using the equivalence presented in equation (2.1) and rearranging; the energy equation transforms to the following:

$$\frac{\partial p}{\partial t} + \frac{u \partial p}{\partial x} = a^2 \left( \frac{\partial \rho}{\partial t} + \frac{u \partial \rho}{\partial x} \right) = (\delta_s - 1) \frac{1}{A} \left( \Omega + \frac{\omega u}{\cos \psi} \right) \quad (2.28)$$

The continuity equation (2.6) contains the partial derivative of  $\rho$  with respect to time, while the momentum equation (2.7) contains the partial derivative of  $u$  with respect to time. For convenience of numerical solution of the three equation of conservation, the energy equation is rewritten such that the term containing partial derivative with respect to time, would be that of  $p$  only. This condition could be achieved by substituting the continuity equation (2.6) into equation (2.28). The resulting equation, which is used in the numerical solution is as follows:



$$\frac{\partial p}{\partial t} + \frac{u \partial p}{\partial x} + a^2 \rho \frac{\partial u}{\partial x} = (\delta_s - 1) \frac{1}{A} \left( \Omega + \frac{\omega u}{\cos \psi} \right) + a^2 \xi \quad (2.29)$$

Equation (2.29) is simpler than equation (2.28). However, in deriving the characteristic and compatibility equations for the numerical method of characteristics, equation (2.28) has to be used instead of equation (2.29) because the latter fails to produce a unique solution. This is explained further in Section 4.3.2.

## 2.4 THERMODYNAMIC AND TRANSPORT PROPERTIES

### 2.4.1 INTRODUCTION

The three basic equation of conservation [Equations (2.6), (2.7) & (2.29)] must be written with dependent variables in such a way that the solution of pressure, velocity, density and temperature could be obtained. This is in general, commonly done by using the equations of state and some other thermodynamic relationships, which are defined by the model used to represent the transient event. An equation of state is an expression which interrelates properties of substances, and we distinguish between two types of equations of state namely the thermal and the caloric equations of state. A gas which obeys the ideal gas thermal equation of state (Equation B-1 in the Appendix) is said to be thermally perfect; and if it has constant specific heats, it is said to be calorically perfect (the terms ideal gas and perfect gas are sometimes used as synonyms). Sections 2.4.2, 2.4.3 and 2.4.4 deal with the thermal equations of state while section 2.4.5 deals with the caloric equations of state.

There are many different ways to approach this problem, for example Van Deen and Reintsema (1983) and Tiley (1989) used the general equation of state for a real gas,

$$P = Z \rho R T \quad (2.30)$$

and the thermodynamic identity based on the Joule-Kelvin effect [Zemansky and Dittman (1983)];

$$dh = C_p dT + \left[ \frac{T}{\rho} \left( \frac{\partial \rho}{\partial T} \right)_P + 1 \right] \frac{dp}{\rho} \quad (2.31)$$

to obtain three equations containing the compressibility factor,  $Z$ , and its partial derivatives. The latter were then substituted in terms of pressure, temperature and velocity; using the Berthelot thermal equation of state.

Generally the thermodynamic process during a transient event can be represented by two major categorisations, namely the perfect or real gas model and the isentropic or non-isentropic (polytropic) decompression model. There is a wide selection of equations of state varying in accuracy and complexity. The choice of which equation to use in a given situation is determined by the type of gas that is being modelled, the level of accuracy required, the temperature and pressure ranges that are likely to be encountered and the amount of available computer space that can economically be used. This subject is covered in the following sections of this chapter, and some of the available equations of state are presented in Appendix B. The perfect gas equation of state holds at low pressures in the vapour and gas regions. The perfect-gas model, whether isentropic or non-isentropic is perhaps the simplest and thus it has been common practice, when predicting transients in a ruptured gas pipeline to assume that the fluid will behave as a perfect gas. The basic premise in making this approximation is that any non-ideal effect that may occur will only affect the initial stages of decompression, and for the majority of the release process, the fluid will behave as a perfect gas. Significant departures can, however occur between the perfect gas and the real fluid decompression behaviour due to condensation effects.

Results from studies by Picard and Bishnoi (1988 and 1989) and Flatt (1985-1989) show that the perfect-gas model can underestimate the transient pressure in gas pipeline ruptures by more than 20%, and underestimate the mass flow rate of gas escaping from the ruptured pipe by up to 50%. One of the major weaknesses of the perfect-gas model is its inability to predict the sudden drop of sound velocity that occurs at the onset of condensation. However, the perfect gas assumption has been used by several workers including Lyczkowski, Grimesey & Solbrig (1978); Lang & Fannelop (1987); Kunsch, Sjøen & Fanneløp (1991); Lang (1991); Chen, Richardson & Saville (1992); and Olorunmaiye & Imide (1993). Lang (1991) admitted that the assumption of a perfect gas leads to errors in the flow rate of about 25% but made the assumption in order to demonstrate the possible use of the spectral method. Kunsch, Sjøen and Fanneløp (1991) made the assumption of an ideal gas just for the sake of simplicity. They expressed the non-ideality of the gas by a compressibility factor, which was taken to be 0.82 for the pressure levels encountered in the investigation. It was claimed that the important results such as mass flow rates were qualitatively well described by the ideal gas model. Another aspect to be considered in using an equation of state for natural gas is the composition of the different substances that make up the gas. For example, Flatt (1985), instead of regarding



natural gas as consisting of diverse  $C_nH_m$  gases of locally differing composition, methane ( $CH_4$ ) was used. Approximately 90 to 95% of natural gas consists of this substance whose thermodynamic characteristics are known. The perfect-gas model is not considered for application in this study, but instead a real-fluid decompression model, which also takes into consideration the mixed nature of natural gas, is used.

## 2.4.2 THERMAL EQUATIONS OF STATE FOR REAL GASES

The term equation of state refers to the equilibrium relation, in the absence of special force fields, between pressure, volume, temperature and composition of a substance, whether it be quite pure or in a uniform mixture. In terms of a functional relation it is expressed as,

$$f(p, v, T, x) = 0 \quad (2.32)$$

An equation of state may be applied to gases, liquids and solids. An equation of state for a real gas accounts for dissociation and ionisation which is important where very high temperatures are encountered. Over five dozen equations of state are known to exist, which represent the liquid, vapour and liquid-vapour regions. These include the Van Der Waals (1873), Clausius (1880) Dietrici (1899), Berthelot(1899-1903), Wohl (1914), Keyes (1917), NBS-National Bureau of Standards (1923) , Beattie-Bridgman (1928), Keyes-Smith-Gerry (1936), Lennard-Jones-Devonshire (1937), Benedict-Webb-Rubin (1940), Hirschfelder-Bird-Spotz (1949), Redlich-Kwong (1949), Bloomer-Rao (1952), Martin-Hou (1955), Hirschfelder-Buehler-McGee-Sutton (1958), Pings-Sage (1959), Storbridge (1962), Costolnick-Thodos (1963), Flory-Orwall-Vrij (1964), McCarty-Stewart (1965), Goodwin (1967), Martin (1967), Soave-Redlich-Kwong (SRK) (1972), Peng-Robinson (PR) (1976), Van Reet-Skogman (1987) and the Kamerlingh-Onnes equations of state.

There are two general approaches to the development of an equation of state, namely the theoretical approach and the empirical or semi-theoretical approach. The theoretical approach is based on either the kinetic theory or statistical mechanics, involving intermolecular forces. The empirical approach has been covered in detail by, among others, Martin (1967). The empirical approach is more of a convenient method of interpolation if it is applied to a pure substance. It can become dangerously inaccurate when used in unfamiliar situations. Empirical equations have been used more widely than theoretical ones because of lack of data to enable the application of the latter equations to various practical



situations and fluids [Münster (1969)]. However, the theoretical approach gives high accuracy and a basis for a wide application.

In the search for an equation of state, one must first make a decision on the amount and kind of data that will be required to obtain the parameters in the equation; range of density to be covered; and the precision with which the pressure, volume and temperature ( $p, v, T$ ) data are to be represented. For some applications it is desirable to have an equation which can be obtained from a minimum of data i.e. the critical temperature, pressure and volume; or the boiling point; or some molecular parameter. In other applications, an equation is sought which will represent a large amount of experimental  $p-v-T$  data within the precision of the experiment. In all pressure-explicit equations, density is paramount. If the same order of precision is to be maintained, a relatively simple short equation will suffice for low densities, whereas a long complicated equation will be required if coverage is to include both high and low densities. High precision equations have many arbitrary constants whose values depend primarily upon the density range and in a minor way upon the temperature range. For example, an equation representing precisely up to a fiftieth of the critical density may need only two constants, while four or five constants will be necessary when in the region of half the critical density. To continue up to the critical density at least a half dozen or more constants will be required and twice that many will be needed if the goal is one and a half, or two times, the critical density.

The Keyes equation of state produces data within the experimental precision for densities of up to a little over half the critical density, while the BWR equation of state, used by Kiuchi (1993), gives good precision for a density range well past the critical density. The Bloomer-Rao equation of state is essentially the same as the BWR equation of state in which the temperature coefficients have been modified to fit nitrogen data. The Keyes-Smith-Gerry equation of state can achieve extremely high precision in calculating thermodynamic properties of steam, but is valid only to a third of the critical density. The Hirschfelder-Buehler-McGee-Sutton and Costolnick-Thodos equations of state cover a wide range of densities and simultaneously maintain a precision which is acceptable for practical applications. In these equations the  $p-v-T$  plateau of data is divided into regions and separate equations are written for the different regions. The Flory-Orwall-Vrij and Lennard-Jones-Devonshire equations of state possess high precision but the range of their applicability is limited to the liquid region where the densities are always significantly greater than critical densities. The Van Der Waals, Clausius, Dietrici, Berthelot, Wohl and

Redlich-Kwong equations of state cover the whole range of density from infinitely attenuated gas to compressed liquid, but with fairly large deviations from experimental results. The Van Der Waals equation is quite accurate at low pressure, but it is inaccurate near the critical point. The Dietrici equation is reliable near the critical point for many organic fluids. However, errors are incurred in other regions far from the critical isotherm and hence it cannot be used for largely varying temperatures. The Berthelot equation produces comparatively accurate results for gases and vapours at low temperatures.

Thorley and Tiley (1987) and Tiley (1989) considered the Van Der Waals, Dietrici and Berthelot equations for application in the analysis of transients in a ruptured high-pressure gas pipeline and found the Berthelot equation to be the most suitable. Picard and Bishnoi (1987) used the Peng-Robinson (PR) and the Soave-Redlich-Kwong (SRK) equations of state to calculate the thermodynamic speed of sound in single-phase fluids consisting of pure components and mixtures and in the two-phase region of a multi-component mixture. Both the PR and SRK equations of state were noted for their ability to provide quite accurate vapour densities and generated reliable equilibrium ratios. However, neither was able to provide liquid densities with the same level of acceptability although the PR equation of state was somehow better than the SRK equation of state. Both the SRK and PR equations of state were weak in predicting sound velocities in liquids, although each was considered to have shown some promise for application to vapours i.e. with errors less than 10%. The Van Reet-Skogman equation of state, used by Kiuchi (1993), is considered adequate for reasonable ranges of pressure and temperature.

It is generally recommended therefore, that for cases where the fluid is transported at conditions near the critical point, more sophisticated equations are required. Also, simple equations of state such as the Redlich-Kwong equation of state fail by far to fit the data within the experimental precision. Even up to the critical density, errors of the order of 5% or more can occur which is considered completely intolerable. These equations can fit data quite precisely over limited ranges but they definitely are not the tools to correlate good p-v-T data within the experimental precision. They cannot therefore be seriously regarded as more than a qualitative tool for predicting p-v-T behaviour. The Beattie-Bridgman equation of state, which contains five adjustable constants, represents with some accuracy the whole range above the triple point. The Martin equation of state, used by Flatt (1985), is the same as the Martin-Hou equation of state with the addition of the exponential terms, which permit the former equation to go to about 2.3 times the critical density as opposed



to 1.5 times the critical density reached by the latter. The equation of Martin has the valuable property that it is also solvable explicitly in respect of temperature. For the practical application, the extra expenditure in computation time with the real gas variant was 13% as compared with the corresponding ideal gas computation.

In deciding on the use of one of the equations of state, or the other, it has been common practice to choose the simplest possible equation. Various workers have justified their choice in different ways. For example Flatt (1985) argued that, in view of the relative simplicity of the one-dimensional flow model used, it was not necessary to demand too high an accuracy from the equation of state and therefore used the Martin equation of state. However, he later admits [Flatt (1993-96)] that the use of the Martin equation of state and an empirical  $C_v(p)$  correlation is inconsistent from the thermodynamic point of view, and therefore recommends the use of a theoretical equation of state of the type  $h = h(p,S)$ . Thorley and Tiley (1987) argued that since the two terms in which the compressibility factor and its derivatives appeared i.e.

$$\frac{T}{Z} \left( \frac{\partial Z}{\partial T} \right)_P \quad \text{and} \quad \frac{p}{Z} \left( \frac{\partial Z}{\partial p} \right)_T$$

are usually relatively small, a complex equation of state would be uneconomical in terms of computer time and therefore used the Berthelot equation of state.

In this study the theoretical approach to equations of state is used. Though more complex, it is as accurate as experimental data. As a result of this high accuracy, the theoretical approach to equations of state is well suited for analysis of high-pressure gas transients and it has been used under similar circumstances by Richardson and Saville (1991), with satisfactory results. As far as possible, real gas properties and data are used in the model.

## **2.4.3 THEORETICAL APPROACH TO EQUATION OF STATE**

### **2.4.3.1 Introduction to the Basic Principles and Equations**

In this approach, the macroscopic properties of the fluid such as pressure and temperature are essentially determined by the interaction of very many particles (atoms, molecules), in contrast to properties definable for single atoms or molecules, even though the latter properties are usually measured in systems with very large number of particles. The



underlying idea is that a probability aggregate can be constructed, with the help of which certain probabilistic statements can be derived about the system under consideration. The theoretical approach to the development of the equations of state has developed over many years, utilising both the principles of classical and quantum mechanics. From the viewpoint of statistical mechanics, a system is considered to consist of an enormous number of molecules, each of which is capable of existing in a set of states at different energy levels. The molecules are assumed to interact with one another by means of collisions or by forces caused by fields. A system of molecules may be perceived to be isolated or, in some cases, considered to be embedded in a set of similar systems or ensemble of systems. Concepts of probability are applied, and the equilibrium state of the system is assumed to be the state of highest probability. The fundamental problem is to find the number of molecules in each of the molecular energy states (population of the states) when equilibrium is reached. It is not the intention of this study to go into the details of these principles but rather to find a useable form of an equation of state based on this approach, that will represent the situation being modelled as accurately as possible. For further details on these principles, the reader is referred to Münster (1969).

On the basis of this theoretical approach, the microscopic description of a system involves specifying many quantities, which are not suggested by our sense perceptions and cannot be measured e.g. configurational, residual, partition, molecular distribution functions etc. The relation between the macroscopic and microscopic points of view lies in the fact that the few directly measurable properties, whose specification constitutes the macroscopic description are really averages over a period of time of a large number of microscopic characteristics. For example, the macroscopic quantity, pressure, is the average rate of change of momentum due to all the molecular collisions made on a unit area. In statistical mechanics, an ideal gas is defined as a system of non-localised particles whose interaction energy can be neglected relative to the total energy of the system. The laws of ideal gas are limiting laws at zero pressure. Their practical significance is due to the fact that they frequently give sufficiently good approximations for simple gases at ordinary pressures. Deviations from the ideal gas laws, which are due to intermolecular forces, arise at finite pressures thus the necessity for real gas considerations. For real gases at ordinary pressures, at least two effects appear, which can only be included by the addition of special constants. These constants are known as the volume correction, which takes account of the volume of the molecules themselves and the pressure correction; which takes account

of the intermolecular forces of attraction. The Van der Waals equation of state was the first to take into account these considerations. The quantitative results of the Van der Waals equation are generally not satisfactory, but nevertheless represent the behaviour of real gases in a fairly satisfactory qualitative manner. The Beattie-Bridgman equation of state proved itself the best from the viewpoint of convenience of computation.

The most general equation of state is the Kammerlingh-Onnes equation of state (Equation B-17). In this formulation, the equation is represented as a power series in  $v^{-n}$ . The equation is commonly called the virial equation of state and the coefficients B, C, D, E, etc. are known as the second, third, fourth, fifth, etc. virial coefficients respectively. The coefficients vary with temperature, and depend on the nature of the gas and are related to molecular properties of the gas. In the pressure range from zero to about forty standard atmospheres, only the first two terms in the expansion are significant. In general, the greater the pressure range, the larger the number of terms in the virial expansion. The equation is used to account for the behaviour of real gases especially at high pressures. The equation is tedious to use but one of its merits is that once the virial coefficients are determined, the behaviour of any real gas can be predicted. An average reduced virial equation of state can be obtained by introducing the reduced state variables  $p_r$ ,  $T_r$  and  $v_r$  in place of  $p$ ,  $T$  and  $v$ . The reduced virial equation of state is:

$$\frac{p_r v_r}{T_r K_c} = \left( 1 + \frac{B_r K_c}{v_r} + \frac{C_r K_c^2}{v_r^2} + \frac{D_r K_c^3}{v_r^3} + \frac{E_r K_c^4}{v_r^4} + \frac{F_r K_c^5}{v_r^5} \right) \quad (2.33)$$

where the reduced state variable are

$$p_r = \frac{p}{p_c} \quad T_r = \frac{T}{T_c} \quad v_r = \frac{v}{v_c} \quad (2.34)$$

and the coefficients  $B_r$ ,  $C_r$ ,  $D_r$  etc. are of the form

$$B_r = b_1 + \frac{b_2}{T_r} + \frac{b_3}{T_r^2} + \frac{b_4}{T_r^3} + \frac{b_5}{T_r^4} \quad (2.35)$$

and the critical coefficient

$$K_c = \frac{N_L R T_c}{p_c v_c} \quad (2.36)$$

( $N_L$  is Avogadro's number). The importance of the reduced form of the equation of state (Principle of Corresponding States-Refer to Section 2.4.3.2) is due to the fact that many substances have almost the same thermal equation of state in the reduced state variables. The value of  $K_c$  evaluated by Münster (1969) from equation (2.36) above, when  $p_r=T_r=v_r=1$  is  $K_c=3.43$ . The remaining 25 numerical coefficients in equation (2.33) are available from Landolt-Bornstein Tables. Also available from this reference are the coefficients of the Van der Waals equation for various substances.

#### 2.4.3.2 The Principle of Corresponding States

The principle of corresponding states is based on the fact that any equation of state

$$f(p, v, T, A, B, C) = 0 \quad (2.37)$$

which does not contain more than three independent constants can by insertion of the critical data be put into the form

$$\varphi(p_r, v_r, T_r) = 0 \quad (2.38)$$

The above change is possible because one of the three constants (A, B, C), i.e. the gas constant is universal and the two others can be eliminated by means of the following equation:

$$\left( \frac{\partial p}{\partial v} \right)_T = \left( \frac{\partial^2 p}{\partial v^2} \right)_T = 0 \quad (2.39)$$

Equation (2.39) holds at the critical point. Equation (2.38), which no longer contains constants relating to specific substances, has universal validity. This is called the principle of corresponding states. In its simplest form, the principle of corresponding states postulates that the surface  $p_r = f(v_r, T_r)$  is the same for all members of a given set of substances.

The fact that any useful empirical equation of state contains more than two specific constants means that this principle can not be rigorous in the strict sense. On the other hand, experience has shown that the principle is obeyed very exactly by a few substances and that for the remainder, all degrees of approximation occur up to complete failure. It was concluded by Münster (1969), that the principle of corresponding states will be obeyed by the heavier inert gases and non-polar diatomic molecules at best. For other substances, deviations will be greater the more unsymmetric and polar the molecule is. The principle



of corresponding states applies only to spherical molecules and to pure substances. Kay (1936) developed a method of calculating the  $p$ - $v$ - $T$  data of hydrocarbon mixtures, based on the principle of corresponding states. The  $p$ - $v$ - $T$  of the mixtures expressed as deviations from the perfect gas law were correlated with similar data on pure hydrocarbons, using the pseudocritical temperature and pressure. This was compared with experimentally determined data for eleven typical hydrocarbon mixtures in the gaseous state, over a wide range of temperature and pressure extending from the saturated condition to the highly superheated condition above the critical region. It was claimed that the accuracy of the method was comparable to that with which the principle of corresponding states was found to hold for pure hydrocarbons. It was observed that the reduced  $p$ - $v$ - $T$  relations of pure hydrocarbons were not exactly the same for different hydrocarbons. However, the differences were, in general, insignificant except at high reduced temperatures. In this region the differences were a function of molecular weight.

#### **2.4.3.3 Extension of the Principle of Corresponding States**

Two major limitations of the principle of corresponding states, namely restriction to a set of substances and restriction to pure substances, necessitated its extension to cover these situations. One such extension is that by Rowlinson and Watson (1969). In their approach, they expressed the residual and configuration properties of a fluid in terms of residual or configuration properties of a pure substance, usually termed the reference substance. Non-spherical molecules were included by the use of shape factors. The principle of corresponding states was defined by a pair of equations that relate the configurational properties. The equations were chosen so that the conventional principle of corresponding states emerges as a special case.

Saville and Szczepanski (1982) presented two methane-based equations of state, one valid over the reduced temperature range of 0.2-2.6, and the other valid over the reduced temperature range of 0.35-2.6. The equations are extended versions of the Benedict-Webb-Rubin equation of state and were intended for use as reference equations of state in the calculation of thermodynamic properties by the principle of corresponding states. The equations reproduced experimentally measured properties of the fluid phase over the whole region for which they exist (reduced temperatures of 0.47 to 3.3). Extension to higher temperatures was made by utilising experimental measurements made

on nitrogen and hydrogen, and an empirical scheme was used for reduced temperatures below 0.47. The two equations were reported to have provided a satisfactory basis for the calculation of thermodynamic properties of hydrogen and the two-phase behaviour of hydrogen-hydrocarbon mixtures, provided the pseudo-critical parameters are used for hydrogen and that the temperature of interest is well above the critical temperature of hydrogen, so that the effect of quantum behaviour of hydrogen molecules is small. Full phase diagrams were calculated for the mixtures including the critical region.

#### **2.4.3.4 Commercial Computer Software**

##### **2.4.3.4.1 IUPAC**

The IUPAC equation of state package is one of a variety of packages supplied by the Physical Property Data Service (PPDS), which is operated by the National Engineering Laboratory, UK and the Institution of Chemical Engineers. The equation of state package has been produced by the IUPAC Thermodynamic Tables Project Centre of Imperial College, London. It comprises a suite of computer programmes to calculate the thermodynamic properties of a small number (currently 10) of pure fluids to an accuracy which is comparable with that of the best experimental data. The fluids covered so far are ethylene, methane, nitrogen, oxygen, propylene, carbon dioxide, argon, hydrogen, propane and ethane. Available experimental results on the fluids have been critically evaluated and selected data fitted to an equation of state using statistical methods. Every property is calculated from a single equation of state for each fluid, which ensures thermodynamic consistency amongst all properties.

The heat capacity, enthalpy and density are available at any point in the fluid region, within wide limits of pressure and temperature, or on the saturation line. The equation of state package is written in FORTRAN IV in the form of a portable sub-programme, which can be readily linked to design programmes. The sub-programme has been developed to suit a number of user applications and computer environments.

##### **2.4.3.4.2 QUANT**

QUANT is a computer programme for thermodynamic and transport properties of real gases and their mixtures. The programme is owned by Silberring Engineering Ltd. of



Zurich, and is based on the virial equation of state. In the present version, calculation is possible only up to the second virial coefficient, but an extension to further virial coefficients is under way. The source code of QUANT is written in the Microsoft Professional BASIC language but could be linked to any particular application programme written in any of the usual Microsoft languages such as FORTRAN, PASCAL, or C. The programme delivers properties of elements, compounds and any of their mixtures; but is restricted to the gaseous phase so far. QUANT uses spectroscopic and other experimental information as a basis for its formulation. Residual properties of pure gases and their mixtures, including partial properties of components in the latter, are calculated using the virial equation of state. The virial equation of state is said to be the only one which allows one to deduce the properties of mixtures from those of pure substances using a sound theoretical basis and moderate amount of additional information. The virial coefficients are represented by proprietary temperature functions which allow a reliable smoothing and interpolations of experimental data as well as their extrapolations beyond the limits of experimental evidence. QUANT operates on IBM compatible personal computers.

A particular variation of QUANT prints extended gas properties in the standard or real state as a function of standard state fugacity or pressure and temperature, in addition to those delivered by the standard version of QUANT. The additional data consists of isochoric heat capacity related to the gas constant ( $C_v/R$ ); isentropic exponent, also equal to the ratio of the isobaric to isochoric heat capacity ( $K = C_p/C_v$ ); and the partial derivatives,  $\alpha_p$ ,  $\beta_v$ ,  $\gamma_T$ ,  $\gamma_S$  and  $\delta_S$ . These properties are available for all substances, mixtures, units parameter ranges and steps covered by QUANT. The data from this variant is very important in relation to the  $\gamma\delta$  method described in Sections 2.3 and 2.4.5.

#### **2.4.3.4.3 PREPROP**

Richardson and Saville (1991) used the extension of the principle of corresponding states, developed by Rowlinson and Watson (1969), and the methane-based reference equations of Saville and Szczepanski (1982) [equations A-19 and B-20], to calculate the thermophysical properties in a computer model for blowdown of pipelines (BLOWDOWN). Using the result of the above mentioned studies, they developed a computer package called PREPROP, for calculation of thermophysical properties of multi-component mixtures. Their choice of the corresponding states package was necessitated by the need for good



prediction of phase equilibrium, enthalpy and density simultaneously. The model has produced results which agree well with experimental results for blowdown of natural gas pipelines.

#### 2.4.4 OTHER APPROACHES FOR REAL-GAS MIXTURES

A much simpler approach for dealing with real-gas mixtures is the use of Dalton's rule of additive pressures or the Amagat rule of additive volumes, described by Holman (1980). The difference between these two and the law of partial pressures is that the individual pressures or volumes are calculated from some real-gas equation of state. This simplified approach neglects interaction between the constituent molecules, and therefore considerable errors are expected. In addition to these simple additive rule, there are many relations which have been developed for the calculation of real-gas mixtures properties.

Kay (1936) developed the simple procedure described in Section 2.4.3.2, which assumes that the mixture may be treated as a pseudo-pure substance with some empirical artifice used to determine the pseudo-critical constants for the mixture. According to Holman (1980), the procedure is accurate to within 10% over a wide range of temperatures and pressures.

#### 2.4.5 CALORIC EQUATIONS OF STATE

For a real gas, the specific heats vary with temperature and pressure, and the caloric equation of state may take the form:

$$C_v = C_v (T, p) \quad (2.40)$$

When a high-pressure natural gas pipeline breaks, the gas can escape from the pipe in a process that is sometimes approximated as isentropic. The isentropic model assumes that heat conduction and wall friction are negligible. However, during isentropic decompression of any gas the temperature falls drastically. With natural gas of high specific gravity, this may lead to pressures and temperatures which fall within the two-phase (gas-liquid) region.

Non-isentropic decompression models are developed based on the thermodynamics of two-phase (liquid-gas) real-fluid, multi-component mixtures and the laws for unsteady non-isentropic processes, i.e. viscous dissipation and heat transfer occurring. There have been various such models developed for different applications, but in this study three

models are considered, namely those by Picard & Bishnoi (1989), Flatt (1985-1989) and Richardson & Saville (1991). These models are briefly discussed here. Both models were developed for analysing transient flows following a rupture in a high-pressure gas pipeline and were used in conjunction with the method of characteristics. The Picard-Bishnoi non-isentropic decompression model utilises the thermodynamics relationship,

$$T dS = dh - \left( \frac{1}{\rho} \right) dp \quad (2.41)$$

It determines the complete decompression histories at all locations inside the pipeline including the rupture point and the emergency shut-down valve. In working with the model, it became apparent that a numerical instability may develop at the rupture plane from problems involving non-isentropic flow if the selected distance between grid nodes is too large in the high gradient region immediately upstream of the rupture plane (numerical instability was not observed for problems involving isentropic flow). In order to overcome the instability problem without creating excessive computational demands, use was made of non-uniform grid spacing (refer to section 4.4) to allow for fine grid spacing near the rupture plane where grid spacing is most critical and coarser spacing further back. Since non-isentropic effects in the region of the rupture plane seemed to be caused by the instability problem, a second strategy was to impose a short isentropic region at the rupture plane. This approximation was considered to be valid assuming the isentropic region is small relative to the total pipe length. The use of the modification completely eliminated the rupture plane instability problem.

The Flatt non-isentropic decompression model is based on the polytropic coefficients of Dzung (1944), which are as follows:

$$\alpha_{\sigma} = \frac{T}{v} \left( \frac{\partial v}{\partial T} \right)_{\psi}, \quad \gamma_{\sigma} = - \frac{v}{p} \left( \frac{\partial p}{\partial v} \right)_{\psi}, \quad \beta_{\sigma} = \frac{T}{p} \left( \frac{\partial p}{\partial T} \right)_{\psi} \quad (2.42)$$

where the subscript  $\sigma$  corresponds to an optional index which represents any set of thermodynamic quantity e.g.  $p, v, T, h, S$ , etc.; the polytropic characteristic number,

$$\psi = v \frac{\partial p}{\partial h} \quad (2.43)$$

and the Gibbs equation which is sometimes described as the "definition of entropy"

$$T ds = dh - v dp \quad (2.44)$$



Flatt (1989), further developed the model by introducing a new coefficient  $\delta_s$ , which enabled it to cover both bi-phase and homogeneous gas-liquid as well as pure liquid flows. This approach is called the gamma delta method and in principle can be generalised to three dimensional flow. The basic relationships for this method, whose complete derivation is given in Section 2.3 is:

$$dh = \frac{\delta}{\delta - 1} v dp + \frac{\gamma}{\gamma - 1} p dv \quad (2.45)$$

where,

$$\delta = 1 - \frac{v}{T} \left( \frac{\partial T}{\partial v} \right)_s \quad (2.46)$$

The delta-coefficient of the gamma-delta method and also the coefficients  $\alpha_p$ ,  $\beta_v$  and  $\gamma_s$  have been incorporated into the real gas software, QUANT, described in Section 2.4.3.4.2. A non-isentropic decompression model and the Flatt gamma delta method have been used in this study.

## 2.5 FRICTIONAL FORCE

### 2.5.1 INTRODUCTION

For gas flow in short and medium length pipelines, frictional effects are often small and localised, hence they have normally been considered relatively unimportant in view of the overall uncertainties involved in modelling most practical problems. However, for long pipelines, the principal reason for change in pressure along the pipeline is due to friction losses. The frictional effects are, cumulative and become important for long term transients. In long pipes they can give rise to significant pressure drop and line packing under transient conditions. Modelling of frictional effects may be done either by numerically evaluating the frictional factor in equation (2.47) using known flow field data or by using experimental correlations. The shear stress at the wall tends to be proportional to the pressure gradient, while the average velocity may be out of phase with the pressure gradient because of the inertia of the main flow.

The friction term in the basic equations is denoted by  $\omega$  and is defined as the friction force per unit length of the pipe opposing the flow. After assuming that the minor

losses are negligible, the frictional force per unit length is expressed by the empirical relationship;

$$\omega = \frac{A}{d} \rho f_D \frac{u|u|}{2} \quad (2.47)$$

As the transients progress, and the high frequency content of the pressure waves dies out, a point is reached where the explicit procedure is no longer suitable. An implicit procedure that allows large time-steps is more appropriate. Consequently, in modelling frictional effects in high-pressure gas pipeline transients, a number of questions have to be answered. These are discussed in the sections of this chapter which follow. Over 20 friction factor expressions have been identified in this study. These include those by Hagen-Poiseuille for laminar flow; Blasius (1911), Uhl (1965), Panhandle "A", Smith (1956) and Chaudhry (1979) for partially developed turbulent flow; Von Karman (1930), Nikuradse (1933) and Smith (1956) for fully developed turbulent flow; Colebrooke (1939), Oliemans (1976), Moody (1947), Swamee-Jain (1976), Zigrang-Sylvester (1982), Shacham (1980), Haaland (1983), Wood (1966), Colebrooke-White or Prandtl-Colebrooke (1938-39), Churchill (1977) and Chen (1979) for the transition region. The relevant expressions for the friction factor are presented in Appendix C.

It should however, be admitted that only very little seems to be known from the theoretical point of view of the real behaviour of frictional effects in transient flow because the problem is non-linear, thus making the finding of analytical solutions unlikely. Flatt (1986) attempted to explain this phenomenon for a rupture at the upstream end of a straight pipe. He illustrated his argument with figures for the cases with and without frictional effects being considered. According to his model a pressure peak would appear somewhere in the middle of the pipe, its location corresponding approximately to the location of the flow reversal i.e. where the velocity is zero. With increasing time, the pressure peak slowly moves towards and until it reaches the closed end.

### **2.5.2 STEADY FLOW FRICTION FACTOR**

The use of a steady flow friction factor to represent the wall shear stress is only justified theoretically for steady flow. For the calculation of unsteady flow in pipes the steady state friction term is usually used, and can produce acceptable results, although it is well known that this term does not describe the real physical phenomenon accurately. Perhaps it is



reasonable to expect this to be valid for small perturbations around a steady flow condition and some experimental evidence exists to support this. However, this would not be expected to be true in the case of large and rapid disturbances.

Van Deen and Reintsema (1983) argued that the Darcy friction factor is weakly dependent on Reynolds number, but it may be considered as constant in the region of interest because of the large Reynolds numbers ( $Re > 10^7$ ) involved. Being aware of the limitation of using a steady flow friction factor for unsteady flow, Thorley and Tiley (1987) recommended its use in modelling of unsteady transient flow of compressible fluids in pipelines. Their justification was that there had been no friction factors defined for transient gas flows, except some time-dependent friction factors for laminar liquid flow and also on the basis that "tuning" of the friction term may be employed when investigating rapid transients. Tiley (1989) used a constant value steady-state friction factor in modelling of pressure transients in a ruptured high-pressure gas pipeline. The basis of this choice was the assumption that fully developed turbulence was achieved and if necessary a flow dependent friction factor could be substituted into the analysis provided that the improvement in the results obtained justified the additional computing involved. The various expressions for steady-state friction factor are presented in Appendix C.

### 2.5.3 FLOW-DEPENDENT FRICTION FACTOR

The flow of fluids in pipelines is categorised, depending on Reynolds number, into either laminar flow, partially or fully developed turbulent flow. Friction factor is dependent on the type of flow as categorised above which may vary from point to point in a pipeline, and in addition on pipe roughness. The traditional way of estimating the friction factor for a Newtonian fluid flowing through a pipe is based on the well known Moody Friction Chart. This chart is made up of various relevant equations for different flow regimes. However, in numerical modelling of flow situations, these charts are unsuitable and equations have to be used. Numerous equations have been developed for estimating friction factors. The most widely used are presented in Appendix C. For laminar flow ( $Re < 2100$ ), the Hagen-Poiseuille equation is used i.e.

$$f_D = \frac{64}{Re} \quad (2.48)$$

It should be noted that the Darcy friction factor is four times the Fanning friction factor.

For fully developed turbulence, the rough pipe law which assumes that the friction factor is solely dependent on the pipe roughness and size is used:

$$\frac{1}{\sqrt{f_D}} = A_1 \log\left(\frac{d}{\epsilon}\right) + B_1 \quad (2.49)$$

where  $A_1$  and  $B_1$  are constants. For partially developed turbulence either the smooth pipe law or the Blasius form of the smooth pipe law are used. Here the friction factor is assumed to be only dependent on the fluid properties and pipe size. The smooth pipe law is traditionally expressed as:

$$\frac{1}{\sqrt{f_D}} = A_2 \log(Re \sqrt{f_D}) + B_2 \quad (2.50)$$

The Blasius form of the smooth pipe law is given as:

$$f_D = A_3 Re^{B_3} \quad (2.51)$$

where  $A_2$ ,  $B_2$ ,  $A_3$  and  $B_3$  are all constants. The above equation is true only over a very limited range of  $Re$ . For the transition zone between partially and fully developed turbulence a combination of both the rough and smooth pipe laws is used. The Colebrooke equation (Equation C-2) has been universally adopted for this regime. However, there are numerous other equations which could be solved explicitly, and with almost the same accuracy as the Colebrooke equation.

The key factor in applying a flow-dependent friction factor is the determination of which flow regime is to represent the flow at a particular point and time. This situation is exacerbated by the fact that, in many practical flow situation many flow regimes exist and thus different equations have to be used. Typical high-pressure gas pipeline flows are characterised by their high Reynolds numbers. The key decision to be made for such flows therefore, is whether it could be assumed that fully developed turbulence has been achieved, so that the rough pipe law which is independent of Reynolds number and hence flow could be employed. If however, the flow is in the partially developed turbulent regime or even in the transition zone between partially and fully developed turbulence, the friction factor would vary with changes in the Reynolds number (for Newtonian fluids this is not a problem).



In this study, an expression for friction factor is selected, which covers as much as possible, all the flow situations i.e.  $Re$  and  $\epsilon/d$  expected during the transient event being modelled. Particular attention is paid to expressions for friction factor, which cover the transition zone from partially to fully developed turbulent flow. As seen in Appendix C, there are more than twenty expressions for the friction factor in this zone. Though the Colebrooke equation is the most accurate (it represents data within 5% of experimental results), it has the disadvantage that solution for the friction factor requires iteration. This makes it less attractive for computer models. Swamee and Jain (1976) presented an explicit equation [Equation C-8], which was found to yield values of the friction factor well within  $\pm 1\%$  of the Colebrooke-White equation for  $10^{-6} \leq \epsilon/d \leq 10^{-2}$  and  $5 \times 10^3 \leq Re \leq 10^8$ . The equation was also found to be applicable over the entire turbulent zone of pipe flow, unlike the Wood equation [Equation C-7] which is not applicable to smooth-turbulent flows and computes the friction factor within  $\pm 5\%$  of the Colebrooke equation. The Swamee-Jain equation was found to be easy to apply.

Zigrang and Sylvester (1985) made a review of nineteen explicit friction factor equations. Three among these were developed in their above mentioned study. They classified the equations, according to precision, into three categories namely simple equations [Equations C-11, C-14 and C-15]; intermediate precision equations [Equations C-16, C-17 and C-18]; and highest precision equations [Equations C-19, C-20, C-21 and C-22]. The equations were compared for precision against the Colebrooke equation, and for complexity, in the range  $2500 \leq Re \leq 10^7$  and  $4 \times 10^{-5} \leq \epsilon \leq 0.005$ . Though the equations have relative errors of up to 13%, all the equations in the intermediate and highest precision categories were found to have relative errors well within 1% of the Colebrooke equation (within 6% of experimental data). The study concluded that the high accuracies in the highest precision category are unnecessary. In this study, more attention will be paid to the range of flow i.e.  $Re$  and  $\epsilon/d$  which the various equations cover, rather than wasting too much time in finding an equation with the highest precision. The accuracy in calculating the friction factor in real systems is influenced by how well the pipe wall roughness and diameter are known. Both these parameters may vary with time and position in the pipe.

At least two expression for friction factor i.e. those by Chen (1979) and Churchill (1977) [equations C-5 and C-6 respectively] exist, which cover the whole range of Reynolds numbers and pipe roughness and which produce results which are nearly the same



as those produced by the Colebrooke equation. The Chen equation was used by Bisgaard, Sørensen and Spangenberg (1987) in modelling of transients in a ruptured high-pressure gas pipeline. This equation is also used in this study, because it is explicit, it covers the whole range of Reynolds number, and it is simpler than the Churchill equation. The most popular method of estimating flow-dependent friction factors is by using the quasi-steady friction formula, whereby the steady-state expressions are used for unsteady flow. The friction factor is calculated for each grid point as a function of Reynolds number without consideration being made to the fluctuation of velocity and the gradient of the other values.

Eichinger and Lein (1992) proposed and investigated two new methods of presenting the unsteady friction term namely based on wall shear stress and on friction power. The formula for unsteady friction term based on wall shear stress is solely dependent on the value of the gradient of velocity in the near wall region. In this case calculation of the velocity profile near the wall is of extreme importance. This applies in particular to turbulent flow because as the Reynolds number increases, so does the gradient near the wall. The formula for the friction term based on the friction power is based on consideration of energy of the incompressible fluid. The difference between the work of the internal and external forces and the increase of the kinetic energy of a volume element of an incompressible fluid is the dissipation per unit of time. Preliminary investigation of unsteady flow using the two unsteady friction terms revealed that the results obtained, using the friction factor based on the wall shear stress, were considerably better than those achieved using the friction term based on the friction power. Moreover, numerical difficulties sometimes arose when using a friction term based on friction power. For this reason the friction term based on wall shear stress was preferred and used as an unsteady friction term. The formula for unsteady friction term based on wall shear stress, which was used by Ohmi, Kyomen and Usui (1985) is as follows:

$$\omega = \frac{4\nu}{gd} \left. \frac{\partial u}{\partial r} \right|_{r=r_0} \quad (2.52)$$

where  $r_0$  is the radius of the pipe.

Thorley and Tiley (1987) recommended the use of a constant friction factor which they claimed will usually be adequate as a first approximation. The basis for their argument was that in practice the basic data for determining the friction factor, even for steady flow, will rarely be known within a few percent. In this study, the explicit equation of Chen (1976) [Equation C-5] and the friction term formula based on wall shear stress are recommended. However, the equation of Chen has been used.



#### 2.5.4 FREQUENCY-DEPENDENT FRICTION FACTOR

In the study which preceded this work i.e. by Tiley (1989) very little attention was paid to the dependence of friction factor on the frequency of transient events. In this study, an extensive investigation is made on studies available on this subject. However, it is admitted that there has not yet been any satisfactory results to justify the application of a frequency-dependent friction factor in this model. The first and most significant work on frequency dependent friction in transient pipe flow was by Zielke (1968). He developed a procedure within the framework of the method of characteristics that utilises the recent history of the transient to take the shift in phase between the boundary film and the main flow into account for the laminar flow case. His equation relates the wall shear stress in transient laminar pipe flow to the instantaneous mean velocity and to the weighted past velocity changes. Based on the pioneering work by Zielke (1968), Brown (1969) developed a quasi-method of characteristics, applied to forcing functions which depend on non-local and non-instantaneous (former) states of the system.

Hirose (1971) was the first to extend the Zielke idea into turbulent flow. He used an empirically developed weighting function to adapt the method of characteristics which is very simple compared to the analytical expression for laminar flow based on Zielke's approach. Trikha (1975) derived a similar expression for frequency-dependent friction in transient laminar flow which approximates the exact expression by Zielke very well in both the time and frequency domains. This approximation is simpler, easy to program, requires significantly less computer storage and computation time and hence is more practical than the exact expression by Zielke. Kagawa et al (1983) developed a model which requires less computer storage and computation time than Zielke's exact model and more accurate than Trikha's approximation model. Kagawa's approximate weighting function is derived by approximating Zielke's function with the first-order lag element one by one so its time constants of the first order lag elements reduce very slowly, which shows that by taking many more terms of the first order lag elements Kagawa's model could reach good accuracy. By comparing predictions with experimental data, Budny, Wiggert and Hatfield (1990) concluded that frequency-dependent friction factor for laminar flow based on Zielke's equation can be extended into the transition zone and beyond, at least to a Reynolds number of 11,000 and is capable of predicting the decay over many cycles.

Yigang and Jing-Chao (1990) developed a new approach for simulating frequency-dependent terms both in the frequency and time domain by using the method of non-linear square integral optimum. Because this new method is optimised over a large frequency range and needs fewer terms of the first order lag elements than Kagawa's model, it possesses an excellent high speed of calculation and accuracy in both frequency and time simulations and is more practical for analysing the frequency and transient responses, pressure surges, and pressure attenuations in hydraulic pipelines. In the Trikha and Kagawa models, the equation of frequency-dependent friction in the time domain includes an unknown current flow rate value. Therefore an interactive algorithm is needed to calculate the frequency-dependent friction in the method of characteristic, which also makes the simulation complex and time consuming. The Yigang-Jing-Chao method does not need iterating and requires only half of the computation time of Trikha and Kagawa models.

Vardy (1992) and Vardy, Hwang and Brown (1993) concluded that the use of expressions similar to that developed by Zielke (1968) for transient laminar friction in pipes, is justified theoretically and experimentally for transient turbulent friction. In this case the weighting function curve ceases to be unique but rather a family of curves exist, one for each value of the product ( $f d Re$ ). The Zielke expression is shown to be an asymptotic limit of the family of weighting function curves. Further work is going on [Vardy (1993)] to provide a theoretical framework at higher Reynolds numbers and to explore the influence of frequency effects in turbulent flows at all Reynolds number. It should also be noted that the expression is applicable only to moderate Reynolds numbers and only to smooth pipes. Some progress has been made in extending the work to higher Reynolds numbers and to rough pipes. All expressions such as Trikha's are limited in the range of time scale for which they are applicable and hence appropriate numerical coefficients have to be chosen.

From this review, it seems rather too early to start applying these frequency-dependent friction terms in the modelling of transients in high-pressure gas pipelines. Since the effects of unsteady friction, in addition to steady friction, are very small in such applications, a frequency-dependent friction factor is not used in this model.

### **2.5.5 FRICTION FACTOR FOR TWO-PHASE HOMOGENEOUS FLOW**

During depressurisation of dense-phase gases in a ruptured pipeline, the existence of two phases, gas and liquid, is likely to occur. In the process of modelling such an event



therefore, one needs to consider how to handle the situation, including the friction term. The friction factor is strongly dependent on the liquid fraction and different calculation techniques give substantially different results. There are two main techniques of presenting the friction term in two-phase flow namely, by modifying the Reynolds number and the roughness term in the equation for friction factor; and including in the expression for friction a multiplier for two-phase friction, which is determined empirically.

The expression by Oliemans (1976) [Equation C-3] is an example of the former technique. Thorley and Tiley (1987) recommended the use of the latter technique because it is relatively simple and had already been adapted by various authors for analysis of transient flow situations. They claimed that modifying the Reynolds number and roughness term is more appropriate for steady flow analysis. The two-phase friction factor is not used in this study.

#### **2.5.6 FRICTION FACTOR WITH RESPECT TO FLUID STRUCTURE INTERACTION**

The phenomenon of Fluid Structure Interaction has been discussed in depth in Section 2.2.3, and need not be repeated here. With respect to Fluid Structure Interaction the friction term in the momentum equation must be corrected for axial motion of the pipe i.e. the relative fluid velocity is of importance. Since it was decided earlier, in Section 2.2.3 not to include the effect of Fluid Structure Interaction in this model, its effect on friction factor is also being neglected. However, this gives an indication of the number of factors that affect the friction and how difficult it is to achieve an accurate representation of the friction term.

#### **2.5.7 APPROXIMATION OF FRICTION FACTOR WHEN SOLVING THE BASIC EQUATIONS**

It has already been stated in Section 2.5.1 that frictional effects in transient flows are highly non-linear. Terms in which finite-differences are used to represent quantities which are integrals rather than derivatives, in particular pipe friction, may introduce numerical instability and require particular care. It has been argued that a linearised friction term does not adequately represent this high frictional effect in gas and so a second-order approximation such as the trapezoidal rule has been used.

However, Suwan and Anderson (1992) discovered an unconditionally stable linear implicit approximations adopted from the method of characteristics, which was the most accurate of the many approximations tested over representative ranges of data. A second-order approximation (refer to section 4.3.2) is used to calculate the friction force in this model.

## **2.6 HEAT TRANSFER**

### **2.6.1 INTRODUCTION**

Whenever a disturbance occurs in pipe flow system, it causes changes in temperature because the change in pressure and velocity of the gas involves an acceleration that in turn derives its energy from the internal energy of the gas. This situation leads to heat transfer between the gas and its surroundings. The heat transfer term,  $\Omega$ , is defined as the heat flow into, or from the pipe wall per unit length of pipe. Although this term is considerably smaller in magnitude than the friction term, it is still a necessary inclusion especially when considering long distance pipelines.

Heat transfer occurs by means of forced convection through the turbulence boundary layer of the gas in the pipe, conduction through the pipe wall, by natural convection outside the pipe and radiation to the surroundings. There are two extreme cases of heat transfer namely isothermal flow and adiabatic flow including the special case of isentropic flow. In the isothermal flow model the temperature is assumed to be constant and therefore there is a net heat flow through the pipe. In this case the energy equation becomes redundant except to calculate the value of the heat transfer,  $\Omega$ . In the adiabatic model, it is assumed that there is no net flow of heat through the pipe. However, in reality some heat transfer will take place between the gas and its surroundings although thermal equilibrium will not always be achieved.

### **2.6.2 HEAT TRANSFER PROCESS**

The most common approach in unsteady flow modelling has been to use either of the two extreme cases described in Section 2.6.1. Isothermal flow relates to slow dynamic changes. If a pipe is long and the change is relatively gradual, the gas will tend to come to thermal equilibrium with the pipe. The mass of the pipe is usually much greater (order of 15 times)



than the gas it contains. In this kind of situation therefore, the assumption of constant temperature is reasonable. Adiabatic flow relates to fast dynamic changes in the gas, where it is assumed that the pressure changes occur instantaneously allowing no time for heat transfer to take place between the pipe and the surroundings.

The subject of whether or not the isothermal flow assumption is adequate for modelling rapid transients, especially those following a ruptured high-pressure gas pipeline, has been discussed by among others Flatt (1993-96). It is generally considered that for such flow situations, the isothermal model is inadequate and thus the energy equation has to be used. However, the isothermal model has continued to be used by various workers including Lang and Fanneløp (1987); Kunsch, Sjøen & Fanneløp (1991); Lang (1991); and Olorunmaiye & Imide (1993). Wilson (1981) investigated the heat transfer to a fluid experimentally. He observed an isothermal condition throughout the length of the pipe, except for about the last 200 diameters, during which the rapidly accelerating flow near the pipe exit was moving too quickly to gain heat from the pipe walls. The justification which is commonly given for this assumption is that the mass flow rate at the rupture shows a negligibly small difference between the isothermal and adiabatic models. Kunsch, Sjøen & Fanneløp (1991) and Lang (1991) used both the adiabatic and isothermal assumptions. Both studies observed the difference in flow rates at the break between the two models to be very small. Kunsch, Sjøen and Fanneløp (1991) attributed this fact to the opposite effects of the critical density (higher for isothermal flow) and the critical velocity (lower for isothermal flow), on the choked mass flow rate, which was observed by Ryhming (1987).

Surprisingly, Olorunmaiye and Imide (1993) found that the flow rate predicted at the broken end of the pipe was lower than that of a model based on the adiabatic flow assumption by about 18%, but at the same time agreeing quite well with that of Lang and Fanneløp (1987), for isothermal flow. However, the  $p(x,t)$ -distributions of the two models are quite different (30% discrepancy). Flatt (1993-1996) believes that this fact was known to some of the workers who have used the isothermal model, but they pretended not to be aware of it. He states that the coincidence explained above comes from the fact that the isothermal flow model leads to almost equal but opposite relative errors in density and velocity, such that their product,  $\rho u$  ( $=m/A$ ) is nearly correct. Flatt (1993-1996) demonstrates analytically that the use of this assumption for gas pipeline rupture problems, is in fact a violation of the second law of thermodynamics.

In his model for unsteady compressible flow following a rupture in a long pipeline, Flatt (1986) used both assumptions of isothermal and adiabatic flow. Admitting that both assumptions are extremely idealised, reality being somewhere in between, he applied the isothermal assumption on the initial conditions and adiabatic flow for the time thereafter. His justification was that the isothermal assumption is not valid if important changes in the thermodynamic state of the particle occur over short distances as is the case near the broken end of a pipeline. Before the rupture, the flow is slow and the time a particle takes to move along the whole pipeline is long. The isothermal flow approximation for the initial condition therefore appears very reasonable. The sudden introduction of the adiabatic hypothesis has almost no effect on that part of the pipeline situated between the upstream end of the pipe and the location of the wave front. This hypothesis is confirmed by experimental results and thermodynamically using the Mollier-entropy diagram for a steady adiabatic pipe flow of a perfect gas with low Mach number. The hypothesis of adiabatic flow, especially near the broken end where particles are accelerated relatively rapidly and over a short distance was considered closer to reality than the hypothesis of isothermal flow. He recommended that for long time intervals the heat transferred into the pipeline should be accounted for though admitting that this would considerably complicate the analysis.

In their similar model Van Deen and Reintsema (1983) started by admitting that since the thermal contact between the pipe and its surroundings is generally difficult to estimate, or is even completely unknown, it is difficult to give a reliable estimate of the heat transfer into the pipe. However, they avoided the problem of estimating the heat transfer by assuming that the temperature and pressure changes during the transient phenomenon could be described by a linear relationship;

$$\nabla T = b \cdot \nabla p \quad (2.53)$$

where  $b$  is a constant to be determined. This representation is more general than the common practice of assuming either isothermal or isentropic flow. Equation (2.53) was substituted into the energy equation and after elimination of  $\Omega + \omega u$  an equation without the unknown  $b$  was obtained. In this study, a non-isothermal non-adiabatic heat transfer model is used.



### 2.6.3 CALCULATION OF HEAT TRANSFER

For fluid flows at high velocities, the velocity of flow varies from zero at the pipe wall to the free stream velocity outside the boundary layer. This velocity distribution, which is shown in Fig. 2.6, sets up viscous stresses which do shearing work on the fluid particles. The work in turn increases the internal energy as well as the temperature of the particles. The resulting temperature gradient causes heat to be transferred through the fluid from the region near the wall to the main body of the fluid, in order to transport the energy dissipated by the shear work.

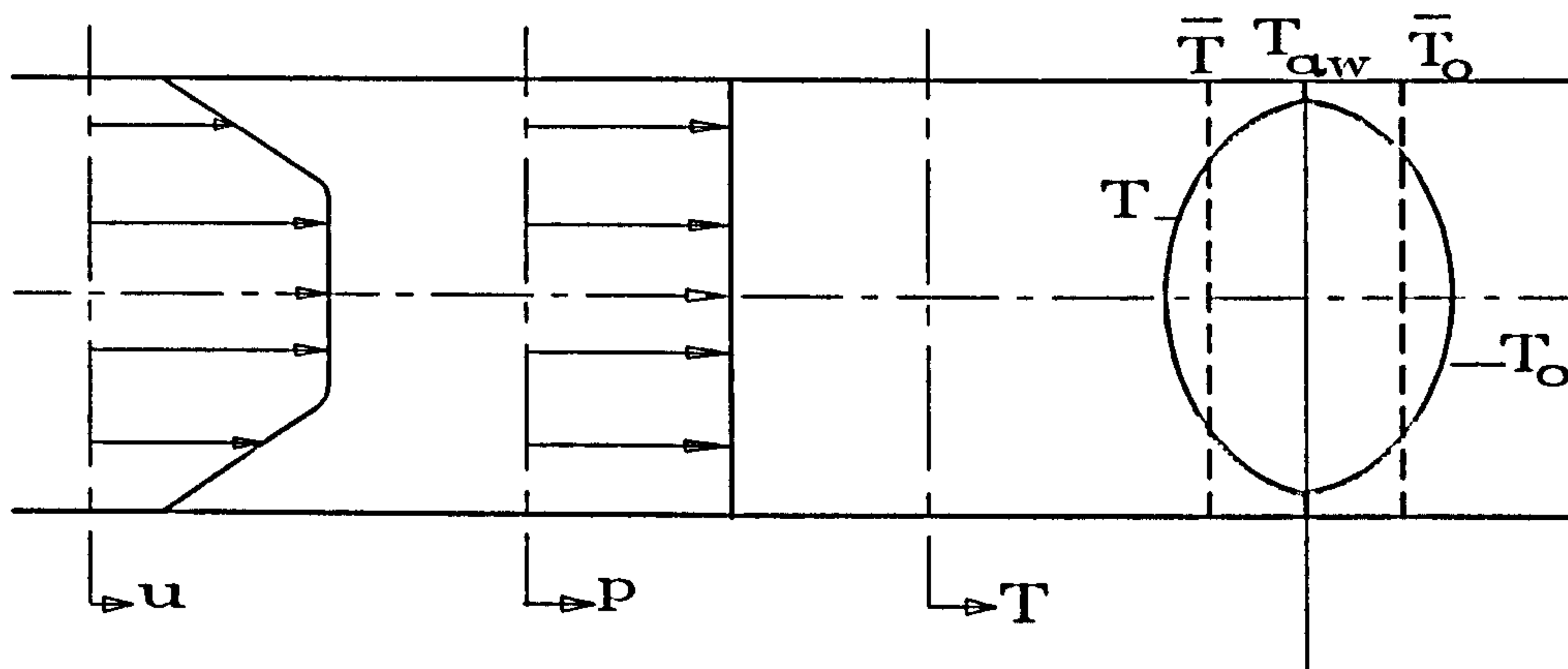


Fig. 2.6 Distribution of Pressure, Temperature and Flow Velocity Along the Pipe Diameter

Two different approaches to calculation of heat transfer to the gas were considered in this study. In the first approach, one of the relationships between the dimensionless numbers, namely  $Re$ ,  $Pr$ ,  $Nu$  and  $St$  is used to calculate the convective heat transfer coefficient across the boundary layer. In the second approach the adiabatic wall temperature and recovery factor are used to calculate the heat transfer. The difference between the two approaches is only the way in which the heat transfer between the fluid and the inner wall of the pipe is calculated. For the rest of the system, the analysis is the same for both approaches. The two alternatives for calculating the heat transfer to the fluid are described in the remaining part of this section:

#### (a) Heat Transfer Calculation by Using Adiabatic Wall Temperature and Recovery Factor

After the effects of viscous shearing work and heat conduction within the boundary layer have been brought to a balance everywhere in the fluid, the pipe wall is at an equilibrium temperature ( $T_{aw}$ ). The temperature distribution in the boundary layer is as shown in

Fig.2.6. The temperature difference responsible for the heat transfer from the pipe wall into the fluid is related to the adiabatic wall temperature and an empirical value,  $R_c$ , known as the recovery factor. The recovery factor is related to the adiabatic wall temperature by the following relationship:

$$R_c = \frac{T_{aw} - \bar{T}}{\bar{T}_o - \bar{T}} \quad (2.54)$$

where  $\bar{T}$  and  $\bar{T}_o$  are average free stream static and stagnation temperatures respectively, as shown in Fig. 2.6.  $T_o$  is calculated by equation (2.75). Shapiro (1953) pointed out that various experiments had yielded values of recovery factor for subsonic pipe flow between 0.87 and 0.91; and for supersonic pipe flow between 0.83 and 0.90.

From equations (2.54) and (2.75):

$$T_{aw} = \bar{T} + R_c \left( \frac{u^2}{2C_p} \right) \quad (2.55)$$

The heat transfer through the pipe wall and from the outside pipe wall to the surrounding atmosphere is given by the equation:

$$\Omega = U_{pw} (T_{wo} - T_{aw}) = U_o (T_A - T_{wo}) \quad (2.56)$$

The overall heat transfer coefficient across the pipe wall is given by the equation:

$$U_{pw} = \frac{k_p}{\ln \left( 1 + \frac{2c}{d} \right)} \quad (2.57)$$

The overall heat transfer coefficient from the outer pipe wall to the surrounding atmosphere is calculated in either of two ways, depending on whether the pipe is exposed to the atmosphere or buried in a medium other than air at atmospheric conditions. In most cases, pipes would be buried in either the ground (for onshore pipelines) or water (for offshore pipelines). The overall heat transfer coefficient outside a buried pipe is given by the equation:

$$U_o = \frac{k_m}{\ln \left( 1 + \frac{2D}{d + 2c} \right)} \quad (2.58)$$

and that for pipes exposed to the atmosphere is given by the equation:



$$U_o = \left( \frac{d}{2} + c \right) h_{CA} \quad (2.59)$$

In equation (2.58) above, it is assumed that heat transfer is uniform in all radial directions of the pipe. For natural convection in air at atmospheric pressure,  $h_{CA}$  is calculated using the following simplified expression:

$$h_{CA} = B \left( \frac{\Delta T}{L} \right)^C \quad (2.60)$$

where B and C are constants depending on the geometry and L is the significant length, also a function of geometry and flow.  $\Delta T$  is the temperature difference between the surface and the bulk air in K.

McAdams suggested values for horizontal cylinders as shown in Table 2.1 below. The values of  $h_{CA}$  calculated from these coefficients have the dimensions of W/m<sup>2</sup>. The constant numbers Pr and Gr are calculated using equations (A-12) and (A-14) respectively. For most cases of high-pressure gas flow in pipes, the product GrPr lies between 10<sup>3</sup> and 10<sup>9</sup>. The first row of Table 2.1 is used, resulting into the following equation for  $h_{CA}$ :

$$h_{CA} = 1.32 \left( \frac{T_A - T_{wo}}{d} \right)^{\frac{1}{4}} \quad (2.61)$$

GrPr	B	C	L
10 <sup>3</sup> <GrPr<10 <sup>9</sup>	1.32	1/4	Diameter
10 <sup>9</sup> <GrPr<10 <sup>12</sup>	1.24	1/3	1

Table 2.1 McAdams Constants for Natural Convection to Air

The value of  $T_{wo}$  is calculated from equation (2.56) as follows:

$$T_{wo} = \frac{U_{pw} T_{aw} + U_o T_A}{U_{pw} + U_o} \quad (2.62)$$

An approximated value of  $T_{wo}$  is used in equation (2.61) to calculate the value of  $h_{CA}$ . In this study, the value of  $T_{wo}$  at the previous grid point is used. However, if a higher degree of accuracy is required, an iteration procedure could be used. The value of  $\Omega$  is calculated using equation (2.56), after the above calculations. The radial temperature distribution over a section of the pipe and its surroundings is shown in Fig. 2.7.

**(b) Heat Transfer Calculation by Using Overall Heat Transfer Coefficient Across the Boundary Layer**

Two relationships are commonly used to calculate the overall heat transfer coefficient across the boundary layer, namely the Colburn equation and the Dittus-Boelter equation (1930). The Colburn equation is as follows:

$$St = 0.023 Re^{-0.2} Pr^{-2/3} \quad (2.63)$$

where  $St$  is evaluated at the average mean fluid temperature,  $Re$  and  $Pr$  are evaluated at the average film temperature,  $Re > 10^4$ ,  $0.7 < Pr < 160$ , and  $L/d > 60$ . The Dittus-Boelter equation (1930) is as follows:

$$Nu = 0.023 Re^{0.8} Pr^n \quad (2.64)$$

where  $n = 0.3$  if the fluid is being cooled

$n = 0.4$  if the fluid is being heated

All the fluid properties are evaluated at the average mean fluid temperature.

$Re > 10^4$ ,  $0.7 < Pr < 100$ , and  $L/d > 60$

Depending on whether equation (2.63) or (2.64) is used, equation (A-7) or (A-13) respectively, are used to calculate the convective heat transfer coefficient across the boundary layer ( $h_{BL}$ ). The overall heat transfer coefficient across the boundary layer is given by the equation:

$$U_{BL} = \frac{d}{2} h_{BL} \quad (2.65)$$

Equation (2.64) is not suitable for transient analysis of linebreak in high-pressure gas pipelines because both cases of fluid being heated and being cooled occur during the transient event. This would require changing the value of  $n$  during the analysis, which makes the procedure more complicated. The other overall heat transfer coefficients i.e.  $U_{pw}$  and  $U_o$  are calculated in the same way as shown in section (a). Referring to Fig.2.7, the heat transfer into the gas is given by the equation:

$$\Omega = U_{BL}(T_{wi} - T) = U_{PW}(T_{wo} - T_{wi}) = U_o(T_A - T_{wo}) \quad (2.66)$$

Equation (2.66) is solved simultaneously for the values of either  $T_{wi}$  and/or  $T_{wo}$ . The values obtained are substituted into equation (2.66) together with the values of respective overall heat transfer coefficients calculated earlier, to obtain  $\Omega$ . From equation (2.66);

$$\begin{aligned} U_{BL}(T_{wi} - T) &= U_{PW}(T_{wo} - T_{wi}) \\ (U_{BL} + U_{PW})T_{wi} - U_{PW}T_{wo} - U_{BL}T &= 0 \end{aligned} \quad (2.67)$$

and



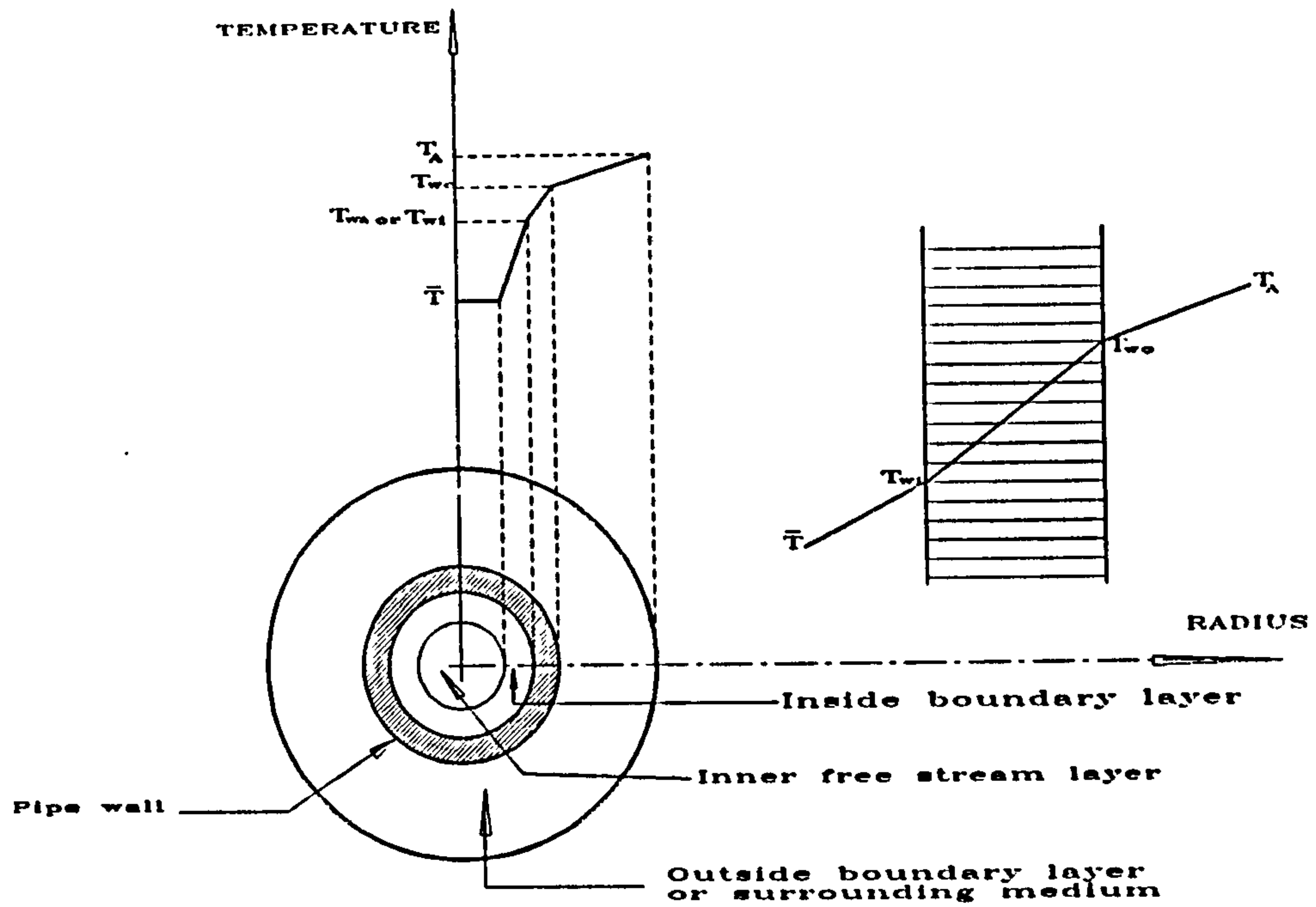


Fig. 2.7 Radial Temperature Distribution Across a Pipe Section and its Surroundings

$$\begin{aligned}
 U_{PW}(T_{wo} - T_{wi}) &= U_o(T_A - T_{wo}) \\
 - U_{PW} T_{wi} + (U_{PW} + U_o)T_{wo} - U_o T_A &= 0
 \end{aligned} \tag{2.68}$$

Multiplying equation (2.67) by  $(U_{PW} + U_o)$  and equation (2.68) by  $U_{PW}$  we get:

$$(U_{PW} + U_o)(U_{BL} + U_{PW})T_{wi} - (U_{PW} + U_o)U_{PW}T_{wo} = (U_{PW} + U_o)U_{BL}T \tag{2.69}$$

$$- (U_{PW})^2 T_{wi} + U_{PW}(U_{PW} + U_o)T_{wo} = U_{PW}U_o T_A \tag{2.70}$$

Adding equation (2.70) to (2.69) we get:

$$T_{wi}[(U_{PW} + U_o)(U_{BL} + U_{PW}) - (U_{PW})^2] = (U_{PW} + U_o)U_{BL}T + U_{PW}U_o T_A$$

$$T_{wi} = \frac{(U_{PW} + U_o)U_{BL}T + U_{PW}U_o T_A}{(U_{PW} + U_o)(U_{BL} + U_{PW}) - U_{PW}^2} \tag{2.71}$$

From equation (2.67)

$$T_{wo} = \frac{(U_{BL} + U_{PW})T_{wi} - U_{BL}T}{U_{PW}} \tag{2.72}$$

Tiley (1989) used a simplified approach of estimating the heat transfer into the pipe. She argued that unless the pipe is lagged, it can be assumed that the higher conductivity of the pipe results in a negligible temperature difference between the internal and external pipe

walls. Therefore the heat transfer may be estimated by the temperature difference between the mean wall temperature and the gas temperature and using the Stanton number method for a circular cross-section pipe;

$$\dot{Q} = \pi d \rho u C_p St(T_w - T) \quad (2.73)$$

The problem now remained to evaluate the Stanton number. Tiley (1989) considered two methods, either using the boundary layer theory or using a function of the Reynolds and Prandtl numbers. She argued that since the heat transfer term in the basic equations is comparatively small and since variation in Stanton number with flow rate are not sufficient to warrant additional computation involved, a constant value Stanton number was used, with provision for "tuning" each situation encountered. In this study, the heat transfer is calculated using the adiabatic wall temperature and recovery factor method described in (a).

## 2.7 OTHER APPROACHES TO THE BASIC EQUATIONS

A new approach to the basic equations of flow has been proposed by Flatt and Trichet (1995). The method is called the gamdeleps method and it utilises the fluid stagnation properties. Stagnation properties are defined as the properties resulting when a fluid is decelerated to zero velocity in a steady flow adiabatic process with no work interaction occurring and also gravitational, magnetic, electric and capillary effects absent. In this report, the stagnation properties will be denoted by a subscript o. According to the first law of thermodynamics, stagnation enthalpy is given by the equation:

$$h_o = h + \frac{u^2}{2} \quad (2.74)$$

For a perfect gas, stagnation temperature is given by the equation:

$$T_o = T + \frac{u^2}{2C_p} \quad (2.75)$$

The stagnation pressure for a compressible fluid flow is:

$$p_o = p \left( \frac{T_o}{T} \right)^{\frac{\gamma}{\gamma-1}} \quad (2.76)$$



The two non-dimensional coefficients  $\gamma$  and  $\delta$  described in Sections 2.3 and 2.4.5 in relation to the gamma delta method developed by Flatt (1993) have been used by Flatt and Trichet (1995), together with a third non-dimensional coefficient  $\epsilon$ , to calculate the stagnation properties for the gaseous, liquid and the two-phase regions of a pure real fluid. The coefficient  $\epsilon$  is calculated using the equation:

$$\epsilon = \gamma + \frac{\rho}{\gamma} \left( \frac{\partial \gamma}{\partial \rho} \right)_s \quad (2.77)$$

This third coefficient  $\epsilon$  enables description of an infinitesimal isentropic process in terms of the Mach number. The three coefficients  $\gamma$ ,  $\delta$  and  $\epsilon$  describe infinitesimal processes in a thermodynamically rigorous manner and are valid for the gaseous, liquid and two-phase regions of a pure real fluid. They were used in a new method named gamdeleps method by Flatt and Trichet (1995), who also used them to describe the relationships between stagnation and static properties of real gases. The relationships are as follows:

$$T_o = T \left[ 1 + \left( \frac{\bar{\epsilon} - 1}{2} \right) M_a^2 \right]^{\frac{\bar{\delta}-1}{\bar{\epsilon}-1}} \quad (2.78)$$

$$\rho_o = \rho \left[ 1 + \left( \frac{\bar{\epsilon} - 1}{2} \right) M_a^2 \right]^{\frac{1}{\bar{\epsilon}-1}} \quad (2.79)$$

$$p_o = p \left[ 1 + \left( \frac{\bar{\epsilon} - 1}{2} \right) M_a^2 \right]^{\frac{\bar{\gamma}}{\bar{\epsilon}-1}} \quad (2.80)$$

$$Z_o = Z \left[ 1 + \left( \frac{\bar{\epsilon} - 1}{2} \right) M_a^2 \right]^{\frac{\bar{\gamma} - \bar{\delta}}{\bar{\epsilon}-1}} \quad (2.81)$$

$$a_o = a \left[ 1 + \left( \frac{\bar{\epsilon} - 1}{2} \right) M_a^2 \right]^{\frac{1}{2}} \quad (2.82)$$

The sign (  $\bar{\phantom{x}}$  ) on top of the dimensionless coefficients denote the arithmetic averages of the values between the two states.

Stagnation properties provide a convenient reference state in studying properties of a flowing fluid. Flatt (1993-1996) suggests that the use of stagnation properties in the equations of conservation for unsteady flow of fluids in pipes avoids many difficulties due to mathematical singularities at the choked end, which are often encountered when static quantities are used. The proposed procedure, which is not yet known to have been used, involves writing the conservation equations in the classical form with static quantities and then substituting stagnation variables for the static ones.

The gamdeleps method enables computer codes to be written without the necessity of distinguishing between the types of phase the fluid is in. This is especially relevant to the study of linebreak in high-pressure gas pipelines where gas/liquid mixtures are anticipated and the location of the beginning or end of vaporisation region varies with time. A computer code written for any real gas can be used for a perfect gas by setting  $\gamma=\delta=\epsilon=K$ . Neither the gamdeleps method nor the stagnation properties have been used in this study. The stagnation properties were not used, as suggested by Flatt (1993-96) because the numerical algorithm did not suffer the singularity problems such as those experienced by Flatt (1986). However, the use of the gamdeleps method is recommended as the next stage of this study. The gamma delta method which has been used in this model is applicable only for gas or liquid or homogeneous liquid/gas mixture phases.



## **CHAPTER 3**

# **METHODS FOR SOLUTION OF THE BASIC EQUATIONS**

### **3.1 INTRODUCTION**

Unsteady flow of fluids in pipelines can adequately be represented by a system of partial differential equations, of first or second order depending on the type of problem, as discussed in Chapter 2. Such systems may either be parabolic or hyperbolic. Methods for solving these equations can quite generally be classified as either analytical or numerical. Analytical methods of solution are very laborious as regards computation and therefore are unsuitable for solving problems of this nature, where the equations are rather complex. Analytical or exact solution is available only for greatly simplified equations and situations and it is very laborious as regards computation. It offers the basis for verifying the accuracy of numerical techniques. As a result of these limitations, the analytical method of solution is not feasible normally for analysis of transient flow conditions in pipe systems. Many numerical methods are available and have been used for the solution of these equations.

Apart from the numerical method to be selected, the analyst is faced with a choice of whether to use a distributed or lumped parameter approach. In the lumped parameter approach, the inertia of the fluid in a particular pipe is treated as a lump as opposed to continuously distributed in the former approach. Distributed parameter modelling requires a relatively complex analytical model and may involve a large number of calculation necessary for fast transients occurring in a time scale which is short compared to system characteristic time. Lumped parameter modelling utilises a much simpler analytical model and requires far fewer calculations. It saves much time and effort and it provides reliable solutions for large complex networks. The time interval must be chosen small enough to account for pressure waves traversing the shortest pipe section in the network, therefore requiring carrying out frequent calculations.

In this chapter, the most commonly used numerical methods are described together with their comparative advantages and drawbacks in various fluid transient phenomena. The methods are the method of characteristics, finite-difference methods, finite-element methods, flux-difference splitting schemes, the method of lines and the wave-plan method. More than three dozen studies, which have used one or the other of the

above methods of solution are summarised and discussed, with the objective of leading to the selection of a method to be used for modelling of high-pressure gas pipe rupture.

## **3.2 NUMERICAL METHODS OF SOLUTION**

### **3.2.1 FINITE-DIFFERENCE METHODS**

#### **3.2.1.1 General Description**

Generally, the basis of finite-difference formulations is that the differentials of the dependent variables appearing in the partial differential equations, are expressed in approximate expressions so that a digital computer which performs only standard arithmetic and logical operations can be employed to obtain a solution. Two methods which are used for approximating the differentials are the Taylor series expansion and the use of polynomials. The approximations of the derivatives may be expressed as either forward, backward or central differences; first-, second-order accurate and so on.

The finite-difference approximations are used to replace the derivatives that appear in the partial differential equations. Finite-difference formulation of the partial differential equations can be done in two ways, namely, explicit and implicit formulations. Finite-difference methods are therefore categorised in the two types mentioned above. Among the other categories of numerical methods, which have been covered separately in this chapter, there are some which are based on finite-difference formulation. These are the method of characteristics, the flux-difference splitting schemes, the method of lines and the wave-plan method. The above methods are covered separately in Sections 3.2.1.3, 3.2.3, 3.2.5 and 3.2.5 respectively. This section therefore, deals with formulations that are entirely based on the explicit and/or implicit finite-difference formulations.

Solution procedures based on the explicit and implicit formulations are different. In the explicit formulation, all unknowns can be solved for directly at each grid point. In the implicit formulation, more than one unknown exists and therefore the finite-difference equations must be written for all spatial grid points, at a given time level, to provide the same number of equations as there are unknowns and which are solved simultaneously. Obviously, the solution of explicit equations is simpler than the implicit equations. However, implicit formulations are more stable than explicit formulations. This review focuses on the explicit and implicit finite-difference methods that are relevant to the solution



of unsteady flow of gas in pipelines. Detailed description of the equations used in conjunction with the Lax-Wendroff second-order two-step method is given in Section 3.2.1.4. The MacCormack second-order method and the Warming-Kutler-Lomax third-order methods are described in detail in Sections 4.3.2 and 4.3.3 respectively.

### **3.2.1.2 Explicit Finite-Difference Methods**

Explicit finite-difference methods integrate the basic partial differential equations by considering the changes in the dependent variables along the direction of the independent variables, producing the solution values at evenly spaced points in the physical plane. The method is classified as explicit because the value of the dependent variable at one particular time level, is calculated directly from values of the dependent variable at previous time levels. Many different explicit finite-difference methods, ranging from single-step first-order accurate to four-step fourth-order accurate schemes, have been developed for the fluid transient equations. Some of the popular methods are listed below:

- (i) Forward Euler Method
- (ii) Method of Lax
- (iii) Lax-Wendroff Single-Step Method
- (iv) Lax-Wendroff Two-Step Method
- (v) Alternating Gradient Method
- (vi) MacCormack Method
- (vi) Rusanov-Burstein-Mirin Method
- (vii) Abarbanel-Gottlieb-Turkel Method
- (viii) Hopscotch Method
- (ix) Leap Frog Method
- (x) Pseudoviscosity Method
- (xi) Warming-Kutler-Lomax Third-Order Method

Explicit finite-difference methods also have their advantages and disadvantages. The major advantage of explicit finite-difference methods especially in comparison with the method of characteristics is that they are very simple to programme. The conservative law form of the hyperbolic equations has the favourable property that conservative finite-difference methods applied to it produce solutions automatically satisfying the Rankine-Hugoniot relations across a shock, which greatly facilitates accurate shock

calculation. No special care need to be taken of the location of shocks, therefore it is suitable for systems in which shocks form. There are no eigenvectors to be computed. Eigenvectors are needed solely for testing stability conditions. There are no linear or non-linear equations to be solved. Explicit finite-difference methods need comparatively little computer memory space since they solve the equations directly rather than simultaneously. The majority of finite-difference methods (including implicit) models neglect the term  $u\partial u/\partial x$  as in the method of characteristics but some also neglect the term  $\partial(\rho u)/\partial t$  to get a creeping flow model. Second-order of accuracy is normally regarded as sufficient for the analysis of gas transients. Finite-difference methods produce solution values at evenly spaced points in the physical plane. One of the major disadvantages of finite-difference methods, other than the method of characteristics, is that continuous initial data may propagate along the characteristics thus making it difficult to handle. Explicit methods suffer from stability problems since they are only conditionally stable. Time steps are restricted by a stability criterion, which result in a large amount of computer time being required. They are therefore not suitable for analysis of large systems or unsteady flows over long periods of time. In the presence of shocks, methods of higher than first-order produce considerable overshoot and oscillatory systems. A smoothing parameter for overshoot can tend to smooth out the transient peaks. Unlike the method of characteristics, finite-difference methods are unable to solve the boundary conditions naturally.

The MacCormack Method is superior to the method of characteristics when Courant number ( $C_n$ ) differs from unity appreciably. It is inherently dissipative i.e. because it is second-order accurate in both space and time, no special shock capturing approach is needed. It is unconditionally stable if  $C_n$  is less than unity and it produces minimal precision loss when  $C_n$  moves away from unity. The method permits the use of a grid spacing that is not overly fine even in highly complex cases. As the method is quite efficient, overall computation effort remains reasonable. The MacCormack method could be very well suited for applications of increasing complexity such as two-phase, gas-liquid flow problems and multi-dimensional flow. It is simple and has low development cost. The complete equations can be used without making any simplification.

The pseudoviscosity method has a relatively good accuracy. It is stable and more suitable for the Lagrangian formulation. Any shock front that occurs in the flow is spread over more than one finite-difference mesh length and the dependent variables; i.e. pressure, velocity, density, internal energy, entropy, etc. are continuous throughout a shock front;



thus eliminating the need for shock fitting. It produces no overshoot in pressure and is more versatile i.e. can be used for variable cross-sectional area ducts.

The Warming-Kutler-Lomax method is third-order accurate both in space and time. It is a simple extension of the second-order schemes. The diffusive and dispersive errors are easily controlled by selecting appropriate numerical parameters. It captures shock without any special treatment.

### **3.2.1.3 Method of Characteristics**

The method of characteristics is the natural numerical method for quasi-linear hyperbolic systems in two independent variables. By an appropriate choice of coordinates, paths can be defined in the  $x$ - $t$  plane, called characteristic lines, along which the system of partial differential equations is converted into a system of ordinary differential equations that may be solved by standard single step finite-difference methods for ordinary differential equations. The basic rationale underlying the use of characteristics is that by an appropriate choice of coordinates, the original system of hyperbolic equations can be replaced by a system whose coordinates are the characteristics. The use of this method becomes particularly simple when applied to two equations in two dependent variables. When the characteristic coordinates are used in this way, the method is known as the natural method of characteristics.

One of the major drawbacks of the method of characteristics is that if the dependent variables are required at fixed time intervals, a two-dimensional interpolation in the characteristic net is required and this may be quite complicated. This drawback has been overcome by the mesh method of characteristics called the method of specified time intervals, which solves the characteristic equations on values for the dependent variables at specified time-distance coordinates. With the mesh points defined in advance, and the interpolation taking place as computation advances, it becomes a one-dimensional interpolation. Although the method of characteristics is most ideal for the solution of quasi-linear hyperbolic equations with two dependent variables on characteristics, which is the natural coordinate system, a great deal of effort has been made to extend the method to other more complicated cases. However, this is at the expense of simplicity and accuracy. The above effort includes the extension for calculating three dependent variables encountered in transient non-isothermal gas flow. Also several methods have been

developed to increase accuracy of solution in these complicated cases. A detailed description of the procedure and derivation of equations used in method of characteristics solutions is given in Section 4.3.1.

The method of characteristics has many advantages compared with the other numerical methods of solution. In the method of characteristics solution, discontinuities in the initial value may propagate along the characteristics, making it easy to handle them. Large time steps are possible in the natural method, since they are not restricted by a stability criterion. The boundary conditions are also properly posed. The method of characteristics is relatively accurate, but requires one to understand how it operates and to choose a suitable time step. The method can be readily adapted to solve for three dependent variables required for the analysis of non-isothermal transient gas flow. It is time consuming to programme on a computer. Discontinuous initial data and shock waves do not lead to solution with overshoot and details are not smeared, in the natural method. Exact solution is possible in the constant coefficient case with two dependent variables regardless of eventual discontinuities in the initial data, in the case of the natural method. No attention needs to be paid to the position of the shocks, in the hybrid method and in general it causes only a small overshoot. The hybrid method is easily generalised to more than two dependent variables. The natural method is unconditionally stable. The method of characteristics also has some disadvantages. If more than two dependent variables are required to describe the system in the natural method, then the complexity increases. If the solution of dependent variables in the natural method is required at fixed time intervals, then two-dimensional interpolation in the characteristic net is required, and this can be very complicated. The hybrid method is comparatively slow because the time steps are restricted by a stability criterion. If calculation is to be performed in terms of an arbitrary set of dependent variables, eigenvalues and eigenvectors are needed at each node (easy with Riemann type variables). Difficulties arise with curved characteristics, because it requires solving for different levels of time at each step, which is tedious and time consuming and increases the complexity. The hybrid method is difficult to apply to networks because of the restriction by the stability criterion i.e.  $\Delta x \geq a \times \Delta t$  (the hybrid method is conditionally stable). If more than two dependent variables are required to describe the system, then the complexity of the computation increases and hence computing costs and time become considerably high. In order to simplify the computation, part of the momentum equation i.e. the term  $u \partial u / \partial x$  in equation 2.7 is neglected and thus yielding straight characteristics.



### 3.2.1.4 Lax-Wendroff Second-Order Two-Step Method

Referring to the finite-difference grid in (Fig. 3.1) and Equation (4.73), the two-step second-order Lax-Wendroff approximation [as developed by Lax and Wendroff (1960)] may be written as follows:

First Step:

$$A_{(i+\frac{1}{2}, j+\frac{1}{2})} = \frac{1}{2}[A_{(i,j)} + A_{(i+1,j)}] - \frac{1}{2} \frac{\Delta t}{\Delta x} [B_{(i,j)} - B_{(i+1,j)}] + \frac{1}{2} \Delta t [C_{(i,j)} + C_{(i+1,j)}] + O(\Delta x^2, \Delta t) \quad (3.1)$$

Second Step:

$$A_{(i,j+1)} = A_{(i,j)} - \frac{\Delta t}{\Delta x} [B_{(i+\frac{1}{2}, j+\frac{1}{2})} - B_{(i-\frac{1}{2}, j+\frac{1}{2})}] + \Delta t [C_{(i+\frac{1}{2}, j+\frac{1}{2})} + C_{(i-\frac{1}{2}, j+\frac{1}{2})}] + O(\Delta x^2, \Delta t^2) \quad (3.2)$$

where  $O(\Delta x^2, \Delta t^2)$  is the truncation or rounding error.

A close examination of Equations (3.1) and (3.2), reveals that the values at all the points at time level  $t = i+\frac{1}{2}$  can be found in the first step. These values are then used in the second step to derive the values at time level  $t = j+1$ . This is illustrated in Fig. 3.1.

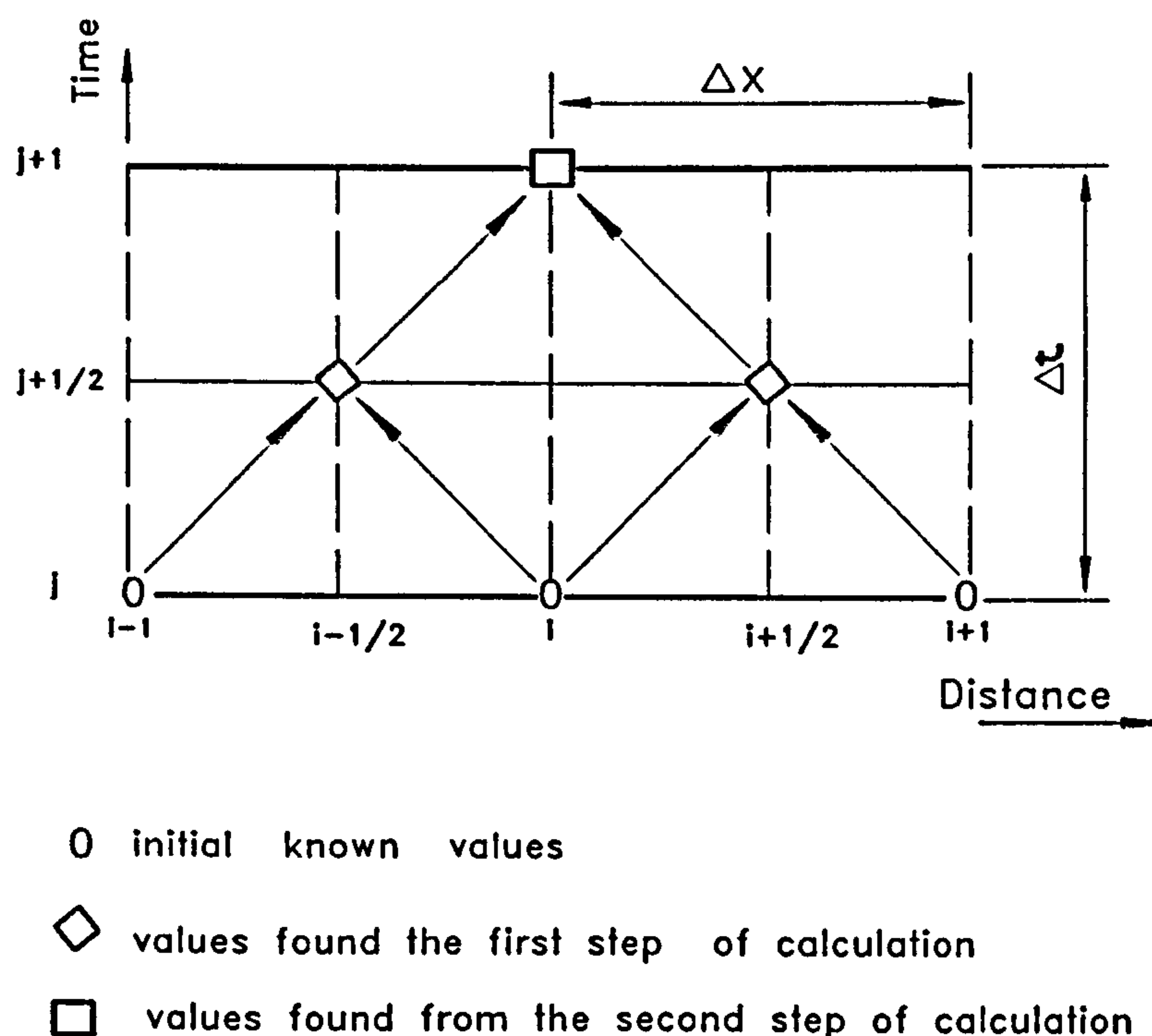


Fig. 3.1 Finite-Difference Grid Illustrating the Two-step Lax-Wendroff Method

The Lax-Wendroff method produces slight overshoot at discontinuities and shocks. It is most suitable for dealing with systems in which shock waves form. With this method, it is easy to deal with the energy equation. It has a relatively good accuracy and it is stable.

It is especially effective for the Eulerian formulation. Any shock front that occurs in the flow is spread over more than one finite-difference mesh length and the dependent variables i.e. pressure, velocity, density, internal energy, entropy etc. are continuous throughout a shock front; thus eliminating the need for shock fitting. The method yields an overshoot in pressure at the shock front, thus reducing accuracy in determining peak pressure.

### **3.2.1.5 Implicit Finite-Difference Methods**

In implicit methods the finite-difference equation contains, at a particular time level, dependent variable which can not all be calculated explicitly from the previous level. Many numerical methods based on this principle have been developed and used for the solution of various engineering problems. Those which have been popular for the solution of the partial differential equations describing unsteady fluid flow in pipelines include the following:

- (i) Fully Implicit Method
- (ii) Crank-Nicolson Method
- (iii) Centred Difference Method
- (iv) Characteristic Finite-Difference Method
- (v) Explicit-Implicit Methods
- (vi) Guy Method
- (vii) Gear Method
- (viii) Backward Euler Method
- (ix) Beam-Warming Method

The major difference between explicit and implicit finite-difference methods is that implicit methods are unconditionally stable. The restriction on time step, which is experienced with other methods is overcome, i.e. no restriction on the maximum allowable time step. The maximum practical time step is limited by the rate of change of the variable imposed at the boundary conditions rather than by limitation required by a stability criterion. In case of rapid transients, where small time-steps and large number of sections are required, the method loses the advantage of fast computation. The major weakness of implicit finite-difference methods is that they can yield unsatisfactory results for rapid transients. They are suitable for the analysis of slow transients on relatively large



networks. Some methods have been known to produce erratic results during the imposition of some types of boundary conditions. Computer programmes based on these methods do not allow easy extension. The methods require the solution of non-linear simultaneous equations usually by Newton-Raphson linearisation at each time step; for complicated gas networks the matrix becomes quite large, the computer storage requirements become very large and the solution time can be excessive. These drawbacks have been minimised by the use of a sparse matrix procedure.

The fully implicit method does not suffer from spurious oscillations but does not have as high asymptotic accuracy as  $\Delta t \rightarrow 0$ , as the Crank-Nicolson method. Though the fully implicit method involves solution of simultaneous non-linear equations, usually by the Newton Raphson method, the jacobians are sparse and therefore full advantage of this is taken in solving the large set of equations economically. Stability of the method depends on convergence tolerance. Rapid transient phenomena such as pulsation is filtered in case of large time-step adopted.

The Crank-Nicolson method has a high-order of accuracy. For sudden changes in the forcing function, the solution is prone to oscillation about the true solution. The method involves the solution of simultaneous non-linear equations, usually by the Newton-Raphson method. It is relatively simple, easier to programme and readily extended to pipeline networks of any size. Consequently, computation is much faster. The centred-difference method requires a large amount of computer storage and lengthy execution times. It has the advantage of using a sparse matrix method. The Beam-Warming method is second-order accurate in space and time. It introduces negligible diffusive errors and captures shock without special treatment.

### **3.2.2 FINITE-ELEMENT METHODS**

The finite-element method is believed to be one of the oldest. It was used by Babylonians to evaluate numbers between those given in tables and by early oriental mathematicians in the approximation of the circumference of a circle. Solving an engineering problem by the finite-element approach involves the following steps:

- (a) Formulation of governing equations and boundary conditions
- (b) Division of the analysis region into finite elements
- (c) Selection of interpolation functions

- (d) Determination of element properties
- (e) Assembling of global equations
- (f) Solution of global equations
- (g) Verification of solution

The finite-element method consists primarily of replacing a set of differential equations in terms of unknown variables with an equivalent but approximate set of algebraic equations where each of the unknown variables is evaluated at a nodal point. Several different approaches may be used in the evaluation of these algebraic equations, and finite-element methods are often classified according to the method used. In order to arrive at a proper method for a particular problem, it may be necessary to examine several methods. The three most common methods of formulation of finite-difference equations are direct methods, variational methods and residual methods.

Division of the solution region into elements can take the form of either one-, two- or three-dimensional elements of varying shapes. There is usually not a single correct way of dividing a particular solution region with all the others being wrong. Decisions on how to divide up the solution region into elements is based on engineering judgment and there are no definitive guidelines available. Depending on the positioning of nodes in the element and whether the sides of the element are straight or curved, finite elements are generally classified as simplex or higher order elements. Regardless of the geometrical shape, finite elements are categorised as either Lagrangian or Hermite elements. In contrast to the Lagrange family of elements, the Hermite category includes derivatives of the variables as well as values defined at the nodes. The theoretical basis of the finite-element methods has been covered extensively by Allaire (1985). Finite-element methods have not been used for gas transients as widely as the finite-difference based methods and thus there are not many of these methods known.

Until recent years, only two methods namely the Galerkin Method, used by Rachford and Dupont (1974), and more recently by Osiadacz and Yedroudj (1989) and Kiuchi (1987); and the moving finite-element method, have been used. Bisgaard, Sørensen and Spangenberg (1987) developed a weighted residual finite-element method which uses the Galerkin finite-element method to discretize the equation. The most popular finite-element methods for fluid transients are therefore the following:

- (i) Galerkin Method
- (ii) Spectral Galerkin Method



- (iii) Spectral Collocation Method
- (iv) Moving Finite-Element Method
- (v) Method of Bisgaard-Sørensen-Spangenberg

Finite-element methods have some advantages over finite-difference methods. The former methods can be used to solve virtually any engineering problem for which a differential equation can be written. They have a higher accuracy because cubic hermite splines which should give errors which are of  $O(h^4)$  could be used. However, this accuracy cannot always be usefully realised due to the geographical nature of networks. Finite element methods are most useful for two and three-dimensional problems. Variational methods are easy to extend to two and three-dimensional problems. Residual methods can be applied to any problem for which a governing boundary value problem can be written. For the case of residual methods, once techniques are learnt, the details are relatively straight forward. The major disadvantage of finite-element methods is that they are somewhat complex, with complexity being proportional to the complexity of the differential equations for that particular problem. Direct methods are difficult to apply to two and three-dimensional problems. Variational methods lack a functional for certain classes of problems, for example those dealing with the flow of viscous fluid. It is difficult to find variational methods for some problems, even though they exist. The procedure for finite-element solution is rather lengthy and not widely used in gas network simulation. When the solution possesses discontinuities, higher-order methods may not always give more accurate solutions.

The Galerkin method requires a lengthy execution time. It is formulated to treat slow transients. Computer resources required are small enough and it has some significant theoretical advantages. In using the moving finite-element method, care needed in treatment of boundary conditions. The method is very complicated to programme.

### **3.2.3 FLUX-DIFFERENCE SPLITTING SCHEMES**

The concept of upwinding has been used in local discrete approximations in finite-difference and finite-element methods for many years. Upwind schemes have become popular since the beginning of the 1980's and these methods now play an important role in computational fluid dynamics. They offer a sound theoretical basis of the characteristic theory for hyperbolic systems and are capable of capturing discontinuities. Some of the most common



methods for the solution of the basic equations for transient gas flow are the  $\lambda$  formulation, flux-vector splitting methods and flux-difference splitting methods.

The flux-vector splitting methods were pioneered by Steger and Warming. Van Leer developed a flux vector splitting with an implicit relaxation algorithm, which is efficient, simple and capable of capturing the sharp shock waves. The simplicity of this method, however, came at a price of reduced accuracy for viscous flows due to the large dissipation. Higher-Order Polynomial Expansion (HOPE) scheme of Lion and Steffen and the Low-Diffusion Flux-Vector Splitting Scheme of Van Leer were aimed at building up a pure flux-vector splitting scheme with vanishing mass diffusion. They did achieve the required split mass but instability and non-monotonicity of the schemes are not acceptable for practical calculations. Efforts have also been made to improve the original Van Leer scheme by using some techniques borrowed from the flux-difference splitting schemes first suggested by Hanel and then extended by Van Leer. The Van Leer-Hanel (1990) Scheme uses the net mass flux and the one side velocity, and the total enthalpy for the transverse momentum and energy equations. A successful and more promising scheme was suggested by Liou and Steffen, the Advection Upstream Splitting Method (AUSM). They introduced an advective Mach number by combining split Mach number contributions from the original Van Leer's mass splitting. In a variety of calculations, this scheme was reported to be as accurate and convergent as the Roe flux-difference splitting scheme, which was considered to be the most accurate by then.

One of the more recent works in this area is that of Zha and Bilgen (1993). A new flux vector splitting scheme, using the velocity component normal to the volume interface as the characteristic speed, and yielding a vanishing individual mass flux at the stagnation has been developed. Flux-difference schemes can correctly capture shock waves and provide criteria to discriminate the correct information carried by propagating waves. The difference in flux between two adjacent node points is split into terms that will affect the flow evolution at points either side of the section under investigation. It is assumed that uniform flow occurs at each node point and over the cell extending one and a half grid intervals each side of the node point. A discontinuity generally separates two neighbouring cells in the middle of the interval, and the evolution in time of this discontinuity provides the criteria for splitting the flux difference over an interval into terms associated with waves that propagate up and down the pipe. The above procedure is known as the Roe method. This method was extended by Pandolfi to hyperbolic equations. The Roe method was used frequently since it can take care of both steady shocks and contact discontinuities.



In an attempt to extend the upwind idea to global methods such as spectral or pseudospectral methods, Huang and Sloan (1993) developed a new upwind pseudospectral method for solution of linear singular perturbation problems without turning points. Glaister (1994) presented a flux difference splitting numerical scheme for the solution of the Euler equations of compressible flow of a gas in a single spatial coordinate. The scheme uses the Riemann solver for the Euler equations for a duct of variable cross-section and using the arithmetic mean (in contrast to the usual square root averaging of Roe's Riemann solver) for computational efficiency.

Flux-difference splitting methods can correctly capture shock waves and provide criteria to discriminate the correct information carried by propagating waves. Good results have been obtained for flux-difference splitting methods, but required numerical experimentation. Flux-difference splitting methods are unconditionally stable and solution at boundaries create no difficulties. The  $\lambda$  formulation method requires comparatively low computing time and is sufficiently accurate. The disadvantage of the  $\lambda$  formulation methods, is that shock waves have to be treated explicitly. Flux-vector splitting techniques of first-order are very diffuse. Higher order flux-splitting methods generate post shock oscillations. A considerable amount of time is required to split the flux-difference. If a second-order method is used the integration in flux-difference splitting methods, the computation time is again increased. Some inaccuracies can develop in flux-difference splitting methods for cases such as interaction of shocks. Flux-difference splitting methods are complex and require large execution times. The Zha-Bilgen Method is very simple and easy to implement. It is efficient and capable of capturing the crisp shock profile. With third-order differencing, it produces results with least oscillations near the shock.

### **3.2.4 METHOD OF LINES**

The method of lines has been studied and used extensively in the former Soviet Union for over forty years and more recently in the USA and other parts of the world. In this method, a system of partial differential equations is transformed into a system of ordinary differential equations by discretizing all the equations in all but one independent variable. The system of ordinary differential equations can then be solved by any suitable numerical method. For the case where the partial differential equations depend on two variables, the method of lines is essentially a technique for replacing the system of partial differential equations in two variables, by an approximate system of ordinary differential equation in one of these variables. Thus for the fluid transient equations, finite differencing in the

space variable leads to a set of time-dependent ordinary differential equations. The number of ordinary differential equations is equal to the number of partial differential equations multiplied by the number of grid points used. In the above example, spatial derivatives are replaced by difference quotients. Since for the numerical solution of the generated system of ordinary differential equations the time variable is in fact discretized too, we finally obtain a full finite-difference system. Many of the known finite-difference methods can be thought of as being generated in this way. The boundary within which the method is applied is taken to be a rectangle. Boundaries of more general shapes can be reduced to this form by suitable coordinate transformations. Boundary conditions are prescribed on all or some sides of the rectangle. For applications in transient gas flow analysis, a parabolic form of the partial differential equations is used, for which the boundary conditions are only needed on three sides.

Presently, there is a general purpose software code based on this method available. Ames (1977), Holt (1984) and Osiadacz (1987) gave theoretical descriptions of this method. In Holt's description, the method is based on a second-order partial differential equation of elliptic or mixed type whereas Osiadacz uses a parabolic partial differential equation. Osiadacz further discusses the application of this method to solve a system of partial differential equations describing the unsteady flow of gas in pipes and problems associated with its use, when dealing with rapidly varying signals and means of avoiding and overcoming them. It has been found that the procedure is satisfactory only where transients are gradual and continuous. There has been some recent studies where this method has been used practically to analyse unsteady flow of gas in pipelines. These are summarised in Section 3.3.

Sophisticated packages based on the method of lines exist for numerical solution of ordinary differential equations. The method of lines is empirical and extremely simple. Higher-order methods can be used for the integration of time, for example fourth-order Runge-Kutta or multi-step predictor-corrector methods, which is approximate for parabolic problems. Numerical time-domain solutions using the method of lines can be compared directly with corresponding method of characteristics solutions. The main advantage of the method of lines is that it offers the possibility of utilizing highly developed software for ordinary differential equations. The method of lines is only suitable for numerical solution of partial differential equations of elliptic, mixed-elliptic and parabolic type. It is usually but not exclusively applied to parabolic problems. Special care must be taken on the



formulation of boundary conditions. The method is convenient in particular where lumped-parameter systems of ordinary differential equations in time is required. Second- and higher-order accurate methods do not give better accuracy for parabolic problems than first-order Euler integration. With the method of lines it is difficult to treat the boundary conditions properly.

### **3.2.5 WAVE-PLAN METHOD**

The wave-plan method is based on a physical description of transient flow as a movement of pressure waves at sonic speed and corresponding pressure-flow relations for the effects of these waves impinging on fluid elements. It has some similarities with the method of characteristics solution because of the technique of tracing sonic disturbances throughout the system. The wave-plan solution is obtained as follows:

- (i) At the point or points in the fluid system where a disturbance is introduced, an incremental change in fluid flow rate because of the disturbance over a short interval of time is computed.
- (ii) The incremental pressure pulse accompanying the flow rate change is then computed.
- (iii) This pressure pulse is propagated throughout the system at sonic speed.
- (iv) The pressure pulse is partly reflected and partly transmitted at all geometrical and physical discontinuities.
- (v) Pressure- and velocity-time histories are computed for any point in the system by summing with time the contributions of the incremental waves.

The relationship between pressure head and flow changes caused by a pressure wave travelling in the fluid filled line can be computed from momentum considerations.

Application of this method has mainly been on liquid systems and therefore the basic partial differential equations have been derived from the equations of continuity and momentum. In the original formulation of this method by Wood, Dorsch and Lightner (1966), the resulting equations for the case where the fluid and pipe are assumed to be elastic, are non-linear partial differential equations. Since this method was formulated, there has not been much published application, until recently by Boulos, Wood and Funk (1990) and again by Wood, Funk and Boulos (1990). Both of these are on hydraulic systems applications.

The wave-plan method is more easily applied to complex unsteady flow systems, in addition to lending itself better to physical interpretation. Complete solution is obtained i.e. both the transient and steady-state response to a suddenly imposed periodic flow disturbance are obtained. The disturbing function can be of arbitrary form and need not be periodic. Non-linear effects are easily included. The wave-plan method is advantageous in making certain types of dynamic response calculations. For example, the response of fluid filled lines having types of axial cross-sectional area distribution for which there would be little hope of obtaining closed-form analytical solutions, can be easily handled. The method readily solves problems in which there is interaction between the structural motion of the conduits and the perturbations in the fluid flowing within the conduit. It offers certain advantages for handling complex networks and it closely represents the actual mechanism of transient pipe flow. The main limitation of the wave-plan method when dealing with pipe networks is that the time interval must be chosen small enough to account for pressure waves traversing the shortest pipe section in the network thus requiring frequent calculations. However, there are economies in time when computing for associated long lines as calculations for intermediate points can be omitted.

### **3.3 A REVIEW OF SOME NUMERICAL STUDIES**

#### **3.3.1 GENERAL STUDIES ON TRANSIENT FLOW**

There have been many studies on fluid transients since the last review by Tiley (1989). These, together with some which were not used in the above study are reviewed. Also some studies which were used in the previous review are deliberately included so as to lead to what is thought to be a more consistent selection of a numerical method for modelling transients in ruptured gas pipelines. Most of the studies are based on gas systems, although a few based on other systems have also been included in order to support some of the arguments used in selecting the optimum method. The studies are generally grouped into three categories. The first category is that of studies consisting of theoretical reviews and comparisons of various numerical methods of solution of fluid transient problems. The second category consists of practical studies on various fluid transient phenomena, other than pipe rupture. The third category is that of studies dealing with pipe rupture and blowdown modelling. The former two are dealt with in this section while the latter is covered in Section 3.3.2.



In the first category i.e. theoretical studies, Ames (1977) made a very comprehensive survey, description and discussion of finite-difference methods for partial differential equations. Some important hints were given to assist in deciding on whether a particular method is suitable for the solution being sought. If the equations are of no great complexity and are known to possess well behaved solutions, finite-difference procedures can be employed providing the limitations imposed by the characteristics are considered in the development. Since parabolic and hyperbolic equations characteristically have open integration domains, explicit methods are applicable to these problems. However, stability questions are crucial to these situations. On the other hand, stability difficulties are not as serious in implicit methods. In many non-linear cases, the use of implicit methods leads to the necessity to solve sets of non-linear algebraic equations. For such cases, there is little to be gained by employing finite-difference methods over that of characteristics. However, in some problems the proper use of implicit methods can lead to linear equations. Finite-difference methods can also be used for single or simultaneous first-order equations, providing the convergence and stability requirements are considered. Methods of treating shocks by finite-difference approximations include the Lax-Wendroff and the pseudoviscosity methods. Numerical evidence shows that in the presence of discontinuous initial values or shock waves, finite-difference methods of higher than first-order produce solutions with non-physical overshoot.

Niessner (1980), compared different numerical methods for calculating one-dimensional unsteady flows. The methods included are the method of characteristics, both explicit and implicit finite-difference methods and the method of lines. Advantages and disadvantages of each are discussed for different fluid transient cases. Implicit methods are appropriate if the time step is more restricted by the stability criterion of implicit methods than by accuracy requirements. Since the accuracy is determined by derivatives of the solution, the application of implicit methods is likely to be successful in the case where the solution varies slowly in space and in time or where the important effects propagate slowly with respect to the acoustic waves. This seldom occurs with unsteady flows, where the system changes significantly with small time intervals so that there is no opportunity for larger time steps. The study concludes that the Lax-Wendroff method seems to present a good compromise between simplicity, accuracy, speed and robustness (moderate overshoot in case of shocks). Because of its simplicity, it can be applied to all points except those on the boundary. Seemingly without loss of overall accuracy, boundary



points can be handled by a proper adaption of the method of Courant-Isaacson-Rees. Application of higher order methods like the method of Abarbanel-Gottlieb-Turkel often prove unhelpful because of the difficulty of a proper treatment of boundary conditions even if they are approximated with one order lower accuracy thereby not destroying the order of the method. Some attractive methods such as the leap-frog and the Hopscotch method produce considerable overshoot in the event of shocks.

Goldwater and Fincham (1981) explained and discussed applications of some of the popular numerical methods, including finite-difference methods, the method of characteristics and finite-element methods in modelling gas supply systems. Osiadacz (1987), gave a theoretical description of various finite-difference methods for computer solution of partial differential equations describing unsteady flow of gas in pipelines. Methods for both the parabolic and hyperbolic systems were presented. Of relevance to unsteady gas flow are explicit and implicit finite-difference methods, the method of characteristics and the method of lines.

Thorley and Tiley (1987), provided a review of theoretical and some experimental studies with dense-phase gas transmission systems, without assumptions such as isothermal and isentropic flow of ideal gas and including the effects of wall friction and heat transfer. The major aim was to be able to choose a numerical method to be used to solve the partial differential equations describing gas flow transients following a pipe rupture. The more popular methods were reviewed including the method of characteristics, explicit and implicit finite-difference methods, finite-element methods and flux-difference splitting schemes. Implicit finite-difference methods were recommended for slow transients because they do not require small time steps for stability, hence provide considerable saving in computational time. The method of characteristics was recommended for rapid transients because of the advantage of using small time steps to model events changing rapidly in space and time. It was further stated that a method of solution that would not accommodate a varying wave speed should not be used for non-isothermal flows. The Lax-Wendroff two-step explicit finite-difference method was recommended as the most suitable for dealing with systems in which shock waves form.

In the second category of studies, Fashbaugh and Widawsky (1972) presented results of an analytical study concerned with a one-dimensional prediction of the propagation of shock waves through air ducting systems, with variable cross-sectional area and including attenuations due to viscous effects at the wall of the duct. Shock fitting



using the method of characteristics, the pseudoviscosity method and the Lax-Wendroff two-step method were considered. It was concluded that shock fitting using the method of characteristics is complicated, especially for problems where more than one shock front is present. The pseudoviscosity finite-difference method in the Lagrange formulation was found to predict with good accuracy shock waves propagating through ducts with increasing cross-sectional areas up to area ratios of at least 10 to 1. Either the pseudoviscosity finite-difference method in Lagrange formulation or the Lax-Wendroff two-step method in the Eulerian formulation can be used for predicting shock attenuation in constant area ducts. The Lax-Wendroff method however, yields an overshoot in pressure at the shock front, which reduces accuracy when determining the peak pressure. The shock velocity differs slightly between the two methods, which is attributed to the pressure overshoot. The addition of the friction term (using a constant friction factor) in the pseudoviscosity and the Lax-Wendroff finite-difference methods brings these methods into fairly good agreement with experimental results. It was recommended that for accurate predictions in very long ducts, an appropriate function for the friction factor is needed and the pseudoviscosity method should be used.

Padmanabhan, Ames and Martin (1978) used the explicit-implicit method which was introduced by McGuire and Morris for a simple boundary-value problem of wave propagation in bubbly two-phase mixtures. The homogeneous model of two-phase flow was used to simulate the transient response of a flowing bubbly air-water mixture subsequent to the rapid closure of a valve at the downstream end of a horizontal pipe 25mm in diameter and 18m long. Computation along the boundary was accomplished using the method of characteristics. It was shown that in the event of discontinuity due to shock-wave formation, the direct numerical integration using the explicit-implicit method is much simpler than the commonly used method of characteristics, which in this case involves a shock fitting procedure. It was concluded that the explicit-implicit method is simple and versatile, and because of the implicit set of computations is more suitable for boundary value problems than such explicit methods as the Lax-Wendroff scheme.

Mathers, Zuzak, McDonald and Hancox (1976) presented a finite-difference scheme using backward-differencing in time and which is structured so that the difference equations resemble, as nearly as possible, the method of characteristics. This method was referred to as the characteristic finite-difference method. Special procedures were presented for treatment of discontinuities associated with phase transition (liquid to two-phase and



vapour to two-phase). Solutions from this method were compared with experimental data for blowdown from subcooled conditions and with solutions obtained using the method of characteristics. It was concluded that the characteristic finite-difference scheme is simpler and more versatile than the method of characteristics and produced good agreement with the method of characteristics. It also demonstrated a potential for the natural treatment of boundary conditions and relative ease with which unequal segment lengths and junctions can be handled. In addition the scheme could readily be extended to more sophisticated flow-boiling models, e.g. models which consider flows with equal phase velocities but unequal temperatures.

Kawabe (1982) developed an analytical method for single and two-phase flow in arbitrary piping networks. In this method, the piping network was represented by flow channels and vessels. The thermal-hydraulic transients in the channel were expressed by partial differential equations, which were solved by an implicit method simultaneously for the whole network with ordinary differential equations describing the change of vessel pressure and enthalpy. Osiadacz and Yedroudj (1989) reported on a comparison of an implicit finite-difference scheme with the Galerkin finite-element method using linear and cubic extrapolating polynomials for the simulation of transient phenomenon caused by the change of capacity of a compressor feeding a gas pipeline. The comparison between the analysed methods was based on the accuracy of results and computation time. In this comparison, the basic equations were derived from the laws of conservation of mass and momentum and further simplified into two types of equations. These are a non-linear parabolic model, which could be simplified into a linear model if variations of flow through the pipe are small; and a second-order parabolic partial differential equation, linear with respect to pressure at every time step. The two methods were compared on both the above forms of the basic equations. The study showed that the finite-difference method has a considerable advantage in computation time over the finite-element method, while both produce results of approximately the same accuracy.

Bhallamudi and Chaudhry (1990) reported on the application of two methods of integrating numerically the non-linear partial differential equations describing transient flows in homogeneous gas-liquid mixtures in pipes. The numerical methods are the third-order explicit finite-difference scheme developed by Warming, Kutler and Lomax (1973) and an implicit second-order finite-difference scheme, which is a variation of the scheme of Beam and Warming (1976). The Warming-Kutler-Lomax scheme is an extension of the presently



available second-order schemes. The diffusive and dispersive errors are easily controlled in this scheme by selecting appropriate numerical parameters, and it is third-order accurate in space and time. The Beam-Warming scheme is second order accurate in both space and time, unconditionally stable and non-dissipative. Both schemes capture shocks without special treatment. They observed that computed results using these two schemes compared satisfactorily with experimental results and also with result obtained using other numerical schemes. The study concluded that the method of characteristics usually employed for analysing transients in single liquid flows is not suitable for mixture flows because of the pressure-dependent coefficients in the governing equations. The wave velocity varies with pressure and shocks may form during the transient state.

Moe and Bendiksen (1993), presented the physics of a new type of multi-dimensional two-fluid model, based on a first-order semi-implicit finite-difference scheme, which is solved in two steps applying a separate equation for pressure. The numerical scheme is based on an extension of one-dimensional models used earlier. A basic difference between this model and the other existing models is in the solution procedure, aiming in particular at improved prediction of transient problems. A volume equation is applied for the pressure, enabling a direct two-step solution procedure, which involves first the solution of pressure and velocities implicitly from the volume and momentum equations and then the solution of the specific masses from the continuity equations. These linearised equation sets are solved directly applying a Gaussian band solver, thus avoiding an iterative solution procedure. In local instantaneous formulations of multi-phase flow, the domain is described by single-phase subsets separated by interphases. The conservation equations for single-phase flow are applied within each subset and local instantaneous transfer rate of mass, momentum and energy are formulated as boundary conditions at the interphase. The model differs from the other models for separated or stratified flow mainly in the ordering of the solution procedure sequence, particularly the stage at which the volume fraction is determined as well as the degree of implicit-explicitness to which the equations are formulated. The model is designed to cover a wide range of separated flows with volumetric gas fractions from zero to unity. Single-phase flow is treated as a special case where the gas fraction or the liquid hold-up is zero. There are no restrictions on the range of fluid properties that can be applied, i.e. in principle the model accepts any fluid, liquid or gas. The model was verified through extensive comparisons with available experimental data as well as through comparisons with



other models. It was shown that this scheme is robust, as well as mass and (with a proper correction) volume conserving. Single-phase simulations show excellent agreement with analytical solutions for laminar pipe and channel flow, including dambreak and collapsing liquid column problems. Four different types of transient two-phase phenomena were simulated. The model predictions compare very well with experimental data and where available with other models such as FLUENT. The dambreak problem illustrates the importance of the horizontal convective term in the momentum equation on the numerical diffusion. More comprehensive studies of two-phase stratified and slug flow problems were reported to be underway.

Kiuchi (1993), described a fully implicit finite-difference method for calculating isothermal unsteady gas flow in pipeline networks. The centred-difference form was used in space and a fully implicit algorithm in time. The algorithm for solving the finite-difference equations is based on the iterative Newton Raphson method. Standard Neumann stability analysis and an iterative convergence method are used. The Neumann stability analysis applied to the equations show that they are unconditionally stable. The iterative calculation method for a junction with three branches, which was proposed by Guy, was used. The second inertia term in the basic equation was neglected. Calculation results of a few valve opening and closure sample cases were compared with those of the method of characteristics, two-step Lax-Wendroff method, Guy's implicit method in which the second inertia term is included and the Crank-Nicolson method. It was found that the method using the Crank-Nicolson implicit method in time, gives an unstable solution in the case of the large time steps adopted, and even in the case of small time steps the method gives unrealistic oscillations. It was concluded that explicit methods give a correct answer when the pipes are sufficiently divided into small sections. Oscillations are greatly damped in Guy's method and the same tendency is seen in the present method when a small number of sections and large time steps are adopted.

Comparisons on network applications were made for the present method, Guy's method and the method of characteristics. Results of the three methods agreed well even if the time step is increased from one minute to thirty minutes. The present method showed a considerable advantage in computation time over Guy's method and most over the method of characteristics. Although the present method applied to a pipe is unconditionally stable, the iterative calculation at connecting points among pipes does not always assure convergence. Therefore convergence has to be confirmed. It was found that stability



depends on the convergence tolerance. Excellent agreement with the method of characteristics and the two-step Lax-Wendroff method regarding accuracy and computation time is greatly reduced compared to the above methods in small time steps. Large time steps can be used compared to explicit methods, which require small time steps according to the Courant condition. The method was found to have advantages in stability and computation time compared with the method of characteristics, the two-step Lax-Wendroff method, Guy's method and the Crank-Nicolson method. It was also found that a rapid transient phenomenon, such as pulsation, is filtered in the case of a large time step adopted with the present method. Such problems require small time steps and a large number of sections and the subject of interest is concentrated on such phenomena, thus losing the advantage of fast computation. Finally it was found that convergence of calculations at connecting points using iterative convergence methods depends on the time step, the number of iterations and pipeline size; but it is predictable in most cases.

Van Deen and Reintsema (1983), used a discrete-space continuous-time approach on a second-order finite-difference method for the solution of the partial differential equations on an analogue computer. Dynamic behaviour of a 90km long, 0.76m (30 inch) diameter main transmission line in the Gasunie system of the Netherlands was used. Gas was injected into the line from both sides and delivered from a series of points. A gate valve in this line was closed and reopened after 45 minutes. Flow, temperature and pressure were measured during and after reopening of the valve at two points. It was found that the form and magnitudes of experimental and model results were quantitatively correct.

Beauchemin and Marche (1992) showed that the use of the method of characteristics over the MacCormack method is no longer justified in contemporary closed-conduit transient analysis where the systems being studied are highly complex and the full equations are used. Details of a numerical scheme, computation procedure and treatment of the boundary conditions of a full model employing the MacCormack scheme, which is a two-step second-order explicit finite-difference scheme of the Lax-Wendroff type, were presented. The model is based on single-step isothermal liquid flow in an elastic pipe. A steady state friction factor was used and no simplification was made on the basic equations. The model was applied to many real world hydraulic transient problems including multiple pump trip-out in branching networks with many different types of pipes (varying wave speeds) and pump failure in a multiple-pipe single-branch system. Most of



these cases had secondary controlling devices such as pressure regulating valves and air inlet valves, already present in the system and involved either the verification or the design of primary control devices such as throttled surge tanks and air chambers. It was found that the MacCormack method is superior to the method of characteristics when the Courant number ( $C_n$ ) differs appreciably from unity. For this, precision rather than cost is the main criterion, especially for well behaved  $C_n$ . When  $C_n$  is much smaller than unity, the MacCormack method produces results with a precision that could not be attained with any reasonable number of computation nodes when the method of characteristics is used. Also an important observation was made regarding the use of the MacCormack method. The use of the first and second alternatives in succession on consecutive time steps could introduce important oscillations in the solution especially where the basic equations are poorly approximated. This can be avoided by using exclusively one of the two calculation alternatives. Directional bias caused by the above is important only when working with two space dimensions, in which case it is recommended that the average with both methods be used. Doing so does seem to smear the shock slightly and the computation time is doubled.

The study concluded that the method of characteristics is the most accurate and least costly for simple systems when  $C_n$  is equal to unity. If  $C_n$  is not equal to unity, linear interpolations (spatial or temporal) are required, which can introduce very significant attenuations and dispersion errors in the solution. On the other hand, the MacCormack method is superior to the method of characteristics when  $C_n$  differs from unity appreciably.

The MacCormack method is inherently dissipative, that is, because it is second-order accurate in both space and time, no special shock capturing approach is needed. It is unconditionally stable if  $C_n$  is less than unity, and produces minimal precision loss when  $C_n$  moves away from unity. The method permits the use of a grid spacing that is not overly fine, even in highly complex cases and as it is quite efficient, overall computation effort remains reasonable. The method could be very well suited for applications of increasing complexity such as two-phase gas-liquid flow problems; and multi-dimensional flow. It is simple and has a low development cost.

Boulos, Wood and Funk (1990), compared procedures based on an exact solution, the method of characteristics and a wave-plan method for solution of two simple pressure surge problems and compared the results. The basic partial differential equations were greatly simplified by assuming isothermal flow and neglecting the distributed frictional



effect within the pipe as well as the convective terms. Friction effects were included in the wave-plan method. Calculations were carried out for all the three methods, using data provided for a case of valve closure for a system of liquid flowing from a reservoir at the upstream end to the downstream end of a line of constant cross-sectional area. Two cases were considered for each method, that is one with an open end connecting the upstream reservoir and the other where the orifice is positioned at the upstream end between the entrance reservoir and the pipeline (simulated friction). It was shown that each of these numerical methods produces a solution which is identical to the exact solution. It was also shown that an exact solution to transient complex piping system is generally not available. Results obtained using the numerical techniques for a network of pipes agreed closely with only minor differences.

Wood, Funk and Boulos (1990), compared a distributed parameter model using the wave-plan method to a lumped parameter model based on a combination of the dynamic line and continuity equations to form a set of difference equations for a path of pipes, for several cases of transient conditions in pipe networks. Two piping systems, a three pipe junction system and a network, were analysed using both methods. Comparison was made for various transient situations, including a ramp change in the head and sinusoidal variation for the former system; and a pump trip, a 50% change in pump speed and a sinusoidal speed change in the pump for the latter. It was observed that a distributed parameter transient analysis of a piping system requires a relatively complex analytical model and may involve a large number of calculations. On the other hand, a lumped parameter analysis utilises a much simpler analytical model and requires far simpler calculations. The time interval for distributed parameter model must be chosen to be small enough to account for pressure waves traversing the shortest pipe section in the network, thus requiring the carrying out of frequent calculations. The number of calculations is generally much larger than the number required utilising the lumped parameter model. The study concluded that for fast transients, i.e. those occurring in a time scale which is short compared to the system characteristic time, it is necessary to use a distributed parameter model to accurately describe pressure and flow at a particular point. For extremely slow transients it is often acceptable to use a quasi-steady model. When the transient is too fast for a quasi-steady description, yet slow relative to the system characteristic time, a lumped parameter model may be used. A technique employed to solve the lumped parameter equations, which comprise the dynamic model,



is similar to the simultaneous path method for steady state flow and provides reliable solutions for large complex networks. The use of the lumped parameter model saves much time and effort.

Suwan and Anderson (1992), developed a reliable basis for lumped-parameter model suitable for stability analysis of self excited perturbations based on the method of lines, discounting the previous conclusion that the procedure is satisfactory only where transients are gradual and continuous. The physical problem used was that of a rapid transient initiated by an instantaneous downstream valve closure. The model was successfully applied to the prediction of compressor surging in a system where fluid compressibility effects are important. The model produced results identical with the method of characteristics. It was found that a linear method of lines solution is not necessarily identical to the linear method of characteristic solution even if  $a \times \Delta t = \Delta x$ , unless it is appropriately formulated and appropriate forward and backward interpolations are adopted to represent information transmission in the characteristic directions. This is clearly most significant in problems where wave fronts are distinct and wave reflections occur, for example with standing wave patterns often associated with self excited oscillations. For slow transients or flood routing problems which are less dominated by either boundary conditions, the above conclusion would not have the same significance. Some significant aspects regarding the use of the method of lines were investigated in the study. The dependent variables have often been taken as the original primitive variables but this study concluded that Riemann or Allievi characteristic variables are preferable.

For the waterhammer hyperbolic equations, at least, a first-order discrete space interpolation polynomial represents the underlying physics better than higher order approximations. The terms in which finite-differences are used to represent quantities which are integrals rather than derivatives, in particular pipe friction, may introduce numerical instability and require particular care. For time-domain simulations, first-order Euler integration is more accurate than higher-order methods, which introduce errors by violating the hyperbolic equation domain of dependence.

Zha and Bilgen (1993), presented a new flux-vector splitting scheme for the numerical solution of the Euler equation, using the velocity component normal to the volume interface as the characteristic speed and yielding vanishing individual split mass flux at stagnation conditions (with Mach number approaching zero). This keeps the advantages of the flux-vector splitting schemes, such as being able to capture crisp shock



profile, simplicity and efficiency. The scheme also leads to vanishing numerical dissipation for the mass and momentum equations with Mach number approaching zero. It was stated that even though one of the diffusive terms of the energy equation does not vanish, theoretical analysis indicates that diffusion may be ensured by using higher-order differencing. Application of the scheme to solve the one-dimensional Euler equation yielded solutions which are monotone and normal shock wave profiles which are crisp. For a one dimensional shock tube problem with shock and contact discontinuities, this scheme and the Roe flux difference splitting scheme, give very similar results, which are the best compared with those from the Van Leer scheme and Liou-Steffen Advection Upstream Splitting Method (AUSM) scheme. For multi-dimensional transonic flows, sharp monotone shock wave profiles with mostly one transition zone are obtained. The results were compared with those from Van Leer scheme, the AUSM scheme and also with experiments.

It was concluded that for viscous flow, the present scheme may be more accurate than the flux vector scheme without the mass flux vanishing at stagnation conditions. The scheme with a Mach number polynomial of degree one, which is the natural and lowest degree, is very simple and easily implemented. The scheme converges well for the cases tested, slightly faster than the AUSM scheme and slower than the Van Leer scheme. With a third-order differencing method, the present scheme produced results with least oscillations near a shock. The results also agreed favourably well with experimental results for a transonic nozzle.

Huang and Sloan (1993) presented a new pseudospectral method with upwind features for numerical solution of linear singular perturbation problems without turning points. It was shown that this upwind pseudospectral method has distinct advantages relative to the standard pseudospectral method and the upwind finite-difference methods for singular perturbation problems without turning points. However, a conclusion was made that it needs further study to apply the upwind pseudospectral method to singular perturbation problems with turning points and to the numerical solution of high Reynolds number flow problems in fluid dynamics. Glaister (1994) presented results produced by his method, which has been described in Section 3.2.3, for five shock tube test problems. These were compared with exact solutions and solutions using other more complex algorithms. It was generally found that the results are comparable. It was concluded that the Glaister method can be used for slab, cylindrically or spherically symmetric problems

with confidence. It was also concluded that the method can be used as a comparison with results from two-dimensional schemes by choosing a large number of mesh points for accuracy and not be expensive on computing.

### **3.3.2 STUDIES ON PIPELINE RUPTURE AND BLOWDOWN**

Work done on this category of studies is somewhat limited both in quantity and quality. One of the earliest models for the analysis of gas pipeline rupture on record is that by Sens, Jouve and Pelletier (1970). This was followed by Lyczkowski, Grimesey and Solbrig (1978). Knox, Atwell, Angle, Willoughby and Dielwart (1980) claimed that three models existed, which adequately predicted the transient release of a gas from a ruptured pipeline. These are described by the Alberta Petroleum Industry, Government Environmental Committee (1978). There have since then been several attempts to develop a computer model for gas pipe rupture analysis, including that by Tiley (1989) which forms the starting point of this study. The majority of those which are discussed in this report are based on the method of characteristics. The rest are based on various finite-element and finite-difference schemes. These studies are summarised in this section.

Sens, Jouve and Pelletier (1970) used an explicit finite-difference method for the numerical solution of partial differential equations to simulate transient flow in a gas pipeline a few seconds after a break. Lyczkowski, Grimesey and Solbrig (1978) investigated several explicit finite-difference numerical schemes for solution of homogeneous equations of change for one-dimensional fluid flow and heat transfer. The Alternating Gradient Method (AGM), which is based on the two-step Lax-Wendroff procedure, was found to be the most successful. Results using the AGM were compared with analytical results for an ideal shock tube and blowdown of an ideal gas, and also experimental results for blowdown of a steam-water mixture. Agreement between the results was very good. Comparison of the AGM with the two-step Lax-Wendroff method for the shock tube indicated that the AGM is more accurate than the Lax-Wendroff scheme, probably due to more numerical damping in the AGM. Although the AGM is restricted by a time-step limitation which is slightly smaller than the standard Courant condition for a given time-step and mesh size, it is at least as accurate as implicit schemes. Since only two cycles per time step are needed, the AGM is faster than a fully implicit scheme. In addition, the AGM is simple to programme.



In the study by the Alberta Petroleum Industry, Government Environmental Committee (1978) to evaluate and improve hydrogen sulphide isopleth prediction the following techniques were used: two dispersion models, the INTERA Environmental Consultants Ltd. (INTERA) model and the Energy Resource Conservation Board (ERCB) model; and two blowdown models, the INTERCOMP Resource Development and Engineering (INTERCOMP) model and a simplified blowdown model. Common blowdown curves generated by the INTERCOMP "TRANSFLOW" blowdown model were used in both the ERCB and INTERA atmospheric dispersion calculations. The INTERCOMP "TRANSFLOW" model uses the basic momentum, mass and energy balances in a numerical simulator to calculate the time curve defining the rate of gas blowdown from the pipeline. Among other things, the model has the capability of including valve closure time, frictional effects and gas flow rate in the line before rupture in the calculations. No further details of the models were given in the report.

Knox, Atwell, Angle, Willoughby and Dielwart (1980), reported on a project to assess the basic source characteristic assumptions relevant to modelling of sour gas pipeline ruptures and well blowouts. A 3.2 kilometres long, 168 millimetre diameter pipeline was ruptured 32 times under varied conditions. A 7.1 kilometres long, 323 millimetre diameter pipeline was also ruptured and results were photographically recorded. The experimental rupturing technique, transient release rate and sensitivity to source configuration were evaluated. Parameters investigated included overburden, wind speed, release angle, fracture length, rupture mode and line pressure. Computer input parameters which needed verification are plume rise, volume dilution and rate of release. The study was based on three computer release rate models which existed [Alberta Petroleum Industry, Government Environmental Committee (1978)] and which have been described in the previous paragraph. It was confirmed that all the three computer release rate models adequately predict the transient release of gas from a ruptured pipeline.

Cronje, Bishnoi and Svrcek (1980) described a procedure to solve the equations for single-phase, one-dimensional, unsteady, compressible, frictional flow with heat transfer. The procedure is based on Hartree's hybrid method for solving the governing hyperbolic partial differential equations. In this numerical method, a rectangular grid is superimposed on the characteristic mesh in the time-distance plane. The values of the variables at points lying on the characteristics at time  $t$  are calculated by linear interpolation from their known values prevailing at the rectangular grid points at the same time,  $t$ . The governing equations

are integrated along their characteristics over a time step  $\partial t$  in time, to obtain the new values of these variables at the grid points at time  $t + \partial t$ , and the process is repeated until the required time interval is covered. The method was applied to shock tube data that simulate a gas pipeline rupture. It was shown that the effect of friction is considerably more important than the effect of heat transfer. For large elapse times, the effect of friction is significant and the numerical model predicted well the available experimental values at these times. However, the numerical model agreed with experimental data at higher pressure ratios, at short elapse times and near the rupture plane.

Jones and Gough (1981) reported on a theoretical model for analysing high-pressure natural gas decompression behaviour. The method was incorporated in a computer programme called DECAY. The model was tested with a series of experimental data, which is reported in Chapter 5 and Section 6.2.2. Jones and Gough (1981) also reported that other organisations, including Exxon Production Research and the University of Calgary, were involved in studies on high-pressure gas decompression behaviour. The two organisation had developed similar models to that of the British Gas. Mallinson (1996) reports about another computer model called PIPEBREAK, which has been validated with recent full-scale pipeline experimental data with reasonable success.

Fanneløp and Ryhming (1982) studied the sudden release of gas from long pipelines. A straight forward solution based on the time-honoured concept of integral methods in boundary-layer theory was used. Spatial profiles of pressure and flow rate were assumed which satisfy the boundary conditions. He defined different time regimes, each requiring a different method of solution. The inviscid regime is often of very short duration, probably much shorter than the time required for a full break to occur. It is followed by a viscous expansion process in which wave and dissipation processes are both important and in which the pressure at the break approaches the ambient value. The combined inviscid and viscous expansion phase were categorised as the early time regime. The time regime when the pressure decreases monotonically towards the open end, such as in the case of a break at the low-pressure end was referred to as the late time regime. The intermediate time regime was defined as the time which lasts from  $t \approx 25$  seconds to the time when the pressure peak has moved to the other (closed) end. Simple solutions were developed for flow cases of prime interest. Validity and accuracy of the methods were checked using two procedures namely variations of profile families and mathematical analysis of the partial differential equations based on an iterative approach carried out to second order. The integral method was shown to have adequate accuracy for engineering studies.



Van Deen and Reintsema (1983), developed a computer model for high-pressure gas transmission lines based on the method of characteristics and compared it with experimental data from the Gasunie transmission system. A leak was simulated by the fast opening of a valve connecting the pipeline to a nearby parallel pipeline at a lower pressure. Pressure responses at a point 10km downstream of the leak were investigated. Lack of agreement in the magnitude of the reflected pressure waves was observed and attributed to imperfect modelling of the boundary conditions. It was also observed that changes in the numerical values of the resistance factor of the pipeline have only a slight influence on the value of the result.

Flatt (1985-1989), studied the use of the method of characteristics for analysis of unsteady compressible flow in long pipelines following a rupture. In his model the simplifying assumptions of isothermal and low Mach number, often applied in the case of unsteady compressible flow in pipelines, were not used. To achieve higher accuracy, higher-order polynomials and an assumption of correspondingly curved characteristic lines were also used. The algorithms used were limited to shock free flows. An accuracy criterion showed that higher numerical accuracy may be obtained if the number of grid points was sufficiently large and if a special modified form of the boundary conditions at the broken section was used. The major difficulty encountered was due to the singularity which resulted from the combined effects of friction and choking ( $M_* = 1$ ), occurring at the broken end. The results confirmed conclusions established earlier that viscous flows with large values of  $4fL/d$  (order of magnitude of 1000) behave very differently from flows without friction. In particular the mass flow escaping through the broken section, and the pressure there fall to much smaller values. On the other hand, at some distance from the broken section the pressure stays at high values much longer than in the case without friction. The study concluded that the method of characteristics is more suited to problems with relatively low values of the parameter  $fL/d$ . Cases with important frictional effects have to be carefully checked regarding the accuracy of the results and require many more grid points than cases without friction.

Bisgaard, Sørensen and Spangenberg (1987), reported on a finite-element method developed for transient compressible flow in pipelines. A weighted residual method with a one-dimensional straight line element with two nodes was combined with an implicit Euler method and applied to the basic equations without making any simplification. Higher-order polynomials were used as interpolating functions, since derivatives must be specified at the nodes in addition to the variable itself. The Galerkin finite-element method was used to discretize the equations. Gauss quadrature was used for the integration, where the order

of the Gauss quadrature was adjusted to the order of the polynomial. A fully implicit Euler integration method was used for time integration after a third-order Runge-Kutta method had failed the stability criterion. The method was used to describe blowout and to determine the performance of a leak detection system. The first derivative of density and the first and second derivatives of velocity were included since small leaks are more easily recognised from derivatives of specified variables than from the variables themselves. A comparison was made between full-scale measurements carried out on a 77.33 kilometres gas transmission line from Neustadt through Sörzen to Unterföhring, in Germany, and corresponding finite element calculations. In the rupture simulation, the fluid was assumed to behave like an ideal gas with constant specific heat flowing through a convergent nozzle and calculations were carried out with 21 elements and a time step length of 0.5 seconds. It was claimed that results from the computer model had successfully been compared with process data from a full-scale pipeline. However, this was not shown in the paper for the case of a pipe rupture. It therefore remains doubtful as to whether the method could accurately and efficiently be used for the analysis of pipe rupture problems.

Lang and Fanneløp (1987) reported on a method for efficient computation of the pipeline break problem. In their method, partial differential equations were reduced to a set of ordinary differential equations by means of procedures in the family of the method of weighted residuals. The reduced equations were integrated by standard numerical techniques. The finite-element method, the spectral Galerkin method and the spectral collocation method were all used and results compared. It was demonstrated that stable, accurate and efficient solutions to the pipeline break problem could be obtained by the method of weighted residuals. Although the approximate functions used with the spectral collocation method would appear to be suited primarily for elliptic problems, it was possible to apply them to the hyperbolic equations by modifying one of the coefficients. Good results were obtained, and it was recommended that the computer time required by this method could be further reduced without loss of accuracy when the number of polynomials in the approximate solutions is reduced successively during the course of the calculation, as the gradients of pressure and velocity become smaller. It was concluded that the best results in terms of stability, accuracy and computing time were obtained with the collocation method.

Cheng and Bowyer (1987) presented a general quasi-one-dimensional unsteady compressible fluid flow code, which adopted the Eulerian approach and used the artificial viscosity method for finite-difference numerical integration of the governing equations. The



numerical method is a generalised two-step explicit Lax-Wendroff finite-difference scheme that includes an adjustable implicit artificial viscosity term. Two sample computations were used to demonstrate the code capability. In the first case, the transient imposed on a system undergoing a pipe rupture was studied for different combinations of the effects of elbows and restrictors. A steam vessel was considered to be the reservoir with a pressure of 1000psi (69bar) and a temperature of 550°F (288°C). A flow restrictor (with a throat whose cross-sectional area is 36% of the duct flow area) was located 8ft (2.5m) downstream of the second elbow. In the second case, transients caused by a sudden pipe rupture at the left side of three-duct system were predicted.

Picard and Bishnoi (1988 and 1989) used their three models, namely the Perfect-gas Isentropic Decompression (PID) model, Real-fluid Isentropic Decompression (RID) model and Real-fluid Non-isentropic Decompression (RND) model to investigate the importance of real-fluid behaviour in modelling of high pressure gas pipeline ruptures. All these models are based on the method of characteristics. Botros, Jungowski and Weiss (1989), discussed some computational models and solution methods for gas pipeline blowdown and assessed the significance of the various assumptions involved. Two physical models, namely a volume model, where a pipe is considered as a volume with stagnation conditions inside; and a pipe model, where a pipeline section is considered as a pipe with velocity increasing towards the exit were considered. The pertinent equations for each model were solved analytically and numerically. The volume model was represented by a set of quasi-linear ordinary differential equations which were solved by a variable order backward differentiation formula method (Gear's method). The pipe model is governed by a set of non-linear first-order parabolic partial differential equations, which were solved by a first-order Euler implicit finite-difference scheme. It was concluded that the accuracy of results obtained from the various models and solution methods depends greatly on the ratio  $fL/d$  of the pipe section under blowdown and the stack relative size with respect to the main pipe size. Generally as  $fL/d$  increases, predictions using all models tend to become inaccurate. For relatively low  $fL/d$  values, all models provide reasonable predictions and therefore the simple analytical volume calculations can be used effectively.

Tiley (1989), used the method of characteristics for pressure transients in a ruptured gas pipeline with friction and thermal effects included. A real gas equation of state (Berthelot equation) was used and the "small terms" in the basic equations were neglected. A reducing grid size was used in the vicinity of the break to be enable rarefaction waves to be modelled following a linebreak. The friction term was represented by a second-order approximation. The values at a state 1 at the base of the characteristic

were found by interpolating the grid points. Hence by solving these equations, a first-order approximation was obtained for the predicted pressure, temperature and flow velocity. Since the required stability and accuracy was not achieved using the first-order approximation, this solution was used as an initial estimate in a second-order procedure.

Although the exact procedure of this second order model is dependent on the type of grid point being examined, in principle, new values for the variable at state 1 were found using quadratic interpolation. The coefficients in the characteristic equations were then calculated using these values. The coefficients were averaged with the previous state 1 coefficients and the results were substituted back into the characteristic equations. By this method, new values for the predicted pressure, temperature and flow velocity were obtained. Results were obtained by performing a number of computer simulations for a set of data and comparing the results with shock tube and full-size pipeline experimental data. Problems were encountered with numerical stability and accuracy of results. For certain grid size and initial conditions, the solution became unstable at random points along the pipeline. It was concluded that although this type of instability could be controlled to an extent by varying the grid size and break boundary conditions, the problem may be totally alleviated by using an alternative numerical method for solving the theoretical equations.

Lang (1991) reported on the computation of gas flow in pipelines following a rupture by a spectral method. The governing partial differential equations were converted into a scheme suitable for solution by a computer by a two step procedure. In the first step, the collocation version of the spectral method was used to calculate the space derivatives. The remaining ordinary differential equations were then integrated by standard numerical techniques in the second step. Accurate results were obtained for short computing times with only a few collocation points. Kunsch, Sjøen and Fanneløp (1991) reported on a study of the flow characteristics close to a shut-down valve for an offshore gas pipeline, and over the length of the segment between the valve and a rupture. Integration of the partial differential equations was performed with the two-step MacCormack method. A fine mesh size was imposed at the boundaries where the gradients can be large. Treatment of boundary conditions, especially those relative to the valve, based on concepts from the method of characteristics, proved to be adequate. The calculations showed a better accuracy than previously used models. In another publication, Kunsch, Sjøen and Fanneløp (1995) concluded that a precise knowledge of the coefficient of friction and other losses coefficients is not necessary. They demonstrated that the mass flow rates are insensitive to the exact geometric shape and contraction ratio of the break, resulting from an accidental



rupture. They also compared their model results with those obtained by Flatt (1985b). They admitted that the results from Flatt's model (which was based on the method of characteristics) were probably more accurate than their's, for the inertia dominated early time regime. They observed that the ideal gas assumption overestimated [Flatt (1993-94)] the mass flow rate. Flatt (1985b) observed the opposite effect, when the perfect gas assumption was used.

Chen, Richardson and Saville (1992) presented a model for simulation of blowdown or rapid depressurisation following a full-bore rupture of pipelines containing perfect gases. The equations of gas dynamics were solved by the method of characteristics using four different algorithms namely the hybrid method, the hybrid method with multi-grid system, wave-tracing and multiple wave-tracing methods. The multiple wave-tracing method was found to be the most efficient and accurate method among the other methods for simulating long gas line rupture problems. This method was used to simulate the blowdown of the sub-sea pipeline between the Piper Alpha and MCP-01 offshore platforms and the result was compared with measurements made during the night of the tragedy on the Piper Alpha platform. The results were found to be in moderate agreement, the discrepancy being due to real fluid behaviour. It was concluded that although the perfect gas blowdown model is not capable of modelling real fluid behaviour, its simplicity and speed combined with the multiple wave-tracing method should provide a quick yet reasonably accurate evaluation of gas dynamics for risk assessment to a gas transmission line.

Chen, Richardson and Saville (1993) developed a simplified finite-difference method to solve transient two-phase pipe flow problems. In this method, the flow channel is discretized using staggered meshes where the flow velocity is defined at the cell edge and all other variables defined at cell centre. Following the guidelines of the Fourier stability analysis, the scheme treats the momentum convection term explicitly and the flow velocity is expressed in terms of pressure. The density in the mass conservation equation is further eliminated using a locally linearised equation of state so that the discretized conservation laws can be reduced to two difference equations in terms of mixture enthalpy and pressure only. The only assumption made is that there is thermodynamic equilibrium between the two phases. The method has several advantages. Since the velocities in the momentum equations are decoupled from other state variables, the extension of this method to other two-phase flow models is very straight forward. The size of time step for the integration is not limited by a Courant number restriction. The choice of mixture enthalpy and pressure permits the method to make transition between single-phase and two-phase without difficulty. Extension to a multi-component system with concentration stratification effects

is possible. Results of the model were presented by way of example for the blowdown of a 100m long pressurised LPG pipeline using a homogeneous two-phase flow model.

Olorunmaiye and Imide (1993) presented a mathematical model based on unsteady isothermal flow theory and solved by the method of characteristics. It was reported that the model predicted results for natural gas pipeline rupture problems consistent with predictions of other workers. The accuracy of the numerical scheme when using linear characteristics with quadratic interpolation was found to be adequate. It was found that the curvature of the characteristics is not as pronounced in isothermal flow as it is in adiabatic flow and therefore it is not necessary to include the effect of curvature of the characteristics in the computation of unsteady isothermal flows. It was concluded that the model is useful in analysing other unsteady flows associated with pipeline operation, such as controlled venting to the atmosphere prior to shutdown or repair, and sudden changes in pressure at either end of the pipeline. The waves generated in these operations cannot be as strong as waves associated with pipeline rupture.

Gasunie of the Netherlands [De Bakker (1993)] have developed a pc-model for gas out flow for complex pipeline networks with different elements and different out flow scenarios all in one model. It can model linebreak, venting and leakage. It can handle elements like valves, vessels, restrictions and elements defining different boundary conditions, which can represent e.g. the behaviour of a compressor. The basic relations are solved using an implicit finite-difference scheme. A graphical user interface makes inputting of the network very easy. In developing the model, emphasis was put on userfriendliness, robustness and the ability to model complex networks. The accuracy of the model is estimated at 5 to 20%, which is considered by Gasunie to be sufficient for hazard analysis purposes.

The Southwest Research Institute (SwRI) [Morrow (1996)] has conducted a study, to simulate venting of natural gas pipelines, for the Gas Research Institute. The computer model which was reported by Olorunmaiye and Imide (1993) was used. One of the aspects which were considered was whether a leak detection system could distinguish between a signal caused by a pipeline leak and other transient signals caused by normal operation, such as compressor startup and shutdown and deliveries of gas through branched lines. Initially, the computed transient results overestimated the gas outflow and pressure drop. In order to match the computed results to experimental data, the throat area of the relief valve was reduced below its physical size. This empirical adjustment, which is called "exit loss factor", resulted in a fairly well agreement between computed and measured pressures.



### 3.4 DISCUSSION OF NUMERICAL METHODS

The criteria upon which a suitable numerical method is selected for analysis of a particular fluid transient problem is based mainly on the accuracy of results and computation cost.

Each numerical method has its own advantages and disadvantages. These have been discussed in Sections 3.3.1 and 3.3.2. In general, higher degrees of accuracy can be achieved at the expense of increased computational labour. The problem is to find, for a given mathematical model of a pipeline, a numerical model which meets the criteria of accuracy at relatively small computation time.

Before proceeding with a discussion of the numerical methods, it is important to understand and define precisely the type of system and transient phenomena to be modelled.

The problem of gas pipe rupture is highly non-linear and no general analytical solution is yet known. The foremost objective of this study, therefore, is to develop a computer model which will lead to a better understanding of the unsteady fluid dynamics behaviour occurring inside the pipeline. One also needs to distinguish between simulation of unsteady gas flow in a single pipe and that in a complex gas pipe network, including the way in which non-pipe elements are provided for in the simulation process. At this initial stage, the model is limited to the simple case of a single pipeline, since the primary interest is long, high-pressure trunk pipelines. However, note is taken of these other more complex cases and a criterion of flexibility for extension to such situations is added in the list of selection criteria. By the same argument and also the conclusion made by Wood, Funk and Boulos (1990), that for fast transients it is necessary to use a distributed parameter model, the same model is used. Despite their advantages of simplicity and fewer calculations, lumped parameter models, including the method of lines are therefore not suitable for application in this particular situation.

Knox, Atwell, Angle, Willoughby and Dielwart (1980), showed that the system response to, and therefore its modelling, depends on among other things the rupture mode. Botros, Jungowski and Weiss (1989) distinguished between two modes of rupture which require different modelling approaches, one in which the exit area is much smaller than that of the main pipe and the other in which the exit area is as large as the main cross-sectional area. This study focuses on the latter case. However, with appropriate specification of the boundary conditions the model should be able to analyse any other mode of rupture. For this case the flow velocity in the pipe becomes high (about 350 m/s)

initially, at the ruptured section, and varies rapidly with time. Shock waves of varying speeds are formed. These travel up and down the pipe and are ultimately transmitted and partly reflected at geometrical and contact discontinuities. For long transmission lines (typically 150km), this could take some time. A method must therefore be chosen that will accurately represent these shock waves and accommodate the varying speeds of the waves without smearing the details or overshooting. With appropriate choice of a numerical method, all shocks may be treated wherever they appear in the pipeline. In addition, shock interactions with boundaries and other shock waves may also be treated.

Having read Sections 3.3.1 and 3.3.2, one would have probably had an answer for which numerical method is to be selected. As regards the review of numerical methods as well as the actual modelling of pipe rupture, the work by Tiley (1989) remains the most recent and comprehensive. However, a major inconsistency is observed in selecting the method of characteristic as the optimum numerical method. This is mainly because it was admitted that the Lax-Wendroff two-step explicit finite-difference method is the most suitable for dealing with systems in which shock waves form. The study could also have benefited from previous similar studies by Flatt (1985-1989) and Picard & Bishnoi (1987-1989), which seems to have arrived at the same results and conclusions. The two strong arguments put forward by Tiley (1989), in favour of the method of characteristics are, small time step requirement and proper handling of the boundary conditions. The discussion in Sections 3.3.1 and 3.3.2 shows that these could both be achieved with other methods such as the explicit finite-difference method used by Beauchemin and Marche (1992). In addition, in both the studies by Van Deen and Reintsema (1983) and by Tiley (1989), there appears to be some problems due to the representation of the boundary conditions. Flatt (1986) claimed to have achieved higher numerical accuracy by using a special modified form of the boundary conditions at the broken section. However, the algorithms he used are limited to shock free flows. It is therefore doubted as to whether the advantage of the method of characteristics on handling the boundary conditions really holds in the case of ruptured gas pipelines.

There are conflicting results regarding the significance of the friction effects on the results, from the studies of Van Deen and Reintsema (1983) and Flatt (1986). Whereas the former concluded that changes in the numerical value of the resistance factor of the pipeline have only a slight influence on the results, the latter confirmed the effect to be the opposite for flows with large value of  $fL/d$ . From the studies on modelling of



transients using the method of characteristics, the selection of whether or not to use the method is based on among other things the ratios of  $fL/d$ , Mach number and Courant number ( $C_n$ ). The method of characteristics is more suited to problems with relatively low values of the parameter  $fL/d$  (order of magnitude of 250). For  $C_n$  values not equal to unity, the method of characteristics produces inaccurate results. Most of the studies on gas pipe rupture, using the method of characteristics have produced unsatisfactory results. Moreover, as stated by Bhallamudi and Chaudhry (1990), the method of characteristics is not suitable for mixture flows, which are likely to occur in high-pressure natural gas pipeline ruptures. Based on this argument, it is therefore concluded that the method of characteristics is not suitable for modelling of transients in ruptured gas pipelines.

Implicit methods are appropriate if the time step is more restricted by the stability criterion of explicit methods than accuracy requirement. Since accuracy is determined by derivatives of the solution, the application of implicit methods is likely to be successful in cases where the solution varies slowly in space and time or where the important effects propagate slowly with respect to the acoustic waves. This occurs seldom with unsteady flows where the system changes significantly with small time intervals so that larger time steps are not applicable. Implicit finite-difference schemes are more economical than the explicit finite-difference schemes and the method of characteristics, although the latter can achieve more accurate results. From the above reasoning, implicit finite-difference methods are not favourable for applications dealing with rapid transients such as in the case of a ruptured gas pipeline.

The method of Moe and Bendiksen reported before, represents a typical model for complex flow analysis incorporating aspects such as multi-phase and multi-dimensional flow. But since it is based on implicit finite-difference formulations, it is doubted as to whether it meets all the requirements for analysis of transients in a ruptured gas pipe. However, the theoretical background and the procedure used, could form a useful basis for developing a model for the particular case being addressed.

The recent applications of finite-element methods in transient compressible flow in pipelines such as the one described by Bisgaard, Sørensen and Spangenberg (1987), indicate a good potential of the methods for such applications. However, compared to finite-difference methods, the latter have considerable advantage in computation time. Adding this to the complexity of formulating the finite-element equations, especially in

unsteady gas flow in pipelines, the method becomes less favourable for such applications. Recently developed flux-difference schemes, such as the Zha-Bilgen flux-vector splitting method, appear to possess most of the properties required for analysis of transient gas flows. Also the wave-plan method looks promising as an alternative solution method, although its application on gas transients analysis is as yet unknown.

Explicit finite-difference methods including the pseudoviscosity method, the second-order two-step Lax-Wendroff method, the Alternating Gradient Method of Grimesey and Solbrig (1978) and MacCormack method and the third-order Warming-Kutler-Lomax method, are by far the most preferred. Despite being efficient and able to capture shock waves with only a slight or no overshoot problems, they can very well be suited for applications of increasing complexity such as two-phase liquid-gas and multidimensional flows and complete equations can be used. The MacCormack second-order method and the third-order Warming-Kutler-Lomax method have particularly been selected, in addition to the method of characteristics.



## CHAPTER 4

# THE COMPUTER MODEL FOR LINEBREAK ANALYSIS

## 4.1 SIMPLIFICATION OF THE BASIC EQUATIONS OF FLOW

### 4.1.1 SHOULD THE SMALL TERMS BE NEGLECTED?

There are two contradictory constraints in developing a computer model for the transient flow of compressible fluid in pipelines. On the one hand, it is required that the description of the phenomenon is accurate and on the other hand, it has to be simple enough that the computational means necessary for solving this model are reasonable. As a common practice, simplified models are sought which present a reasonable compromise between the accuracy of the description, computation time and storage requirements. Simplified models are obtained by neglecting some terms in the basic equations, based on quantitative estimations of the particular elements of the equation, for some given conditions of operation of the pipeline. Different authors have used various simplifications and have neglected or retained one term or the other. The terms which are commonly neglected in the simplification of the basic equations are the inertia or acceleration terms,  $\rho u \partial u / \partial x$ ; the convective term,  $u \partial \rho / \partial x$ ; and the gravity term  $\rho g \sin \theta$ . To decide which terms may be neglected, magnitudes for each term for characteristic values of the variable are needed.

By considering a high-pressure transmission line, where the dynamic variations are determined by the fluctuations in demand with significant changes occurring on the time scale of hours, Goldwater and Fincham (1981) concluded that it is reasonable to neglect the inertia terms as they contribute less than one per cent of the friction term. This approximation is referred to as the creeping motion approximation. However, if the disturbances are more rapid, the values of the inertia terms in the region of the disturbances will be significant. The creeping motion approximation is therefore not likely to be satisfactory in that region, though it may still be a reasonable approximation to the gross behaviour of the whole system. Weimann (1978) concluded that the second inertia term,  $\rho u \partial u / \partial x$ , can be neglected, but the first inertia term,  $\rho \partial u / \partial t$ , should be retained if disturbances with a cycle time of less than eight minutes are important.

Assuming steady-state conditions and using a steady-state flow computation procedure, Osiadacz (1987) calculated the approximate values of the particular terms of the momentum equation. His results showed that the first inertia term, second inertia term,



gravity term and the friction term, amounted to 0.170 to 3.407%, 0.053%, 6.424% and 145.9% respectively; of the term describing the pressure drop along the pipe. The majority of workers have neglected the second inertia term, but have retained the first term. Goldwater and Fincham (1981) stated that this decision is influenced by the convenience of this approximation in applying the method of characteristics. Kiuchi (1993) argued that the second inertia term can be eliminated by assuming that the convective term is negligible, and the flow velocity is small compared to the speed of sound. He justified his assumption by the observation by Guy (1967) that for most cases of operations in actual gas pipelines, the ratio of the values of the pressure term : first inertia term : the second inertia term is approximately 1:0.1:0.01. However, in the case of high flow velocity, where the above assumption is not valid he recommended that the energy equation should be considered because of the Joule-Thompson effect. A strong argument for retention of both the inertia terms was put forward by Rachford (1972) and again by Rachford & Dupont (1974), on the basis that their deletion is justified where models are used only to simulate slow transients.

A simplification whereby the convective term has been neglected is known as the acoustic approximation. Lavooij and Tijsseling (1990) argued that the convective term can be neglected if the fluid velocity is much smaller than the propagation speed of the pressure waves. Moe and Bendiksen (1993) used the dambreak problem to illustrate the importance of the horizontal convective term, in the momentum equation, on the numerical diffusion. The gravity term is neglected in simplifications whereby it is assumed that the pipeline is horizontal. The majority of workers have used this approximation in their models. Flatt (1993-1996) argued, by using the momentum equation of a stationary one-dimensional flow with friction and gravity terms included, that for a typical pipe flow situation, the influence of the gravity term is small compared to that of the frictional effects. He argued that since the friction factor is not known accurately, the error made by neglecting the gravity term is less important than the error in the friction factor plus the error due to the one-dimensional flow assumption. For unsteady flow, the uncertainty on the friction factor is actually very large. He noted the case of two-phase flow is a totally different one as gravity affects even horizontal flows. Such flows are extremely sensitive to how well the two phases are mixed. Gravity, having the tendency to unmix the liquid and gaseous components, can result in a significant error in the solution. However, this later effect is not taken into account in the simplified model used in this study.



Two other terms in the basic equations which need to be considered are the term  $u\partial H/\partial x$  for the geometric variation of the pipe cross-sectional area, and the term  $u\partial \rho/\partial x$  for variation in cross-sectional area of the pipe due to the elasticity of the pipe material. For high-pressure gas pipelines, where thick walled and uniform diameter pipes are used, these terms are normally omitted. However, some workers including Flatt (1989) and Beauchemin & Marche (1992), have included these terms. In the study by Tiley (1989); all the four terms discussed earlier i.e. the two inertia terms, the convective term and the gravity term; were included. This was despite the fact that the method of characteristics was used for numerical solution of the basic equations. However, the model did not take into consideration the terms representing the variation of the pipe cross-sectional area. Exaggerated simplification of the basic equations may lead to distorted understanding of reality and false conclusions. On the other hand if the model is too complicated, it may prove impractical. Following on from the foregoing argument, it is concluded that the three basic partial differential equations will be used in their "accurate" form i.e. Equations (2.6), (2.7) and (2.29) with the exception that the term for variation of cross-section area i.e.  $\xi$  is set to zero. In addition the pipe diameter is assumed to be uniform i.e.  $\cos\psi = 1$ . The resolution equations are as follows:

#### Continuity equation

$$\frac{\partial \rho}{\partial t} + u \frac{\partial \rho}{\partial x} + \rho \frac{\partial u}{\partial x} = 0 \quad (4.1)$$

#### Momentum equation

$$\frac{\partial u}{\partial t} + \frac{1}{\rho} \frac{\partial p}{\partial x} + u \frac{\partial u}{\partial x} = - \frac{\omega}{\rho A} - g \sin \theta \quad (4.2)$$

#### Energy equation

$$\frac{\partial p}{\partial t} + u \frac{\partial p}{\partial x} + a^2 \rho \frac{\partial u}{\partial x} = \frac{1}{A} (\delta_s - 1)(\Omega + \omega u) \quad (4.3)$$

### 4.1.2 SOLUTION PROCEDURE

The basic partial differential form of the three conservation equations are to be solved using a suitable numerical method. Different workers have used different approaches in manipulating and solving such equations. Cronje, Bishnoi and Svrcek (1980) developed the three equations of conservation in a very similar manner to the one used in this study. They

used the thermodynamic relationships for a perfect gas to obtain a set of transformed equations, which were then solved numerically. Van Deen and Reintsema (1983) reduced the three conservation equations and the equation of state into two partial differential equations (with respect to pressure, velocity and temperature), which were then solved numerically. By introducing the so-called molar flow and substituting it to the continuity and momentum equations, Osiadacz (1987) reduced the two equations into one second-order partial differential equation.

As it can be seen above, there are various ways of manipulating the basic conservation equations, which could result in different numbers and forms of the equations. However, the majority of workers have used the basic equations (after the simplifications discussed in Section 4.1.1), without manipulating or combining them as shown above. For the case of non-isothermal flow, an equation of state is added (in some cases combined with the conservation equation). The basic principle in manipulating these equations is to ensure mathematical consistency, i.e. the number of equations should be the same as the number of unknown dependent variables.

It has already been stated, in Section 2.3, that the three equations of conservation have been developed in a way which enables them to be valid for real (or perfect) gas homogeneous liquid-vapour mixtures and pure liquids. The form of the equations is almost identical to the one required for a perfect gas, which simplifies considerably computer codes and can deal with problems where several of these three fluid forms appear simultaneously. The three equations of conservation contain three dependent variables, namely  $p$ ,  $u$  and  $\rho$ . In addition,  $T$ , which is also required in calculating  $\Omega$ , needs to be determined. This necessitates the addition of another equation, the equation of state, in order to ensure mathematical consistency. These four equations will be solved simultaneously by a computer, using a suitable numerical scheme. In Section 2.4, a detailed discussion is made of the available options which can represent the equations of state. This work will be greatly simplified if one of the computer software packages available is obtained and used as a sub-routine of the main programme. The QUANT software is strongly recommended because apart from the usual thermodynamic and transport properties of the gas, it also gives the values of the partial derivatives  $\alpha_p$ ,  $\beta_v$ ,  $\gamma_T$ ,  $\gamma_s$  and  $\delta_s$  required for the  $\gamma\delta$  method, which is used in this study.

The Chen expression for friction factor [equation (C-5)] is used to account for the friction losses. The formula for unsteady friction loss based on wall shear stress has been found unsuitable for this study because it requires two-dimensional flow consideration. Also the two-phase friction multiplier has not been used at this stage. Using the two-phase



friction multiplier, the expression for the friction term becomes

$$\omega = \frac{A}{d} \rho f_D \frac{u|u|}{2} \Phi^2 \quad (4.4)$$

where  $\Phi^2$  is the multiplier for two-phase flow. The heat transfer is calculated using the recovery factor and adiabatic wall temperature method. The fluid properties used to calculate both the friction force and heat transfer are flow dependent, rather than the constant value Reynolds and Stanton numbers used by Tiley (1989).

### 4.1.3 REPRESENTATION OF NON-LINEAR TERMS

The basic equations for the unsteady flow of fluid in pipelines contain terms which cannot be represented directly by finite differences. These terms are the pipe friction term, the second inertia term, the convective term, and the term representing the geometric variation of cross-sectional area. Some workers have avoided this problem by neglecting as many of the above terms as possible. However, finite-difference methods can take into account these non-linearities in the basic partial differential equations, which are neglected in the linear transfer techniques but which do have an influence on the flow. A second-order approximation is used to calculate the frictional force.

## 4.2 INITIAL AND BOUNDARY CONDITIONS

### 4.2.1 INTRODUCTION

Partial differential equations are classified according to their order as first-, second-order etc.; as either linear, or quasi-linear or non-linear; and either elliptic, or parabolic, or hyperbolic. The criteria for this classification is explained in most literature dealing with partial differential equations, including Ames (1977), Hoffman (1989) and Lapidus & Pinder (1982). Further classification is made through the engineering and physical problems described by these partial differential equations as either equilibrium (boundary value), or eigenvalue, or propagation (initial value) problems; according to the type of initial and boundary conditions existing. Equilibrium problems are problems of steady-state nature. Very often, but not always, the integration domain is closed and bounded. The governing equations for equilibrium problems are elliptic. Eigenvalue problems may be thought of as extensions of equilibrium problems, wherein critical values of certain parameters are to be determined in addition to the corresponding steady-state configurations. Propagation

problems are initial value problems that are unsteady-state or transient by nature. Prediction of subsequent behaviour of the system, given the initial steady-state, is achieved by solving the differential equation within the domain when the initial steady-state is prescribed and subject to prescribed conditions on the boundaries. The integration domain is open. The problem of propagation of pressure waves in fluids, falls under the classification of propagation or initial value problems. Propagation problems are described by parabolic and hyperbolic partial differential equations.

In order to obtain a unique solution to a partial differential equation, a set of supplementary (initial and boundary conditions) must be provided, in order to determine the arbitrary functions which result from the integration of the partial differential equations. An initial condition is a requirement that the dependent variable is specified at some initial state. A boundary condition is a requirement that the dependent variable or its derivative must satisfy at the boundary of the domain of the partial differential equation. Four different types of boundary conditions are distinguished, namely the Dirichlet, Neumann, Robin and mixed boundary conditions. In the Dirichlet boundary conditions, the dependent variable is prescribed along the boundary; in the Neumann boundary condition, the normal gradient of the dependent variable along the boundary is prescribed; in the Robin boundary condition, the imposed boundary condition is a linear combination of Dirichlet and Neumann types; and in mixed boundary conditions, the boundary condition along a certain portion of the boundary is frequently of the Dirichlet type and on another portion of the boundary is of the Neumann type.

The initial condition is the steady-state condition in the pipe prior to the initiation of unsteady flow. The initial conditions are also specified at the boundaries at the initial time. Boundary conditions require values only at full node points (points which have an integral number in the spatial index) and do not involve any tentative locations. Lyczkowski, Grimesey and Solbrig (1978) stated that when the numerical scheme is of the higher order than the differential equations, as is often the case, more boundary conditions are required for the partial difference equations than for the partial differential equations. The additional conditions are referred to as missing boundary conditions. However, the theory of characteristics applied to differential equations restricts the boundary conditions which may be specified. The boundary conditions which can be prescribed are inlet (upstream), outlet (downstream) and closed boundary conditions. Missing boundary conditions only occur for the inflow boundary. This additional information is obtained by



extrapolating from the interior. At an inflow boundary, the theory of characteristics permits only two items to be specified; and for an outflow boundary, only one item can be specified. Only a zero velocity may be specified at a closed boundary, in the case of gas flow. For liquid flow, cavitation can occur and for a vapour condensation may occur.

When flow reversal occurs at a boundary which was initially prescribed to be an outflow boundary, the pressure at the boundary remain the same. However, the internal energy at the inflow boundary that was previously at the outflow boundary becomes the internal energy from the previous time step. In the case of ruptures in pipelines, boundary conditions are specified at the break. As already stated in Chapter 3, one of the main advantages of the method of characteristics is that the boundary conditions are properly posed. Moreover, when using finite-difference methods of higher than first-order, it is not possible to solve the boundary nodes directly. Beauchemin and Marche (1992) gave the two methods which are generally used in conjunction with the MacCormack scheme. The first method involves using the appropriate characteristic equation at each boundary. The second method involves extrapolation of interior fluxes at fictitious calculation nodes beyond the boundaries. The presence of these fictitious nodes permits differencing in both directions even at the boundaries. The use of characteristic equations is preferred to the flux extrapolation method because the former method generally yields better overall results. When using a third-order scheme, it is only possible to solve for nodes  $j = 3, 4, \dots, N-2$ ; where  $N$  is the number of reaches. In this situation, a second-order scheme without the third level is used at the nodes adjacent to the boundary.

## **4.2.2 STEADY STATE ANALYSIS**

### **4.2.2.1 Basic Equations for Steady State Flow**

The details of the programmes developed in this study are given in Section 4.6. After prompting for system data and in the case of variable grid size generating the distance grid, steady state analysis is performed for all the distance grid points in both the upstream and downstream sections of the pipe. Two separate programmes have been written one for each of the pipe sections. The programme for the downstream section depends on data calculated by the programme for the upstream section. This makes it necessary for the former programme to be run in succession to the latter programme.

The steady state model assumes a fully developed flow, with the fluid properties being known at the initial grid point. The basic equations for steady state flow analysis are derived from the basic equations for unsteady flow (Equations (4.1), (4.2) and (4.3)). All the partial derivatives with respect to  $t$  are set to zero, thus resulting in ordinary differential equations with respect to  $x$ . Assuming that the cross-section area of the pipe is constant, the three ordinary differential equations are as follows:

**Continuity equation:**

$$u \frac{d\rho}{dx} + \rho \frac{du}{dx} = 0 \quad (4.5)$$

**Momentum equation:**

$$\frac{dp}{dx} + \rho u \frac{du}{dx} + \left( \frac{\omega}{\rho A} + g \sin \theta \right) \rho = 0 \quad (4.6)$$

**Energy equation:**

$$\frac{dp}{dx} + \rho \frac{a^2}{u} \frac{du}{dx} - \frac{1}{A} (\delta_s - 1) \left( \frac{Q}{u} + \omega \right) = 0 \quad (4.7)$$

In addition to the above three equations, the QUANT software is used to calculate the thermodynamic and transport properties of the fluid. Also the equation of state can be used in any form which is convenient for the type of assumptions used. Given the fluid properties at one grid point, the equations are solved simultaneously to obtain the properties at the next grid point. Four different models all of which assume viscous flow, were developed in this study. The models are an incompressible flow model and three compressible flow models based on isothermal, adiabatic and non-isothermal non-adiabatic flow assumptions.

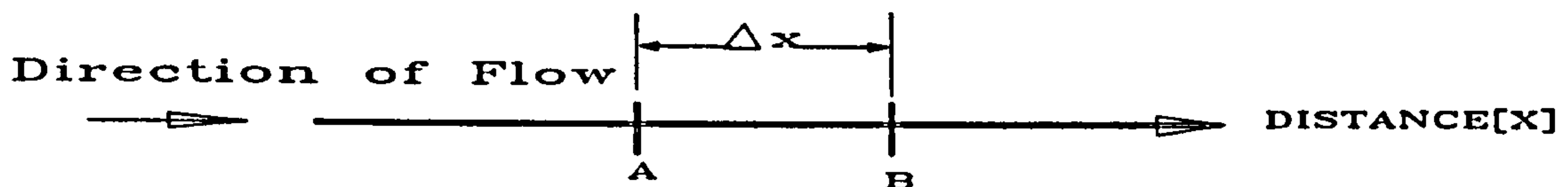


Fig. 4.1 Grid Mesh for Steady State Analysis

Three numerical methods of solution are compared (only for incompressible adiabatic flow assumption). The methods are first-order backward, first-order forward and second-order finite difference methods. For the rest of the flow assumptions only the first-order backward finite difference method is used. After calculating  $p$ ,  $u$  and  $\rho$ ; the temperature of the fluid is calculated using either the QUANT software or the general equation of state [equation (B-2)]. The speed of sound is calculated using either equation (A-10) or (A-11), depending on the assumptions made.



#### 4.2.2.2 Incompressible Flow

The incompressible flow assumption means that

$$\frac{d\rho}{dx} = 0$$

which according to the continuity equation (4.5) implies that

$$\frac{du}{dx} = 0$$

From the momentum equation (equation (4.6))

$$\frac{dp}{dx} = - \left( \frac{\omega}{\rho A} + g \sin \theta \right) \rho$$

In one variation of the model, it is assumed that temperature is constant i.e. isothermal flow while in another variation an adiabatic flow is assumed. In both the variations, numerical analysis is performed using a finite-difference method in which the fluid properties at the previous grid point are used to calculate the new fluid properties at the new grid point. This numerical method is referred to as the backward difference method, and is of the first-order of accuracy. Using this method and referring to Fig. 4.1, the pressure difference between the two points is given by the following equation:

$$\Delta p = - \left( \frac{\omega}{\rho A} + g \sin \theta \right) \rho \Delta x \quad (4.8)$$

$\rho$  and  $u$  are constant for both the isothermal and adiabatic models and  $T$  is also constant for the isothermal model. The temperature drop in the adiabatic model is obtained by differentiating the equation of state [equation (B-2)]. The resulting equation is as follows:

$$dp = Z R \rho dT$$

Rearranging the above equation, we get:

$$dT = \frac{dp}{Z R \rho}$$

which in finite differences becomes

$$\Delta T = \frac{\Delta p}{Z R \rho} \quad (4.9)$$

#### 4.2.2.3 Isothermal Compressible Flow

From the continuity equation (equation (4.5))

$$d\rho = - \rho \frac{du}{u} \quad (4.10)$$

and from the momentum equation (equation (4.6))

$$dp = - \left[ \rho u du + \left( \frac{\omega}{\rho A} + g \sin \theta \right) \rho dx \right] \quad (4.11)$$

Differentiating the equation of state (equation (B-2)), with respect to  $\rho$ , we get:

$$d\rho = \frac{dp}{Z R T} \quad (4.12)$$

Equating the right hand side of equations (4.10) and (4.11) results in the following equation:

$$\frac{dp}{Z R T} = - \rho \frac{du}{u}$$

and rearranging we get

$$du = - \frac{u}{\rho Z R T} dp \quad (4.13)$$

Substituting equation (4.13) into equation (4.11), results in the following equation:

$$dp = - \left[ - \frac{\rho u^2}{\rho Z R T} dp + \left( \frac{\omega}{\rho A} + g \sin \theta \right) \rho dx \right]$$

which upon solving for  $dp$  gives

$$dp = - \frac{\left( \frac{\omega}{\rho A} + g \sin \theta \right)}{\left( 1 - \frac{u^2}{Z R T} \right)} \rho dx$$

Based on the proceeding equations and referring to Fig. 4.1, the finite difference equations based on the fluid properties at the previous grid point are as follows:

$$\Delta p = - \frac{\left( \frac{\omega}{\rho A} + g \sin \theta \right)}{\left( 1 - \frac{u^2}{Z R T} \right)} \rho \Delta x \quad (4.14)$$

$$\Delta u = - \frac{u}{\rho Z R T} \Delta p \quad (4.15)$$

$$\Delta \rho = - \frac{\rho}{u} \Delta u \quad (4.16)$$

and  $T$  is constant.



#### 4.2.2.4 Adiabatic Compressible Flow

Equations (4.10) and (4.11) are also used for this model. In addition, the equation of state for adiabatic flow is used. The equation is as follows:

$$p = \rho^n \quad (4.17)$$

where  $n$  is the polytropic coefficient of the gas. Expressing equation (4.17) in natural logarithms we get the following:

$$\ln p = n \ln \rho$$

Assuming  $n$  is constant and differentiating we get:

$$\frac{dp}{p} = \frac{n}{\rho} \frac{d\rho}{\rho} \quad (4.18)$$

Similarly from equation (B-2) and assuming that  $Z$  is constant.

$$dT = \left( \frac{dp}{p} - \frac{d\rho}{\rho} \right) T \quad (4.19)$$

Three different numerical methods are used, in this thesis, to solve the four differential equations (4.10), (4.11), (4.18) and (4.19). The three methods differ in the properties of the fluid used to calculate the dependent variables at the new grid point i.e. point B in Fig. 4.1. In the first method, the fluid properties used are those at the previous grid point (point A). This method is referred to as first-order backward difference method. In the second method, the properties used are those at the new grid point (point B) and the method is called first-order forward difference method. The third method, is referred to as a second-order difference method and uses the average of the properties at the previous and new grid points i.e. points A and B respectively in Fig. 4.1. A comparison is made between the three models with regard to their accuracy, and simplicity. Since most of the data used are for relatively short pipelines and zero initial flow velocity, it is generally found that there is not much difference in the results from the three methods to justify further investigation and validation. The first-order backward method was selected for use in all the steady state analysis programmes, especially because of its simplicity. Also since the steady state model is by itself a very inaccurate representation of the flow of gas in high-pressure pipelines, it is concluded that there is no justification for using a more accurate numerical method. However, for longer pipelines and flow velocities which are significantly greater than zero, variations in the results from the three numerical methods are expected.

### (a) First-order Backward Difference Method

In this method, the dependent properties of the gas  $p$ ,  $u$ ,  $\rho$  and  $T$ ; are calculated based on the properties of the gas at the previous grid point. The four differential equations (4.10), (4.11), (4.18) and (4.19) are used to derive the finite-difference equations for this method.

From equations (4.10) and (4.18)

$$\Delta u = -\frac{u}{n} \frac{\Delta p}{p} \quad (4.20)$$

From equations (4.11) and (4.20):

$$\Delta p = \frac{\left( \frac{\omega}{\rho A} + g \sin \theta \right)}{\left( \frac{\rho u^2}{n p} - 1 \right)} \rho \Delta x \quad (4.21)$$

and

$$\Delta \rho = -\rho \frac{\Delta u}{u} \quad (4.22)$$

or

$$\Delta \rho = \frac{\rho}{n} \frac{\Delta p}{p} \quad (4.23)$$

From equation (4.19)

$$\Delta T = \left( \frac{\Delta p}{p} - \frac{\Delta \rho}{\rho} \right) T \quad (4.24)$$

Alternatively, equation (4.12) could be used instead of equation (4.18), in which case equations (4.20) and (4.21) would be replaced by equations (4.15) and (4.14) respectively. The other thermodynamic and transport properties of the fluid are also calculated, based on the state of the fluid at the previous grid point.

### (b) First-order Forward Difference Method

Calculation of the four dependent gas properties  $p$ ,  $u$ ,  $\rho$  and  $T$  at the new grid point is effected using values of the same properties at the new grid point. But in this study, the other thermodynamic properties and also the transport properties used are based on the previous grid point. Equation (4.6) expressed in finite differences is as follows:

$$\Delta p + (\rho + \Delta \rho) (u + \Delta u) \Delta u + (\rho + \Delta \rho) l \Delta x = 0 \quad (4.25)$$

where

$$l = \frac{\omega}{\rho A} + g \sin \theta \quad (4.26)$$

Equations (4.23) and (4.20) are used to calculate  $\Delta \rho$  and  $\Delta u$  respectively.



**Calculation of  $\Delta p$ :**

$$\begin{aligned}
 \Delta p &= \frac{(p+\Delta p)}{n} \frac{\Delta p}{(p+\Delta p)} = \frac{p \Delta p}{n(p+\Delta p)} + \frac{\Delta p \Delta p}{n(p+\Delta p)} \\
 \Delta p \left( 1 - \frac{\Delta p}{n(p+\Delta p)} \right) &= \frac{p \Delta p}{n(p+\Delta p)} \\
 \Delta p &= \frac{p \Delta p}{n(p+\Delta p) \left( 1 - \frac{\Delta p}{n(p+\Delta p)} \right)} = \frac{n(p+\Delta p) p \Delta p}{n(p+\Delta p)[n(p+\Delta p) - \Delta p]} \\
 \Delta p &= \frac{p \Delta p}{n p + (n-1) \Delta p} \quad (4.27)
 \end{aligned}$$

**Calculation of  $\Delta u$ :**

$$\begin{aligned}
 \Delta u &= -\frac{(u+\Delta u)\Delta p}{n(p+\Delta p)} \\
 &= -\frac{u \Delta p}{n(p+\Delta p)} - \frac{\Delta u \Delta p}{n(p+\Delta p)} \\
 \Delta u \left( 1 + \frac{\Delta p}{n(p+\Delta p)} \right) &= -\frac{u \Delta p}{n(p+\Delta p)} \\
 \Delta u &= -\frac{u \Delta p}{n(p+\Delta p) \left( 1 + \frac{\Delta p}{n(p+\Delta p)} \right)} \\
 \Delta u &= -\frac{u \Delta p}{n(p+\Delta p) + \Delta p} \\
 \Delta u &= -\frac{u \Delta p}{n p + (n+1) \Delta p} \quad (4.28)
 \end{aligned}$$

**Calculation of  $\Delta p$ :**

Equations (4.27) and (4.28) are substituted into equation (4.25) and rearranged to form a polynomial function in  $\Delta p$ . The polynomial is solved for  $\Delta p$ , which is then substituted into equations (4.27) and (4.28) to obtain  $\Delta p$  and  $\Delta u$  respectively. Substituting equations (4.27) and (4.28) into (4.25) we get:

$$\Delta p + \left[ \left( \rho + \frac{\rho \Delta p}{np + (n-1)\Delta p} \right) \left( u - \frac{u \Delta p}{np + (n+1)\Delta p} \right) \left( - \frac{u \Delta p}{np + (n+1)\Delta p} \right) \right] + \left( \rho + \frac{\rho \Delta p}{np + (n-1)\Delta p} \right) l \Delta x = 0$$

Multiplying throughout by  $[np + (n-1)\Delta p]$  and  $[np + (n+1)\Delta p]^2$

$$\{[np + (n-1)\Delta p][np + (n+1)\Delta p]^2 \Delta p\} + \{[np + (n-1)\Delta p] \rho + \rho \Delta p\} \{[np + (n+1)\Delta p] u - u \Delta p\} \{-u \Delta p\} + \{[np + (n-1)\Delta p][np + (n+1)\Delta p]^2 \rho + [np + (n+1)\Delta p]^2 \rho \Delta p\} l \Delta x = 0 \quad (4.29)$$

Equation (4.29) can be considered as having three terms I, II, and III on the left hand side, represented by the first, second and third lines respectively. The three terms of equation (4.29) are simplified as follows:

**Term I:**

$$\begin{aligned} I &= [np + (n-1)\Delta p][n^2 p^2 + 2np(n+1)\Delta p + (n+1)^2 (\Delta p)^2] \Delta p \\ &= [n^3 p^3 + n^2(n-1)p^2 \Delta p + 2n^2 p^2(n+1) \Delta p + 2n(n+1)(n-1)p(\Delta p)^2 + n(n+1)^2 p (\Delta p)^2 + (n-1)(n+1)^2 (\Delta p)^3] \Delta p \\ I &= n^3 p^3 (\underline{\Delta p}) + n^2(n-1)p^2 (\underline{\Delta p})^2 + 2n^2 (n+1)p^2 (\underline{\Delta p})^2 + 2n(n+1)(n-1)p(\underline{\Delta p})^3 + n(n+1)^2 p(\underline{\Delta p})^3 + (n+1)^2(n-1)(\underline{\Delta p})^4 \end{aligned} \quad (4.30)$$

**Term II:**

$$\begin{aligned} II &= [np\rho + (n-1)\rho \Delta p + \rho \Delta p][np u + (n+1)u \Delta p - u \Delta p][-u \Delta p] \\ &= (np\rho + n\rho \Delta p)(np u + nu \Delta p)(-u \Delta p) \\ &= -u \Delta p[n^2 p^2 \rho u + n^2 p \rho u \Delta p + n^2 p \rho u \Delta p + n^2 \rho u (\Delta p)^2] \\ II &= -n^2 u^2 \rho (\underline{\Delta p})^3 - 2n^2 u^2 \rho p (\underline{\Delta p})^2 - n^2 u^2 \rho p^2 (\underline{\Delta p}) \end{aligned} \quad (4.31)$$

**Term III:**

$$\begin{aligned} III &= [n^2 p^2 + 2n(n+1)p \Delta p + (n+1)^2 (\Delta p)^2][np + (n-1) \Delta p + \Delta p]\rho l \Delta x \\ &= [n^2 p^2 + 2n(n+1)p \Delta p + (n+1)^2 (\Delta p)^2][np + n \Delta p]\rho l \Delta x \\ &= [n^3 p^3 + 2n^2 (n+1)p^2 \Delta p + n(n+1)^2 p(\Delta p)^2 + n^3 p^2 \Delta p + 2n^2 (n+1)p(\Delta p)^2 + n(n+1)^2 (\Delta p)^3]\rho l \Delta x \\ III &= n(n+1)^2 \rho l \Delta x (\underline{\Delta p})^3 + n(n+1)(3n+1)p\rho l \Delta x (\underline{\Delta p})^2 + n^2(3n+2)p^2 \rho l \Delta x (\underline{\Delta p}) + n^3 p^3 \rho l \Delta x \end{aligned} \quad (4.32)$$

Substituting equations (4.30), (4.31) and (4.32) into equation (4.29) we get:

$$\begin{aligned} &[(n+1)^2 (n-1)](\underline{\Delta p})^4 + [2n(n+1)(n-1)p + n(n+1)^2 p - n^2 \rho u^2 + n(n+1)^2 \rho l \Delta x](\underline{\Delta p})^3 + \\ &[2n^2 (n+1)p^2 + n^2 (n-1) p^2 - 2n^2 p\rho u^2 + n(n+1)(3n+1)p\rho l \Delta x](\underline{\Delta p})^2 + \\ &[n^3 p^3 - n^2 p^2 \rho u^2 + n^2(3n+2)p^2 \rho l \Delta x](\underline{\Delta p}) + n^3 p^3 \rho l \Delta x = 0 \end{aligned} \quad (4.33)$$



Equation (4.33) is a fourth order polynomial in  $\Delta p$  and is solved using a recipe XZRHQR4, which is a modified version of recipe XZRHQR from Press, Teukolsky, Vetterling, and Flannery (1992) and Vetterling, Teukosky, Press, and Flannery (1992). The polynomial equation (4.33) can be expressed in a simplified form as follows:

$$a_1 (\Delta p)^4 + a_2 (\Delta p)^3 + a_3 (\Delta p)^2 + a_4 (\Delta p) + a_5 = 0 \quad (4.34)$$

where the coefficients  $a_1$  to  $a_5$  are defined as follows:

$$a_1 = (n-1)(n+1)^2 \quad (4.35)$$

$$a_2 = 2n(n+1)(n-1)p + n(n+1)^2 p - n^2 \rho u^2 + n(n+1)^2 \rho / \Delta x \quad (4.36)$$

$$a_3 = 2n^2 (n+1)p^2 + n^2 (n-1)p^2 - 2n^2 p \rho u^2 + n(n+1)(3n+1)p \rho / \Delta x$$

$$a_3 = (3n+1)n^2 p^2 - 2\rho u^2 n^2 p + n(n+1)(3n+1)p \rho / \Delta x \quad (4.37)$$

$$a_4 = n^3 p^3 - n^2 p^2 \rho u^2 + n^2 (3n+2)p^2 \rho / \Delta x \quad (4.38)$$

$$a_5 = n^3 p^3 \rho / \Delta x \quad (4.39)$$

The fluid temperature is calculated using equation (4.19) as follows:

$$\begin{aligned} \Delta T &= \left( \frac{\Delta p}{p} - \frac{\Delta \rho}{\rho} \right) (T + \Delta T) \\ &= \left( \frac{\Delta p}{p} - \frac{\Delta \rho}{\rho} \right) T + \left( \frac{\Delta p}{p} - \frac{\Delta \rho}{\rho} \right) \Delta T \\ \Delta T &= \frac{\left( \frac{\Delta p}{p} - \frac{\Delta \rho}{\rho} \right) T}{1 - \left( \frac{\Delta p}{p} - \frac{\Delta \rho}{\rho} \right)} \end{aligned} \quad (4.40)$$

### (c) Second-order Difference Method

In this method, the fluid properties are based on the averages between the properties at the previous and new grid points i.e. points A and B respectively, in Fig. 4.1. Equation (4.6) expressed in finite differences for this method is as follows:

$$\Delta p + \left[ \left( u + \frac{\Delta u}{2} \right) \Delta u \left( \rho + \frac{\Delta \rho}{2} \right) \right] + \left[ l \Delta x \left( \rho + \frac{\Delta \rho}{2} \right) \right] = 0 \quad (4.41)$$

Equations (4.23) and (4.21) are used to calculate  $\Delta p$  and  $\Delta u$  respectively.

**Calculation of  $\Delta \rho$ :**

$$\begin{aligned}
 \Delta \rho &= \frac{\left(\rho + \frac{\Delta \rho}{2}\right) \Delta p}{n \left(p + \frac{\Delta p}{2}\right)} = \frac{2\rho \Delta p}{n(2p + \Delta p)} + \frac{\Delta p \Delta \rho}{n(2p + \Delta p)} \\
 \Delta \rho \left(1 - \frac{\Delta p}{n(2p + \Delta p)}\right) &= \frac{2\rho \Delta p}{n(2p + \Delta p)} \\
 \Delta \rho &= \frac{2\rho \Delta p}{n(2p + \Delta p) \left(1 - \frac{\Delta p}{n(2p + \Delta p)}\right)} \\
 \Delta \rho &= \frac{2\rho \Delta p}{n(2p + \Delta p) - \Delta p} = \frac{2\rho \Delta p}{2np + (n-1)\Delta p} \\
 \Delta \rho &= \frac{2\rho \Delta p}{2np + (n-1)\Delta p} \quad (4.42)
 \end{aligned}$$

**Calculation of  $\Delta u$ :**

$$\begin{aligned}
 \Delta u &= -\frac{\left(u + \frac{\Delta u}{2}\right) \Delta p}{n \left(p + \frac{\Delta p}{2}\right)} = -\frac{(2u + \Delta u) \Delta p}{n(2p + \Delta p)} = -\frac{(2u \Delta p + \Delta u \Delta p)}{n(2p + \Delta p)} \\
 \Delta u \left(1 + \frac{\Delta p}{n(2p + \Delta p)}\right) &= -\frac{2u \Delta p}{n(2p + \Delta p)} \\
 \Delta u &= \frac{-2u \Delta p}{n(2p + \Delta p) \left(1 + \frac{\Delta p}{n(2p + \Delta p)}\right)} = \frac{-2u \Delta p}{n(2p + \Delta p) + \Delta p} \\
 \Delta u &= \frac{-2u \Delta p}{2np + (n+1)\Delta p} \quad (4.43)
 \end{aligned}$$

**Calculation of  $\Delta p$ :**

In a similar way as for the first-order forward difference method, substitution of equations (4.42) and (4.43) into (4.41) leads to a fourth order polynomial function in  $\Delta p$ , which is also solved by the numerical recipe XZRHQR4. Substitution of equations (4.42) and (4.43) into (4.41) gives the following equation:

$$\Delta p \cdot \left[ \left( u + \frac{(-)u \Delta p}{2np + (n+1)\Delta p} \right) \left( \frac{-2u \Delta p}{2np + (n+1)\Delta p} \right) \left( \rho + \frac{\rho \Delta p}{2np + (n-1)\Delta p} \right) \right] + \left[ l \Delta x \left( \rho + \frac{\rho \Delta p}{2np + (n-1)\Delta p} \right) \right] = 0$$



**NB:** For equations (4.42) and (4.43),

$$2np + (n+1) \Delta p = n(2p + \Delta p) + \Delta p \quad \text{and}$$

$$2np + (n-1) \Delta p = n(2p + \Delta p) - \Delta p$$

Therefore multiplying throughout the above finite-difference equation by  $[2np + (n+1)\Delta p]^2$  and  $2np + (n-1) \Delta p$  we get

$$\begin{aligned} & [2np + (n-1) \Delta p][2np + (n+1)\Delta p]^2 \Delta p + \\ & \{[2np + (n+1)\Delta p]u - u \Delta p\} \{-2u \Delta p\} \{[2np + (n-1) \Delta p] \rho + \rho \Delta p\} + \\ & \{[2np + (n-1)\Delta p][2np + (n+1)\Delta p]^2 \rho / \Delta x + [2np + (n+1)\Delta p]^2 \rho / \Delta x \Delta p\} = 0 \end{aligned} \quad (4.44)$$

The above equation is split into three terms I, II and III represented by the left hand side first, second and third lines respectively. The three terms are simplified as follows:

**Term I:**

$$\begin{aligned} I &= [4n^2 p^2 + 4np(n+1)\Delta p + (n+1)^2 (\Delta p)^2][2np + (n-1)\Delta p]\Delta p \\ &= [8n^3 p^3 + 4n^2 p^2 (n-1)\Delta p + 8n^2 p^2 (n+1)\Delta p + 4np(n+1)(n-1)(\Delta p)^2 + \\ & \quad 2np(n+1)^2 (\Delta p)^2 + (n-1)(n+1)^2 (\Delta p)^3]\Delta p \\ I &= 8n^3 p^3 (\underline{\Delta p}) + 4n^2 p^2 (3n+1) (\underline{\Delta p})^2 + 4np(n+1)(n-1)(\underline{\Delta p})^3 + \\ & \quad 2np(n+1)^2 (\underline{\Delta p})^3 + (n-1)(n+1)^2 (\underline{\Delta p})^4 \end{aligned}$$

**Term II:**

$$\begin{aligned} II &= [(2np + n \Delta p + \Delta p)u - u \Delta p] \{-2u \Delta p\} [(2np + n \Delta p - \Delta p)\rho + \rho \Delta p] \\ &= (2np + n \Delta p)(-2u \Delta p)(2np\rho + n\rho \Delta p) \\ &= -[4np^2 u \Delta p + 2nu^2 (\Delta p)^2][2np\rho + n\rho \Delta p] \\ &= -8n^2 p^2 u^2 \rho \Delta p - 4n^2 u^2 p\rho (\Delta p)^2 - 4n^2 u^2 p\rho (\Delta p)^2 - 2n^2 u^2 \rho (\Delta p)^3 \\ II &= -8n^2 p^2 u^2 \rho (\underline{\Delta p}) - 8n^2 u^2 p\rho (\underline{\Delta p})^2 - 2n^2 u^2 \rho (\underline{\Delta p})^3 \end{aligned}$$

**Term III:**

$$\begin{aligned} III &= [2np + (n-1)\Delta p + \Delta p][4n^2 p^2 + 4n(n+1)p \Delta p + (n+1)^2 (\Delta p)^2]\rho / \Delta x \\ &= [2np + n \Delta p][4n^2 p^2 + 4n(n+1)p \Delta p + (n+1)^2 (\Delta p)^2]\rho / \Delta x \\ &= [8n^3 p^3 + 4n^3 p^2 \Delta p + 8n^2 (n+1)p^2 \Delta p + 4n^2 (n+1)p(\Delta p)^2 + \\ & \quad 2n(n+1)^2 p(\Delta p)^2 + n(n+1)^2 (\Delta p)^3]\rho / \Delta x \\ III &= n(n+1)^2 \rho / \Delta x (\underline{\Delta p})^3 + 2n(n+1)(3n+1)p\rho / \Delta x (\underline{\Delta p})^2 + \\ & \quad 4n^2 p^2 (3n+2) \rho / \Delta x (\underline{\Delta p}) + 8n^3 p^3 \rho / \Delta x \end{aligned}$$

Substituting the three terms I, II and III back into the original equation (4.44) we get the following equation:

$$\begin{aligned}
 & (n-1)(n+1)^2 (\underline{\Delta p})^4 + \\
 & [2np(n+1)^2 + 4np(n+1)(n-1) - 2n^2 u^2 \rho + n(n+1)^2 \rho / \Delta x](\underline{\Delta p})^3 + \\
 & [4n^2 p^2 (3n+1) - 8n^2 u^2 p\rho + 2n(n+1)(3n+1)p\rho / \Delta x](\underline{\Delta p})^2 + \\
 & [8n^3 p^3 - 8n^2 p^2 u^2 \rho + 4n^2 p^2 (3n+2) \rho / \Delta x](\underline{\Delta p}) + 8n^3 p^3 \rho / \Delta x = 0
 \end{aligned} \tag{4.45}$$

Equation (4.45) is a fourth-order polynomial in  $\Delta p$  and could also be expressed in the same form as equation (4.34). The coefficients of the polynomial are as follows:

$$a_1 = (n-1)(n+1)^2 \tag{4.46}$$

$$a_2 = 2n(n+1)^2 p + 4n(n+1)(n-1)p - 2n^2 u^2 \rho + n(n+1)^2 \rho / \Delta x \tag{4.47}$$

$$a_3 = 4n^2 (3n+1)p^2 - 8n^2 u^2 p\rho + 2n(n+1)(3n+1)p\rho / \Delta x \tag{4.48}$$

$$a_4 = 8n^3 p^3 - 8n^2 p^2 u^2 \rho + 4n^2 (3n+2)p^2 \rho / \Delta x \tag{4.49}$$

$$a_5 = 8n^3 p^3 \rho / \Delta x \tag{4.50}$$

The fluid temperature is calculated using equation (4.19) as follows:

$$\begin{aligned}
 \Delta T &= \left( \frac{\Delta p}{p} - \frac{\Delta \rho}{\rho} \right) \left( T + \frac{\Delta T}{2} \right) \\
 2\Delta T &= \left( \frac{\Delta p}{p} - \frac{\Delta \rho}{\rho} \right) 2T + \left( \frac{\Delta p}{p} - \frac{\Delta \rho}{\rho} \right) \Delta T \\
 \Delta T &= \frac{2T \left( \frac{\Delta p}{p} - \frac{\Delta \rho}{\rho} \right)}{2 - \left( \frac{\Delta p}{p} - \frac{\Delta \rho}{\rho} \right)}
 \end{aligned} \tag{4.51}$$

#### 4.2.2.5 Non-isothermal Non-adiabatic Compressible Flow

All the three basic equations for steady state flow analysis, equations (4.5), (4.6) and (4.7), are used in the non-isothermal non-adiabatic compressible flow model. The QUANT software is used to calculate the thermodynamic and transport properties of the fluid. The procedure used is as follows:

- (i) The fluid properties at the previous grid point are calculated using the QUANT software.
- (ii) Using the properties determined in (i) above,  $\Omega$  and  $\omega$  are calculated.
- (iii) Solving equations (4.5), (4.6) and (4.7) simultaneously for  $dp$ ,  $du$  and  $dp$  and transforming the resulting equations into finite-difference equations to obtain  $\Delta p$ ,



$\Delta u$  and  $\Delta p$ . In all the calculations, the fluid properties are based on the properties at the previous grid point.

(iv) Calculation of the values of  $p$ ,  $u$  and  $\rho$  at the new grid point.

(v) Repeating the procedure for the subsequent grid points.

Solution of equations (4.6) and (4.7) simultaneously, results in the following equations:

$$\frac{du}{dx} \left( \rho u - \frac{\rho a^2}{u} \right) + \left( \frac{\omega}{\rho A} + g \sin \theta \right) \rho + (\delta_{s-1}) \left( \frac{\Omega + \omega u}{A} \right) \frac{1}{u} = 0$$

$$du = - \frac{\left[ (\delta_{s-1}) \left( \frac{\Omega + \omega u}{A} \right) \frac{1}{u} + \left( \frac{\omega}{\rho A} + g \sin \theta \right) \rho \right]}{\rho u - \rho \frac{a^2}{u}} dx$$

$$du = - \frac{\left[ (\delta_{s-1}) \left( \frac{\Omega + \omega u}{A} \right) \frac{1}{u} + \left( \frac{\omega}{\rho A} + g \sin \theta \right) \rho \right]}{\rho u \left[ 1 - \left( \frac{a}{u} \right)^2 \right]} dx$$

Transforming into finite-difference equations, we get the following equation:

$$\Delta u = - \frac{\left[ (\delta_{s-1}) \left( \frac{\Omega + \omega u}{A} \right) \frac{1}{u} + \left( \frac{\omega}{\rho A} + g \sin \theta \right) \rho \right]}{\rho u \left[ 1 - \left( \frac{a}{u} \right)^2 \right]} \Delta x \quad (4.52)$$

Expressing equation (4.6) in finite differences we get the following equation

$$\Delta p = - \rho u \Delta u - \left( \frac{\omega}{\rho A} + g \sin \theta \right) \rho \Delta x \quad (4.53)$$

The temperature at the new grid point is calculated using the QUANT software.

#### 4.2.3 BREAK BOUNDARY CONDITIONS

Correct approximation of the initial values of the dependent variables,  $p$ ,  $u$ ,  $\rho$  and  $T$ , at the break point at the time of the break is equally as crucial as developing an accurate model for analysis of the transient flow which follows. No matter how accurate the transient analysis model is, it will give incorrect results if the initial break conditions are incorrect.

When a full-bore break of a pipe occurs, the gas escapes from the full area of the pipe and

the properties of the gas such as  $p$ ,  $u$ ,  $\rho$  and  $T$  change drastically. In reality, the break could be different from a full-bore break. The former is considered to be the worst situation. Although the gas properties change almost instantaneously after the break, this happens in a finite interval of time. The problem here is to find a physical model to represent this process. There have been several models to calculate the initial conditions after the break of high pressure vessels and pipelines containing gas. Some of these are presented and discussed in this section.

British Gas [Jones and Gough (1981)] developed a single-phase decompression model which assumes that when a pipeline breaks, the gas escapes from the full area of the pipe in a process that is essentially isentropic. The decompression disturbance travels back into the pipe, with each pressure level propagating at a fixed speed. At the break, the pressure level falls until the gas is escaping at sonic speed with corresponding equalisation pressure given by the following equation:

$$p_e = p_o \left( \frac{2}{K+1} \right)^{\frac{2K}{K-1}} \quad (4.54)$$

where the subscripts  $e$  and  $o$  denote equalisation pressure and initial pressure before the break respectively.

Flatt (1986) developed a homentropic decompression model which is represented in Fig. 4.2. The initial conditions before the break are calculated by the appropriate steady state and/or transient analysis programmes and are represented by curves ①-②-③ and A-B-D for  $p$  and  $u$  respectively. A sudden break at the broken end at time  $t=0s$  is accompanied by an instantaneous drop in static pressure from point 3 to a much lower pressure at point 4, corresponding to choked flow i.e.  $M_{a(x=L)} = 1$  for  $t>0s$ . The initial values  $p_e(x)$ ,  $\rho_e(x)$ ,  $a_e(x)$  and  $u_e(x)$  for  $L^1 \leq x \leq L$ , whereby the arbitrary value  $L-L^1$  may cover one or more  $\Delta x$  meshes, are calculated by equations (4.55) to (4.62) [Flatt (1986)]. The subscripts  $e$  and  $o$  are as defined earlier.

$$u_e = \left[ 1 + \left( \frac{K-1}{2} \right) \left( \frac{u_o}{a_o} \right)^2 - \left( \frac{1-\xi}{\tau_o} \right) \right] a_o \quad (4.55)$$

$$a_e = \left[ 1 - \left( \frac{K-1}{2} \right) \left( \frac{u_e - u_o}{a_o} \right)^2 \right] a_o \quad (4.56)$$



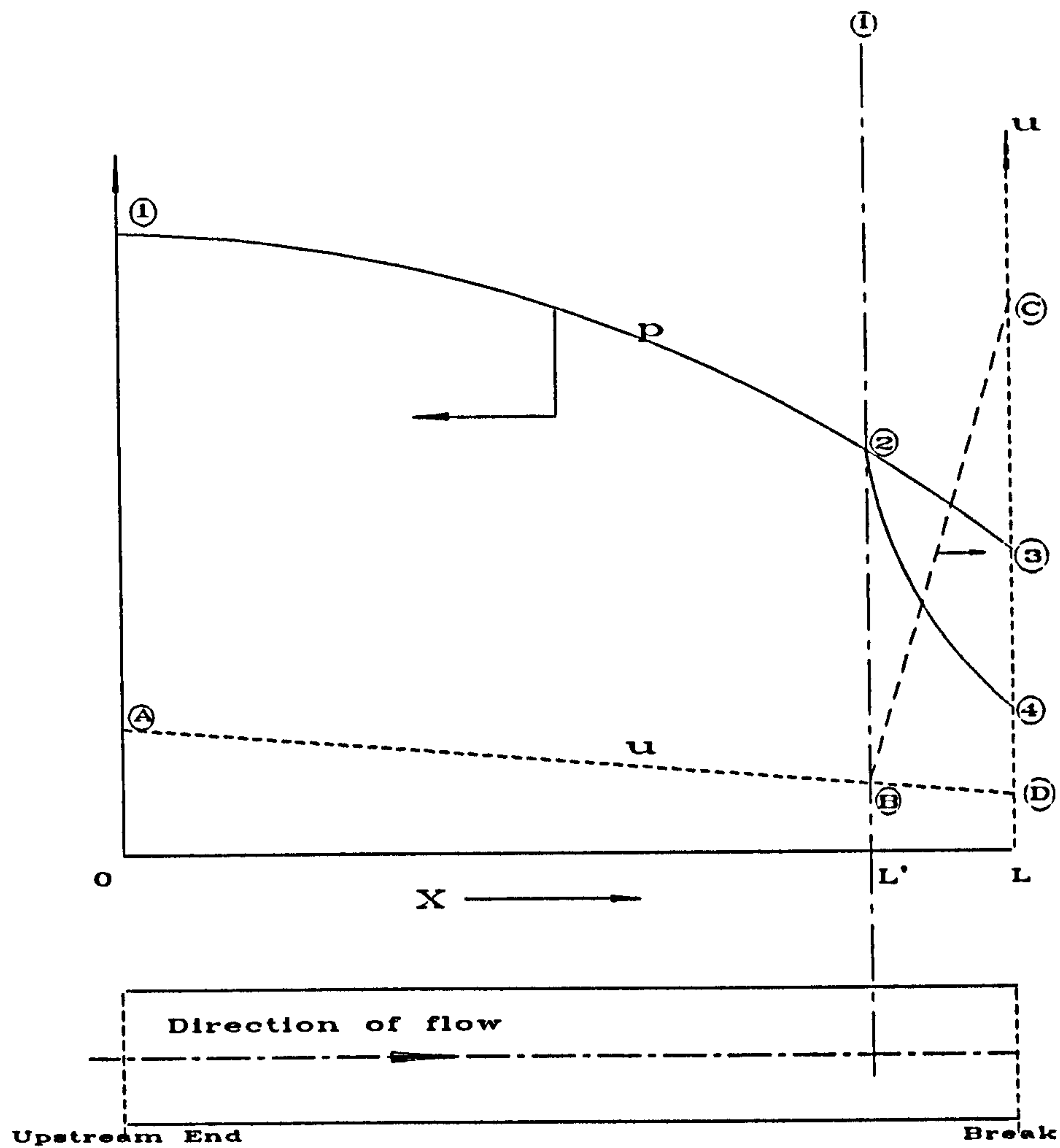


Fig. 4.2 Diagrammatic Representation of the Flatt Decompression Model

$$\rho_e = \left[ \frac{a_e}{a_o} \right]^{\frac{2}{K-1}} \left( \frac{p_o}{R T_o} \right) \quad (4.57)$$

$$p_e = \left[ \frac{a_e}{a_o} \right]^{\frac{2}{K-1}} p_o \quad (4.58)$$

where

$$a_o = \sqrt{K R T_o} \quad (4.59)$$

$$\tau_o = \frac{\Delta t'}{L} a_o \quad (4.60)$$

$$\xi = \frac{x}{L} \quad (4.61)$$

and

$$\Delta t' = \frac{L - L^1}{a_o} \quad (4.62)$$

Kunsch, Sjøen and Fanneløp (1991) developed an isothermal model which is very similar to that developed by Flatt (1986). The resulting equations for the former model are:

$$u_e = a_o - \left( \frac{x - L}{L^1 - L} \right) (a_o - u_o) \quad (4.63)$$

$$a_e = a_o \quad (4.64)$$

$$P_e = P_o + \left( \frac{u_o}{a_o} - 1 \right) \left( 1 - \left( \frac{x - L}{L^1 - L} \right) \right) \quad (4.65)$$

where

$$P = \ln p \quad (4.66)$$

Tiley (1989) used a different approach, in which linebreak was considered as the situation occurring in a shock tube when the diaphragm is suddenly ruptured. The equations for particle velocity for rarefaction wave assuming isentropic conditions and that of particle velocity of the compression wave derived by Earnshaw (1860) and Bannister and Mucklow (1948) respectively were used. The Earnshaw equation is as follows:

$$u_e = \frac{2}{K - 1} a_o \left( 1 - \left[ \frac{p_e}{p_o} \right]^{\frac{K-1}{2K}} \right) \quad (4.67)$$

and the Bannister and Mucklow equation is as follows:

$$u_e = \frac{a_a \left( \left( \frac{p_e}{p_a} \right) - 1 \right)}{\sqrt{\frac{K_a}{2} \left( (K_a + 1) \left( \frac{p_e}{p_a} \right) + (K_a - 1) \right)}} \quad (4.68)$$

The subscripts e and o are as defined before and the subscript  $a$  denote the properties at



the resulting ambient conditions (low pressure zone). The equalisation pressure,  $p_e$ , was determined by equating equation (4.67) to (4.68) and solving for  $p_e$  by iteration. Tiley (1989) also defined the critical value of the equalisation pressure as given by the following equation:

$$p_e^* = \left[ \frac{2}{K+1} \right]^{\frac{2K}{K-1}} p_o \quad (4.69)$$

All the three models discussed above, those by Flatt (1986), Tiley (1989) and Kunsch, Sjøen and Fanneløp (1991) were considered in this study. All except Tiley's iteration method were found to overestimate the equalisation pressure, thus causing severe problems with the numerical method for transient analysis after the break. Even the Tiley's equation for critical equalisation pressure overestimated the equalisation pressure. Tiley's iterative method resulted in equalisation pressure and wave speed which are lower than the critical values. Although this situation does not cause any problem with the numerical method, it results in underestimation of the initial gas outflow and therefore underestimation of the release rates and blowdown time. In addition, this method produces good results only if the low pressure zone (in this case ambient) state is defined close enough to its actual value. This requires a trial and error procedure. It should be noted that the properties on the outside of the pipe at the break are not the final ambient conditions. For example, a break problem involving a pipeline with initial conditions before the break as  $p_o=3.14\text{MPa}$ ,  $a_o=378\text{m/s}$  and  $T_o=281\text{K}$ , the speed of sound at the low pressure zone after the break is  $220\text{m/s}$  while the speed of sound at the final ambient conditions is  $399\text{m/s}$ . It has also been found that the arbitrary length  $L-L^*$ , in Fig. 4.2, of one  $\Delta x$  mesh is adequate as a starting point for transient analysis after the break.

A much simpler and more accurate method than any of the four methods discussed above is developed and used in this study. This method assumes that the flow velocity and wave speed at time  $t=0$ s after the break, at the break point ( $x=L$ ) is the same as the speed of sound at the break. In equation form, this is expressed by equations (4.63) when  $x=L$  i.e.

$$u_e = a_o \quad (4.70)$$

and equation (4.64).

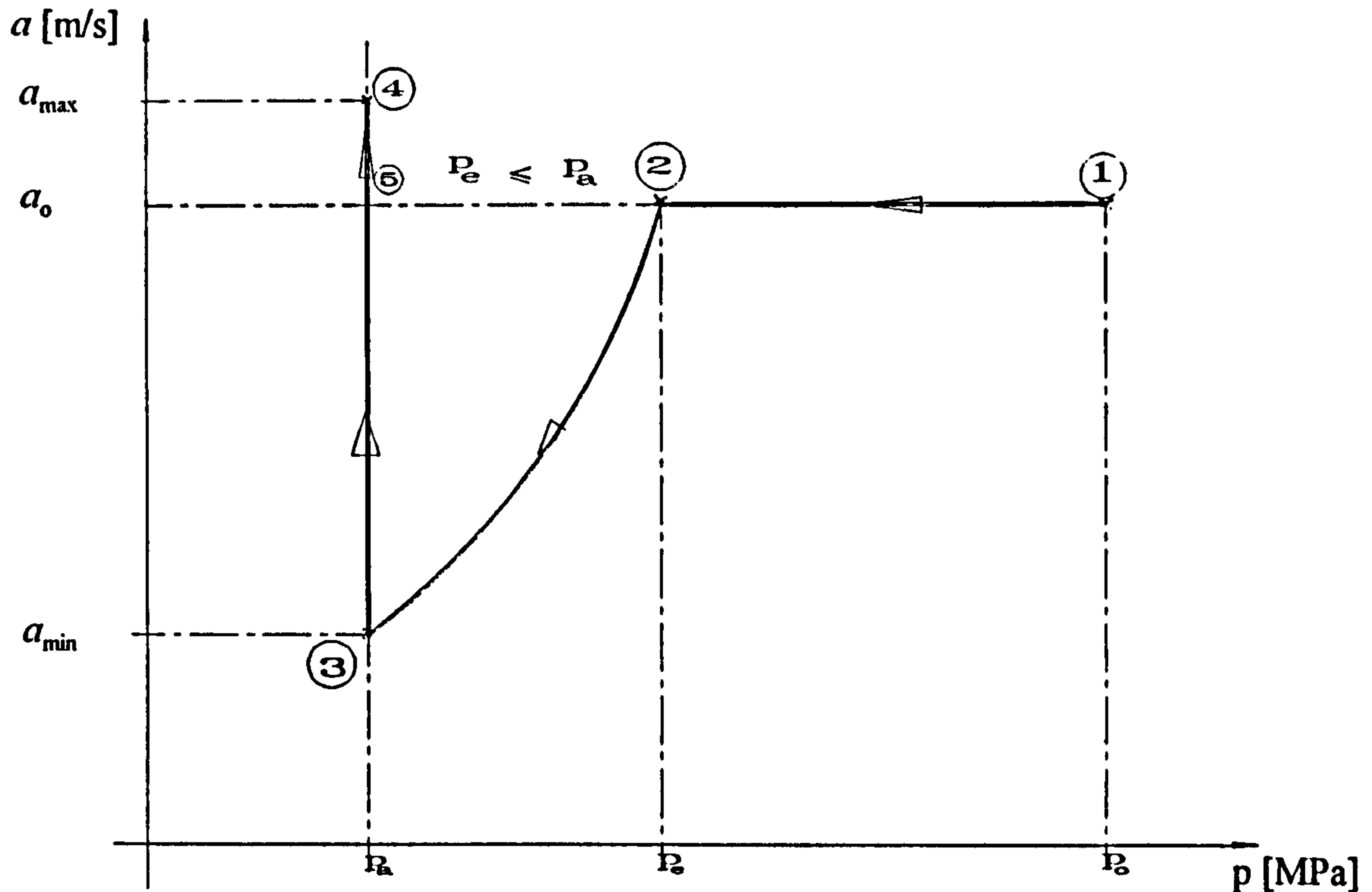


Fig. 4.3 Typical Decompression Curve at the Break Boundary

The equalisation pressure is calculated explicitly by substituting equation (4.70) into the Earnshaw equation (4.67). The resulting equation is as follows:

$$p_e = \left[ \frac{3 - K}{2} \right]^{\frac{2K}{K-1}} p_0 \quad (4.71)$$

The values calculated by equations (4.64), (4.70) and (4.71) represent the fluid properties at the critical equalisation pressure i.e. point 2 in Fig. 4.3. Using this model, the maximum possible gas flow speed is achieved and thus reducing the possibility of underestimating the gas outflow. The transient analysis programme then models the flow after the break and the state of the gas at the break point, ideally, follows the path shown in Fig. 4.3 as ①-②-③-④.

Referring to Fig. 4.3, two distinct time regimes are considered at the broken end. As long as the pressure at the boundary  $x=L$  (Refer Fig. 4.2) is higher than the external pressure, there will be choking of the flow i.e.  $M_{x=L}(t) = 1$ . When the pressure at  $x=L$  reaches the exterior pressure, the choking condition no longer holds and the boundary



condition is replaced by the condition that  $p_{x=L}(t) = p_a$ . The choking and constant pressure boundary conditions are represented by the straight lines ①-② and ③-④ respectively, of the curve in Fig. 4.3.

It could be seen clearly, from equation (4.71) that the equalisation pressure is independent of the external conditions, but finally the conditions inside the pipe (at the break) will converge to those outside the pipe, through the path shown by the curve ①-②-③-④. At the start of the break, the state outside the pipe at the break point is marked as point ③. This state represents a low wave speed resulting from the temperature drop due to the sudden pressure drop at the break. As the gas heats up, the wave speed rises to the value marked as point ④, which corresponds to the final ambient temperature. However, a situation could exist whereby the exterior pressure is greater or equal to the equalisation pressure. A typical example could be in pipes buried under water. In such cases, no choking flow would occur and the constant pressure boundary condition will be the only existing one. The resulting process would be as represented by the path ①-②-⑤-④ in Fig.4.3.

Any model which produces equalisation pressure which is higher than the critical equalisation pressure (point ② in Fig. 4.3), for the case where  $p_e > p_a$ , will suffer severe problems with the numerical analysis which follows after the break.

## 4.3 NUMERICAL SOLUTION OF THE BASIC EQUATIONS FOR UNSTEADY FLOW

### 4.3.1 INTRODUCTION

The various numerical methods for solution of the basic partial differential equations of unsteady fluid flow in a pipeline and a detailed discussion of their applications and suitability for the solution of the unsteady flow equations for a ruptured high-pressure gas pipeline are presented in Chapter 3. The shock-capturing explicit finite-difference methods of solution are preferred to the shock fitting scheme using the method of characteristics. Both Tiley (1989) and Niessner (1980) gave presentations of the basic partial difference equations for the more popular numerical methods. It is not intended to repeat this presentation here, but nevertheless a presentation will be made for those methods which are used in this study. Explicit finite-difference schemes range from the single-step first-order schemes to four-step fourth-order schemes. Explicit finite-difference methods integrate the basic partial

differential equations by considering the changes in the dependent variables along the directions of the independent variables. This produces the solution values at evenly spaced points in the physical plane.

Various explicit finite-difference schemes were presented by Thorley & Tiley (1987), Tiley (1989) and Niessner (1980). Niessner (1980) included higher-order methods. This study focuses on the MacCormack and also the non-centred third-order Warming-Kutler-Lomax method. These methods allow explicit calculation of approximate values  $A_{(i,j+1)}$  of the solution at certain node points  $(i, j+1)$  of a rectangular grid from known exact or approximate values  $A_{(i,j)}$  of the solution at another node point  $(i, j)$ , preferably belonging to the past. No eigenvectors need to be calculated. Eigenvalues are required only for testing stability conditions. Here "explicit" means that no linear or non-linear equations are to be solved. In order to write the equations for the third-order Warming-Kutler-Lomax finite-difference numerical method, the basic partial differential equations have to be expressed in the following form:

$$\frac{\partial A}{\partial t} + B \frac{\partial A}{\partial x} + C = 0 \quad (4.72)$$

The form expressed in equation (4.72) above, also applies for the method of characteristics. The form stipulated for the MacCormack method is as follows:

$$\frac{\partial(A)}{\partial t} + \frac{\partial(B)}{\partial x} = C \quad (4.73)$$

MacCormack (1971) used his method for the time dependent Navier-Stokes equations in two dimensions. The equations are linear i.e. body forces and heat transfer were neglected. However, the method can be used in situations where the basic equations are not linear as done by Beauchemin and Marche (1992) for analysis of transient flow of a compressible single-phase liquid in an elastic pipe. The basic equations in that case were quasi-linear i.e. in the same form as equation (4.72). The same approach as used by Beauchemin and Marche (1992) is used in this study.

The three basic partial differential equations (4.1), (4.2) and (4.3) can be expressed in the matrix form of equation (4.72), where the matrices A, B and C are as follows:

$$A = \begin{bmatrix} p \\ u \\ \rho \end{bmatrix} \quad (4.74)$$



$$\underline{B} = \begin{bmatrix} u & \rho a^2 & 0 \\ \frac{1}{\rho} & u & 0 \\ 0 & \rho & u \end{bmatrix} \quad (4.75)$$

$$\underline{C} = \begin{bmatrix} (1 - \delta_s) \frac{(\Omega + \omega u)}{A} \\ \frac{\omega}{\rho A} + g \sin \theta \\ 0 \end{bmatrix} \quad (4.76)$$

Before performing transient analyses, a steady state analysis has to be performed in order to establish the initial conditions (conditions at  $t = 0s$ ) in the pipeline. This could be followed by transient analysis before introducing the break boundary conditions.

The discussion in Chapter 3 concluded that explicit finite-difference methods are the most suitable for solution of the basic equations for analysis of linebreak problems. In this case the equations to be solved are equations (4.1), (4.2) and (4.3). The second order-method developed by MacCormack (1971) and the third-order method developed by Warming, Kutler and Lomax (1973) are the most preferable for this study. The method of characteristic could also be used, but it was selected for solution at the boundary points, while the MacCormack method was selected for solution at the nodes next to the boundary. The three different numerical methods of solution mentioned above are used for complete solution of the basic equations. The method of characteristics is studied in two forms namely the first-and second-order. The different methods were compared with regard to accuracy of their numerical results, stability and economy in computing resources.

### 4.3.2 METHOD OF CHARACTERISTICS

The theory of the method of characteristic is very well known and documented. It is therefore not intended to repeat it in this study. For more details on the method, the reader is referenced to among others Courant and Friedrichs (1948), Hartree (1955), Lister (1960) and Ames (1977). The major weakness of the natural method of characteristics arises in the event that spatial distribution of the dependent variables are required at fixed time. This is normally the case in many fluid transient flow analyses. In such cases, a two-dimensional

interpolation in the characteristic net would be necessary and it could be complicated depending upon the form of the equations. However, the problem can be avoided by using hybrid methods, which define the mesh points in advance in space and time. In the hybrid methods, the interpolation is done as computation advances and consequently the interpolation becomes one-dimensional.

Two common hybrid methods are those by Courant, Isaacson and Rees (1952) which is a first-order method and Hartree (1955) which is a second-order method. According to Ames (1977) the Hartree method is more accurate than the Courant-Isaacson-Rees method. Ames (1977) also stated that the former method could be applied to second-order systems with only minor changes. Referring to Fig. 4.4, the hybrid method starts by assuming that the solution is known at the mesh points on time level  $t$ . The intersections of the characteristic lines with the time level  $t$  line i.e. points Q, R and S are unknown. These together with the values of the dependent variables at point P are determined using the characteristic and compatibility equations. Interpolation for the values of the dependent variables and the positions of points Q, R and S is necessary at each step.

The first step in the method of characteristics solution is to convert the basic partial differential equations of flow into ordinary differential equations. Two most common methods of achieving this are the matrix transformation method, such as the one used by Tiley (1989) and that of multiplying the basic equations by an unknown parameter and summing them. The latter method was used by Lister (1960), Wylie and Streeter (1978) for isothermal flow (only two equations) and by Zucrow and Hoffman (1977) for non-isothermal flow (three equations). The method used by Zucrow and Hoffman (1977) is adapted for this study because of its simplicity, mathematical rigour and also because the equations used in this study are very similar to those used by Zucrow and Hoffman (1977).

The common practice in the method of characteristics solution is to use first-order and linear approximations to calculate values at the next time level. Values obtained in the first-order calculation are used as initial estimates for the iterative solution in the second-order approximation. In the case of hybrid methods, the first step is to find the positions of the intersections of the characteristic curves with the distance axis at time  $t$ , point Q, R, and S. This also could be done using either first- or second-order approximation. Tiley (1989) used linear interpolation to determine the intersection points Q, R and S, based on values of  $u$  and  $a$  which were averaged between the respective surrounding grid points for each of the characteristic curves. First-order approximation was used to calculate the



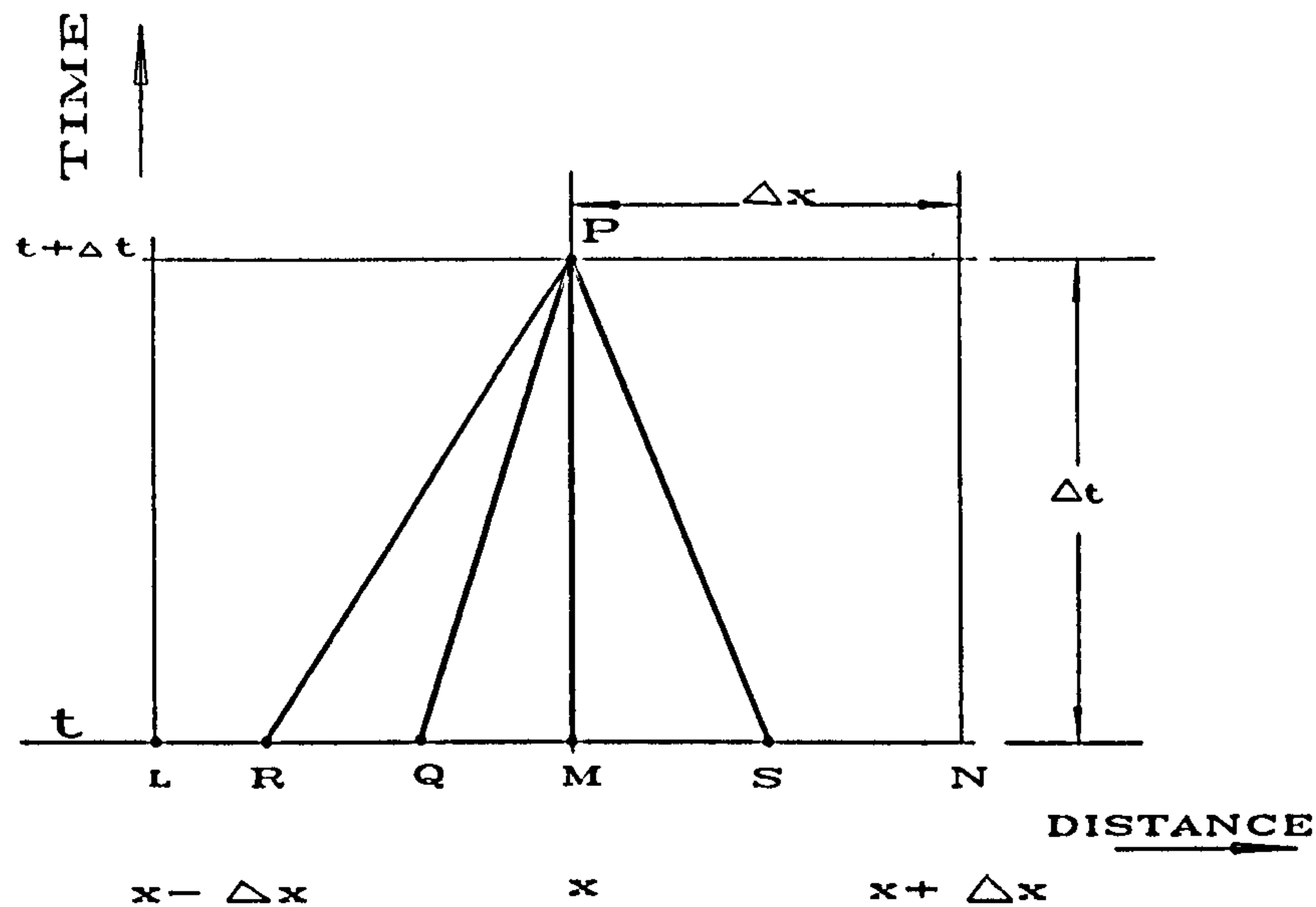


Fig. 4.4 Hybrid Method of Characteristics Solution Grid

properties of the fluid at the next time step i.e. the interaction of the characteristic curves or point P in Fig. 4.4. New positions of points Q, R and S were defined using the previously calculated intersection points and the newly calculated point P. Taylor's theorem was used to derive equations for quadratic interpolation so that new values of the fluid properties could be calculated at the bases of the characteristics. These values were then averaged with the predicted values obtained from the first-order approximation or previous second-order approximations. The results were used as variables in the characteristic and compatibility equations.

There are other methods which have been developed for application in the method of characteristics, with the aim of simplifying the process, improving accuracy and reducing computation costs. For example, Flatt (1985) developed a singly-iterative second-order method which was based on the use of curved characteristic lines within each numerical space-time mesh. No iteration was needed in determining points Q, R and S. Iteration was required only in determining the values at the next time level. Flatt (1985) claimed that with his algorithm, the overall procedure needed only a single iteration and was as good as a second-order method, giving more accurate results with less computing time.

In this study, both the first- and second-order approximations are used in succession and taking full advantage of the flexibility of the C programming language. Different subroutines have been written for each of the two orders of approximation. For the first-order method, points Q, R and S are calculated using the characteristic equations and the

values of  $u$  and  $a$  at point  $M$  initially, and the averages between the values at  $M$  and those estimates at  $P$  in subsequent iterations. The fluid properties at  $Q$ ,  $R$  and  $S$  are calculated using linear interpolation between those at the respective surrounding grid points. A first-order approximation is used to calculate the properties at the next time step i.e. point  $P$ , in the first-order method. In the second-order approximation, the procedure is exactly the same as that used by Tiley (1989), which was described earlier, with the exception that values calculated by the second-order approximation are not averaged with those calculated using the first-order approximation. The latter values are only used in the first iteration of the second-order approximation.

## DERIVATION OF THE CHARACTERISTIC AND COMPATIBILITY EQUATIONS

The basic equations for unsteady flow are derived from first principles in Chapter 2 and further simplified in Section 4.1.1. The resulting equations are given as equations (4.1), (4.2) and (4.3) for the continuity, momentum and energy equations respectively. The characteristic and compatibility equations corresponding to equations (4.1), (4.2) and (4.3) are derived by multiplying equations (4.1), (4.2) and (4.3) by unknown parameters  $\delta_1$ ,  $\delta_2$  and  $\delta_3$  respectively, summing the products and equating it to zero. In this procedure reference is made to Fig. 4.4. For the sake of convenience of mathematical manipulation the energy equation used is that given by equation (2.28), but after making the same simplifications as those made to equation (2.29). The use of equation (4.3) leads to a coefficient matrix in which the elements of one row are all zeros. This results in equation (4.88) with both sides being zeros and therefore no solution for  $\lambda$ . The starting equation is as follows:

$$\delta_1 (4.1) + \delta_2 (4.2) + \delta_3 (4.3) = 0 \quad (4.77)$$

Substituting equations (4.1), (4.2) and (4.3) into (4.77) we get the following equations:

$$\delta_1 \left( \frac{\partial \rho}{\partial t} + u \frac{\partial \rho}{\partial x} + \rho \frac{\partial u}{\partial x} \right) + \delta_2 \left( \frac{\partial u}{\partial t} + \frac{1}{\rho} \frac{\partial p}{\partial x} + u \frac{\partial u}{\partial x} + \frac{\omega}{\rho A} + g \sin \theta \right) + \delta_3 \left( \frac{\partial p}{\partial t} + u \frac{\partial p}{\partial x} - a^2 \frac{\partial \rho}{\partial t} - a^2 u \frac{\partial \rho}{\partial x} + (1 - \delta_s) \left( \frac{\Omega + \omega u}{A} \right) \right) = 0$$



$$\begin{aligned}
& \delta_1 \frac{\partial \rho}{\partial t} + \delta_1 u \frac{\partial \rho}{\partial x} + \delta_1 \rho \frac{\partial u}{\partial x} + \delta_2 \frac{\partial u}{\partial t} + \frac{\delta_2}{\rho} \frac{\partial p}{\partial x} + \delta_2 u \frac{\partial u}{\partial x} + \\
& \delta_2 \left( \frac{\omega}{\rho A} + g \sin \theta \right) + \delta_3 \frac{\partial p}{\partial t} + \delta_3 u \frac{\partial p}{\partial x} - \delta_3 a^2 \frac{\partial \rho}{\partial t} - \delta_3 a^2 u \frac{\partial \rho}{\partial x} + \delta_3 (1 - \delta_s) \left( \frac{\Omega + \omega u}{A} \right) = 0 \\
& (\delta_1 - \delta_3 a^2) \frac{\partial \rho}{\partial t} + (\delta_1 u - \delta_3 u a^2) \frac{\partial \rho}{\partial x} + \delta_2 \frac{\partial u}{\partial t} + (\delta_1 \rho + \delta_2 u) \frac{\partial u}{\partial x} + \\
& \delta_3 \frac{\partial p}{\partial t} + \left( \frac{\delta_2}{\rho} + \delta_3 u \right) \frac{\partial p}{\partial x} + \delta_2 \left( \frac{\omega}{\rho A} + g \sin \theta \right) + \delta_3 \left[ (1 - \delta_s) \left( \frac{\Omega + \omega u}{A} \right) \right] = 0
\end{aligned}$$

Factoring out the coefficients of the x derivatives we obtain the following equation:

$$\begin{aligned}
& (\delta_1 u - \delta_3 u a^2) \left[ \frac{\partial \rho}{\partial x} + \frac{\delta_1 - \delta_3 a^2}{\delta_1 u - \delta_3 u a^2} \frac{\partial \rho}{\partial t} \right] + \\
& (\delta_1 \rho + \delta_2 u) \left[ \frac{\partial u}{\partial x} + \frac{\delta_2}{\delta_1 \rho + \delta_2 u} \frac{\partial u}{\partial t} \right] + \\
& \left( \frac{\delta_2}{\rho} + \delta_3 u \right) \left[ \frac{\partial p}{\partial x} + \frac{\delta_3 \rho}{\delta_2 + \delta_3 \rho u} \frac{\partial p}{\partial t} \right] + \\
& \delta_2 \left( \frac{\omega}{\rho A} + g \sin \theta \right) + \delta_3 \left[ (1 - \delta_s) \left( \frac{\Omega + \omega u}{A} \right) \right] = 0 \quad (4.78)
\end{aligned}$$

The slopes of the characteristic curves  $dt/dx = \lambda$ , are the coefficients of the partial derivatives of  $\rho$ ,  $u$  and  $p$  with respect to  $t$ . Therefore:

$$\lambda = \frac{\delta_1 - \delta_3 a^2}{\delta_1 u - \delta_3 u a^2} = \frac{\delta_2}{\delta_1 \rho + \delta_2 u} = \frac{\delta_3 \rho}{\delta_2 + \delta_3 \rho u} \quad (4.79)$$

Assuming  $\rho$ ,  $u$  and  $p$  are continuous, then

$$\frac{du}{dx} = \frac{\partial u}{\partial x} + \lambda \frac{\partial u}{\partial t} \quad (4.80)$$

$$\frac{d\rho}{dx} = \frac{\partial \rho}{\partial x} + \lambda \frac{\partial \rho}{\partial t} \quad (4.81)$$

$$\frac{dp}{dx} = \frac{\partial p}{\partial x} + \lambda \frac{\partial p}{\partial t} \quad (4.82)$$

Substituting equations (4.80), (4.81) and (4.82) into equations (4.78) we get the following equation:

$$(\delta_1 u - \delta_3 u a^2) d\rho + (\delta_1 \rho + \delta_2 u) du + \left( \frac{\delta_2}{\rho} + \delta_3 u \right) dp + \left[ \delta_2 \left( \frac{\omega}{\rho A} + g \sin \theta \right) + \delta_3 \left( (1 - \delta_s) \left( \frac{\Omega + \omega u}{A} \right) \right) \right] dx = 0 \quad (4.83)$$

Equation (4.83) is the compatibility equation, which is valid along the characteristic curves determined by equation (4.79). What is required now is to eliminate the unknown parameters  $\delta_1$ ,  $\delta_2$  and  $\delta_3$  from equations (4.79) and (4.83). Solving for  $\delta_1$ ,  $\delta_2$  and  $\delta_3$  from equation (4.79) we get the following equations:

$$(\lambda u - 1) \delta_1 + (0) \delta_2 - a^2 (\lambda u - 1) \delta_3 = 0 \quad (4.84)$$

$$(\lambda \rho) \delta_1 + (\lambda u - 1) \delta_2 + (0) \delta_3 = 0 \quad (4.85)$$

$$(0) \delta_1 + (\lambda) \delta_2 + \rho (\lambda u - 1) \delta_3 = 0 \quad (4.86)$$

For equations (4.84) to (4.86) to have a solution other than  $\delta_1 = \delta_2 = \delta_3 = 0$ , the determinant of the coefficient matrix for the system of those equations must vanish. Thus

$$\begin{vmatrix} \lambda u - 1 & 0 & -a^2(\lambda u - 1) \\ \lambda \rho & \lambda u - 1 & 0 \\ 0 & \lambda & \rho(\lambda u - 1) \end{vmatrix} = 0 \quad (4.87)$$

The above determinant is expressed as follows:

$$(\lambda u - 1) [(\lambda u - 1)^2 - a^2 \lambda^2] = 0 \quad (4.88)$$

Equation (4.88) is a cubic polynomial in  $\lambda$  whose roots are as follows:

$$\lambda_o = \left( \frac{dt}{dx} \right)_o = \frac{1}{u} \quad (4.89)$$

$$\lambda_+ = \left( \frac{dt}{dx} \right)_+ = \frac{1}{u + a} \quad (4.90)$$

$$\lambda_- = \left( \frac{dt}{dx} \right)_- = \frac{1}{u - a} \quad (4.91)$$

Equation (4.89), (4.90) and (4.91) represent the three characteristic lines namely the path line characteristic  $C_o$  and the right- and left-running Mach lines  $C_+$  and  $C_-$  respectively. The compatibility equation along the path line is obtained by substituting the equation for the path line i.e.  $(\lambda u - 1) = 0$  into equations (4.84) to (4.86). This substitution results into the following solution:



$$\delta_1 = 0 \quad \delta_2 = 0 \quad \delta_3 \text{ is arbitrary} \quad (4.92)$$

Substituting equation (4.92) into (4.83) we get the following equation:

$$dp - a^2 d\rho = - \left[ (1-\delta_s) \frac{(\Omega + \omega u)}{Au} \right] dx \quad (4.93)$$

Similarly for the Mach lines, equations (4.84) to (4.86) are solved for the  $\delta$ 's as follows:

$$\delta_1 = - \frac{(\lambda u - 1)\delta_2}{\lambda \rho} = a^2 \delta_3 \quad (4.94)$$

$$\delta_2 = - \frac{\lambda \rho a^2 \delta_3}{(\lambda u - 1)} = - \frac{\rho (\lambda u - 1)\delta_3}{\lambda} \quad (4.95)$$

$$\delta_1 = a^2 \delta_3 \quad (4.96)$$

Equations (4.94) and (4.95) are not independent and consequently there are only two independent relationships between  $\delta_1$ ,  $\delta_2$  and  $\delta_3$ . This implies that one of the three  $\delta$ 's is arbitrary.  $\delta_3$  is chosen to be arbitrary and equations (4.95) and (4.96) are substituted into equation (4.83). The resulting equation is as follows:

$$\left[ u - \frac{\lambda a^2}{(\lambda u - 1)} \right] dp - \left[ \frac{\rho a^2}{\lambda u - 1} \right] du + \left[ (1-\delta_s) \left( \frac{\Omega + \omega u}{A} \right) - \frac{\lambda \rho a^2}{(\lambda u - 1)} \left( \frac{\omega}{\rho A} + g \sin \theta \right) \right] dx = 0 \quad (4.97)$$

Using the equation for the Mach line characteristics in equation (4.88) i.e.  $(\lambda u - 1)^2 = a^2 \lambda^2$ , equation (4.97) is simplified to:

$$\frac{1}{\lambda} dp - \frac{(\lambda u - 1)}{\lambda^2} \rho du + \left[ (1-\delta_s) \left( \frac{\Omega + \omega u}{A} \right) - \frac{(\lambda u - 1)}{\lambda} \rho \left( \frac{\omega}{\rho A} + g \sin \theta \right) \right] dx = 0 \quad (4.98)$$

Multiplying throughout equation (4.98) by  $\lambda$  we get the following equation

$$dp - \frac{(\lambda u - 1)}{\lambda} \rho du + \left[ \lambda (1-\delta_s) \left( \frac{\Omega + \omega u}{A} \right) - (\lambda u - 1) \rho \left( \frac{\omega}{\rho A} + g \sin \theta \right) \right] dx = 0 \quad (4.99)$$

Substituting the equation for the Mach line characteristics i.e. equations (4.90) and (4.91), we get the compatibility equations for Mach line characteristics, which are as follows:

**Right-running Mach line characteristic:**

$$dp + \rho a du = - \left[ \frac{1}{u+a} (1-\delta_s) \left( \frac{\Omega + \omega u}{A} \right) + \frac{a}{u+a} \rho \left( \frac{\omega}{\rho A} + g \sin \theta \right) \right] dx \quad (4.100)$$

**Left-running Mach line characteristic:**

$$dp - \rho a du = - \left[ \frac{1}{u-a} (1-\delta_s) \left( \frac{\Omega + \omega u}{A} \right) - \frac{a}{u-a} \rho \left( \frac{\omega}{\rho A} + g \sin \theta \right) \right] dx \quad (4.101)$$

Substituting equations (4.90) and (4.91) into equations (4.100) and (4.101) respectively, we obtain the following equations:

$$dp + \rho a du = - \left[ \rho a \left( \frac{\omega}{\rho A} + g \sin \theta \right) + (1-\delta_s) \left( \frac{\Omega + \omega u}{A} \right) \right] dt \quad (4.102)$$

$$dp - \rho a du = - \left[ - \rho a \left( \frac{\omega}{\rho A} + g \sin \theta \right) + (1-\delta_s) \left( \frac{\Omega + \omega u}{A} \right) \right] dt \quad (4.103)$$

Equations (4.93), (4.102) and (4.103) are the compatibility equations along the path line characteristic  $C_0$  and the right- and left-running Mach lines  $C_+$  and  $C_-$  respectively. According to the theory of characteristics [Courant and Friedrichs (1948)], every solution of the original system of partial differential equations should satisfy the characteristic and compatibility equations. The converse is also true and therefore every solution of the characteristic and compatibility equations must satisfy the original system of partial differential equations.

A second-order approximation of the friction term is obtained by differentiating equation (A-4), which gives:

$$\begin{aligned} d\omega &= \frac{\partial \omega}{\partial \rho} d\rho + \frac{\partial \omega}{\partial u} du \\ d\omega &= \frac{\omega}{\rho} d\rho + \frac{2\omega}{u} du \end{aligned} \quad (4.104)$$

The average value between two given points, 1 and 2, is given by:

$$\bar{\omega} = \frac{\omega_1 + \omega_2}{2}$$



If  $\omega$  is the value at point 1 and  $\omega+d\omega$  is the value at point 2, then

$$\begin{aligned}\bar{\omega} &= \frac{\omega + (\omega + d\omega)}{2} = \omega + \frac{d\omega}{2} \\ \bar{\omega} &= \omega + \frac{d\omega}{2}\end{aligned}\quad (4.105)$$

Substituting equation (4.104) into (4.105) we get:

$$\begin{aligned}\bar{\omega} &= \omega + \frac{1}{2} \left( \omega \frac{d\rho}{\rho} + 2\omega \frac{du}{u} \right) \\ \bar{\omega} &= \omega \left( 1 + \frac{d\rho}{2\rho} + \frac{du}{u} \right)\end{aligned}\quad (4.106)$$

The right hand side of equation (4.106) is substituted for  $\omega$  in the compatibility equations (4.93), (4.102) and (4.103) resulting in the following equations:

**Along the path line characteristic:** (NB:  $dx/u$  is substituted by  $dt$ )

$$\begin{aligned}dp - a^2 d\rho &= - \left[ (1-\delta_s) \left( \Omega + \omega u \left( 1 + \frac{d\rho}{2\rho} + \frac{du}{u} \right) \right) \right] \frac{dt}{A} \\ \frac{A}{(1-\delta_s)} \frac{dp}{dt} - \frac{a^2 A}{(1-\delta_s)} \frac{d\rho}{dt} &= - \Omega - \omega u \left[ 1 + \frac{d\rho}{2\rho} + \frac{du}{u} \right] \\ \frac{A}{(1-\delta_s)} \frac{dp}{dt} - \frac{a^2 A}{(1-\delta_s)} \frac{d\rho}{dt} &= - \Omega - \omega u - \frac{\omega u}{2} \frac{d\rho}{\rho} - \omega du \\ \left[ \frac{A}{(1-\delta_s)dt} \right] dp - \left[ \frac{a^2 A}{(1-\delta_s)dt} - \frac{\omega u}{2\rho} \right] d\rho + \omega du &= - \Omega - \omega u\end{aligned}\quad (4.107)$$

**Along the right-running Mach line characteristic:**

$$\begin{aligned}dp + \rho a du &= - \left( a\rho \left( \frac{\omega}{\rho A} + g \sin \theta \right) + \left[ (1-\delta_s) \frac{(\Omega + \omega u)}{A} \right] \right) dt \\ \frac{1}{dt} dp + \frac{\rho a du}{dt} &= - \frac{\rho a \omega}{\rho A} - \rho a g \sin \theta - \frac{1}{A} (1-\delta_s) \Omega - \frac{(1-\delta_s) \omega u}{A} \\ \frac{A}{dt} dp + \frac{\rho a A}{dt} du &= - \left[ u(1-\delta_s) + \frac{\rho a}{\rho} \right] \omega - \rho a A g \sin \theta - (1-\delta_s) \Omega\end{aligned}$$

Substituting equation (4.106) for  $\bar{\omega}$  we get the following equations:

$$\begin{aligned} \frac{A}{dt} dp + \frac{\rho a A}{dt} du &= \left[ -u(1-\delta_s) - \frac{\rho a}{\rho} \right] \omega \left[ 1 + \frac{d\rho}{2\rho} + \frac{du}{u} \right] - \rho a A g \sin \theta - (1-\delta_s) \Omega \\ \left[ \frac{A}{dt} \right] dp + \left[ \frac{\omega}{2} \left( \frac{u}{\rho} (1-\delta_s) + \frac{a}{\rho} \right) \right] d\rho + \left[ \frac{\rho a A}{dt} + \omega \left( (1-\delta_s) + \frac{a}{u} \right) \right] du &= \\ \left[ -u(1-\delta_s) - \rho \frac{a}{\rho} \right] \omega - \rho a A g \sin \theta - (1-\delta_s) \Omega & \quad (4.108) \end{aligned}$$

Along the left-running Mach line characteristic:

$$\begin{aligned} dp - \rho a du &= - \left( -a\rho \left[ \frac{\omega}{\rho A} + g \sin \theta \right] + \left[ (1-\delta_s) \frac{(\Omega + \omega u)}{A} \right] \right) dt \\ \frac{1}{dt} dp - \frac{\rho a}{dt} du &= \frac{\rho a \omega}{\rho A} + \rho a g \sin \theta - \frac{1}{A} (1-\delta_s) \Omega - \frac{(1-\delta_s) \omega u}{A} \\ \frac{A}{dt} dp - \frac{\rho a A}{dt} du &= \frac{\rho a \omega}{\rho} + A \rho a g \sin \theta - (1-\delta_s) \Omega - (1-\delta_s) \omega u \\ \frac{A}{dt} dp - \frac{\rho a A}{dt} du &= - \left[ u(1-\delta_s) - \frac{\rho a}{\rho} \right] \omega + \rho a A g \sin \theta - (1-\delta_s) \Omega \end{aligned}$$

Substituting equation (4.106) for  $\bar{\omega}$ , the following equations are obtained:

$$\begin{aligned} \frac{A}{dt} dp - \frac{\rho a A}{dt} du &= - \left[ u(1-\delta_s) - \frac{\rho a}{\rho} \right] \omega \left[ 1 + \frac{d\rho}{2\rho} + \frac{du}{u} \right] + \rho a A g \sin \theta - (1-\delta_s) \Omega \\ \frac{A}{dt} dp + \left[ \frac{\omega}{2} \left( \frac{u}{\rho} (1-\delta_s) - \frac{a}{\rho} \right) \right] d\rho - \left[ \frac{\rho a A}{dt} - \omega \left( (1-\delta_s) - \frac{a}{u} \right) \right] du &= \\ - \left[ u(1-\delta_s) - \frac{\rho a}{\rho} \right] \omega + \rho a A g \sin \theta - (1-\delta_s) \Omega & \quad (4.109) \end{aligned}$$

Equations (4.107), (4.108) and (4.109) are simultaneous equations with three unknowns, namely  $dp$ ,  $d\rho$  and  $du$ . The equations can be expressed in a simplified form as follows

$$a_{11} dp + a_{12} d\rho + a_{13} du = b_{11} \quad (4.110)$$

$$a_{21} dp + a_{22} d\rho + a_{23} du = b_{21} \quad (4.111)$$

$$a_{31} dp + a_{32} d\rho + a_{33} du = b_{31} \quad (4.112)$$

Equations (4.110), (4.111) and (4.112) are solved simultaneously together with the characteristic equations (4.89), (4.90) and (4.91). The coefficients of equations (4.110), (4.111) and (4.112) are as follows:

$$a_{11} = \frac{A}{(1 - \delta_s) dt} \quad (4.113)$$



$$a_{12} = - \left[ \frac{A a^2}{(1 - \delta_s) dt} - \frac{\omega u}{2\rho} \right] \quad (4.114)$$

$$a_{13} = \omega \quad (4.115)$$

$$a_{21} = \frac{A}{dt} \quad (4.116)$$

$$a_{22} = \frac{\omega}{2} \left[ \frac{u}{\rho} (1 - \delta_s) + \frac{a}{\rho} \right] \quad (4.117)$$

$$a_{23} = \frac{\rho a A}{dt} + \omega \left[ (1 - \delta_s) + \frac{a}{u} \right] \quad (4.118)$$

$$a_{31} = \frac{A}{dt} \quad (4.119)$$

$$a_{32} = \frac{\omega}{2} \left[ \frac{u}{\rho} (1 - \delta_s) - \frac{a}{\rho} \right] \quad (4.120)$$

$$a_{33} = - \left[ \frac{\rho a A}{dt} - \omega \left[ 1 - \delta_s - \frac{a}{u} \right] \right] \quad (4.121)$$

$$b_{11} = -(\Omega + \omega u) \quad (4.122)$$

$$b_{21} = [-u(1 - \delta_s) - a]\omega - \rho a A g \sin\theta - (1 - \delta_s)\Omega \quad (4.123)$$

$$b_{31} = -[u(1 - \delta_s) - a]\omega + \rho a A g \sin\theta - (1 - \delta_s)\Omega \quad (4.124)$$

Whereas the natural method of characteristics is unconditionally stable, the hybrid method of characteristics is only conditionally stable. The stability criterion used is that of Courant, Friedrichs and Levy, which states that the domain of dependence of the exact solution is contained within the domain of dependence of the numerical solution. In symbols the Courant-Friedrichs-Levy stability criterion is represented as:

$$\frac{\Delta t}{\Delta x} \leq \frac{1}{(|u| + a)_{\max}} \quad (4.125)$$

The solution of characteristic and compatibility equations could be obtained using either a first- or second-order approximation. In the first-order method, one finite-difference approximation is expressed as:

$$\int_x^{x+\Delta x} f(x) dx = f(x) \Delta x \quad (4.126)$$

and in the second-order method, the approximation is expressed by the trapezoidal rule as follows:

$$\int_x^{x+\Delta x} f(x) dx \approx \frac{1}{2}[f(x) + f(x+\Delta x)] \Delta x \quad (4.127)$$

## FINITE DIFFERENCE SOLUTION OF THE CHARACTERISTIC AND COMPATIBILITY EQUATIONS

The following procedure is used to calculate the fluid properties at a point distance  $x$ , for a new time level  $t+\Delta t$ , using the characteristic and compatibility equations:

### First Stage: First-order Approximation:

- (i) **Determination of the positions Q, R and S by first-order approximation of the characteristic equations:** Referring to Fig. 4.4.

$$x_Q = x - u_M^t \Delta t \quad (4.128)$$

$$x_R = x - (u_M^t + a_M^t) \Delta t \quad (4.129)$$

$$x_S = x - (u_M^t - a_M^t) \Delta t \quad (4.130)$$

where the subscripts denote the point on the  $x$ - $t$  plane and the superscripts denote the time level.

- (ii) **Determination of the fluid properties at Q, R and S by linear interpolation:**

It is customary to assume that the characteristic lines are positioned as shown in Fig. 4.4. However, the positions may not necessarily be the same always. For example, if  $u$  is negative (opposite to the direction of positive  $x$  shown in Fig. 4.4), the characteristic curve  $QP$  would shift to the opposite side of line  $MP$ . Also if the flow is choked or supersonic the characteristic line  $SP$  would coincide with line  $MP$  or shift to the opposite side of  $MP$  respectively. In this way the values of fluid properties at position  $Q$ , for example, calculated assuming that it is between points  $L$  and  $M$  while it is in fact between  $M$  and  $N$  will be incorrect. To avoid such problems, a two-stage procedure is used. In this procedure, a check is first performed to establish the position of points  $Q$ ,  $R$  and  $S$  in relation to points  $L$ ,  $M$  and  $N$ . Such provision was not included in the model by Tiley (1989). The only properties which are approximated using this method are  $p$ ,  $\rho$  and  $u$ . The remaining fluid properties are calculated by the QUANT software using the values of  $p$  and  $\rho$  obtained in the first-order approximation as input values. The equations for first-order approximation of fluid properties at points  $Q$ ,  $R$  and  $S$  are as follows:



Fluid properties at position Q:

If  $x_Q < x$

$$p_Q^t = \left( \frac{x - x_Q}{\Delta x} \right) p_{x-\Delta x}^t + \left[ 1 - \left( \frac{x - x_Q}{\Delta x} \right) \right] p_x^t \quad (4.131)$$

$$u_Q^t = \left( \frac{x - x_Q}{\Delta x} \right) u_{x-\Delta x}^t + \left[ 1 - \left( \frac{x - x_Q}{\Delta x} \right) \right] u_x^t \quad (4.132)$$

$$\rho_Q^t = \left( \frac{x - x_Q}{\Delta x} \right) \rho_{x-\Delta x}^t + \left[ 1 - \left( \frac{x - x_Q}{\Delta x} \right) \right] \rho_x^t \quad (4.133)$$

If  $x_Q > x$

$$p_Q^t = \left( \frac{x_Q - x}{\Delta x} \right) p_{x+\Delta x}^t + \left[ 1 - \left( \frac{x_Q - x}{\Delta x} \right) \right] p_x^t \quad (4.134)$$

$$u_Q^t = \left( \frac{x_Q - x}{\Delta x} \right) u_{x+\Delta x}^t + \left[ 1 - \left( \frac{x_Q - x}{\Delta x} \right) \right] u_x^t \quad (4.135)$$

$$\rho_Q^t = \left( \frac{x_Q - x}{\Delta x} \right) \rho_{x+\Delta x}^t + \left[ 1 - \left( \frac{x_Q - x}{\Delta x} \right) \right] \rho_x^t \quad (4.136)$$

Fluid properties at position R:

If  $x_R < x$

$$p_Q^t = \left( \frac{x - x_R}{\Delta x} \right) p_{x-\Delta x}^t + \left[ 1 - \left( \frac{x - x_R}{\Delta x} \right) \right] p_x^t \quad (4.137)$$

$$u_R^t = \left( \frac{x - x_R}{\Delta x} \right) u_{x-\Delta x}^t + \left[ 1 - \left( \frac{x - x_R}{\Delta x} \right) \right] u_x^t \quad (4.138)$$

$$\rho_Q^t = \left( \frac{x - x_R}{\Delta x} \right) \rho_{x-\Delta x}^t + \left[ 1 - \left( \frac{x - x_R}{\Delta x} \right) \right] \rho_x^t \quad (4.139)$$

If  $x_R > x$

$$p_R^t = \left( \frac{x_R - x}{\Delta x} \right) p_{x+\Delta x}^t + \left[ 1 - \left( \frac{x_R - x}{\Delta x} \right) \right] p_x^t \quad (4.140)$$

$$u_R^t = \left( \frac{x_R - x}{\Delta x} \right) u_{x+\Delta x}^t + \left[ 1 - \left( \frac{x_R - x}{\Delta x} \right) \right] u_x^t \quad (4.141)$$

$$\rho_R^t = \left( \frac{x_R - x}{\Delta x} \right) \rho_{x+\Delta x}^t + \left[ 1 - \left( \frac{x_R - x}{\Delta x} \right) \right] \rho_x^t \quad (4.142)$$

Fluid properties at position S:

If  $x_S < x$

$$p_S^t = \left( \frac{x - x_S}{\Delta x} \right) p_{x-\Delta x}^t + \left[ 1 - \left( \frac{x - x_S}{\Delta x} \right) \right] p_x^t \quad (4.143)$$

$$u_S^t = \left( \frac{x - x_S}{\Delta x} \right) u_{x-\Delta x}^t + \left[ 1 - \left( \frac{x - x_S}{\Delta x} \right) \right] u_x^t \quad (4.144)$$

$$\rho_S^t = \left( \frac{x - x_S}{\Delta x} \right) \rho_{x-\Delta x}^t + \left[ 1 - \left( \frac{x - x_S}{\Delta x} \right) \right] \rho_x^t \quad (4.145)$$

If  $x_S > x$

$$p_S^t = \left( \frac{x_S - x}{\Delta x} \right) p_{x+\Delta x}^t + \left[ 1 - \left( \frac{x_S - x}{\Delta x} \right) \right] p_x^t \quad (4.146)$$

$$u_S^t = \left( \frac{x_S - x}{\Delta x} \right) u_{x+\Delta x}^t + \left[ 1 - \left( \frac{x_S - x}{\Delta x} \right) \right] u_x^t \quad (4.147)$$

$$\rho_S^t = \left( \frac{x_S - x}{\Delta x} \right) \rho_{x+\Delta x}^t + \left[ 1 - \left( \frac{x_S - x}{\Delta x} \right) \right] \rho_x^t \quad (4.148)$$

(iii) **Calculation of p, u and  $\rho$  at position P using first-order approximation:**

The values of p, u and  $\rho$  at position P are obtained by expressing the three differential equation (4.110), (4.111) and (4.112) in finite differences and solving them simultaneously. The fluid properties used to calculate the coefficients of the equations are evaluated at position M. The finite difference equations are as follows:



Along the path line characteristic, equation (4.110) becomes

$$a_{11}(p_P - p_Q) + a_{12}(\rho_P - \rho_Q) + a_{13}(u_P - u_Q) = b_{11}$$

$$a_{11} p_P + a_{12} \rho_P + a_{13} u_P = a_{11} p_Q + a_{12} \rho_Q + a_{13} u_Q + b_{11} \quad (4.149)$$

Similarly, equations (4.150) and (4.151) below, are obtained from equations (4.111) and (4.112) along the right- and left-running Mach line characteristics respectively. The equations are as follows:

$$a_{21} p_P + a_{22} \rho_P + a_{23} u_P = a_{21} p_R + a_{22} \rho_R + a_{23} u_R + b_{21} \quad (4.150)$$

$$a_{31} p_P + a_{32} \rho_P + a_{33} u_P = a_{31} p_S + a_{32} \rho_S + a_{33} u_S + b_{31} \quad (4.151)$$

Equations (4.149), (4.150) and (4.151) are simplified as follows:

$$A_{11} p_P + A_{12} \rho_P + A_{13} u_P = B_{11} \quad (4.152)$$

$$A_{21} p_P + A_{22} \rho_P + A_{23} u_P = B_{21} \quad (4.153)$$

$$A_{31} p_P + A_{32} \rho_P + A_{33} u_P = B_{31} \quad (4.154)$$

where the coefficients are as follows:

$$A_{11} = a_{11} \quad (4.155)$$

$$A_{12} = a_{12} \quad (4.156)$$

$$A_{13} = a_{13} \quad (4.157)$$

$$A_{21} = a_{21} \quad (4.158)$$

$$A_{22} = a_{22} \quad (4.159)$$

$$A_{23} = a_{23} \quad (4.160)$$

$$A_{31} = a_{31} \quad (4.161)$$

$$A_{32} = a_{32} \quad (4.162)$$

$$A_{33} = a_{33} \quad (4.163)$$

$$B_{11} = a_{11} p_Q + a_{12} \rho_Q + a_{13} u_Q + b_{11} \quad (4.164)$$

$$B_{21} = a_{21} p_R + a_{22} \rho_R + a_{23} u_R + b_{21} \quad (4.165)$$

$$B_{31} = a_{31} p_S + a_{32} \rho_S + a_{33} u_S + b_{31} \quad (4.166)$$

### Second Stage: Second-order Approximation:

In order to achieve a higher degree of accuracy, the second-order method is used after all iterations of the first-order method have been completed. The values of  $p_P$ ,  $\rho_P$  and  $u_P$  calculated using the first-order approximation are used as initial estimates.

- (i) **Determination of the positions Q, R and S by second-order approximation of the characteristic equations:** Referring to Fig. 4.4.

$$x_Q^{k+1} = x - \left[ \frac{2\Delta t}{\frac{1}{u_Q^k} + \frac{1}{u_P^k}} \right] \quad (4.167)$$

$$x_R^{k+1} = x - \left[ \frac{2\Delta t}{\frac{1}{(u+a)_R^k} + \frac{1}{(u+a)_P^k}} \right] \quad (4.168)$$

$$x_S^{k+1} = x - \left[ \frac{2\Delta t}{\frac{1}{(u-a)_S^k} + \frac{1}{(u-a)_P^k}} \right] \quad (4.169)$$

where the subscripts k and k+1 represent the iteration numbers.

- (ii) **Determination of the fluid properties at Q, R and S by quadratic interpolation:**

The very well known Taylor's theorem is used. The theorem produces a set of equations for quadratic approximation of the fluid properties at points Q, R and S. If higher accuracy is required, a higher order polynomial could be used. Referring to Fig. 4.4, the Taylor's expansion around point M which is at a distance x, for a property, say p, is as follows:

$$p(x+\Delta x) = p(x) + \Delta x p'(x) + \frac{(\Delta x)^2}{2} p''(x) + \frac{(\Delta x)^3}{6} p'''(x) + \dots \quad (4.170)$$

$$p(x-\Delta x) = p(x) - \Delta x p'(x) + \frac{(\Delta x)^2}{2} p''(x) - \frac{(\Delta x)^3}{6} p'''(x) + \dots \quad (4.171)$$

Adding equation (4.171) to (4.170) and neglecting terms with higher order than two we get:

$$\begin{aligned} p(x+\Delta x) + p(x-\Delta x) &= 2p(x) + (\Delta x)^2 p''(x) \\ p''(x) &= \frac{1}{(\Delta x)^2} [p(x+\Delta x) + p(x-\Delta x) - 2p(x)] \end{aligned} \quad (4.172)$$

Subtracting equation (4.171) from (4.170) and neglecting higher order terms we get:

$$\begin{aligned} p(x+\Delta x) - p(x-\Delta x) &= 2\Delta x p'(x) \\ p'(x) &= \frac{1}{2\Delta x} [p(x+\Delta x) - p(x-\Delta x)] \end{aligned} \quad (4.173)$$

⋮



Substituting equations (4.172) and (4.173) into equations (4.170) and (4.171), neglecting higher order terms and interpolating for properties at position Q we get the following equations:

$$p(x+\Delta x_Q) = p(x) + \Delta x_Q \frac{1}{2\Delta x} [p(x+\Delta x) - p(x-\Delta x)] + \frac{(\Delta x)^2}{2} \frac{1}{(\Delta x)^2} [(p(x+\Delta x) + p(x-\Delta x) - 2p(x))] \quad (4.174)$$

$$p(x-\Delta x_Q) = p(x) - \Delta x_Q \frac{1}{2\Delta x} [p(x+\Delta x) - p(x-\Delta x)] + \frac{(\Delta x)^2}{2} \frac{1}{(\Delta x)^2} [p(x+\Delta x) + p(x-\Delta x) - 2p(x)] \quad (4.175)$$

Equations (4.131) to (4.148) transform into equations (4.176) to (4.184), which follow:

Fluid properties at position Q:

$$p_Q^{k+1} = p_M \pm \frac{1}{2\Delta x} (p_L + p_N) (x_Q^{k+1} - x) + \frac{1}{2(\Delta x)^2} (p_L + p_N - 2p_M) (x_Q^{k+1} - x)^2 \quad (4.176)$$

$$\rho_Q^{k+1} = \rho_M \pm \frac{1}{2\Delta x} (\rho_L + \rho_N) (x_Q^{k+1} - x) + \frac{1}{2(\Delta x)^2} (\rho_L + \rho_N - 2\rho_M) (x_Q^{k+1} - x)^2 \quad (4.177)$$

$$u_Q^{k+1} = u_M \pm \frac{1}{2\Delta x} (u_L + u_N) (x_Q^{k+1} - x) + \frac{1}{2(\Delta x)^2} (u_L + u_N - 2u_M) (x_Q^{k+1} - x)^2 \quad (4.178)$$

Fluid properties at position R:

$$p_R^{k+1} = p_M \pm \frac{1}{2\Delta x} (p_L + p_N) (x_R^{k+1} - x) + \frac{1}{2(\Delta x)^2} (p_L + p_N - 2p_M) (x_R^{k+1} - x)^2 \quad (4.179)$$

$$\rho_R^{k+1} = \rho_M \pm \frac{1}{2\Delta x} (\rho_L + \rho_N) (x_R^{k+1} - x) + \frac{1}{2(\Delta x)^2} (\rho_L + \rho_N - 2\rho_M) (x_R^{k+1} - x)^2 \quad (4.180)$$

$$u_R^{k+1} = u_M \pm \frac{1}{2\Delta x} (u_L + u_N) (x_R^{k+1} - x) + \frac{1}{2(\Delta x)^2} (u_L + u_N - 2u_M) (x_R^{k+1} - x)^2 \quad (4.181)$$

Fluid properties at position S:

$$p_S^{k+1} = p_M \pm \frac{1}{2\Delta x} (p_L + p_N) (x_S^{k+1} - x) + \frac{1}{2(\Delta x)^2} (p_L + p_N - 2p_M) (x_S^{k+1} - x)^2 \quad (4.182)$$

$$\rho_S^{k+1} = \rho_M \pm \frac{1}{2\Delta x} (\rho_L + \rho_N) (x_S^{k+1} - x) + \frac{1}{2(\Delta x)^2} (\rho_L + \rho_N - 2\rho_M) (x_S^{k+1} - x)^2 \quad (4.183)$$

$$u_S^{k+1} = u_M \pm \frac{1}{2\Delta x} (u_L + u_N) (x_S^{k+1} - x) + \frac{1}{2(\Delta x)^2} (u_L + u_N - 2u_M) (x_S^{k+1} - x)^2 \quad (4.184)$$

The positive and negative signs are used if the position of Q or R or S is between M and N and L and M respectively.

(iii) **Calculation of p, u and ρ at position P using second-order approximation:**

The same equations as used in the first-order approximation, equations (4.152), (4.153) and (4.154) are used. The fluid properties used to calculate the coefficients of the equations are averaged between those at the newly established positions of Q, R and S and those previously calculated at point P. Therefore, the coefficients of equations (4.152), (4.153) and (4.154) are calculated as follows:

$$A_{11} = \frac{1}{2}\{[a_{11}]^{k+1}_Q + [a_{11}]^k_P\} \quad (4.185)$$

$$A_{12} = \frac{1}{2}\{[a_{12}]^{k+1}_Q + [a_{12}]^k_P\} \quad (4.186)$$

$$A_{13} = \frac{1}{2}\{[a_{13}]^{k+1}_Q + [a_{13}]^k_P\} \quad (4.187)$$

$$A_{21} = \frac{1}{2}\{[a_{21}]^{k+1}_R + [a_{21}]^k_P\} \quad (4.188)$$

$$A_{22} = \frac{1}{2}\{[a_{22}]^{k+1}_R + [a_{22}]^k_P\} \quad (4.189)$$

$$A_{23} = \frac{1}{2}\{[a_{23}]^{k+1}_R + [a_{23}]^k_P\} \quad (4.190)$$

$$A_{31} = \frac{1}{2}\{[a_{31}]^{k+1}_S + [a_{31}]^k_P\} \quad (4.191)$$

$$A_{32} = \frac{1}{2}\{[a_{32}]^{k+1}_S + [a_{32}]^k_P\} \quad (4.192)$$

$$A_{33} = \frac{1}{2}\{[a_{33}]^{k+1}_S + [a_{33}]^k_P\} \quad (4.193)$$

$$B_{11} = \frac{1}{2}\{[a_{11}]^{k+1}_Q + [a_{11}]^k_P\}p^{k+1}_Q + \frac{1}{2}\{[a_{12}]^{k+1}_Q + [a_{12}]^k_P\}\rho^{k+1}_Q + \frac{1}{2}\{[a_{13}]^{k+1}_Q + [a_{13}]^k_P\}u^{k+1}_Q + \frac{1}{2}\{[b_{11}]^{k+1}_Q + [b_{11}]^k_P\} \quad (4.194)$$

$$B_{21} = \frac{1}{2}\{[a_{21}]^{k+1}_R + [a_{21}]^k_P\}p^{k+1}_R + \frac{1}{2}\{[a_{22}]^{k+1}_R + [a_{22}]^k_P\}\rho^{k+1}_R + \frac{1}{2}\{[a_{23}]^{k+1}_R + [a_{23}]^k_P\}u^{k+1}_R + \frac{1}{2}\{[b_{21}]^{k+1}_R + [b_{21}]^k_P\} \quad (4.195)$$

$$B_{31} = \frac{1}{2}\{[a_{31}]^{k+1}_S + [a_{31}]^k_P\}p^{k+1}_S + \frac{1}{2}\{[a_{32}]^{k+1}_S + [a_{32}]^k_P\}\rho^{k+1}_S + \frac{1}{2}\{[a_{33}]^{k+1}_S + [a_{33}]^k_P\}u^{k+1}_S + \frac{1}{2}\{[b_{31}]^{k+1}_S + [b_{31}]^k_P\} \quad (4.196)$$

The values of p, ρ and u calculated using the above coefficients are to be used in the (k+1)<sup>th</sup> iteration. The iteration would continue until the required accuracy criterion is met.

## **SOLUTION OF THE THREE SIMULTANEOUS LINEAR ALGEBRAIC EQUATIONS**

Equations (4.152), (4.153) and (4.154) are simultaneous linear algebraic equations with three unknowns  $p_P$ ,  $\rho_P$  and  $u_P$  which are to be determined. A brief review of the various forms and behaviour of such equations is given in this section. For further details reference should be made in specialised literature. If there are as many equations as there are unknowns, the system of equations is known as non-singular, and there is a good chance that a unique solution exists. A system of equations is singular if it fails to produce a unique solution analytically. The latter situation could result even though the number of equations



is equal to the number of unknowns, if one or more of the equations is a linear combination of the other (row degeneracy) or if all the equations contain certain variables only in exactly the same linear combination (column degeneracy). For equations with the same number of variables as the number of equations, row degeneracy implies column and vice versa.

Some equations may be too close to linearly dependent that round off errors in the computer render them linearly dependent at some stage in the solution process. In such cases the numerical procedure fails. Also sometimes accumulated round-off errors in the solution process can swamp the true solution. This problem emerges particularly if the number of unknowns is too large. In this case the numerical procedure does not fail algorithmically but it returns a set of solutions that are wrong. The closer a set of equations is to being singular, the more this situation is likely to happen. Much of the sophistication of complicated linear equations solving methods is devoted to the detection and/or correction of these two pathologies.

Methods of solution of linear algebraic equations are generally classified into two categories, namely direct and iterative methods. Direct methods execute in a predictable number of operations, while iterative methods attempt to converge to the desired solution in however many steps are necessary. Iterative methods are preferred when the loss of significance is critical either due to large number of unknowns or because the problem is close to singularity. On the borderline between direct and iterative methods, there is a technique called iterative improvement of a solution that has been obtained by direct methods. At the extreme end of the spectrum, there are linear problems which by their underlying nature are close to singular. In this case sophisticated methods are necessary. However, a technique called singular value decomposition can sometimes turn singular problems into non-singular ones, thus additional sophistication becomes unnecessary.

Several packages are available for the solution of algebraic equations, although not always in the C language. These include LINPACK, developed by Argonne National Laboratories, which was published and is available for free use. A successor of LINPACK, called LAPACK is now available. Packages available commercially include those in the IMSL and NAG libraries. Routines for various tasks are usually provided in several possible simplifications in the form of the input coefficient matrix e.g. symmetric, triangular, sparse, banded, positive definite etc. Special routines for these special case have advantages of higher efficiency than the form provided for general matrices. Press, Teukolsky, Vetterling and Flannery (1992) presented a series of packages which include the Gauss-



Jordan elimination method, LU decomposition methods, tridiagonal systems, band diagonal systems, iterative improvement of a solution to linear equations, singular value decomposition and packages for sparse linear systems.

Some workers have reported the problem of singularity in the solution of the equations for unsteady flow following linebreak in high-pressure gas in pipelines, especially near the break. Flatt (1986) explained this as being caused by the pressure gradient near the break approaching infinity i.e.  $(\partial p / \partial x)_t \rightarrow -\infty$  owing to the choking condition ( $M_a=1$ ) and the cumulative effect of friction over long pipelines. He proved analytically that as Mach number tends towards unity, the solution tends towards infinity. Flatt (1993-1996) suggests that this problem could be eliminated by using stagnation properties of the fluid, in place of the conventional static properties. Tiley (1989) also reported similar problems with her model. She described it as instability which occurred at some grid sizes and initial conditions, at random points along the pipe. No such problems have been observed in this study. The model has been tested with pipelines of up to 68km length and pressure of up to 12.5MPa. At some stage during the development of the model, it was thought that singularity problems existed but it was later found that they were caused by machine round off error, incorrect initial break conditions and mistakes in the numerical algorithm. A numerical recipe called XSVBKS from Press, Teukolsky, Vetterling and Flannery (1992) and Vetterling, Teukolsky, Press and Flannery (1992) was modified and adopted for use with the programmes developed in this study. The recipe is based on the singular value decomposition, which sometimes can turn singular sets of equations into non-singular ones. However, it was found that the recipes XSVBKS could not handle the kind of singularity problems which were experienced during this study. In addition, the use of numerical recipes from Press, Teukolsky, Vetterling and Flannery (1992) and Vetterling, Teukolsky, Press and Flannery (1992) presented an additional problem in that more computer capacity is required to compile and run the recipes. This problem could be reduced by doing separate compilation of the recipes. However, since singularity is no longer a problems in this model, it was decided to solve the equations using a simple analytical procedure. The procedure is as follows:

**(i) Solution at interior points:**

For interior grid points, solution using the method is as follows: We first multiply equations (4.152) and (4.153) by  $A_{21}$  and  $A_{11}$  respectively, obtaining the following equations:



$$A_{11} A_{21} p_p + A_{12} A_{21} \rho_p + A_{13} A_{21} u_p = B_{11} A_{21} \quad (4.197)$$

$$A_{21} A_{11} p_p + A_{22} A_{11} \rho_p + A_{23} A_{11} u_p = B_{21} A_{11} \quad (4.198)$$

Subtracting equation (4.198) from (4.197) we get:

$$(A_{12}A_{21} - A_{22}A_{11})\rho_p + (A_{13}A_{21} - A_{23}A_{11})u_p = B_{11}A_{21} - B_{21}A_{11} \quad (4.199)$$

Similarly, multiplying equations (4.153) and (4.154) by  $A_{31}$  and  $A_{21}$  respectively we get

$$A_{21} A_{31} p_p + A_{22} A_{31} \rho_p + A_{23} A_{31} u_p = B_{21} A_{31} \quad (4.200)$$

$$A_{31} A_{21} p_p + A_{32} A_{21} \rho_p + A_{33} A_{21} u_p = B_{31} A_{21} \quad (4.201)$$

Subtracting equation (4.201) from (4.200) we get:

$$(A_{22}A_{31} - A_{32}A_{21})\rho_p + (A_{23}A_{31} - A_{33}A_{21})u_p = B_{21}A_{31} - B_{31}A_{21} \quad (4.202)$$

Equations (4.199) and (4.202) are then solved simultaneously for  $u_p$  by multiplying equation (4.199) by  $(A_{22}A_{31}-A_{32}A_{21})$  and equation (4.202) by  $(A_{12}A_{21}-A_{22}A_{11})$  and subtracting. The resulting equation is as follows:

$$\begin{aligned} & [(A_{13}A_{21}-A_{32}A_{11})(A_{22}A_{31}-A_{32}A_{21})-(A_{23}A_{31}-A_{33}A_{21})(A_{12}A_{21}-A_{22}A_{11})]u_p = \\ & [(B_{11}A_{21}-B_{21}A_{11})(A_{22}A_{31}-A_{32}A_{21})-(B_{21}A_{31}-B_{31}A_{21})(A_{12}A_{21}-A_{22}A_{11})] \\ u_p = & \frac{[(B_{11}A_{21} - B_{21}A_{11}) (A_{22}A_{31} - A_{32}A_{21}) - (B_{21}A_{31} - B_{31}A_{21}) (A_{12}A_{21} - A_{22}A_{11})]}{[(A_{13}A_{21} - A_{32}A_{11}) (A_{22}A_{31} - A_{32}A_{21}) - (A_{23}A_{31} - A_{33}A_{21}) (A_{12}A_{21} - A_{22}A_{11})]} \quad (4.203) \end{aligned}$$

Examination of equations (4.116) and (4.119) show that, for constant diameter pipes and same  $\Delta t$  values for both the RP and SP characteristics, the values of  $A_{21}$  and  $A_{31}$  are the same. Consequently, equation (4.203) could be simplified further. However, this simplification is not made because in some cases the break is such that the cross-section area at the exit is not the same as in the rest of the pipeline. Either equation (4.199) or (4.202) could be used to solve for  $\rho_p$ . Using equation (4.199)

$$\rho_p = \frac{(B_{11}A_{21} - B_{21}A_{11}) - (A_{13}A_{21} - A_{23}A_{11})u_p}{(A_{12}A_{21} - A_{22}A_{11})} \quad (4.204)$$

Similarly, either equation (4.152), (4.153) or (4.154) could be used to calculate  $p_p$ . Using equation (4.152)

$$p_p = \frac{B_{11} - A_{12} \rho_p - A_{13} u_p}{A_{11}} \quad (4.205)$$

The value of  $u_p$  calculated by equation (4.203) is used in equations (4.204) and (4.205), and the value of  $\rho_p$  calculated by equation (4.204) is used in equation (4.205). Equations (4.203), (4.204) and (4.205) are also used for the case of choked flow at the broken end, since all the three characteristics exist in the domain.

## **(ii) Solution at boundary points:**

Solution at interior points by the method described in section (i) would enable solution within the domain bounded with circles in Fig. 4.5. This means that at each time level, one distance mesh is lost on each end of the pipe section. Consequently, for any transient analysis, a solution could not be obtained for the whole length of the pipe unless the calculation started with a pipe extending beyond both ends of the pipe section. The length of the pipe should be such that after calculation for the required number of time levels, the whole length of the test section would still be covered. Apart from the fact that such a procedure would be unnecessarily time consuming, it is also not practical especially if the boundaries are fixed or the analysis takes place over a long period of time. A typical example of the latter condition is in this study, where the break boundary is fixed and it has to be modelled throughout the run time.

In order to enable the boundary points to be fixed and modelled, some boundary conditions have to be specified. Boundary conditions are additional parameters to the characteristic and compatibility equations, which exist at the boundary points. They may be the equation of the boundary in the  $x$ - $t$  plane and various specifications of the dependent variables as a function of the independent variables. To obtain a solution at a boundary point, the number of additional equations required is the same as the number of characteristic curves lacking at the boundary point. Let us consider a pipe flow from an upstream boundary which is at a distance  $x_0$  to a downstream boundary which is at a distance  $x_n$ . The equations of the boundary points on the  $x$ - $t$  plane are fixed at  $x=x_0$  and  $x=x_n$  for the upstream and downstream boundaries respectively. For calculation between time levels  $t_0$  and  $t_1$ , the meshes next to both boundaries are represented in Fig. 4.6. The characteristic curves defined in Fig. 4.4 are superimposed on the boundary meshes. The requirement is to find a solution at point P in Fig. 4.6 (a) and (b). It is assumed that  $u$  is positive in the downstream direction and also the flow is subsonic at both the boundary points. The same procedure as for the interior points is used to calculate the solution at point P, but in this case the number of characteristics and hence the number of equations is less than the number of unknowns i.e. two equations less in Fig. 4.6(a) and one equation less in Fig. 4.6(b). In order to obtain a unique solution at the boundary points, the missing equations must be replaced by specifications for some of the dependent variables.



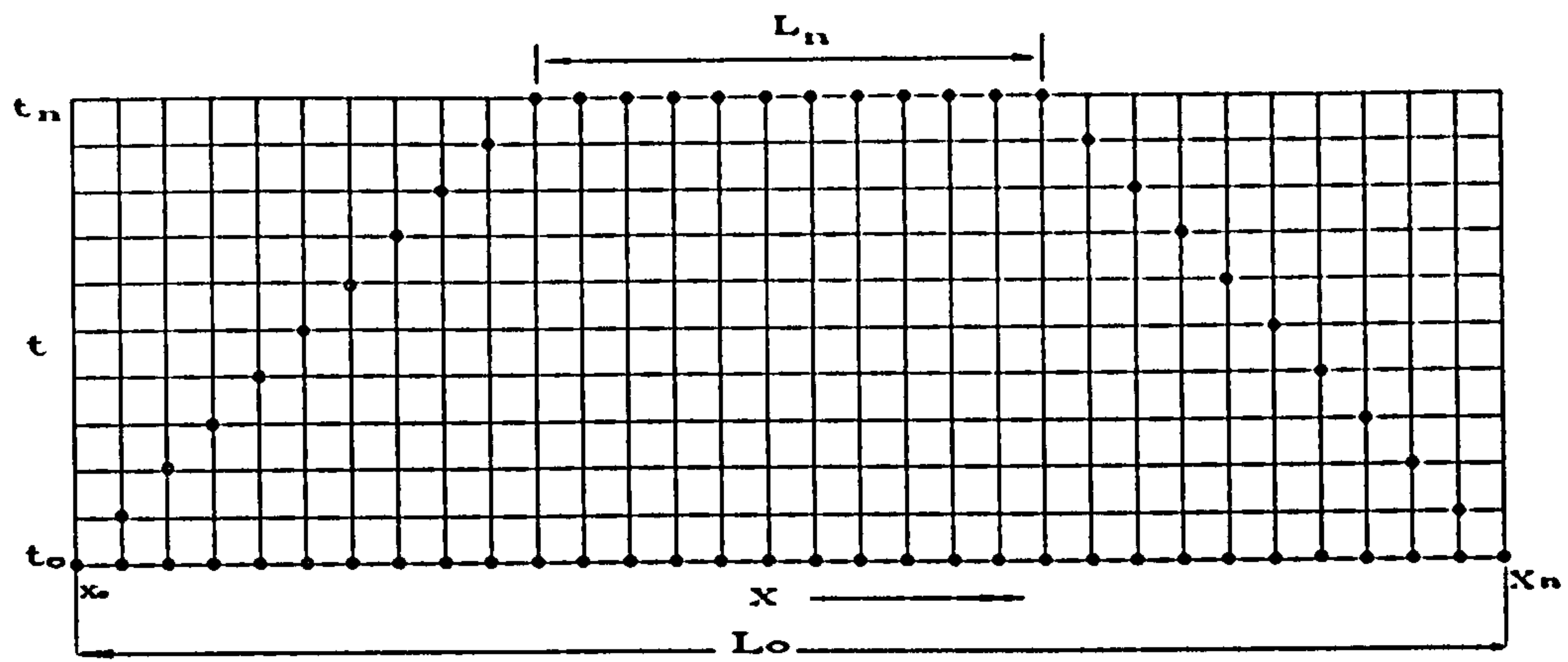


Fig. 4.5 Solution Domain in the x-t Plain Using Interior

However, the flow could be such that the two assumptions made in Fig. 4.6 do not apply. A typical example in linebreak problems is that  $u$  could be negative in the downstream direction in Fig. 4.6(b). If the magnitude of  $u$  is less than that of  $a$  i.e.  $M_a < 1$ , then there will be only one characteristic curve present in Fig 19(b) i.e. the RP characteristic curve. In order to obtain a unique solution at point P, two specific boundary conditions have to be specified. If the magnitude of  $u$  is greater than or equal to that of  $a$  i.e.  $M_a \geq 1$ , then there will be no characteristic curve existing in the x-t domain of dependence for solution at point P. In this case, the solution at point P will have to be evaluated entirely from the specific boundary conditions. However, if  $u$  is positive in the downstream and the flow is such that  $M_a \geq 1$ , all the three characteristic curves would exist in the domain of dependence and no additional boundary condition needs to be specified. A typical example of this situation is choked flow resulting after linebreak in high-pressure gas pipelines. A similar situation would occur in the upstream section [Fig. 4.6(a)]. If  $M_a \geq 1$ , and  $u$  is negative in the downstream direction, there would be no characteristic curves in the domain of dependence. The solution at point P would have to be calculated in a manner based entirely on the specific boundary conditions. But if  $u$  is positive in the downstream direction, all the three characteristic curves would exist in the domain of dependence and no additional boundary conditions would be required. This is the other case of choked flow in linebreak problems. If  $u$  is negative in the downstream direction and  $M_a < 1$ , two characteristic curves would exist in the domain of dependence and only one additional boundary conditions would have to be specified in order to obtain a unique solution at point P.

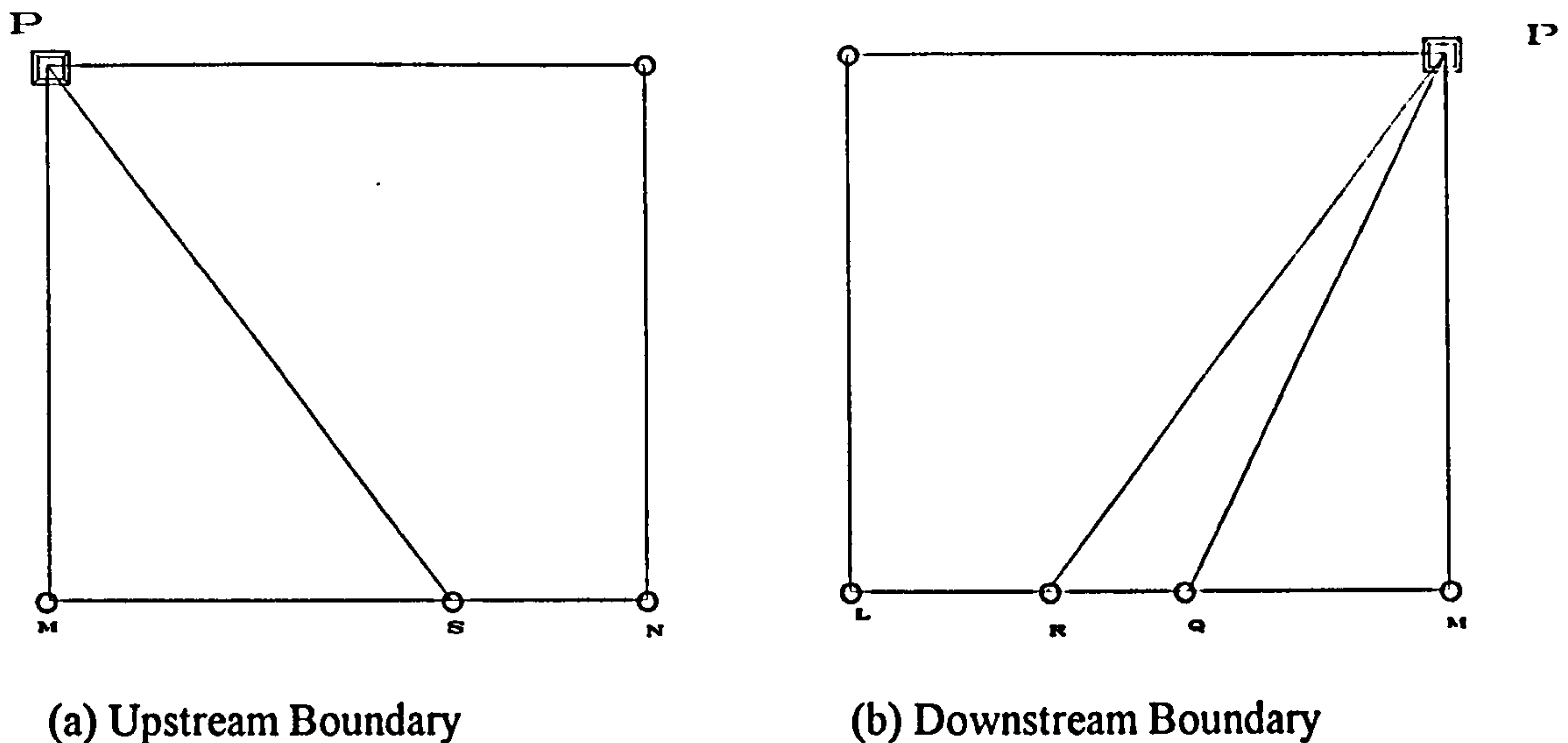


Fig. 4.6 Solution at Boundary Points

In general, there are four different cases of boundary condition specification for each of the upstream and downstream boundaries. The four cases are summarised in Table 4.1. However, in most steady and slow transient flows in pipelines, alternatives 3 and 6 in Table 4.1 are the most common. In rapid transients following linebreak of high-pressure gas pipelines, any one combination of alternatives 3, 4, 5, 6, 7 and 8 could occur. Before performing a transient analysis all the necessary boundary condition required to obtain unique solutions at the boundary throughout the run time should be specified. Sometimes it is not easy to specify accurate boundary conditions and some approximations and assumptions have to be made. Examples of boundary conditions which are commonly used are constant  $p$ , constant mass flow rate, constant  $T$ , the prescription of  $p$  as a function of  $t$  and the prescription of  $u$  as a function of  $t$ .

#### Calculation of the solution at boundary points when two characteristic curves exist:

**Boundary condition:  $p$  at point  $P$  is given**

In this case equations (4.152), (4.153) and (4.154) transform to:

$$A_{12} \rho_p + A_{13} u_p = B_1 \quad (4.206)$$

$$A_{22} \rho_p + A_{23} u_p = B_2 \quad (4.207)$$

$$A_{32} \rho_p + A_{33} u_p = B_3 \quad (4.208)$$

where

$$B_1 = B_{11} - A_{11} p_p \quad (4.209)$$



$$B2 = B21 - A21 p_P \quad (4.210)$$

$$B3 = B31 - A31 p_P \quad (4.211)$$

UPSTREAM BOUNDARY	CHARACTERISTICS AVAILABLE	DOWNSTREAM BOUNDARY
1. $u > a$ u Positive	NONE	2. $u > a$ u Negative
3. $u < a$ u Positive	SP RP	4. $u < a$ u Negative
5. $u < a$ u Negative	SP QP RP	6. $u \leq a$ u Positive
7. $u \geq a$ u Negative	THREE QP, RP & SP	8. $u \geq a$ u Positive

Table 4.1: Possible Boundary conditions

Dividing equations (4.206) by  $A12$ , (4.207) by  $A22$  and (4.208) by  $A32$  we get the following equations:

$$\rho_P + \frac{A13}{A12} u_P = \frac{B1}{A12} \quad (4.212)$$

$$\rho_P + \frac{A23}{A22} u_P = \frac{B2}{A22} \quad (4.213)$$

$$\rho_P + \frac{A33}{A32} u_P = \frac{B3}{A32} \quad (4.214)$$

Referring to Fig. 4.4, the characteristic curves available could either be QP and RP, RP and SP or QP and SP. If the characteristics available are QP and RP, equations (4.212) and (4.213) are solved simultaneously, obtaining the following equations:

$$u_P = \frac{\frac{B1}{A12} - \frac{B2}{A22}}{\frac{A13}{A12} - \frac{A23}{A22}}$$

$$u_P = \frac{B1 A22 - B2 A12}{A13 A22 - A23 A12} \quad (4.215)$$

From equation (4.212)

$$\rho_P = \frac{B1 - A13 u_P}{A12} \quad (4.216)$$

If the characteristic curves available are QP and SP, equations (4.212) and (4.214) are solved simultaneously, obtaining the following equations:

$$u_P = \frac{\frac{B1}{A12} - \frac{B3}{A32}}{\frac{A13}{A12} - \frac{A33}{A32}}$$

$$u_P = \frac{B1 A32 - B3 A12}{A13 A32 - A33 A12} \quad (4.217)$$

As in the previous case, equation (4.216) is used to calculate  $\rho_P$ . If the characteristic curves existing are RP and SP, equations (4.213) and (4.214) are solved simultaneously resulting into the following equations:

$$u_P = \frac{\frac{B2}{A22} - \frac{B3}{A32}}{\frac{A23}{A22} - \frac{A33}{A32}}$$

$$u_P = \frac{B2 A32 - B3 A22}{A23 A32 - A33 A22} \quad (4.218)$$

From equation (4.213)

$$\rho_P = \frac{B2 - A23 u_P}{A22} \quad (4.219)$$

**Boundary condition: u at point P is given**

The same procedure as for the case when p was given as the boundary conditions used. Equations (4.152), (4.153) and (4.154) transform into the following equations:

$$p_P + \frac{A12 \rho_P}{A11} = \frac{B1}{A11} \quad (4.220)$$

$$p_P + \frac{A22 \rho_P}{A21} = \frac{B2}{A21} \quad (4.221)$$

$$p_P + \frac{A32 \rho_P}{A31} = \frac{B3}{A31} \quad (4.222)$$

where

$$B1 = B11 - A13 u_P \quad (4.223)$$

$$B2 = B21 - A23 u_P \quad (4.224)$$

$$B3 = B31 - A33 u_P \quad (4.225)$$



If the characteristic curves available are QP and RP, equations (4.220) and (4.221) are solved simultaneously, obtaining the following equations

$$\rho_P = \frac{B1 \ A21 - B2 \ A11}{A12 \ A21 - A22 \ A11} \quad (4.226)$$

Using equation (4.220)

$$p_P = \frac{B1 - A12 \ \rho_P}{A11} \quad (4.227)$$

If characteristic curves available are QP and SP, equations (4.220) and (4.222) are solved simultaneously, thus obtaining the following equation:

$$\rho_P = \frac{B1 \ A31 - B3 \ A11}{A12 \ A31 - A32 \ A11} \quad (4.228)$$

Equation (4.227) is used to calculate p at position P. If the characteristic curves available are RP and SP, equations (4.221) and (4.222) are solved simultaneously, thus obtaining the following equation:

$$\rho_P = \frac{B2 \ A31 - B3 \ A21}{A31 \ A22 - A32 \ A21} \quad (4.229)$$

Equation (4.221) is used to calculate p at position P as follows:

$$p_P = \frac{B2 - A22 \ \rho_P}{A21} \quad (4.230)$$

**Boundary condition: p at point P is given**

Using the same procedure as for the two case where p and u are give, the following equations are obtained:

$$p_P + \frac{A13 \ u_P}{A11} = \frac{B1}{A11} \quad (4.231)$$

$$p_P + \frac{A23 \ u_P}{A21} = \frac{B2}{A21} \quad (4.232)$$

$$p_P + \frac{A33 \ u_P}{A31} = \frac{B1}{A31} \quad (4.233)$$

where

$$B1 = B11 - A12 \ \rho_P \quad (4.234)$$

$$B2 = B21 - A22 \ \rho_P \quad (4.235)$$

$$B3 = B31 - A32 \ \rho_P \quad (4.236)$$

If the characteristic curves available are QP and RP, equations (4.231) and (4.232) are solved simultaneously, obtaining the following equations

$$u_P = \frac{B1 A21 - B2 A11}{A13 A21 - A23 A11} \quad (4.237)$$

Using equation (4.221)

$$p_P = \frac{B1 - A13 u_P}{A11} \quad (4.238)$$

If characteristic curves available are QP and SP, equations (4.221) and (4.223) are solved simultaneously, thus obtaining the following equation:

$$u_P = \frac{B1 A31 - B3 A11}{A13 A31 - A33 A11} \quad (4.239)$$

Equation (4.238) is used to calculate p at position P. If the characteristic curves available are RP and SP, equations (4.222) and (4.223) are solved simultaneously, thus obtaining the following equation:

$$u_P = \frac{B2 A31 - B3 A21}{A23 A31 - A33 A21} \quad (4.240)$$

From equation (4.232)

$$p_P = \frac{B2 - A23 u_P}{A21} \quad (4.241)$$

**Boundary condition: Mass flow rate at point P is given**

Substituting equation (A-2) into equations (4.152) (4.153) and (4.154), we get the following equations:

$$p_P = \frac{A12 \rho_P}{A11} + \frac{A13}{A11} \frac{\dot{m}}{A \rho_P} = \frac{B11}{A11} \quad (4.242)$$

$$p_P = \frac{A22 \rho_P}{A21} + \frac{A23}{A21} \frac{\dot{m}}{A \rho_P} = \frac{B21}{A21} \quad (4.243)$$

$$p_P = \frac{A32 \rho_P}{A31} + \frac{A33}{A31} \frac{\dot{m}}{A \rho_P} = \frac{B31}{A31} \quad (4.244)$$

If the characteristic curves available are QP and RP; equations (4.242) and (4.243) are solved simultaneously, obtaining the following quadratic equation in  $\rho_P$ :

$$\left( \frac{A12}{A11} - \frac{A22}{A21} \right) \rho_P^2 - \left( \frac{B11}{A11} - \frac{B21}{A21} \right) \rho_P + \left( \frac{A13}{A11} - \frac{A23}{A21} \right) \frac{\dot{m}}{A} = 0$$



The quadratic equation is solved for  $\rho_P$  as follows:

$$\rho_P = \frac{\left(\frac{B11}{A11} - \frac{B21}{A21}\right) \pm \sqrt{\left(\frac{B21}{A21} - \frac{B11}{A11}\right)^2 - 4\left(\frac{A12}{A11} - \frac{A22}{A21}\right)\left(\frac{A13}{A11} - \frac{A23}{A21}\right)\frac{\dot{m}}{A}}}{2\left(\frac{A12}{A11} - \frac{A22}{A21}\right)} \quad (4.245)$$

From equation (4.242)

$$p_P = \frac{B11 - A12 \rho_P - A13 \frac{\dot{m}}{A \rho_P}}{A11} \quad (4.246)$$

The value of  $u$  at position  $P$  is calculated using equation (A-2). If characteristic curves available are  $QP$  and  $SP$ , equations (4.242) and (4.244) are solved simultaneously, thus obtaining the following quadratic equation in  $\rho_P$ :

$$\left(\frac{A12}{A11} - \frac{A32}{A31}\right) \rho_P^2 - \left(\frac{B11}{A11} - \frac{B31}{A31}\right) \rho_P + \left(\frac{A13}{A11} - \frac{A33}{A31}\right) \frac{\dot{m}}{A} = 0$$

The quadratic equation is solved for  $\rho_P$  as follows:

$$\rho_P = \frac{\left(\frac{B11}{A11} - \frac{B31}{A31}\right) \pm \sqrt{\left(\frac{B31}{A31} - \frac{B11}{A11}\right)^2 - 4\left(\frac{A12}{A11} - \frac{A32}{A31}\right)\left(\frac{A13}{A11} - \frac{A33}{A31}\right)\frac{\dot{m}}{A}}}{2\left(\frac{A12}{A11} - \frac{A32}{A31}\right)} \quad (4.247)$$

As for the previous case, the values of  $p$  and  $u$  at position  $P$  are calculated using equations (4.246) and (A-2) respectively. If the characteristic curves available are  $RP$  and  $SP$ , equations (4.243) and (4.244) are solved simultaneously, thus obtaining the following quadratic equation in  $\rho_P$ :

$$\left(\frac{A22}{A21} - \frac{A32}{A31}\right) \rho_P^2 - \left(\frac{B21}{A21} - \frac{B31}{A31}\right) \rho_P + \left(\frac{A23}{A21} - \frac{A33}{A31}\right) \frac{\dot{m}}{A} = 0$$

The quadratic equation is solved for  $\rho_P$  as follows:

$$\rho_P = \frac{\left(\frac{B21}{A21} - \frac{B31}{A31}\right) \pm \sqrt{\left(\frac{B31}{A31} - \frac{B21}{A21}\right)^2 - 4\left(\frac{A22}{A21} - \frac{A32}{A31}\right)\left(\frac{A23}{A21} - \frac{A33}{A31}\right)\frac{\dot{m}}{A}}}{2\left(\frac{A22}{A21} - \frac{A32}{A31}\right)} \quad (4.248)$$

From equation (4.243)

$$p_P = \frac{B21 - A22 \rho_P - A23 \frac{\dot{m}}{A \rho_P}}{A21} \quad (4.249)$$

The value of  $u$  at position  $P$  is calculated using equation (A-2).

**Calculation of the solution at boundary points when only one characteristic curve exists:**

**Boundary condition:  $u$  and  $p$  at position  $P$  are given**

In this case equations (4.152), (4.153) and (4.154) are used. If the characteristic curve which exists in the domain is QP:

$$\rho_P = \frac{B11 - A11 p_P - A13 u_P}{A21} \quad (4.250)$$

If the characteristic curve which exists in the domain is RP:

$$\rho_P = \frac{B21 - A21 p_P - A23 u_P}{A22} \quad (4.251)$$

If the characteristic curve which exists in the domain is SP:

$$\rho_P = \frac{B31 - A31 p_P - A33 u_P}{A32} \quad (4.252)$$

**Boundary condition:  $p$  and  $\rho$  at position  $P$  are given**

Using the same equations as for the previous case, if the characteristic curve which exists in the domain is QP:

$$u_P = \frac{B11 - A11 p_P - A12 \rho_P}{A13} \quad (4.253)$$

If the characteristic curve which exists in the domain is RP:

$$u_P = \frac{B21 - A21 p_P - A22 \rho_P}{A23} \quad (4.254)$$

If the characteristic curve which exists in the domain is SP:

$$u_P = \frac{B31 - A31 p_P - A32 \rho_P}{A33} \quad (4.255)$$

**Boundary condition:  $u$  and  $\rho$  at position  $P$  are given**

The same equations as for the previous two cases are used. If the characteristic curve which exists in the domain is QP:

$$p_P = \frac{B11 - A12 \rho_P - A13 u_P}{A11} \quad (4.256)$$

If the characteristic curve which exists in the domain is RP:

$$p_P = \frac{B21 - A22 \rho_P - A23 u_P}{A21} \quad (4.257)$$



If the characteristic curve which exists in the domain is SP:

$$p_P = \frac{B_{31} - A_{32} \rho_P - A_{23} u_P}{A_{31}} \quad (4.258)$$

**Boundary condition: Mass flow rate at position P is given**

Equation (4.242), (4.243) and (4.244) are used to calculate  $\rho$  at position P, and equation (A-2) is used to calculate  $u$  at position P. If the characteristic curve which exists in the domain is QP, equation (4.242) is used and the following quadratic equation in  $\rho_P$  is obtained:

$$A_{12} \rho_P^2 + (A_{11} p_P - B_{11}) \rho_P + A_{13} \frac{\dot{m}}{A} = 0$$

The quadratic equation is solved for  $\rho_P$  as follows:

$$\rho_P = \frac{(B_{11} - A_{11} p_P) \pm \sqrt{(A_{11} p_P - B_{11})^2 - 4 A_{12} A_{13} \frac{\dot{m}}{A}}}{2 A_{12}} \quad (4.259)$$

If the characteristic curve which exists in the domain is RP, equation (4.243) is used and the following quadratic equation in  $\rho_P$  is obtained:

$$A_{22} \rho_P^2 + (A_{21} p_P - B_{21}) \rho_P + A_{23} \frac{\dot{m}}{A} = 0$$

The quadratic equation is solved for  $\rho_P$  as follows:

$$\rho_P = \frac{(B_{21} - A_{21} p_P) \pm \sqrt{(A_{21} p_P - B_{21})^2 - 4 A_{22} A_{23} \frac{\dot{m}}{A}}}{2 A_{22}} \quad (4.260)$$

If the characteristic curve which exists in the domain is SP, equation (4.244) is used and the following quadratic equation in  $\rho_P$  is obtained:

$$A_{32} \rho_P^2 + (A_{31} p_P - B_{31}) \rho_P + A_{33} \frac{\dot{m}}{A} = 0$$

The quadratic equation is solved for  $\rho_P$  as follows:

$$\rho_P = \frac{(B_{31} - A_{31} p_P) \pm \sqrt{(A_{31} p_P - B_{31})^2 - 4 A_{32} A_{33} \frac{\dot{m}}{A}}}{2 A_{32}} \quad (4.261)$$

### 4.3.3 MACCORMACK SECOND-ORDER TWO-STEP METHOD

The finite difference form of equation (4.73) using the MacCormack method can be written in either of the two alternatives 1 or 2 described below. The subscripts and superscripts used refer to Fig. 4.7.

#### ALTERNATIVE 1:

**Predictor step (forward difference):**

$$A_i^P = A_i^t - B_i^t \frac{\Delta t}{\Delta x} (A_{i+1}^t - A_i^t) - C_i^t \Delta t \quad (4.262)$$

**Corrector step (backward difference):**

$$A_i^C = A_i^P - B_i^P \frac{\Delta t}{\Delta x} (A_i^P - A_{i+1}^P) - C_i^P \Delta t \quad (4.263)$$

#### ALTERNATIVE 2:

**Predictor step (backward difference):**

$$A_i^P = A_i^t - B_i^t \frac{\Delta t}{\Delta x} (A_i^t - A_{i+1}^t) - C_i^t \Delta t \quad (4.264)$$

**Corrector step (forward difference):**

$$A_i^C = A_i^P - B_i^P \frac{\Delta t}{\Delta x} (A_{i+1}^P - A_i^P) - C_i^P \Delta t \quad (4.265)$$

Applying the method used by Beauchemin and Marche (1992), to write the finite difference equations for equations (4.1), (4.2) and (4.3), the following equations are obtained:

#### ALTERNATIVE 1:

**Predictor step (forward difference):**

$$\rho_i^{PI} = \rho_i^t - u_i^t \frac{\Delta t}{\Delta x} (\rho_{i+1}^t - \rho_i^t) - \rho_i^t \frac{\Delta t}{\Delta x} (u_{i+1}^t - u_i^t) \quad (4.266)$$

$$u_i^{PI} = u_i^t - \frac{1}{\rho_i^t} \frac{\Delta t}{\Delta x} (p_{i+1}^t - p_i^t) - u_i^t \frac{\Delta t}{\Delta x} (u_{i+1}^t - u_i^t) + \Delta t \left( \frac{\omega_i^t}{\rho_i^t A} + g \sin \theta \right) \quad (4.267)$$

$$p_i^{PI} = p_i^t - u_i^t \frac{\Delta t}{\Delta x} (p_{i+1}^t - p_i^t) - [a_i^t]^2 \rho_i^t \frac{\Delta t}{\Delta x} (u_{i+1}^t - u_i^t) + \Delta t \left[ (1 - [\delta_s]_i^t) \left( \frac{\Omega_i^t + \omega_i^t u_i^t}{A} \right) \right] \quad (4.268)$$



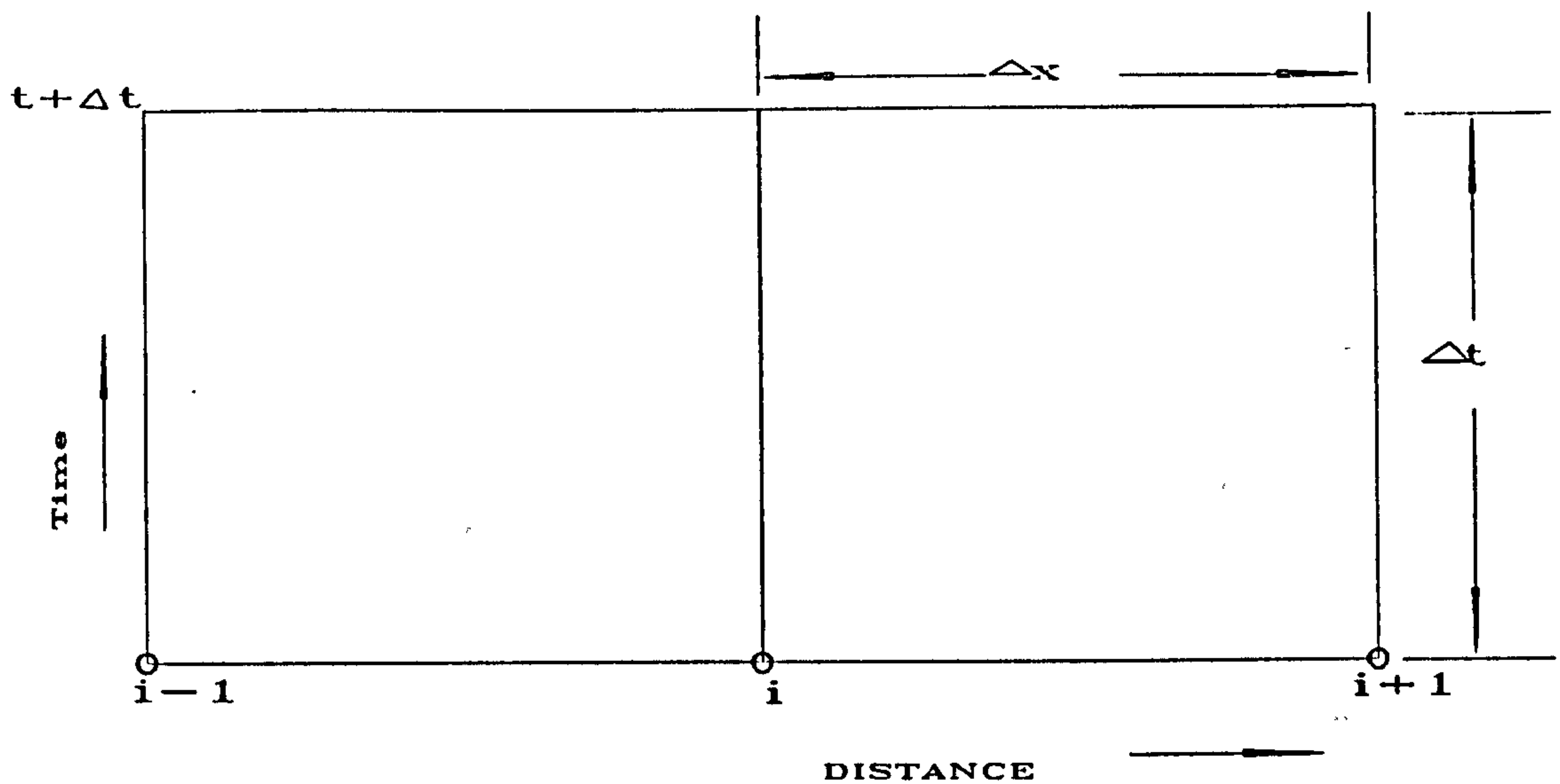


Fig. 4.7 Calculation Mesh for the Second-order MacCormack Method

**Corrector step (backward difference):**

$$\rho_i^{CI} = \rho_i^{PI} - u_i^{PI} \frac{\Delta t}{\Delta x} (\rho_i^t - \rho_{i-1}^t) - \rho_i^t \frac{\Delta t}{\Delta x} (u_i^{PI} - u_{i-1}^{PI}) \quad (4.269)$$

$$u_i^{CI} = u_i^{PI} - \frac{1}{\rho_i^{PI}} \frac{\Delta t}{\Delta x} (p_i^{PI} - p_{i-1}^{PI}) - u_i^{PI} \frac{\Delta t}{\Delta x} (u_i^{PI} - u_{i-1}^{PI}) + \Delta t \left( \frac{\omega_i^{PI}}{\rho_i^{PI} A} + g \sin \theta \right) \quad (4.270)$$

$$p_i^{CI} = p_i^{PI} - u_i^{PI} \frac{\Delta t}{\Delta x} (p_i^t - p_{i-1}^{PI}) - [a_i^{PI}]^2 \rho_i^{PI} \frac{\Delta t}{\Delta x} (u_i^{PI} - u_{i-1}^{PI}) + \Delta t \left[ (1 - [\delta s]_i^{PI}) \left( \frac{\Omega_i^{PI} + \omega_i^{PI} u_i^{PI}}{A} \right) \right] \quad (4.271)$$

**ALTERNATIVE 2:**

**Predictor step (backward difference):**

$$\rho_i^{P2} = \rho_i^t - u_i^t \frac{\Delta t}{\Delta x} (\rho_i^t - \rho_{i-1}^t) - \rho_i^t \frac{\Delta t}{\Delta x} (u_i^t - u_{i-1}^t) \quad (4.272)$$

$$u_i^{P2} = u_i^t - \frac{1}{\rho_i^t} \frac{\Delta t}{\Delta x} (p_i^t - p_{i-1}^t) - u_i^t \frac{\Delta t}{\Delta x} (u_i^t - u_{i-1}^t) + \Delta t \left( \frac{\omega_i^t}{\rho_i^t A} + g \sin \theta \right) \quad (4.273)$$

$$p_i^{P2} = p_i^t - u_i^t \frac{\Delta t}{\Delta x} (p_i^t - p_{i-1}^t) - [a_i^t]^2 \rho_i^t \frac{\Delta t}{\Delta x} (u_i^t - u_{i-1}^t) + \Delta t \left[ (1 - [\delta s]_i^t) \left( \frac{\Omega_i^t + \omega_i^t u_i^t}{A} \right) \right] \quad (4.274)$$

**Corrector step (forward difference):**

$$\rho_i^{C2} = \rho_i^{P2} - u_i^{P2} \frac{\Delta t}{\Delta x} (\rho_{i+1}^{P2} - \rho_i^{P2}) - \rho_i^{P2} \frac{\Delta t}{\Delta x} (u_{i+1}^t - u_i^{P2}) \quad (4.275)$$

$$u_i^{C2} = u_i^{P2} - \frac{1}{\rho_i^{P2}} \frac{\Delta t}{\Delta x} (\rho_{i+1}^{P2} - \rho_i^{P2}) - u_i^{P2} \frac{\Delta t}{\Delta x} (u_{i+1}^{P2} - u_i^{P2}) + \Delta t \left( \frac{\omega_i^{P2}}{\rho} A + g \sin \theta \right) \quad (4.276)$$

$$p_i^{C2} = p_i^{P2} - u_i^{P2} \frac{\Delta t}{\Delta x} (\rho_{i+1}^{P2} - \rho_i^{P2}) - [a_i^{P2}]^2 \rho_i^{P2} \frac{\Delta t}{\Delta x} (u_{i+1}^{P2} - u_i^{P2}) - \Delta t \left[ (1 - [\delta_s]_i^{P2}) \left( \frac{\Omega_i^{P2} + \omega_i^{P2} u_i^{P2}}{A} \right) \right] \quad (4.277)$$

The value of each variable at the end of a time step is the average of the variables' values at the beginning of the time step and its corrected values.

$$\rho_i^{t+\Delta t} = \frac{1}{2}(\rho_i^t + \rho_i^{C1}) \quad \text{or} \quad \rho_i^{t+\Delta t} = \frac{1}{2}(\rho_i^t + \rho_i^{C2}) \quad (4.278)$$

$$u_i^{t+\Delta t} = \frac{1}{2}(u_i^t + u_i^{C1}) \quad \text{or} \quad u_i^{t+\Delta t} = \frac{1}{2}(u_i^t + u_i^{C2}) \quad (4.279)$$

$$p_i^{t+\Delta t} = \frac{1}{2}(p_i^t + p_i^{C1}) \quad \text{or} \quad p_i^{t+\Delta t} = \frac{1}{2}(p_i^t + p_i^{C2}) \quad (4.280)$$

It is possible to use each of the two alternatives exclusively or alternatively at each time step. Another more complicated alternative is to use an average of the corrected values obtained when both alternatives are carried out at every time step. In equation form, this alternative is expressed as follows:

$$\rho_i^{t+\Delta t} = \frac{1}{2} \rho_i^t + \frac{1}{4} \rho_i^{C1} + \frac{1}{4} \rho_i^{C2} \quad (4.281)$$

$$u_i^{t+\Delta t} = \frac{1}{2} u_i^t + \frac{1}{4} u_i^{C1} + \frac{1}{4} u_i^{C2} \quad (4.282)$$

$$p_i^{t+\Delta t} = \frac{1}{2} p_i^t + \frac{1}{4} p_i^{C1} + \frac{1}{4} p_i^{C2} \quad (4.283)$$

The merits, demerits and suitability for application of the three alternatives of using the MacCormack method are discussed in Chapter 3. In this study, the three alternatives are compared. The main reason for his selection is that alternative 1 is simple. Using alternative 2 would make it necessary to calculate predicted values at the subsequent distance point, which makes the procedure more complicated and requires more computer storage capacity. However, it should be noted that Beauchemin and Marche (1992) recommended the use of average values with both alternatives, in cases where it is important that the signal be transmitted at the correct speed.



### 3.3.2 WARMING-KUTLER-LOMAX THIRD-ORDER METHOD

The finite-difference equations for the third-order Warming-Kutler-Lomax method for hyperbolic equations of the form of equation (4.72), and with reference to Fig. 4.8, are as follows:

$$A_i^{(1)} = A_i^J - \frac{2}{3} \frac{\Delta t}{\Delta x} B_i^J (A_{i+1}^J - A_i^J) - \frac{2}{3} \Delta t C_i^J \quad (4.284)$$

$$A_i^{(2)} = \frac{1}{2} \left[ A_i^J + A_i^{(1)} - \frac{2}{3} \frac{\Delta t}{\Delta x} B_i^J (A_i^{(1)} - A_{i+1}^{(1)}) - \frac{2}{3} \Delta t C_i^{(1)} \right] \quad (4.285)$$

$$A_{i+1}^{(1)} = A_{i+1}^J - \frac{2}{3} \frac{\Delta t}{\Delta x} B_{i+1}^J (A_i^J - A_{i+1}^J) - \frac{2}{3} \Delta t C_{i+1}^J \quad (4.286)$$

$$A_{i+1}^{(2)} = \frac{1}{2} \left[ A_{i+1}^J + A_{i+1}^{(1)} - \frac{2}{3} \frac{\Delta t}{\Delta x} B_{i+1}^J (A_{i+1}^{(1)} - A_{i+2}^{(1)}) - \frac{2}{3} \Delta t C_{i+1}^{(1)} \right] \quad (4.287)$$

$$A_{i+1}^{(1)} = A_{i+1}^J - \frac{2}{3} \frac{\Delta t}{\Delta x} B_{i+1}^J (A_{i+1}^J - A_{i+1}^J) - \frac{2}{3} \Delta t C_{i+1}^J \quad (4.288)$$

$$A_{i+1}^{(2)} = \frac{1}{2} \left[ A_{i+1}^J + A_{i+1}^{(1)} - \frac{2}{3} \frac{\Delta t}{\Delta x} B_{i+1}^J (A_{i+1}^{(1)} - A_i^{(1)}) - \frac{2}{3} \Delta t C_{i+1}^{(1)} \right] \quad (4.289)$$

In order to be able to obtain the solutions for all the above equations, it is necessary to calculate the values of  $A_{i+2}^{(1)}$ ,  $C_{i+2}^{(1)}$ ,  $C_{i+1}^{(1)}$ ,  $C_i^{(1)}$ . These values are calculated as follows:

$$A_{i+2}^{(1)} = A_{i+2}^J - \frac{2}{3} \frac{\Delta t}{\Delta x} B_{i+2}^J (A_{i+1}^J - A_{i+2}^J) - \frac{2}{3} \Delta t C_{i+2}^J \quad (4.290)$$

The values  $C_{i+1}^{(1)}$ ,  $C_i^{(1)}$  and  $C_{i+1}^{(1)}$  are calculated after solving for  $A_{i+1}^{(1)}$ ,  $A_i^{(1)}$  and  $A_{i+1}^{(1)}$ . The values of the dependent variables at the new time level are calculated using the following equation:

$$A_i^{(j+1)} = A_i^J - \frac{1}{24} \frac{\Delta t}{\Delta x} B_i^J \left( -2A_{i+2}^J + 7A_i^J - 7A_{i+1}^J - 2A_{i+2}^J \right) - \frac{3}{8} \frac{\Delta t}{\Delta x} B_i^J (A_{i+2}^{(2)} - A_{i+1}^{(2)}) - \Delta t C_i^J - \frac{\varphi}{24} (A_{i+2}^{(1,2)} - 4A_{i+1}^{(1,2)} + 6A_i^J - 4A_{i+1}^{(1,2)} + A_{i+2}^{(1,2)}) \quad (4.291)$$

After developing the finite-difference equations for the Warming-Kutler-Lomax method, what is required now is to express the basic equations of flow [equations (4.1), (4.2) and (4.3)] in the form of equation (4.72). The value of  $\varphi$  in equation (4.291), which is called the free parameter, is chosen such that dissipation and dispersion errors are minimum. The

following equations are used:

$$\varphi = 4C_n^2 - C_n^4 \quad (4.292)$$

$$\varphi = \frac{(4C_n^2 + 1)(4 - C_n^2)}{5} \quad (4.293)$$

where

$$C_n = \frac{\Delta t}{\Delta x} a_{\max} \leq 1 \quad (4.294)$$

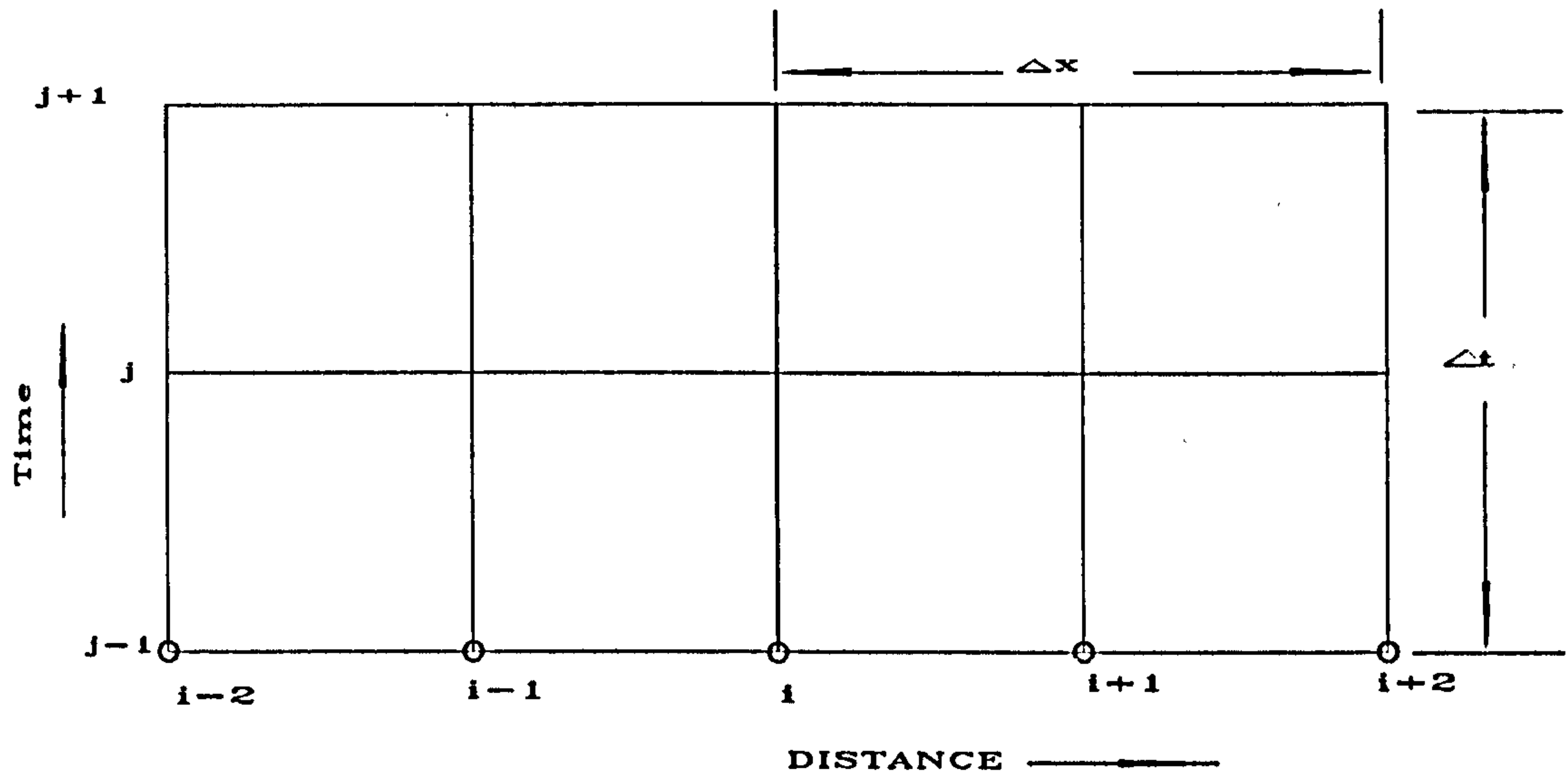


Fig. 4.8 A Finite Difference Grid Illustrating the Three-step Warming-Kutler-Lomax Method

Warming, Kutler and Lomax (1973) recommended that for practical purposes and for a given value of Courant number such that  $|C_n| \leq 1$ , the value of the free parameter  $\varphi$  should fall in between the values calculated by equations (4.292) and (4.293). In this model, an average of values calculated by the two equations above is used. For equations (4.1), (4.2) and (4.3) to be expressed in the same form as equation (4.72), the former equations have to be expressed in a matrix form, where the matrices  $\underline{A}$ ,  $\underline{B}$  and  $\underline{C}$  are as follows:

$$\underline{A} = \begin{pmatrix} \rho \\ u \\ p \end{pmatrix} \quad (4.295)$$

$$\underline{B} = \begin{pmatrix} u & p & 0 \\ 0 & u & \frac{1}{\rho} \\ 0 & a^2 p & u \end{pmatrix} \quad (4.296)$$



$$C = \begin{pmatrix} 0 \\ \frac{\omega}{\rho a} + g \sin \theta \\ (1-\delta s) \left( \frac{\Omega + \omega u}{A} \right) \end{pmatrix} \quad (4.297)$$

#### 4.4 VARIABLE GRID SIZE

The concept of variable grid size in the solution of the partial differential equations, was introduced in order to be able to model adequately the physical behaviour following a break in a pipeline; to reduce the CPU time; and to increase accuracy and stability of solution is not very new. Press, Teukolsky, Vetterling and Flannery (1992) reported that practical multigrid methods which are commonly used to solve elliptic partial differential equations were first introduced in the 1970's. In such problems, conventional elimination methods can be quite inefficient and traditional iterative (or relaxation) methods tend to become ineffective as the problem size grows. These limitations can be eliminated by multigrid methods. Multigrid methods increase the speed of convergence of solution.

In hyperbolic problems, such as in this study, the situation is somewhat different. In the case of linebreak problems, the pressure drop is very rapid and as a result very rapid transients occur in the vicinity of the break at the early times after the break. These transients are transmitted to the side of the broken section which is away from the break and tend to die away as one moves away from the break. Even in the vicinity of the break, rapid transients die out with increasing time after the break. With such rapid transients in the vicinity of the break, a very fine grid mesh is required in order to model the flow accurately. The effect of grid size on accuracy, convergence and stability in linebreak problems has been investigated by among others Flatt (1986) and Picard and Bishnoi (1989). It is generally concluded that stable solutions are obtained if the grid size is less than or equal to some critical value. For typical pipelines (1km and above), the critical grid size would result in excessive computational load.

The practical solution to the above problem is to use what is referred to, in this study, as the variable grid size in order to avoid confusion with the multigrid methods used for elliptic equations. The variable grid method involves the use non-uniform grid spacing in order to allow for fine grid spacing in the vicinity of the break, where grid spacing is most critical and coarser spacing further away from the break. The use of this method was first

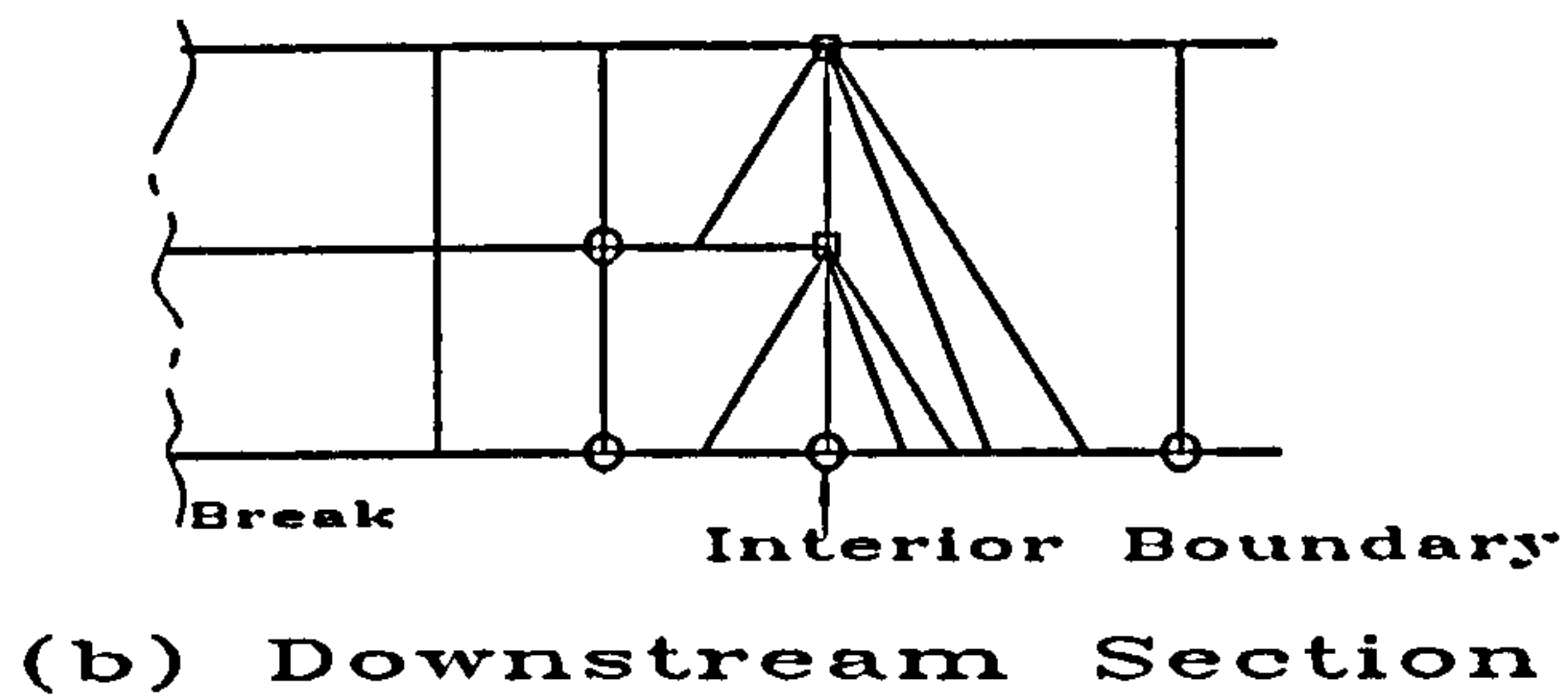
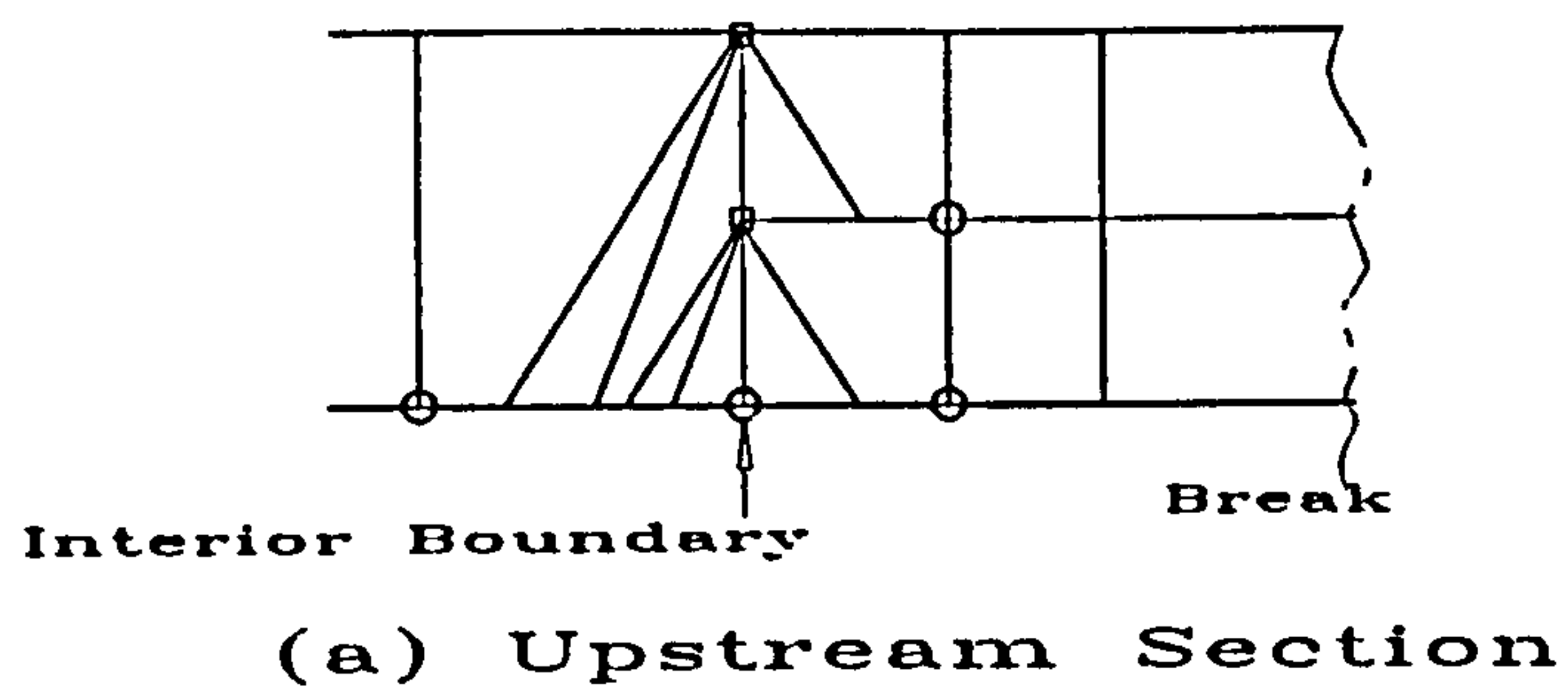
reported by Tiley (1989) and Picard and Bishnoi (1989). Since then it has become the common practice for linebreak problems and it has been used by among others Kunsch, Sjøen and Fanneløp (1991) and Chen, Richardson and Saville (1992).

In using the variable grid size method, an important parameter to be determined is the factor between successive grid sizes. Tiley (1989) tried first a factor of ten and found that such a dramatic grid size difference caused numerical instability in the solution. This was probably caused by interpolation error between the bigger grid mesh. A factor of two was found to produce minimum instability. Chen, Richardson and Saville (1992) used a factor of five. There is no study known which has attempted to reduce the computation load further by increasing the grid size in the vicinity of the break after the rapid variations have died out. This would result in a more efficient programme, but the procedure would be more complicated.

In this study, a variable grid size is used and a factor of 2 is used between the size of two successive grid sizes. The finest grid size is selected first, based on the stability of the solution and also the length of the pipe section being modelled. If the grid size selected is not small enough, problems could be encountered with stability in the solution. On the other extreme, if the finest mesh size is too small, it may not be possible to model the whole length of the pipe within reasonable CPU time and computer memory. A computer programme for generating distance grid mesh has been written. It can generate up to a dozen different mesh sizes. The number of different mesh sizes and the number of grids in each size depends on the size of the smallest mesh size selected and the length of the pipe being modelled. The grid generation programme generates only the distance mesh and the time mesh is generated by the transient analysis programme as the computation proceeds. A typical grid mesh for a variable grid analysis is shown in Fig. 4.9. Also the criteria for selecting the smallest grid size is discussed in Section 4.7.

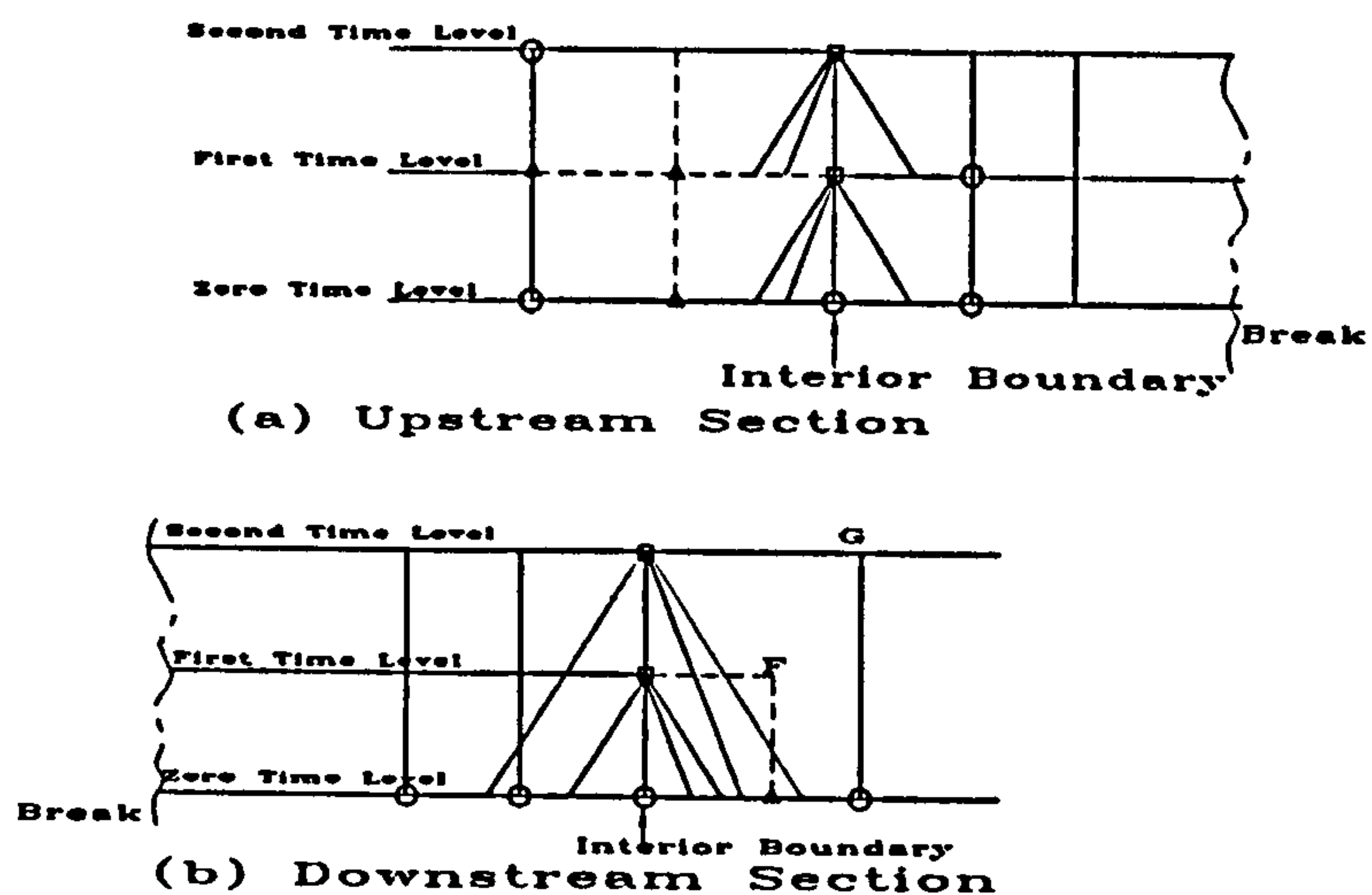
Solution at the boundaries between different mesh sizes (interior boundary points) may be performed in two different ways. In the first alternative, there is no interpolation used and calculation is performed with different  $\Delta x$  and  $\Delta t$  on each side of the boundary point. The finite-difference grid mesh for this alternative is shown in Fig. 4.9 above. In the second alternative, interpolation is performed first, before the transient analysis, so as to ensure the same grid size on both sides of the interior boundary point. Quadratic interpolation based on the Taylor's theorem, such as the one used in Section 4.3.2 for the second order method of characteristics is used. The grid layout for this alternative is shown





○ - initial known values;  
 □ - calculated values for the time level

Fig. 4.9 Finite-difference Grid Illustrating Solution at Interior Boundary Without Interpolation



○ - Initial known values;  
 △ - Values calculated by interpolation  
 □ - Values calculated by transient analysis programme at new time level.

Fig. 4.10 Finite-difference Grid Illustrating Solution at Interior Boundary With Interpolation

in Fig. 4.10. The smaller grid sizes are used at the interior boundary points throughout the upstream section, while in the downstream section the bigger sizes are used for the second time level calculation.

The reason for using the bigger grid size for the downstream section is that it is not possible to interpolate for point F in Fig. 4.10(b) without knowing the properties at point G. At the time of calculating the new values at the second time level at the interior boundary point, the values at point G will still be unknown. Tiley (1989) used the first alternative for the second-order method of characteristics. In this study, the second alternative is used for all the programmes using numerical methods of high than the first-order of accuracy. A first-order accurate programme, using the first alternative for the interior boundary points has been written. The programme could be extended to the second-order of accuracy. The interpolation procedure which ensures the same  $\Delta x$  and  $\Delta t$  on each side of the interior boundary point i.e. the second alternative, is more convenient especially when using the explicit finite-difference methods.

#### **4.5 APPLICATION OF THE QUANT SOFTWARE FOR THERMODYNAMIC AND TRANSPORT PROPERTIES OF FLUIDS**

The thermodynamic and transport properties of the fluid are calculated using the QUANT software which was described briefly in Section 2.4.3.4.2. The QUANT software is presently available in a version which can be used only on personal computers operating under the MS-DOS environment and it can be run in two different ways. In the first way, any quantity of data books can be printed (as hard copies or disk files) for any of the gases included in the coverage range or any of their mixtures. This method requires the selection of such a spacing of parameter entries that is adequate for the application being sought. Such files can be read by almost any programme, written in any programming language and in any operating system. In this way, retrieval of information generated by QUANT may be more rapid (in particular if the files necessary for any particular case are copied to the RAMDRIVE) because once performed, QUANT calculations may be used as many times as necessary. The data books written by QUANT deliver everything as a function of pressure and temperature. Therefore some manipulation by either linear or polynomial interpolation, in order to get the sought information as a function of pressure and temperature, is necessary. The output of specific volume is given in a dimensionless form



of compressibility factor, from which the former could be calculated. The temperature can also be found therefrom as a function of pressure and specific volume but an iteration of the compressibility factor becomes necessary.

Calculation can be simplified further and accelerated by restricting the storage of data to properties at the standard state and to the virial coefficients, including their temperature derivatives. These sets of data are dependent only on the nature of a pure gas or on the composition of the gas mixture and on temperature. They are independent of pressure and specific volume. But everything else (except transport properties) for real gases can be calculated from this data, using equations which are provided in the software literature. This procedure would, however, not deliver any information about the parameter limits within which QUANT delivers valid data of real gases and care must be taken not to exceed them.

In the second way of running the QUANT programme, output data for any requested set of input parameters is returned and could be displayed on the screen or returned to the calling programme for further processing. A master programme written in this way, can be used to prepare or modify the input parameters or any part of them for any other master programme and to store them on disk files for repetitive use. Any pair of the five thermodynamic properties, namely  $p$ ,  $T$ ,  $v$ ,  $H/R$  and  $S/R$  can be used as input. Alternatively, only one of the five properties could be used as input parameter, if the properties are required at the dew point of an individual gas or the dew point of such a component of a mixture which starts to condense at the highest temperature or at the lowest total pressure. Running the QUANT software in this way produces the output data at precisely the input parameter state, with iterations being performed automatically by the QUANT programme. The output data is registered in a random access file in the virtual drive. The data is stored in the file as binary data in single precision numbers in IEEE format. This method is expected to be more practical for such applications as in this study.

Regardless of which of the two options of using the QUANT software described above is used, there are additional input parameters to be specified. These include data on the substances used and units of the input and output data. The present version of QUANT covers over 100 individual substances including hydrocarbons, alkenes, cycloalkanes, inorganic compounds, noble gases and other gases. The input data in this case includes the chemical formulae of the substances, isomer number, hyperfine structure variant number (HFS) and fractional composition of each substance in the mixture. The HFS number is a



number which indicates which of the different isotopes are contained in the compound. For example the HFS number for substances composed of the most abundant or most stable isotopes, would have HFS value of zero. The other HFS variants are designated by numbers e.g. 1 to 3 for hydrogen. For the first three parameters i.e. chemical formula, isomer number and HFS number; QUANT offers two options for their inputting namely selecting from the QUANT default data and user selected inputting. In a similar way, the units for  $T$ ,  $p$ ,  $v$ ,  $\mu$  and  $k$  have to be specified before running QUANT. The input parameters are store in appropriate records in the respective random access files in the virtual disk. The data contained in those files is stored in a binary form, each record representing either a single precision number, an integer or a character in IEEE format or an ASCII code. A typical example of input data required for a particular mixture in order to fully specify the substances used is shown in Table 6.2.

A call to any of the QUANT programme variants returns the thermodynamic and transport properties of individual gas or of a gas mixture, including the input parameters, in the units selected by the user. The speed of execution of the QUANT programme can be increased by restricting the frequency of modifications of the list of substances. It can also be increased to a lesser extent by restricting the frequency of modification of mixture composition. On the other hand, the speed of execution decreases with the increasing number of components. The speed is not affected by changing units and is highest if  $p$  and  $T$  are the input parameters. It is slightly lower when the other pairs of independent parameters are the known input properties and it is significantly lower whenever output is requested at the dew point. A mathematical co-processor greatly increases the speed of execution. For example, in this study, it was observed that it took over two minutes to calculate the output properties using the option in which output properties are produced for an individual set of input parameters. The calculation involved a mixture of twelve substances and was performed on a 486SX personal computer with 8MB RAM capacity and a CPU speed of 25MHz, but without a mathematical co-processor. The same calculation was performed within a few seconds on a 486DX personal computer with 4MB RAM, CPU speed of 33MHz and which is equipped with a mathematical co-processor. When a pure gas was used on the former machine, the computation speed was comparable with that of the latter machine for the mixture of twelve substances.

The QUANT software produces a wide range of output thermodynamic and transport properties, but less than a dozen are relevant for the programmes developed in



this study. The properties are  $M$ ,  $p$ ,  $T$ ,  $v$ ,  $C_p/R$ ,  $K$ ,  $\gamma$ ,  $\delta$ ,  $\mu$ ,  $k$ . A big challenge was encountered in linking the QUANT programmes to the CFD programmes written during this study. The CFD programmes produced output in  $p$ ,  $\rho$  (from which  $v$  can easily be calculated) and  $u$ . The ideal situation would be to use the values of  $p$  and  $v$  calculated by the CFD programmes as input properties to the QUANT programme, which in turn produces output data including  $T$  and the other properties required for further calculations. Either of the two ways of running the QUANT programme, which are discussed above, could be used. It is evident, from previous discussions, that the latter option in which QUANT is run for individual sets of input data is the most convenient. A procedure was designed for this method, whereby after registering the list of substances and units (both of which remain unchanged for a particular pipeline analysis), the set of input values i.e.  $p$  and  $v$  produced by the CFD programme are written in the form stipulated by QUANT to a random access file PARAS.USR which resides in the virtual disk. The QUANT programme is then called, only for doing calculation of properties and to produce output in a random access file PROPS.DAT in the same fashion as the input data file PARAS.USR. Another programme reads the binary data from the random access binary file PROPS.DAT and returns the data in ASCII form to the calling CFD programme. Both the programmes for writing and reading input and output data respectively, in the random access files have successfully been written in the C language. What remains to be done is to write a programme which could be called by the CFD programme, to invoke the QUANT programme to do the calculation of output properties and write the output data in the output file PROPS.DAT automatically. Either of the variant programmes QDB or QDF supplied with the QUANT software, on request, was used but manual execution was necessary due to the menu structure through which they operate. This made it impractical in this application where the call to QUANT programme needs to be done numerous times. Moreover, the procedure is very slow, and thus it results in very long execution time if the programmes are run using this method directly.

The alternative method i.e. using ASCII data books produced by QUANT, also proved to be difficult. This is because the known properties produced by the CFD programmes are  $p$  and  $v$ , while the required input parameters for the QUANT data books are  $p$  and  $T$ . However, it is possible to use the values of  $p$  and  $v$  as input parameters, but the procedure is cumbersome and requires iteration because of the fact that the data books contain the output of  $v$  in the dimensionless form of  $Z$ . Efforts to develop a programme



which would invoke the QUANT programme to produce output data in the random access file PROPS.DAT automatically have yet to be completed. The task proved to be too difficult, especially because of incompatibility of the QUANT programme with compilers available, and insufficient information concerning the QUANT programmes. After some correspondence with the supplier, a different programme, QTS, which is designed to co-operate repetitively with any user's programme which delivers its input information as many times as necessary and handles the output information from each consecutive run was supplied. QTS was found not to be well suited for application in this study, where for each calculation point, both thermodynamic and input parameters vary independently. The QTS programme is limited to loops. Moreover, the programme is unnecessarily complicated and difficult to run with large user's programmes, of the kind developed in this study. Flatt (1993-1996) developed a programme RGAS1 by modifying one of demonstration programmes (FODEMO) supplied together with the programme QTS. The programme is expected to be able to produce thermodynamic data for a given gas or mixture of gases, one thermodynamic parameter e.g. pressure being fixed and the other one being varied to convenience. The result of this loop is written in a formatted ASCII file and its contents may be displayed on the screen or sent to a printer.

The most practical approach for CFD programmes for unsteady flow of gas in pipelines would be to include it as a programme unit containing tabulated values of all thermodynamic properties required, expressed as functions of  $p$  and  $\rho$  for the domain of the solution. This should include an interpolation procedure which for a given pair of values of  $p$  and  $\rho$ , would produce the thermodynamic values of the remaining parameter. A programme such as the one which was written by Flatt (1993-96) i.e. RGASI, would serve to prepare the required data tables. A substantial economy is achieved in computing time by using this approach, which was finally adopted for application in this study. The most ideal procedure is the one in which the input thermodynamic properties are written in the random access file PARAS.USR, in the virtual disk and the output data read by a programme written in C language. What is required now is a programme which will invoke the QUANT software to do the calculation for each set of input data automatically. The main disadvantage of this procedure is that it is very uneconomical in computing time.

The task of incorporating the QUANT software with the CFD programmes has proved to be much more demanding than it had previously been anticipated. The QUANT software has proved to have some limitations as far as its application in modelling of high-



pressure gas linebreak is concerned. However, the implications of the limitations have been appreciated fully and the performance of the software is considered to be adequate. Constant communication with the supplier was necessary and proved to be very useful. Two major limitations of the QUANT software are lack of output at high pressures, typical of those encountered in high-pressure gas pipelines, and also lack of output at very low temperatures (minimum temperature at which QUANT delivers output is 200K for most natural gas mixtures). The software is constantly being improved by the suppliers and a later version which is expected to be released soon, but not soon enough for this programme of study, is expected to be capable of producing output at higher pressures, typical of those encountered in high-pressure gas pipeline applications. The substance coverage range of QUANT is adequate to represent most natural gas mixtures.

## **4.6 COMPUTER CODES**

One of the reasons for keeping the basic equations of flow as simple as possible is to economise on computation labour, time and memory requirement. However, in the case of modelling transients in ruptured high-pressure gas pipelines, the potential for the realisation of the above is very limited. The reason for this is that, as seen in Section 4.1.1, the basic equations have to be used almost without any further simplifications in order to achieve the required accuracy criteria. On the other hand, Taylor (1992) stated that the general rule of thumb is that the value of software exceeds that of the associated hardware. Also since most engineering programming occurs in some group context, continuity and ease of maintenance are significant factors to be considered. A computer programme is therefore required to be easy to develop and maintain, as well as robust.

Most computer programmes for engineering applications use FORTRAN-77, PASCAL and C. The latter two provide a richer programming environment, but FORTRAN is generally faster in compilation speed. Programmes may actually be using several languages, but many of the numerical utilities that are available are written in FORTRAN. Justification for using FORTRAN includes, for example, that FORTRAN is the acceptable language for the industry. Tiley (1989) used FORTRAN-77 to write her computer model for analysis of transients in ruptured high-pressure gas pipelines. The model consisted of two programmes, one performing the transient analysis and the other converting the required section of the numerical output of the first programme into a



graphical form. In this study, it is recommended that the C language be used and a pc based compiler adopted to compile and run the programme. The C language is efficient, compact and also flexible. C is considered to be more professional and user friendly than FORTRAN. The advantages of the C language over FORTRAN are even greater when using the UNIX system because C is the programming language for the UNIX system (99% of UNIX is in C). Also due to the fact that the author had no previous knowledge of either FORTRAN or C, it is more profitable to learn C which is the most up-to-date language. When using other sub-routines, such as the QUANT software for thermodynamic and transport properties of the gas, problems may be encountered if these would be written in other languages than C. However, if data is output to an ASCII file, it can be picked up by programmes written in another language. QUANT is written in BASIC! and PREPROP in FORTRAN. The QUANT software could be linked with programmes written in any other language. Another aspect which needs to be considered is the computer hardware requirement. Most workers, Tiley (1989) in particular, have justified their simplifications of the basic equations with limitations in the computational labour, time and storage capacity which could be utilised economically. With the present state-of-the-art of computer hardware development (super computers), this may not be a big problem. However, the main problem is the present accessibility of such computers, not only to the author but also to most of the potential users of such programmes. If a computer programme is to have wider application therefore, it should be designed such that it can be handled by the type of computer hardware which is commonly available to the intended users. It is therefore intended that all computer programmes which are developed in this study, should be able to run on a pc.

Tiley (1989) used a Gould PN 9005 main computer to run her programme. However, Richardson (1993-96) is using a 286 PC to run the BLOWDOWN programme. This has been possible after inclusion of a special card, Microway-i860 which can increase the RAM memory capacity to 8-32MB. The full size card costs about £2000.00. It is argued that the performance of these cards is at best using a 286 PC, compared to the later models such as 386 and 486 PC's, because the bigger box of the former allows for better cooling. This possibility enables such programmes to be run almost anywhere. The SHELL Group is presently using this technology.

With the new generation of computers i.e. faster and higher capacity computers such as the PENTIUM series of personal computers and supercomputers, the size of



problems which can be solved is greatly increased. Application of these computers to engineering problems is increasing. Gathmann, Hebeker and Schöffel (1991) reported on a new FORTRAN code called PICUS, which simulates shock wave propagation in complex geometries. Special emphasis was given to its implementation on modern supercomputers, which in this case was an IBM ES/3090 with a vector facility. The PICUS code has been developed to treat some more sophisticated effects; including three-dimensional geometry, non-equilibrium chemistry and coupling with external heat conduction material. Even for much simplified cases, the requirement for very fine computational grids for resolving the intended physical phenomena with sufficient accuracy underscores the need for supercomputers. The final version of PICUS is faster, by a factor of 20, than a previous code with related objectives in mind. However, it should be noted that these machines require a different computational approach to obtain the most effective results. The UNIX system can be operated as a supercomputer using the Convex OS facility. This facility is presently available at the University College, London (UCL) and it can be accessed through networking. At least one project in the Department of Mechanical Engineering and Aeronautics at City University is benefitting by networking with the UCL Convex OS-UNIX supercomputing.

### **An Outline of the Main Features of TILEY'S Model**

The main features of the Tiley model, which was developed in the previous work at City University are listed in the following section. These will help to indicate improvements which have been included in the new model which is developed in this study. The main features of the Tiley model are as follows:

- (a) It allows the possibility of flow reversal downstream the break to be modelled.
- (b) Handling grid size reduction in the vicinity of the break is possible.
- (c) It can perform transient analysis on a given shock tube or single pipe.
- (d) It gives numerical output for pressure, flow velocity and temperature at each time step.
- (e) A second programme converts the required section of the numerical output into graphical form.
- (f) Both programmes were written in FORTRAN 77 for use on a Gould PN 9005 mainframe computer.

- (g) The computer model consists of a transient analysis programme and a graphics programme.
- (h) The transient analysis programme consists of a main programme and sixteen subroutines

The transient analysis programme (main programme) performs the following functions:

- (1) Prompting for gas and system data.
- (2) Grid formation.
- (3) Calling subroutines STEAD1 and STEAD2 to perform isothermal steady flow analyses upstream and downstream respectively, producing initial values ( $p$ ,  $T$  and  $u$ ) at every grid point.
- (4) Calculate  $\rho$ ,  $Z$  and their partial derivatives with respect to  $T$  and  $p$ ,  $\omega$ ,  $\Omega$  and isentropic and isothermal wave speeds.
- (5) Maximum time step calculated on the basis of a stability criterion so that the required time step and run time may be entered.
- (6) Calling subroutines SUB1 to SUB6 and BREAK1 and BREAK2 to perform method of characteristic calculation of new values of  $p$ ,  $T$  and  $u$  at first time level.
- (7) Calculate  $\rho$ ,  $Z$  and their partial derivatives with respect to  $T$  and  $p$ ,  $\omega$ ,  $\Omega$  and isentropic and isothermal wave speeds for the points.
- (8) Calling subroutines SUB1 to SUB6 and BREAK1 and BREAK2 to perform method of characteristic calculation of new values of  $p$ ,  $T$  and  $u$  at the next time level.
- (9) Procedure repeated until all time steps have been completed.
- (10) Calling subroutines SUBUP and DOWN1 to calculate new values of  $p$ ,  $T$  and  $u$  at upstream and downstream boundaries respectively.
- (11) Printing out these initial values at the specified grid points.
- (12) Initiate the pipe break.
- (13) Calculate the equalisation pressure at the break.
- (14) Determine the number of time steps over which the pressure drop occurs.
- (15) Calculate new values of pressure at the break one time step after the rupture occurs.
- (16) Calling subroutines BREAK3 and BREAK4 to calculate  $T$  and  $u$  at the break one time step after the rupture occurs.
- (17) Calling subroutines SUB1 to SUB6 to calculate new values of  $p$ ,  $T$  and  $u$  at each of the internal points.
- (18) Calling subroutines SUBUP and DOWN1 to calculate values at the pipe ends.



(19) Continue looping.

(20) Printing out results after each major time step until run time is reached.

The flow chart for the Tiley's model is presented in Fig. 4.11 and a list of its subroutines is as follows:

- STEAD1 - isothermal steady state flow analysis upstream
- STEAD2 - isothermal steady state flow analysis downstream
- SUB1 - normal internal points upstream of the break
- SUB2 - internal boundary points between different grid sizes upstream of the break
- SUB3 - internal boundary points between different grid sizes downstream of the break
- SUB4 - normal internal points downstream of the break
- SUB5 - internal boundary points linking different grid sizes upstream of the break
- SUB6 - internal boundary points linking different grid sizes downstream of the break
- BREAK1 - method of characteristics analysis at break point prior to the break
- BREAK2 - defines those values at the break downstream as the same as those upstream
- BREAK3 - calculates T and u at the break point, in the upstream section
- BREAK4 - calculates T and u at the break point, in the downstream section
- SUBUP - calculates new values of p, T and u at the upstream boundary
- DOWN1 - calculates new values of p, T and u at the downstream boundary
- GETFIL - opens data file
- DMINV - calculates the inverse of a matrix

### **Programme Achitecture**

The new model which is developed in this study, was intended to be an improvement on the Tiley model. Therefore, the same approach as that used by Tiley has been followed, as much as possible. However, in order to achieve the above objective, some significant changes have

been made to the approach which was followed by Tiley. The main features of the new model, which are not present in the Tiley model, are as follows:

- (a) A different form of the basic equations.
- (b) The QUANT software is used to calculate thermodynamic and transport properties of the fluid.

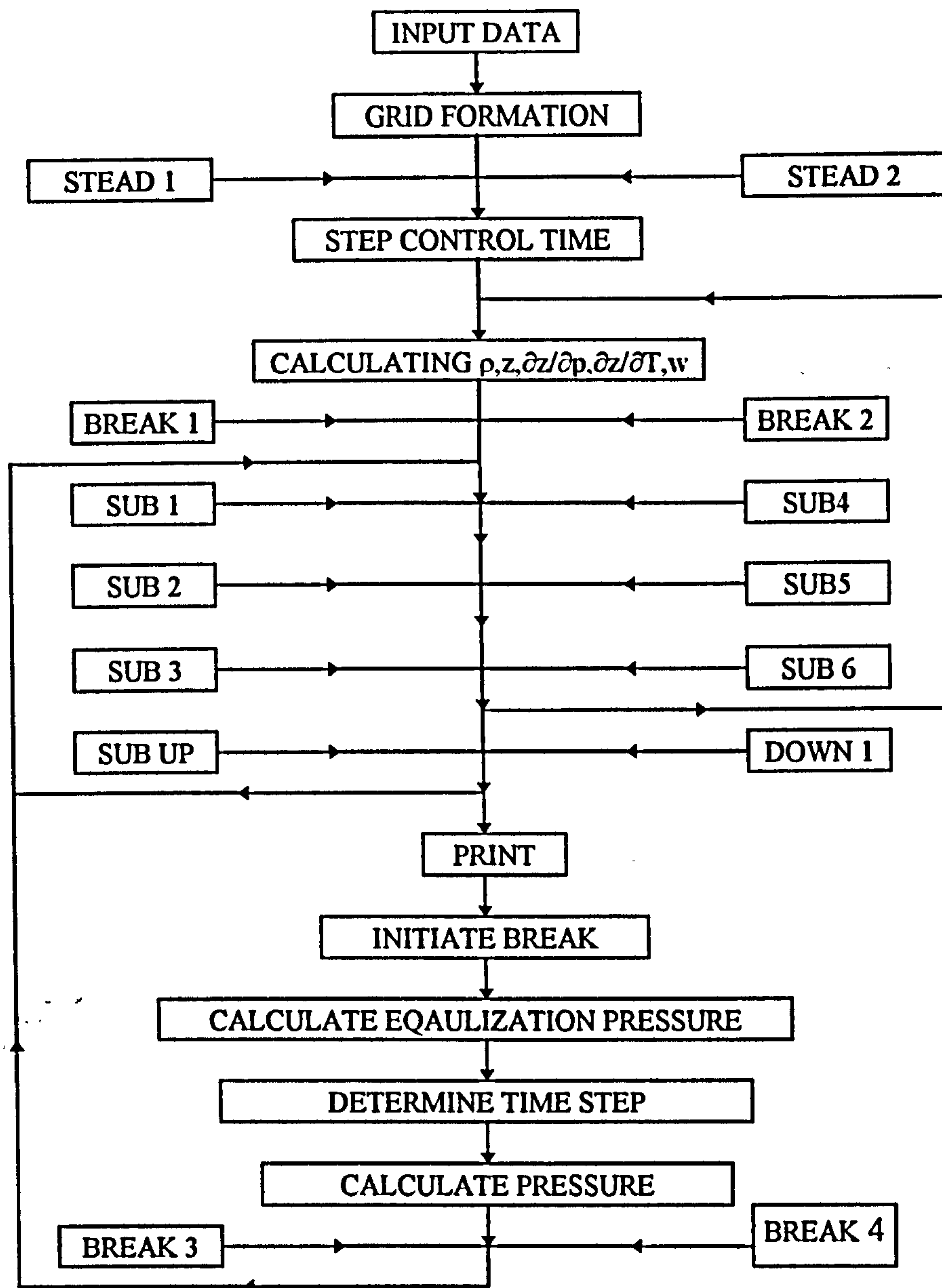


Fig. 4.11 Flow Chart for Tiley's Computer Programme



- (c) Various numerical methods of solution, including finite-difference methods of second- and third-order are used.
  - (d) The C programming language has been adopted.
  - (e) The programme has been devised for use on pc machines.
  - (f) Validation with full-scale experimental data has been undertaken.
  - (g) Fewer simplifications have been made on the basic equations.
  - (h) Various models for steady state analysis, including incompressible and compressible adiabatic, isothermal and non-isothermal non-adiabatic flow models, have been considered.
  - (i) Heat transfer models have been developed for both buried pipes and pipes exposed to the atmosphere.
  - (j) Numerical output data is printed at the required distance and time intervals.
- The other features, which are also included in the Tiley model are as follows:
- (i) Transient analysis can be performed for a given shock tube or single pipe.
  - (ii) Numerical output data is produced for  $p$ ,  $u$ ,  $T$ ,  $\rho$  and  $a$  at each grid point.
  - (iii) Allows the possibility of flow reversal downstream of the break.
  - (iv) Grid size reduction in the vicinity of the break can be handled.
  - (v) Graphical output is produced from numerical data, but in this case using commercially available graphics programmes.

The layout and architecture of this programme is more complex and contains many more subroutines than the Tiley model. The advantages of the C programming language, including the possibility of writing many small subroutines have been fully exploited. The main programme consists of subroutines INITIAL (for initialising the execution of the main programme) and SYSDATA (for inputting the general system and gas data); and sub-programmes STEAD (for performing steady state analysis), TRANS (for performing transient analysis before the break) and BREAK (for performing transient analysis after the break has been initiated). Each of the three sub-programs prints numerical output in data files at the required interval. In addition, there are two other subroutines, GRIDGEN (for performing grid generation, in the case of variable grid size) and BRINC (for initiating the break and calculating the fluid properties at the break, on both the up and downstream sides). For each of the three sub-programmes, namely STEAD, TRANS and BREAK there exists the different combinations and permutations for all the different steady state models, numerical methods of solution and heat transfer models; programmes for analysis of the flow up and downstream the break; and uniform and variable grid size models.

The same programmes are used for transient analysis before and after the break. The only alterations made, are on the equations for calculating the fluid properties at the boundary points, which applies only for the method of characteristics. The uniform grid size programmes have been included because the procedure for developing this programme involved the use of a uniform grid size first. Otherwise the variable grid size programme takes care of this condition. The programme was compiled and run on a personal computer. An IBM compatible personal computer with a RAM memory of 8MB and CPU speed of 25MHz (486SX) performed as good as one with a RAM memory of 16MB and CPU speed of 33MHz (upgraded 486DX2). Personal computers are more convenient than mainframe computers, especially because of their portability which makes it possible for them to be used almost everywhere. This factor is very important, especially for this study, where sometimes it may be necessary to perform the analysis on site. In addition, the QUANT software for thermodynamic and transport properties of fluids is available for use only with personal computers.

The main problem with personal computers is their relatively low computation speed, especially if a small time and distance mesh is used and or if the pipe section is long. The time used to complete the analysis for a one second run time could be as long as five to six days (120 to 150 hours). At the time when this simulation was performed, constant values for the thermodynamic and transport properties of the fluid were used. The inclusion of the QUANT data files reduced the execution speed to less than a half. Also, in order to be able to simulate the flow in a pipeline of say 10km, in the same way as above, a run time of around thirty seconds is required. With the same computing resources as above, such an analysis would last up to a total of five months. Obviously such CPU time is highly excessive and should be reduced by using either a bigger grid mesh or a faster computer. For example, by using  $\Delta x=1\text{m}$ , instead of  $\Delta x=0.1\text{m}$  which was used for the case described above, the CPU time would be reduced by a factor of ten. However, the increase in the in the grid size is limited by the stability criteria of the numerical methods and the accuracy required for the results. Whatever the case, the option of using a faster computer needs to be considered seriously. The use of chips such as the microway number smasher card containing an i860 chip, which is presently being used at Imperial College [Richardson (1993-1996)], is strongly recommended. The card costs about two thousand Sterling pounds and it makes the personal computer 5 to 10 times faster than a 486 personal computer. The I860 chip is to be found in Sun spark stations. The use of Sun spark



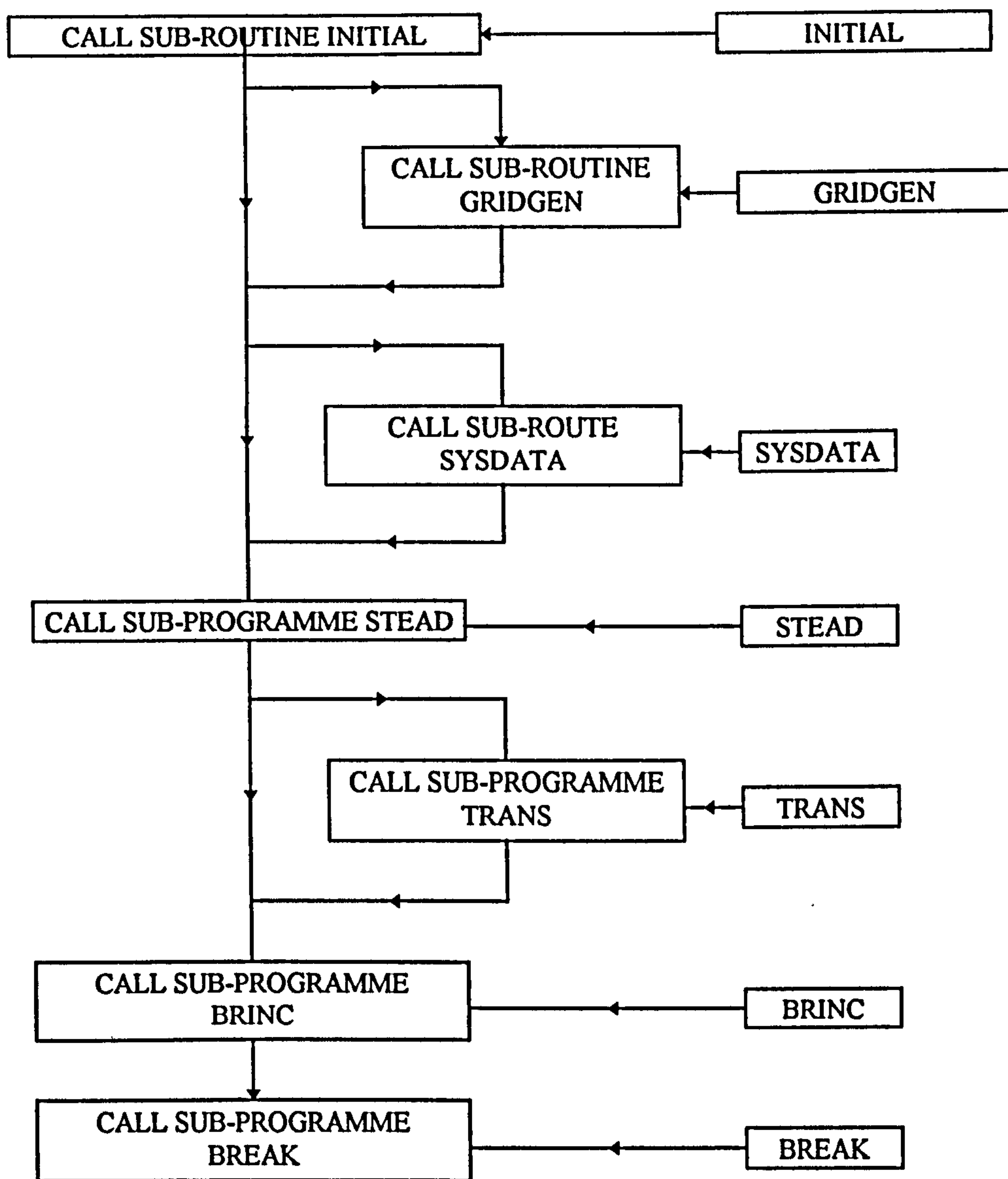


Fig. 4.12 Flow Chart for the Main Computer Programme.

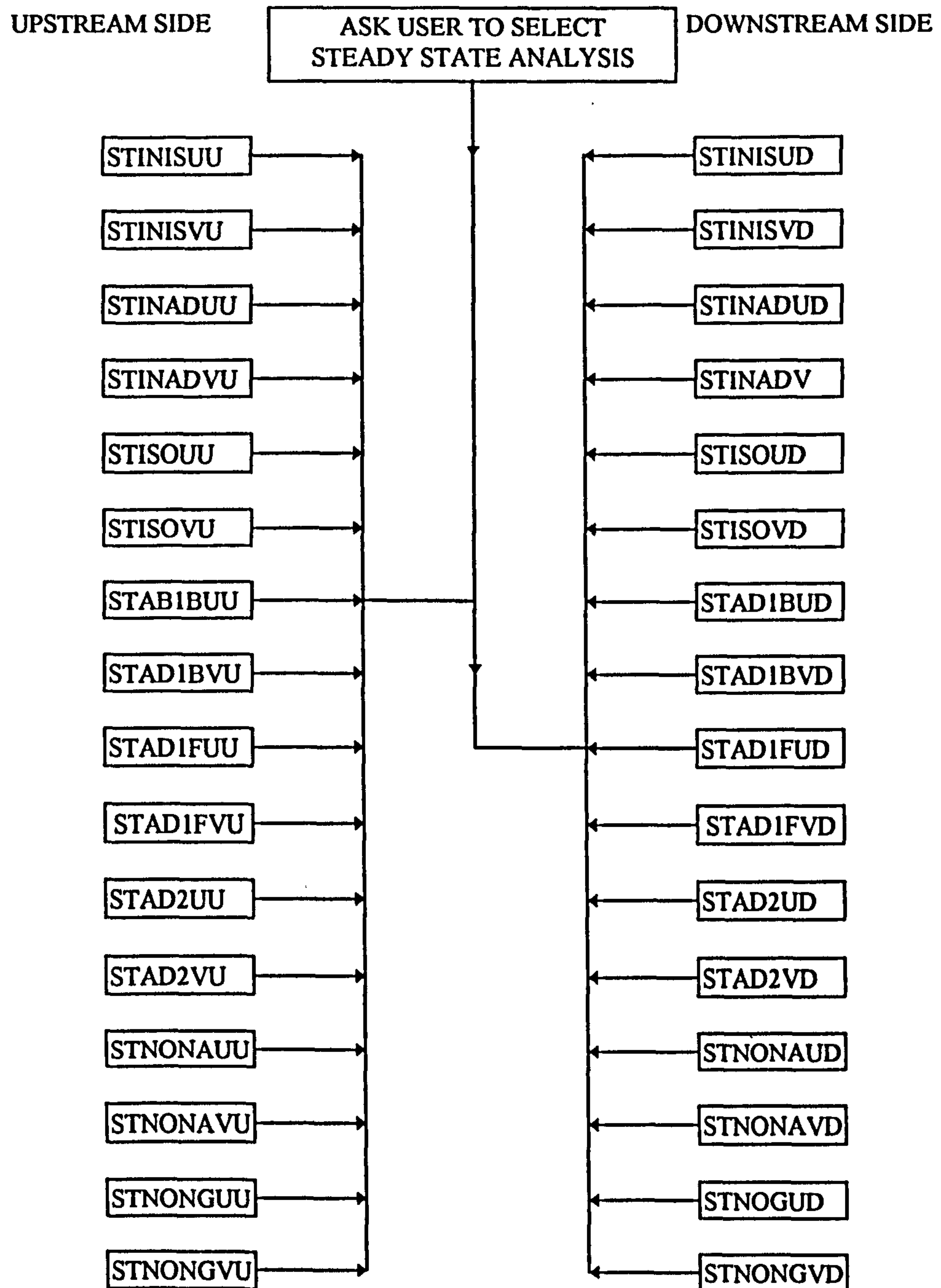
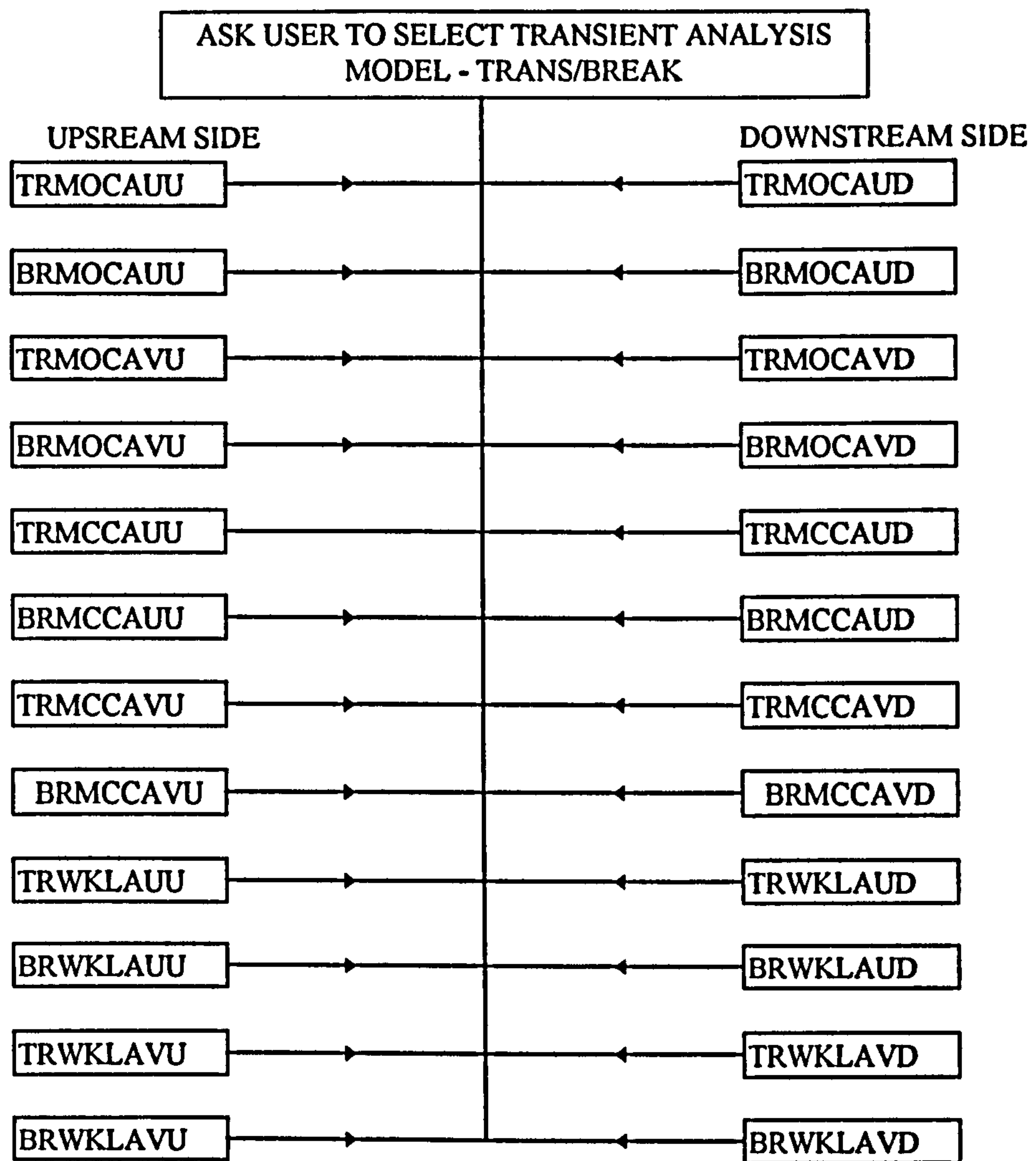


Fig. 4.13 Flow Chart for Sub-programme STEAD Call





NB: These sub-programmes are for the case of pipes exposed to the atmosphere. For buried pipes, "A" is replaced with "G".

Fig. 4.14 Flow Chart for Sub-programmes TRANS and BREAK Calls

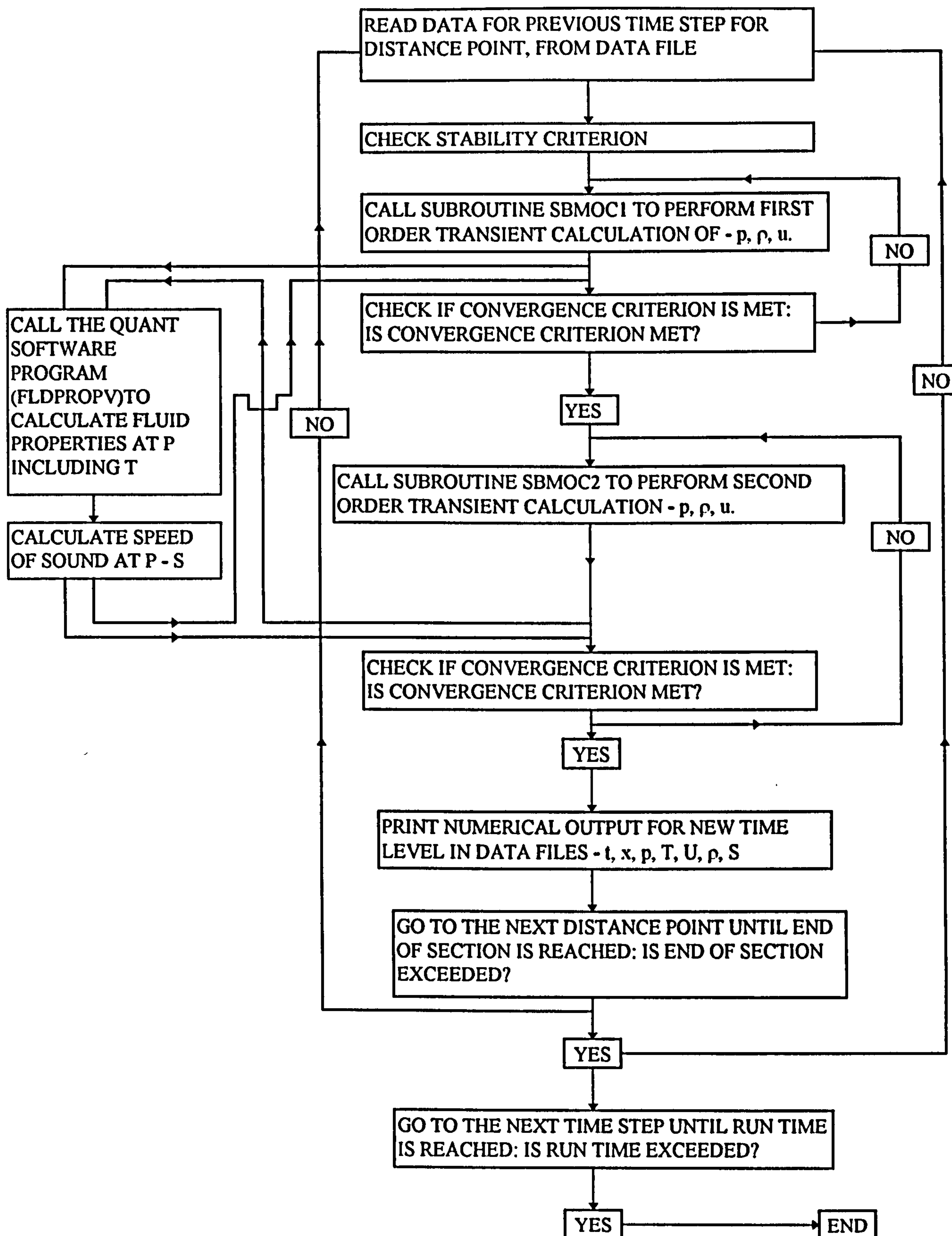


Fig. 4.15 Flow Chart for a Typical Method of Characteristic Programme.



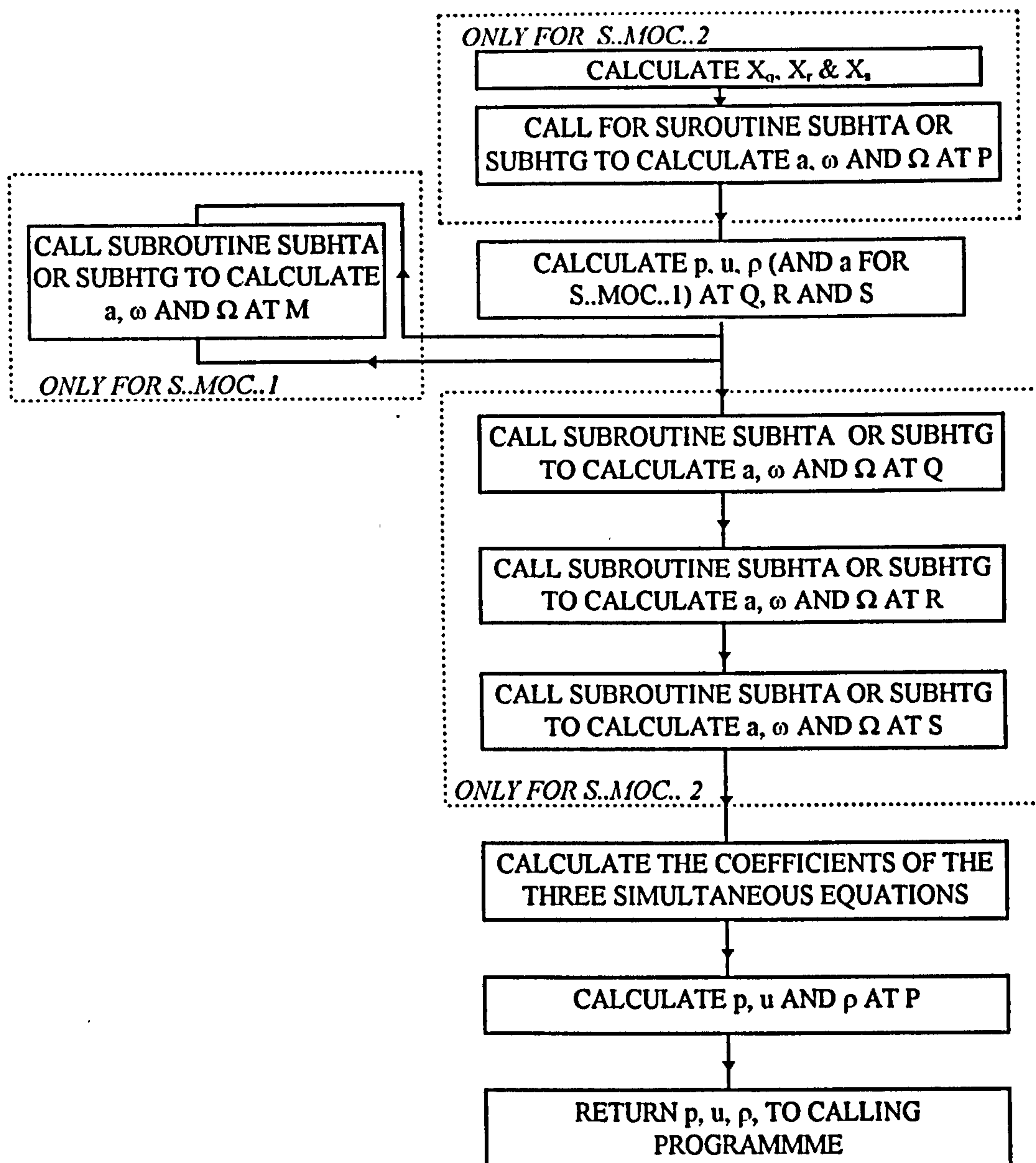


Fig. 4.16 Flow Chart for the Sub-routines S..MOC..1 and S..MOC..2

stations could therefore be another option for increasing the CPU speed, especially if data files produced from the QUANT software are used rather than running the software to produce output at each grid point. The programme was compiled and run using a Borland C++ compiler version 2.1, which is based on the MS-DOS operating system. The compiler is compatible with the Unix version used in Sun spark stations, and the programmes require very minor alterations to enable them to run on the latter system.

Fig. 4.12 through 4.16, illustrate the various subroutines and sub-programmes developed in this study. The listing of all subroutines and sub-programmes is given in Appendix E.

## 4.7 PREPARATION OF GENERAL GAS AND SYSTEM DATA

Before any of the programmes described in Section 4.6 can run, all the required general data about the system and the fluid must be obtained and stored in ASCII form in a data file called SYSTEM.DAT. The data is stored in the sequence shown in Table 4.2 and read as an array ID. Only the numeric values i.e. the column designated value is stored in the SYSTEM.DAT file.

### Pipe lengths: ID[0], ID[6], ID[7] and ID[8]

All the subroutines are based on the arrangement of the pipe shown in Fig. 4.17 below. The test section consists of a straight pipe of length ID[6], extending from a point at distance ID[0] to a point at distance ID[0]+ID[6]. Direction of flow before the break is to the right. The break occurs at a point at a distance ID[0]+ID[8] along the test section, which could be anywhere between the two ends or at one of the ends. Therefore the length from the upstream end of the section to the break point is ID[8], and that from the break point to the downstream end of the section is ID[7].

Unless otherwise specified, the distance to the point at the upstream end of the test section i.e. ID[0] is taken to be zero. Assuming the break takes place on a plane perpendicular to the axis of the pipe, and that no part of the pipe is lost during the break, the total length of the test section is the sum of the length of the section upstream the break and that downstream the break i.e.  $ID[6] = ID[8] + ID[7]$ .



No	Array Element	Description	Value	Units
1	ID[0]	Length of pipe at upstream end		[m]
2	ID[1]	Outer pipe wall temperature at upstream end		[K]
3	ID[2]	Thermal conductivity of pipe material		[W/mK]
4	ID[3]	Thermal conductivity of surrounding medium		[W/mK]
5	ID[4]	Pipe diameter		[m]
6	ID[5]	Angle of inclination of pipe to horizontal		[Rads.]
7	ID[6]	Total length of pipe section		[m]
8	ID[7]	Length of pipe section downstream the break		[m]
9	ID[8]	Length of pipe section upstream the break		[m]
10	ID[9]	Finest distance mesh		[m]
11	ID[10]	Inner pipe wall surface roughness		[m]
12	ID[11]	Pipe wall thickness		[m]
13	ID[12]	Depth of the pipe below the surface		[m]
14	ID[13]	Temperature of the surrounding atmosphere		[K]
15	ID[14]	Pressure of the surroundings		[MPa]
16	ID[15]	Initial temperature of gas at upstream end		[K]
17	ID[16]	Initial pressure of gas at upstream end		[MPa]
18	ID[17]	Mass flow rate of gas		[kg/s]
19	ID[18]	Finest time step for transient analysis		[s]
20	ID[19]	Run time for transient analysis		[s]
21	ID[20]	Coefficient of dynamic viscosity of gas		[Ns/m <sup>2</sup> ]
22	ID[21]	Initial density of gas at upstream end		[kg/m <sup>3</sup> ]
23	ID[22]	Polytropic coefficient of gas		[-]
24	ID[23]	Compressibility factor of the gas at initial conditions		[-]
25	ID[24]	Starting time for transient analysis		[s]
26	ID[25]	Density of gas at final conditions		[kg/m <sup>3</sup> ]
27	ID[26]	Temperature of gas at final conditions		[K]
28	ID[27]	Speed of sound of gas at final conditions		[m/s]
29	ID[28]	Molecular weight of gas		[g/mol.]
30	ID[29]	Equivalent pipe diameter at the broken end		[m]
31	ID[30]	Compressibility factor of gas at final conditions		[-]
32	ID[31]	Ratio of specific heats of gas at final conditions		[-]

Table 4.2: General Gas and System Data Layout

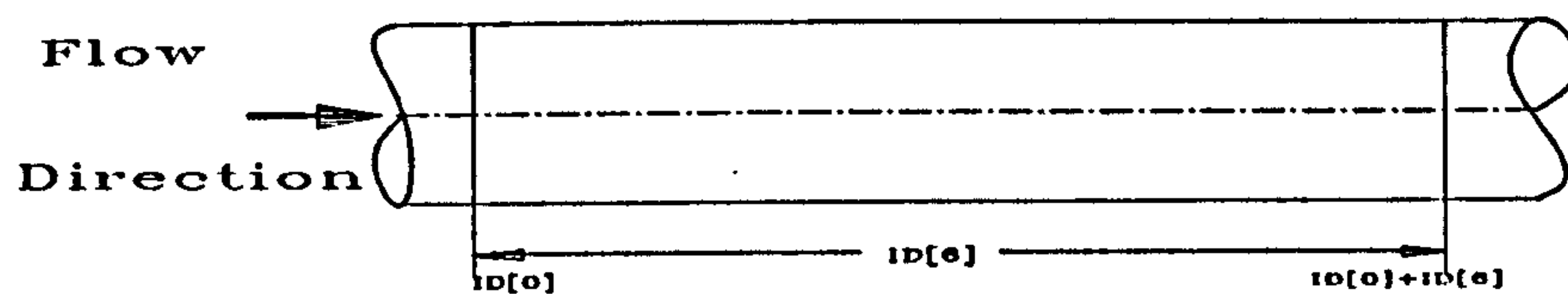


Fig. 4.17a Test Section of Pipe Before the Break.

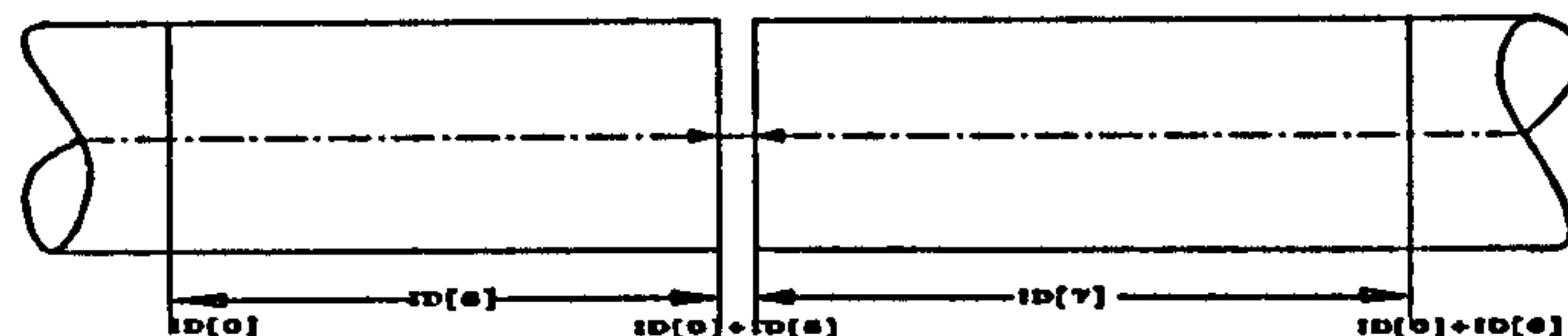


Fig. 4.17b Test Section After the Break

### Pipe Diameters: ID[4] and ID[29]

The basic equations derived for this study can handle situations in which the cross-section area of the pipe varies with distance along the axis of the pipe. However, in this model it is assumed that the cross-section area and hence the diameter of the pipe is constant throughout the test section. This assumption is reasonable for typical gas pipeline systems.

The diameter of the pipe is defined as ID[4]. Very often the break is not full-bore i.e. the cross-section area at the break is different from that at the rest of the pipe. This situation is taken care of by the equivalent diameter at the break (ID[29]). A typical arrangement for such a system is shown in Fig. 4.18.

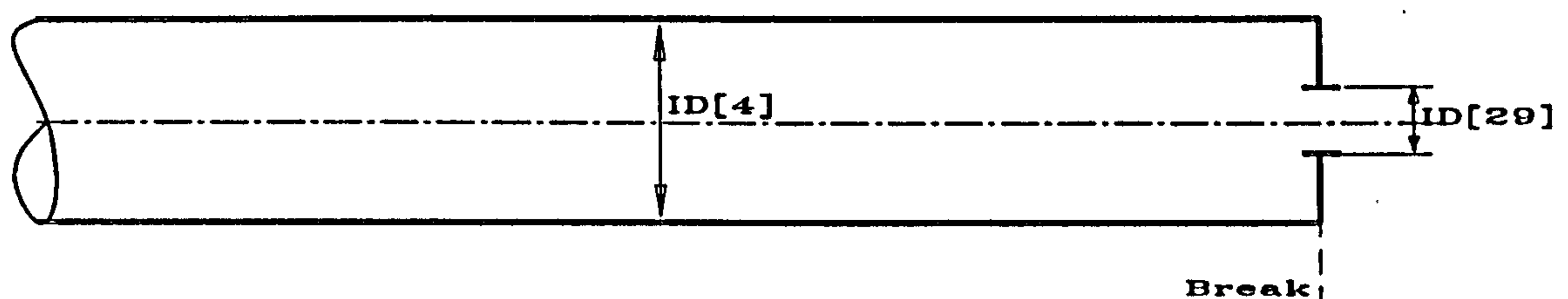


Fig. 4.18 Diameters of the Pipe at Test Section

### Angle of Inclination of the Pipe to the Horizontal: ID[5]

This is the angle which the pipe section forms with the horizontal. In most cases the angle is zero i.e. the pipe is horizontal or for the sake of simplicity, it is assumed to be horizontal.



### **Mesh Size: ID[9] and ID[18]**

With the hybrid method of characteristics and the explicit finite-difference methods used in this model, a rectangular co-ordinate grid is required. To enable the grid mesh to be generated for both the uniform and variable size cases, only two parameters need to be specified, namely ID[9] and ID[18]. ID[9] is the finest distance mesh which in the cases of uniform grid size is the same throughout the length of the test section. In the case of variable grid size, the distance mesh size increases by a factor of two from one mesh size to the next and away from the break. Values of ID[9] smaller than 0.1m presented difficulties because of computer floating point error. It is therefore recommended that an ID[9] value of 0.1m be taken as the smallest. The finest time step ID[18], is determined in relation to the finest distance mesh, according to the Courant-Friedrich-Levy stability criterion. ID[18] also varies in a similar fashion as ID[9] away from the break. For typical high-pressure natural gas linebreak problems, the ratio between ID[9] and ID[18] is around 1000.

The decision on whether to use a uniform or variable grid size depends mainly on the length of the pipe section being modelled. The variable grid size model enables a much longer section to be analysed. The maximum number of grid points which can be handled depends on the capacity of computer used for the analysis. For a 486 personal computer with a RAM memory of 8MB, the maximum number of distance grids which could be handled is around 120. An optimum number is chosen that will ensure the required accuracy criterion and reasonable CPU time are met. The grid mesh for both the sections of the pipe i.e. upstream and downstream of the break are shown in Fig. 4.19.

### **Starting and Run Times: ID[24] and ID[19]**

The run time for a particular transient analysis programme, ID[19], is the time during which the transient event is being modelled. In the case of transient analysis after the break, this is taken to be the time interval from when the break occurs until when the transient event stops. The starting time in this case is taken to be zero.

For transient events taking place over long intervals of time, it may be convenient to do the analyses in batches. After each batch, the values of ID[19] and ID[24] should be changed in the SYSTEM.DAT file. ID[24] is given the value of ID[19] in the previous batch and ID[19] is given a new value, until the required run time is reached. Care should

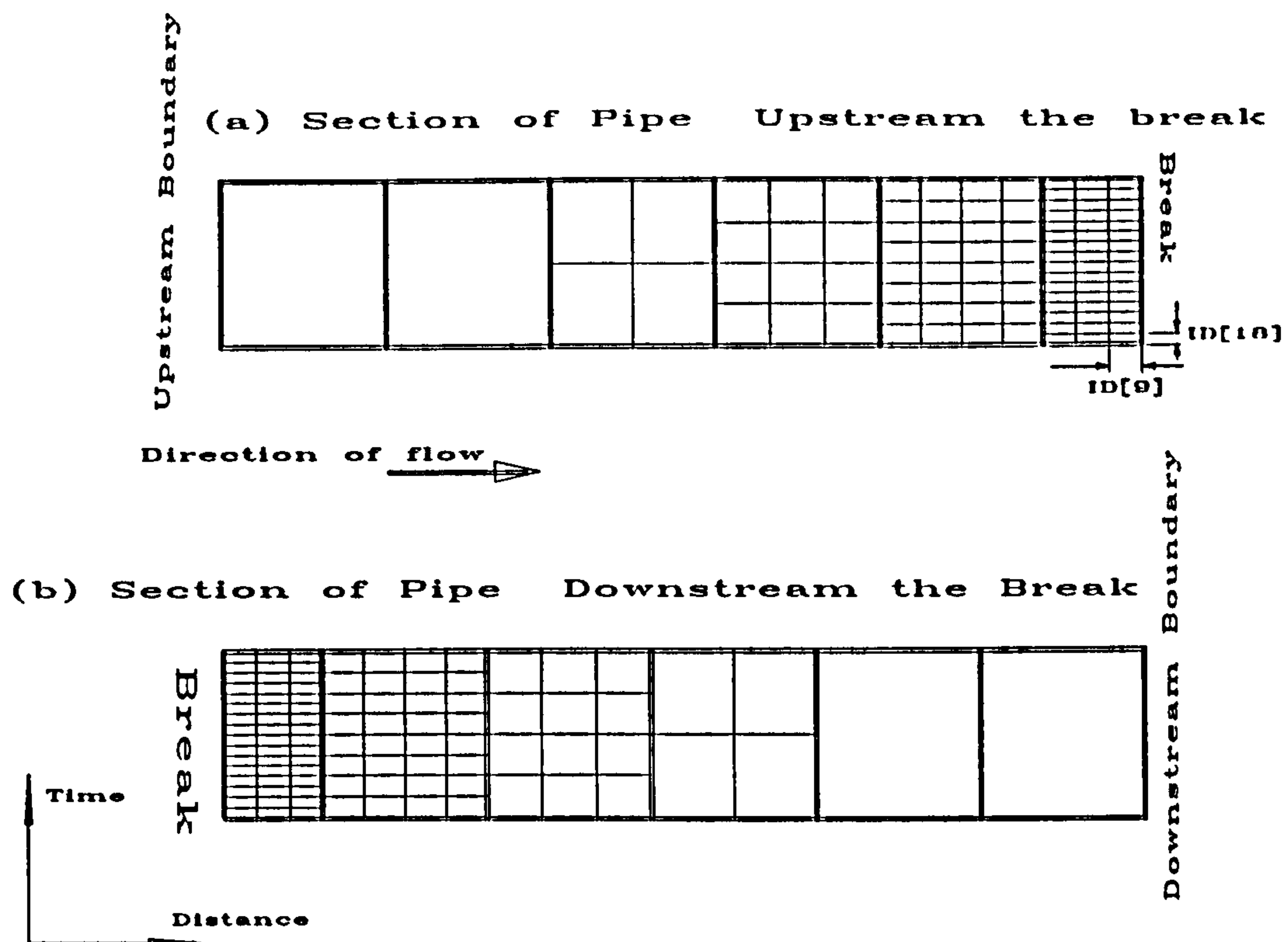


Fig. 4.19 Variable Grid Mesh Layout

be taken to ensure that the respective data files for the last time step of the previous batch are kept intact before starting the next batch analysis.

#### Physical Properties of the Pipe Material: ID[2], ID[10] AND ID[11]

ID[2] is the thermal conductivity of the pipe material and it is used in the non-isothermal non-adiabatic steady state analysis programmes and in the transient analysis programmes to calculate the heat transfer through the pipe wall. The pipe wall thickness (ID[11]) is also required and used in exactly the same way as ID[2]. The inner pipe wall roughness (ID[10]) is used by all the steady state and transient analysis programmes to calculate the frictional force.

#### Physical Properties of the Surrounding Environment: ID[1], ID[3], ID[12], ID[13] and ID[14]

The outer pipe wall temperature and temperature of the surrounding atmosphere (ID[13]) are used by all the non-isothermal non-adiabatic steady state and transient analysis programmes to calculate the heat transfer through the pipe wall and from the pipe to the surrounding environment. The pipe wall temperature needs to be specified only at the



upstream end. In situations where this data is not available, an estimated value is used. The estimated value should be based on the temperature of the surroundings or of the gas, and allow for a reasonable temperature drop. If the value of ID[1] estimated is not accurate enough and also for points other than the upstream end, the programmes will calculate the precise value through iterations.

The thermal conductivity of the surrounding media (ID[13]) and the depth of the pipe below the surface (ID[12]) apply only in cases where the pipe is buried and for non-isothermal non-adiabatic programmes. They are used to calculate the heat transfer through the medium, from the pipe outer wall to the surrounding atmosphere. In most cases the pipes are buried either under ground or water. The surrounding media in these cases are the media in which the pipes are buried, and ID[12] is the depth of the pipe in the medium, below the atmosphere.

Pressure of the surroundings (ID[14]) is the pressure of the place at which the broken pipe discharges. If the broken pipe is open to the atmosphere, the surrounding pressure will be the local atmospheric pressure. In some cases, for example pipes buried under water, the broken pipe would discharge the gas under water and the surrounding pressure will be higher than the atmospheric pressure. In such case, the surrounding pressure is given by the following equation:

$$ID[14] = p_A + (\rho_w \cdot g \cdot ID[12]) \quad (4.298)$$

where  $p_A$  is atmospheric pressure and  $\rho_w$  is density of the water and ID[12] is the depth of the pipe in the water.

**Physical Properties of the Gas: ID[15], ID[16], ID[17], ID[20], ID[21], ID[22], ID[23], ID[25], ID[26], ID[27], ID[28], ID[30] and ID[31]**

Among the above data the primary data which must be specified in all the steady state and transient analysis programmes is the initial temperature, pressure and density of the gas at the upstream end i.e. ID[15], ID[16] AND ID[21] respectively and mass flow rate of gas before the break (ID[17]). With programmes which use the QUANT software i.e. the non-isothermal non-adiabatic steady state and all transient analysis programmes it is not necessary to specify both T and  $\rho$ . The most practical way is to specify T and calculate  $\rho$  using the QUANT software, although the opposite could also be used. This applies only when the domain range of the parameters lies within the range in which the QUANT software delivers output. Otherwise both T and  $\rho$  have to be specified.

The fluid properties  $\mu$  (ID[20]),  $n$  (ID[22]),  $Z$  (ID[23]) all at the initial state of the gas and  $M$  (ID[28]) are not required for the non-isothermal non-adiabatic steady state and the transient analysis programmes. They are used by the other steady state analysis programmes, and they are not all required by each of the programmes. For the programmes using the QUANT software, all the fluid properties mentioned in this paragraph can be calculated from it and need not necessarily be specified in the data file SYSTEM.DAT.

The fluid properties at the final conditions, are the properties of the gas at the state in which the gas is expected to be after the transient event has ended. The properties which need to be specified at the final condition are  $\rho$  (ID[25]),  $T$  (ID[26]),  $a$  (ID[27]),  $Z$  (ID[30]) and  $K$  (ID[31]). These together with the pressure and temperature of the surroundings (ID[14] and ID[15] respectively) are used by the programme for transient analysis after the break as the properties of the gas at the final state, and to which the programme must finally converge.



## CHAPTER 5

### A REVIEW OF SOME EXPERIMENTAL AND NUMERICAL DATA

#### 5.1 INTRODUCTION

Experiments on high-pressure gas pipeline rupture are commonly divided in two categories, namely laboratory experiments and full-scale pipeline experiments. Laboratory experiments have traditionally been performed using shock tubes although other variations are also used. Full-scale pipeline experiments represent more realistically the situation being modelled, but are very expensive, hazardous and entail significant practical problems. Data of this type is therefore very scarce compared with laboratory data, and is in most cases restricted. Laboratory experiments, on the other hand, are more practicable but do not accurately represent the full-scale situation. However, results from shock tubes tests, especially those using modified shock tubes (to include the effects of heat transfer, change in cross-sectional area, etc.) are good enough and have been used in the absence of full-scale experimental data.

Laboratory experiments have traditionally been performed using shock tubes although other variations are also used. An alternative to performing full-scale pipeline experiments would be to wait until a pipeline ruptures accidentally and collect the required data. But since accidents occur unexpectedly, are inherently unsafe, and often when people are ill prepared to collect the required data, it is not possible to collect all the required data. The other alternative data available, is results from other similar computer models. However, this type of data should be used with great caution. Experimental data on linebreak problems and especially full-scale experimental data is becoming increasingly available. Very often, experimental data is available in a form which can not be used directly without modifications, assumptions, extrapolations and interpolations.

Result of transient analysis in ruptured pipelines, whether produced by experiments or computer models, are normally presented in a set of graphs. The more commonly used are the  $p$ - $x$ ,  $T$ - $x$ ,  $u$ - $x$ ,  $p$ - $t$ ,  $T$ - $t$ ,  $u$ - $t$ ,  $I$ - $t$ ,  $m$ - $t$  and  $p$ - $a$  curves. A review of experimental data which is available on pipeline rupture has shown that it consists of data from shock tube tests; laboratory rupture experiments on short sections of pipes; linebreak simulation experiments on full-scale pipelines such as those reported by Bisgaard, Sørensen and Spangenberg (1987) and Van Deen & Reintsema (1983); rupture and blowdown tests on

sections of full-scale pipeline such as the Foothills Pipelines (Yukon) Ltd. (1981); and measurements on full-scale pipeline system during accidental rupture such as the Piper Alpha disaster.

One essential requirement before performing computer modelling of a given pipeline rupture is that the test data, specific gas data and pipeline system data must be prepared in the form required by the computer programme. Often this involves making a number of assumptions and simplifications, such as assuming some parameters to be constant for some interval. Computer software for calculation of thermophysical properties of fluids such as PPDS-IUPAC, QUANT, ASPEN PLUS and PREPROP are available and make the process much easier and accurate, while maintaining a sound computation speed. System data such as pipeline dimensions, is usually included in experimental data. However, some variables such as grid size, friction factor, Stanton number etc. need to be determined. A suitable grid size needs to be chosen in order to meet the required quality of results. Transient analysis in the vicinity of the break is very crucial. However, it is often not easy to obtain the required experimental data and with the required accuracy in this area. In that case, the only available option is to use computer models. Consequently, a review of the available computer models is made, from which suitable results are to be selected for comparison with the model being developed.

## **5.2 LABORATORY EXPERIMENTS**

### **5.2.1 DESCRIPTION OF THE SHOCK TUBE TEST**

A simple shock tube consists of a tube of constant cross-section, in which a diaphragm initially separates two bodies of gas at different pressures. Rapid removal of the diaphragm generates a flow of short duration containing waves of finite amplitudes separated by quasi-steady regions. Initially, after diaphragm removal, a shock wave travels into the low pressure gas while an expansion or rarefaction wave travels into the high pressure gas. The quasi-steady flow regions induced behind these waves are separated by a contact surface across which pressure and velocity are equal, but density and temperature are in general different. The shock heating of the low pressure gas and the expansion cooling of the high-pressure gas, permit a very wide range of flow temperatures to be achieved. There is a very wide range of research applications of shock tubes, including the study of the propagation of pressure waves in unsteady fluid flow situations. A large number of results from shock



tube experiments exist and some of these are specifically on the modelling of unsteady fluid flow, similar to that occurring in ruptured high-pressure pipelines.

Stronger shock waves can be produced with various modifications to the simple shock tube. These modifications include driver gas heating and area reduction from driver to driven sections. The theory and performance of simple shock tubes has been described by Glass (1958); and Hall (1958) covers modified shock tubes.

### **5.2.2 REVIEW OF SOME LABORATORY EXPERIMENTS**

There is a wide range of experimental results from shock tubes available. These have been presented and discussed by Glass (1958), Issa (1970), Thorley & Tiley (1987) and Tiley (1989). There seems to be not much published recently, on shock tube modelling of ruptures in high-pressure gas pipelines. Most of the recent work is based on full-scale pipeline experiments, which are becoming increasingly available.

Based on a three point criteria, described in Section 5.5, Tiley (1989) selected the Groves-Bishnoi-Wallbridge (1978) [referred to as the Groves data] shock tube data and the British Gas shock tube data [Jones and Gough (1981)]. The Groves data was also used by Cronje, Bishnoi and Svrcek (1980) to simulate gas pipeline rupture, with successful results. In using the Groves data, Tiley (1989) had to make various assumptions regarding shock tube material (in order to estimate the friction factor and Stanton number); the effective rupture time of the diaphragm and the accuracy and sensitivity of the measuring and recording devices. Therefore, no assessment could be made of the experimental errors incurred. No such problems were experienced with the British Gas data.

Lyszkowski, Grimesey and Solbrig (1978) used experimental results from ideal gas shock tube tests and blowdown of an ideal gas from a 13ft (approximately 4m) long pipe. In the case of the shock tube tests, the length of the pipe was 20ft (approximately 6m) and the initial pressure ratio at the middle was 7.9 to 1 [114.7lb/in<sup>2</sup> abs. to 14.7lb/in<sup>2</sup> abs. (7.9 to 1 bar)]. The velocity was uniformly zero and the internal energy was uniformly 80.62Btu/lb (187.5kJ/kg) initially. A diatomic gas having a specific heat capacity ratio ( $K$ ) of 1.4 was used. Results were presented in the form of graphs of pressure, velocity and internal energy; all as functions of the pipe length. The same gas was used in the blowdown experiment. The ratio of the initial pressure in the pipe to ambient pressure was



2.83 and the initial pressure was 1,000 lb/in<sup>2</sup> abs (69 bar). Results were presented in the form of closed end pressure and break velocity as functions of time after the break.

Ilic (1987) determined experimentally the rate of transient mass discharge of a two-phase mixture through a short pipe. An initially stagnant and saturated column of Freon-12 liquid stored in a 0.25 litre glass vessel was used. Blowdown was initiated through a 3.2mm bore brass tube, 50mm long by opening a quick acting ball valve located downstream from the pipe. Strain gauge pressure transducers with natural frequency of about 20kHz were used to measure vapour pressure in the space above the liquid in the glass vessel and the pressure of the liquid at the exit of the discharge pipe. A Bourdon tube compound pressure gauge was used to indicate the initial and final receiver pressures. The fluid temperature was measured at the exit plane of the pipe with a 0.2mm diameter chromel/alumel thermocouple whose bare hot junction was machined flush with the pipe bore and thermally insulated from the pipe wall by a resin plug (1.6mm diameter) in which the thermocouple wires were embedded. A similar thermocouple mounted on the discharge pipe wall showed that the temperature drop was insignificant throughout the blowdown period, except during the vapour stage. The pressure transducer and temperature signals were recorded on a high speed chart recorder. Results have been presented in terms of photographs taken at 0.33 seconds intervals, discharging vessel mass inventory variation with time and discharge tube exit characteristics and driving pressure history. An initial delay period was observed before the start of ebullition by the formation of vapour at the bottom of the vessel. Discrete bubbles eventually combined to form a slug of vapour which displaced the descending liquid surface and caused considerable mixing in its wake. At the end of blowdown, only vapour issued from the vessel. The criterion of choking was taken to be the independence of the pipe exit pressure from the receiver pressure changes. This condition was confirmed by the simultaneous measurement of the fluid exit temperature, which showed similar trends to the exit pressure.

Haque, Richardson, Saville and Chamberlain (1990) reported on experiments conducted on rapid depressurisation of large pressure vessels at the Imperial College, London. The aim of the experiments was to enable understanding of the physical processes involved during blowdown. The experiments involved the depressurisation of three vessels ranging in diameter from 5 to 110cm, with length to diameter ratios from 10 to 3 respectively. Most of the measurements were made on vertical vessels blowdown from the top and from the bottom. However, measurements were also made on horizontal vessel



blowdown through an exit on the axis of the end closure of the vessel. Measurements recorded included pressure, temperature and composition; all as a function of time during the blowdown process. The vessels were instrumented with pressure transducers to measure the internal pressure and thermocouples to measure temperature within the gas space in the vessel and the surface temperatures of the vessel wall, both inside and outside. Pressurisation was with nitrogen at 150 bar and depressurisation was through an orifice down to atmospheric pressure. A data logger was used to record all the pressures and temperatures once every 3 seconds.

Haque, Richardson, Saville, Chamberlain and Shirvill (1992) presented and discussed experimental measurements which were taken to validate their computer model, BLOWDOWN. The experiments were conducted using different sized vessels oriented vertically and horizontally; containing a range of different fluids; and with blowdown from the top, bottom and side through chokes of various sizes. The experiments were conducted using three vessels of different sizes, in order to check the effect of vessel size on the model predictions. The model showed that the predictions are scale-independent. The three vessels used were named as Vessel 1 to 3; and had lengths of 3.240m, 1.524m and 0.671m; inside diameters of 1.130m, 0.273m and 0.040m; and thickness of 59mm, 25mm and 5mm respectively. Transducers were used to measure the pressure in the vessels to an estimated accuracy of  $\pm 0.2$  bar. Pressure gauges were also used to give direct measurements. Bare-wire thermocouples were used to measure the temperature of the fluid within the vessel and also of the inside and outside walls to an estimated accuracy of  $\pm 0.5$ K. It was also possible to withdraw samples of the fluid from the top and bottom of the vessel at arbitrary stages during blowdown, and to measure the composition of the samples using a mass spectrometer and a gas chromatograph. In addition, a windowed port was attached to the upper part of the vessel and a mirror set at an angle of  $45^\circ$  to the vertical within the vessel. A video camera was then used to view the fluid within the vessel both horizontally, across the upper part of the vessel occupied by gas; and vertically downwards, from the part occupied by gas to the part occupied by liquid. In this way condensation in the gas and evaporation in the liquid could be monitored directly and continuously during the blowdown. All measurements were transmitted to data logging systems and thence to micro-computers for subsequent data reduction. The experiments were carried out at the Imperial College (for Vessel 2) and the British Gas test site at Spadeadam (for Vessel 1).



Experiments using Vessel 1 at Spadeadam were conducted on mixtures of methane, ethane and propane; together with some on nitrogen (for comparison with the Imperial College experiments). Some eighteen and fifteen sets of experiments, which were referred to as S1 to S18 and I1 to I15 were conducted at Spadeadam and Imperial College respectively. The experiments covered a wide range of different fluid compositions, vessel orientation, blowdown directions and choke sizes. The experiments at Imperial College were, for safety reasons, confined to non-inflammable but representative fluids. Nitrogen was used as a representative gas phase since its critical properties are in the same range as those of methane; and carbon dioxide was used as a representative condensable phase such as propane. The initial pressure was, except in two cases 120 bar for the Spadeadam tests; and 50 bar for the Imperial College tests. Blowdown times were of the order of 1,500 seconds for the Spadeadam experiments and 100 seconds for the Imperial College experiments. Three experiments, namely I1, S9 and S12; all of which were conducted with a vertical orientation of the vessels and blowdown at the top position; were selected as representative comparisons for the BLOWDOWN model. However, in the case of the pipeline rupture model, experiments carried out at a horizontal orientation of the vessels are more representative. Richardson (1993-96) reports on further experimental blowdown tests on a 1.6m long, 0.3m diameter vessel at Imperial College; a 3.0m high, 1.3m diameter vessel conducted by SHELL at Spadeadam; and a 0.3m high, 0.15m diameter vessel at Imperial College for a number of flashing flow tests.

### **5.3 REVIEW OF SOME FULL-SCALE PIPELINE EXPERIMENTS**

Perhaps the earliest full-scale pipeline rupture tests are those reported by Sens, Jouve & Pelletier (1970). The test was conducted on an 11,800m long 0.1065m internal diameter natural gas pipeline at a pressure of 31.4bar. The results in form of p-t and u-t curves were compared with calculated results and said to be identical. However, this is one of the simplest cases of natural gas flow, since the pressure was relatively low and measurements were taken away from the vicinity of the break. In most cases, the pressure would be so high that the modelling would involve handling of liquid and gas phases. In a test programme conducted by Alberta Petroleum Industry Government Environmental Committee (1979), an existing 168.3mm outside diameter pipeline which was typical of sour gas lines in the province was used. The test section, approximately 4.0km in length,



was burst at the midpoint. In addition, one rupture was performed on a pipeline of 323.9mm diameter and approximately 7.1km long. Of the results presented, only the p-t and m-t curves are relevant for this case.

Tiley (1989) used results from some full-scale tests on high-pressure gas pipelines including those reported by Jones & Gough (1981) and Foothills Pipelines (Yukon) Ltd. (1981). As for the results presented by Jones and Gough (1981), the tests were conducted with natural gas and using short sections of pipe. Tests, sections were 1.22m diameter and approximately 50m long with reservoir sections at both ends. The pipe was pressurised to approximately 90bar and a crack was initiated at the centre of the test section. Pressure histories were recorded at points either side of the break, and results were presented as p-a curves. Similar results; for tests carried out by BMI, on behalf of British Gas; and for tests that British Gas conducted for SHELL; were also presented. In these cases, the initial pressures were 120 and 140 bar respectively. The experiments reported by Foothills Pipeline (Yukon) Ltd. (1981) were carried out between 1979 and 1981 at the Northern Alberta Test Facility. Short sections of about 120m long and 1.4m and 1.2m diameter pipe were charged with natural gas of known composition and pressurised to between 74bar and 87 bar. Fracture was initiated at the centre of the test section and results were presented in the form of p-t and p-a curves.

Van Deen & Reintsema (1983) used experimental data from GASUNIE to validate their theoretical model. In the experiment, a linebreak was simulated by rapidly opening a valve which connected the test pipe to a parallel pipe at a lower pressure. Another set of data from full-scale pipeline simulation of a rupture is that reported and used by Bisgaard, Sørensen and Spangenberg (1987), and which was carried out in 1979 on a 77.33km gas pipeline from Neustadt through Sörzen to Unterföhring in Germany. Gradle (1984) presented blowdown curves for natural gas i.e. graphs of blowdown time versus pipeline volume (t-V curves), for different types of pipeline and at line pressures ranging from 13.8bar to 103.4bar. Knox, Atwell, Angle, Willoughby and Dielwart (1980) presented results of sour gas pipeline rupture experiments. Two pipelines of a 3.8km, 168mm diameter and a 7.1km, 323mm diameter were ruptured at the midpoints of the test sections. m-t curves were presented for the two pipelines at an initial pressure of 69bar and gas temperature of 10°C. The total mass of gas released was also measured. Wilson (1981) also reported on full-scale rupture tests performed in 1978 by Alberta Petroleum Industry, Government Environmental Committee (1979). Botros, Jungowski and Weiss (1989) used

the data obtained during the blowdown of a straight gas pipeline section and a three-unit compressor station for comparison with their models. Results were presented in the form of p-t curves.

Richardson and Saville (1991) used experimental data from one of three ruptures of lines connected to the Piper Alpha platform, which was monitored sufficiently well to give useful validity information; and also data from a line of length 100m and bore 150mm, containing LPG. In the latter case, initial pressures of up to 21bar, and initial temperatures of about 293K were used. The blowdown was done through orifices ranging in equivalent diameter from 0.01m to 0.15m (full-bore). Results were presented in the form of p-t and p-T curves, at the intact end of the line; and m-t, M-p curves. Some of these results were also used by Chen, Richardson and Saville (1992). Chen, Richardson and Saville (1993) reported on a 100m long pipe with an internal diameter of 150mm, which was fully ruptured at one end. Pressure at the intact end and total mass in the pipeline were recorded as a function of time. The pipe was filled with 95% propane and 5% butane mixture at a pressure of 11bar and temperature of 20°C. Much more data resulting from laboratory experiments and also full-scale tests, but which has not been published, exist. However, the data was not available for this study.

Mallinson (1996) reports of recent experimental data, which have been acquired by British Gas in addition to the ones reported by Jones and Gough (1981). The new data were obtained through full-scale pipeline tests, in collaboration with several other companies. Mallinson (1996) further states that the cost of the experiments was very high, and as such the results are both valuable and also commercially sensitive. This data was therefore not available for this study.

Morrow (1996) reports on other recent full-scale pipeline venting tests, which were performed by a gas transportation company, in order to evaluate leak detection systems. The pipeline system consisted of parallel pipelines with interconnections or cross-overs that could be opened or closed. The interconnections were spaced at regular intervals between compressor stations. A partial linebreak was simulated by venting gas through a smaller diameter branch line terminated by a remotely actuated quick acting relief valve. A full linebreak was not simulated. P and T data were recorded. This information was received too late to be able to follow up on the possibility of the data being made available.



## 5.4 REVIEW OF SOME NUMERICAL DATA

Sens, Jouve and Pelletier (1970) claimed that results from their model was identical with their experimental results described in Section 5.3. Arrison, Hancox, Sulatisky and Banerjee (1977) compared predictions by their RODFLOW code with experimental data for blowdown of a recirculating water loop containing two pumps, two heated sections and two heat exchangers arranged in a figure-of-eight geometry. Results were presented as p-t and T-t curves at different sections of the loop and different break sizes.

Groves, Bishnoi and Wallbridge (1978) developed a computer model to calculate decompression wave velocities in natural gas pipelines. The model was validated with the experimental data of Groves (1976). Results were presented as p-a curves. Cheng and Bowyer (1978) used their quasi-one-dimensional unsteady compressible fluid flow code to simulate two cases of transient flow. Transients caused by a sudden pipe rupture at the left hand side of a three duct steam system were predicted. Results were presented as p-t curves. Lyczkowski, Grimesey and Solbrig (1978) presented comparative results of their alternating gradient method with analytical results and also their experimental data described in Section 3.2. The results were presented as p-x, u-x and e-x in an ideal shock tube 5ms after the break; p-t and u-t at the closed end of the pipe for an ideal gas; and p-t for a blowdown of steam-water mixture pipe.

A study by Alberta Petroleum Industry, Government Environmental Committee (1978) reported on existing two isopleth prediction models, one blowdown model and a simplified blowdown model developed during the study. Predictions from the blowdown models were presented as m-t curves and validated with experimental results in a subsequent study [Alberta Petroleum Industry Government Environmental Committee (1979)]. Knox, Atwell, Angle, Willoughby and Dielwart (1980), presented M-t curves resulting from their theoretical model and compared them with their experimental data reported in Section 5.3. Cronje, Bishnoi and Svrcek (1980) presented graphs of results from their adiabatic model and compared them with the experimental data of Groves (1976). Results were presented as p-a curves for pure methane and argon. Wilson (1981) presented an M-t and exit pressure ration against time for the full-scale pipeline rupture experiments described by Knox, Atwell, Angle, Willoughby and Dielwart (1980).

Fanneløp and Ryhming (1982) presented several graphs which model the pressure profiles and release rates following the rupture of a gas pipeline. No experimental data was

used, and in the simulation the break took place at the high pressure end. Van Deen and Reintsema (1983) compared results from their numerical model with full-scale pipeline experiments which were designed to simulate a linebreak. Graphs of pressure against time were presented for the two simulation experiments. Flatt (1985 and 1986), presented various graphs resulting from predictions of his model. However, no experimental data was used to validate his model predictions. The graphs presented include p-x, u-x, S-x, a-x and m-x; and m-t curves.

Bisgaard, Sørensen and Spangenberg (1987) compared results from the linebreak simulation experiments reported in Section 5.3 with results of their numerical model. Results were presented as p-t curves for the above case and also for simulation of a rupture in a straight pipeline using their numerical model. Lang and Fanneløp (1987) presented m-t curves, resulting from simulations with three different methods and compared them with those calculated by Fanneløp and Ryhming (1982). They also presented p-x and u-x curves for various times after the rupture.

Picard and Bishnoi (1988) compared results from their computer models with experimental data from the Northern Alberta Burst Tests [Foothills Pipeline (Yukon) Ltd. (1981)]. Graph of pressure ratio  $p/p_L$  (where  $p_L$  is the pressure at the initial condition) versus expansion wave velocity were presented. Picard and Bishnoi (1989) used their three models to demonstrate the importance of real-fluid behaviour in modelling of high pressure gas pipeline ruptures. A case was considered whereby after a sudden rupture of a 168.3mm diameter sour-gas pipeline, an upstream emergency shutdown valve closes, restricting the blowdown length to 1000m. Pressure of the gas was 110bar. Results were presented as m-t, p-t, u-t, a-t, and T-t curves.

Tiley (1989) used the shock tube data used by Groves, Bishnoi & Wallbridge (1978) i.e. that of Groves (1976) and that of Jones & Gough (1981); and also the full-scale pipeline experimental results of Foothills Pipeline (Yukon) Ltd. (1981) to validate her computer model. Results were presented as p-a and p-t curves. Botros, Jungowski and Weiss (1989) presented a series of p-t profiles resulting from their models predictions. Comparisons were made with their field measurements reported in Section 5.3. Lang (1991) presented p-x, m-x and m-t curves, resulting from his numerical model. Kunsch, Sjøen and Fanneløp (1991) presented m-t, I-t, u-t, p-t and p-x curves produced by their computer model for rupture of sub-sea pipeline connected to process equipment on the platform through a vertical segment.



Richardson and Saville (1991) presented a series of graphs comparing predictions from their model BLOWDOWN with experimental results. The results consist of p-t, T-t and I-t curves at the intact end of the pipe; m-t and mass efflux curves against time at the ruptured end; and mass flux through the orifice with upstream pressure. Chen, Richardson and Saville (1992) presented m-t, p-t curves at both the open and intact ends of the pipe. The graphs consist of results obtained from the BLOWDOWN model and from experiments. Haque, Richardson, Saville, Chamberlain and Shirvill (1992) presented p-t, T-t and m-t following blowdown of a gas vessel. The data calculated using the BLOWDOWN model was compared with experimental results. Chen, Richardson and Saville (1993) presented p-t curves at the intact end and m-t curves of the line predicted by their homogeneous two-phase model and also resulting from experiments.

Olorunmaiye and Imide (1993) presented m-t curves, produced by their model and compared them with results calculated by Flatt(1986) and also Lang and Fanneløp (1987).

## **5.5 SELECTION OF TEST DATA**

In her selection of experimental data for comparison with the theoretical model, Tiley (1989) used the following criteria:

- (i) The variables required by the programme must either be given in the experimental data or be calculated from it.
- (ii) The experimental results must be of a form that can be directly compared with the theoretical computer output.
- (iii) Details of the apparatus and procedure are necessary in order to be able to assess the experimental error and evaluate the results obtained.

The same criteria will be used in this study. All the recent data described in Section 5.3 was not available for this study, despite the big effort made to secure it. The discussion of the data which could be obtained and its screening for suitability in this study is covered in this section.

When a break occurs in a high-pressure gas pipeline, the pressure of the gas drops virtually instantaneously at the break and rarefaction waves are transmitted up and down the pipeline and rapidly dissipated when the fluid in the pipe is a gas. A flow reversal occurs in the section of the pipe down stream the break. In order to model these waves properly, a reduced grid size is normally required in the vicinity of the break. Mass release rates from pipeline ruptures was studied by Wilson (1981). The behaviour of gas during

its initial release, expansion and plume rise was studied by carrying out an exact momentum analysis of the expanding jet outside the pipe rupture, and developing a more sophisticated model for both the mass release rate and the plume rise of the momentum jet. The most hazardous portion of the gas released during a pipeline rupture is emitted during the first 10 to 20 seconds, when the high initial mass flow causes the largest downwind concentrations. There have been other but simpler models for predicting the initial release rates from high-pressure gas pipeline rupture, including those by Flatt (1986) and Kunsch, Sjøen and Fanneløp (1991). Another factor which affects the release rates is the rupture mode. This was studied by Knox, Atwell, Angle, Willoughby and Dielwart (1980). In most cases a full bore rupture is assumed. Wilson (1981) also studied the heat transfer to the moving gas through the pipe walls and observed from experiments almost an isothermal condition throughout the length of the pipe, except for about the last 200 diameters during which the rapidly accelerating flow near the pipe exit was moving too quickly to gain heat from the pipe walls.

To be able to produce comparable results, a model developed for such as above conditions and assumptions, should be validated with data obtained from experiments performed under similar conditions. Criteria such as the one used by Tiley (1989), and listed in this section, is very useful in selecting experimental data for comparison with theoretical models. The review of experimental data available has revealed that the criteria are very seldom met, and consequently a number of test sets have to be used in order to validate a particular model. Also some assumptions have to be made for some data, thus reducing the accuracy of the data. For example, in using the Groves data, Tiley (1989) had to make various assumptions regarding shock tube material in order to estimate the friction factor and Stanton number; the effective rupture time of the diaphragm and the accuracy and sensitivity of the measuring and recording devices. Therefore, no assessment could be made of the experimental errors incurred.

Four different categories of data for validating computer models have been reviewed in this chapter. The main disadvantage of laboratory experimental data, including shock tube data, is that of its much smaller scale compared to full-scale pipelines. The small diameter effects observed by Groves, Bishnoi and Wallbridge (1978), thermal effects included by among others Tiley (1989) and frictional effects discussed by Flatt (1986) are some of the important factors against laboratory experiments data. Under such a situation, many of the assumptions such as frictionless, adiabatic flow etc. which would not normally apply to full scale pipelines, hold true. This means that a model developed under such



assumptions and validated with such data would produce comparable results, but it would not produce correct results when applied to a full-scale pipeline. However, one the positive aspects of laboratory experiments, is that high compression ratios could be used, thus producing strong shock waves. On the other side, simulated rupture experiments represent a more realistic presentation of all the effects encountered in a full pipeline rupture, but operate under very small pressure ratios. For example in the experiments used by Van Deen and Reintsema (1983) and Bisgaard Sørensen and Spangenberg (1987) the pressures varied by approximately 0.2bar in 400 second and 2.3bar in 2 hours. In a typical high-pressure gas pipeline rupture, the pressure at the break would be reduced to near ambient pressure within a fraction of a second. Simulated full-scale pipeline experiments therefore represent rather slower transients compared to actual rupture experiments.

Full-scale pipeline rupture tests provide the most suitable data for validating numerical models. But even with full-scale pipeline experimental data, often measurements do not exist for the section of the pipeline in the vicinity of the break and at the time interval required to show all the important variations of the properties. Some models for simulating pipeline ruptures were claimed to have passed simply because the data used to validate them was based on laboratory experiments which could not represent all the effects existing in a full-scale pipeline. The claim by Haque, Richardson, Saville, Chamberlain and Shirvill (1992) that their model predictions were scale-independent, should be treated with great caution, since the study was on vessels and not pipelines. In such cases the effects mentioned above are not significant. Numerical results from other models are only useful as a qualitative comparison when developing a computer model and preliminary evaluation and comparison of results. They should not be regarded as final validity evidence.

Although as seen in this review, there is plenty of experimental data for validation of computer models, it is not easily available. When available, it is often in a form of printed graphs which requires one to translate it into numerical data. In some cases, the specification of the gas and test condition is not fully given and even when given, it is not always easy for workers to obtain the properties of such mixtures. All these are some of the factors that significantly affect the accuracy and validation of computer models for rupture in natural gas pipelines. Even with a working model, there is a need to regularly update the gas composition since as observed by Foothills Pipeline (Yukon) Ltd. (1981), it changes with time.

Computer models for simulation of transient flow of gas following a rupture in high-pressure pipelines must be validated with suitable experimental data. Although all types of data discussed in this paper are useful at some stage of development of a computer model, full-scale pipeline rupture tests provide the most suitable and reliable data for validating computer models for such events. Whenever possible this category of data should be used as the final and most reliable validity test for computer models. The review of experimental data available has revealed that a number of test sets have to be used in order to provide all the necessary data required to fully validate a particular model. Also some assumptions have to be made for some data, thus reducing the accuracy of the data. Although as seen in this review, there is plenty of experimental data for validation of computer models, it is not easily available.

Based on this review, four sets of experimental data are selected for validation of this computer model. The data is that reported by Jones & Gough (1981), Foothills Pipeline (Yukon) Ltd. (1981), Alberta Petroleum Industry Government Environmental Committee (1979) and Sens, Jouve and Pelletier (1970). The test data is referred to in this study as the British Gas, Foothills, API and SNGSO test data respectively. More details about the tests and the data are presented in Chapter 6.



## CHAPTER 6

# VALIDATION OF THE COMPUTER MODEL

### 6.1 VALIDATION PROCEDURE

It was decided in Chapter 5 that four sets of full scale pipeline experimental data on pipe sections of varying lengths, diameters and operating conditions will be used to validate the computer model predictions. The tests, which are referred to as British Gas, Foothills, APT and SNGSO; are briefly described in this chapter. The necessary gas and system data which was provided is presented in tabular form and the experimental and predicted results from the computer models are presented in graphical form. The results are discussed in Section 6.3. The procedure used in validating the computer model is as follows:

- (i) All the data provided concerning the gas and the test system is stored in relevant files in the QUANT software and transient analysis programme. Data which is not provided, is estimated based on some known parameter of the system or of similar systems.
- (ii) A data file of thermodynamic and transport properties of the fluid which covers all the range of dependable variables ( $p$ ,  $\rho$  and  $T$ ) encountered during the transient event is produced using the QUANT software.
- (iii) Computer simulation is performed for the test sections described in section 4.6 and numerical results are stored in a data file at intervals for the dependant variables  $t$  and  $x$  sufficient to produce good graphical output.
- (iv) The computer programme DSORT is used to process the data generated in (iii) in to a form which can be used by standard graphical packages to plot the require graphs.
- (v) A commercial graphical software EXCEL is used to plot the required graphs, combining both the experimental data generated in (v) and the data predicted by the computer model, which is generated in (iv). Both sets of data are plotted in the same graph in order to provide good comparison.
- (vi) Experimental data which are available in graphical form are converted into numerical data and stored in ASCII files which can be used by standard graphical packages to plot graphs. If the experimental data is available in numerical form, in ASCII data files, then this step is not required. However, if the data file is too big,

then step (iv) may be applied also to the experimental data. In this study, all the data used to validate the computer models are available in the form of printed graphs.

Four sets of experimental data have been selected to validate the computer model. Only data which is believed to represent rapid transient behaviour has been used. For all the four sets of data, the pipes are effectively horizontal, and are exposed to the atmosphere. Therefore only the heat transfer model based on pipes exposed to the atmosphere is used.

## **6.2 COMPARISON OF COMPUTER MODEL PREDICTIONS WITH EXPERIMENTAL RESULTS**

### **6.2.1 FOOTHILLS TEST DATA**

The tests which were reported by Foothills Pipeline(Yukon)Ltd.(1981), were carried out between December 1979 and April 1981 at the Northern Alberta Burst Test Facility (NABTF). A total of six tests, which are denoted as NABTF1, NABTF3, NABTF4, NABTF5, NABTF6 and NABTF7, were carried out and were reported. The main purpose of the test was to examine the effect of gas composition on the fracture behaviour of the pipe. Shorts lengths of a total of 243m and diameters of approximately 1.2 and 1.4m were charged with natural gas of known composition and pressurised to between 74 and 87 bar. Fracture was initiated at the centre of the test section by detonating an explosive cutter. Results were presented in the form of pressure histories and timing wire data showing the crack tip position. The data is presented for each section of the broken pipe which are denoted as West and East. In relation to the computer model they are referred to as downstream and upstream sections respectively.

Out of the results presented, of relevance to this study are the p-t and a-p curves. Although the data can be used to some extent to validate computer models for linebreak analysis, it was not intended for that purpose. The major reason which makes this data unsuitable for validating line break models is the fact that the fracture was designed to propagate along the axial direction of the pipe covering some considerable lengths. This makes it difficult to model the break boundary, especially using this model where the break boundary is assumed to be fixed in the x-t plane. The shorter the axial distance covered by the fracture propagation the more suitable the results are for validating the computer model.



Two major weaknesses have been observed in the FOOTHILLS data. The first is that of p-t curves crossing each other. The second is that of non-identical curves for the two identical halves of the broken pipe section. During the depressurisation of a broken pipe, the pressure at the intact end remains higher than that at the broken end and the pressure gradient follows the same direction throughout the depressurisation process. Therefore, it is not possible for the pressure at a point in the pipe which is further away from the break to be lower than that of a point which is nearer to the broken end, during the first transient of the pressure wave following the break. The fact that this rule is not followed by the FOOTHILLS test results, indicates that the data presented in this report must be used with extreme caution.

The state of the gas inside the pipe was stationary before the break. Assuming a uniform temperature throughout the length of the pipe, there is a symmetry in all the properties of the fluid and the geometry of the pipe about the cross section at the middle of the pipe. The symmetry should be maintained even after the break, if the fracture propagation is the same on both sections of the pipe, unless if there are strong external factors such as wind which would affect the out flow of gas from the broken ends. In the FOOTHILLS results, this condition is also not well followed.

PARAMETER\TEST	NABTF1	NABTF3	NABTF4	NABTF5	NABTF6	NABTF7
Outer diameter (mm)	1422	1219	1219	1422	1219	1219
Wall thickness	13.71	15.24	13.71	13.71	15.24	13.71
P [kPa]	7446	8687	8687	7446	8697	8143
T [C]	23-26	(-3)-(-4)	18.5	1819	(-4)-(-5)	(-5)-(-6)
Pipe Material	Gr.483	Gr.483	Gr.483	Gr.483	Gr.483	Gr.483
Gas composition [%]						
CH <sub>4</sub>	86.59	85.36	85.36	84.7	85.19	85.71
C <sub>2</sub> H <sub>6</sub>	6.8	8.22	7.68	8.21	8.07	7.94
C <sub>3</sub> H <sub>8</sub>	4.03	4.34	4.46	4.38	4.4	4.27
i-C <sub>4</sub> H <sub>10</sub>	0.262	0.182	0.238	0.201	0.203	0.214
n-C <sub>4</sub> H <sub>10</sub>	0.421	0.278	0.331	0.235	0.3	0.311
i-C <sub>5</sub> H <sub>12</sub>	0.057	0.029	0.032	0.029	0.029	0.033
n-C <sub>5</sub> H <sub>12</sub>	0.034	0.028	0.032	0.03	0.029	0.03
n-C <sub>6</sub> H <sub>14</sub>	0.008	0.013	0.011	0.008	0.01	0.009
CO <sub>2</sub>	0.076	1.56	0.049	2.212	1.177	1.1409
N <sub>2</sub>	1.71	1.56	1.804	2.212	1.177	1.1409
Ar	0.016	1.56	0.013	2.212	1.177	1.1409
O <sub>2</sub>	0.016	1.56	0.013	2.212	1.177	1.1409

Source: Foothills Pipeline (Yukon) Ltd (1981)

Table 6.1: Foothills Test General Data

Two test results, namely NABTF1 EAST and NABTF7 WEST, are selected for validation of the computer model. The result NABTF1 EAST are used to validate the model for flow reversal in the downstream section of the broken pipe and the NABTF7 WEST results are used for the upstream section. Both the NABTF1 and NABTF7 tests were performed with relatively short axial fracture propagation (approximately 5m and 18m respectively). The length of the axial fracture propagation is more than three times higher in NABTF7 test than in the NABTF1 test. The test results produced for test NABTF7 WEST seem to be more promising for validating of the model. Two main reasons for this are the lower timing wire velocity used for NABTF7 compared to that used for NABTF1; and the long distance away from the broken end (18.28m compared with 4.2m for NABTF1) used as the shortest distance to present the results. The schematic of the Foothills test NABTF1 and NABTF7 are presented in Figs. 6.1 and 6.2 respectively.

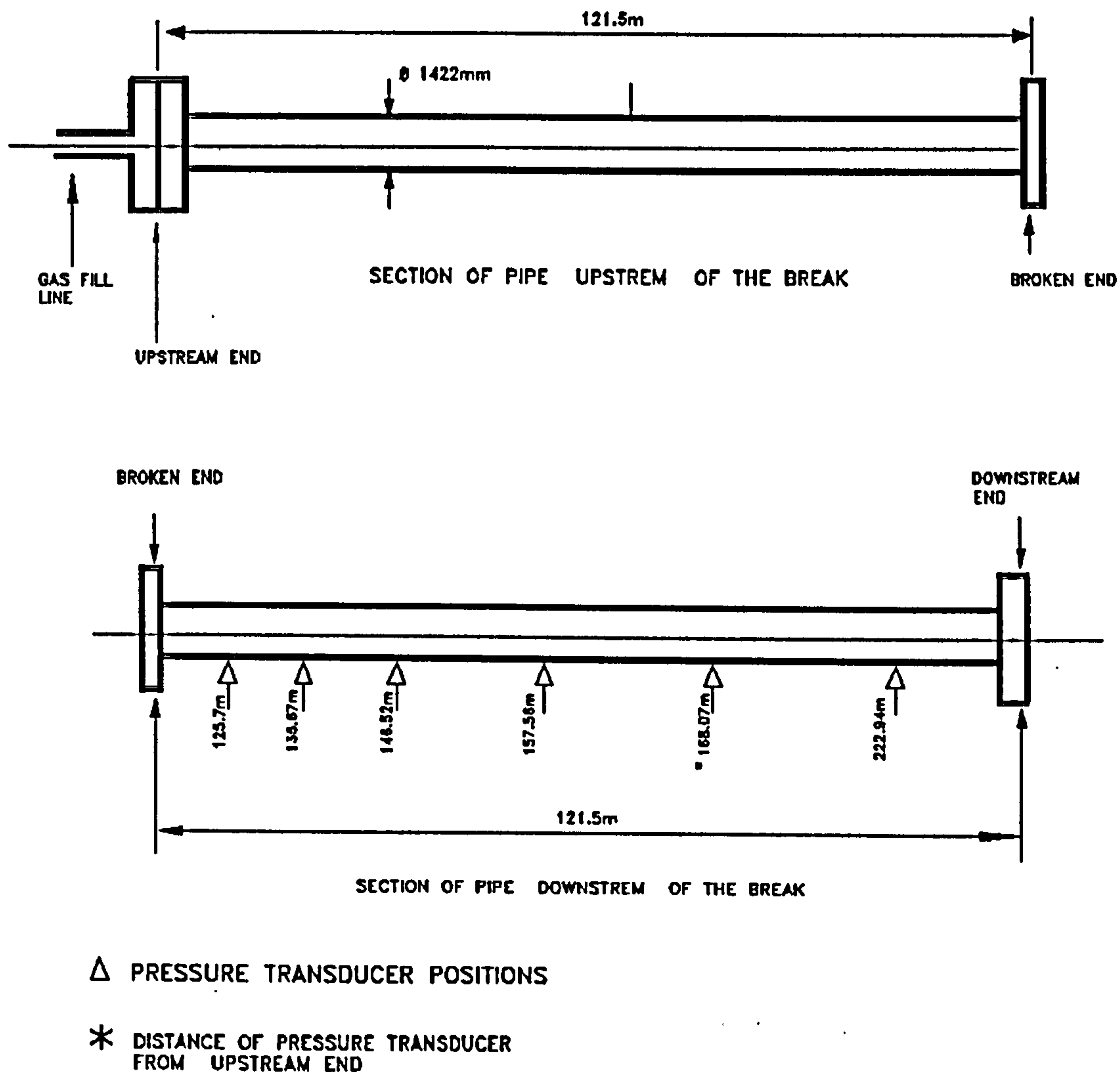


Fig. 6.1 Schematic of Foothills Test NABTF1



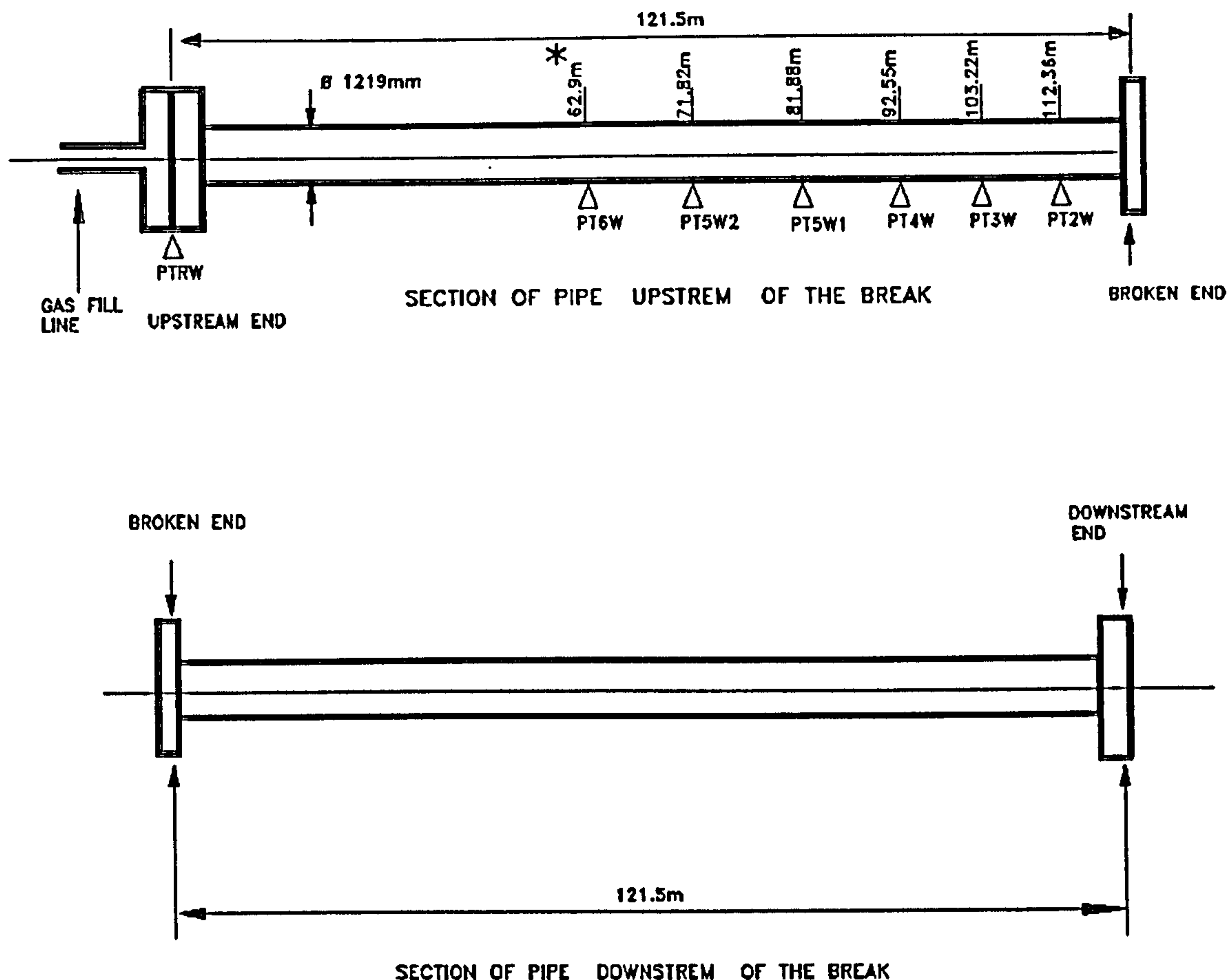


Fig. 6.2 Schematic of Foothills Test NABTF7

Sufficient data was provided concerning the test gas, to enable determination of the rest of the required fluid properties using the QUANT software. The former are summarised in Table 6.1. The average composition of the gas used in the seven test which is given in Table 6.2 is used as the input data to the QUANT software. A data file FLUID.DAT is generated using the routine DFGEN, to cover the whole range of the dependent variables( $p$ ,  $T$  and  $\rho$ ) which will be covered by the transient event.

Results produced by the computer model are summarised in Figs.6.7 to 6.11, together with the experimental results presented by Foothills Pipelines (Yukon) Ltd. (1981). A grid spacing of  $\Delta x = 0.1\text{m}$  and  $\Delta t = 0.0001\text{s}$ , at the broken end is used in the numerical model and a variable grid spacing is used.

Chemical Formula	ISM	HES	%Composition
CH <sub>4</sub>	0	0	85.10
C <sub>2</sub> H <sub>6</sub>	0	0	8.00
C <sub>3</sub> H <sub>8</sub>	0	0	4.40
i-C <sub>4</sub> H <sub>10</sub>	1	0	0.20
n-C <sub>4</sub> H <sub>10</sub>	2	0	0.30
i-C <sub>5</sub> H <sub>12</sub>	1	0	0.03
n-C <sub>5</sub> H <sub>12</sub>	2	0	0.03
n-C <sub>6</sub> H <sub>14</sub>	1	0	0.01
CO <sub>2</sub>	0	0	0.07
N <sub>2</sub>	0	0	1.70
Ar	0	0	0.08
O <sub>2</sub>	0	0	0.08

Table 6.2 Average Gas Composition for Foothills Test

### 6.2.2 BRITISH GAS TEST DATA

The tests referred to as British Gas Tests are those which were reported by Jones and Gough (1981). They include a series of experiments which were carried out using short pipe sections of 120ft (36.6m) length and 4in (0.1016m) diameter, with a bursting disc at one end. The aim of the tests was to validate a theoretical model developed by British Gas. The computer model, DECAY, could be used to predict the decompression behaviour of any gas mixture from any starting conditions of pressure and temperature.

Three gas mixtures, namely methane/ethane, methane/propane and a typical rich gas mixture, were used. The decompression was performed from pressures ranging from 70 to 125 bar (7.0MPa to 12.5MPa) and temperatures ranging from 13 to 30°C. Gas of known composition was pumped into the pipe until the required conditions (p and T) were attained. The bursting disc was explosively ruptured and the resulting decompression behaviour was recorded by pressure transducers at a number of locations along the pipe. p and T curves together with the appropriate details on the gas composition, initial conditions of p and T were presented. The curves include both the experimental results and predictions by the British Gas DECAY model.

Also presented in the report, are four sets of experimental p-a curves which were obtained from BMI using a 20 ft (6.1m) long 4in (0.1016m) diameter pipe; full-scale fracture tests carried out by British Gas for Shell and North America sponsors; and full-scale fracture tests carried out by BMI for Artic Gas Pipeline companies. For these tests, only the p-a data is presented together with predicted results using the British Gas DECAY



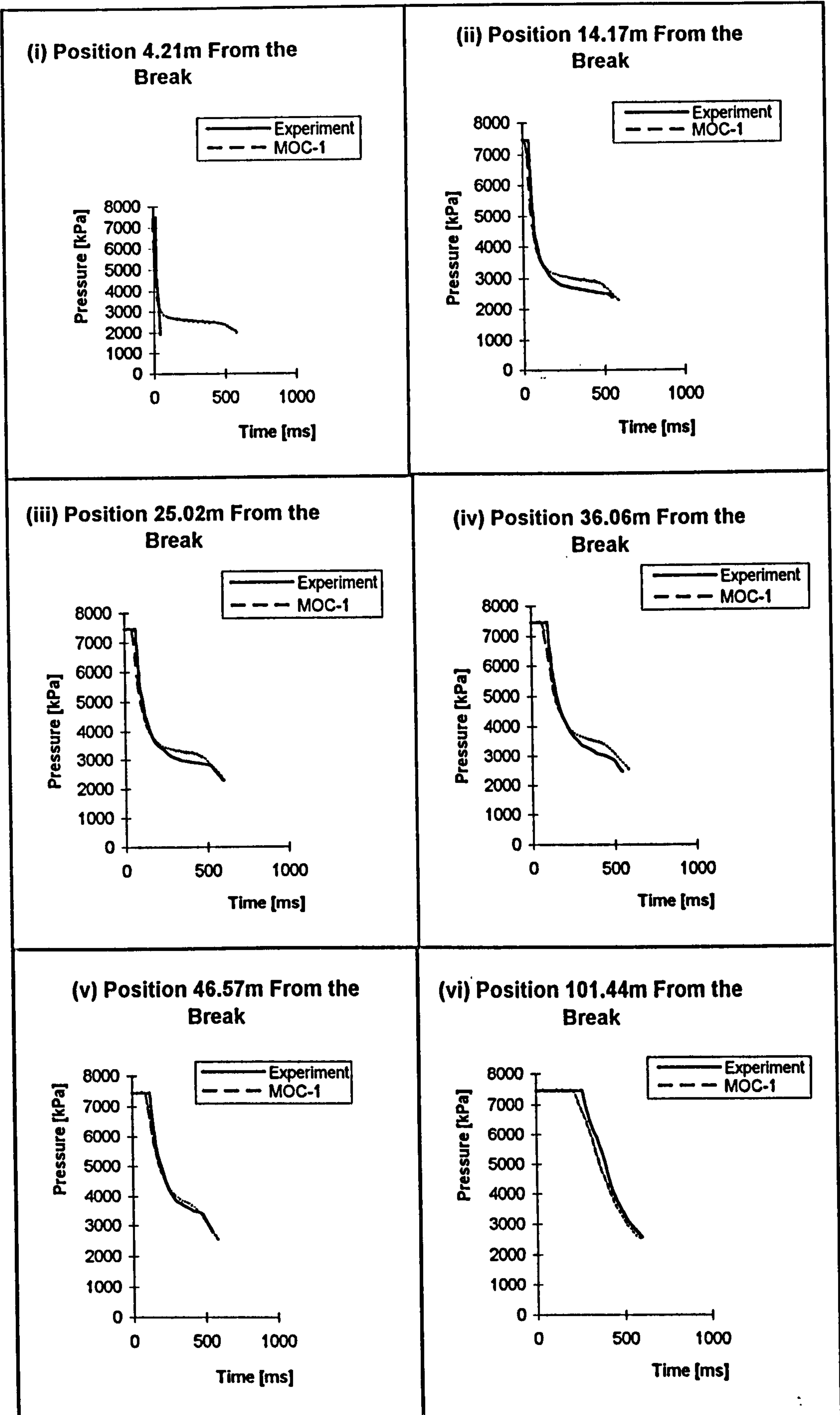


Fig. 6.3 p-t Curves for Foothills Test NABTF1 East Comparison With First-order Method of Characteristics Predictions

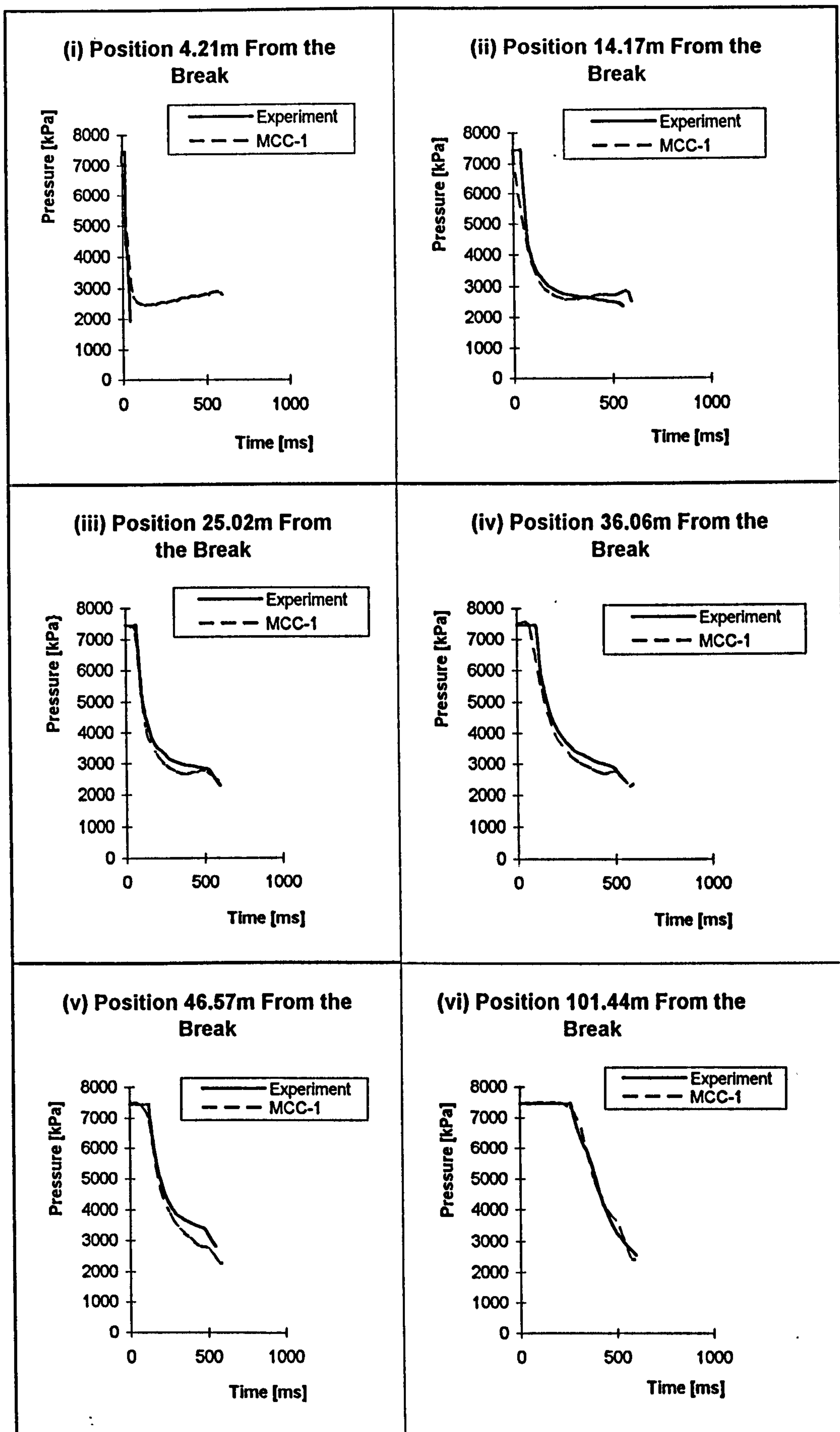
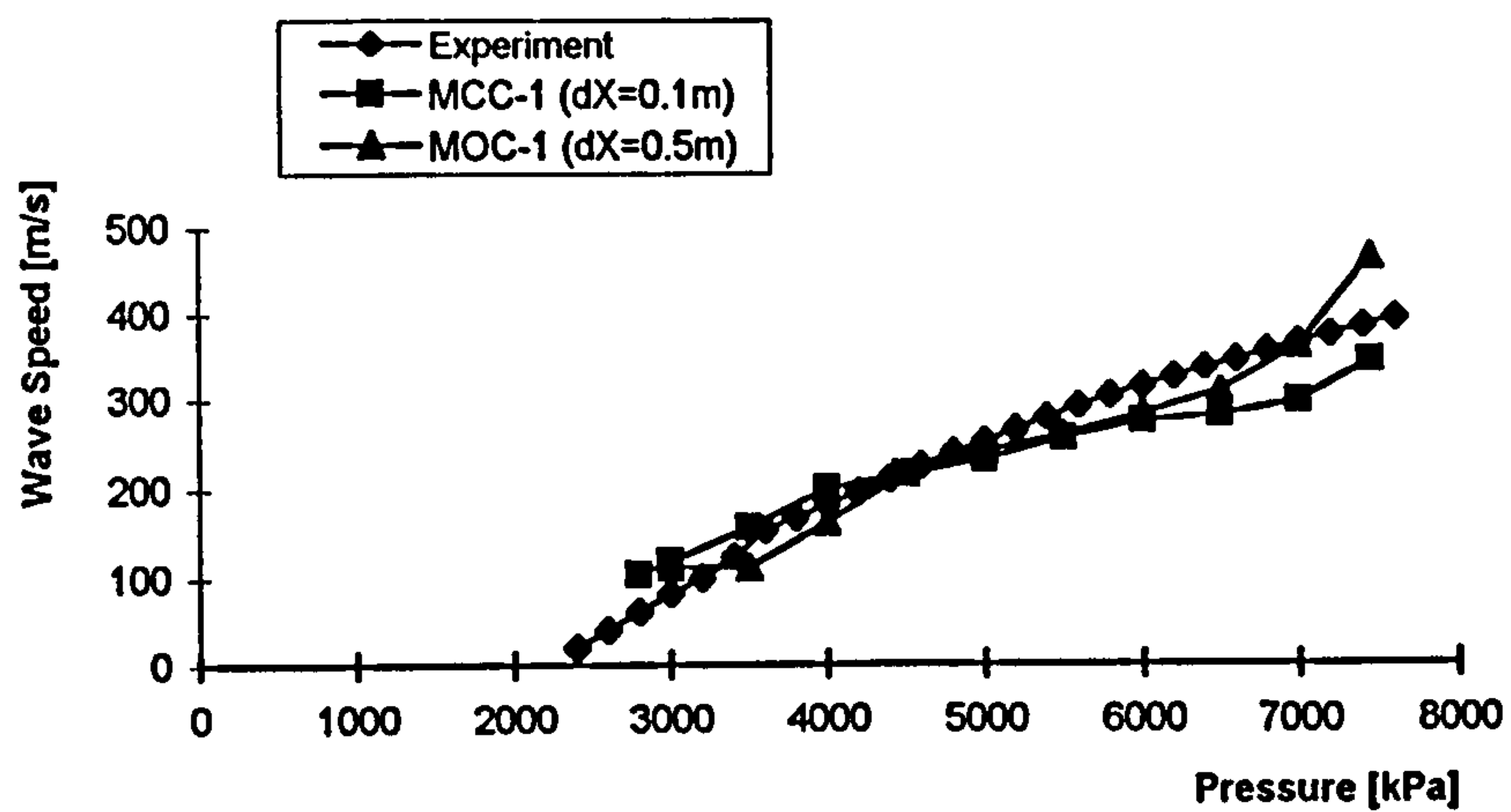
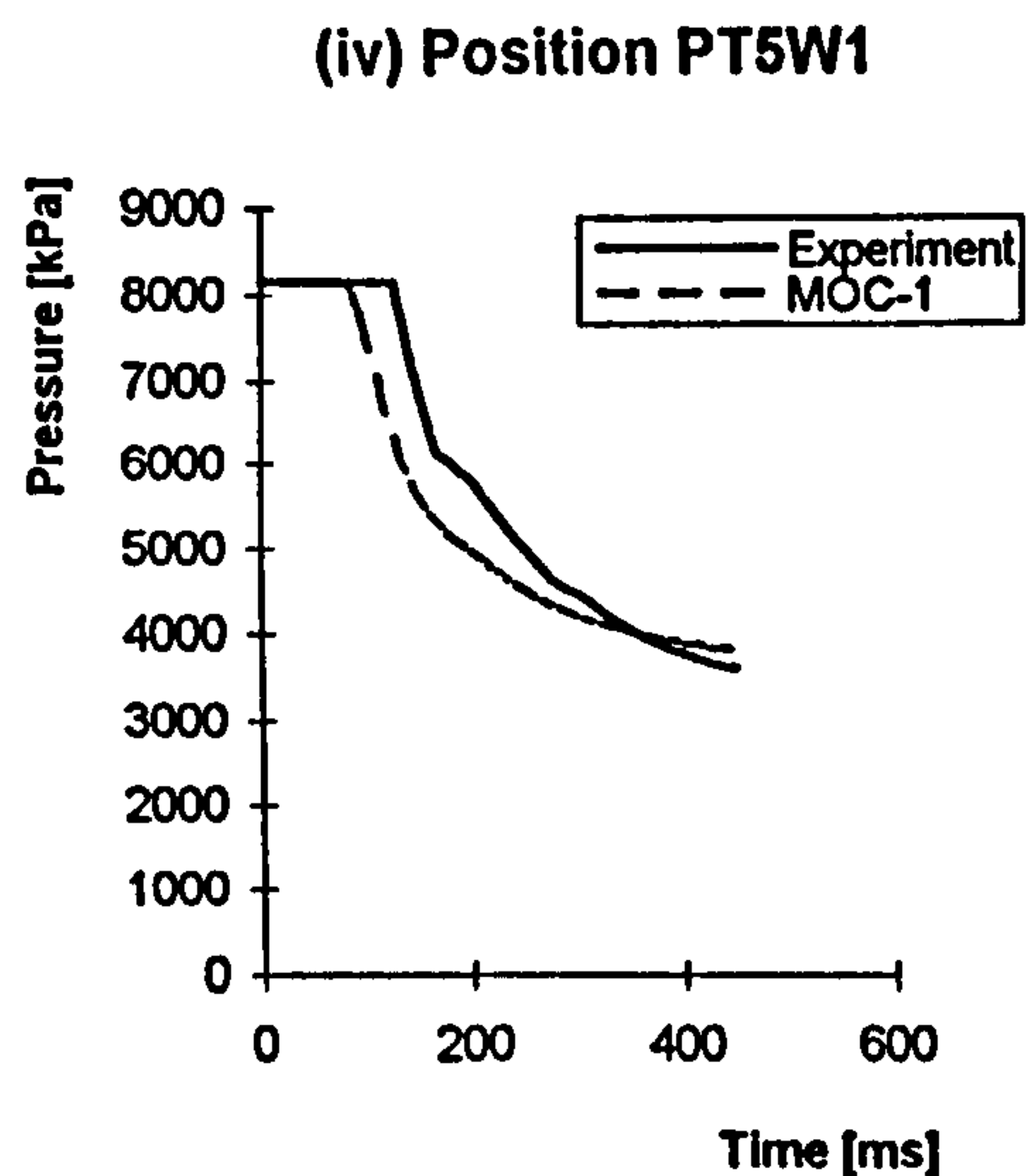
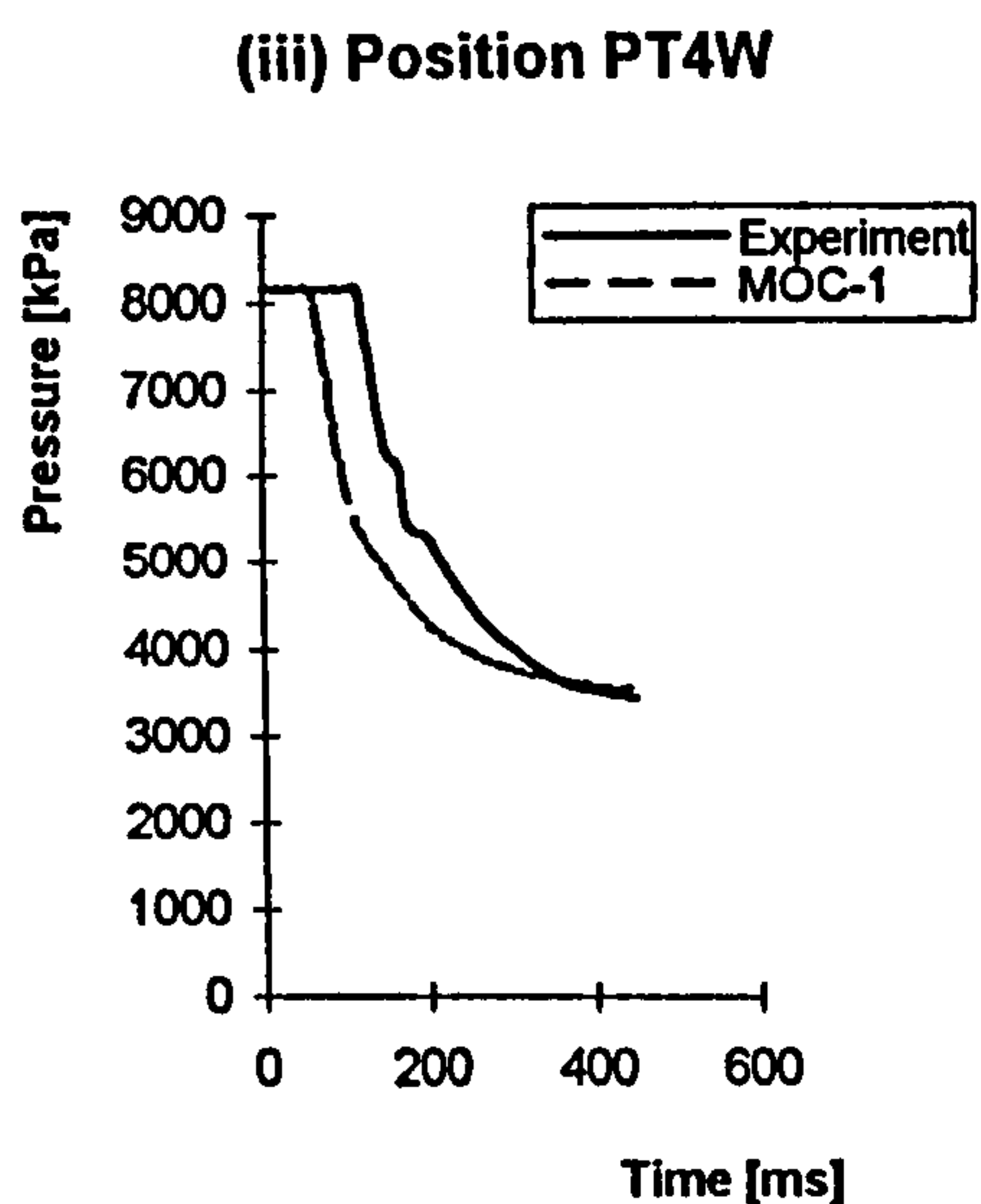
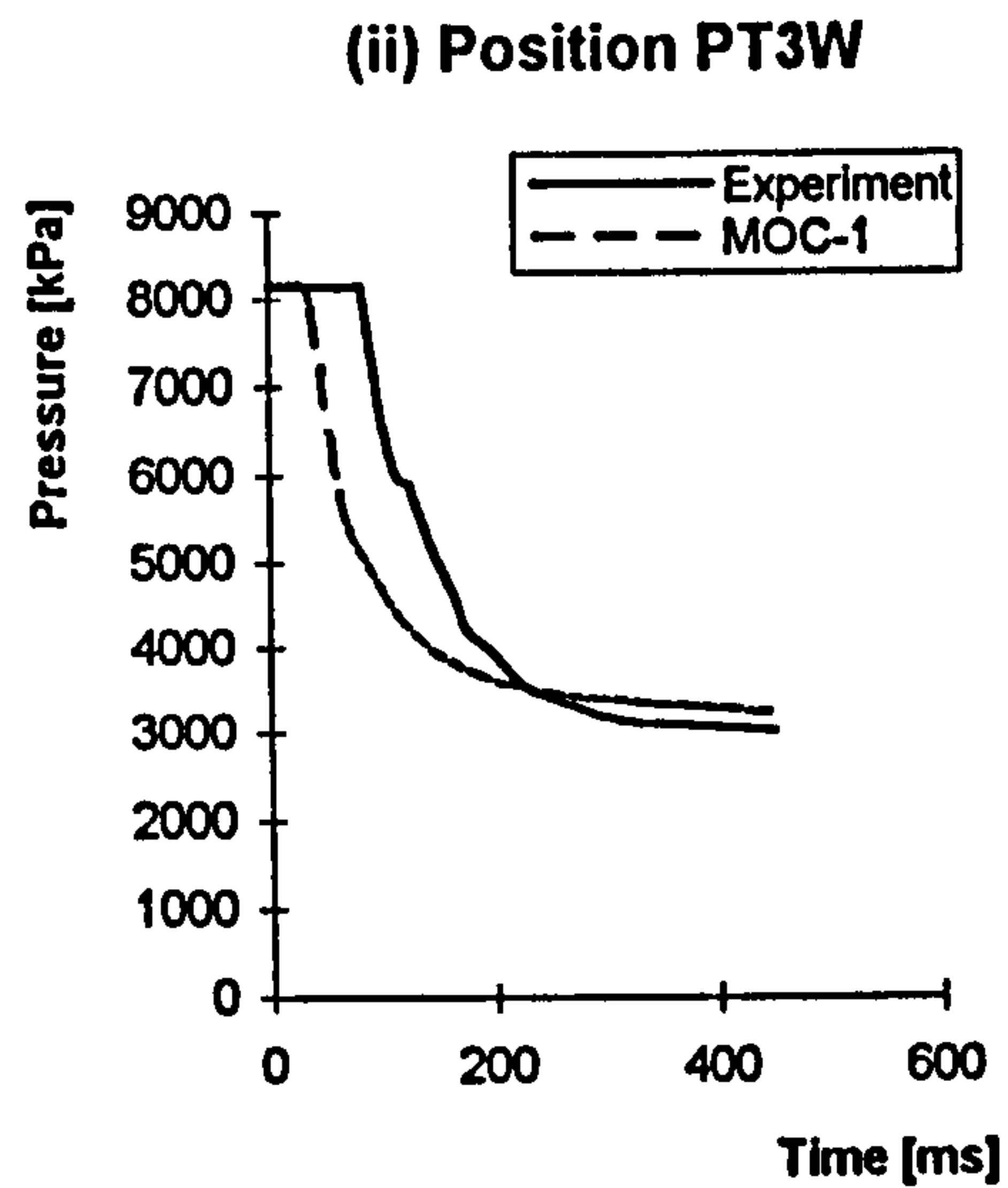
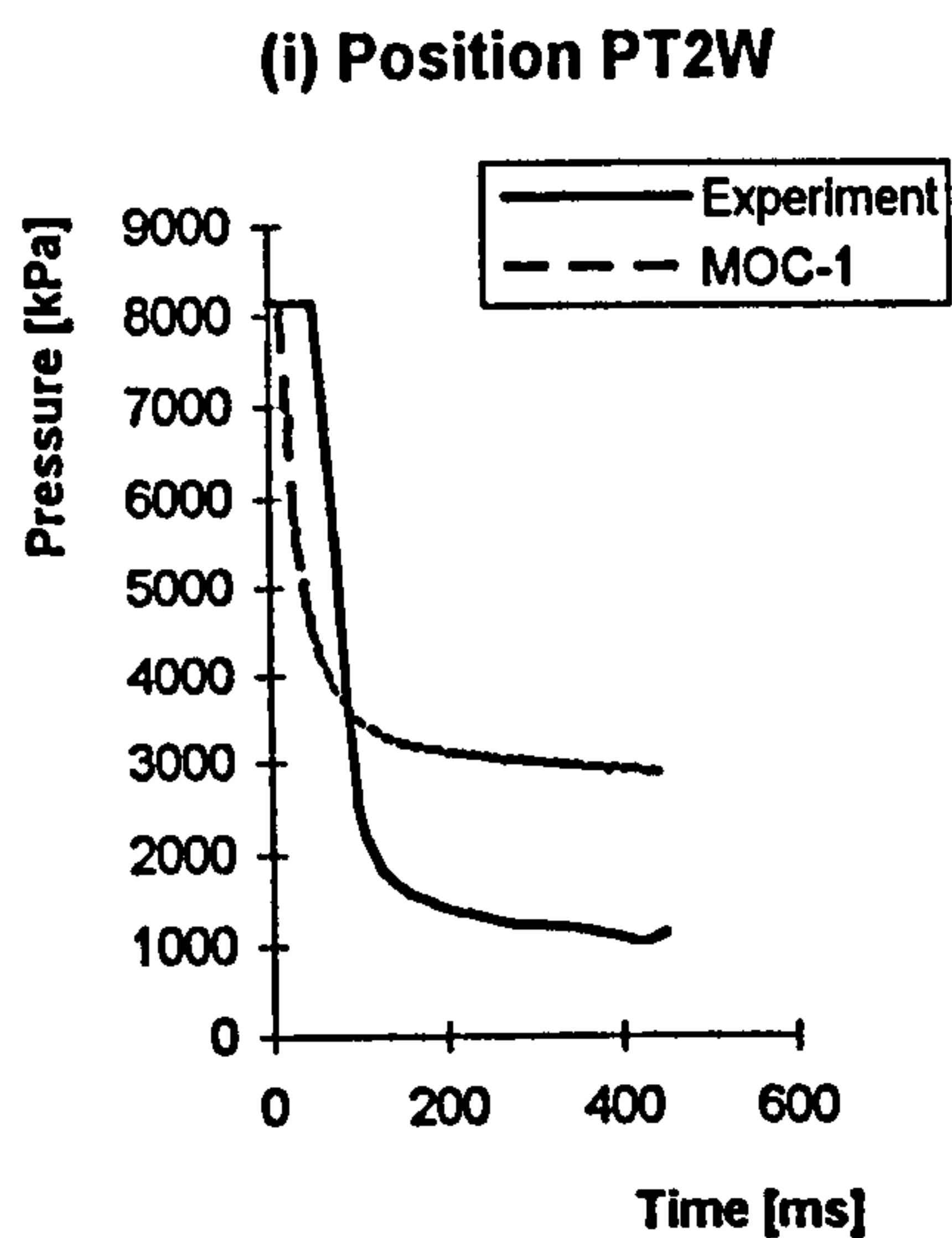


Fig. 6.4 p-t Curves for Foothills Test NABTF1 East Comparison With MacCormack Method Predictions





**Fig. 6.5 Pressure Wave Propagation Speed for Foothills Test NABTF1 East**



**Fig. 6.6 p-t Curves for Foothills Test NABTF7 West Comparison With First-order Method of Characteristics Predictions**

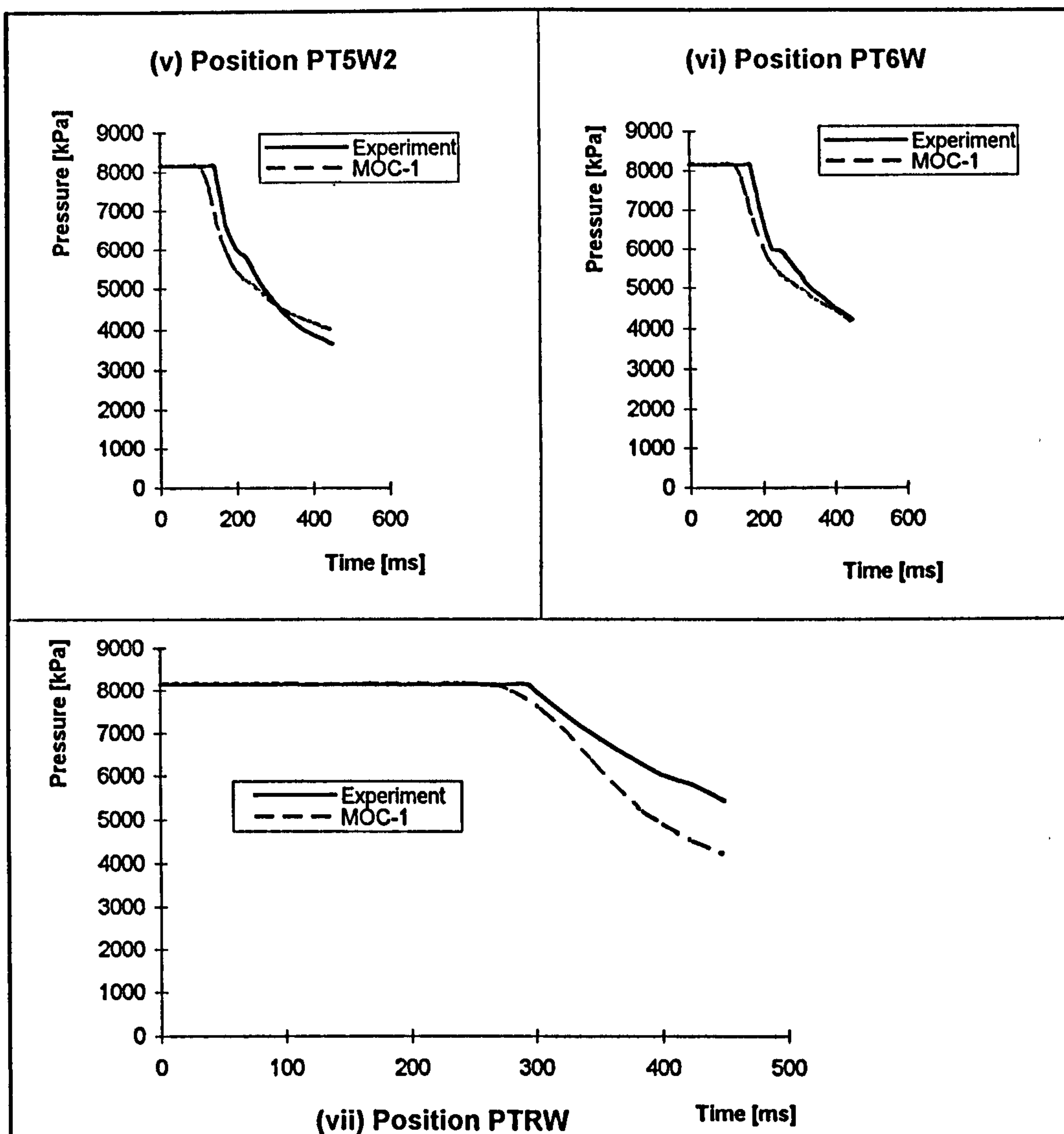


**Fig. 6.6 p-t Curves for Foothills Test NABTF7 West Comparison With First-order Method of Characteristics Predictions**

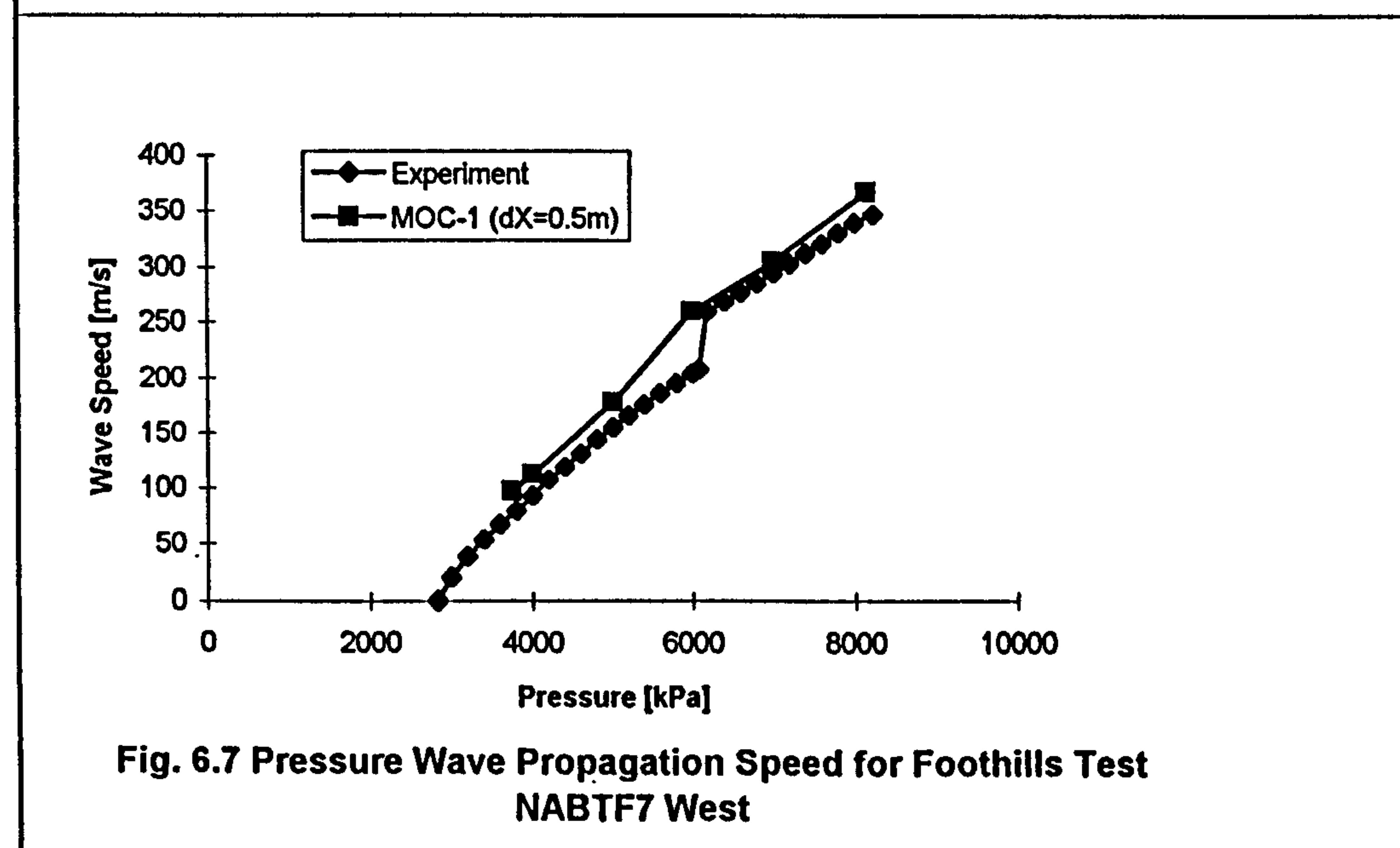


**Fig. 6.7 Pressure Wave Propagation Speed for Foothills Test NABTF7 West**



model and two other existing computer models. The other models were developed by the Exxon Production Research Company and the University of Calgary, and were based on a similar theoretical approach to the one used in developing the British Gas model.

No further details were given on the full-scale tests, apart from the gas compositions and the initial conditions of  $p$  and  $T$ . The full-scale results cannot therefore be used to validate this computer model. The pattern of the experimental results presented by Jones and Gough (1981) is in general more consistent than that presented by Foothills Pipelines (Yukon) Ltd (1981). The problem of  $p$ - $t$  curves for different positions on the pipe crossing each other, which was reported in Section 6.2.1, is not so present in the data described in this section. The three tests performed by British Gas using a multi-constituent (typical) natural gas mixture are used to validate this computer model. The initial pressures for the test were 70bar, 100bar and 125bar, and the initial temperatures were 29°C, 25°C and 25°C respectively. The three tests are referred to as British Gas Test 1, 2 and 3 respectively. These results are used to validate the computer model only in relation to the  $p$ - $t$  curves. As for the  $p$ - $a$  curves, only the BMI (PRUDHOE BAY 1), BMI (PRUDHOE BAY 2) and the University of Calgary tests are used. These tests are referred to as BMI1, BMI2 and UCT respectively. There are two main reasons for this selection of data, apart from that of availability of all the necessary data to enable computer modelling. The two reasons are: firstly, the fact that the multi-constituent gas mixture represents more closely a typical natural gas mixture. The second reason is one which is of convenience. The procedure used to prepare the fluid property data file using the QUANT software, (refer to Sections 4.5 and 6.1.1) has the major deficiency in that manual operation is necessary for each set of input data. Consequently, this procedure is very tedious and time consuming. Test data on gas with compositions which are closest to that of the Foothills tests (refer to Section 6.2.1), is selected so that the same fluid property data file could be used.

The composition data used for the gas mixtures in all the tests selected is presented in Table 6.2 and results produced by the computer model together with their corresponding experimental data, are presented in Figs. 6.9 to 6.21. The same grid spacing at the break is used as for the Foothills tests, including a variable grid spacing. A grid spacing of  $\Delta x = 0.1\text{m}$  and  $\Delta t = 0.0001\text{s}$  is used for all the tests, at the broken end. The Schematic of the British Gas tests is presented in Fig. 6.8.

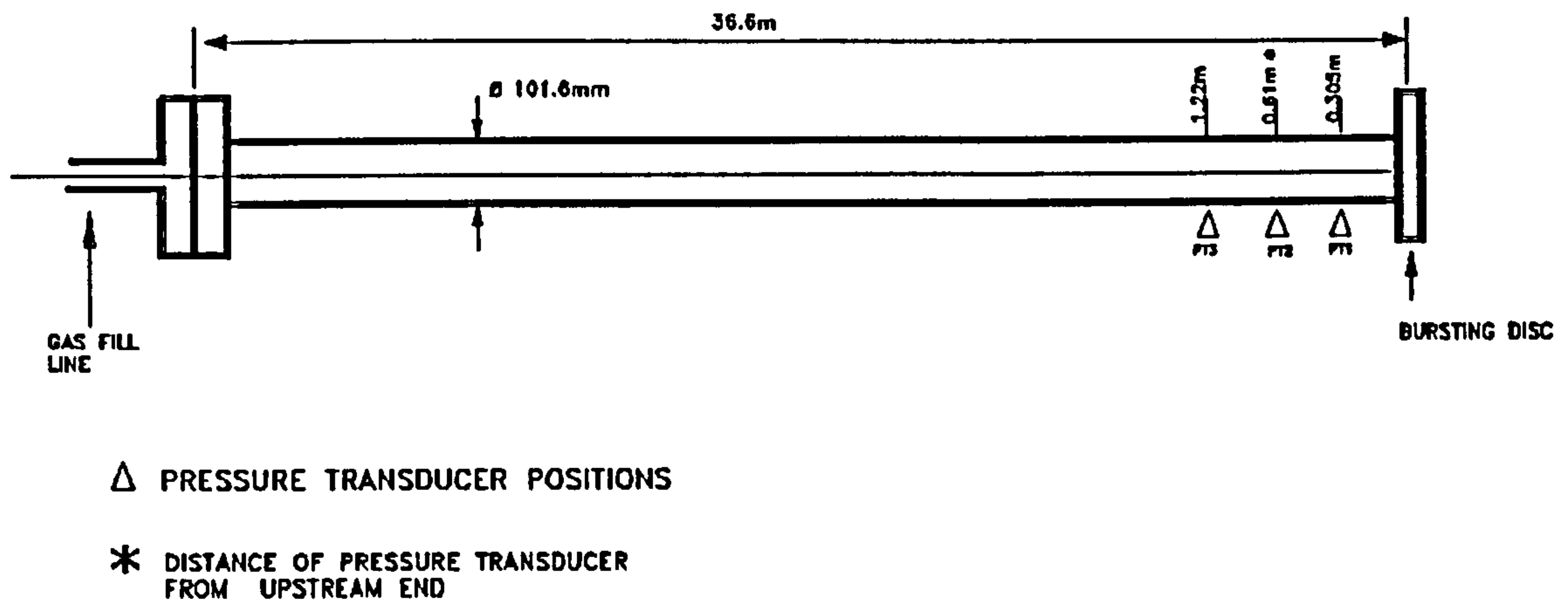


Fig. 6.8 Schematic of British Gas Tests BGT1, BGT2 and BGT3

### 6.2.3 SNGSO TEST DATA

The experimental data used to validate this model so far, were carried out using rather short pipe sections. The significance of using full-scale pipeline experimental data was discussed in Chapter 5. In this section, and also the one which follows full-scale pipeline experiments are used in order to obtain a better validity evidence for the model. In this section the test results which were reported by Sens, Jouve, and Pelletier (1970) are used

The test was carried out on a 11,800m long 0.1065m internal diameter natural gas pipeline, at a pressure of 3.14MPa, on the S.N.G.S.O gas system. A section of a pipe was duplicated and taken out of service temporarily. One end of the pipe could be connected to the system or isolated, while the other end was equipped with a venting assembly with a cylindrical passage of 0.1m diameter. The assembly permitted venting of the pipe to the atmosphere by either bursting a disc or by rapid operation of a stop-cock. It was observed that the two methods of venting the pipe were indistinguishable from one another when the decompression behaviour at a point 6.159m from the broken end were considered. However, substantial differences were observed at the broken end during the first few milliseconds after the break occurred. No details were provided regarding the gas composition, but it is assumed that the gas used was a typical natural gas mixture of composition close to that of the Foothills tests (refer to Table 6.2). Consequently, the same data file for the fluid properties as used for the Foothills test is used.

Comparative model prediction and experimental results are presented in Figs. 6.23, 6.24 and 6.25. A much bigger grid spacing at the break (ten times that used for the



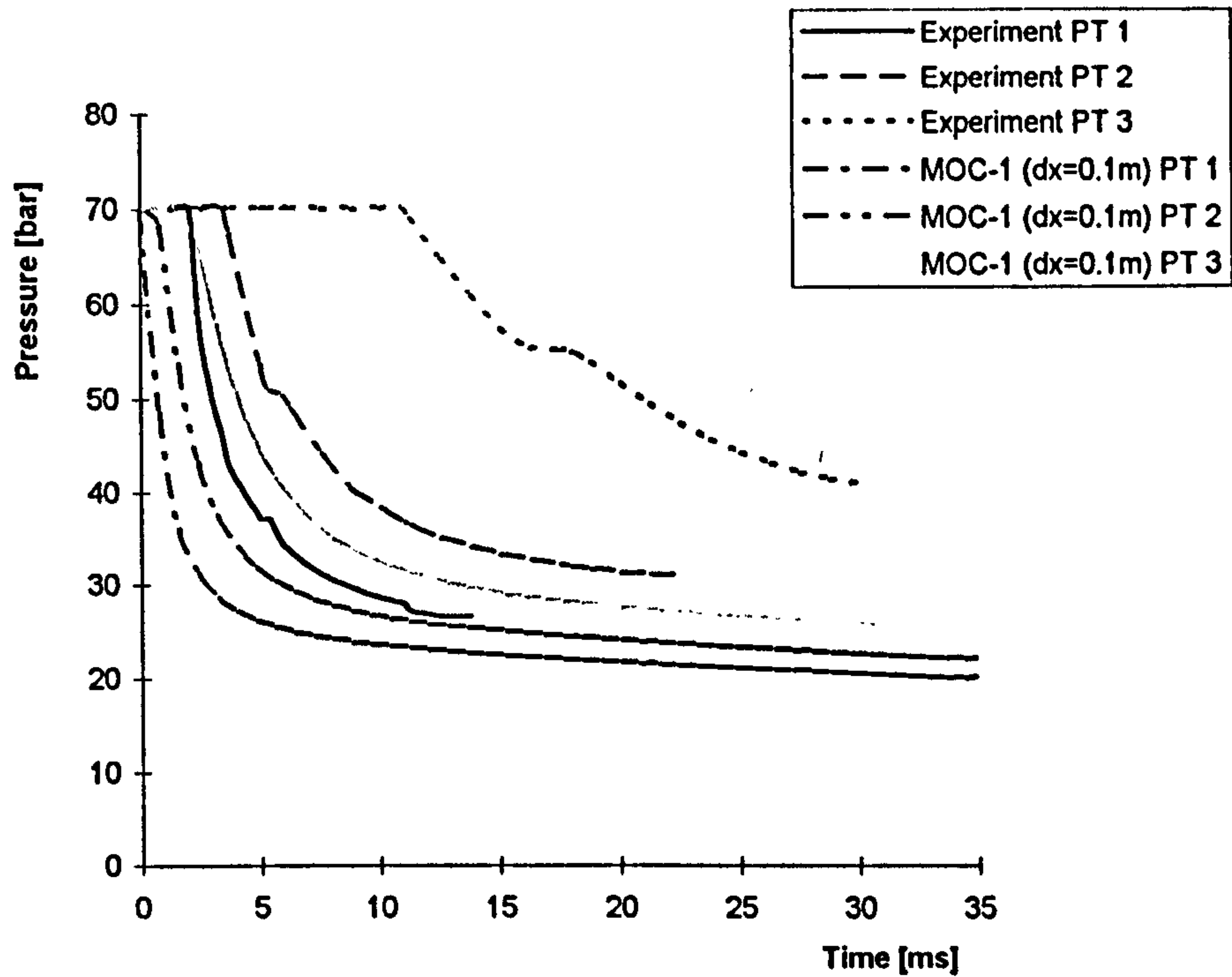


**Fig. 6.9 p-t Curves for British Gas Test BGT1 Comparison with First-order Method of Characteristics Predictions**

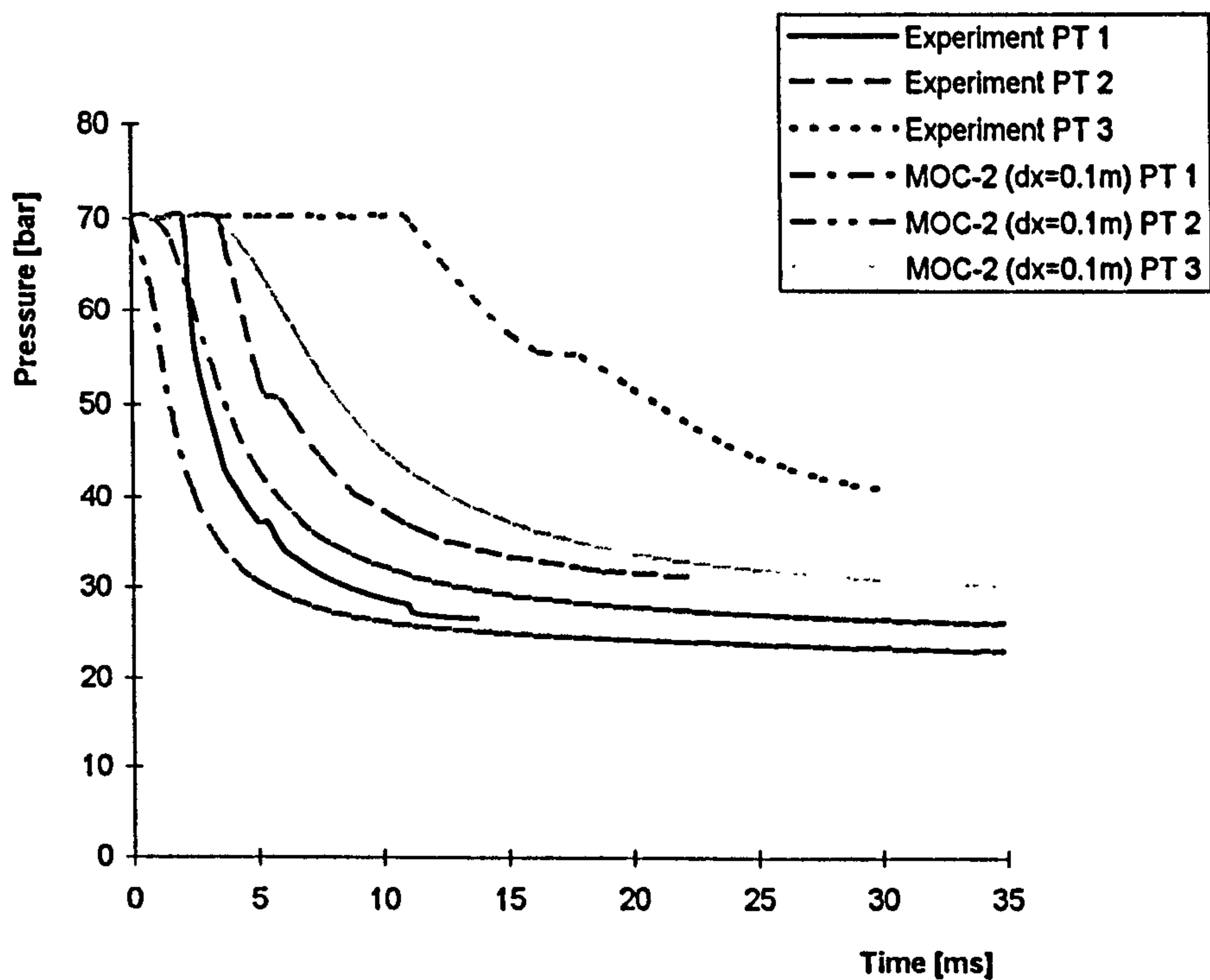


**Fig. 6.10 p-t Curves for British Gas Test BGT1 Comparison with Second-order Method of Characteristics Predictions**

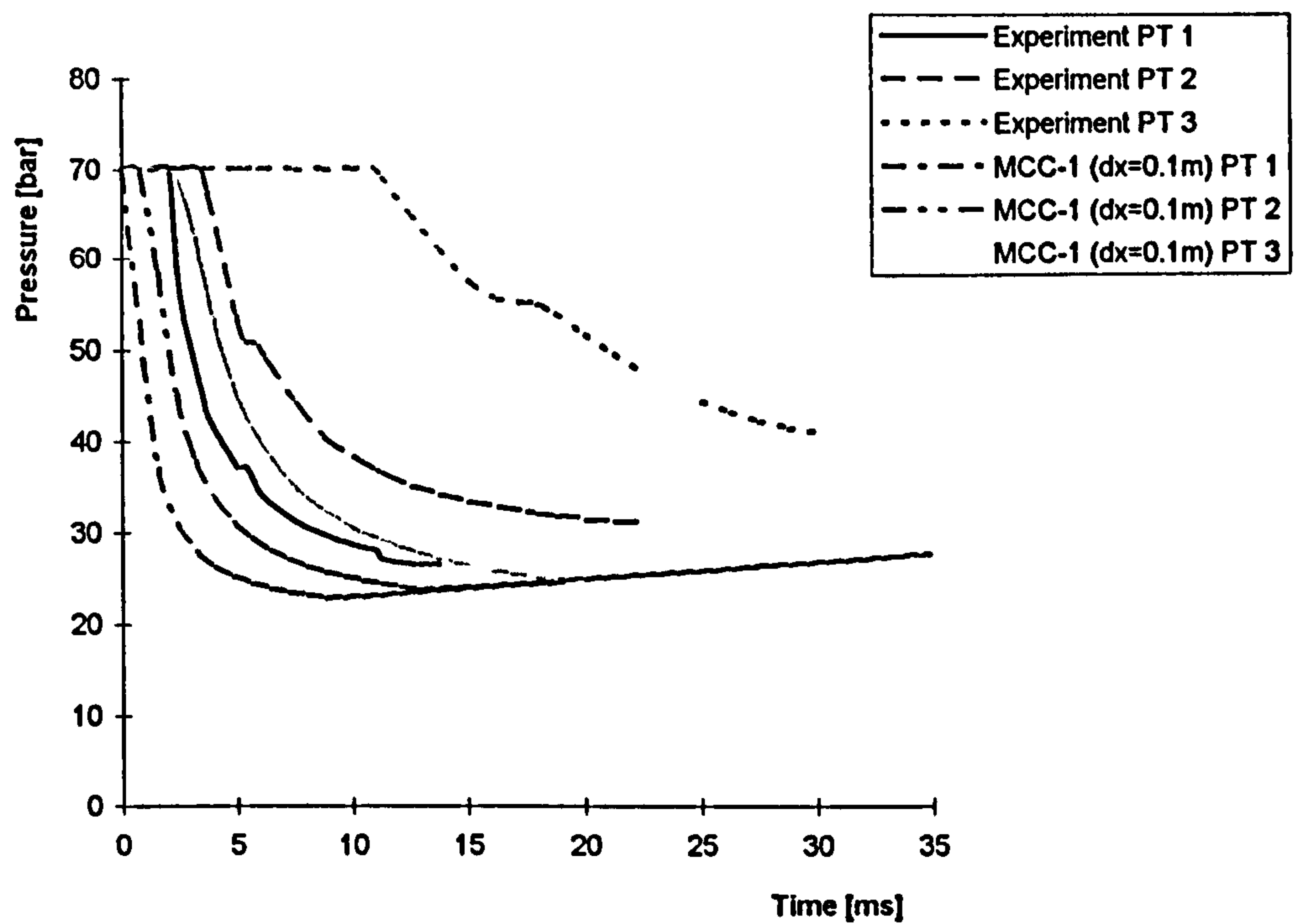


**Fig. 6.11 p-t Curves for British Gas Test BGT1 Comparison with MacCormack Method (Alternative 1) Predictions**

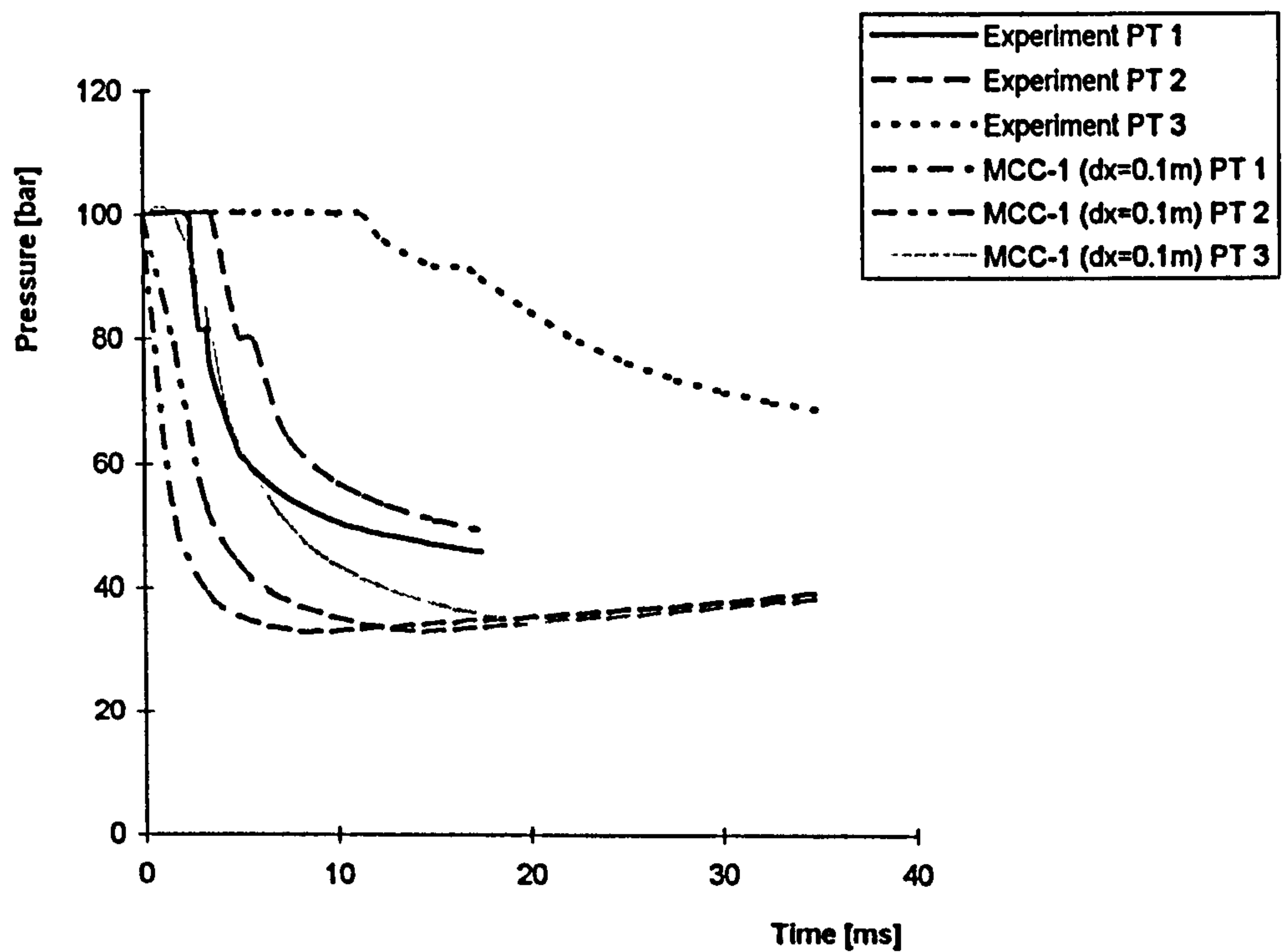


**Fig. 6.12 p-t Curves for British Gas Test BGT2 Comparison with MacCormack Method (Alternative 1) Predictions**



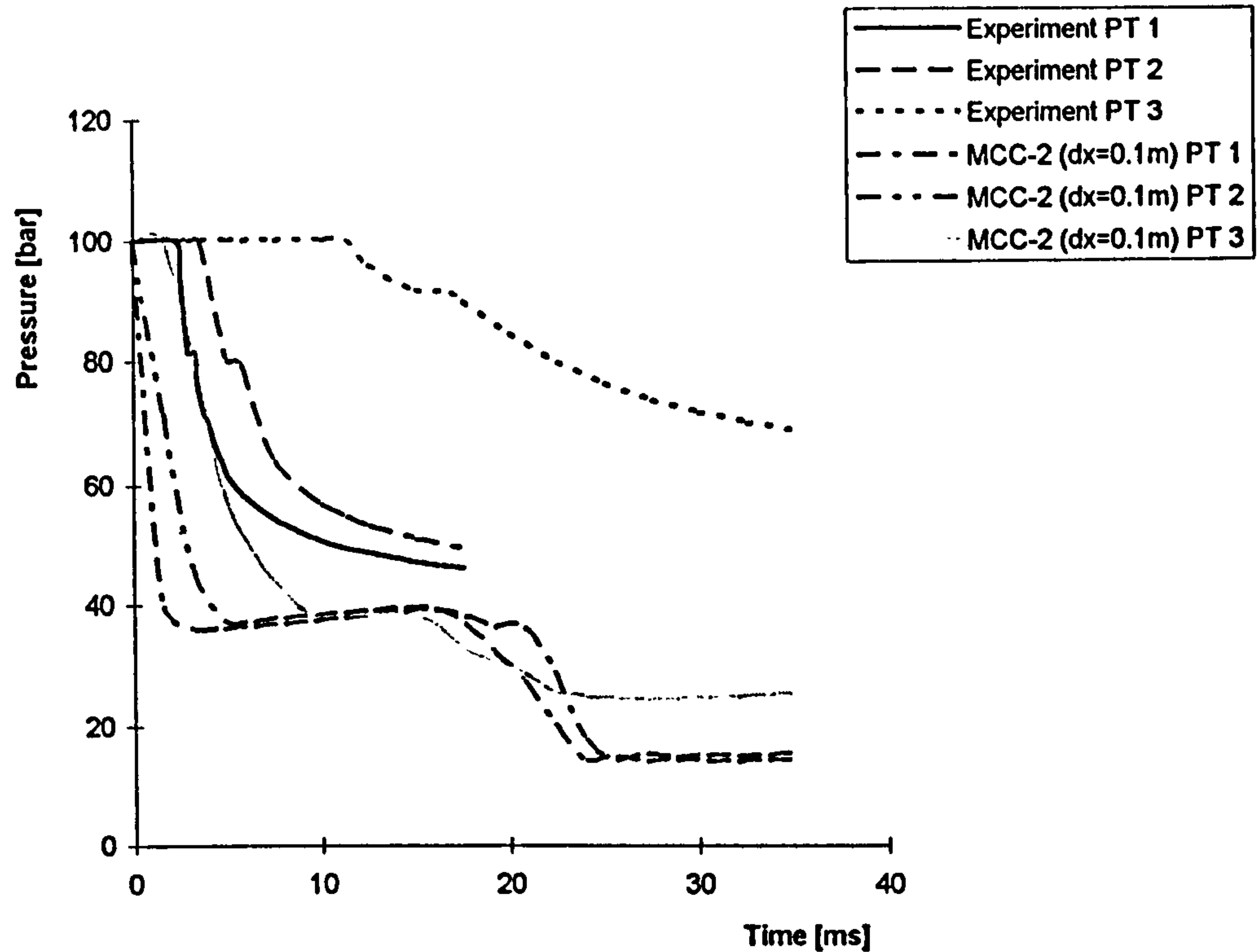


**Fig. 6.13 p-t Curves for British Gas Test BGT2 Comparison with MacCormack Method (Alternative 2) Predictions**

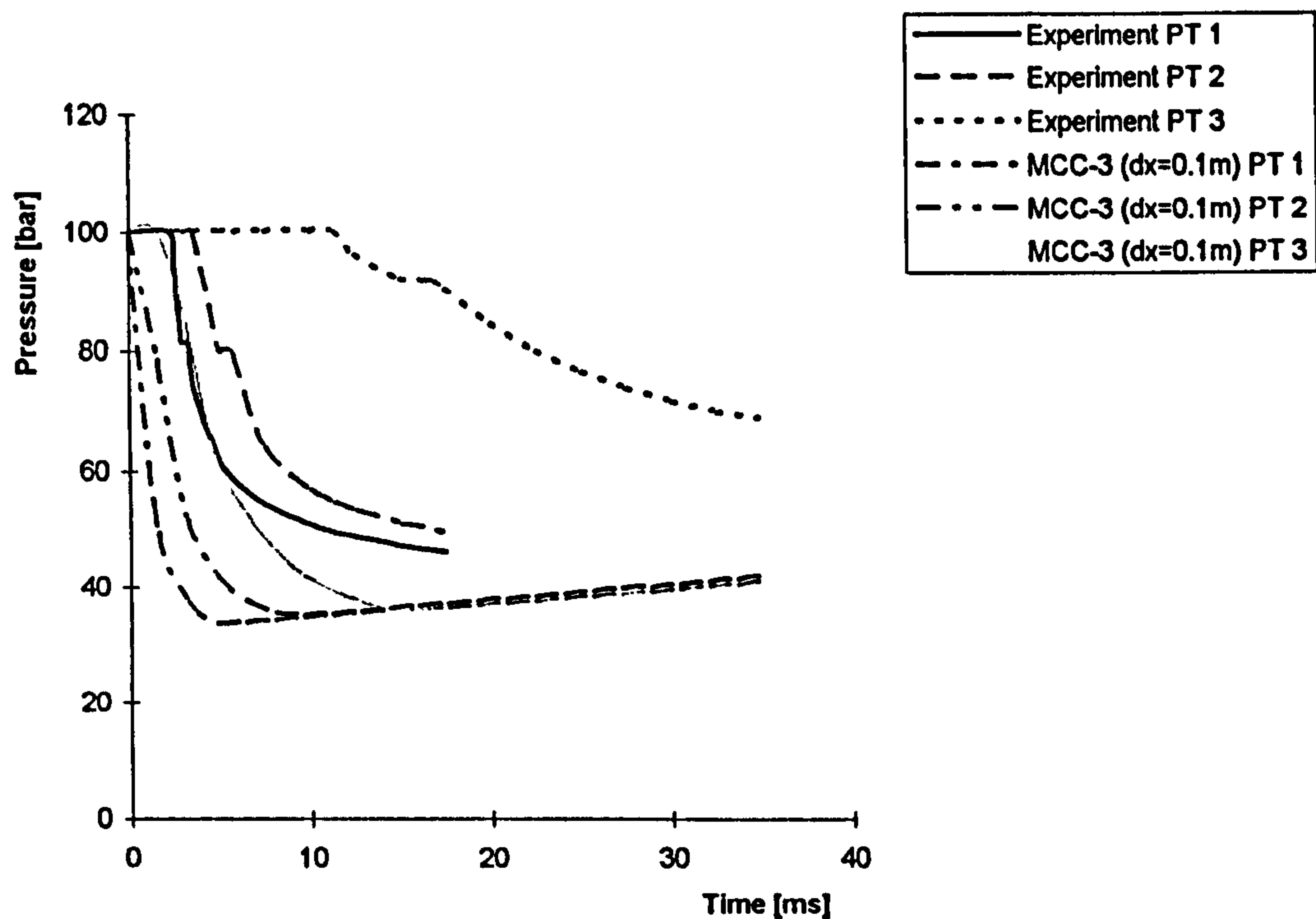


**Fig. 6.14 p-t Curves for British Gas Test BGT2 Comparison with MacCormack Method (Alternative 3) Predictions**

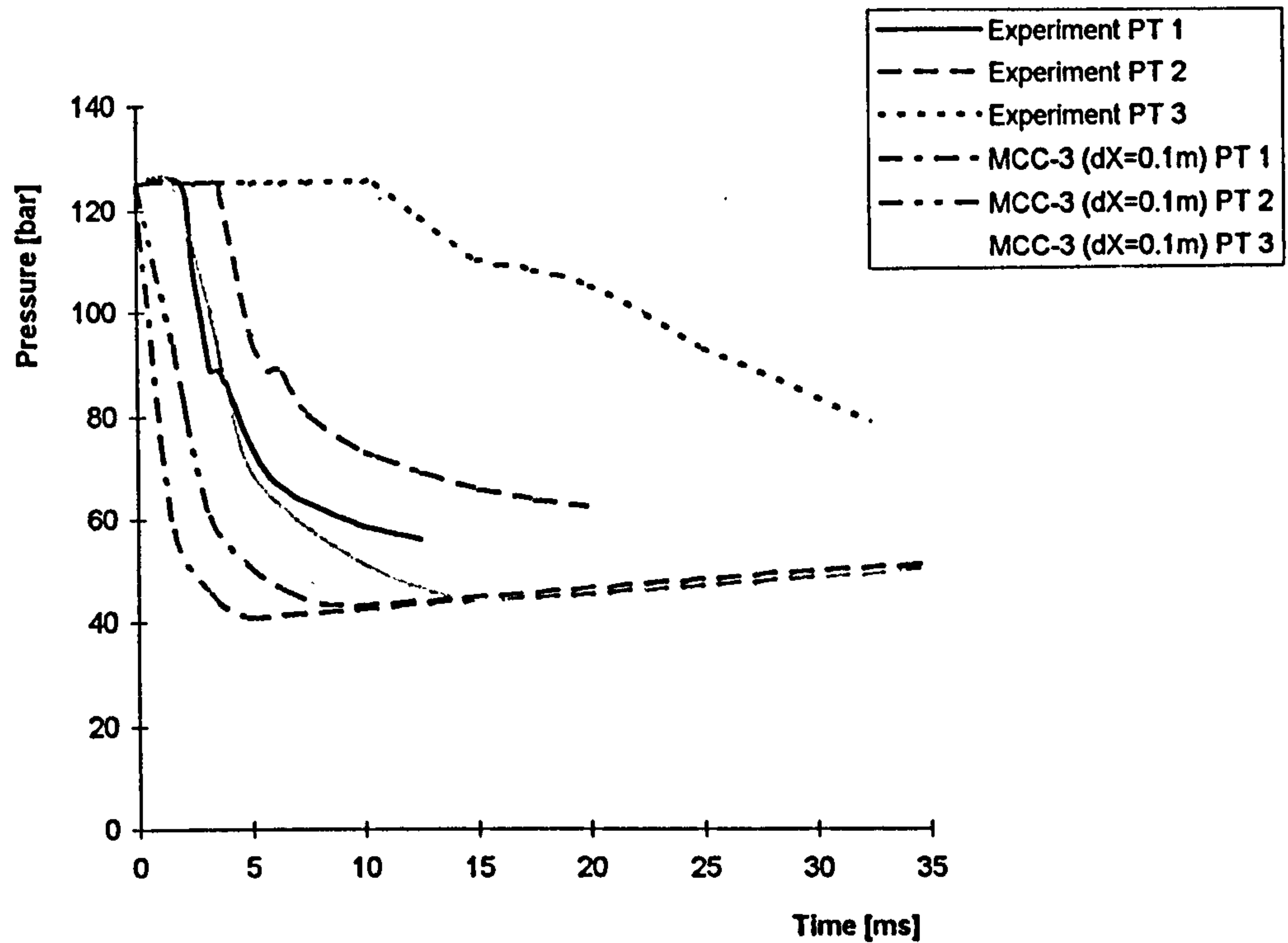


**Fig. 6.15 p-t Curves for British Gas Test BGT3 Comparison with MacCormack Method (Alternative 3) Predictions**

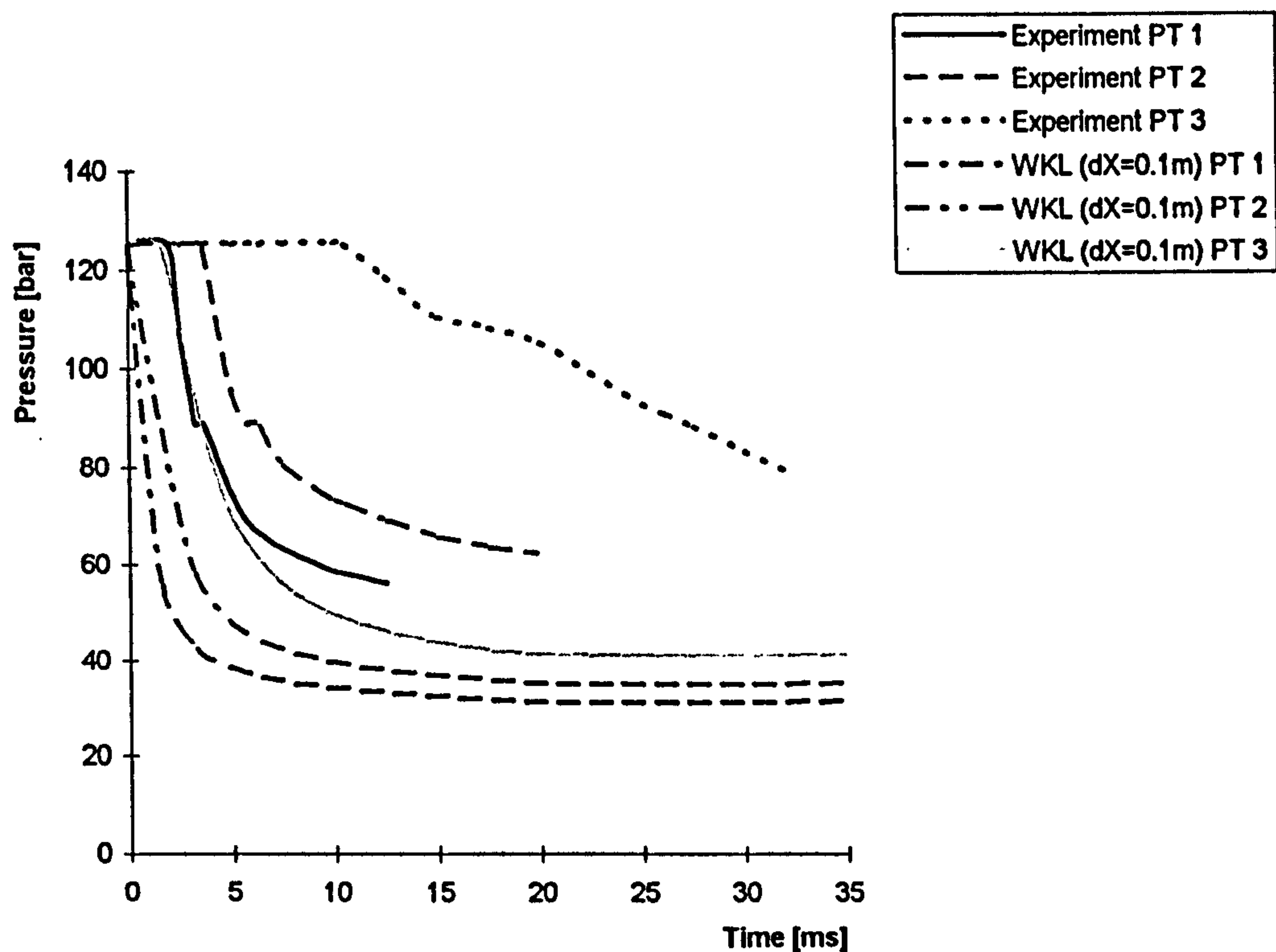


**Fig. 6.16 p-t Curves for British Gas Test BGT3 Comparison with Warming-Kutler-Lomax Method Predictions**



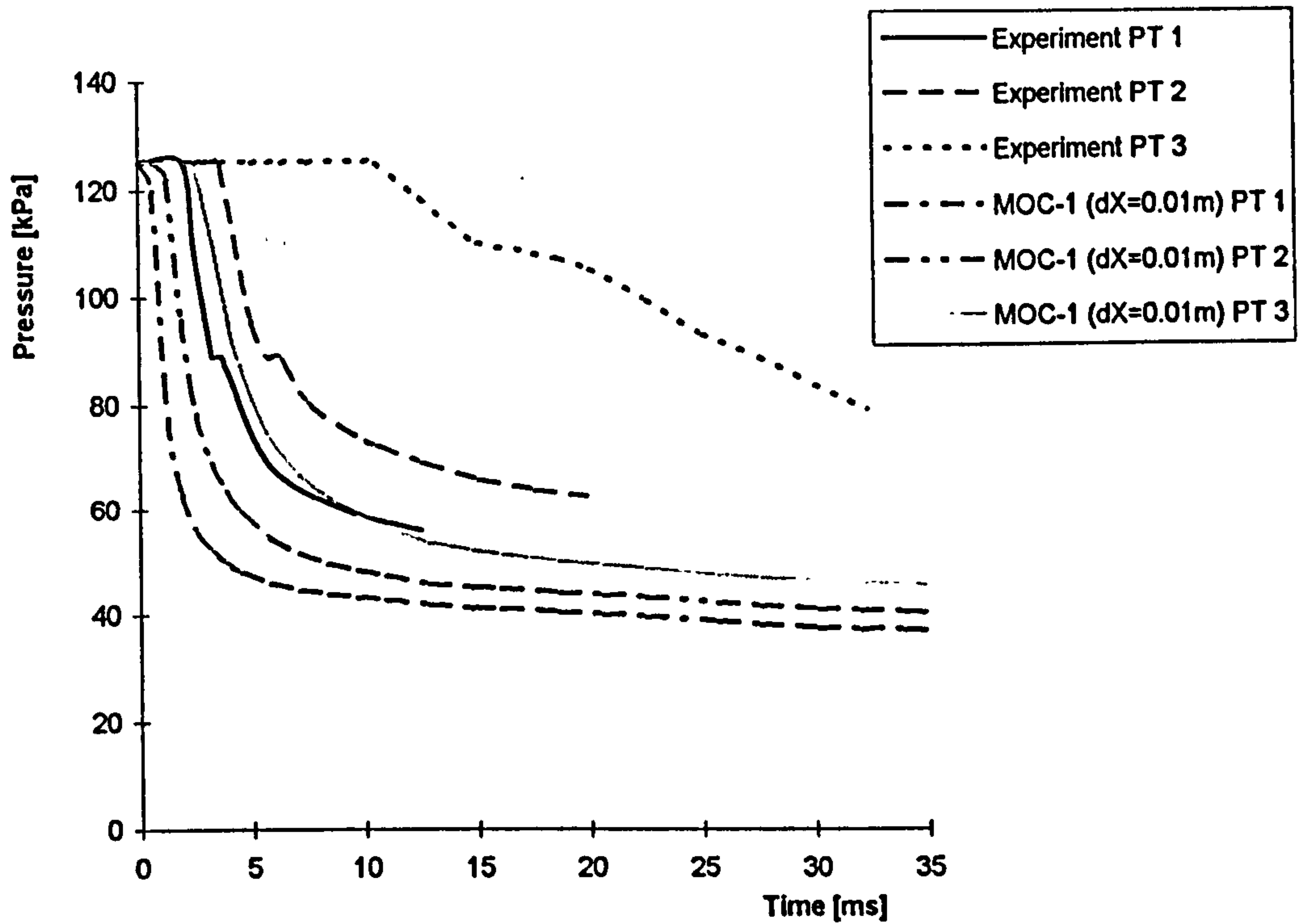


**Fig. 6.17 p-t Curves for British Gas Test BGT3 Comparison With First-order Method of Characteristics Predictions ( $dX=0.01\text{m}$ )**

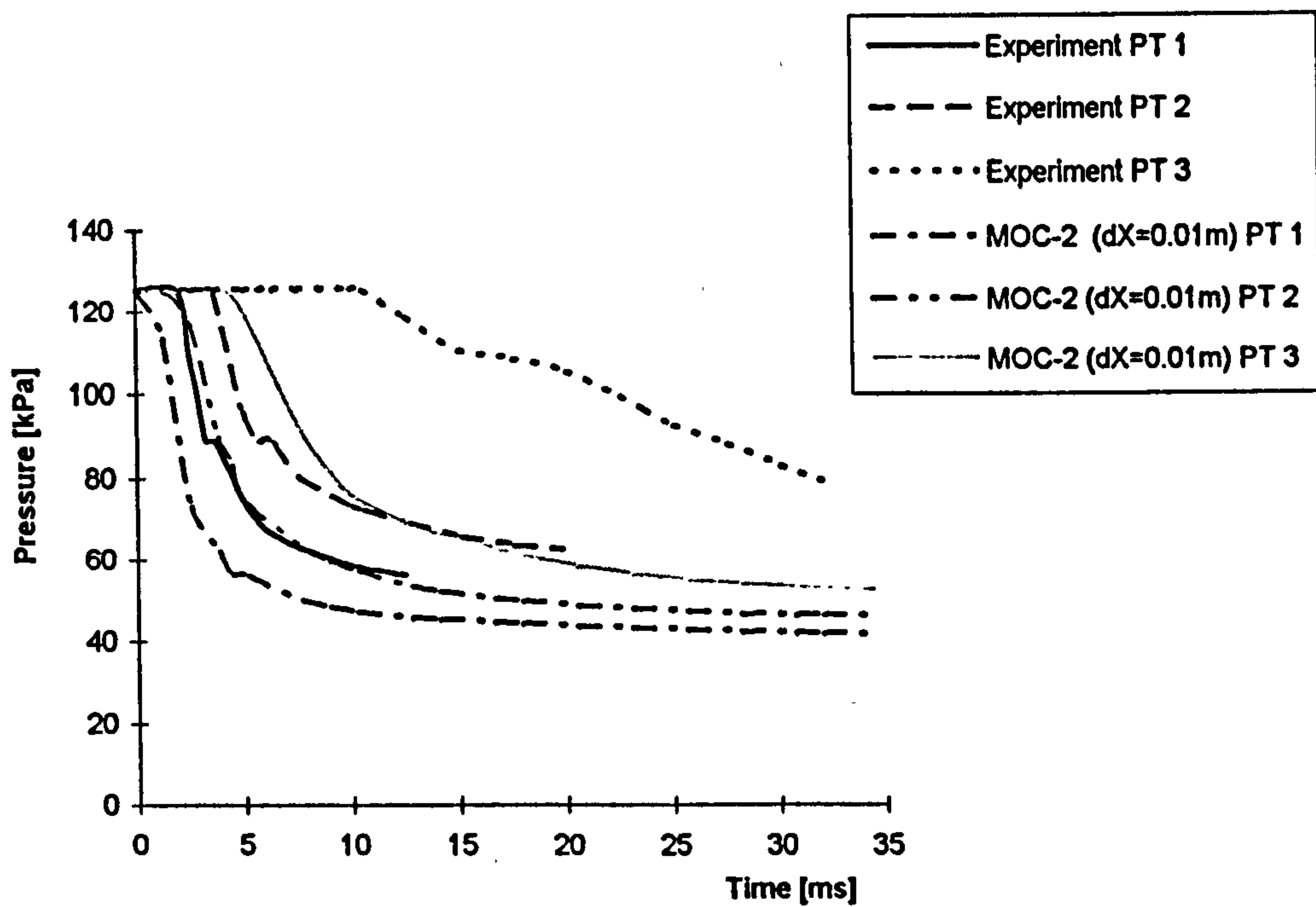


**Fig. 6.18 p-t Curves for British Gas Test BGT3 Comparison with Second-order Method of Characteristics Prediction ( $dX=0.01\text{m}$ )**

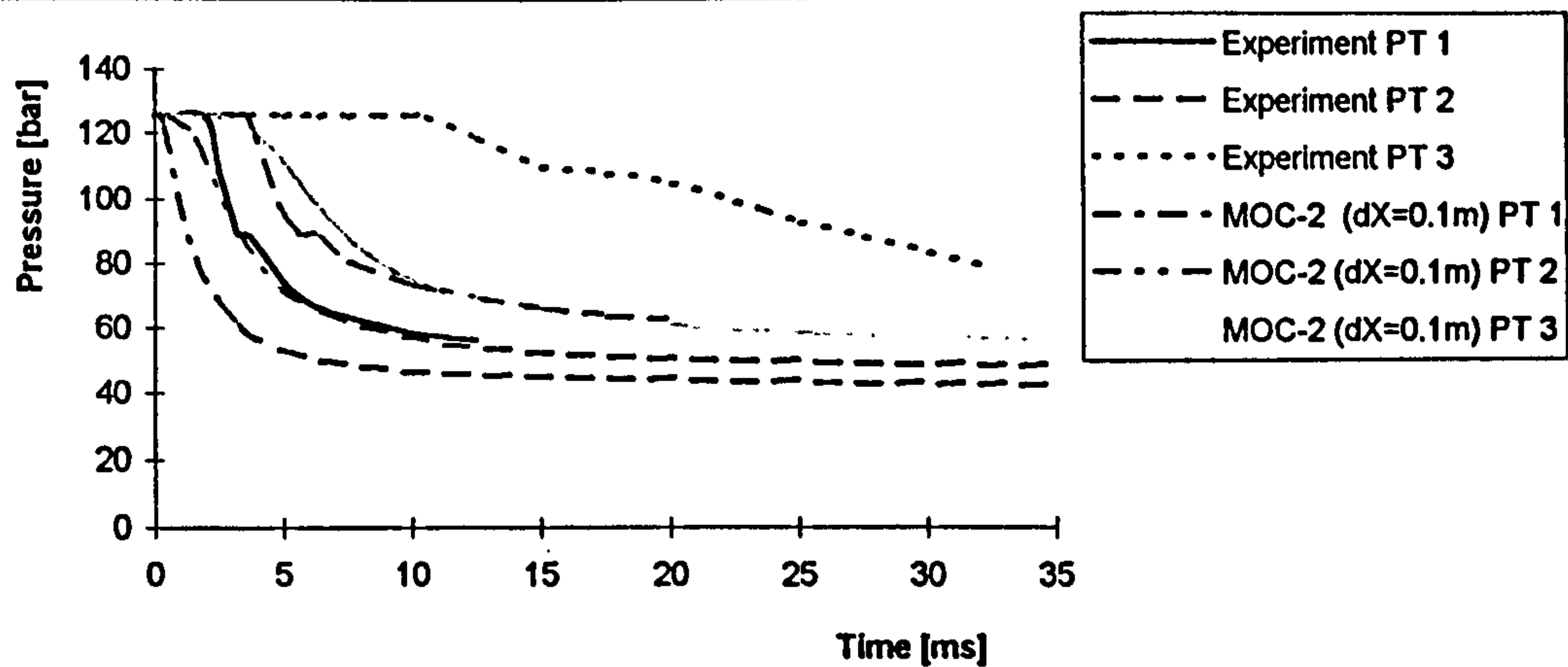


**Fig. 6.19 p-t Curves for British Gas Test BGT3 Comparison with Second-order Method of Characteristics Predictions (dX=0.1m)**

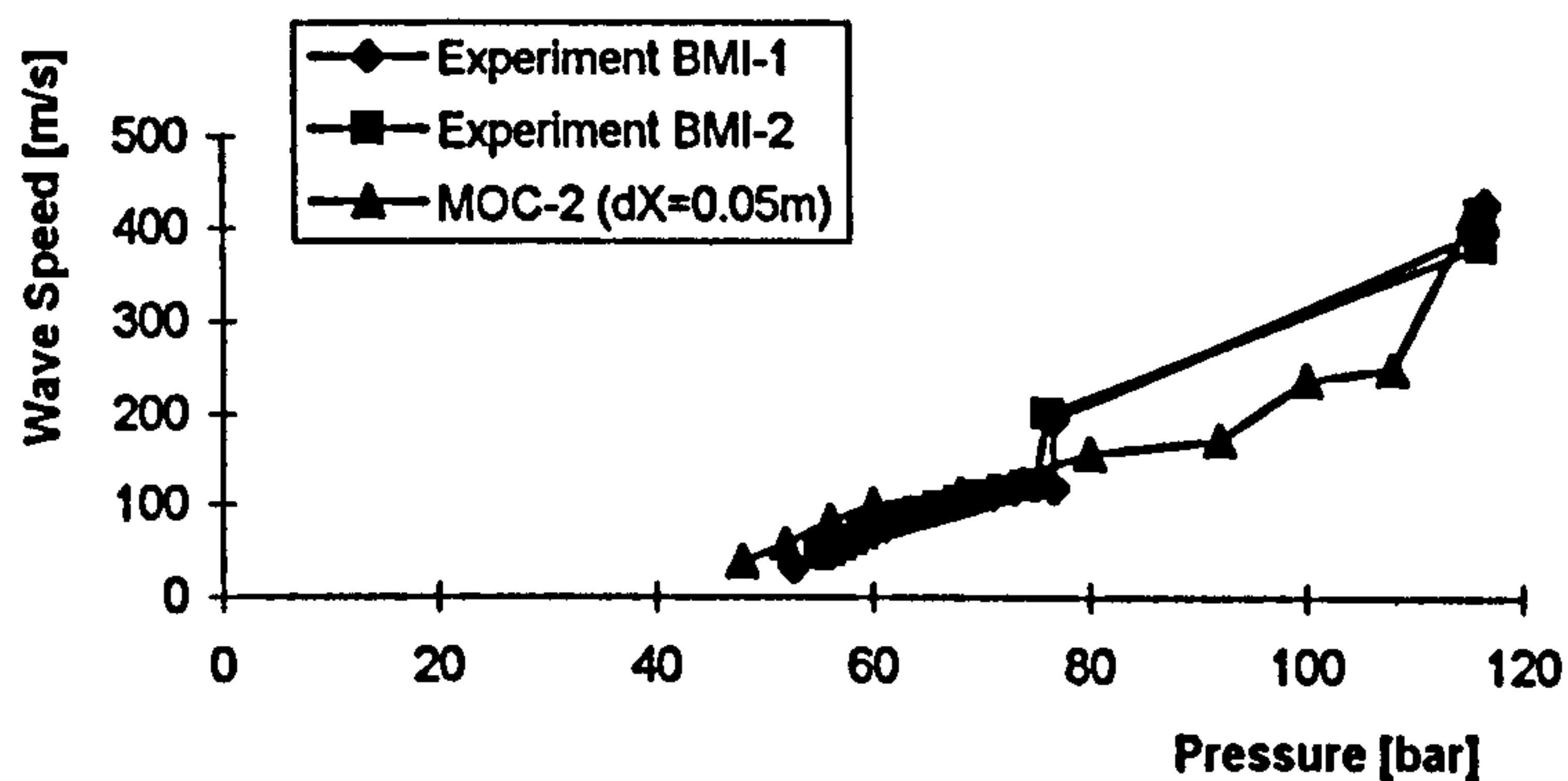


**Fig. 6.20 Pressure Wave Propagation Speed Curves for BMI Tests**

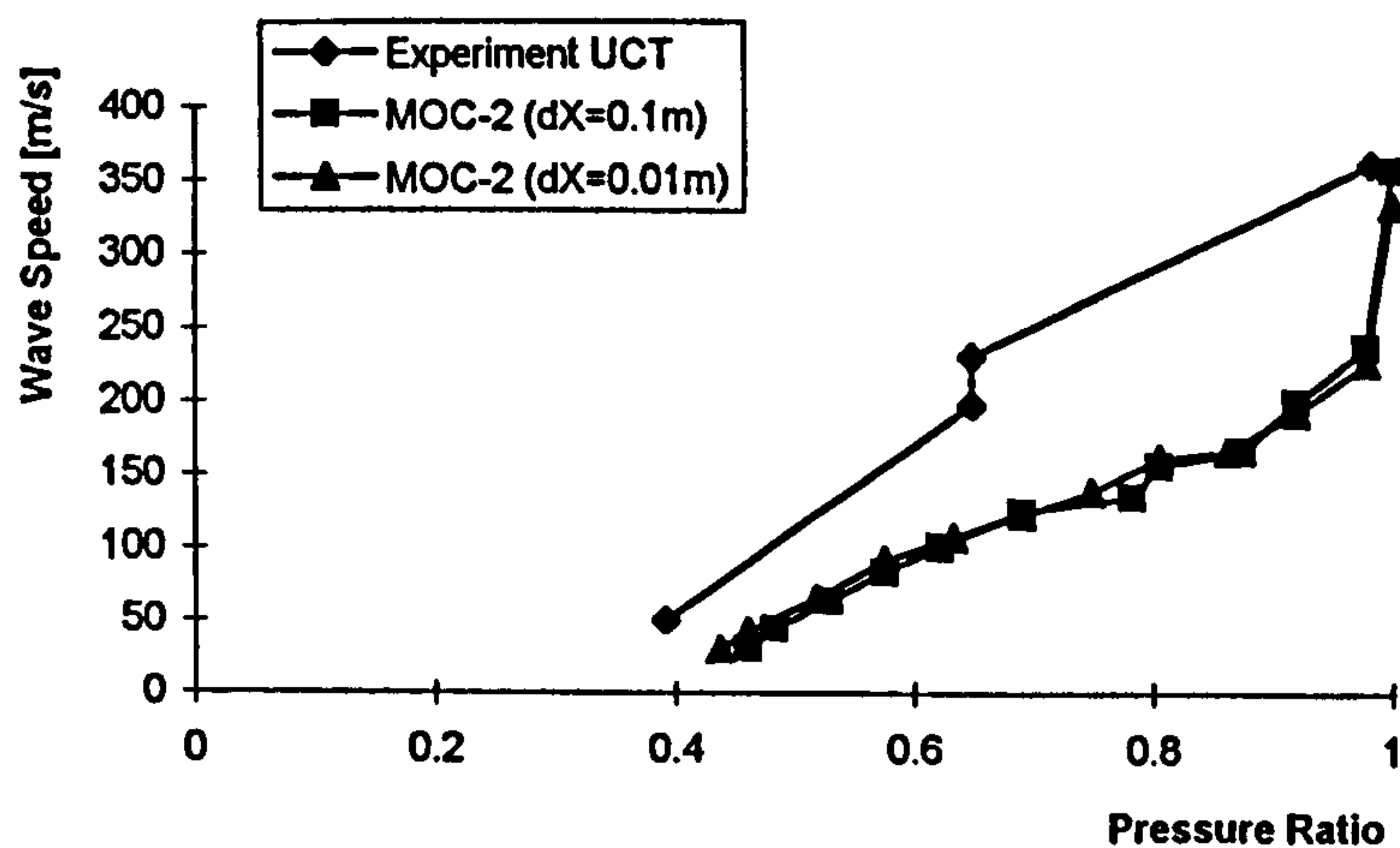


**Fig. 6.21 Pressure Wave Propagation Speed Curves for University of Calgary Test**



Foothills and British Gas Test) is used. The reason for using such a big spacing is to minimise CPU time. The analysis in this case is performed for a much longer time (25s) compared with the hundreds and tens of milliseconds used in the Foothills and British gas tests respectively. No problems were experienced with the numerical algorithm due to the selection of this large grid spacing at the broken end ( $\Delta x=1\text{m}$ ,  $\Delta t=0.0001\text{s}$ ). A variable grid spacing is used and the largest  $\Delta x=512\text{m}$ .

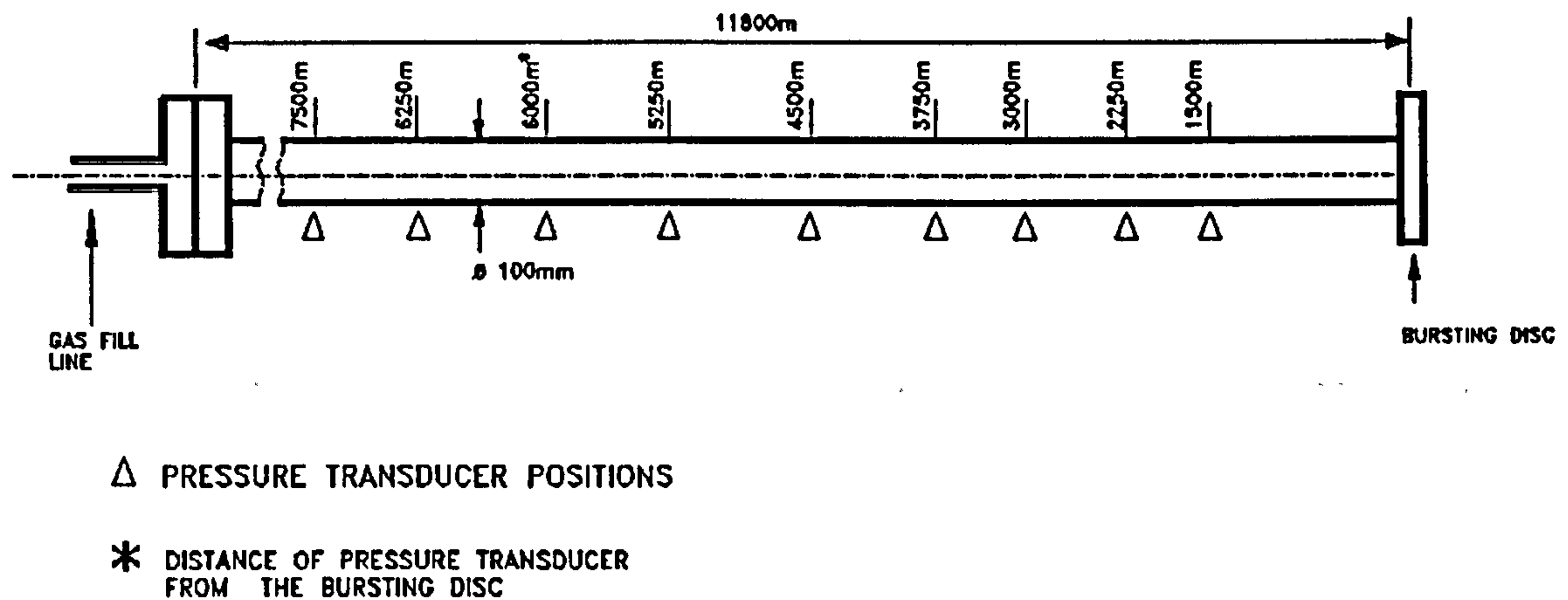


Fig. 6.22 Figure 6.22 Schematic of SNGSO Test

#### 6.2.4 API TEST DATA

The second set of full-scale experimental data is that which was reported by the Alberta Petroleum Industry, Government Environmental Committee (1979). The tests were performed as the second phase for a field verification programme of isopleth prediction techniques. It involved a full-scale field programme to investigate, among other things, the behaviour of gas emissions resulting from a pipeline rupture. The rupture mode was the most critical variable examined. Two tests setups were used at the test site, which is located in the Western gas field in Southwestern Alberta. The first and second tests are referred to here as APIT1 and APIT2. The tests were carried out using an existing 168.3mm outside diameter pipeline which was typical of sour gas pipelines in the province at pressures of 6.9 and 3.45MPa respectively. The tests section was approximately 4.0km long. It was burst at the mid point. The third test is referred to in the report as APIT3. It was performed on a 323.9mm outside diameter and approximately 7.1km long pipeline. Also in this test the pipeline was pressurised to 6.9MPa pressure and ruptured at the middle. The specification of the pipes used in the two tests was provided. As with SNGSO test, no

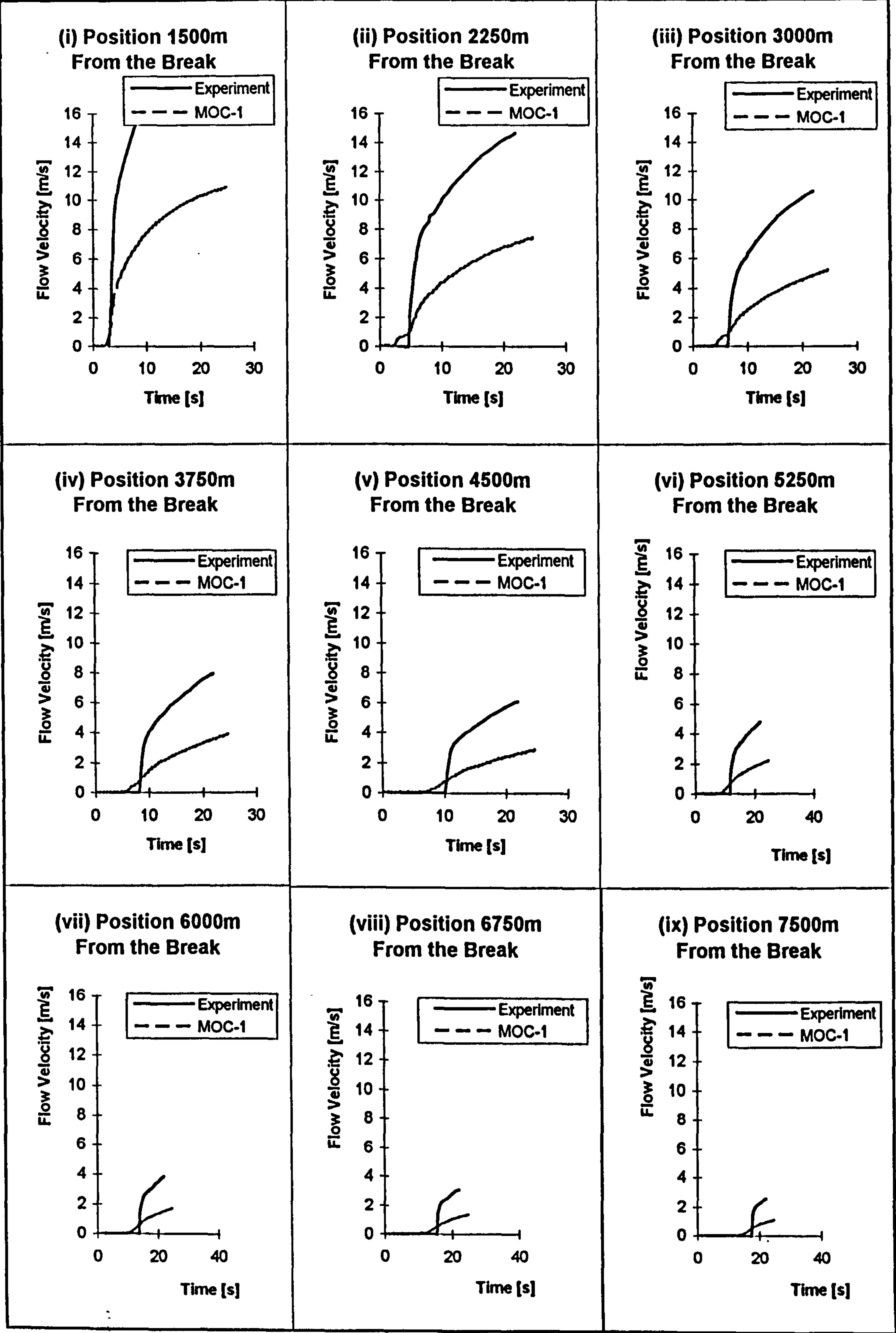


Fig. 6.23 u-t Curves for SNGSO Test Comparison With First-order Method of Characteristics Predictions



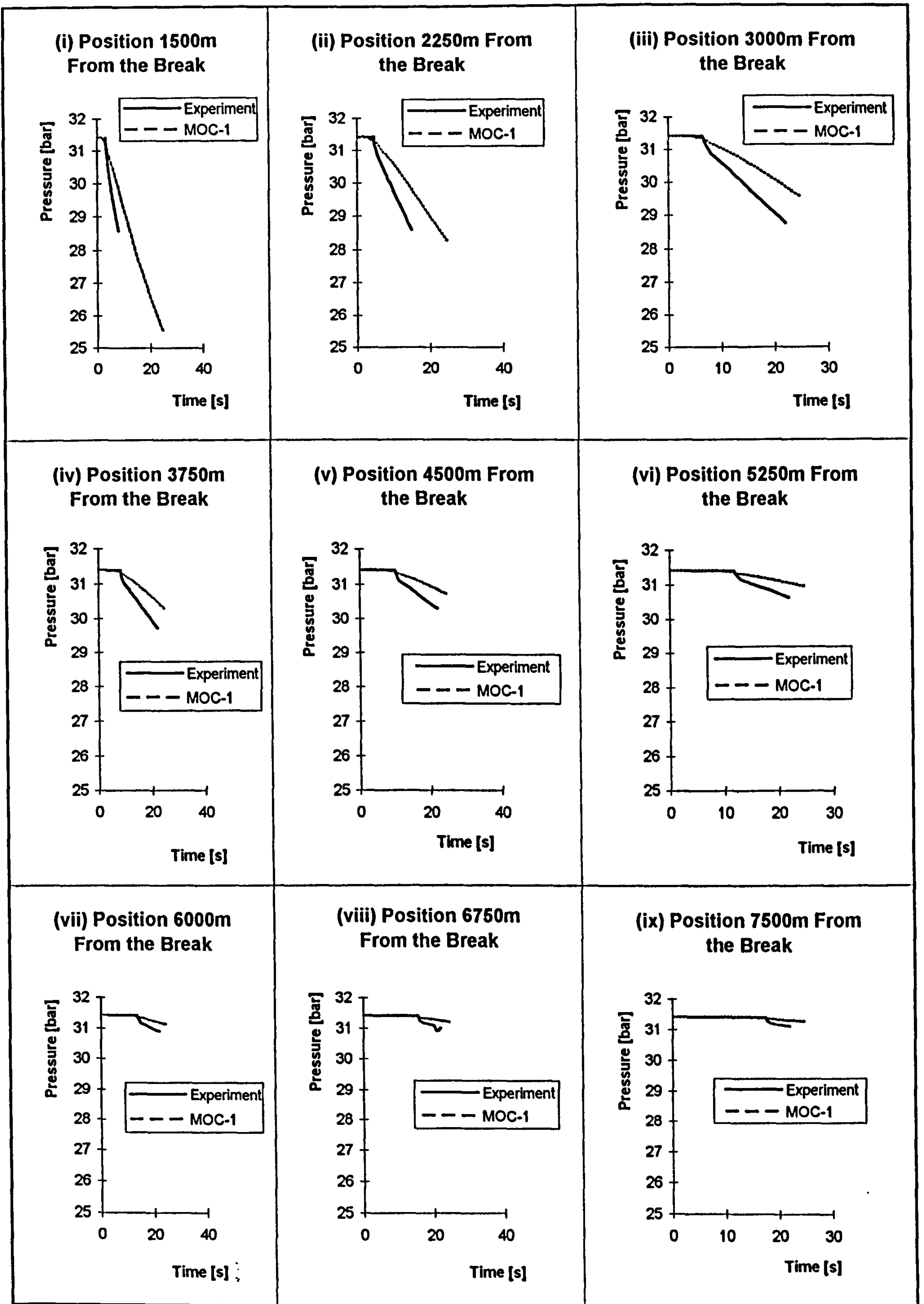


Fig. 6.24 p-t Curves for SNGSO Test Comparison With First-order Method of Characteristics Predictions

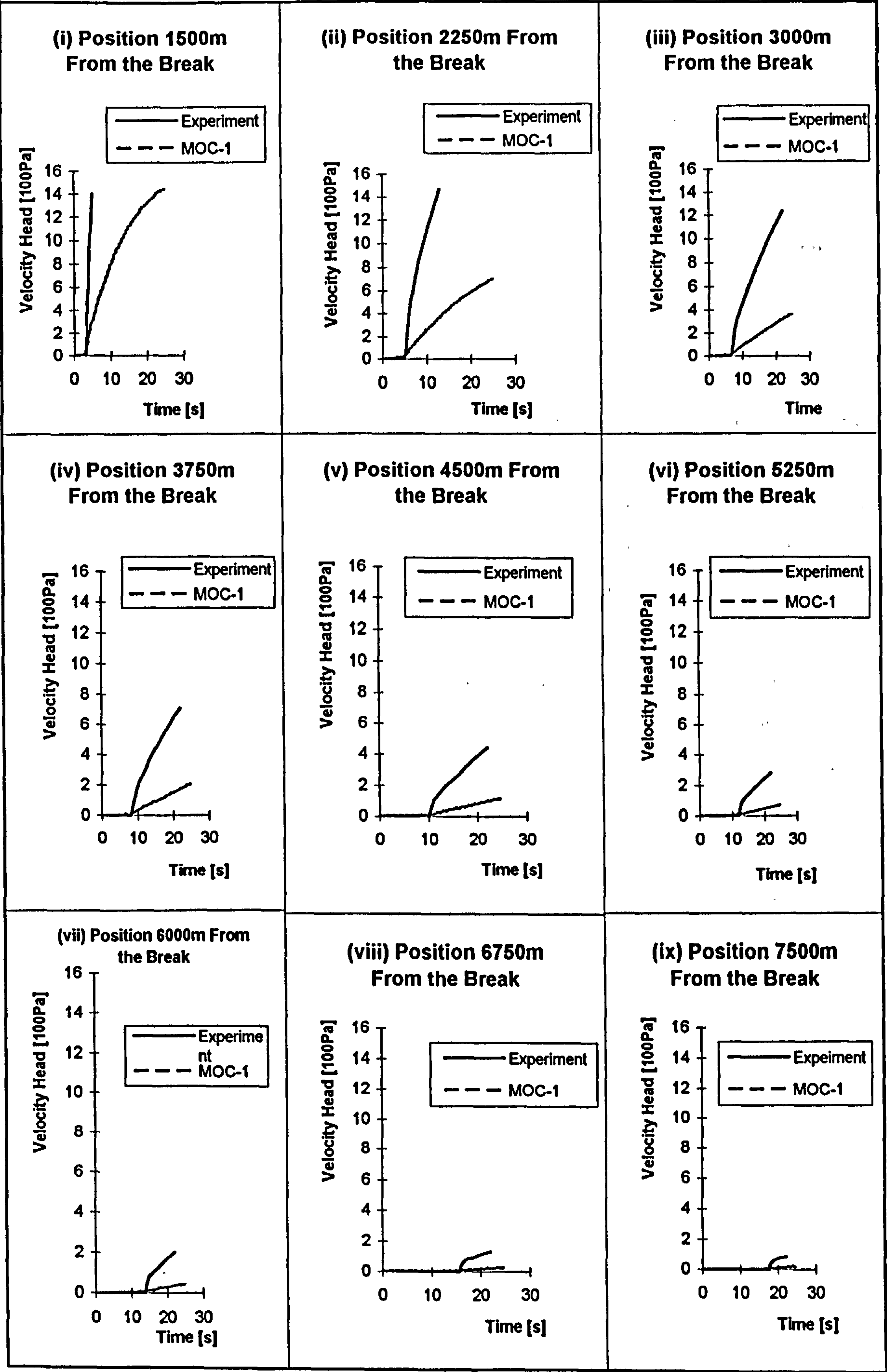


Fig. 6.25 Velocity Head for SNGSO Test Comparison With First-order Method of Characteristics Predictions



data was provided for the gas composition. The same data which was used in the previous sections is used for the fluid properties. Due to the long run times required, a coarse grid spacing is used in order to reduce the CPU time. A grid spacing of  $\Delta x=5\text{m}$  and  $\Delta t=0.005\text{s}$  is used for APIT1 and APIT2 tests, and a grid spacing  $\Delta x=10\text{m}$  and  $\Delta t=0.01\text{s}$  is used for APIT3 test. A variable grid spacing is used in all the computer predictions.

It was observed [Alberta Petroleum Industry, Government Environmental Committee (1979)] that the rupture mode was unpredictable and difficult to control. It was found that under similar test conditions any of three different rupture modes could occur. The three rupture modes are bell opening, ring-off and a combination of the two in which one end is bell and the other ring-off. In bell rupture, the fracture is propagated a short distance along the longitudinal axis with the pipe remaining intact. In ring-off rupture, the fracture is propagated a short distance along the longitudinal axis and then turned circumferential around the pipe. The rupture section would either be blown completely out of the line or remain attached to the pipe by a small tab at either end.

A pressure sensor was placed within 1m of the rupture point in order to ensure that the measurements obtained were in the critical flow zone. It was observed that the instruments were subjected to extreme forces by the exiting gas jet and often they were blown off the line if, the rupture mode was a ring-off. When the rupture mode was a bell opening, the instruments were unaffected. A total of eleven experiments were conducted for measuring flow rate data, six of which could not provide complete data because the instrument to measure the critical flow were lost during the blowdown. The remaining five tests produced sufficient data to validate the computer models. Data from three tests (two bottom ring-off and one side bell) were combined to form a set of experimental data for the 168.3mm diameter pipe at an initial pressure of 6.9MPa (APIT1). Another test, in which the rupture was top ring-off was used for the same pipeline but pressurised to 3.45MPa (APIT2). The last of the five good tests was carried on with the 323.9mm diameter pipe. The line was pressurised to 6.9MPa and the rupture mode was bottom bell. This provided the data for test APIT3. The data for tests APIT1, APIT2 and APIT3, which is described in this section and the corresponding prediction from the computer model developed in this study, are presented in Figs 6.28 to 6.33.

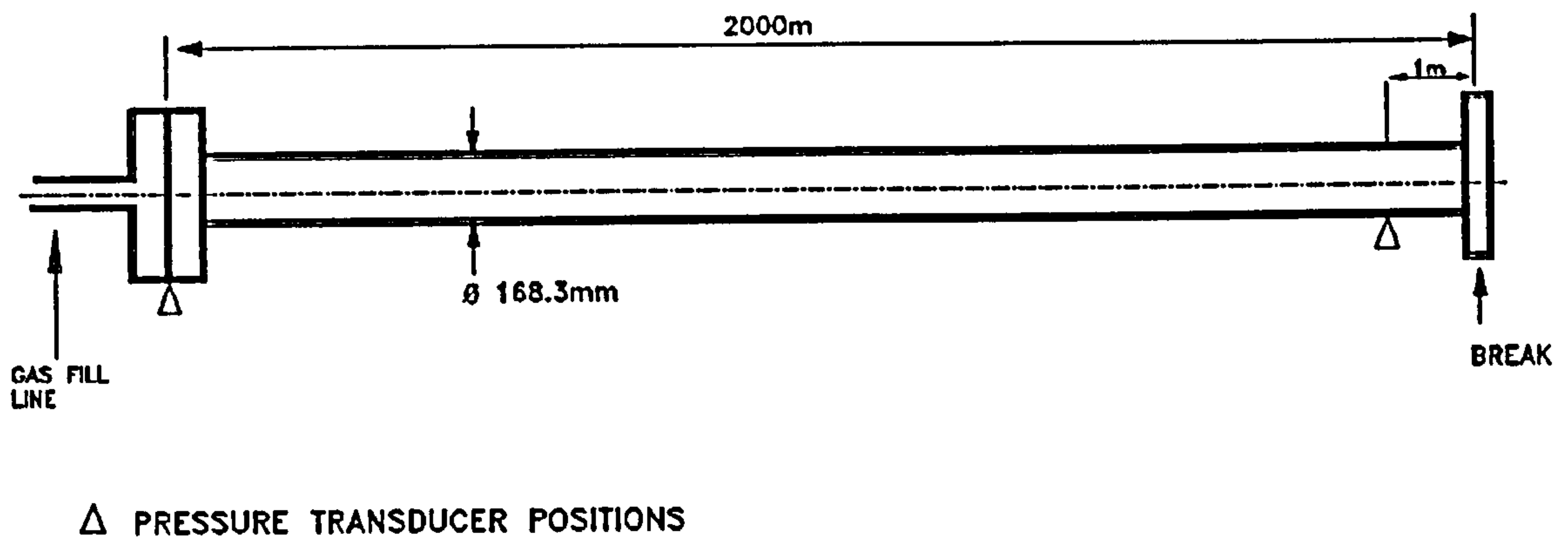


Fig. 6.26 Schematic of Alberta Petroleum Industry Tests APIT1 and APIT2

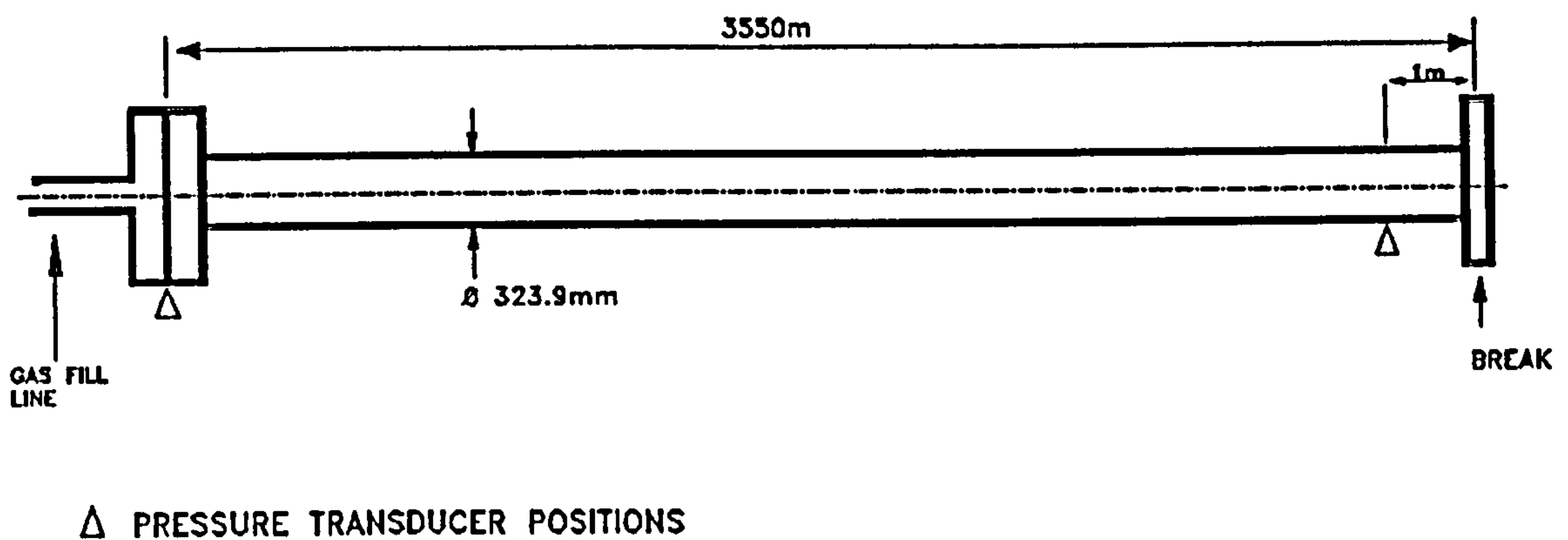


Fig. 6.27 Schematic of Alberta Petroleum Industry Tests APIT3

## 6.3 DISCUSSION OF VALIDATION RESULTS

### GENERAL DISCUSSION

Fanneløp and Ryming (1982) defined the different time regimes following a linebreak, each requiring a different method of solution. These are described in Section 3.3.2. Also Knox, Atwell, Willoughby and Dielwart (1980) discussed the different rupture modes, which require different modelling approaches. In this study, both the early and late time regimes, which were defined by Fanneløp and Ryming (1982), are modelled using the various data presented in this chapter. The same theoretical and numerical models are used for both time regimes. Unless the pipe diameter and/or cross-section area is specified differently at



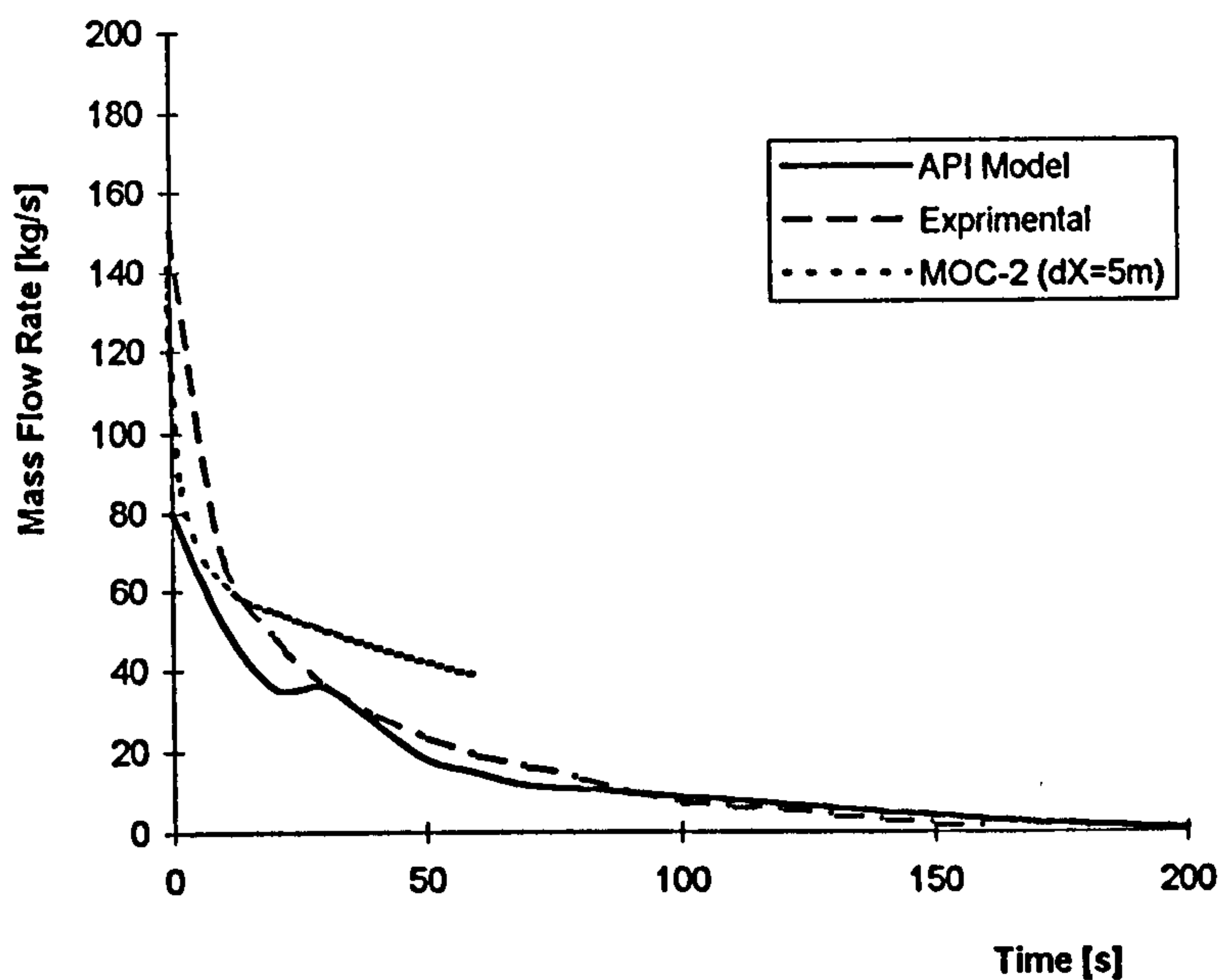


**Fig. 6.28 Mass Flow Rate for Alberta Petroleum Industry Test APIT1 Comparison with Second-order Method of Characteristics Prediction**

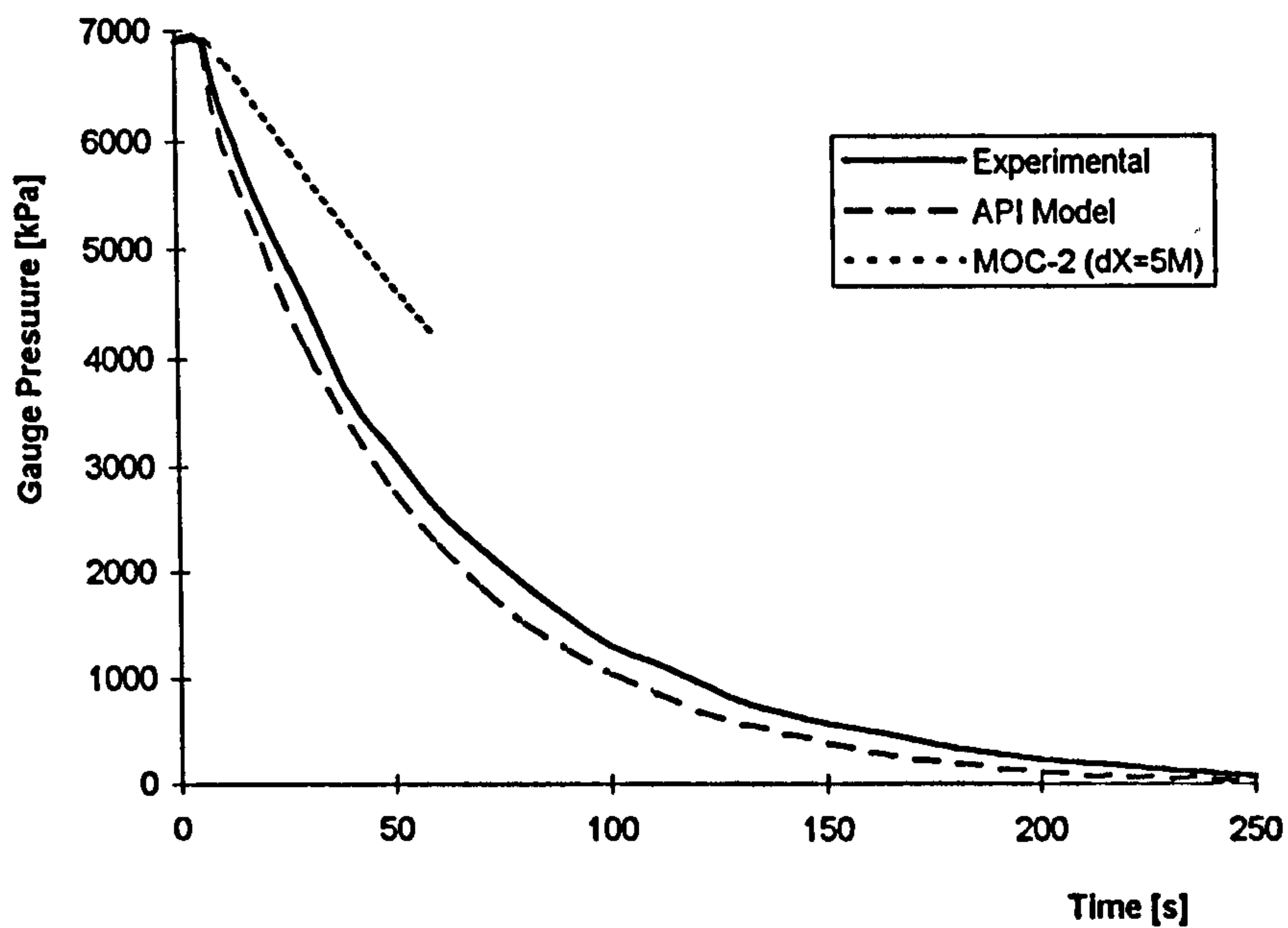


**Fig. 6.29 Pressure at the Intact End for Alberta Petroleum Industry Test APIT1 Comparison with Second-order Method of Characteristics Prediction**

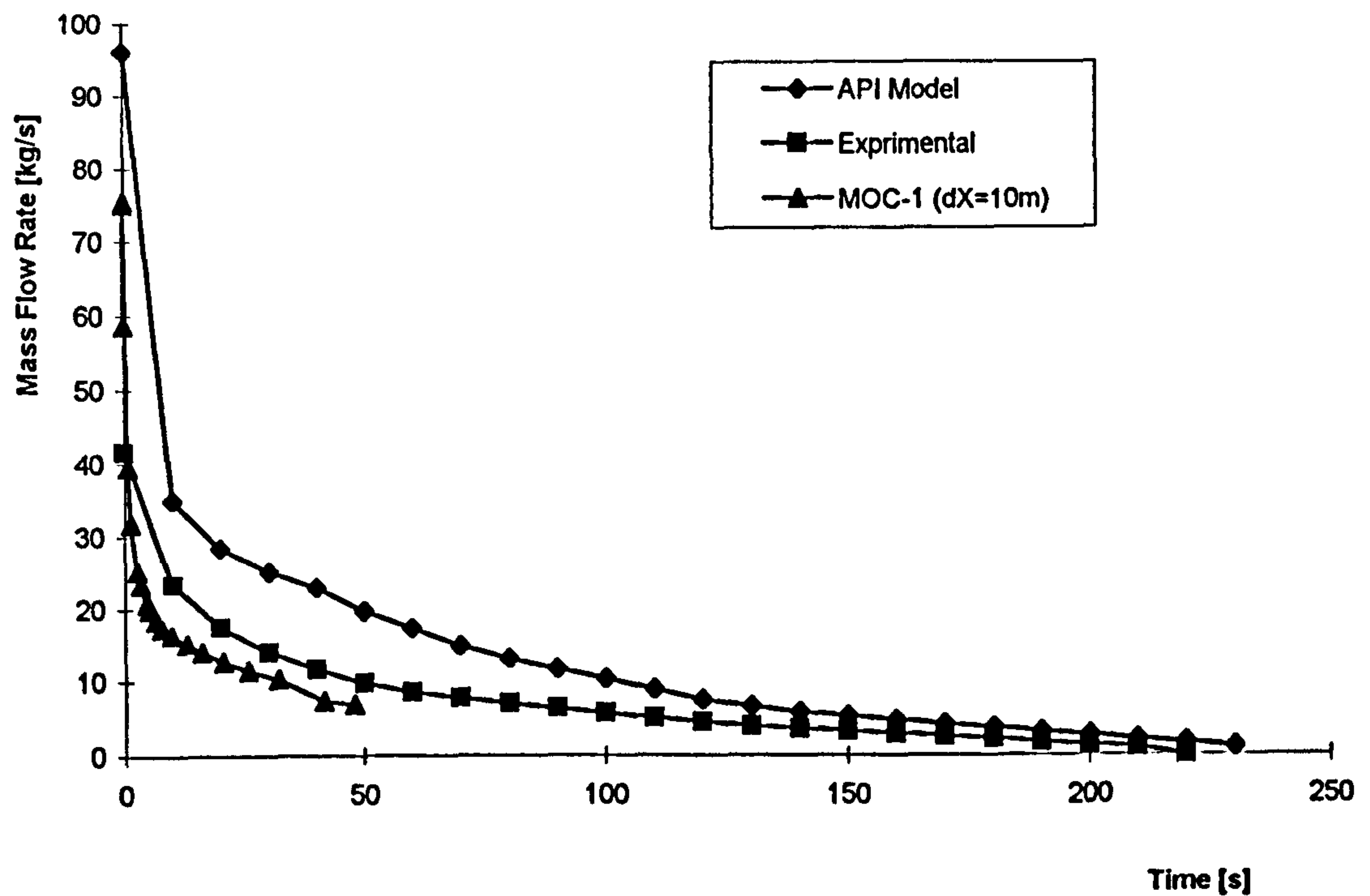


**Fig. 6.30 Mass Flow Rate for Alberta Petroleum Industry Test APIT2 Comparison with First-order Method of Characteristics Prediction**

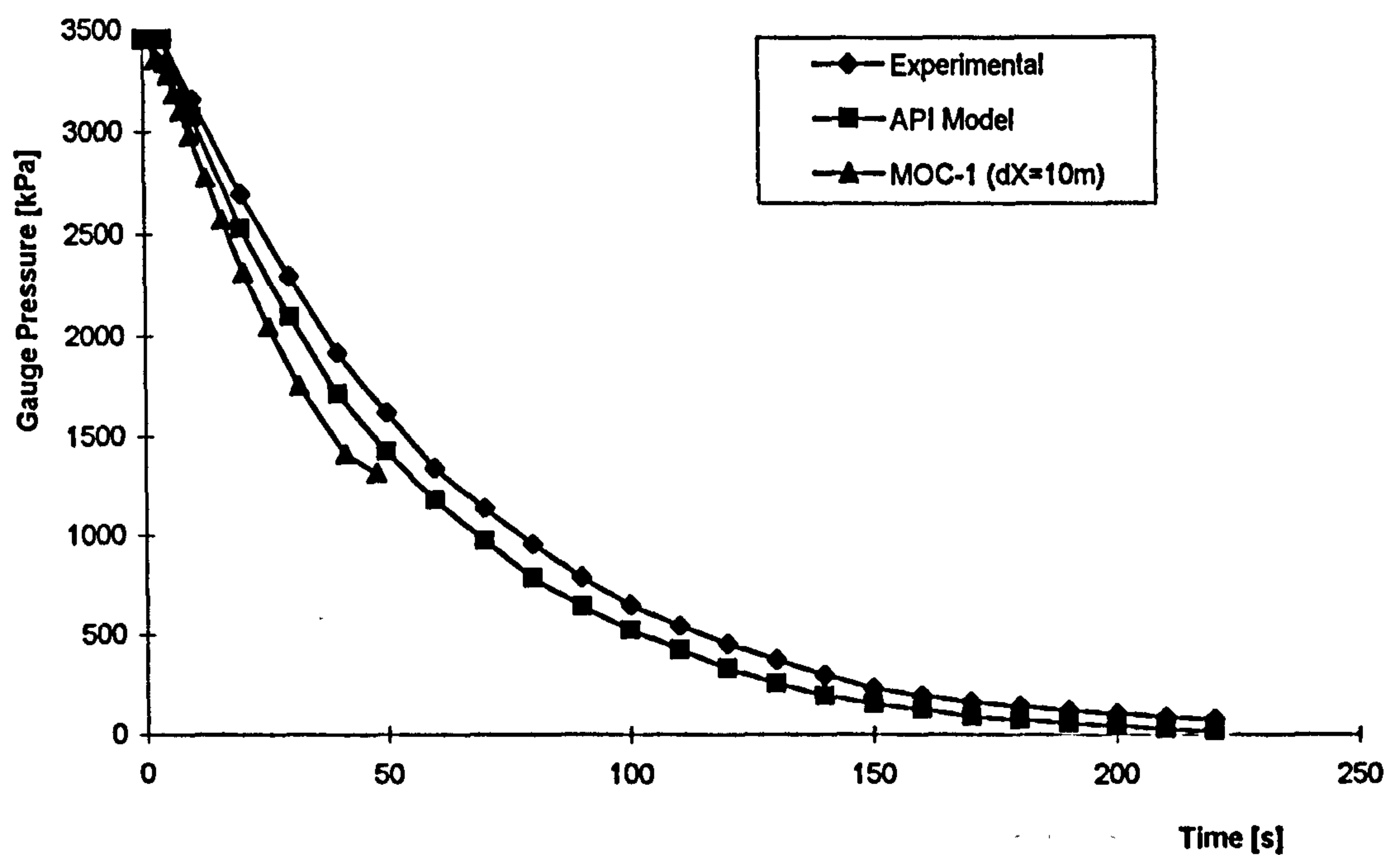


**Fig. 6.31 Pressure at the Intact End for Alberta Petroleum Industry Test APIT2 Comparison with First-order Method of Characteristics Predictions**



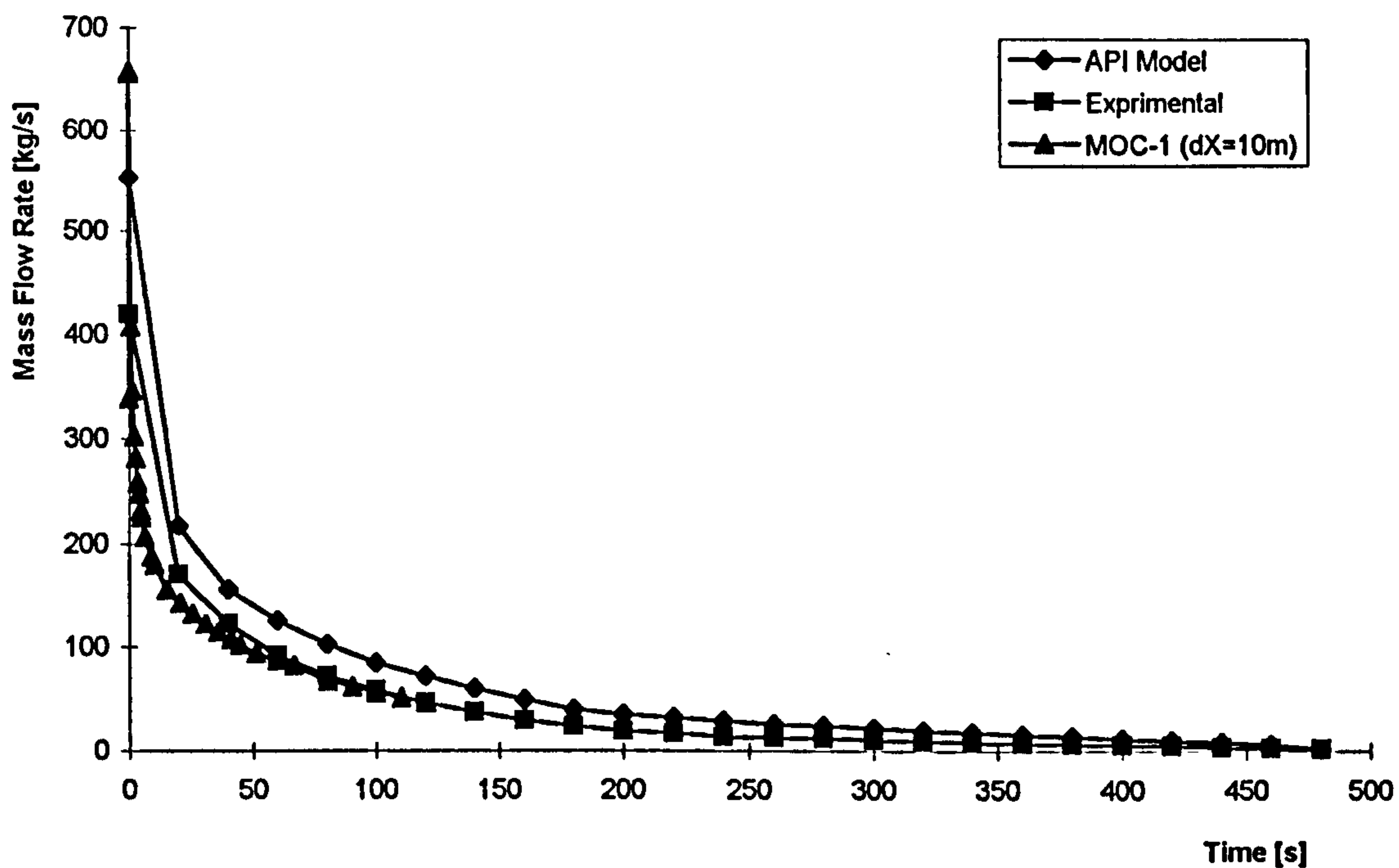


**Fig. 6.32 Mass Flow Rate for Alberta Petroleum Industry Test APIT3 Comparison with First-order Method of Characteristics Prediction**

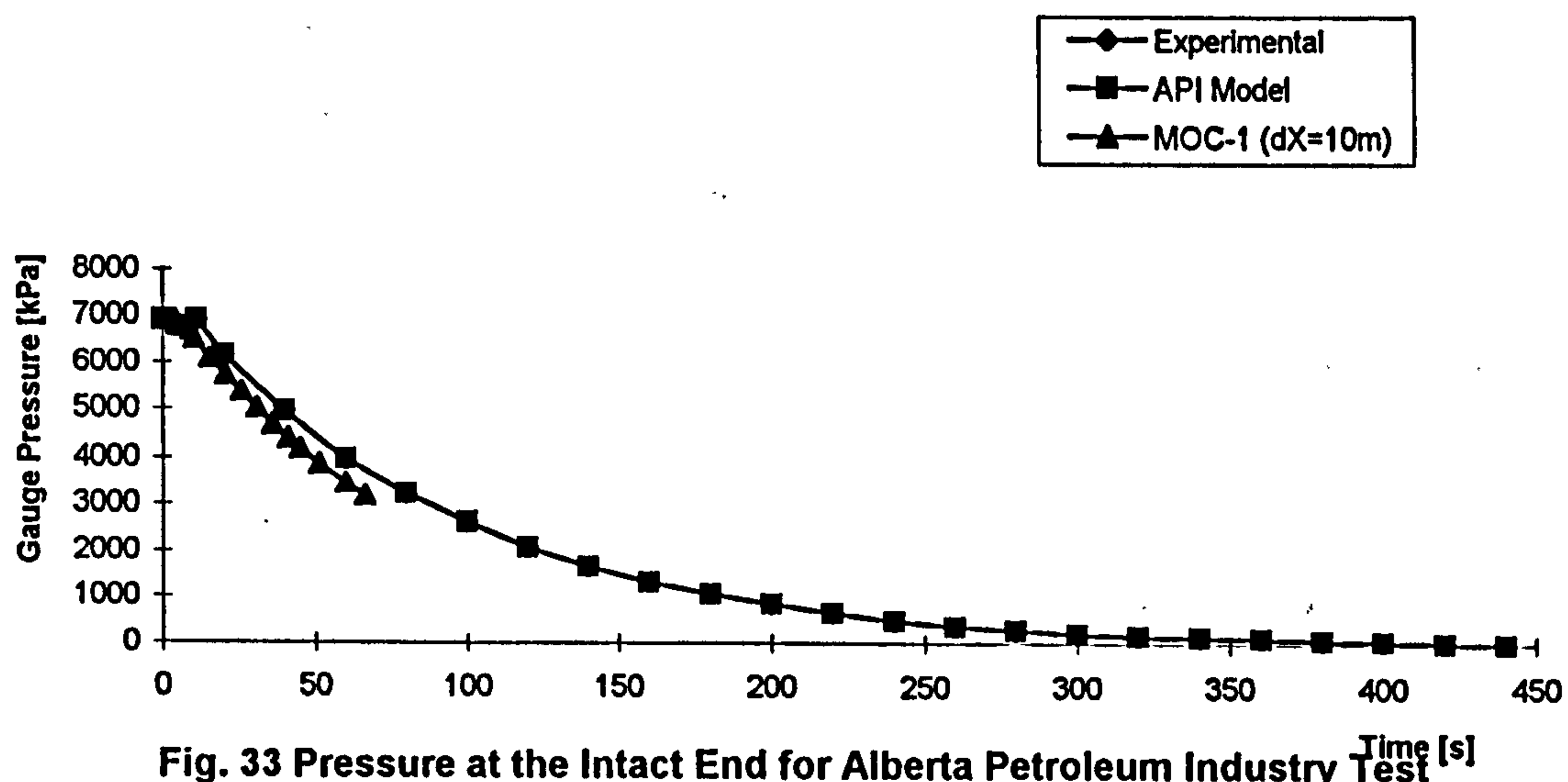


**Fig. 33 Pressure at the Intact End for Alberta Petroleum Industry Test APIT3 Comparison with First-order Method of Characteristics Prediction**

broken end, full bore rupture mode is assumed. The model is limited to analysis of the flow following a linebreak in a straight section of pipeline. Various aspects of the model and the predicted results are discussed, based on results obtained from the computer modelling which is described in sections 6.2.1 to 6.2.4 and previous trial runs. The symbols used in the graphs are defined as follows:

- MOC-1            First-order method of characteristics
- MOC-2            Second-order method of characteristics
- MCC-1            MacCormack method using alternative 1
- MCC-2            MacCormack method using alternative 2
- MCC-3            MacCormack method using alternative 3
- WKL              Warming-Kutler-Lomax method

Two sets of experimental data which were used by Tiley (1989), have been used in this study. These are the British Gas test data and [Jones and Gough (1981)] and the Foothills test data [Foothills Pipeline (Yukon) Ltd. (1981)]. A better comparison has been achieved in this study with the two sets of data than in the study by Tiley (1989). In the study by Tiley (1989), the length of the time step, grid size and break conditions were varied for each simulation, in order to optimize convergence towards a stable solution. In this study, the ratio between the time step and the distance grid is selected such that the Courant-Friedrichs-Levy stability criterion is satisfied. In this uniform grid spacing, the time step varies proportionally as the distance grid varies. For the test data used in this study, the maximum value of speed of sound and hence the maximum flow velocity was above 400m/s, but never it never reached 500m/s. Therefore, in order to ensure that the stability criterion is satisfied, a constant ratio of  $\Delta x/\Delta t=1000\text{m/s}$  was used. This ratio could handle situations in which the flow velocity and wave speed are each 500m/s, without failing the stability criterion. In every calculation step the programme checks to ensure that the Courant-Friedrichs-Levy stability criterion is satisfied. If the stability criterion is not satisfied, the programme stops automatically. Under no circumstance did the programme stop during the simulations reported in this study due to failure of the stability criterion.

In most of the simulations, the grid sizes used at the break boundary were coarser than those which were used by Tiley. Tiley used a grid size of 0.0254m for the British Gas tests but she could not achieve stable results for some of the tests. Tests for which stable results could not be achieved are those for which the initial pressure was high and the initial flow rate was zero. No such problems were encountered in this study, even with grid size



of up to 0.1m for the British Gas tests. The only problem encountered for such tests was that the execution speed of the programme was very slow and the boundary conditions, in some cases, were not properly modelled. This condition is explained further in the discussion of the method of characteristics.

Tiley (1989) also noticed that the theoretical p-t curves tended to begin their pressure drop too early. This effect was more noticeable the further the transducer was from the break. She attributed this phenomenon to the response time of pressure transducers, which causes a delay in recording the pressure drop. In this study, only the transducers which are close to the break have been investigated. The same phenomenon as was observed by Tiley was repeated. However, a comparison of the pressure wave speeds predicted by the computer model, with those obtained from the BMI and University of Calgary tests show a good agreement. Since there were no p-t curves provided for the latter two test, it was not possible to compare the pattern of the p-t curves. Also since there are no pressure wave curves for the British Gas test which have been used in this study, it was not possible to compare the pressure wave speed. However, the fact that the pressure waves predicted by the model compare favourably with experimental values from the BMI, University of Calgary and Foothills tests indicate that there is a problem with the British Gas test data. Tiley (1989) did contact the British Gas in order to ascertain the accuracy of their data. She reported that they could not ascertain the accuracy of their data, but they indicated that they were not entirely satisfied with it. Although not conclusively confirmed, they believed that one of their transducers, PT2, was malfunctioning.

Tiley noticed inconsistency in the final pressure reached after the break. In some cases the pressure was higher and in some cases lower. She attributed this condition to inaccuracies incurred in the calculation of equalization pressure at the break. No such problems were encountered in this study due to the accurate model developed for calculating equalization pressure. It should be noted that the data for the curve PT1 in the British gas test BGT1 are those obtained from predictions using the British Gas theoretical model and not from experiments.

In simulating the Foothills test, Tiley (1989) used a grid spacing of 0.01m at the break. This spacing is much finer than that which is used in this study (0.1m to 0.5m, and it would be expected to produce better results. However, Tiley used time steps varying from 0.65 to 0.75ms (quoted as s in her thesis). This time step is too big for the value of  $\Delta x$  used and fails the Courant-Friedrichs-Levy stability criterion. The ratio  $\Delta x/\Delta t$  used by



Tiley was between 13.33 and 15.39m/s, which is much less than 1000m/s which is used in this study. This gross error in the time step is probably the main reason for the instability problems encountered by Tiley. The argument by Tiley that decreasing the time step could have lead to an increase in the accumulative round-off error in the results is not valid.

Simulation results produced in this study using the method of characteristics compare very well with the experimental data, as the p-t curves and the pressure wave speeds are modelled correctly. Tiley argued that a possible reason for her model's overestimation of the wave speeds was the second-order approximation used near the break. This argument is not correct because the second order approximation has an opposite effect i.e. producing lower wave speeds than those produced using the first order approximation. As was the case with Tiley's simulations, the final pressures calculated for the Foothill tests were slightly higher than the experimental values. The reason for this is that the theoretical models did not account for the crack propagation along the length of the pipe. The crack propagation has the effect of moving the point at which the equalization would occur along the pipe. In this study, this effect was more severe with test NABTF7 than with test NABTF1 because of the long crack propagation in the former test (18.28m in NABTF7 compared with 4.21m in NABTF1). The crossing of the p-t curves, which was attributed to temperature related zero drift during testing [Foothills Pipeline (Yukon) Ltd. (1981)] does not exist in prediction obtained using the method of characteristics and the Warming-Kutler-Lomax methods. However, this phenomenon was observed when the MacCormack method, indicating that the method is not suitable for analysis of transient flow following a break in a high-pressure gas pipelines.

The two other sets of data, namely the SNGSO and the Alberta Petroleum Industry data, were not used by Tiley. Both sets involved relatively long pipes and the data seem to be consistent and satisfactory. A good agreement was obtained between the experimental data and the prediction results, even with the big grid size used. The major weakness of the data is that they do not contain sufficient information about the gas used, some specifications of the testing system and accuracy of measurements recorded. The intact end pressure which was calculated using the Alberta Petroleum Industry data differ from the experimental and their model prediction data considerably. The second-order method results show the biggest discrepancy. Also the mass flow rates calculated using the second order-method are higher. The values produced with the first-order method compare much better with the experimental data than those obtained using the second-order method.



The values mass flow rates produced by the first-order method of characteristics are lower than the experimental values. The reasons for this discrepancy are errors in calculating the gas density and the big grid spacing used. The results obtained from this simulation give an indication that the first-order method of characteristics is the most suitable in situations where a big grid spacing is used.

A comparison of the model prediction and experimental data for the SNGSO test show a reasonably good agreement. The pressure starts to drop at the same time (Figs. 6.23 and 6.24), which indicate that the wave speeds predicted by the computer model are correct. However, the magnitudes of the pressure drop and flow velocity predicted by the computer model are less than experimental values. This discrepancy is caused by interpolation error and the big grid spacing used. Data which was obtained using a smaller grid spacing ( $\Delta x=1\text{m}$ ) and the second-order method of characteristics could not be used for validation because the interpolation error and round-off error of the computer affected the results very much. This effect is explained in detail in the grid size discussion.

## **THE QUANT SOFTWARE FOR THERMODYNAMIC AND TRANSPORT PROPERTIES OF FLUIDS**

The fluid property data, which are used by the programmes, are calculated using the QUANT Software. Heat transfer is calculated using the recovery factor and adiabatic wall temperature method and therefore the values of  $Pr$ , thermal conductivity of the fluid and  $C_p/R$  are not required. However, the three values listed above are used in other variations of the computer model. Three main limitations of the QUANT software are unavailability of  $Pr$ ,  $k_f$  and  $\mu$  at some low temperatures, unavailability of all output values at much lower temperatures and temperatures below 200K and lack of all outputs at high pressures. The composition of the gas mixture used in this study is given in Table 6.2. The highest pressure for which output is available, but only for part of the temperature range required, is around 7MPa. This limitation has been overcome by using the fluid properties which are available at the closest state of the fluid and additional data for the gas mixture which was provided by the suppliers of the QUANT software on request [Silberring (1995)]. The additional data was calculated using a later version of QUANT which is still being developed. The later version of QUANT is expected to be able to produce output at higher pressures, similar to those encountered in high-pressure natural gas pipelines.

It is observed that the temperature of the gas near the break boundary drops to values below the 200K minimum limit of the QUANT. This situation occurs when the initial pressure of the gas in the pipeline is sufficiently high and the initial temperature of the gas is relatively low. This means that in order for QUANT software to be able to cover all linebreak events in high-pressure natural gas fully, its range of temperature coverage has to be extended to temperatures lower than the present minimum limit of 200K. Silberring (1993-95) and Flatt (1993-96) argued that the temperatures could never drop below the 200K limit.

The routine FLDPROPV calculates the fluid properties from the data file FLUID.DAT, using an interpolation procedure. When used with the transient analysis programmes problems were encountered due to the limited computer memory available. An alternative procedure in which the closest properties are used, produced satisfactory results. However the alternative procedure requires that a close spacing of the input parameter be used. A spacing of 0.1MPa and 5K was used for pressure and temperature respectively. A comparison of execution times when constant fluid properties were used and when the procedure described above was used, revealed that the biggest proportion of the execution time is spent in calculating the fluid properties from the data file generated by QUANT. As explained in Section 4.5, the procedure which is used in this study is the fastest option available.

## **INITIAL CONDITIONS BEFORE THE BREAK**

In all the analyses reported in this chapter, calculation of the initial conditions of the gas is greatly simplified by the fact that the initial flow velocity is zero. Any of the different steady state analysis models presented in Section 4.2.2 would have produced the same results. However, the non-adiabatic non-isothermal steady state analysis model is used.

Also since the flow velocity is zero, transient analysis before the break would produce the same results as those produced by steady state analysis. An application of the transient analysis before the break are presented in section 7.4.

## **CONDITIONS AT THE BREAK BOUNDARY**

The method of characteristics is used for solution at the boundary nodes, in all the transient analysis programmes. In the case of the break boundary the initial break conditions are calculated as described in Section 4.2.3. The initial conditions calculated, enabled results



which are numerically stable be attained. Using this procedure, the pressure at time  $t = 0$  drops to its equalisation value which is calculated as described in Section 4.2.3. The temperature drop is small at first but keeps on falling as time passes. Also the density of the gas drops during the decompression process. The speed of sound at the break remains the same at  $t=0s$ , but drops as the temperature drops. The pressure drop at the break boundary, below the equalisation pressure is natural. There is no time dependent curve such as the one used by Tiley (1989) to model the pressure drop at the broken end. The time dependent curve may lead to incorrect results because the exact rate of pressure drop is not known.

When using the MacCormack second-order method, solution at the node next to the boundary node produced an overshoot in the velocity. This has been controlled by limiting the magnitude of flow velocity from exceeding its corresponding speed of sound.

## **NUMERICAL METHODS OF SOLUTION**

### **(i) The Method of Characteristics**

Tiley (1989) used the second-order method because the first-order method did not meet the required accuracy and stability criteria. Even with the second-order method, she encountered problems of numerical instability and accuracy of results. For certain grid points and initial conditions, the solution became unstable at random points along the pipeline. She recommended that the problem could be alleviated totally by using an alternative numerical method. The same problems were encountered by Picard and bishnoi (1989). Flatt (1989) encountered similar problems which he called singularity. Problems such as those encountered by Flatt (1986) and Tiley (1989), do not exist with this model. A convergence tolerance of  $\pm 5\%$  and  $\pm 1\%$  is used for the first and second-order calculations, respectively. The number of iterations required is very small. In most calculations, one or two iterations for each order are sufficient. The fluid properties used for calculation of the coefficients of the three simultaneous equations, in the first-order step, are those at position M in Fig. 4.4. The use of the fluid properties at position M rather than those at positions Q, R and S was made in order to reduce the size of the programme. However, a significant error could be introduced due to this simplification, especially if the fluid properties vary considerably between two grid points, such as is the case in ruptured high-pressure natural gas pipelines. Since in this case the first-order method is used as a

rough estimate for the second-order calculation, the error introduced by the first-order calculation is corrected by the second-order method. In the case that only the first-order method is used for the complete solution, then values of the fluid properties at respective positions Q, R and S should be used in the first iteration, and their averages with values at position P for the previous iteration should be used in the subsequent iterations. For the second-order method, the fluid properties used to calculate the coefficients of the simultaneous equations are averages between the newly established position of Q, R and S and those previously calculated at position P.

It was observed in this study that in situations where there are sharp changes in the fluid properties, such as during the first few  $\Delta t$ 's in the region around the break, the second-order step fails numerically. For such cases, the first-order method is used throughout the calculation.

When the method of characteristics was used to model the flow reversal in the section of the pipeline downstream of the break, it produced results which tend to lean on the values at the intact end of the pipeline section. This directional bias results in a very slow pressure drop in the broken section of the pipeline, including the broken boundary. The problem of directional bias does not exist either in the programme based on the MacCormack method, nor the one based on the method of characteristics for the section of the pipeline upstream of the break. An investigation into the problem did not reveal any error in the calculation procedure or computer coding. In fact the values calculated at various stages are comparable in magnitude with those calculated by the programme for the pipeline section upstream of the break and the characteristic curves are positioned correctly. The problem of directional bias with the method of characteristics was observed only when the second-order approximation was used. Both the upstream and downstream models produce comparable results, when the first-order method is used.

It was observed that the second-order method of characteristics is more accurate than the first-order method, especially if the simulation involves the area in the vicinity of the break and very small grid size. The second-order method produces outputs which are beyond the range of maximum and minimum output around the leading edge of the of the decompression wave. This causes severe problems with the numerical algorithm. The situation is controlled by using the first-order approximation. The computer programme includes a provision to check if the condition is encountered and calls the programme for the first-order approximation to correct the situation. It was also observed that the use of



a smaller grid size helps to minimize the problem to some extent. Computation speed of the first-order method is over twice as fast as that of the second-order method. For some boundary conditions and initial conditions of the gas, the second-order method becomes slower. For example, when modelling the British Gas test BGT3 (initial pressure and temperature are 12.4MPa and 273K respectively and  $\Delta x=0.01\text{m}$ ), the second-order method was ten times slower than the first-order method. Also the second-order method failed to handle the choking boundary condition well. The first-order method was used in this case and produced satisfactory results. When a larger grid size ( $\Delta x=0.1\text{m}$ ) was used, the problem with the second-order method was minimal and computational speed was the same as with the other British Gas test data. The problem of modelling the choking condition was caused by the failure of the numerical procedure to model properly the temperature drop and therefore increase in density, which follows the initial decompression. The situation was corrected by tuning in the temperature drop and also increasing the convergence interval of the second-order method.

The major difference between the first- and second-order methods is that the pressure drops predicted by the second-order method are smaller than those predicted by the first-order method. Also the speed of propagation of the pressure waves is slightly faster with the first-order method. However, both results compare well with experimental data. The main reason for the discrepancy in the first- and second-order methods is the different convergence criteria used (1% and 5% for the first- and second-order methods respectively). The two values were selected, firstly because they are thought to correspond with relative accuracies of the two methods, and secondly because the first-order method is also used as a rough approximation of the second-order method. Ideally, a more accurate criterion should be used if the first-order method is used on its own to calculate the final solution. However, it is thought that a value which is smaller than 5% would not be too fine in relative to the overall accuracy of the first-order approximation. Unfortunately, the pressure wave propagation speeds of the two methods could not be compared at further positions from the broken boundary and for a longer run time. A comparison of the predicted mass flow rates and pressure at the intact end, using the first- and second-order methods and the Alberta Petroleum Industry data, shows a better agreement with the first-order method than with the second-order method. This result was achieved even though a finer grid spacing was used with the second order method. An explanation for the discrepancy is given under the general discussion.



## **(ii) The MacCormack Second-order Method**

Beauchemin and Marche (1992) concluded that the MacCormack method is superior to the method of characteristics when  $C_n$  differs appreciably from unity. When  $C_n$  is much smaller than unity, the MacCormack method produces results with a precision that could not be attained with any reasonable number of computation nodes, when the method of the characteristic is used. They also concluded that the use of the alternatives 1 and 2 which are described in Section 3.3.1, in succession on time steps could introduce significant oscillations in the solution, especially where the basic equations are poorly approximated. Directional bias could be avoided by using exclusively one of the two calculation alternatives. The directional bias is important only when working with two space dimensions, in which case it was recommended that the average of both methods (alternative 3) be used. Beauchemin and Marche (1992) claimed that doing so did seem to smear the shock slightly and the computation time was doubled.

In this study the computer programme is written in a way that any of the three alternatives could be used. This is despite the fact that it is recommended in Section 3.3.1 that alternative 1 be used exclusively. Results from the three alternatives are presented in Fig. 6.12, 6.13 and 6.14, for British Gas BGT2. Due to limited computer memory, only the first-order calculation of the method of characteristics could be used at the boundary points, when using alternative 3. The MacCormack method is extremely simple to programme, compared with the method of characteristics. The execution speed of the MacCormack method is faster than that of the method of characteristics. But in this case, where the time used to calculate the fluid properties from the QUANT software constitutes the biggest proportion of the CPU time, the two methods have execution speeds which do not differ much. The same argument applies for the difference which is to be expected between alternative 3 and the other two alternatives of the MacCormack method.

It is stated in Section 3.2.2.2 that in the presence of shocks, explicit finite-difference methods of higher than first order produce considerable overshoot and oscillatory systems. Results obtained from the MacCormack method are oscillatory especially near the broken end. The oscillations are more severe for smaller  $L/D$  values. Also an overshoot was observed in the flow velocity, at the node next to the boundary node at the break. The overshoot was controlled by limiting the magnitude of the flow velocity to that of the corresponding speed of sound. These problems were not encountered with the method of



characteristics. With the MacCormack method the problem of directional bias which was encountered with the method of characteristics, in the section of the pipeline down stream the break, does not exist.

The three alternatives of using the MacCormack method were compared using the British Gas test BGT2 data. Results are presented in Figs. 6.12, 6.13 and 6.14. Alternatives 1 and 3 produced similar results. Alternative 2 produced the worst results, with much bigger oscillations and pressures falling fastest. The computation speed of alternative 1 is higher than that of alternative 3.

### **(iii) The Warming -Kutler - Lomax Method**

The computer programme for the Warming-Kutler-Lomax method was written and compiled successfully, but it could not run fully because of the limited computer memory. Even in the main frame computer, the memory of 20MB which was allocated is not enough. In order to simplify the programme, the method of characteristics was used both for the boundary node and the node next to the boundary. Bhallamudi and Chaudhry (1990) recommended that the MacCormack second-order method be used for solution at the node next to the boundary node. Even this did not make it possible to run the programme on a pc. However, by using constant values for the thermodynamic and transport properties of the fluid, it was possible to run the programme for the third-order Warming-Kutler-Lomax method on a PENTIUM P75 pc.

The method failed to produce good results in the region of sharp changes in fluid properties. Results produced in this region included negative velocities (while all other velocities were positive) and pressures which are higher than the initial pressure before the break. The first-order method of characteristics was used to smoothen the sharp edge of the decompression wave, and also the flow velocity and pressure were limited to above zero and within the initial pressure before the break. The British Gas test BGT3, whose run time is 35ms, was used to test the Warming-Kutler-Lomax method. The first-order method of characteristics was used during the first 10ms, but this was not enough to smoothen the sharp edge of the pressure profile so that the Warming-Kutler-Lomax method could be applied. Finally the initial 20ms of the run time were found to be sufficient, for "smoothing" by the method of characteristics and the Warming-Kutler-Lomax method was used for the remaining 15ms. Under this condition, good and stable results were obtained. No oscillations or overshoot, such as those observed with the MacCormack method were

present. Results produced with the Warming-Kutler-Lomax method are compared with those produced by the second-order method of characteristics, the MacCormack method and experimental data. The results are presented in Figs. 6.16 to 6.19.

#### **(iv) Comparison of the Different Numerical Methods**

The transient analysis models based on the method of characteristics, the MacCormack method and the Warming-Kutler-Lomax method are compared based on accuracy, stability of results and computational economy. The main reason for including the MacCormack and Warming-Kutler-Lomax methods in this study was to confirm whether the two methods are suitable for modelling the transient flow following a break in high-pressure gas pipelines. The literature review which was conducted during this study and summarized in Chapter 3, indicated that these methods could be more suitable for high-pressure gas linebreak applications than the method of characteristics. Tiley (1989) used the second-order method of characteristics, but concluded that better results could be obtained by using an alternative numerical method of solution. In a previous publication [Thorley and Tiley (1987)], the MacCormack method was recommended as the most suitable for linebreak problems.

Based on the comparison made in this study, it is concluded that the method of characteristics is the best of all the three methods investigated, for linebreak applications. The criteria used in comparing the three models is accuracy and stability of results, computer memory and CPU time requirements. The third-order Warming-Kutler-Lomax method, in combination with the method of characteristics, produced results which are close to those produced by the second-order method of characteristics. The computer memory requirement of the latter method was too big. The MacCormack method was found to be unsuitable for modelling transient flow following a linebreak in high-pressure natural gas pipelines. It produced oscillating results in the low pressure region, which resulted in p-t curves crossing each other. It predicts the wave speeds reasonably well in the low pressure region, but it underestimates it in the high pressure region. The magnitude of equalization pressure is slightly higher than that calculated with the method of characteristics. The computation speed of the MacCormack method is one and a half times faster than that of the second-order method of characteristics, when the first or second alternatives are used. When the third alternative is used, the computation speed of the MacCormack method is the same as that of the second order-method of characteristics.



## GRID SIZE

The factor of two which is used between one grid spacing and the next, and the second-order polynomial interpolation using the Taylor's theorem, produce good results. A problem was encountered with the variable grid method, when modelling the flow in long pipelines. The round-off error of the computer results in some node points whose next time level for calculation has not been reached, being included in the calculations.

The error occurs because of the big difference between the grid spacing at the break boundary and nodes which are nearer to the intact end. Even when a value of  $\Delta x = 1\text{m}$  is used at the broken end, for a pipeline which is 11.8km long ( $\Delta x = 512\text{m}$  at the intact end), the error still affects the programme. Although this error does not seem to affect the pressure predictions much, it has a significant negative effect on the flow velocity predictions. In some cases negative velocities are obtained at some internal boundaries between different grid sizes, while the rest of the velocities are positive. The net effect is an underestimation of the magnitudes of the flow velocity. An example of a case where this error affected the prediction results is shown in Fig 6.23. For simulations involving shorter pipelines, this error does not affect the programme and the variable grid model produces good results.

A bigger grid spacing, of  $\Delta x = 10\text{m}$  at the break, was used for the SNGSO data. Simulation results are presented in Figs. 6.23 to 6.25. The computer round-off error did not cause serious problems in the solution. The first-order method of characteristics was used. The biggest grid size (at the intact end) was  $\Delta x = 320\text{m}$ . Better results than those produced with the second-order method and  $\Delta x = 1\text{m}$ , at the break, were obtained. With the first-order method and the bigger grid spacing, the equalization pressure reached the ambient value within a few tens of milliseconds, while with the second-order method and the smaller grid spacing, ambient pressure was not reached during the 25s run time. This illustrated the significance of the grid size on the predicted decompression behaviour. This is one of the parameters which were investigated in this study. It was observed that for tests in which the positions of the transducers were very close to the broken end, such as the British Gas tests, a finer grid size was required. For tests in which the transducers are positioned further away from the broken end, such as the Foothills tests a coarser grid size produced sufficiently accurate results. A grid size of 0.1m at the broken end was adequate for the Foothills tests, where most transducers were positioned tens of metres away from the break. For the British Gas tests, where the transducers were positioned within two metres away from the broken end, a grid spacing of 0.1m was not adequate. As seen in

Fig. 6.21, the wave speeds produced by the grid spacings of 0.01 and 0.1m are almost the same. However, Figs. 6.17 to 6.19 show that the time taken for the pressure to start falling is longer when a smaller grid spacing is used. With test where the results are required thousands of metres away from the break,  $\Delta x$  values of up to 10m, at the broken end, produced satisfactory results. This was the case even for the Alberta Petroleum Industry tests, where the mass flow rate was calculated at a position which is 1m away from the break.

A simple rule of thumb is recommended for selection of grid sizes. If the result is required at a position which is a few metres away from the break and/or the length of the pipe section is less than 100m long, a value of  $\Delta x$  ranging between 0.01 and 0.1 should be used. If the result is required at a position which is tens of metres away from the break and/or the pipe is hundreds of metres long, a value of  $\Delta x$  ranging between 0.1 and 1.0m should be used. For longer pipe sections and/or if the result is required further than 100m away from the break, values of  $\Delta x$  of up to 10m could be used.

## **EXPERIMENTAL DATA**

All the experimental data used to validate the computer model were available in the form of printed graphs. The data was converted into a numerical form in order to enable plotting of the predicted results together with the experimental data on the same graph. In order to simplify the conversion of the data and also to minimize errors, the graphs were scanned and the necessary coordinates required to reproduce the graphs were read using the Autocad graphics software. The accuracy of the data obtained is just as good as that of the original graphs.

## **PRESSURE**

Both the method of characteristics and the MacCormack method predict the pressure following a break reasonably well. With the MacCormack method predictions, the pressure flattened faster than with the method of characteristics. This is because of the higher speeds of sound which are obtained from the MacCormack method predictions. Unlike with the MacCormack method, the method of characteristics results are not oscillatory and a consistent pattern is maintained, whereby the pressure decreases as the broken boundary is approached and for any particular position in the pipeline it decreases with time.

The pressure plateau which was demonstrated by Jones and Gough (1981), signifying the two-phase region, was not observed. The reason is that the QUANT



software data does not produce output for the liquid phase and for the transition region from liquid to gas phases.

## TEMPERATURE

Temperature variations in a gas undergoing decompression from a high-pressure pipeline, is one of the parameters which has not been studied much. Experimental data for temperature variations is very scarce and none were obtained for validation of the computer model.

It is obvious that the temperature drops after the pipeline breaks. There is a debate over the uncertainty which exists regarding the relative magnitude of maximum temperature drops resulting from high-pressure pipeline breaks. Richardson (1993-96) argues that the temperature drop could be as high as 50K at the break. In this study temperatures fell to below the 200K minimum limit of output for the QUANT software (drops of up to 100K) in the region near the break, when the method of characteristics was used. With the MacCormack method, the temperature drops were much lower. Flatt (1993-96) and Silberring (1993-95) argue that the temperature drop could not be that big and should not fall below the minimum limit of the QUANT software.

The temperature drops predicted using the method of characteristics are much higher than those predicted using the MacCormack method. In some cases the temperatures fell below 200K when using the method of characteristics, but stayed well above 200K when using the MacCormack method. For the same initial conditions of the gas, the temperature drop was higher when pipes of smaller  $L/d$  were used. Also in some cases, for example the Foothills test NABTF7, the temperature at the broken boundary fell below 200K just when the break condition was introduced i.e.  $t = 0s$ . It was not possible to know exactly what the temperature was, in cases where it fell below 200K. For such cases, the value of 200K was used for temperature and the values at the 200K temperature were used for the other fluid properties required from the QUANT software. An error would be introduced in the calculation especially in the heat transfer. However, the error introduced is small because the pressure in such situations is low and therefore variations in temperature would cause a small variations in the thermodynamic and transport properties of the gas.

## **FLOW VELOCITY**

The flow velocity at the broken end at time  $t = 0$ s after the break is equal to the speed of sound before the break. The flow velocity at the break falls as the speed of sound falls when flow is choked ( $M_a = 1$ ) according to the choking condition  $|u| = a$ . When the pressure at the broken end falls to ambient pressure, the choking condition no longer exists and the magnitude of the flow velocity will be lower than the speed of sound. The flow in this low pressure regime is not investigated because of the long time required for the condition to be attained and the limited time which is available to test the model.

The flow velocity predicted using the MacCormack method is higher than that predicted using the method of characteristics. Also when using the former method, the flow velocity increases faster and spreads out faster than with the latter method. As a result, the velocity gradient is much less with the MacCormack method than with the method of characteristics.

## **FLUID DENSITY**

After the break, the density of the fluid falls in a similar manner as the pressure but by a lesser proportion. With the MacCormack method density predictions are lower than those predicted using the method of characteristics.

## **PRESSURE WAVES PROPAGATION SPEED**

The value of the speed of sound in the fluid ( $a$ ), at the break, remains the same at  $t = 0$ s as it was before the break (Refer to Fig. 4.3). Due to the temperature drop which continues to take place thereafter, the density of the fluid at the break increases slightly. The increase in density results in a drop in the speed of sound, according to equation (A-11), and hence a drop in the flow velocity according to the choking condition  $|u| = a$ . Since the drop in pressure is higher in proportion than the drop in density, the speed of sound drops as the pressure drops. This pattern is transmitted towards the intact end of the pipe as time goes on and is less rapid away from the break and as time passes.

The predicted output of " $a$ " differs significantly from the pressure wave speeds presented in experimental data. However, the predicted output values of " $a$ " compare well with those presented in other data such as the additional data provided by Silberring (1995) and the data presented by Straty (1974) and Tsumura and Straty (1977). The reason for



the discrepancy between experimental wave speeds and predicted values of "a" is that the values of the speed of sound measured in the experiments is not surprising. The value given in experimental data is the speed at which a pressure wave propagates in the fluid i.e. it is calculated by measuring the time it takes for a particular pressure wave to travel from one known position to another known position in the pipe. The values of "a", which are calculated using equation (A-11), refer to the leading edge of the pressure wave front. This will be faster than a mean value calculated from the p-t curves. The pressure wave speed is influenced by both the values of a and u as explained by the theory of characteristics in Section 4.3.1. The value of the pressure wave propagation speed calculated from the p-t curves resulting from the computer simulation were compared with experimental data for the Foothills NABTF1 and NABTF7 tests, the BMI tests and the University of Calgary test. The results are presented in Figs. 6.5, 6.7, 6.20 and 6.21. Only the method of characteristics and the MacCormack methods were used. It could be seen from the graphs that apart from the University of Calgary test, the method of characteristics produces results which are very close to the experimental data. The wave speeds calculated using the second-order method of characteristics are slightly lower than those calculated using the first-order method. The MacCormack method underestimates the wave speeds at higher pressures and produces values which are slightly higher than experimental value at lower pressures.

Data which was obtained using the second-order method of characteristics for the Foothills NABTF7 test could not be used for validation because a wrong value was used for the initial density. The wave speeds obtained were very much lower than the experimental values. A finer grid spacing  $\Delta x=0.01\text{m}$  was used for the University of Calgary test, in an attempt to obtain a better agreement with experimental data. The result obtained is almost the same as with the grid spacing of  $\Delta x=0.1\text{m}$ . It has been confirmed that further reduction of the grid spacings would not produce more accurate results. Also since the computer model has produced good results for all the other tests, it is believed that the discrepancy between the two sets of data in the University of Calgary test is caused by experimental error.

## COMPUTING RESOURCES

The biggest constraint, as far as the computer memory requirement and computation speed are concerned, was introduced when non-constant fluid property data were used. Initially,

the programmes were run with constant fluid property data, which were obtained from the QUANT software. Even though the basic equations are used almost without any simplifications, the computation was very fast. The introduction of varying fluid data greatly reduced the computation speed.

In situations where the initial pressure before the break is low and temperature output is not required, the use of constant fluid property data will greatly increase the computation speed while maintaining a reasonably good accuracy of results. When the programmes were run in this manner, it was possible to use a 486 pc with a RAM memory of 8MB. When varying fluid property data was used the 486 pc could not cope and a PENTIUM P75 was sufficient to run all the programmes based on the method of characteristic and the MacCormack method. The programmes based on the third-order Warming-Kutler-Lomax method was successfully compiled but could not run on the PENTIUM pc because of insufficient memory.

The problem of insufficient memory could be solved by either using a bigger pc or a mainframe computer. The UNIX based C++ compilers run the programmes which are using pc based Borland C++ (in this case Version 2.1) compilers with very few alterations, namely adding an "include file" `stdlib.h` and changing the commands in the "system()" statements to correspond with those used by the UNIX operating system.

A user memory of 20MB on the mainframe computer could only perform as well as the 486 pc. Even by using the "temporary" directory in the mainframe computer, which should have more capacity available, did not improve the situation. The remaining options are therefore to use either a more powerful pc than PENTIUM P75 or the mainframe computer with more memory allocation than the present 20MB. Computation speed of the pc could be increased by installing a chip similar to the Microway-i860 which is being used at present on a 286 pc, at the Imperial College [Richardson (1993-96)].

## **DISCUSSION OF ERRORS**

Three main categories of error in validating computer models for linebreak analysis, with experimental data were discussed by Tiley (1989). The three categories are

- (i) Calibration, measurement and recording of experimental data.
- (ii) Assumptions and simplifications made in the basic theoretical equations.
- (iii) Errors inherent in the numerical modelling procedure.



The error in experimental data also includes the error in converting graphical data into numerical data. Regarding the error in performing the experiments and recording experimental data, the best one could do is obtain an estimate of the error so that it could be accounted for in the simulation. No error estimate was provided with the experimental data. Even the rupture time was not provided and in some cases not all parameters required by the computer model e.g. gas composition, pipe material etc were provided. Through private communication with British Gas, Tiley (1989) was informed that the pressure measuring system as a whole, in the British Gas tests was believed to be within 5%. The error in converting experimental data which is provided in graphical form into numerical data has been reduced significantly by employing the scanning techniques and Autocad. With this procedure, the accuracy of the results is as good as those of the computer software used, which is much better than using a manual technique such as the one which was used by Tiley. Tiley (1989) quoted an accuracy of  $\pm 0.01$  and 5m/s for pressure ratio and wave speed respectively.

The error due to assumptions and simplifications in the theoretical model has greatly been minimized in this model, compared with Tiley's. This model still contains some simplifications such as one-dimensional flow, single-phase flow, non-elastic pipe, no fluid structure interaction and neglecting minor losses. However, the error introduced by these assumptions should be minimal since in this study, only straight horizontal pipes with constant cross-section area have been used. The error due to inaccurate fluid properties has also been minimized by using the QUANT software for thermodynamic and transport properties of fluids. There still remains some possible error in calculating the fluid properties due to the limitations of the QUANT software. These have been discussed under the discussion of the QUANT software. The error is significant in simulations where the initial gas pressure exceeds 5 to 6MPa and temperatures after the break fall below the 200K minimum limit of QUANT. The errors in estimating the friction factor and heat transfer have been minimized by using flow dependent values, which are specific for each calculation step. Tiley assumed that the friction factor and Stanton number (used to calculate heat transfer) were constant along the length of the pipe.

The errors inherent in the numerical modelling procedure include smearing, when a fixed grid is used; round-off error in case of iterative methods; and computer round-off error. Tiley (1989) argued that the smearing error is minimized by using a smaller grid size, while the round-off error is increased by reducing the grid size. There seems to be a contradiction in this argument and the whole idea of using a fine grid spacing. The round-off error of iterative methods depends on a predetermined accuracy criteria (as long as the

solution converges) rather than the grid size. In the model developed in this study, an accuracy of 5% and 1% was specified for the first- and second-order methods of characteristics. It has been observed in this study that interpolation error is not necessarily reduced by using higher-order approximations. In actual fact, approximations of higher order than one produce wrong results for rapidly varying flows. first-order approximation has proved to be the most popular in modelling transient flow following linebreak in high-pressure gas pipelines. Tiley's model contained an additional error because of the method used to obtain the final result at the required positions along the length of the pipe. The method used by Tiley was to approximate the result to the values at the nearest grid point. Such approximation could introduce a very big error in the solution, especially if the position concerned is close to the broken boundary and in the early time regime where the fluid properties vary rapidly. The approximation could also introduce significant error at positions far from the break because of the bigger grid size. In the model developed during this study, linear interpolation is used to calculate the final result at the required positions.

It is not possible to establish the magnitude of the accuracy of the computer model developed in this study, with certainty, because of the poor quality of the experimental data which has been used for validation. However, in most cases the predicted results are in good agreement with the experimental data used.



## **CHAPTER 7**

### **CASE STUDY: THE SONGO SONGO-DAR ES SALAAM NATURAL GAS PIPELINE**

#### **7.1 A BRIEF OVERVIEW OF TANZANIA'S ENERGY SECTOR**

The United Republic of Tanzania is located on the Eastern Coast of Africa, just south of the Equator. The country has a total area of 945000 square kilometres, 6% of which is covered by water. Nearly half of the land is covered by forest reserves, which explains the great overdependence of Tanzania on woodfuel as a source of energy. The present population of Tanzania is about 29 million, with a population growth of 2.55% per annum. Dar es Salaam is the capital of Tanzania and its population is about 5% of the total population. The economy of Tanzania is predominantly agricultural. Other economic activities include manufacturing and processing industries, mining and tourism. Most of the industries are concentrated in urban centres and in particular Dar es Salaam.

Tanzania's indigenous energy resources are large and diverse, although they have not yet been exploited to an appreciable extent. At present, the major energy sources are woodfuel, imported petroleum, hydroelectricity and indigenous coal. Tanzania's hydroelectric power potential is in excess of 4700MW of installed capacity, but only about 10% of it has actually been developed. Coal reserves are estimated at about 1900 million tonnes, of which 304 million tonnes are considered proven. Exploration activities for petroleum based fuels have taken place in Tanzania for several decades, with the resulting discovery of natural gas. No oil discoveries have been made yet and exploration is still under way, with prospects of finding more natural gas and possibly oil. The proven natural gas resource is 20.7 million tonnes oil equivalent (toe), but it is estimated to increase to 47 million toe.

The total energy consumption in Tanzania in 1990 was just over 17 million tonnes of oil equivalent (toe) which came from woodfuel (88.5%), biomass (6%), electricity (0.6%), imported crude oil and refined petroleum products (5%) and coal (0.1%). More than 70% of Tanzania's electricity is generated from hydropower. In the past six years, Tanzania's electricity demand has been growing at an average of 12% per annum. The present electricity demand is estimated at 400MW, but the demand is suppressed due to the shortage of generation capacity. The demand is estimated to double by the turn of this

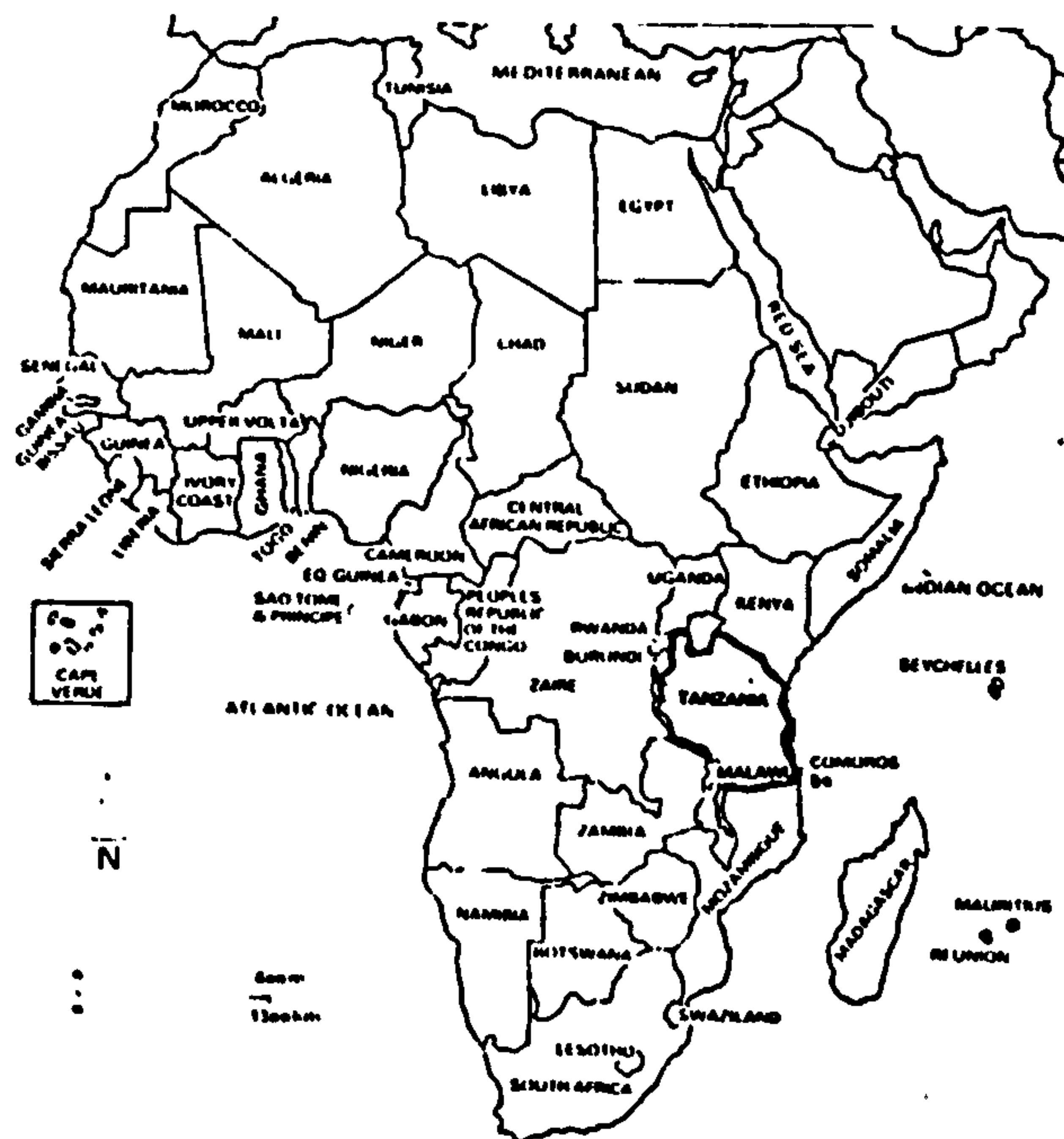


Fig. 7.1 Map of Africa Showing the Location of Tanzania

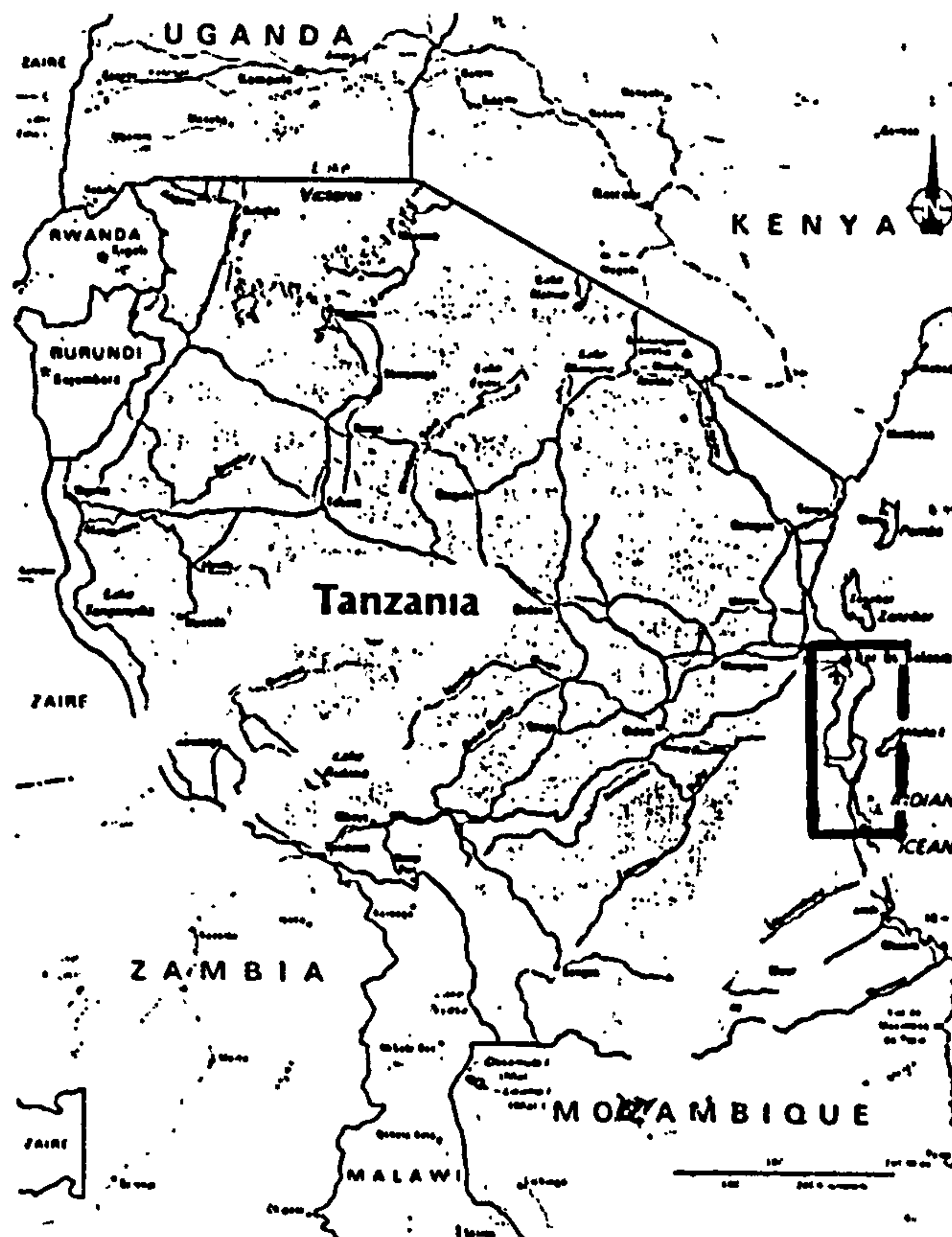


Fig. 7.2 Map of Tanzania Indicating the Location of the Songo Songo Gas Development Project



century. A twenty five year (1985-2010) investment and development programme was set. The programme is aimed at reducing dependence on hydropower and cutting the oil import bill that consumes about 60% of the country's foreign currency earnings each year. During the early years of the 1990's, Tanzania suffered serious power problems, as a result of prolonged drought which reduced water levels in the reservoirs of hydropower plants. Power rationing had to be imposed and as a result industrial production fell drastically and people had to change their lifestyles to adjust to the situation.

The Tanzanian government is implementing an Emergency Power Project (EPP). A 40MW diesel powered plant has been commissioned in Dar es Salaam. Electricity from the plant, which could also use natural gas as a fuel, is linked to the national power grid thereby boosting its output. On the longer term, there are other projects including the construction of a 200MW hydropower plant at Kihansi, development of the coal resource and the Songo Songo Natural Gas Development Project, which is the focus of this study. The project is described in detail in Section 7.2.

## **7.2 DESCRIPTION OF THE SONGO SONGO GAS DEVELOPMENT PROJECT**

### **7.2.1 BACKGROUND INFORMATION**

Natural gas was discovered at Songo Songo, which is a tiny island off the Tanzanian coast, in the Indian ocean south of Dar es Salaam, in 1974. Apart from the Songo Songo gas reserve, there are other smaller reserves, including one at Mnazi Bay. The discovery was followed by proving between 1976 and 1983 and subsequent pre-feasibility and feasibility studies. Several options for developing the resource were considered, including export of the gas to earn foreign exchange, production of ammonia and urea fertilizer and uses in the domestic markets. The latter option includes power generation; pipeline to local markets; and fertilizer, methanol and compressed natural gas facilities. It was considered that, although the gas pool was large, it was not large enough to warrant the development of a major compressed natural gas export facility. The remaining options are being implemented and in addition, there are plans to export some of the gas to neighbouring Kenya.

The Songo Songo Gas Development Project features development of five existing gas wells, of which three are offshore and two are onshore; tying these wells to a central

gas processing plant in Songo Songo island; constructing a pipeline (25km marine and 207km onshore) to transport the gas to Dar es Salaam; building a 60MW power plant in Dar es Salaam to generate electricity; and supplying gas to the 40MW dual fuel power plant described in Section 7.1, which is already operational in Dar es Salaam and also to other users. Another, but different, project is being implemented for the Mnazi Bay reserve.

The Songo Songo project is being implemented jointly by the Ministry of Water Energy and Minerals, which plays a coordinating role for all stake holders in the project; Ocelot Tanzania Inc.; and TransCanada Pipelines Limited. The Tanzania Petroleum Development Corporation (TPDC) is a partner in the project and the Tanzania Electric Supply Company (TANESCO) will be the major consumer of the gas. The project is anticipated to be in service in 1997.

## **7.2.2 GAS PROPERTIES**

Natural gas is found naturally in rock reservoirs below the ground. In its pure state (methane) it is a non-toxic, colourless and odourless gas. Methane is lighter than air. The Songo Songo gas is almost pure natural gas, containing no sulphur compounds and only small amounts of heavy hydrocarbons. Only minimal processing is required to make the gas suitable for pipeline transport and subsequent application by the end users.

The Songo Songo gas field underlies Songo Songo island. The proximity of the field Fig. 7.3 to the island is very convenient in that the shore based facilities can be located on the island and the wells drilled onshore or in very shallow water. Three wells have been drilled onshore and a further six have been drilled in the shallow waters around the island. The nine wells are named as SS1 to SS9. Five of the wells have proven reserves in various parts of the field structure. Of the remaining four wells, three have provided disappointing results in satellite structures and one did not reach the main reservoir objective as a result of blowout and fire.

The main area of the field has been appraised by the five wells which have proven the gas volumes in the main block i.e. wells SS3, SS4, SS5, SS7 and SS9. The reservoir fluid properties were determined in a study by Scientific Software-Intercomp (1990), for simulation purposes. The data includes the relevant physical properties of gas and water. A total of 21 analyses of samples obtained from wells SS5, SS7 and SS9 were conducted. The samples were very consistent in composition, exhibiting a high methane content of



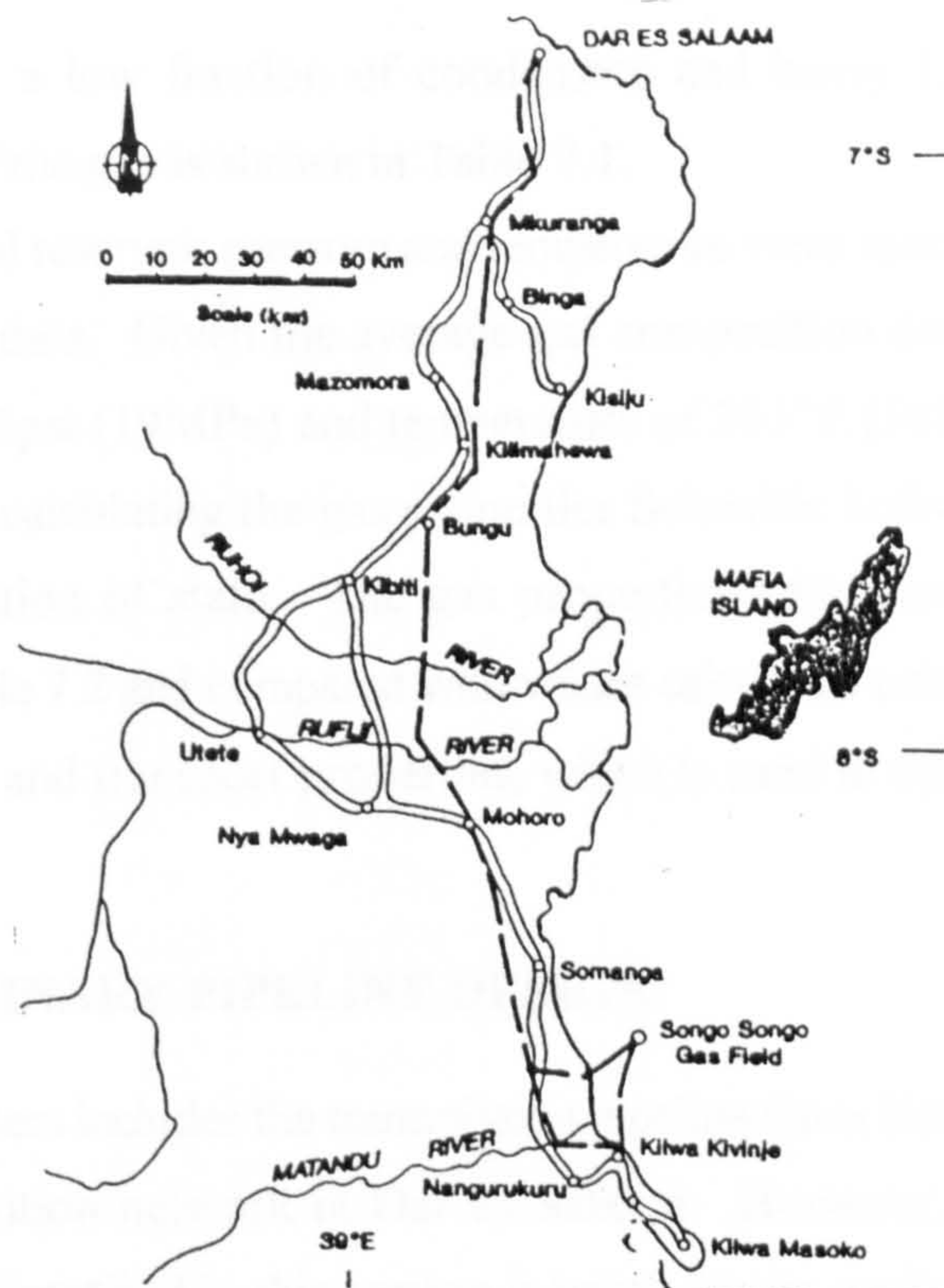


Fig. 7.3 Kilwa Kivinje-Dar es Salaam Gas Pipeline Location Map

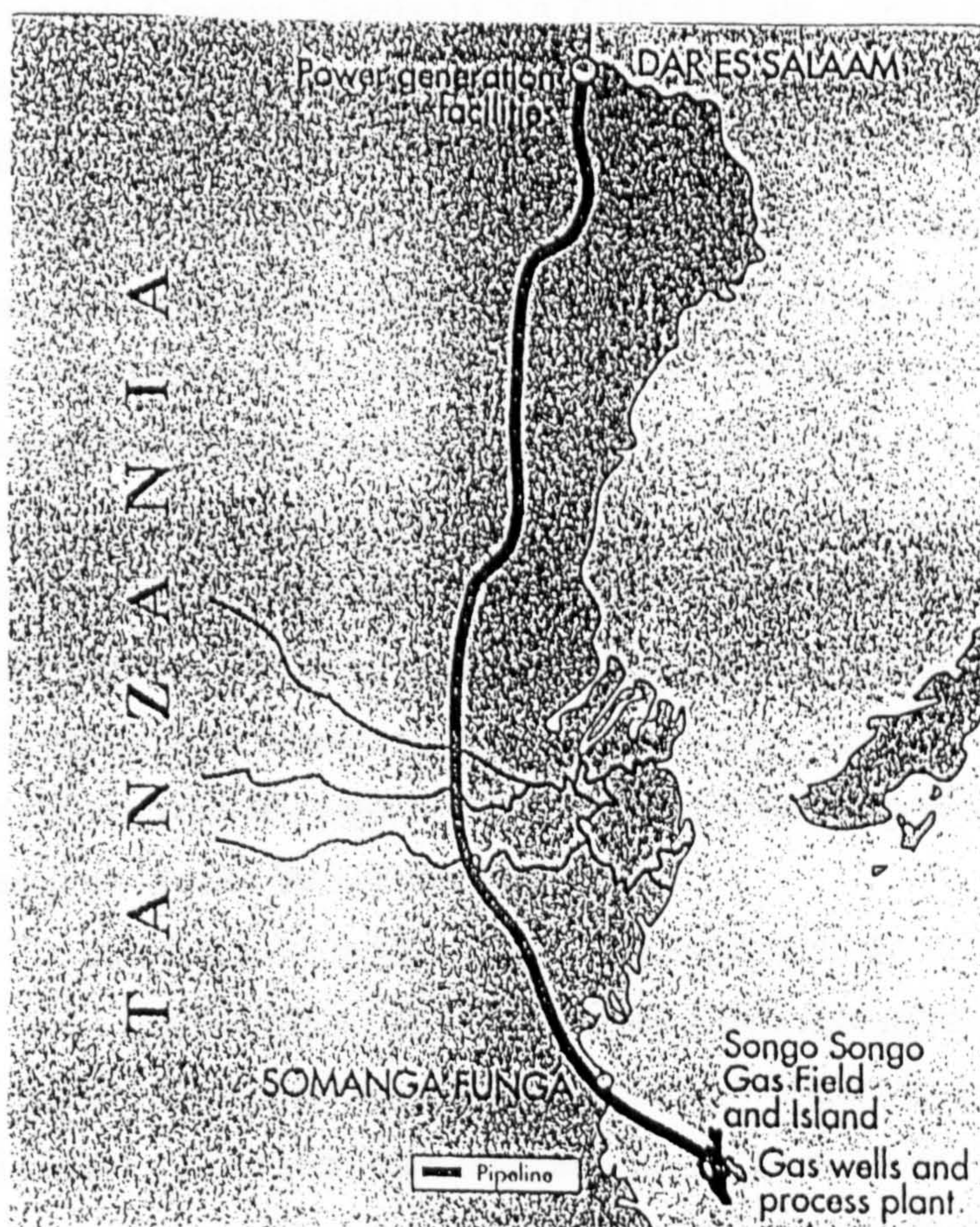


Fig. 7.4 Pipeline Route from Songo Songo Island to Dar es Salaam



about 97% and a low fraction of condensate and heavy hydrocarbons. The average compositions of the gas is shown in Table 7.1.

The initial reservoir pressure and temperature were specified in order to process the fluid properties data. Given the average gas composition data in Table 7.1 and reservoir pressure of 2755psi (19MPa) and temperature of 203°F (368K), the gas properties were determined. In calculating the gas properties Scientific Software-Intercomp (1990) used their own equation of state. The gas properties which are relevant to this study are presented in Table 7.2 and compared with values calculated using the QUANT software for thermodynamic and transport properties, which is used in this study.

### **7.2.3 PRELIMINARY PIPELINE DESIGN**

The pipeline system includes the transmission pipeline from Songo Songo to Dar es Salaam and the distribution network in Dar es Salaam. However, it should be noted that the pipeline design described in this section is based on the preliminary design done by Hardy BBT Ltd. (1989). The gas distribution system consists of a pipeline network which would deliver gas from the city gate station to each individual consumer. The design is in accordance with Canadian Standard CSA Z184.M Code. Three demand scenarios namely low, medium and high were considered. The three scenarios are based on a 20 year life time of the project and projections for power generation by TANESCO. The 20 year life time is based on the design of a fertilizer plant at Kilwa Masoko (refer to Fig. 7.3). According to the design, the proven gas reserve of 20.53bcm (726bcf) was to be drawn at a rate of 0.56bcm/year (19.75bcf/year), by the fertilizer plant, so that its allocation of 11.18bcm (395bcf) is consumed in 20 years. The operation of the gas gathering facilities, dehydration plant and marine pipeline to Kilwa Kivinje was to be under one management to supply gas to the fertilizer plant and the Dar es Salaam pipeline. Therefore, since the Dar es Salaam pipeline was to be dependent on the fertilizer plant operating, all design and economic studies were based on a 20 years of operation only. However, in the likely event that the proven reserves were to be enlarged as production proceeded, the pipeline was sized based on growth through the year 2016.

The design based conditions were a pressure of 101kPa (14.65psig), a temperature of 15°C and a specific gravity of 0.60. The maximum allowable operating pressures were set at 7.93MPa for the low demand scenario and 9.65MPa for both the medium and high demand scenarios. The maximum allowable gas temperature is 49°C, while the maximum design gas temperature was set at 38°C. The design gas volume took into consideration



the average and the peak flow requirements to the year 2016. The projected gas demands under the three scenarios for the years 2011 and 2016 are presented in Table 7.3.

GAS	SS9	SS5	SS7	MEAN	ISM NO.	HFS VAR
N2	0.860	0.68	0.600	0.713	0.000	0.000
CO2	0.47	0.350	0.290	0.370	0.000	0.000
CH4	96.820	97.193	97.440	97.151	0.000	0.000
C2H6	1.050	1.100	0.940	1.030	0.000	0.000
C3H8	0.320	0.300	0.310	0.310	0.000	0.000
i-C4H10	0.070	0.070	0.073	0.070	1.000	0.000
n-C4H10	0.090	0.089	0.088	0.089	2.000	0.000
i-C5H12	0.030	0.025	0.028	0.027	1.000	0.000
n-C5H12	0.030	0.026	0.030	0.029	2.000	0.000
C6H14	0.040	0.030	0.025	0.032	1.000	0.000
C7H16	0.150	0.075	0.100	0.109	1.000	0.000
C8H18	0.060	0.044	0.053	0.052	1.000	0.000
C9H20	0.010	0.018	0.023	0.017	1.000	0.000
TOTAL	100.000	100.000	100.000	100.000	-	-

Source of Gas Composition Data: Scientific Software-Intercomp [1990]

Table 7.1 Average [Mol. %] Composition of Songo Songo Gas

Pipe sizes and flow capacity of the pipeline were determined using the Panhandle formula, which considers gas pressure, temperature and velocity. Steel, plastic and aluminium were all considered as possible materials for construction of the pipeline. However, it was later decided that only a steel pipe would be able to carry the volumes and pressures required for the transmission line. The gas velocities in the pipeline, for each scenario and pipe size, were estimated as shown in Table 7.4. The pipe sizes allow fluctuations which may occur between the peak day demand and the average flow, and the expected velocities are well below the target velocity for the pipeline design. In this particular case flow velocities of 457m/min and 610m/min were given as target and maximum velocities respectively.

Property	SSI
Initial Pressure [psia]	2755
Reservoir Temperature [°F] [K]	203
Molecular weight	16.746
Specific Gravity	0.579
Density (Reservoir) [lb/ft <sup>3</sup> ] [Kg/m <sup>3</sup> ]	7.1007
Density (Surface) [lb/ft <sup>3</sup> ] [Kg/m <sup>3</sup> ]	0.0441
Viscosity (reservoir) [cp]	0.018
Compressibility [psi <sup>-1</sup> ]	3.45x10 <sup>-4</sup>

Source: Scientific Software-Intercomp (1990)

Table 7.2 Songosongo Gas Properties

Pipe sizes were chosen for the three scenarios, based on the initial pressure of 4.80MPa available at Kilwa Kivinje and a minimum terminal pressure of 2.07MPa (300psig) at the city gate station in Dar es Salaam. For both the medium and high demand scenarios, compression must be added at Kilwa Kivinje. The selected pipe sizes, compressor and resulting capacity are summarized in Table 7.5.

DEMAND	AVERAGE DAILY DEMAND		PEAK DAILY DEMAND [MCM]	
	YEAR 2011	YEAR 2016	YEAR 2011	YEAR 2016
LOW	0.56	0.68	0.7	0.85
MEDIUM	1.21	1.33	2.37	2.49
HIGH	2.31	2.43	3.47	5.59

Source: Hardy BBT Ltd (1989)

Table 7.3 Projected gas demand for three scenarios for year 2011 and 2016

Predicted pressure profiles for the line for all the three scenarios are presented in Figs. 7.5, 7.6 and 7.7. For each scenario there are three curves representing maximum sustainable flow consistent with a discharge pressure of 2.07MPa (300psig), design flow rate similar to maximum average daily demands for the three scenarios and flow rate of 70% of the above design flow rate. The distribution system is comparatively small so that while it serves to smooth out local variations in demand, it can not be considered as a major component of storage. The major storage in this case is provided by on-line storage in the transmission pipeline.

SCENARIO	VELOCITY		NOMINAL PIPE SIZE	
	[m/s]	[ft/min]	[mm]	[in]
LOW	198	650	254	10
MEDIUM	235	770	254	10
HIGH	256	840	305	12

Source: Hardy BBT Ltd (1989)

Table 7.4: Estimated Gas Velocities and Pipe Sizes

Three block valve locations were proposed in the preliminary pipeline design. These would permit each section of the transmission line between the valves to be isolated and blown down during repair, maintenance or in an emergency situation. Operation of the block valves would be in the manual mode. Automatic linebreak control was not considered in the preliminary design. It was suggested that additional block valves could be added to the system during the final stage of the project depending on operational considerations. The three block valve locations are presented in Fig. 7.7. The



sectionalizing block will be full-bore valves in order to facilitate pigging of the line. The blowdown valves will be sized to deplete the line section in less than 4 hours. The block valve parameters and blowdown time for each of the three demand scenarios are summarized in Table 7.6. However, it was not specified to which of the pipeline sections in Fig. 7.7 or demand scenarios the blowdown times in Table 7.6 refer.

Demand Scenario	Pipe size Actual size x Wall thickness [mm]	Pressure [MPa]	Compressor Size [MW]	Capacity Flow [MCM/day]
Low	273.1x4.78	-	-	0.78
Medium	273.1x5.20	9.65	2.16	1.83
High	323.9x6.35	9.65	3.39	2.85

Source: Hardy BBT Ltd (1989)

Table 7.5 Pipe Parameters

The original design of the pipeline, as presented by Hardy BBT Ltd. (1989), was for the pipeline to pass through Kilwa Kivinje and also to be tied to the project for the fertilizer plant at Kilwa Masoko. Recent information, including a brochure published by the Ministry of Water, Energy and Minerals and the two Canadian companies involved in the implementation of the project, indicate that a new pipeline route is being followed. The new route is shown in Fig. 7.4. According to the new route, the pipeline is from Songo Songo directly to Dar es Salaam, through Somanga Funga and not Kilwa Kivinje. The new pipeline route does not seem to be tied to any other project apart from the power station and other users in Dar es Salaam. Although it is expected that design details for the new route have been finalised, it was not possible to get them for this study. However, since the pipeline length does not differ much from the one in the proposed old route, and assuming that the gas demand scenarios in Dar es Salaam remain the same, the same data which was proposed for the old pipeline design is used.

DEMAND SCENARIO	Block Valve Size [mm]	Blowdown Stack [mm]	Blowdown Time [hours]
LOW	254	102	3.5
MEDIUM	254	102	4.0
HIGH	305	152	3.3

Source: Hardy BBT Ltd (198

Table 7.6 Block Valves

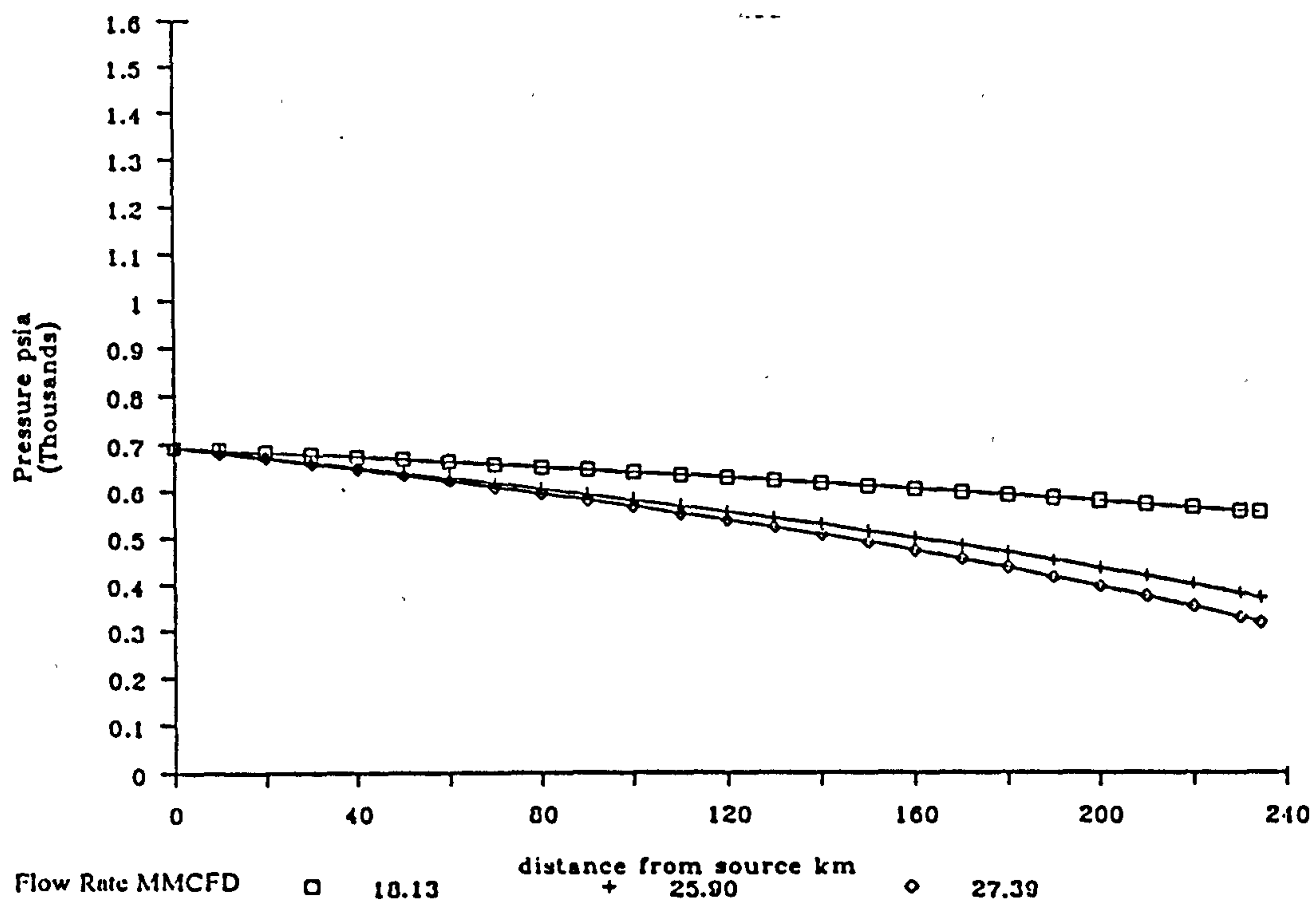
### **7.3 COMPUTER SIMULATION OF A LINEBREAK IN THE SONGO SONGO DAR ES SALAAM GAS PIPELINE**

In this section, the information and data presented in the preceding sections of this report and the computer model developed in this study are used to simulate a linebreak in the Songo Songo Dar es Salaam natural gas pipeline. It is known that a more recent study was conducted by Hardy BBT Limited in 1994, to assess the environmental impact of the pipeline. However, the study report could not be made available for this study. Also as pointed out in the previous section, no further details on the new pipeline route could be obtained. Due to these constraints, it was decided that the data given in the preliminary pipeline design by Hardy BBT Ltd. (1989), which are presented in Section 7.2.3, be used for this simulation exercise.

The main reasons for this analysis are firstly, to simulate the flow following a linebreak in the Songo Songo Dar es Salaam pipeline and secondly to test if the computer programme is capable of handling such a long pipeline as the pipe sections between the block valve location shown in Fig. 7.7 (73.2km). Pipelines are equipped with block valves at different locations along their lengths. The valves enable parts of the pipeline to be isolated for maintenance and in the event of a leak, blowdown or accidental rupture. The valve locations serve as boundary points when performing the computer analysis. Even in situations where such valves are not provided and the pipeline is considerably long, it is convenient to impose boundary conditions in such a way that the length of the pipeline between the boundary points could be handled with the computer programme.

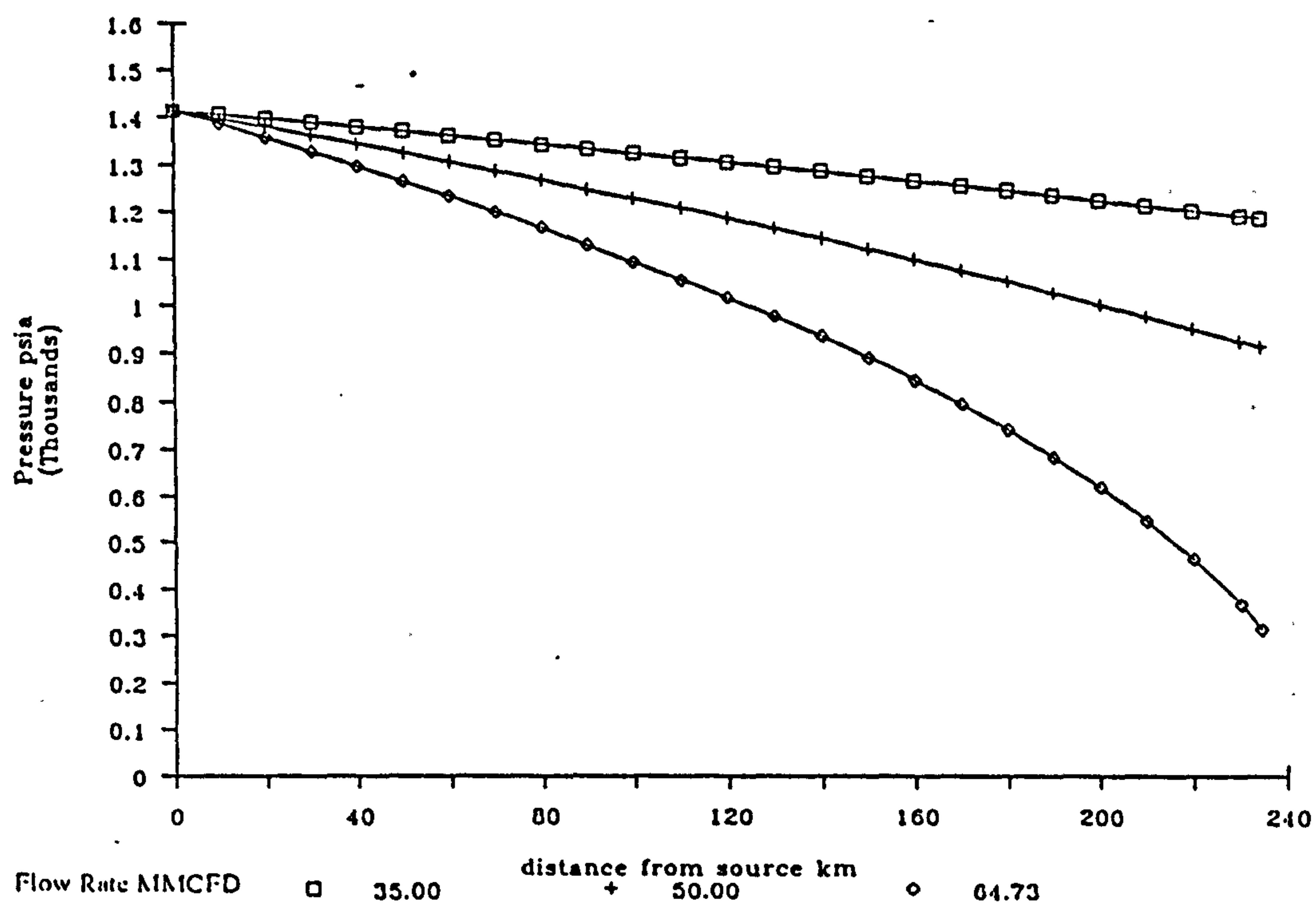
Two main parameters are of interest, namely the time it takes for a pressure wave to be transmitted from the break point to the nearest block valve location and the time taken for the section of the pipeline between the two valves on each side of the break to be emptied. The former parameter determines how quickly the valve operation would be initiated. The limited time available for this study does not permit simulation of the flow until all the gas has escaped from the pipeline, because of the very long CPU time required to carry out the simulation. The simulation is performed only for the early time regime. Referring to Fig. 7.7, it is assumed that a rupture occurs at Marendego, just next to the block valve, on the side of Kilwa Kivinje. The interest is to determine how long it takes for the initial pressure wave to reach Kilwa Kivinje, which is 68.0km away, and initiate the operation of a block valve situated at the exit of the compressor station. The high demand scenario and maximum sustainable flow (the bottom curve in Fig. 7.8) are used.





Source: Hardy BBT Ltd. (1989)

Fig. 7.5 Line Pressure Profile for Low Scenario



Source: Hardy BBT Ltd. (1989)

Fig. 7.6 Line Pressure Profile for Medium Scenario

The average composition of the Songo Songo gas, which is presented in Table 7.1, is used as input data to the QUANT software. A data file to be used by the CFD model is generated from the QUANT software. The initial pressure and mass flow rate of the gas at Kilwa Kivinje are as presented in Fig. 7.8 i.e. 1410psi (9.65MPa) and 100.79MMCFD (25kg/s). The maximum operating temperature of the gas is 311K. The rest of the gas properties at the initial conditions at Kilwa Kivinje are calculated using the QUANT software. A minimum grid spacing of  $\Delta x = 10\text{m}$  and  $\Delta t = 0.01\text{s}$  at the broken end and the variable grid model are used. This rather coarse grid spacing is chosen in order to minimise the CPU time required for the simulation and also to minimise the effect of the computer round off error, which is explained in Section 6.3, when applying the variable grid model on long pipelines. Results from the computer simulation are presented in Figs. 7.9 and 7.10.

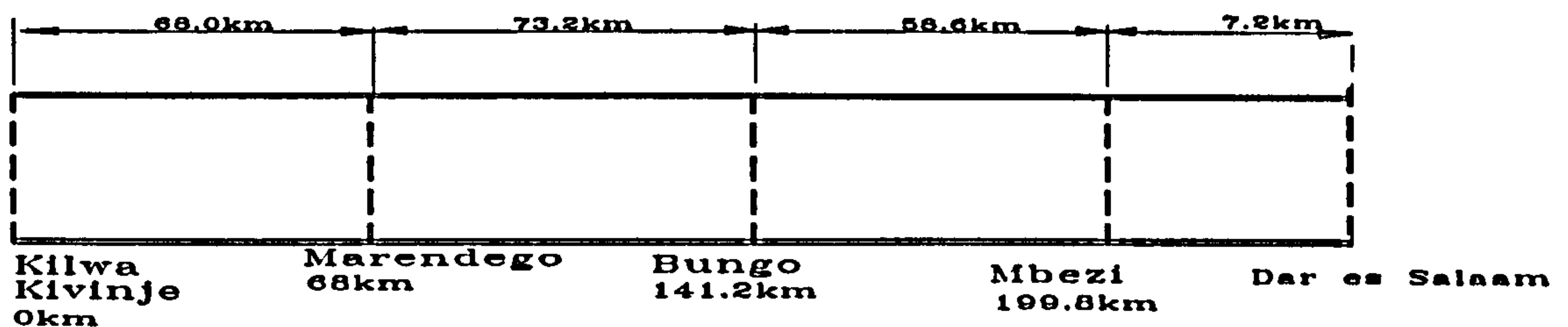


Fig. 7.7 Block Valve Location

The Hardy BBT prediction data which is presented in Figs. 7.8 are used for comparison with the data calculated using the non-isothermal non-adiabatic steady state analysis model presented in Section 4.2.2 and also the transient analysis, before the break, using the method of characteristics. The prediction results obtained are included in Figs. 7.8. All the rupture tests whose data are used, in Chapter 6, to validate the linebreak model were carried out using pipelines in which the gas was initially stationary. As a result of this situation, transient analysis before the break was not necessary. In the case of the Songo Songo-Dar es Salaam pipeline, the initial flow velocity before the break is not zero. Transient analysis before the break was performed in order to establish the initial unsteady flow condition. Results are presented in Fig. 7.8. In both the steady state and transient analyses before the rupture, the variable grid spacing programmes are used. The heat transfer model which was used is that for buried pipeline.



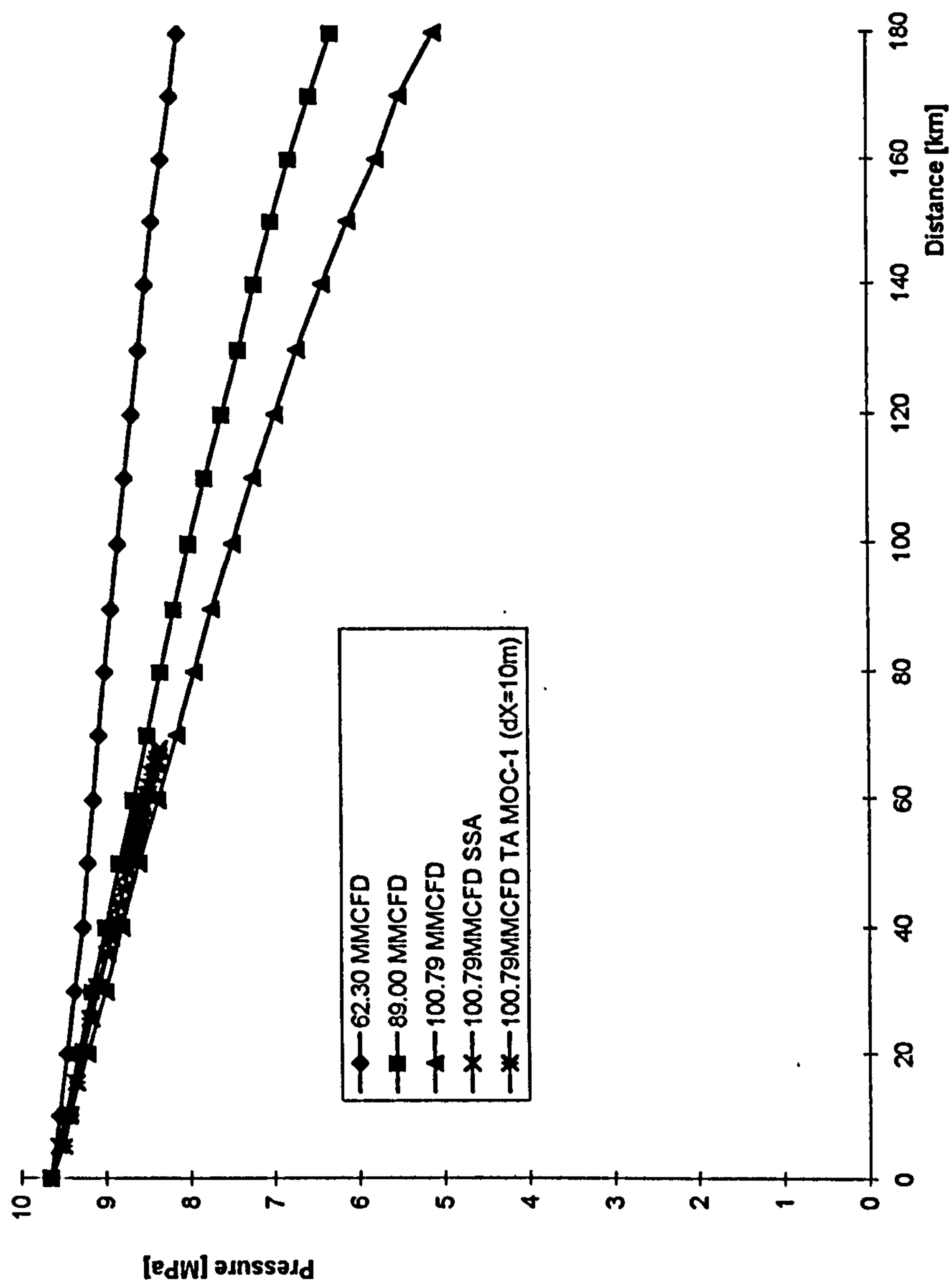
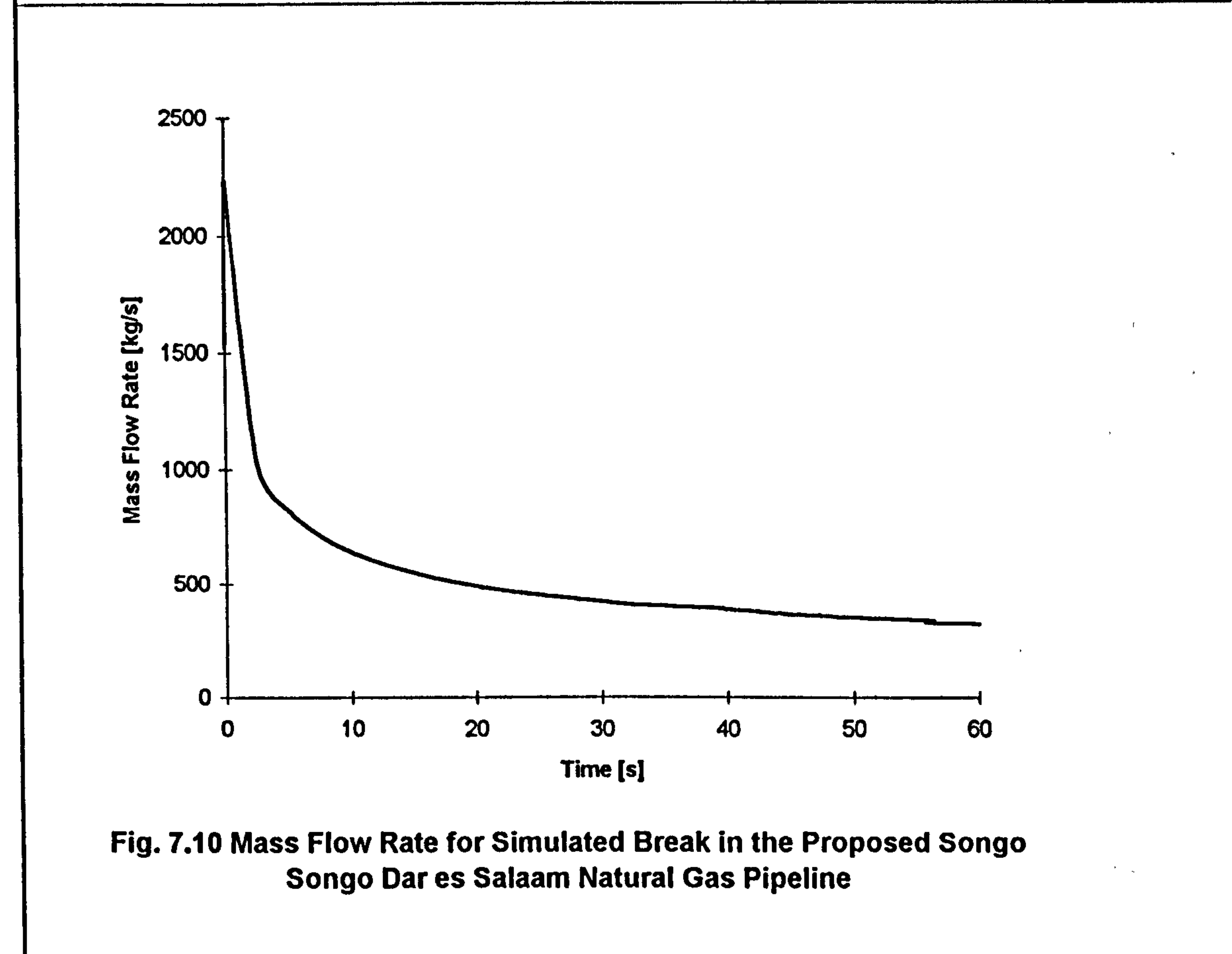
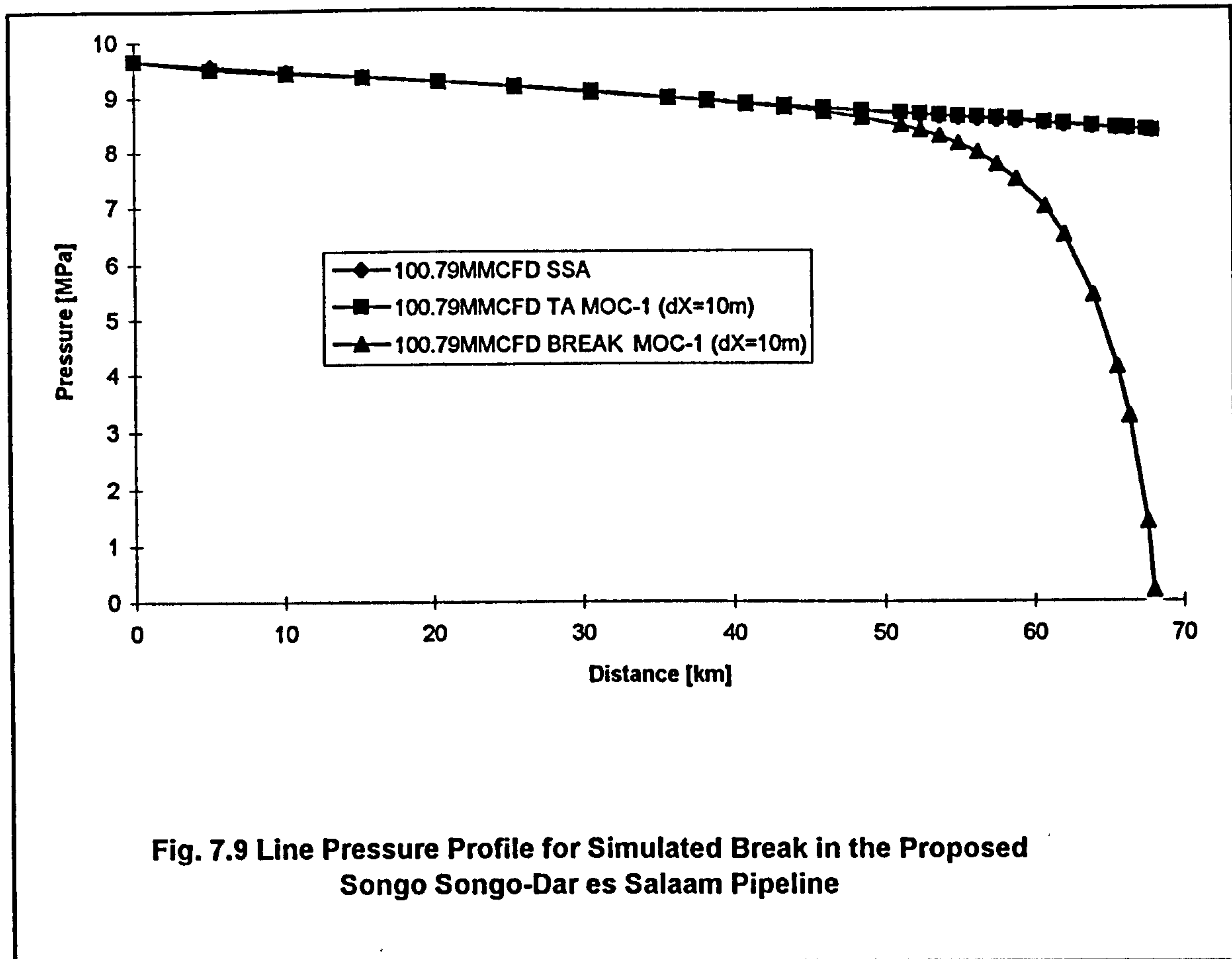


Fig. 7.8 Line Pressure Profile for High Scenario Comparison with Model Predictions





## 7.4 DISCUSSION OF SIMULATION RESULTS

Simulation results for the pressure profile using the steady state analysis (SSA) and transient analysis (TA) models before the break are presented in Fig. 7.8, together with the original data provided by Hardy BBT Ltd. (1989). The pressure profiles for steady state analysis and transient analysis before the break are also presented in Fig. 7.9, together with the pressure profile 60s after the break. The mass flow rate variation is presented in Fig. 7.10.

In calculating the pressure profile using the steady state analysis model problems were encountered when the pipe diameter of 0.305m, which was specified was used. Using this pipe diameter and gas flow rate of 25kg/s, which were given, resulted in a much bigger pressure drop in the pipeline. The pressure predicted at Marendego (68km from Kilwa Kivinje) was around 4MPa, which is less than a half of the pressure presented by Hardy BBT Ltd. Transient analysis using the second-order method of characteristics was performed, in order to confirm whether the problem was with the steady state analysis model or the design data provided by Hardy BBT Ltd. When a boundary condition corresponding with the pressure presented in the Hardy BBT curves (8.2MPa) was imposed negative velocities were obtained at the low pressure end. The negative velocities indicate that the pressure imposed at the boundary was higher than the actual pressure for the parameters given. The mass flow rate was reduced by a half in order to see if the pressure drop would decrease to the required value, but the pressure drop remained higher. When the pipe diameter was increased to 0.5m, the same pressure profile as that presented by Hardy BBT was obtained. Transient analysis was then performed and produced the same pressure profile as the steady state analysis. However, after the transient analysis, the flow velocity was slightly higher than that obtained using the steady state analysis model, but within the limit specified by Hardy BBT. This result indicates that the pipe diameter of 0.305m which was specified is too small. The first-order method of characteristics failed to produce good results in the transient analysis before the break. Consequently, the second-order method was used.

There was no output from the QUANT software for  $P_r$ ,  $\mu$  and  $k_f$  for all the range of pressure and temperature used. Of the three missing properties, only  $\mu$  is required by the computer programme. A constant value was used throughout the range of pressure and temperature encountered. In the fluid data used for validation of the model in Chapter 6, a maximum variation in  $\mu$  was 36.5% within the range of  $p$  and  $T$  used. The constant value was chosen such that it is in the middle of the range, therefore reducing the error in estimating  $\mu$  to a maximum of 18.25%. The error introduced is not significant.

The first-order method of characteristics was used in order to minimize on CPU time. The pressure profile after the break, which is shown in Fig. 7.9, indicates that the leading edge of the pressure wave had not reached the compressor station at Kilwa Kivinje 60s after the break. It had reached a position which is 43.52km from Kilwa Kivinje (24.48km from the break). Due to the limited time available for this study, no further simulations could be performed. The mass flow rate variation is presented in Fig. 7.10. The initial mass flow rate at time  $t=0$ s after the break is less than the peak flow rate. The increase in mass flow rate is caused by increase in the gas density, which occurs after the break because of drop in temperature. During the period of 60s which the flow was simulated, most of the rapid variations in gas outflow took place. The mass flow rate would continue to decay exponentially. The flow rate of around 300kg/s, which was reached after the 60s is comparable in magnitude with the initial flow rate in Alberta Petroleum Industry test APIT3. Assuming that the time taken for the pipe to be emptied is directly proportional to the length of the pipeline and that the flow rate would continue to fall at the same rate as in test APIT3, the time required for the section of the pipe to be emptied is 2.6hours. However, since the flow rate of 300kg/s, in this case is reached when the decay rate is much smaller than in the initial flow after the break in test APIT3, a blowdown time which is longer than 2.6hours is expected. Therefore the 3.3hours blowdown time presented by Hardy BBT Ltd is probably correct.



## CHAPTER 8

### RECOMMENDATIONS FOR FURTHER WORK

In the previous study by Tiley (1989), further work was recommended in four areas namely investigation of the wave speed error, further testing of the model, improvement of the stability of solution and further refinement of the model. Through the different approach which has been used in this model, all the four areas of investigation recommended by Tiley (1989), have been successfully covered. The method of characteristics model which has been developed in this study is sufficiently accurate and reliable for simulating linebreak situations in full-scale pipelines. The only weakness of the model is the directional bias which occurs when modelling the flow reversal in the section of the pipe downstream of the break. This is the only area recommended for further investigation in the model based on the method characteristics. In the meantime, the programme for analysing the flow in the section of the pipeline upstream of the rupture, could be used for the downstream section after the necessary adjustment of the input data. Alternatively, either the programmes based on the MacCormack or Warming-Kutler-Lomax methods could be used.

Two numerical models in addition to the method of characteristics, which is the only one covered by Tiley(1989), have been used in this study. Both the MacCormack and Warming-Kutler-Lomax models, have successfully been developed. What remains to be done is to test further the models. Specifically, the problems of overshoot and oscillating results, which are associated with the MacCormack numerical method, need to be investigated.

Another numerical problem which needs to be solved, is that of round-off error, when modelling flow in long pipelines using the variable grid spacing method and with very small  $\Delta x$  at the broken end.

The QUANT software, in its present version and with all its limitations, provides a sufficiently accurate and optimum means of incorporating real gas properties into the model. However, better results are expected if the current limitation of the software is overcome. The limitations are lack of output for some values of input parameters and for some gases and lack of output at high pressure and temperatures lower than 200K. The former limitation of lack of output at high pressures has already been overcome [Silberring (1993-95)]. But the version of the updated software is not yet available commercially. It is important to follow up on further updates of the software, which would improve the performance of the model.

A great deal of time was devoted to exploring, acquiring and developing an optimum method of incorporating the data produced by the software into the numerical programmes. The method adopted in this study [refer to Section 4.5] provides a compromise as far as accuracy and economy in computational resources are concerned. Two areas are recommended for further work in the application of the QUANT software. The first area is in relation to the routine DFGEN for generating the fluid property data file FLUID.DAT. A programme for automatic execution of the QDB programme of the QUANT software is required, in order to make the process simpler and less time consuming. A detailed explanation of this procedure is given in Section 6.3. The second area, which is also described in section 6.3, concerns the retrieval of data from the file FLUID.DAT. An interpolation procedure has proved to be impossible due to the limited computer memory, when running the transient analysis programmes. The alternative method i.e. generating fluid property data in which the input parameters (p & T) are so close such that the values which are closest to the parameters for which fluid data is required are used. The latter method is less practical with the presently available computing resources. In this study a spacing of 0.1MPa in pressure and 5K in temperature was used. A finer spacing could be used if the domain for the particular analysis is smaller. Further investigation of the possibility of using interpolation procedures is required especially if bigger computing resources are available.

The biggest challenge in developing and also applying the computer programmes in this study, has been that of limited computing resources available. It was decided from the beginning (refer to Section 4.6) that the computer codes developed in this study should be capable of being run on personal computers. The best computer which could be used was the best that was available at the time. But even this requirement could not be met due to limited financial resources which were available for acquiring such computers and also the high speed at which computer technology advances. At first it was thought that a 486DX personal computer would be sufficient. This was true even for the transient analysis including the variable grid method before varying fluid property data was introduced. A PENTIUM P75 is sufficient to run the complete programmes for transient analysis at a speed which is much faster than the one which could be achieved using the 486DX personal computer for the simpler version for the transient analysis programme i.e. with constant fluid property data. Better performance is expected if a more powerful pc such as a PENTIUM P166, is used. It is also thought that such a powerful pc's could



handle a larger number of grid points on one section of pipeline being modelled, than the present maximum number of grid points of around 120. This could eliminate the problem of round-off error experienced when modelling long pipelines with the variable grid programmes. It is therefore recommended that a more powerful pc than the PENTIUM P75 be used to test the programmes. Also the possibility of incorporating a chip similar to the Microway-i860 [refer to Section 4.6], into the present series of personal computers in order to increase their computational speed is worth exploring.

A detailed presentation of experimental data which exist for validating linebreak models is given in Chapter 5. Sufficient experimental data, which covers both short and long pipelines sections were acquired and used in this study. However, it was not possible to get data which are recent and consequently rather old data were used. The data which are used in this study were gathered using tests which were conducted during the past 16 to 20 years. It is expected that in such a long time, there would be a considerable improvement in instrumentation and experimental techniques which could result in more accurate experimental data. Some of the tests reported in Chapter 5, were carried out within the past two years. Data from such tests are therefore expected to be more accurate than the one used in this study and should if possible be used. Unfortunately, it was not possible to have access to this data because of commercial sensitivity.

The model developed in this study assumes that the fluid is a homogeneous gas mixture and that the flow is one-dimensional. These assumptions are adequate for practical linebreak modelling. Better results could be obtained if the simplifications of homogenous and one-dimensional flow are not used. In terms of priority, investigation into these aspects should come as the last step. In order of preference, multiphase effects including frictional forces are probably the most significant, and should be investigated first. The gamdeleps method [Flatt and Trichet (1995)] which is briefly described in section 2.7, is recommended.

## CHAPTER 9

# CONCLUSIONS

After a critical review of the previous study by Tiley (1989), a theoretical model has been developed for analysis of the transient flow following linebreak in high-pressure natural gas pipelines. An improvement has been made in many aspects of the model which was used by Tiley (1989). These include derivation of the basic equations of flow and subsequent simplifications; calculation of frictional force, thermodynamic and transport properties of the fluid, heat transfer to the fluid and numerical method of solution. The basic equations of flow are based on the gamma delta method which was developed by Flatt (1989). The three partial differential equations of flow are derived for unsteady quasi-one-dimensional flow of a real gas through a non-rigid non-constant cross-sectional area pipe. Two further simplifications are made on the basic equations of flow before applying them in the development of the computer model for analysis of the flow following a linebreak. The QUANT software for thermodynamic and transport properties of the fluids is used. The flow dependent explicit equation which was developed by Chen (1979) is used to calculate frictional force. The heat transfer through the pipe is calculated using a formula which is based on the adiabatic wall temperature and recovery factor. The heat transfer is also flow dependent; and the calculation procedure includes both pipes exposed to the atmosphere and buried pipes. An improved and more accurate equation for calculating the initial break conditions at the break is used. This improved equation avoids the problem of underestimating the flow velocity at the outlet end and overestimating the temperature drop at the break.

A non-uniform grid spacing which is very similar to that used by Tiley (1989) is used, in order to be able to handle long pipelines, to produce stable results and to also adequately model the physical behaviour of the gas, following a rupture. This method involves the use of a fine grid spacing in the vicinity of the break and a coarser spacing as one moves away from the break. A possibility of modelling the flow reversal in the section of the pipeline downstream of the break, similar to the one developed by Tiley (1989) is provided. Four different models for calculating the initial steady-state conditions, before the break have been developed. The four models, all of which are viscous flow models are based on the assumptions of incompressible flow and compressible isothermal, adiabatic or non-isothermal non-adiabatic flow. Three different numerical methods for solution of



the theoretical models have been developed. The three numerical methods are a first-order backward method, a first-order forward method and a second-order method. The numerical and theoretical models have been compared with predictions made for the proposed Songo Songo Dar es Salaam Natural Gas Pipeline [Hardy BBT Ltd.(1989)].

The theoretical transient analysis model is developed into a pc based computer code using the C programming language and three different numerical methods of solution. The three numerical methods are the method of characteristics, which was used by Tiley (1989); the two-step second-order explicit finite-difference method of MacCormack; and the third-order Warming-Kutler-Lomax explicit finite-difference method. Predictions using the three numerical methods of solution have been compared with data obtained through both full-scale pipeline and laboratory experiments. The test sections vary from 6.1m to 11.8km in length and 0.1 to 1.4m in diameter .

The transient analysis models, based on the method of characteristics, produce results which are in agreement with experimental data. Also the steady-state analysis models prediction are in good agreement with the predictions made for the Songo Songo Dar es Salaam pipeline. A PENTIUM P75 is just adequate to run the transient analysis programmes which are based on the method of characteristics and the second-order MacCormack method. The programmes based on the third-order Warming-Kutler-Lomax method require a computer with a greater capacity. They could be run on the PENTIUM P75 pc available, when constant fluid properties were used. The Warming-Kutler-Lomax method produced good results, when it was used in cooperation with the method of characteristics in order to smoothen the rapid variations the flow. The predictions which are made using the MacCormack method are not satisfactory (refer to section 6.3).

The QUANT software for thermodynamic and transport properties of fluids contains enough substances to cover all natural gas mixtures at pressure of up to around 6MPa and temperatures of 200K and above. In most high-pressure natural gas pipelines the pressures are much higher than 6MPa and during a linebreak the temperature of the gas near the break falls below the 200K lower limit of QUANT. Additional data were provided at high pressures, for the particular natural gas mixture used for validation. The present version of QUANT together with the additional data have successfully been incorporated with the numerical programmes. An updated version of the QUANT which covers the high-pressure zone was not available in time for this study. The optimum way of incorporating the QUANT software into the numerical programmes is by producing

data files for each particular gas mixture and range of parameter and using an interpolation procedure to obtain the fluid properties at each required state of the gas. Due to limitations in computer memory the interpolation procedure could not be used and instead the nearest data are used.

Sufficient and suitable experimental data were secured and used to validate the model. Both full-scale pipeline experimental data and data obtained from experiments on short pipeline sections of up to 243m have been used. All the data used were obtained from experiments carried out within the past 16 to 26 years. There is plenty of more recent experimental data but its availability for application in this study has proved to be too difficult.

It was stated in Section 1.3 that one of the objectives of this study was to investigate further the linebreak phenomenon, especially at the broken boundary in order to understand it better. The other objective was to develop a computer model for analysis of linebreak in high-pressure natural gas pipeline, based on the previous model which was developed by Tiley (1989). Both these objectives have been implemented satisfactorily. The theoretical decompression a-p curve Fig 4.3 at the broken boundary, has been confirmed by computer the predictions.

The computer model, which is based on the numerical method of characteristics, is very stable numerically, unlike the Tiley (1989) and Picard and Bishnoi (1989) model and also does not suffer singularity problems such as those experienced by Flatt (1986). Predictions from this model compare better with experimental results than the Tiley's model and the wave speeds are correctly estimated. The model developed in this study contains the additional feature of being able to model heat transfer for cases where the pipeline is buried under water, ground or any other medium whose thermal conductivity, and also the depth of the pipe in the medium are known. In addition to the method of characteristics model, computer models based on two other numerical methods have been developed. These two methods were not used by Tiley (1989). The model based on the MacCormack method does not seem to be suitable for high-pressure linebreak applications. The Warming-Kutler-Lomax method produces results which are comparable with the method of characteristics prediction. However, the former methods depends too much on the latter method, in order to be able to produces those results. Further testing of the models is necessary before making a definite judgement on the suitability and merits of each of these models.



It has been confirmed in this study that for typical high-pressure gas pipeline ruptures, the lowest gas temperature at the break could sometimes drop below the 200K minimum limit of the QUANT software. This is contrary to the argument by Silberring (1993-95) and Flatt (1993-96) that the temperature can never drop to such low values. The model based on the MacCormack method predicts lower temperature drops than the method of characteristics model. The former model also predicts higher flow velocities than the latter.

The comparison which was made between the first-order methods and the second-order method for solution of the steady-state flow equations reveals that the second-order method produces results which are significantly different and more accurate than the first-order methods. In this study the steady-state analysis results are used just as initial estimates, and are later improved by a transient analysis. Therefore the first-order backward method is sufficient. In cases where more accurate steady-state analysis results are required, the second-order method should be used. Comparison between the first-order and the second-order method of characteristics results indicate that the second-order method is significantly more accurate than the first-order method, only when the flow in the vicinity of the break is considered. However, the second-order method fails to handle the rapid variations of fluid properties at the initial  $\Delta t$ 's near the break. In such situations the first-order method is used.

A major weakness, which is yet to be explained, was discovered when the method of characteristics was used to model the flow reversal on the downstream section of the broken pipeline (negative flow velocity and  $x$  increasing away from the break). The model calculates accurately the fluid properties and the positions on the  $t$ - $x$  plane for the intersections of the characteristics curves with the time level  $t$  line (Refer to Fig. 4.4). However it produces results which always tend to be biased to the values at the intact end. This directional bias has the overall effect of predicting a decompression process which is extremely slow. No such problems were experienced with the other numerical methods.

The computer models for transient analysis have been validated with experimental data involving linebreak of pipelines which are as long as 11.8km. It has also been used to simulate the flow following a rupture in a pipeline which is 68km long. Due to the big difference between the grid spacings at the broken and the intact ends, the round off error of the computer results in a failure of the variable grid method to function properly. This error does not result in failure of the programme to run. But the model produces results which are wrong at some grid points. The net effect is to underestimate the flow velocity. For shorter pipe sections, such a problem does not exist.

Since the method of characteristics is iterative while the explicit finite-difference method are not, it is expected that the computation time of the method of characteristics would be much longer than those of the explicit finite-difference methods. In this study the method of characteristic and explicit finite-difference have computation speeds which do not differ much. The reasons for this situation are the extremely quick convergence of the method of characteristics model and comparatively long time taken to retrieve the variable thermodynamic and transport fluid data from the data file produced using the QUANT software.

The main sources of error in the model prediction and validation results include round off error of the computer and its related errors especially those caused on the variable grid method, which were explained earlier. More errors result from interpolation and also conversion of experimental data from graphical into numerical form. The latter error has been minimised by using the scanning technique and graphics Autocad software. The other errors are caused by the use of estimated fluid properties, and some other parameters such as gas composition, initial temperature etc. Estimated values were used because of lack of output from the QUANT software and also because some parameters necessary for the computer model are not provided with experimental data.

The previous model by Tiley (1989) had two major weaknesses, namely overestimating the wave speeds and instability if the solution. Both these weaknesses have been eliminated in this study. The method of characteristics, which was also used by Tiley has proved to be the most suitable numerical of solution for analysis of transient flow following linebreak in high-pressure gas pipelines. The first- and second-order methods produce results that are very close together, with the second-order method producing slightly lower wave speeds than the first-order method. The first-order method is over two times faster than the second-order method in computation speed and in some cases the former method handles the boundary conditions better than the latter method. At positions which are further away from the break, the first order method seems to produce better results than the second-order method. The first order method is therefore preferred if the results are required for positions which are further away from the break, and the analysis involves long pipelines. The first-order approximation has proved to a very important tool in modelling of transient flow following linebreak in high-pressure gas pipelines. It is the only numerical method, out of those studied, which can handle all the initial gas conditions, flow variation and grid sizes best. It produces sufficiently accurate results, with the least



computational resources. It therefore provides a practical method for simulating the flow in long pipelines. Except for the problem of directional bias in the second-order method of characteristics when modelling the flow in the section of the pipeline downstream of the break, this study has produced an accurate computer programme, based on the method of characteristics, for analysis of the flow following a break in high-pressure gas pipelines.

The MacCormack second-order method was previously thought of as being potentially better for linebreak problems than the method of characteristics. In contrast, this study has confirmed that the MacCormack method is completely unsuitable for modelling of the flow following linebreak in high-pressure gas pipelines. The third-order Warming-Kutler-Lomax method produces results which are comparable with those produced by the second order method of characteristics. However, it depends too much on the method of characteristics, to smoothen the rapid flow following a break. This makes one wonder whether the results are produced by the Warming-Kutler-Lomax method or the method of characteristics. Due to this over-dependence on the method of characteristics, it was not possible to determine the execution speed of the Warming-Kutler-Lomax method. It requires a lot more computer memory than the second-order method of characteristics.

## REFERENCES AND BIBLIOGRAPHY

- Adkins, C. J. (1983), "Equilibrium Thermodynamics", 3<sup>rd</sup> Edition, Cambridge University Press.
- Alberta Petroleum Industry Government Environmental Committee (1979), "Hydrogen Sulphide Isopleth Prediction-Phase II: Pipe Burst Study".
- Alberta Petroleum Industry Government Environmental Committee (1978), "Hydrogen Sulphide Isopleth Prediction-Phase I: Model Sensitivity Study".
- Allaire, P. E. (1985), "Basics of the Finite Element Method: Solid Mechanics, Heat Transfer and Fluid Mechanics", Wm. C. Brown Publishers, Dubuque, Iowa.
- Ames, W. F. (1977), "Numerical Methods for Partial Differential Equations", Second Edition, Academic Press, New York.
- Ansari, J. S. (1972), "Influence of Including Radial Flow on the Solution of Unsteady Pipe Flow Equations", Transactions of the ASME, Paper No. 72-FE-28.
- Arrison, N. L., Hancox, W. T., Sulatisky, M. T. (1977), "Blowdown of a Recirculating Loop With Heat Addition", IMECHE, C202/77, pp. 77-82.
- Bannister, F. K. and Mucklow, G. F. (1948), "Wave Action Following Sudden Release of Compressed Gas fro a Cylinder", Proc. IMECHE, 159, pp. 269.
- Batchelor, G. K. (1992), "An Introduction to Fluid Dynamics", Cambridge University Press.
- Beauchemin, P. and Marche, C. (1992), "Transients in Complex Closed-Conduit Systems: Second-Order Explicit Finite Difference Schemes", in Bettess, R. and Watts, J. (Ed.), "Unsteady Flow and Fluid Transients", A. A. Balkema, Rotterdam, pp. 31-39.
- Bhallamudi, M. S. and Chaudhry, M. H. (1990), "Analysis of Transients in Homogeneous Gas-Liquid Mixtures", in Thorley, A. R. D. (Ed.), "Pressure Surges: Proceedings of the 6<sup>th</sup> International Conference", BHRA, pp. 343-348.
- Bisgaard, C. Sørensen, H. H. and Spangenberg, S. (1987), "A Finite Element Method for Transient Compressible Flow in Pipelines", Int. J. Num. Meth. Fluids, 7, pp. 291-303.
- Bornstein, R. and Roth, W. A. (1920), "Landolt-Bornstein Physikalisch-Chemische Tabellen", Verlag von Julius Springer, Berlin.
- Botros, K. K., Jungowski, W. M. and Weiss, M. H. (1989), "Models and Methods of Simulating Gas Pipeline Blowdown", Can. J. Chem. Eng., 67, pp. 529-539.
- Boulos, P. F., Wood, D. J. and Funk, J. E. (1990), "A Comparison of Numerical and Exact Solution of Pressure Surge Analysis", in Thorley, A. R. D., (Ed.), "Pressure Surges- Proceedings of the 6th International Conference", BHRA, pp. 149-159.



Bratland, O. and Jensen, P. (1990), "Simulation Models of Pressure-Steps in Very Long Hoses or Pipes With Visco-Elastic Walls", in Thorley, A. R. D. (Ed.), "Pressure Surges: Proceedings of the 6<sup>th</sup> International Conference, BHRA, pp. 59-68.

Brown, F. T. (1969) "A Quasi Method of Characteristics With Application to Fluid Lines With Frequency-Dependent Wall Shear and Heat Transfer", Journal of Basic of Engineering Transactions of the ASME Series D, 91(2), pp. 217-227.

Budny, D. D., Wiggert, D. C. and Hatfield, F. J. (1990), "Energy Dissipation in the Axially-Coupled Model for Transient Flow", in Thorley, A. R. D. (Ed.), "Pressure Surges- Proceedings of the 6<sup>th</sup> International Conference", BHRA, pp. 15-26.

Chen, N. H. (1979), "An Explicit Equation for Friction Factor in Pipe", Ind. Eng. Chem. Fund. 18(3), pp. 296-297.

Chen, J. R., Richardson, S. M. and Saville, G. (1992), "Numerical Simulation of Full-Bore Ruptures of Pipelines Containing Perfect Gases", Trans. IChemE, 70(B), pp. 59-69.

Chen, J. R., Richardson, S. M. and Saville, G. (1993), "A Simplified Numerical Method for Two-Phase Pipe Flow", Trans. IChemE, 71(A), pp. 304-306.

Cheng, L. C. and Bowyer, J. M. (1978), "Tube-Transient Compressible Flow Code", in Papadakis, C. and Scarton, H. (Eds.), "Fluid Transients and Acoustics in the Power Industry", Proceedings of the Winter Annual Meeting of the American Society of Mechanical Engineers, pp. 31-35.

Courant, R. Isaacson, E. and Rees, M. (1952), "Communs. Pure Appl. Maths., 5, pp. 243.

Courant, R. and Friedrichs, K. O. (1948), "Supersonic Flow and Shock-Waves", Interscience Publishers.

Cronje, J. S., Bishnoi, P. R. and Svrcek, W. K. (1980), "The Application of the Characteristic Method to Shock Tube Data that Simulate a Gas Pipeline Rupture", Can. J. Chem. Eng., 58, pp. 289-294.

De Bakker, A. G. (1993), GASUNIE, The Netherlands, "Private Communication".

Dzung, L. S. (1944), "Beitrage zur Thermodynamik Realer Gase", Schweiz, Archiv Bd. 10, No. 11, pp. 305-313 (German).

Earnshaw, S. (1860), "On the Mathematical Theory of Sound", Phil. Trans., Royal Society, 150, pp. 133.

Eichinger, P. and Lein, G. (1992), "The Influence of Friction on Unsteady Pipe Flow", in Bettess, J. and Watts, J., "Unsteady Flow and Fluid Transients", Balkema, Rotterdam, pp. 41-50.

Fan, D. and Tijsseling, A. (1990), "Fluid Structure Interaction With Cavitation in Transient Pipe Flow", ASME J. Fl. Eng., 114(2), pp. 268-274.

- Fanneløp, T. K. and Ryhming, I. L. (1982), "Massive Release of Gas From Long Pipelines", *Journal of Energy*, 6(2), pp. 132-140.
- Fashbaugh, R. H. and Widawsky, A. (1972), "On the Difference Methods for Shock Wave Propagation in Variable Ducts Including Wall Friction", Naval Civil Engineering Laboratory, Port Hueneme, California/ASME.
- Feuer, A. (1982), "The Puzzle Book: Puzzles for the C Programming Language", Prentice-Hall.
- Flatt, R. (1985a), "A Singly-Iterative Second Order Method of Characteristics for Unsteady Compressible One-Dimensional Flows", *Communications in Applied Numerical Methods*, 1, pp. 269-274.
- Flatt, R. (1985b), "On the Application of Numerical Methods of Fluid Mechanics to the Dynamics of Real Gases", *Forschung im Ingenieurwesen*, 51(2), pp. 41-52, in German (English translation: British Gas Translation No. T07823/BG/LRS/LRST817/86).
- Flatt, R. (1986), "Unsteady Compressible Flow in Long Pipelines Following a Rupture", *Int. J. Num. Meth. Fluids*, 6, pp. 83-100.
- Flatt, R. (1989), "Unified Approach of Calculation of Monophase and Biphasic/Homogeneous Flows of Condensable Pure Fluids", *Entropie*, 149, pp. 48-55 (French).
- Flatt, R. (1993a), "Derivation of the Conservation Equations for Unsteady Quasi-One-Dimensional Flow of Real Gases Through Non-Rigid Non-Constant-Area Ducts", Swiss Federal Institute of Technology, Lausanne (unpublished).
- Flatt, R. (1993b), "The Basic Relation of the  $\gamma\delta$  Method", Swiss Federal Institute of Technology, Lausanne (unpublished).
- Flatt, R. (1993-1996), Swiss Federal Institute of Technology, Lausanne, "Private Communication".
- Flatt, R. and Trichet, J. C. (1995), "CFD Oriented Thermodynamics for Single and 2-Phase/Equilibrium Flows of Real Gases", *EUROMECH Colloquium 331: Flow With Phase Transition*, Gottingen.
- Foothills Pipe Lines (Yukon)Ltd (1981), "Final Report on the Test Program at the Northern Alberta Burst Test Facility", Report No. 18031.
- Gathmann, R. J., Hebeker, F. K. and Schöffel, S. (1991), "On the Numerical Simulation of Shock Waves in an Annular Crevice and its Implementation on the IBM ES/3090 with Vector Facility", in Brebbia, C. A., Howard, D. and Peters, A. (Eds.), "Application of Supercomputers in Engineering II", Computational Mechanics Publications and Elsevier Applied Science, London, pp. 319-330.



- Glaister, P. (1994), "An Efficient Shock-Capturing Algorithm for Compressible Flows in a Duct of Variable Cross-Section", *Int. J. Num. Meth. Fluids*, Vol. 18, pp. 107-122.
- Glass, I. I. (1958), "Shock Tubes-Part I: Theory and Performance of Simple Shock Tubes", *UTIA Review*, 2(I).
- Goldwater M. H. and Fincham, A. E (1981), "Modelling of Gas Supply Systems" in Nicholson, H. (Ed.), "Modelling of Dynamical Systems, Vol.2", IEE-Control Engineering Series 13.
- Govier, G. W. and Aziz, K. (1972), "Flow of Complex Mixtures in Pipes", van Nostrand Reinhold.
- Gradle, R. J. (1984) "Design of Gas Pipeline Blowdowns", *Energy Processing*, Jan-Feb.
- Groves, T. K., Bishnoi, P. R. and Wallbridge, J. E. (1978), "Decompression Wave Velocities in Natural Gases in Pipelines", *Can. J. Chem. Eng.*, 56, pp. 664-668.
- Groves, T. K. (1976), "Measured Velocity of Decompression Waves in Natural Gas in Pipelines", Foothills Pipelines (Yukon) Ltd.
- Guy, J. J. (1967), "Computation of Unsteady Gas Flow in Pipe Networks", *ICHEME Symposium Series*, 23, pp. 139-145.
- Hall, J. G. (1958), "Shock Tubes-Part II: Production of Strong Shock Waves; Shock Tube Applications, Design and Instrumentation", *UTIA Review*, 2(II).
- Haque, M. A., Richardson, S. M., Saville, G., Chamberlain, G. and Shirvill, L. (1992), "Blowdown of Pressure Vessels: II. Experimental Validation of Computer Model and Case Studies", *Trans. IChemE*, 70(B), pp. 10-17.
- Haque, M. A., Richardson, S. M. and Saville, G. (1992), "Blowdown of Pressure Vessels: I. Computer Model", *Trans. IChemE*, Vol. 70(B), pp. 3-9.
- Haque, M. A., Richardson, S. M., Saville, G. and Chamberlain, G. (1990), "Rapid Depressurization of Pressure Vessels", *J. Loss Prev. Process Ind.*, Vol. 3, pp. 4-7.
- Hardy BBT Ltd. (1989), "Kilwa Kivinje-Dar es Salaam Gas Pipeline Feasibility Study", Tanzania Petroleum Development Corporation, Project No. CG10305 (R).
- Hartree, D. R. (1964), "Numerical Analysis", Second Edition, Oxford University Press.
- Hirose, M. (1971), "Frequency-Dependent Wall Shear in Transient Fluid Flow: Simulation of Unsteady Turbulent Flow", MSc. Dissertation, Massachusetts Institute of Technology.
- Hoffmann, K. A. (1989), "Computational Fluid Dynamics for Engineers", Engineering Education Systems (EES), Texas.
- Holman, J. P. (1980), "Thermodynamic", Third Edition, McGraw-Hill, New York.

- Holt, M. (1984), "Numerical Methods in Fluid Dynamics", 2<sup>nd</sup> Edition, Springer-Verlag, Berlin.
- Huang, W. and Sloan, D. M. (1993), "A New Pseudospectral Method With Upwind Features", IMA Journal of Numerical Analysis, 13, pp. 413-430.
- Ilic, V. (1987), "Two-Phase Blowdown Through a Short Tube", in Dodge, F. T. and Moody, F. J., "Fluid Transients in Fluid-Structure Interaction-1987", FED, 56, ASME, pp. 87-92.
- IPS (1995.a), Dar es Salaam, 20<sup>th</sup> July.
- IPS (1995.b), Dar es Salaam, 27<sup>th</sup> Sept.
- Issa, R. I. (1970), "One-Dimensional Unsteady Compressible Flow With Friction and Heat Transfer", MSc Dissertation, Imperial College of Science and Technology, University of London.
- Jones, D. G. and Gough, D. W. (1981), "Rich Gas Decompression Behaviour in Pipelines", AGA-EPRG Linepipe Research Seminar IV, Duisburg, British Gas, Report No. ERS E 293.
- Kagawa, T., et al. (1983) " High Speed and Accurate Computing Method of Frequency-Dependent Friction in Laminar Pipe Flow for Characteristics Method", JSME, 49(447), pp. 26- 38 (Japanese).
- Kawabe, R. (1982), "An Analytical Method for Thermal-Hydraulic Transients in Piping Networks", Nucl. Eng. and Design, 73, pp. 441-446.
- Kay, W. B. (1936), "Density of Hydrocarbon Gases and Vapours", Ind. Eng. Chem., 28(9), pp. 1014-1019.
- Kernighan, B. W. and Ritchie, D. (1978), "The C Programming Language", Prentice-Hall.
- Kernighan, B. W. and Pike, R. (1984), "The Unix Programming Environment", Prentice-Hall.
- Kimambo, C. Z. M. (1987), "Energy in Tanzania", Paper Presented at a Seminar Organised by Development Education Centre, Energy for All Project, Cumbria, Feb. 1987.
- Kimambo, C. Z. M. and Thorley, A. (1995), "Computer Modelling of Transients Ruptured High Pressure Natural Gas Pipelines: A Review of Experimental and Numerical Studies", C502/003, IMECHE.
- Kiuchi, T. (1993), "An Implicit Method for Transient Flow in Pipe Networks", Paper Submitted for Publication.



- Knox, H. W., Atwell, L. D., Angle, R., Willoughby, R. and Dielwart, J. (1980), "Field Verification of Assumptions for Modelling Sour Gas Pipelines and Well Blowouts", Petroleum Society of CIM, Paper No. 80-31-46.
- Kunsch, J. P., Sjøen, K. and Fanneløp, T. K. (1991), "Loss Control by Subsea Barrier Valve for Offshore Gas Pipeline", 23<sup>rd</sup> Annual Offshore Technology Conference, Houston, Texas, OTC 6616.
- Kunsch, J. P., Sjøen, K. and Fanneløp, T. K. (1995), "Simulation of Unsteady Flow, Massive Releases and Blowdown of Long, High-Pressure Pipelines", 1995 International Gas Research Conference, Cannes, France.
- Kuo, S. S. (1972), "Computer Applications of Numerical Methods", Addison-Wesley, Reading.
- Lang, E. and Fanneløp, T. K. (1987), "Efficient Computation of the Pipeline Break Problem", in Dodge, F. T. and Moody, F. J. (Eds.), "Fluid Transient in Fluid-Structure Interaction", FED 56, ASME, pp. 115-123.
- Lang, E. (1991), "Gas Flow in Pipelines Following a Rupture Computed by a Spectral Method", J. Appl. Maths. and Physics (ZAMP), 42, pp. 183-197.
- Lapidus, L. and Pinder, G. F. (1982), "Numerical Solution of Partial Differential Equations in Science and Engineering", John Wiley and Sons, New York.
- Lavooij, C. S. W and Tijsseling, A. S. (1990), "Fluid Structure Interaction in Compliant Piping Systems", in Thorley, A. R. D. (Ed), "Pressure Surges-Proceedings of the 6<sup>th</sup> International Conference, BHRA, pp.85-100.
- Lax, P. and Wendroff, B. (1960), "Systems of Conservation Laws", Comm. Pure Appl. Math., 13, pp. 217-237.
- Lister, M. (1960), "The Numerical Solution of Hyperbolic Partial Differential Equations by the Method of Characteristics", in Ralston, A. and Wilf, H. S. (Eds.), "Mathematical Methods for Digital Computers", John Wiley & Sons, pp. 165-179.
- Lyczkowski, R. W., Grimesey, R. A. and Solbrig, C. W. (1978), "Pipe Blowdown Analyses Using Explicit Numerical Schemes", AIChE Symposium Series, 74 (14), pp. 129-140.
- MacCormack, R. (1971), "Numerical Solution of the Interaction of a Shock Wave with a Laminar Boundary Layer", in Holt, M. (Ed.), Lecture Notes in Physics, Vol. 8, Springer-Verlag, New York, pp. 151-163.
- MacCormick, S. F. [Ed.] (1987), "Multigrid Methods: Frontiers in Applied Mathematics", Society for Industrial and Applied Mathematics, Philadelphia, Pennsylvania.
- Mallinson, J. (1996), British Gas, Gas Research Centre, Loughborough, "Private Communication".

Martin, D. J. (1967), "Equations of State", *Ind. Eng. Chem.*, 59(12), pp. 34-52.

Mathers, W. G., Zuzak, W. W., McDonald, B. H. and Hancox, W. T. (1976), "On Finite Difference Solutions to the Transient Flow-Boiling Equations", *Committee on Safety of Nuclear Installations Specialists Meeting on Transient Two-Phase Flow*, Toronto, Ontario, Pergamon Press, pp. 278-315.

Meissner, L. P. and Organick, E. I. (1980), "FORTRAN 77: Featuring Structured Programming", Addison-Wesley Publishing Company, Reading.

Ministry of Water Energy and Minerals, Ocelot Tanzania Inc. and TransCanada Pipelines Ltd. (1994), "Songo Songo Gas Development Project", Brochure.

Ministry of Water Energy and Minerals (1990), "Energy Balance: Tanzania, 1990" Dar es Salaam.

Moe, R. and Bendiksen, K. H. (1993), "Transient Simulation of 2D and 3D Stratified and Intermittent Two-Phase Flows. PART I: Theory", *Int. J. Num. Meth. Fluids*, 16, pp. 461-487.

Monro, D. M. (1985), "FORTRAN 77", Edward Arnold Ltd, London.

Morrow, T. (1996), Southwest Research Institute, San Antonio, Texas, "Private Communication".

Münster, A. (1969), "Statistical Thermodynamics: Volume I", Springer-Verlag, Berlin.

Niessner, H. (1980), "Comparison of Different Numerical Methods for Calculating One Dimensional Unsteady Flows", *Lecture Series 1980-1, Lecture No. 16*, von Karman Institute for Fluid Dynamics, Sweden.

Ohmi, M., Kyomen, S., and Usui, T. (1985), "Numerical Analysis of Transient Turbulent Flow in a Liquid Line", *Bulletin of JSME*, Vol. 28, No. 239, pp. 799-806.

Oliemans, R. V. A. (1987), "Modelling of Two-Phase Flow of Gas and Condensate in Horizontal and Inclined Pipes", *Paper for Presentation at the 6<sup>th</sup> ASME Annual Pipeline Engineering Symposium*, Dallas.

Olorunmaiye, J. A. and Imide, N. E. (1993), "Computation of Natural Gas Pipeline Rupture Problems Using the Method of Characteristics", *J. Hazardous Materials*, 34, pp. 81-98.

Osiadacz, A. J. and Yedroudj, M. (1989), "A Comparison of a Finite Element Method and a Finite Difference Method for Transient Simulation of a Gas Pipeline", *Appl. Math. Modelling*, 13, pp 79-85.

Osiadacz, A. J (1987), "Simulation of Analysis of Gas Networks", Spon, London.

Otwell, R. S., Wiggert, D. C. and Hatfield, F. J. (1985), "The Effect of Elbow Restraint on Pressure Transients", *Journal of Fluids Engineering*, Vol. 107, No. 3, ASME.



- Padmanabhan, M., Ames, W. F. and Martin, C. S. (1978), "Numerical Analysis of Pressure Transients in Bubbly Two-Phase Mixtures by Explicit-Implicit Methods", *J. Eng. Maths.*, 12(1), pp. 83-93.
- Picard, D. J. and Bishnoi, P. R. (1988), "The Importance of Real-Fluid Behaviour and Nonisentropic Effects in Modelling Decompression Characteristics of Pipeline Fluids for Application in Ductile Fracture Propagation Analysis", *Can. J. Chem. Eng.*, 66, pp. 3-12.
- Picard, D. J. and Bishnoi, P. R. (1987), "Calculation of the Thermodynamic Sound Velocity in Two-Phase Multicomponent Fluids", *Int. J. Multiphase Flow*, 13(3), pp. 295-308.
- Picard, D. J. and Bishnoi, P. R. (1989), "The Importance of Real-Fluid Behaviour in Predicting Release Rates Resulting From High-Pressure Sour-Gas Pipeline Ruptures", *Can. J. Chem Eng.*, 67, pp. 3-9.
- Press, W. H., Teukolsky, S. A., Vetterling, W. T. and Flannery, B. P. (1992), "Numerical Recipes in C: The Art of Scientific Computing", Cambridge University Press, 2<sup>nd</sup> Edition.
- Rachford, H. H. Jr. and Dupont, T. (1974), "A Fast Highly Accurate Means of Modelling Transient Flow in Gas Pipeline Systems by Variational Methods", *Soc. Pet. Eng. J.*, 14, pp. 165-178.
- Rachford, H. H. Jr. (1972), "Transient Pipeline Calculations Improve Design", *Oil and Gas J.*, 70(44), pp. 54-57.
- Rachid, F. B. F. and Stuckenbruck, S. (1990), "Transients in Liquid and Structure in Viscoelastic Pipes", in Thorley, A. R. D. (Ed.), "Pressure Surges: Proceedings of the 6<sup>th</sup> International Conference, BHRA, pp. 69-84.
- Ralston, A. and Wilf, H. S. [Ed.] (1964), "Mathematical Methods for Digital computers", John Wiley & Sons, Inc., New York.
- Richardson, S. M. and Saville, G. (1991), "Blowdown of Pipelines", *Society of Petroleum Engineers*, SPE23070, pp. 369-377.
- Richardson, S. M. (1993-1996), Department of Chemical Engineering and Chemical Technology, Imperial College, London, "Private Communication".
- Richtmyer, R. D. (1957), "Difference Methods for Initial-Value Problems", *Interscience Tracts in Pure and Applied Mathematics*, Number 4, Interscience Publishers, Inc., New York, Chapter X.
- Rowlinson, J. S. and Watson, I. D. (1969), "The Prediction of Thermodynamic Properties of Fluids and Fluid mixtures-I: The Principle of Corresponding States and its Extensions", *Chem. Eng. Sc.*, 24, pp. 1565-1574.
- Ryhming I. L. (1987), "On the Expansion Wave Problem in a Long Pipe with Wall Friction", *ZAMP*, 38.

- Saad, M. A., (1985) "Compressible Fluid Flow", Prentice-Hall, Inc., Englewood Cliffs, New Jersey.
- Saville, G. and Szczepanski, R. (1982), "Methane-Based Equations of State for a Corresponding States Reference Substance", Chem. Eng. Sc., 37(5), pp. 719-725.
- Schildt, H. (1989), "ANSI C Made Easy", McGraw-Hill.
- Schmidt, F. W., Henderson, R. E. and Wolgemuth, C. H. (1984), "Introduction to Thermal Sciences: Thermodynamics, Fluid Dynamics, Heat Transfer", John Wiley & Sons.
- Scientific Software-Intercomp (1990), "Songo Songo Reservoir Study", Tanzania Petroleum Development Corporation.
- Sens, M., Jouve, P. and Pelletier, R. (1970), "Detection of a Break in a Gas Line", 11<sup>th</sup> International Gas Conference, Moscow, Paper No. IGU/C37-70, in French, (English Translation: British Gas, Translation No. BG. TRANS 4910).
- Shin, Y. W. (1978), "Two-Dimensional Fluid Transient Analysis by the Method of Characteristics", in Papadakis C. and Scarton H. (Ed.), "Fluid Transients and Acoustics in the Power Industry", ASME, New York, pp. 179-185.
- Silberring, L. (1990), "Thermodynamic and Transport Properties of Gases for Computer Aided Engineering", Paper Presented at the 21<sup>st</sup> International CODATA Conference, Columbus, Ohio.
- Silberring, L. (1991), "A Temperature Function for the Virial Coefficients", Entropie, No. 164/165, pp. 139-140.
- Silberring, L. (1991), "A Computer Program System for Thermodynamic and Transport Properties of Real Gases", Silberring Engineering Ltd., Zurich.
- Silberring, L. (1993-1996), Silberring Engineering Ltd., Zurich, "Private Communication".
- Silberring, L. (1995), "Thermodynamic and Transport Property Data for a Typical Natural Gas Mixture at High Pressures", Supplied in a Diskette on Request (Unpublished).
- Silvester, P. P. (1984), "The Unix System Guidebook: An Introductory Guide for Serious Users", Springer-Verlag.
- Stittgen, M. and Zielke, W. (1990), "Fluid Structure Interaction in Flexible Curved Pipes", in Thorley, A. R. D. (Ed.), "Pressure Surges-Proceedings of the 6<sup>th</sup> International Conference, BHRA, pp. 101-120.
- Straty, G. C. (1974), "Velocity of Sound in Dense Fluid Methane", Cryogenics, July 1974.
- Suwan, K. and Anderson, A. (1992), "Method of Lines Applied to Hyperbolic Fluid Transient Equations", Int. J. Num. Meth. Eng., 33, pp. 1501-1511.



- Swaffield, J. A. (1967), "A Study of the Influence of Bends on Fluid Transients in Pipelines", MPhil Thesis, City University, London.
- Swaffield, J. A. (1968-69), "The Influence of Bends on Fluid Transients Propagated in Incompressible Pipe Flow", Proc. Inst. Mech. Engrs., Vol. 183, Part 1, No.29, pp. 603-614.
- Swamee, P. K. and Jain, A. K. (1976), "Explicit Equations for Pipe-Flow Problems", ASCE J. Hydr. Div., pp. 657-664.
- Taylor, D. L. (1992), "Computer-Aided Design", Addison-Wesley Publishing Company, Reading.
- The Guardian (1995), Tanzanian Newspaper, 13<sup>th</sup> Oct.
- Thorley, A. R. D. (1991), "Fluid Transients in Pipeline Systems", D. & L. George Ltd.
- Thorley, A. R. D. and Tiley, C. H. (1987), "Unsteady and Transient Flow of Compressible Fluids in Pipelines: A Review of Theoretical and Some Experimental Studies", Int. J. of Heat and Fluid Flow, 8(1), pp. 3-15.
- Tijsseling, A. S. and Lavooij, C. S. W (1990), "Fluid Structure Interaction and Column Separation in a Straight Elastic Pipe", in Thorley, A. R. D. (Ed.), "Pressure Surges: Proceedings of the 6<sup>th</sup> International Conference", BHRA, pp. 27-42.
- Tijsseling, A. S. (1993), "Fluid-Structure Interaction in the Case of Waterhammer With Cavitation", Communications on Hydraulic and Geotechnical Engineering of the Faculty of Civil Engineering, University of Dundee, Report No. 93-6, ISSN. 0169-6548.
- Tiley, C. H. (1989), "Pressure Transients in a Ruptured Gas Pipeline With Friction and Thermal Effects Included", PhD Thesis, City University, London.
- Trikha, A. K. (1975), "An Efficient Method for Simulating Frequency Dependent Friction in Transient Liquid Flow", Trans. ASME, J. Fluid Eng., 97, pp. 97-105.
- Tsumura, R. and Straty, G. C. (1977), "Speed of Sound in Saturated and Compressed Fluid Ethane", Cryogenics, April 1977.
- Van Reet, J. D. and Skogman, K. D. (1987), "The Effect of Measurement Uncertainty on Real Time Pipeline Modelling Applications", 1987 ASME Pipeline Engineering Symposium-ETCE, Dallas, Tx.
- Van Deen, J. K. and Reintsema, S. R. (1983), "Modelling of High-Pressure Gas Transmission Lines", Appl. Math. Modelling, 7, pp. 268-273.
- Vardy, A. E. (1993), Faculty of Civil Engineering, University of Dundee, "Private Communication".
- Vardy, A. E., Hwang, K. L. and Brown, J. M. B. (1993) "A Weighting Function Model of Transient Turbulent Pipe Friction", J. Hyd. Res., 31(4), pp. 533-548.

Vardy, A (1992) , " Approximating Unsteady Friction at High Reynolds Numbers", in Bettess, R. and Watts, J. (Eds.), "Unsteady Flow and Fluid Transients", Balkema, Rotterdam, pp. 21-29.

Vardy, A. E. and Fan, D. (1990), "Flexural Waves in a Closed Tube", in Thorley, A. R. D. (Ed.), "Pressure Surges: Proceedings of the 6<sup>th</sup> International Conference", BHRA, pp. 43-58.

Vetterling, W. T., Teukosky, S. A., Press, W. H. and Flannery, B. P. (1992), "Numerical Recipes: Example Book (C)", 2<sup>nd</sup> Edition Cambridge University Press.

Warming, R. F., Kutler, P. and Lomax, H. (1973), "Second-and Third-Order Noncentered Difference Schemes for Nonlinear Hyperbolic Equations", AIAA Journal, 11, pp. 189-196.

Weber Systems Inc. Staff (1984), "C Users' Handbook", Addison-Wesley, Reading.

Weimann, A. (1978), "Gas Distribution Network Dynamic Modelling and Simulation with Respect to Network Control and Monitoring", Thesis, Technical University of Munich, in German (English Translation: British Gas Translation No. LRS T 435).

Welty, J. R. (1978), "Engineering Heat Transfer", John Wiley & Sons.

White F. M. (1988), "Fluid Mechanics", Second Edition, McGraw-Hill, New York.

Wilson, D. J. (1981), "Expansion and Plume Rise of Gas Jets from High Pressure Pipeline Ruptures", Alberta Environment, Pollution Control Division.

Wood, D. J., Dorsch, R. G. and Lightner, C. (1966), "Wave-Plan Analysis of Unsteady Flow in Closed Conduits", ASCE-Journal of Hydraulics Division, 92(HY2), pp. 83-92.

Wood, D. J., Funk, J. E. and Boulos, P. F. (1990), "Pipe Network Transients-Distributed and Lumped Parameter Modelling", in Thorley, A. R. D. (Ed.), "Pressure Surges-Proceedings of the 6th International Conference", BHRA, pp. 131-142.

Wortman, L. A. and Sidebottom, T. O. (1984), "The C Programming Tutor", Prentice-Hall.

Wu, H. L., Pots, B. F. M., Hollenberg, J. F. and Meerhoff, R. (1987), "Two-Phase, Gas/Condensate Flow at High Pressure in an 8-Inch Horizontal Pipe", Paper for Presentation at the 3<sup>rd</sup> International Conference on Multiphase Flow, The Hague.

Wylie, E. B. and Streeter, V. L. (1978), "Fluid Transients", McGraw-Hill.

Wylie, E. B. (1982), "Fluid Transient in Two Spatial Dimensions", Paper for Presentation at the 1982 Pressure Vessel and Piping Conference, ASME, Orlando, Florida.

Yigang, C. and Jing-Chao, S. (1990), "An Efficient Approximate Expression for Transient Flow of High Viscous Fluid in Hydraulic Pipelines", in Thorley, A. R. D. (Ed.) "Pressure Surges-Proceedings of the 6<sup>th</sup> International Conference", BHRA, pp. 15-26.



Zemansky, M. W. and Dittman, R. H. (1983), "Heat and Thermodynamics", 6<sup>th</sup> Edition, McGraw-Hill, New York, Chapter 13.

Zha, G. C. and Bilgen, E. (1993), "Numerical Solution of Euler Equations by Using a New Flux Vector Splitting Scheme", Int. J. Num. Meth. Fluids, 17, pp. 115-144.

Zielke, W. (1968), "Frequency-Dependent Friction in Pipe Flow", Journal of Basic Engineering, March, pp. 109-115.

Zigrang, D. J. and Sylvester, N. D. (1985), "A Review of Explicit Friction Factor Equations", J. Energy Resources Technology, Trans. ASME, 107(2), pp. 280-283.

Zucrow, M. J. and Hoffman, J. D. (1977), "Gas Dynamics: Multidimensional Flow, Vol. 2", John Wiley & Sons, Chapter 19, pp. 295-399.

# APPENDICES

## A GENERAL EQUATIONS

Cross-section area of the pipe:

$$A = \frac{\pi d^2}{4} \quad (A-1)$$

Flow velocity of fluid:

$$u = \frac{\dot{m}}{\rho A} \quad (A-2)$$

Friction factor calculated using the Chen's explicit equation:

$$\frac{1}{\sqrt{f_D}} = -2.0 \log \left( \frac{\epsilon}{3.7065 d} + \frac{5.0452}{Re} \left( \log \left( \frac{1}{2.82577} \right) \frac{\epsilon}{D}^{1.1098} + \frac{5.8506}{Re^{0.8981}} \right) \right) \quad (A-3)$$

Frictional force per unit length of the pipe:

$$\omega = \frac{A}{d} \rho f_D \frac{u|u|}{2} \quad (A-4)$$

Reynold's number:

$$Re = \frac{\rho u d}{\mu} \quad (A-5)$$

Heat transfer across the pipe calculated by the Stanton number method:

$$\Omega = \pi d \rho u C_p St (T_w - T) \quad (A-6)$$

Stanton number:

$$St = \frac{Nu}{Pr Re} = \frac{h}{\rho u C_p} \quad (A-7)$$

$$St = f(Pr, Re) \quad (A-8)$$

Static pressure:

$$p = H \rho g \quad (A-9)$$

Speed of sound/wave speed for a perfect gas:

$$a = \sqrt{\gamma \frac{p}{\rho}} = \sqrt{\gamma Z R T} \quad (A-10)$$

and for a real gas:

$$a = \sqrt{\frac{\gamma_s p}{\rho}} = \sqrt{\gamma_s Z R T} \quad (A-11)$$



Prandtl number

$$Pr = \frac{C_p \mu}{k} \quad (A-12)$$

Nusselt number:

$$Nu = \frac{h d}{k} \quad (A-13)$$

Grasshoff number:

$$Gr = \frac{\beta g \rho^2 d^3 \Delta T}{\mu^2} \quad (A-14)$$

Mach number:

$$Ma = \frac{u}{a} \quad (A-15)$$

## B EXPRESSIONS FOR EQUATION OF STATE

The equation of state for a perfect gas is

$$p = \rho RT \quad (B-1)$$

The general equation of state for a real-gas is

$$P = Z \rho RT \quad (B-2)$$

Van Der Waal equation of state (1873)

$$p = \frac{NRT}{V-NB} - \frac{N^2 A}{V^2} \quad (B-3)$$

Where  $N$  is the number of moles

Dietrici equation of state (1899)

$$p = \frac{RT}{V-B} \exp\left(-\frac{A}{RTV}\right) \quad (B-4)$$

Berthelot equation of state (1903)

$$P = \frac{RT}{V-B} - \frac{A}{TV^2} \quad (B-5)$$

where  $A$  and  $B$  in equation (B-3) to (B-5) are constants.

Redlich-Kwong equation of state (1949)

$$P_R = \frac{T_R}{Z_c(V_R - 0.08664/Z_c)} - \frac{0.42748}{T_R^{0.5} Z_c^2 V_R(V_R + 0.08664/Z_c)^2} \quad (B-6)$$

Soave-Redlich-Kwong (SRK) equation of state (1972)

$$P = \frac{RT}{\tilde{v} - \hat{b}} - \frac{\hat{a}T}{\tilde{v}(\tilde{v} + \hat{b})} \quad (B-7)$$

where

$$\begin{aligned} \hat{b} &= 0.08664 \frac{RT_c}{P_c} \\ \hat{a}(T) &= \hat{a}(T_c) \hat{\alpha}(T_r, w) \\ \hat{a}(T_c) &= 0.4247747 \frac{R^2 T_c^2}{P_c} \\ \hat{\alpha}(T_r, w) &= [1 + \hat{m}(1 - T_r^{0.5})]^2 \\ \hat{m} &= 0.480 + 1.574 W - 0.176 W^2 \end{aligned}$$

Peng-Robinson (PR) equation of state (1976)

$$P = \frac{RT}{\tilde{v} - \hat{b}} - \frac{\hat{a}(T)}{\tilde{v}(\tilde{v} + \hat{b}) + \hat{b}(\tilde{v} - \hat{b})} \quad (B-8)$$

where

$$\begin{aligned} \hat{b} &= 0.077780 \frac{RT_c}{P_c} \\ \hat{a}(T) &= \hat{a}(T_c) \hat{\alpha}(T_r, w) \\ \hat{a}(T_c) &= 0.45724 \frac{R^2 T_c^2}{P_c} \\ \hat{\alpha}(T_r, w) &= [1 + \hat{m}(1 - T_r^{0.5})] \\ \hat{m} &= 0.377464 + 1.54226 w - 0.26992 w^2 \end{aligned}$$

Martin equation of state (1949)

$$\begin{aligned} P = \frac{RT}{v-b} + \frac{A_2 \cdot B_2 T \cdot C_2 e^{-KT}}{(v-b)^2} + \frac{A_3 \cdot B_3 T \cdot C_3 e^{-KT}}{(v-b)^3} + \frac{A_4 \cdot B_4 T \cdot C_4 e^{-KT}}{(v-b)^4} + \\ \frac{A_5 \cdot b_5 T \cdot C_5 e^{-KT}}{(v-b)^5} + \frac{A_6 \cdot B_6 T \cdot C_6 e^{-KT}}{e^{av}} + \frac{A_7 \cdot B_7 T \cdot C_7 e^{-KT}}{e^{-2av}} \end{aligned} \quad (B-9)$$

where a, b, K, A<sub>1</sub> to A<sub>7</sub>, B<sub>1</sub> to B<sub>7</sub> and C<sub>1</sub> to C<sub>7</sub> are constants.

The two parameter thermal equation of state of Martin based on the principle of corresponding states is

$$p_r = \frac{T_r}{Z_c \cdot v_r - 0.085} - \frac{9(4 - T_r)}{64(Z_c \cdot v_r - 0.04)^2} \quad (B-10)$$



where

$$p_r = \frac{p}{p_c} \quad T_r = \frac{T}{T_c} \quad v_r = \frac{p_c}{p} \quad Z_c = 0.28366$$

Note  $Z_c$  is the pseudo-critical real gas factor

The Martin equation solved explicitly with respect to  $T_r$  is

$$T_r = \frac{(Z_c \cdot v_r - 0.085)[36.64(Z_c \cdot v_r + 0.04)^2 p_r]}{9(Z_c \cdot v_r - 0.085) + 64(Z_c \cdot v_r + 0.04)^2} \quad (B-11)$$

Van Reet-Skogman equation of state (1987)

$$\frac{1}{Z} - 1 \approx \frac{P}{T^y} \quad (B-12)$$

*where y is a constant .*

Clausius equation of state (1930)

$$p(\tilde{v}-b) = RT \quad (B-13)$$

Benedict-Webb-Rubin equation of state

$$P = \frac{RT}{\tilde{v}} + \frac{RTB_0 - A_0 - \frac{C_0}{T^2}}{\tilde{v}^2} + \frac{RTb - a}{\tilde{v}^3} + \frac{a\alpha}{\tilde{v}^6} + \frac{C}{\tilde{v}^3 T^2} \left(1 + \frac{\omega}{\tilde{v}^2}\right) e \quad (B-14)$$

*where  $A_0, B_0, C_0, a, b, c, \alpha, \omega$  are empirical constants*

Redlich-Kwong equation of state

$$P = \frac{RT}{\tilde{v}-b} - \frac{a}{\tilde{v}(\tilde{v}+b)T^{0.5}} \quad (B-15)$$

*where*

$$a = 0.427 \frac{(48 R^2 T_c^{5/2})}{p_c} \quad b = 0.086 \frac{(64 R T_c)}{p_c}$$

Beattie-Bridgeman equation of state (1928)

$$P = RT \frac{(1-\epsilon)}{v^2} (v + \dot{B}) - \frac{A}{v^2} \quad (B-16)$$

$$\text{where } A = A_0 \left(1 - \frac{a}{v}\right), \quad \dot{B} = B_0 \left(1 - \frac{\dot{b}}{v}\right), \quad \epsilon = \frac{C}{v T^3}$$

The values of the five constants  $A_0, a, B_0, b$ , are in literature for some gases.

Kamerlingh-Onnes equation of state (1902), in the virial form:

$$pv = NRT \left(1 + \frac{B}{v} + \frac{C}{v^2} + \dots\right) \quad (B-17)$$

An expression in terms of powers of the pressure may be used as shown below;

$$pv = NRT + \dot{B}p + \dot{C}p^2 + \dots \quad (B-18)$$

Saville-Szczepanski methane-based equations of state

$$\begin{aligned}
 p = & \rho RT + \rho^2(A_1T + A_2T^{1/2} + A_3 + A_4/T + A_5/T^2) \\
 & + \rho^3(A_6T + A_7T^{1/2} + A_8 + A_9/T^2) \\
 & + \rho^4(A_{10}T + A_{11} + A_{12}/T) \\
 & + \rho^5A_{13} + \rho^6(A_{14}/T + A_{15}/T^2) + \rho^7A_{16}/T \\
 & + \rho^8(A_{17}/T + A_{18}/T^2) \\
 & + \rho^9A_{19}/T^2 + \rho^3 e^{-\gamma\rho^2} [ (A_{20}/T^2 + A_{21}/T^3) \\
 & + \rho^2(A_{22}/T^2 + A_{23}/T^4) + \rho^4(A_7/T^2 + A_{25}/T^3) \\
 & + \rho^6(A_{26}/T^2 + A_{27}/T^4) + \rho^8(A_{28}/T^2 + A_{29}/T^3) \\
 & + \rho^{10}(A_{30}/T^2 + A_{31}/T^3 + A_{32}/T^4) ] \quad (A2.19)
 \end{aligned}$$

$$\begin{aligned}
 p = & \rho RT + \rho^2(B_1T + B_2T^{1/2} + B_3 + B_4/T + B_5/T^2) \\
 & + \rho^3(B_6T + B_7/T^3) + \rho^4(B_8 + B_9/T + B_{10}/T^3) \\
 & + \rho^5(B_{11}T^2 + B_{12}/T^2) + \rho^6B_{13}/T^2 \\
 & + \rho^8B_{14}/T + \rho^9B_{15}/T + \rho^{11}B_{16}/T^2 \\
 & + \rho^3 e^{-\gamma\rho^2} [(B_{17}/T^2 + B_{18}/T^4) + \rho^2B_{19}/T^4 \\
 & + \rho^4B_{20}/T^2 + \rho^6B_{21}/T^2 + \rho^8(B_{22}/T^2 + B_{23}/T^4)] \quad (A2.20)
 \end{aligned}$$



## C EXPRESSIONS FOR FRICTION FACTOR

### C-1 LAMINAR FLOW: $Re < 2100$

Hagen-Poiseuille equation

$$f_D = \frac{64}{Re} \quad (C-1)$$

### C-2 TRANSITION ZONE

#### C-2.1 Implicit Equations

Colebrooke equation (1938)

$$\begin{aligned} & \text{Valid up to } \frac{\frac{d}{\epsilon}}{(Re \sqrt{f_D})} = 0.01 \\ & \frac{1}{\sqrt{f_D}} = -2.0 \log \left( \frac{\epsilon}{3.7065 d} + \frac{2.5226}{Re \sqrt{f_D}} \right) \end{aligned} \quad (C-2)$$

Oliemans expression for two-phase flow (1976)

$$\frac{1}{\sqrt{f_D}} = -2.0 \log \left( \frac{2\epsilon}{d_{eff}} + \frac{18.7}{Re \sqrt{f_D}} \right) + 1.74 \quad (C-3)$$

$Re$  is a two-phase Reynolds number and  $d_{eff}$  is the effective diameter for the two - phase mixture.

Colebrooke-White (1938-39) or Prandtl-Colebrooke equation

$$\begin{aligned} & \frac{1}{\sqrt{f_D}} = -2.0 \log \left( \frac{\epsilon}{3.7 d} + \frac{2.53}{Re \sqrt{f_D}} \right) \\ & \frac{1}{\sqrt{f_D}} = 2 \log \frac{\epsilon}{d} + 1.14 - 2 \log \frac{(1 + 9.35 d)}{\epsilon Re \sqrt{f_D}} \end{aligned} \quad (C-4)$$

#### C-2.2 Explicit Equations

Chen equation (1979) : All values of  $Re$  and  $\epsilon/d$

$$\frac{1}{\sqrt{f_D}} = -2.0 \log \left( \frac{\epsilon}{3.7065 d} + \frac{5.0452}{Re} \left( \log \left( \frac{1}{2.82577} \right) \frac{\epsilon}{D} \right)^{1.1098} + \frac{5.8506}{Re^{0.8981}} \right) \quad (C-5)$$

Churchill equation (1977) : For all  $Re$  and  $\epsilon/d$

$$f_D = 8 \left( \left( \frac{8}{Re} \right)^{12} + \frac{1}{(A \cdot B)^{\frac{3}{2}}} \right)^{\frac{1}{12}} \quad (C-6)$$

where

$$A = 2.4547 \ln \left( \frac{1}{\left( \frac{7}{Re} \right)^{0.9} + 0.277 \left( \frac{\epsilon}{d} \right)} \right)^{16} \quad B = \left( \frac{37530}{Re} \right)^{16}$$

Wood equation (1966):  $Re > 10,000$  and  $10^5 < \epsilon/d < 0.04$

$$f_D = a + bRe^{-c} \quad (C-7)$$

$$\text{where } a = 0.094 \left( \frac{\epsilon}{d} \right)^{0.225} + 0.53 \left( \frac{\epsilon}{d} \right) \quad b = 88.0 \left( \frac{\epsilon}{d} \right)^{0.44} \quad c = 1.62 \left( \frac{\epsilon}{d} \right)^{0.134}$$

Swamee-Jain equation (1976):  $5000 \leq Re \leq 10^8$  and  $10^{-6} \leq \epsilon/d \leq 10^{-2}$

$$\frac{1}{\sqrt{f_D}} = 2 \log \left( \frac{\epsilon}{3.7d} + \frac{5.74}{Re^{0.9}} \right) \quad (C-8)$$

$$f_D = \frac{1.325}{\left( \ln \left( \frac{\epsilon}{37d} + \frac{5.74}{Re^{0.9}} \right) \right)^2}$$

Generalised Haaland equation (1983):  $n=3$  recommended for gas transmission lines

$$\frac{1}{\sqrt{f_D}} = \frac{1.8}{n} \log \left( \left( \frac{6.9}{Re} \right)^n + \left( \frac{\epsilon}{3.7d} \right)^{1.11n} \right) \quad (C-9)$$

Shacham equation (1980)

$$\frac{1}{\sqrt{f_D}} = -2.0 \log \left( \frac{\epsilon}{3.7d} + \frac{14.5}{Re} \right) \quad (C-10)$$

Simple Zigrang-Sylvester equation (1982)

$$\frac{1}{\sqrt{f_D}} = -2.0 \log \left( \frac{\epsilon}{3.7d} + \frac{13}{Re} \right) \quad (C-11)$$

Moody equation (1976)

$$f_D = 0.0055 \left( 1 + \left( 20,000 \left( \frac{\epsilon}{d} \right) + \frac{10^6}{Re} \right)^{\frac{1}{3}} \right) \quad (C-12)$$

Jain equation (1947)

$$\frac{1}{\sqrt{f_D}} = 1.14 - 2 \log \left( \frac{\epsilon}{d} + \frac{21.25}{Re^{0.9}} \right) \quad (C-13)$$

Simple equation of Chen (1979)

$$\frac{1}{\sqrt{f_D}} = -2.0 \log \left( \left( \frac{\epsilon}{2.549d} \right)^{1.11} + \left( \frac{7.15}{Re} \right)^{0.9} \right) \quad (C-14)$$



Simple equation of Serghides (1984)

$$\frac{1}{\sqrt{f_D}} = -2.0 \log \left( \frac{\epsilon}{3.7d} + \frac{12}{Re} \right) \quad (C-15)$$

Intermediate Zigrang-Sylvester equation (1982)

$$\frac{1}{\sqrt{f_D}} = 2.0 \log \left( \frac{\epsilon}{3.7d} - \frac{5.02}{Re} \log \left( \frac{\epsilon}{3.7d} + \frac{13}{Re} \right) \right) \quad (C-16)$$

Intermediate Zigrang-Sylvester equations (1985)

$$\frac{1}{\sqrt{f_D}} = -2.0 \log \left( \frac{\epsilon}{3.7d} - \frac{2.51}{Re} \left( 1.14 - 2 \log \left( \frac{\epsilon}{d} + \frac{21.25}{Re^{0.9}} \right) \right) \right) \quad (C-17)$$

$$\frac{1}{\sqrt{f_D}} = -2.0 \log \left( \frac{\epsilon}{3.7d} - \frac{4.518}{Re} \log \left( \frac{6.9}{Re} + \left( \frac{\epsilon}{3.7d} \right)^{1.11} \right) \right) \quad (C-18)$$

Zigrang-Sylvester equation of highest precision (1982)

$$\frac{1}{\sqrt{f_D}} = -2.0 \log \left( \frac{\epsilon}{3.7d} - \frac{5.02}{Re} \log \left( \frac{\epsilon}{3.7d} - \frac{5.02}{Re} \log \left( \frac{\epsilon}{3.7d} + \frac{13}{Re} \right) \right) \right) \quad (C-19)$$

Serghides equations of highest precision (1984)

$$\frac{1}{\sqrt{f_D}} = -2.0 \log \left( \frac{\epsilon}{3.7d} - \frac{5.02}{Re} \log \left( \frac{\epsilon}{3.7d} - \frac{5.02}{Re} \log \left( \frac{\epsilon}{3.7d} - \frac{5.02}{Re} \log \left( \frac{\epsilon}{3.7d} + \frac{13}{Re} \right) \right) \right) \right) \quad (C-20)$$

Zigrang-Sylvester equation of highest precision (1985)

$$f_D = \left( A - \frac{(C-A)^2}{C-2B+A} \right)^{-2} \quad (C-21)$$

and

$$f_D = \left( 4.781 - \frac{(A - 4.781)^2}{B - 2A + 4.781} \right)^{-2} \quad (C-22)$$

where

$$A = -2 \log \left( \frac{\epsilon}{3.7d} + \frac{12}{Re} \right) \quad (C-22a)$$

$$B = -2 \log \left( \frac{\epsilon}{3.7d} + \frac{2.51 A}{Re} \right) \quad (C-22b)$$

$$C = -2 \log \left( \frac{\epsilon}{3.7d} + \frac{2.51 B}{Re} \right) \quad (C-22c)$$

### C-2.3 PARTIALLY DEVELOPED TURBULENCE

Chaudhry equation (1979) :  $Re > 2000$

$$f_D = 0.046 Re^{-0.2} \quad (C-23)$$

Panhandle 'A' equation

$$\frac{1}{\sqrt{f_D}} = 3.39 Re^{0.0773} E \quad (C-24)$$

where E is the efficiency of the system and is an adjustable parameter which allows for the effects of the minor losses and variation in pipe roughness.

Uhl equation (1965)

$$\frac{1}{\sqrt{f_D}} = -2 F \log \left( 4 \frac{\sqrt{f_D}}{Re} \right) \quad (C-25)$$

Where F is the drag factor to account for the effect of bends and fittings.

Smith equation (1956)

$$\frac{1}{\sqrt{f_D}} = 2 \log \left( Re \frac{\sqrt{f_D}}{2} \right) - 0.3 \quad (C-26)$$

Blasius equation (1911) :  $Re > 10^5$

$$f_D = 0.3160 Re^{-0.25} \quad (C-27)$$

### C-2.4 FULLY DEVELOPED TURBULENCE

Smith equation (1956)

$$\frac{1}{\sqrt{f_D}} = 2 \log \left( \frac{3.7d}{\epsilon} \right) + 2.2773 \quad (C-28)$$

Nikuradse equation (1932) : Smooth pipe and  $3000 < Re < 3.4 \times 10^6$

$$\frac{1}{f_D} = 2.0 \log (Re \sqrt{f_D}) - 0.8 \quad (C-29)$$

Von Karman equation (1932): Rough pipe and  $(d/\epsilon)/(Re\sqrt{f_D}) > 0.01$

$$\frac{1}{\sqrt{f_D}} = 2 \log \left( \frac{d}{\epsilon} \right) + 1.74 \quad (C-30)$$



## **D LIST OF PROGRAMMES AND SUB-ROUTINES**

<b>BREAK</b>	driver routine for transient analysis after the break
<b>BRINC</b>	driver routine for initiating the break and calculating initial fluid properties at the break
<b>BRINCUC</b>	routine for calculating initial break conditions in both upstream and downstream sections with uniform grid size.
<b>BRINCV</b>	routine for calculating initial break conditions in both upstream and downstream sections with variable grid size.
<b>BRMCCAUD</b>	transient analysis downstream after the break with uniform grid size and pipe exposed to the atmosphere
<b>BRMCCAUC</b>	transient analysis upstream after the break with uniform grid size and pipe exposed to the atmosphere
<b>BRMCCAUDV</b>	transient analysis downstream after the break with variable grid size and pipe exposed to the atmosphere
<b>BRMCCAUCV</b>	transient analysis upstream after the break with variable grid size and pipe exposed to the atmosphere
<b>BRMOCAUD</b>	transient analysis downstream after the break with uniform grid size and pipe exposed to the atmosphere
<b>BRMOCAUC</b>	transient analysis upstream after the break with uniform grid size and pipe exposed to the atmosphere
<b>BRMOCAUDV</b>	transient analysis downstream after the break with variable grid size and pipe exposed to the atmosphere
<b>BRMOCAUCV</b>	transient analysis upstream after the break with variable grid size and pipe exposed to the atmosphere
<b>BRWKLAUD</b>	transient analysis downstream after the break with uniform grid size and pipe exposed to the atmosphere
<b>BRWKLAUC</b>	transient analysis upstream after the break with uniform grid size and pipe exposed to the atmosphere
<b>BRWKLAUDV</b>	transient analysis downstream after the break with variable grid size and pipe exposed to the atmosphere
<b>BRWKLAUCV</b>	transient analysis upstream after the break with variable grid size and pipe exposed to the atmosphere

<b>CALCQDB</b>	execution of MS-DOS commands for automatic execution of QDB programme in the QUANT software
<b>CLEARSCR</b>	clearing the screen
<b>CTWORK</b>	prompting the user to indicate whether or not he wishes to continue running the programme
<b>DFGEN</b>	Creating ASCII data books from the QUANT programme for the domain of fluid parameter
<b>FLDPARAS</b>	writing input parameters in binary random access file paras.usr for running the QUANT programme
<b>FLDPROPB</b>	Reading output data from binary random access file props.dat produced by the QUANT programme
<b>FLDPROPS</b>	Reading output data from ASCII file produced by the FLDPROPB
<b>FLDPROPV</b>	Reading output data from ASCII data book produced by the subroutine and interpolating for the required input parameters
<b>GRIDGEN</b>	sub-programme for grid generation
<b>HEATATM</b>	Calculation of heat transfer through a pipe exposed to the atmosphere
<b>HEATGR</b>	Calculation of heat transfer through a buried pipe
<b>INIQDB</b>	execution of MS-DOS commands to call the programme QDB in the QUANT software, for manual inputting of the input parameters and execution of calculation
<b>INITIAL</b>	initiating the execution of the main programme
<b>MCC</b>	sub-programme for second-order analysis using the MacCormack method
<b>MOCD</b>	sub-programme for second-order method of characteristics analysis downstream the break
<b>MOCU</b>	sub-programme for second-order method of characteristics analysis upstream the break
<b>MTRANS</b>	main/driver routine
<b>SBMOCAU1</b>	first-order calculation of new dependent parameters $p$ , $u$ and $\rho$ using the method of characteristics, with uniform grid size and pipe exposed to the atmosphere
<b>SBMOCAU2</b>	second-order calculation of new dependent parameters $p$ , $u$ and $\rho$ using the method of characteristics and with uniform grid size



- SBMOCAV1** first-order calculation of new dependent parameters  $p$ ,  $u$  and  $\rho$  using the method of characteristics, with variable grid size and pipe exposed to the atmosphere
- SBMOCAV2** second-order calculation of new dependent parameters  $p$ ,  $u$  and  $\rho$  using the method of characteristics, with variable grid size and pipe exposed to the atmosphere
- SBMOCGU1** first-order calculation of new dependent parameters  $p$ ,  $u$  and  $\rho$  using the method of characteristics, with uniform grid size and buried pipe
- SBMOCGU2** second-order calculation of new dependent parameters  $p$ ,  $u$  and  $\rho$  using the method of characteristics, with uniform grid size and buried pipe
- SBMOCGV1** first-order calculation of new dependent parameters  $p$ ,  $u$  and  $\rho$  using the method of characteristics, with variable grid size and buried pipe
- SBMOCGV2** second-order calculation of new dependent parameters  $p$ ,  $u$  and  $\rho$  using the method of characteristics, with variable grid size and buried pipe
- SBMOCVU1** first-order calculation of new dependent parameters  $p$ ,  $u$  and  $\rho$  using the method of characteristics and with variable grid size and without interpolation
- SDMOCAV2** second-order calculation of new dependent parameters  $p$ ,  $u$  and  $\rho$  for the downstream section, using the method of characteristics, with variable grid size and pipe exposed to the atmosphere
- SDMOCGV2** second-order calculation of new dependent parameters  $p$ ,  $u$  and  $\rho$  for the downstream section, using the method of characteristics, with variable grid size and pipe exposed to the atmosphere
- STAD1BUD** adiabatic compressible downstream with backward differencing and uniform grid size
- STAD1BUU** adiabatic compressible upstream with backward differencing and uniform grid size
- STAD1BVD** adiabatic compressible downstream with backward differencing and variable grid size
- STAD1BVU** adiabatic compressible upstream with backward differencing and variable grid size
- STAD1FUD** adiabatic compressible downstream with forward differencing and uniform grid size

<b>STAD1FUU</b>	adiabatic compressible upstream with forward differencing and uniform grid size
<b>STAD1FVD</b>	adiabatic compressible downstream with forward differencing and variable grid size
<b>STAD1FVU</b>	adiabatic compressible upstream with forward differencing and variable grid size
<b>STAD2UD</b>	adiabatic compressible downstream with second-order differencing and uniform grid size
<b>STAD2UU</b>	adiabatic compressible upstream with second-order differencing and uniform grid size
<b>STAD2VD</b>	adiabatic compressible downstream with second-order differencing and variable grid size
<b>STAD2VU</b>	adiabatic compressible upstream with second-order differencing and variable grid size
<b>STEAD</b>	driver routine for steady state analysis routines
<b>STINADUD</b>	adiabatic incompressible downstream of the break with uniform grid size
<b>STINADUU</b>	adiabatic incompressible upstream of the break with uniform grid size
<b>STINADVD</b>	adiabatic incompressible downstream of the break with variable grid size
<b>STINADVU</b>	adiabatic incompressible upstream the break with variable grid size
<b>STINISUD</b>	isothermal incompressible downstream of the break with uniform grid size
<b>STINISUU</b>	isothermal incompressible upstream of the break with uniform grid size
<b>STINISVD</b>	isothermal incompressible downstream of the break with variable grid size
<b>STINISVU</b>	isothermal incompressible upstream the break with variable grid size
<b>STISOUD</b>	isothermal compressible downstream with uniform grid size
<b>STISOUU</b>	isothermal compressible upstream with uniform grid size
<b>STISOVD</b>	isothermal compressible downstream with variable grid size
<b>STISOVU</b>	isothermal compressible upstream with variable grid size
<b>STNONAUD</b>	non-adiabatic non-isothermal compressible downstream with uniform grid size and pipe exposed to the atmosphere
<b>STNONAUU</b>	non-adiabatic non-isothermal compressible upstream with uniform grid size and pipe exposed to the atmosphere
<b>STNONAVD</b>	non-adiabatic non-isothermal compressible downstream with variable grid size and pipe exposed to the atmosphere



<b>STNONAVU</b>	non-adiabatic non-isothermal compressible upstream with variable grid size and pipe exposed to the atmosphere
<b>SUBHTA</b>	Calculation of frictional force and heat transfer through a pipe exposed to the atmosphere
<b>SUBHTG</b>	Calculation of frictional force and heat transfer through a buried pipe
<b>SYSDATA</b>	inputting general system and gas data
<b>TRANS</b>	driver routine for transient analysis before the break
<b>WKL</b>	sub-programme for third-order analysis using the Warming-Kutler-Lomax method
<b>XSVBKS</b>	driver routine for solution of linear simultaneous equations
<b>XZRHQR4</b>	driver routine for solution of fourth-order polynomial.
<b>YESNO</b>	prompting the user to answer YES (Y) or NO (N)

**NOTE:**

- (i) The names of the subroutines used for first- and second-order approximations in the method of characteristics, for transient analysis before the break are obtained by replacing the first two letters of those used after the break, i.e. SB with letters SN.
- (ii) The names of routines used for transient analysis are obtained by replacing the first two letters of those used after the break, i.e. BR with letters TR.
- (iii) The names of sub-routines and routines used in the case of buried pipeline are obtained by replacing the letter A in the names of those used for pipeline which are exposed to the atmosphere, by the letter G.